Thesis reference number:

University of Science and Technology of Hanoi

PHYTOCHEMICAL CONSTITUENTS AND BIOACTIVITIES OF *PANDANUS TECTORIUS* AND *PANDANUS AMARYLLIFOLIUS*

Ph.D. THESIS IN PHARMACOLOGICAL, MEDICAL, AND AGRONOMICAL BIOTECHNOLOGY

DO HOANG GIANG

DEPARTMENT OF LIFE SCIENCES

Hanoi, May 2026

University of Science and Technology of Hanoi

PHYTOCHEMICAL CONSTITUENTS AND BIOACTIVITIES OF *PANDANUS TECTORIUS* AND *PANDANUS AMARYLLIFOLIUS*

Ph.D. THESIS IN PHARMACOLOGICAL, MEDICAL, AND AGRONOMICAL BIOTECHNOLOGY

Candidate: Do Hoang Giang

Supervisor
Assoc. Prof. Nguyen Tien Dat

Co-supervisor
Assoc. Prof. Nguyen Hai Dang

Hanoi, May 2026

Acceptance of Supervisors

1. **Assoc. Prof. Dr. Nguyen Tien Dat**, Center for High Technology Research and Development, Vietnam Academy of Science and Technology

I approve all the modifications and corrections made in the revised version of the thesis

Assoc. Prof. Dr. Nguyen Tien Dat

2. **Assoc. Prof. Dr. Nguyen Hai Dang**, University of Science and Technology of Hanoi, Vietnam Academy of Science and Technology

I approve all the modifications and corrections made in the revised version of the thesis

Assoc. Prof. Dr. Nguyen Hai Dang

Acceptance of the Chairman of the Examination Jury

Prof. Dr. Nguyen Van Hung, Institue of Chemistry, Vietnam Academy of Science and Technology

I approve all the modifications and corrections made in the revised version of the thesis

Prof. Dr. Nguyen Van Hung

DECLARATION

I hereby declare on my honour that I conducted this thesis under the supervision of Assoc. Prof. Dr. Nguyen Tien Dat and Assoc. Prof. Dr. Nguyen Hai Dang. The results presented in the thesis are truthful and have not been previously published, except where they appear in my own publications.

A decade has gone by since this journey started. I'm endlessly grateful to the dear souls who stood with me through every up and down.

ACKNOWLEDGEMENT

First and foremost, I wish to extend my profound gratitude to my supervisors, Assoc. Prof. Dr. Nguyen Tien Dat and Assoc. Prof. Dr. Nguyen Hai Dang, for their invaluable guidance and unwavering support, not only in the completion of this Ph.D. thesis but also throughout my eleven years of study and research. Their mentorship has been instrumental to my academic and professional development, and this work would not have been possible without their encouragement and instruction.

I am equally indebted to the faculty members and staff of the University of Science and Technology of Hanoi (USTH). The opportunity to learn and work under your guidance has been immensely rewarding, and I sincerely hope to continue this fruitful collaboration in the future. I would particularly like to acknowledge my colleagues in the Phytomed group (USTH), whose assistance and cooperation have greatly contributed to the successful completion of this dissertation.

My deepest appreciation is also extended to my colleagues at the Center for High Technology Research and Development, as well as to my former labmates at the Department of Agro-Pharmaceutical Research, now the Department of Applied Chemistry and Biology. Their companionship in laboratory work, moral support, and constant encouragement—often embodied in the recurrent question, *"When will you defend your thesis?"*—have provided invaluable motivation throughout this journey. I am further grateful to the Project under the grant number NCXS01.02/23-25 of the Center for High Technology Research and Development, Vietnam Academy of Science and Technology, for providing the essential resources and facilities that supported my research.

I also wish to acknowledge with gratitude my friends and colleagues from various institutions, both within and beyond Vietnam, for their kind assistance and encouragement over the years.

Finally, my deepest thanks are reserved for my family—for my mother, who has raised me with love and devotion for 35 years; for my beloved wife, who has endured hardships with me and once promised she would support me for a lifetime so that I could pursue my passion for science; and for my son, who brings me joy and strength to overcome life's challenges.

I firmly believe that the experiences and support I have received will serve as a lasting foundation for the continuation of my scientific endeavors.

To all, I extend my deepest and most respectful gratitude!

Do Hoang Giang

ABSTRACT

This thesis investigates the phytochemistry and selected bioactivities of *Pandanus tectorius* and *Pandanus amaryllifolius* through comparative screening of extracts from multiple taxa, targeted isolation and characterization of metabolites from *P. tectorius* leaves, response-surface-based optimization of phenolic- and saponin-enriched fractions from *P. tectorius* fruits, and a phenolic enrichment from *P. amaryllifolius* leaves. Bioassays comprised radical-scavenging (DPPH, hydroxyl), α-amylase inhibition, cytotoxicity (A549, K562, MCF7), and nitric-oxide (NO) production inhibition in LPS-stimulated RAW 264.7 cells.

Comparative profiling revealed pronounced interspecific and organ-level differences: *P. tectorius* was consistently rich in phenolics, flavonoids, and saponins and showed the strongest antioxidant activity, whereas *P. amaryllifolius* accumulated exceptionally high alkaloid levels with attendant cytotoxic and anti-inflammatory effects.

From *P. tectorius* leaves, two new benzofuran epimers (Pandanusfuran A and B) and four known lignans (pinoresinol, pinoresinol monomethyl ether, arctigenin, matairesinol) were characterized by HR-ESI-MS/NMR with absolute configurations assigned via ECD/Snatzke's $Mo_2(OAc)_4$-induced ECD; HPLC-DAD verified the benzofurans as native constituents. Lignans showed comparatively stronger radical-scavenging than benzofurans, while the benzofurans displayed α-amylase inhibition approaching acarbose and selective cytotoxicity toward A549, with minimal activity against K562/MCF7 and negligible NO inhibition.

Box–Behnken Design optimization of *P. tectorius* fruits yielded statistically robust quadratic models for total phenolics (TPC) and total saponins (TSC). Multi-response optimization produced seven validated operating windows that trade off phenolic-rich vs saponin-rich outcomes: TPC-prioritized conditions favor higher ethanol (70–90%) and 80 °C; TSC-prioritized conditions favor 45–55% ethanol and longer extraction times (>175 min); an intermediate "Balance" setting achieves good simultaneous yields. Phenolic-rich extracts showed stronger antioxidant effects, whereas saponin-rich extracts exhibited higher NO inhibition but potential cytotoxicity at the highest saponin levels.

For *P. amaryllifolius* leaves, an optimized phenolic enrichment displayed potent antioxidant activity (comparable to ascorbic acid and catechin) and stronger NO inhibition than separated alkaloid and non-alkaloid fractions, consistent with synergism between phenolic and alkaloid constituents; isolation identified a suite of phenolics and shikimate-derived metabolites (e.g., methyl shikimate, n-butyl shikimate, pinoresinol 4-*O*-*β*-D-glucoside, methyl gallate, vanillic, 4-hydroxybenzoic acids and related esters, vanillin, n-butyl-D-galactopyranoside).

Overall, the outcomes of this work enrich current phytochemical knowledge of *P. tectorius* and *P. amaryllifolius*, elucidate species- and organ-specific bioactivity patterns, and establish optimized extraction strategies that can guide future pharmacological and functional applications.

TÓM TẮT

Luận án này nghiên cứu thành phần hoá học và một số hoạt tính sinh học của các loài *Pandanus tectorius* và *Pandanus amaryllifolius* thông qua các nghiên cứu cụ thể gồm: (i) sàng lọc thành phần và hoạt tính sinh học của cao chiết từ các loài đã thu thập; (ii) phân lập và xác định cấu trúc các hợp chất chuyển hóa thứ cấp từ lá dứa dại (*P. tectorius)*; (iii) tối ưu hóa điều kiện trích ly bằng phương pháp bề mặt đáp ứng nhằm thu được các phân đoạn giàu phenolic và saponin từ quả dứa dại (*P. tectorius*); và (iv) tối ưu hóa quá trình làm giàu phenolic từ lá dứa thơm (*P. amaryllifolius*). Các hoạt tính sinh học được đánh giá bao gồm khả năng quét gốc tự do (DPPH, hydroxyl), ức chế enzyme α-amylase, gây độc tế bào trên các dòng A549, K562, MCF7, và ức chế tạo nitric oxide (NO) trên đại thực bào RAW 264.7 được kích thích bằng LPS.

Kết quả phân tích so sánh cho thấy sự khác biệt rõ rệt giữa các loài và giữa các bộ phận của cây: *P. tectorius* có hàm lượng phenolic, flavonoid và saponin cao nhất, thể hiện hoạt tính kháng oxy hóa mạnh nhất; *P. amaryllifolius* tích lũy hàm lượng alkaloid rất cao, liên quan đến khả năng gây độc tế bào và kháng viêm.

Từ lá *P. tectorius*, hai epimer benzofuran mới (Pandanusfuran A và B) cùng bốn lignan đã biết (pinoresinol, pinoresinol monomethyl ether, arctigenin, matairesinol) được xác định cấu trúc bằng HR-ESI-MS và NMR; cấu hình tuyệt đối được xác định thông qua ECD và phương pháp Snatzke's $Mo_2(OAc)_4$-induced ECD. Phân tích HPLC-DAD khẳng định hai benzofuran này là các thành phần tự nhiên có trong lá cây. Các lignan thể hiện khả năng khử gốc tự do mạnh hơn benzofuran, trong khi benzofuran có hoạt tính ức chế α-amylase gần tương đương acarbose và chọn lọc gây độc tế bào trên dòng A549, cùng với hoạt tính gây độc yếu trên K562 và MCF7, cũng như khả năng ức chế NO ở mức yếu.

Tối ưu hóa bằng thiết kế Box–Behnken đối với quá trình chiết xuất quả *P. tectorius* cho thấy các mô hình bậc hai có ý nghĩa thống kê cao cho tổng hàm lượng phenolic (TPC) và saponin (TSC). Phân tích đa đáp ứng đã xác định bảy điều kiện hoạt động tối ưu tương ứng với các mục tiêu trích ly khác nhau: điều kiện ưu tiên TPC đạt hiệu quả cao nhất khi dùng ethanol 70–90% ở 80 °C; điều kiện ưu tiên TSC đạt tối ưu với ethanol 45–55% và thời gian trích ly kéo dài (>175 phút); trong khi điều kiện "cân bằng" đạt hiệu quả đồng thời ở cả hai chỉ tiêu. Các dịch chiết giàu phenolic thể hiện khả năng

kháng oxy hóa mạnh, trong khi các dịch chiết giàu saponin có khả năng ức chế NO cao hơn nhưng có thể gây độc tế bào ở nồng độ saponin lớn nhất.

Đối với lá *P. amaryllifolius*, phân đoạn phenolic được tối ưu thể hiện hoạt tính kháng oxy hóa mạnh (tương đương acid ascorbic và catechin) và khả năng ức chế NO cao hơn so với các phân đoạn alkaloid và không-alkaloid riêng lẻ, cho thấy hiệu ứng hiệp đồng giữa hai nhóm hợp chất này. Quá trình phân lập đã xác định được nhiều hợp chất phenolic và dẫn xuất của shikimate như methyl shikimate, *n*-butyl shikimate, pinoresinol 4-*O*-*β*-D-glucoside, methyl gallate, vanillic acid, 4-hydroxybenzoic acid cùng các este liên quan, vanillin và *n*-butyl-D-galactopyranoside.

Tổng thể, kết quả của nghiên cứu này góp phần mở rộng hiểu biết hiện có về thành phần hoạt chất chuyển hoá thứ cấp của hai loài *P. tectorius* và *P. amaryllifolius*, làm rõ các đặc trưng về hoạt tính sinh học theo loài và theo bộ phận của cây, đồng thời xây dựng các phương pháp trích ly tối ưu có thể định hướng cho các ứng dụng sản xuất dược phẩm và thực phẩm chức năng trong tương lai.

TABLE OF CONTENTS

LIST OF ABBREVIATIONS

Abbreviation	Full form
^{13}C NMR	Carbon-13 nuclear magnetic resonance spectroscopy
^{1}H NMR	Proton nuclear magnetic resonance spectroscopy
ANOVA	Analysis of Variance
ATCC	American Type Culture Collection
BBD	Box–Behnken Design
CC	Column chromatography
CD_3OD	Tetradeuteromethanol (Methanol-d_4)
$CDCl_3$	Deuterochloroform (Chloroform-*d*)
CH_2Cl_2	Dichloromethane
COSY	^{1}H-^{1}H- correlation spectroscopy
DAD	Diode Array Detector
DEPT	Distortionless enhancement by polarization transfer
DMSO	Dimethyl sulfoxide
DMSO-d_6	Deuterated dimethyl sulfoxide
DNSA	3,5-Dinitrosalicylic acid
DPPH	2,2-Diphenyl-1-picrylhydrazyl
EA	Ethyl acetate
ESI	Electrospray Ionization
FBS	Fetal Bovine Serum
HMBC	Heteronuclear multiple bond correlation
HPLC	High-Performance Liquid Chromatography
HRESIMS	High-Resolution Electrospray Ionization Mass Spectrometry
HSQC	Heteronuclear single quantum correlation
IC_{50}	Inhibitory concentration at 50%
MIC	Minimum Inhibitory Concentration
NO	Nitric Oxide
OD	Optical Density
PLSR	Partial Least Squares Regression
RSM	Response surface method
TAC	Total alkaloid content
TFC	Total flavonoid content
TPC	Total phenolic content
TSC	Total Saponin content

LIST OF TABLES

LIST OF FIGURES

CHAPTER 1. GENERAL INTRODUCTION

1.1. Scientific classification, distribution, and uses of *Pandanus tectorius* and *Pandanus amaryllifolius*

The *Pandanus* genus encompasses a diverse group of tropical plants known for their distinctive features and widespread distribution across tropical and subtropical regions worldwide [1]. Belonging to the family Pandanaceae, these plants are characterized by their unique foliage, often featuring long, narrow leaves arranged in spirals around the trunk, giving them a screw-like appearance. While there are over 750 species within the genus, they share common traits such as aerial prop roots, which help provide stability in sandy or coastal environments [1]. *Pandanus* species play multifaceted roles in various ecosystems and cultures. Ecologically, they contribute to coastal stabilization, providing habitat and food for diverse wildlife. Culturally, they hold significant importance, with their leaves utilized for weaving traditional crafts, such as mats, baskets, and thatched roofs. Moreover, in some culinary traditions, *Pandanus* leaves are employed to infuse a distinctive aroma and flavor into dishes, ranging from savory to sweet. From the lush rainforests of Asia to the remote islands of the Pacific, *Pandanus* plants thrive in a variety of habitats, adapting to diverse environmental conditions. Their resilience, coupled with their cultural and ecological significance, makes the *Pandanus* genus a fascinating subject of study and admiration for botanists, ecologists, and enthusiasts alike [1]. In Vietnam, about 17 species in the genus were determined, such as *Pandanus tectorius*, *Pandanus amaryllifolius*, *Pandanus odoratissimus, Pandanus tonkinensis,* etc [2, 3].

Pandanus tectorius Parkinson ex Du Roi is a species in the genus *Pandanus*, of the family Pandanaceae [1]. The species branches off on the top of trees, which can be about 3-4 meters tall with many roots dropping into the ground, leaves grow in long bunches 1-2 meters, and the middle veins and the edge of the leaf have sharp edges. Male flowers grow at the top of trees and drop down with white, separate buds. The flowers are very fragrant, and female flowers are solitary, with multiple carpels. The fruit cluster is ovate-shaped, about 16-22 centimetres, with an orange petiole, consisting of fruits with angles split into many cells, and fruiting in the summer [2, 3]. The tree is moisture-loving, grows into a rather large bush, produces annual fruit in large quantities,

and is not cut down [4]. *P. tectorius* is widely distributed in tropical forests, mangrove forests, and coastal areas from South Asia to the islands of the Pacific Ocean. In some places, parts of the *Pandanus* plant are commonly used as food, beverage, or flavouring [1]. Meanwhile, the genus *Pandanus* can be easily found from the mountainous midlands regions to the coast of Khanh Hoa. Roots are used in folk medicine to treat oedema, painful urination, urinary frequency, and urinary stones, or to treat fractures and protrusions. The young leaves are also used to cure kidney stones and epilepsy in children [4].

Pandanus amaryllifolius Roxb is an evergreen tree with fragrantly-scented leaves. The tree produces an erect stem, 2 - 4.5 metres tall and 15 cm in diameter [2, 3]. The female inflorescence is unknown, but it produces a male inflorescence on exceedingly rare occasions. The leaves are widely used as a flavouring throughout Southeast Asia. The plant is cultivated for its leaves in gardens in Vietnam, Indonesia, Malaysia, Thailand, New Guinea, Sri Lanka, and the Philippines [2-4].

1.2. Chemical constituents of *Pandanus* species

1.2.1. Lignans

Lignan is one of the most common groups of substances in the *Pandanus* species in general and *P. tectorius* in particular. Three lignans, including pinoresinol **(1)**, (+)-syringaresinol **(2)**, and (+)-medioresinol **(3),** were isolated in the chloroform extract from the *Pandanus odoratissimus* fruits by Cuong *et al.* in 2015 [5].

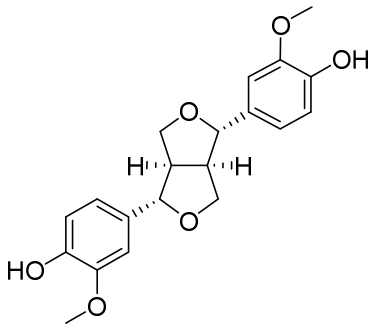

1)

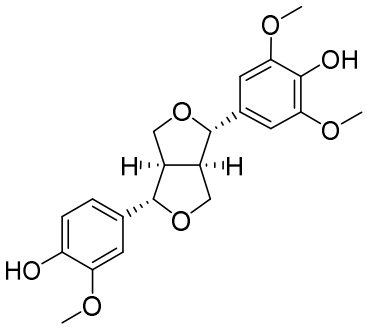

(2)

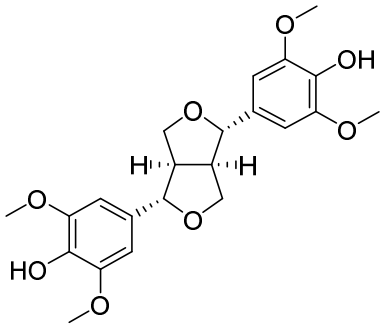

(3)

Meanwhile, previous studies reported lignans in some species of *Pandanus*. In 1998, six lignans, such as eudesmin **(4)**, kobusin **(5)**, pinoresinol **(1)**, epipinoresinol **(6)**, de-4'-*O*-methyleudesmin **(7)**, and 3,4-bis(4-hydroxy-3-methoxy-benzyl)-tetrahydrofuran **(8)** were determined from the root of *Pandanus odoratissimus* by Jong and his colleagues. Besides, five lignans, including (+)-pinoresinol **(1)**, (+)-eudesmin **(4)**, kobusin **(5)**, (+)-sesamin **(9)**, and salicifoliol **(10)** were also identified by Inada *et al*. in 2005 [6]

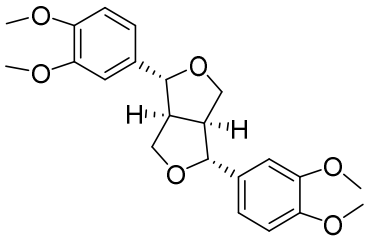

(4)

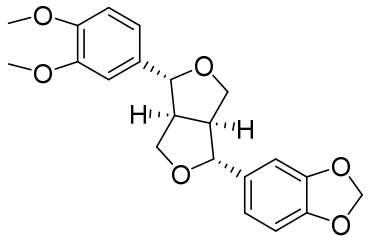

(5)

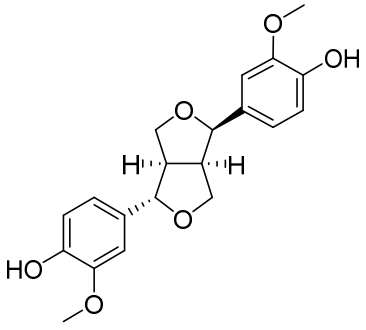

(6)

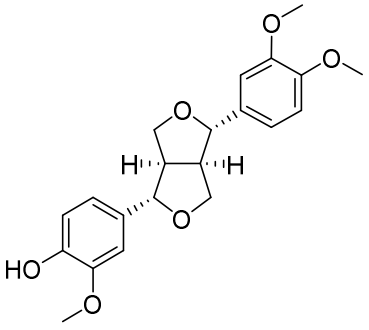

(7)

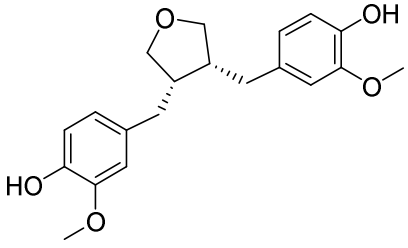

(8)

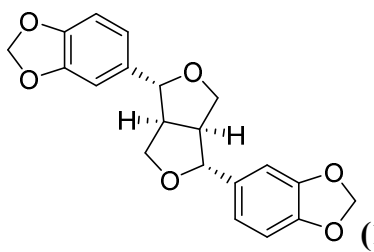

(9)

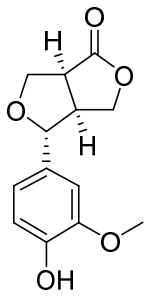

(10)

The lignans include (+)-pinoresinol **(1)**, (+)-syringaresinol **(2)**, (+)-medioresinol **(3),** (+)-lyoniresinol **(11)** and (−)-balanophonin **(12)** were also found in the composition of fruit parts of the *P. tectorius*, as announced by Phat *et al.* in 2016 [7]. The compounds showed better *α*-glucosidase inhibitory activity (IC_{50} = 26.7 – 68.1 μM) than the positive control, acarbose (IC_{50} = 214.5 μM) under the same experimental conditions.

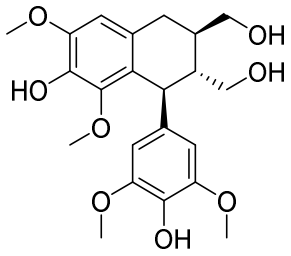

(11)

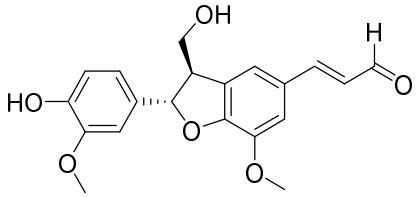

(12)

1.2.2. Flavonoids

In 2013, vitexin **(13)** and tricin **(14)** were isolated from the roots of *P. tectorius* [8]. Previously, five flavonoids, such as tangeretin **(15)**, sakranetin **(16)**, chrysin **(17)**, naringenin **(18)**, and 5,8-dihydroxy-7-methoxy-flavone **(19)** were isolated from fruits of *P. tectorius* by Zhang *et al.* in 2012 [9].

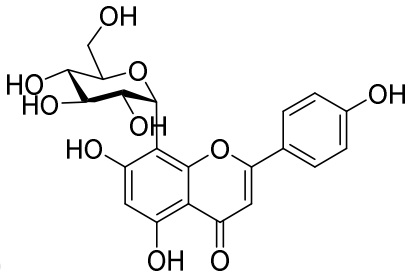

(13)

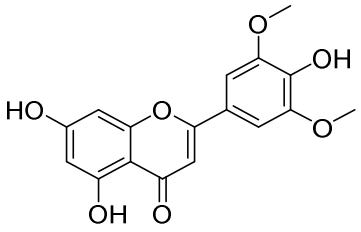

(14)

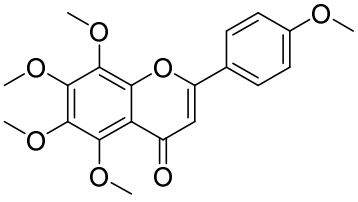

(15)

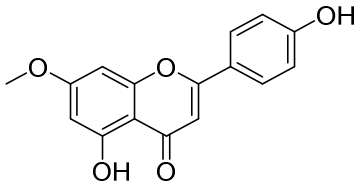

(16)

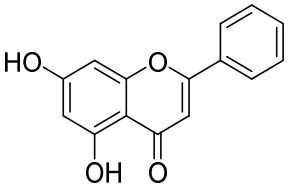

(17)

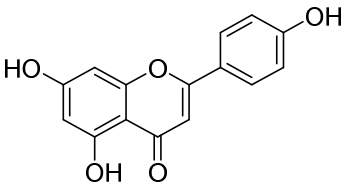

(18)

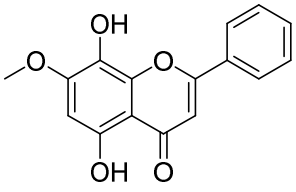

(19)

1.2.3. Coumarin derivatives

Four coumarins, including *Pandanus*in A **(20)**, bergapten **(21)**, 6-(6′-hydroxy-3′,7′-dimethylocta-2′,7′-dienyl)-7-hydroxycoumarin **(22)**, and 6-(6′,7′-dihydroxy-3′,7′-dimethyloct-2′-enyl)-7-hydroxycoumarin **(23)**, were determined from *P. tectorius* fruits by Phat *et al*. These compounds showed better enzyme *α*-glucosidase inhibitory activity (IC_{50} = 36.5 – 84.7 μM) than the positive control, acarbose (IC_{50} = 214.5 μM) [7].

20)

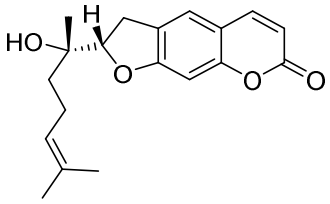

(21)

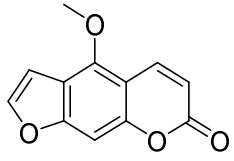

(22)

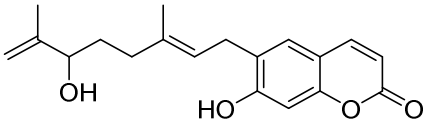

(23)

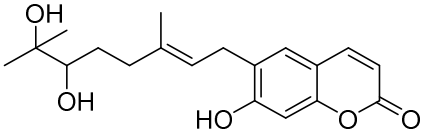

1.2.4. Other phenolics

Besides the three compound classes mentioned above, several other phenolics have been isolated from plants of the genus *Pandanus*. In 1998, 4-hydroxy-3-(2’,3’-dihydroxy-3’-methylbutyl)-benzoic acid methyl ester **(24)** was isolated by Jong *et al*. Meanwhile, *p*-coumaric **(25)** and three isomeric mixtures *E, Z* của *p*-coumaroyl dimethyl maleate **(26*E*, 26*Z*),** *p*-coumaroyl malate **(27*E*, 27*Z*),** *p*-coumaroyl monomethyl malate **(28*E*, 28*Z*)** were determined from the leaves of *Pandanus amaryllifolius* by Suzuki *et al*. [10]

24)

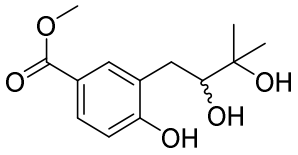

(25)

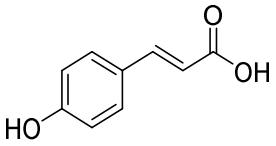

(26E)

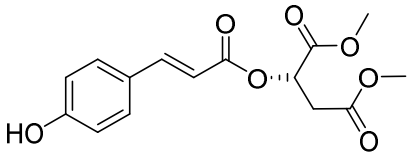

(26Z)

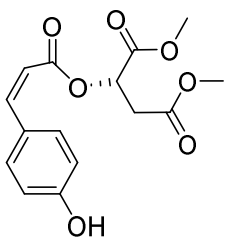

(27E) 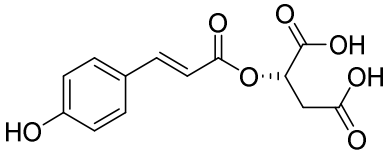

(27Z) 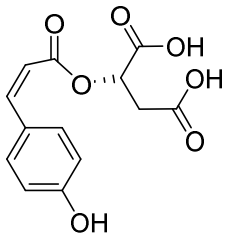

(28E) 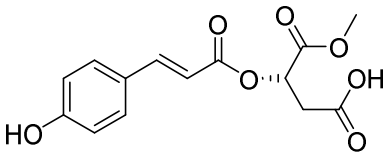

(28Z) 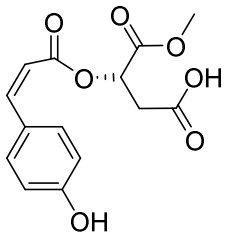

The phenolics were also found in the chemical composition of *P. tectorius*. Protocatechuic aldehyde **(29)** and (*7R, 8R*)-guaiacyl glycerol **(30)** were identified from the ethyl acetate of *Pandanus* fruit by Mai Dinh Tri *et al.* in 2012 [11]. Another study in 2015, six aromatic aldehydes include a new compound *(Z)*-4-hydroxy-3-(4-hydroxy-3-methylbut-2-en-1-yl) benzaldehyde **(31)**, and five known compounds, *p*-hydroxybenzaldehyde **(32)**, syringaldehyde **(33)**, *(Z)*-ferulaldehyde **(34)**, vanillin **(35)**, *(Z)*-sinapinaldehyde **(36)** were isolated from *Pandanus* fruit by these group authors. [12]. These compounds showed a considerable enzyme *α*-glucosidase inhibitory effect at IC_{50} = 36.5 – 192.4 µM, which was much lower than the positive control, acarbose (IC_{50} = 214.5 µM). In addition, ten phenolic derivatives, including vanillin **(35)**, *trans*-ethyl caffeate **(37)**, *cis*-ethyl caffeate **(38)**, *p*-ethyl coumarate **(39)**, sinapaldehyde **(40)**, *trans*-3,4-dihydroxy cinnamaldehyde **(41)**, dihydroconiferyl alcohol **(42)**, coniferyl alcohol **(43)**, 3-hydroxyl-1-(4-hydroxyl-3-methoxyphenyl) propane-1-one **(44)**, salicylaldehyde **(45**) were also determined [9]**.** Moreover**,** three phenolic compounds: 3-bis-(4-hydroxy-3-methoxyphenyl)-3-methoxy-propanol **(46)**, tachioside **(47),** and *p*-hydroxycinamaldehyde **(48)** were also isolated by Phat *et al.*, along with some lignans **(1-3, 11, 12)** as mentioned [7, 12]. Among them, 3-bis-(4-hydroxy-3-methoxyphenyl)-3-methoxypropanol **(46)** and *p*-hydroxycinamaldehyde **(48)** showed significant enzyme *α*-glucosidase inhibiting activity with IC_{50} = 81.5 and 43.8 µM, respectively.

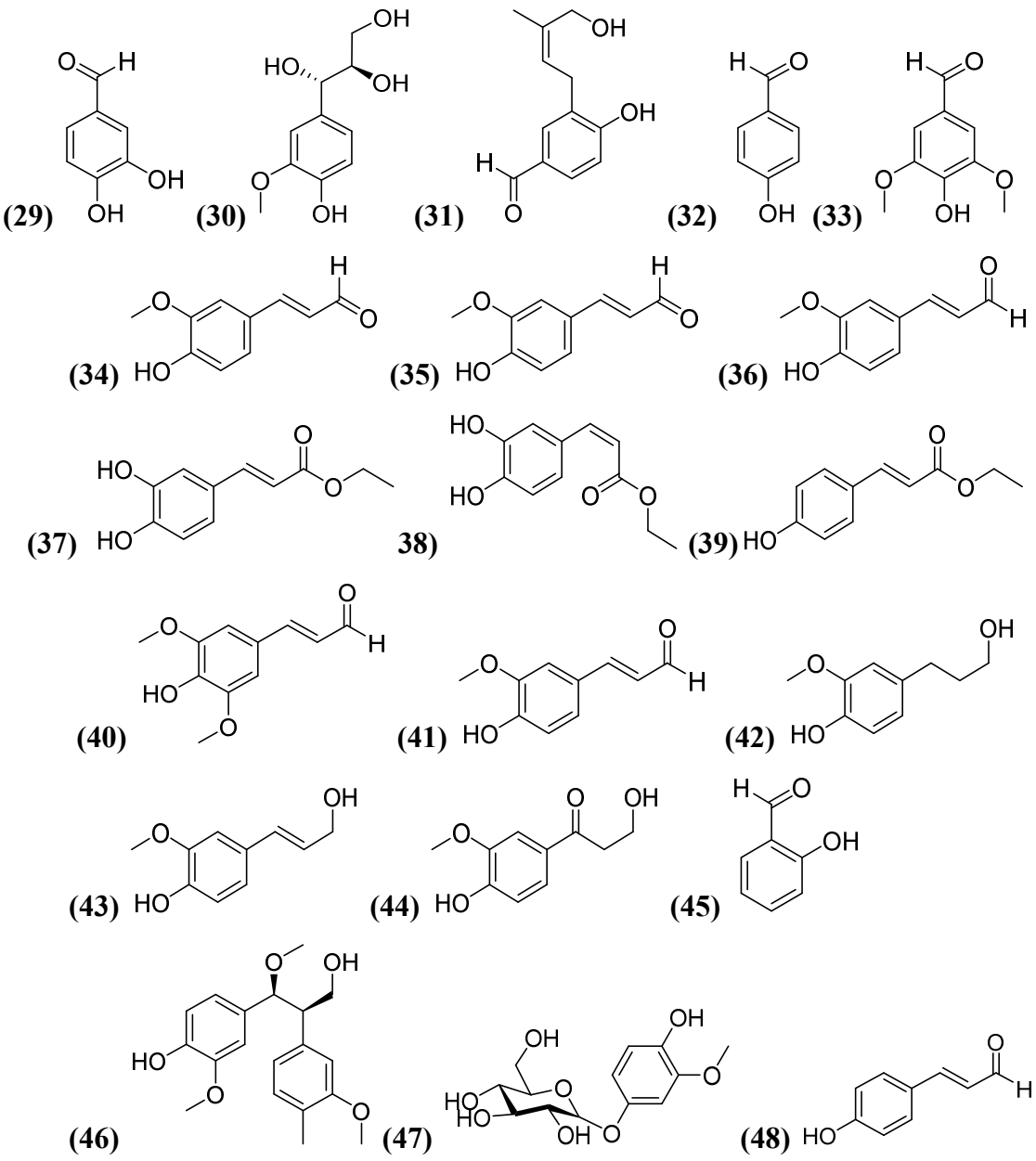

Several phenolics **(49-54)** were recently determined from the roots of *Pandanus tonkinensis* by Trang *et al*. These compounds showed antioxidant activity and inhibition of NO production in RAW264.7 cells. [13].

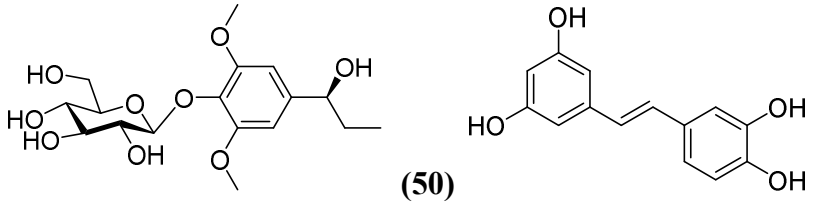

(51)

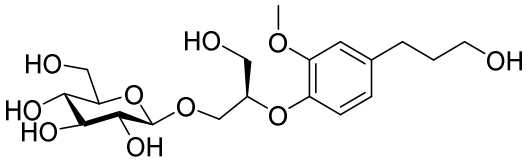

(52)

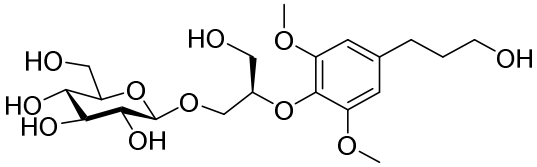

(53)

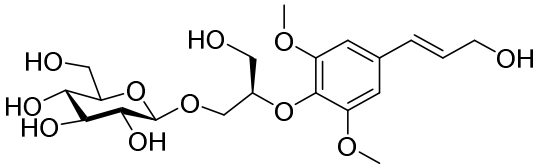

(54)

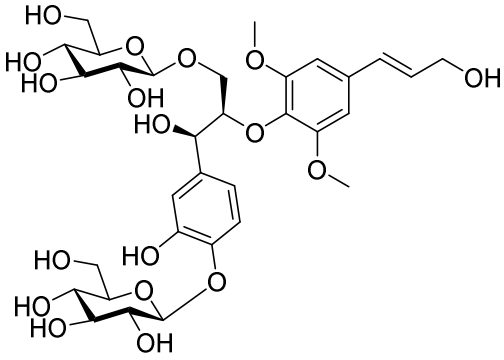

1.2.5. Alkaloids

Three alkaloids, including 2-acetyl-1-pyrroline **(55)**, pandamarine **(56)**, and pandanamine **(57)**, were isolated from the leaves of *P. amaryllifolius* by Byrne [14]. Four other alkaloids, pandanamine **(57)**, pandamarilactonine-A **(58)**, pandamarilactonine-B **(59)**, and pandamarilactone-1 **(60)**, were also determined from the leaves of *P. amaryllifolius* by Takayama *et al.* [15]. In the next study on the same object, four other alkaloids, including norpandamarilactonine-A **(61)**, norpandamarilactonine-B **(62)**, pandamarilactonine-C **(63)**, and pandamarilactonine-D **(64)**, were identified by the author [16, 17].

(55) 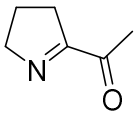

(56) 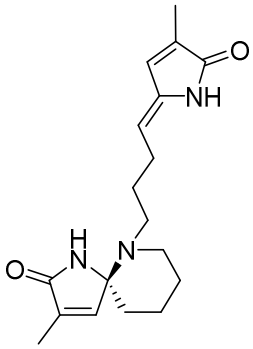

(57) 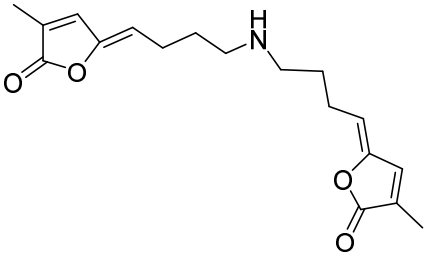

(58) 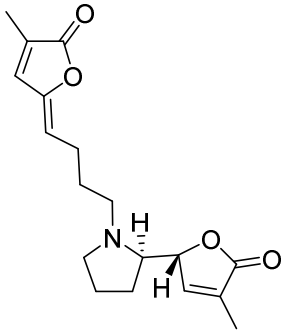

(59) 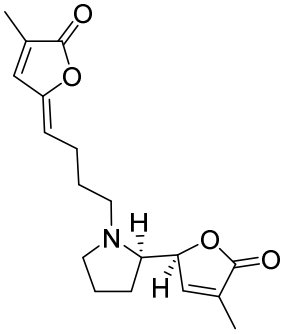

(60) 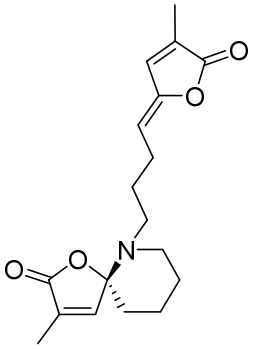

(61) 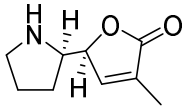

(62) 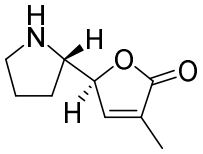

(63) 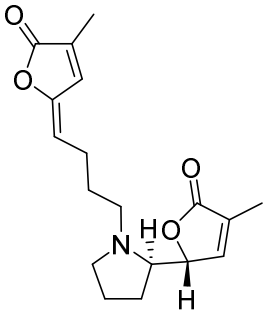

(64) 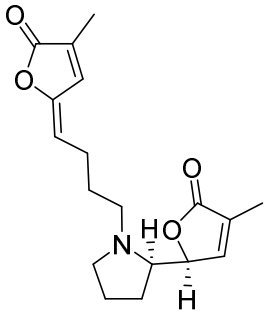

A series of alkaloids, including pandamarilactonine-A **(58)**, pandamarilactonine-B **(62)**, pandamarilactonine-C **(63)**, pandamarilactonine-D **(64)**, pandamarilactonine-E **(65)**, pandamarilactonine-F **(66)**, pandamarilactonine-F-*N*-oxide **(67)**, pandamarilactonine-G **(68)**, pandamarilactonine-H **(69)**, were isolated from the roots of *P. amaryllifolius* by Tan *et al.* in 2010 [18]. *Epi*-pandamarilactonine-H **(70)** is synthesized into isomeric enantiomers. Two alkaloids, such as dubiusamine-A **(71)**, and

dubiusamine-B **(72)** were determined from the leaves of *Pandanus dubius* by these group authors in the same year [18, 19].

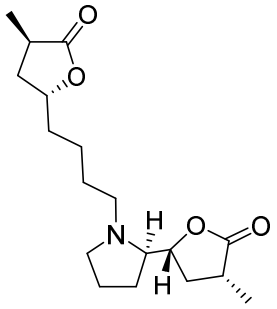

65)

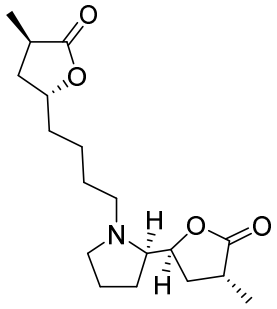

(66)

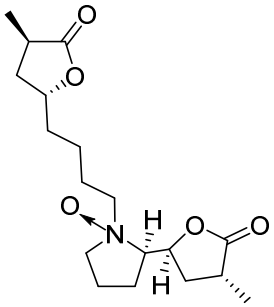

(67)

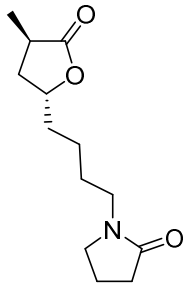

(68)

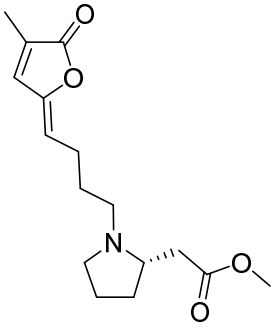

(69)

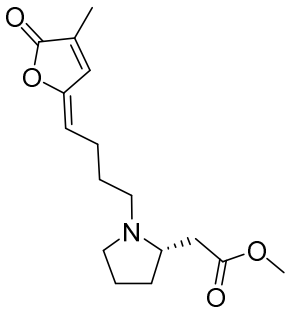

(70)

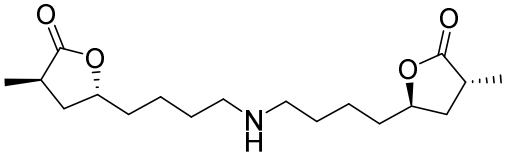

(71)

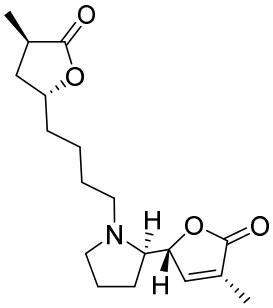

(72)

In 2017, seven alkaloids, such as *Pandanus*ines A and B **(73-74)**, pandalizines C–E **(75-77)**, norpandamarilactonines C and D **(78-79)** were identified from the aboveground part of *P. amaryllifolius* by Cheng *et al.* [20]. Two years earlier, two other alkaloids, including pandalisines A and B **(80-81),** were also isolated from the leaves of *Pandanus utilis* by these authors [21].

(73) 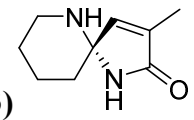

(74) 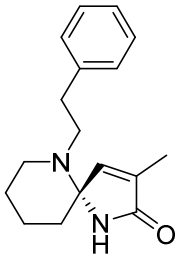

(75) 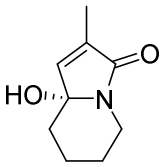

(76) 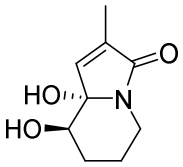

(77) 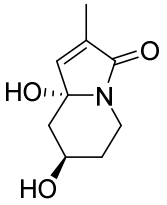

(78) 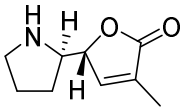

(79) 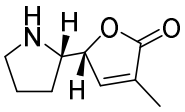

(80) 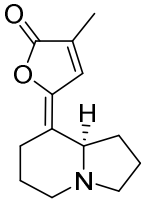

(81) 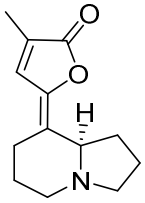

Nine alkaloids, including *N*-acetylnorpandamarilactonines A and B **(82-83)**, pandalizines A and B **(84-85)**, pandanmenyamine **(86)**, pandamarilactones-2 **(87)**, pandamarilactones-3 **(88)**, 5(*E*)-pandamarilactonine-32 **(89),** and pandalactonine **(90),** were determined from the above-ground part of *P. amaryllifolius* by Tsai *et al.* [22].

82) 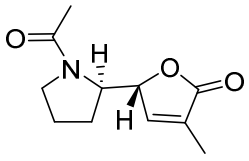

(83) 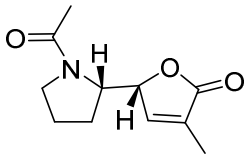

(84) 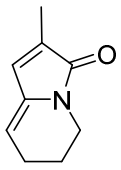

(85) 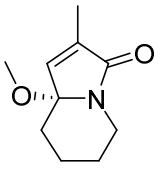

(86) 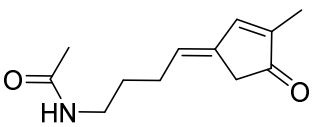

(87) 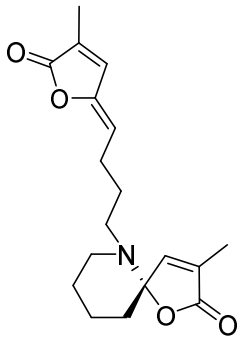

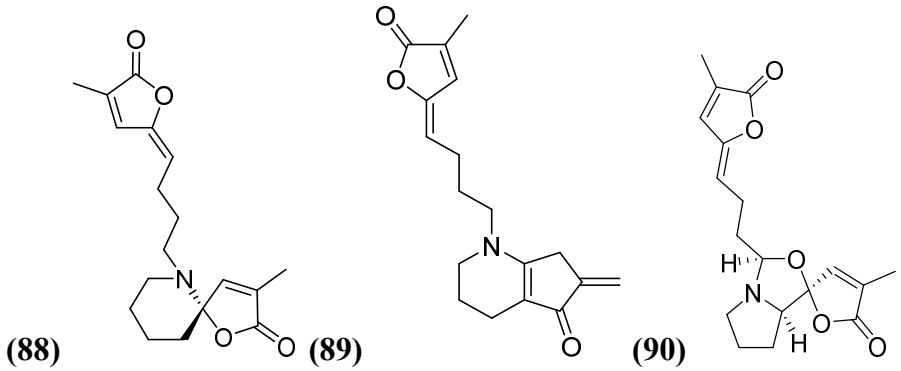

(88) **(89)** **(90)**

The study of Laluces et al about the antibacterial ability of some alkaloids from *Pandanus* showed that pandamarilactonine-A **(58)** exhibited considerable antibacterial activity against *Escherichia coli, Pseudomonas aeruginosa,* and *Staphylococcus aureus,* with the minimum inhibitory concentrations (MIC) on these three bacteria are 62.5, 15.6, and 250 µg/mL, respectively [24].

1.2.6. Benzofurans

Besides phenolics and alkaloids, some benzofuran derivatives have been found in several species of the genus *Pandanus*. Three benzofuran compounds **(91-93)** were isolated from the roots of *P. odoratissimus* by Jong *et al*.[23] .

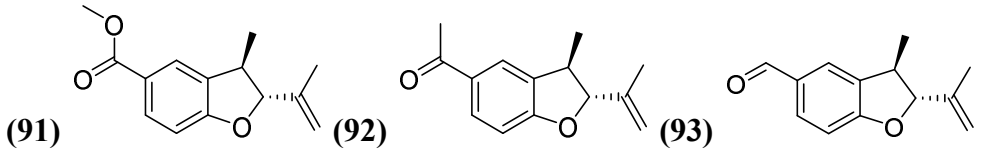

(91) **(92)** **(93)**

Recently, twelve benzofuran compounds **(94-105)** were identified from roots and rhizomes of *Pandanus tectorius* in a recent study [24].

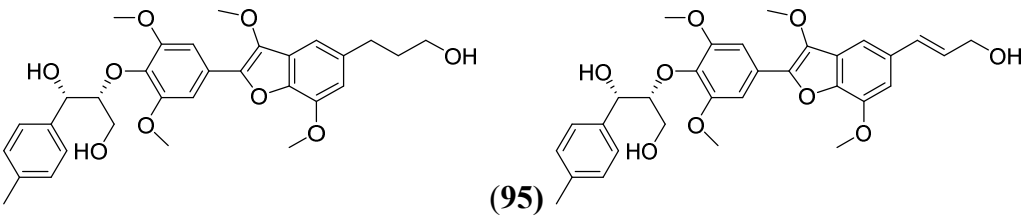

(94) **(95)**

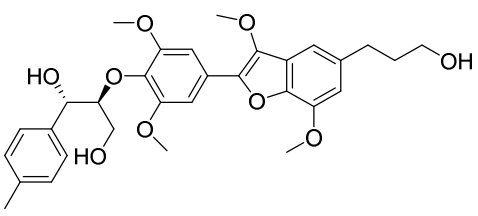

(96)

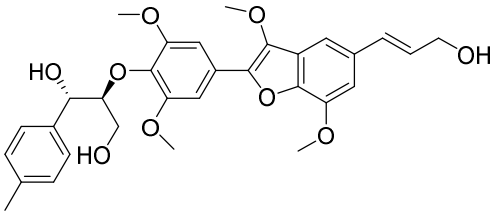

(97)

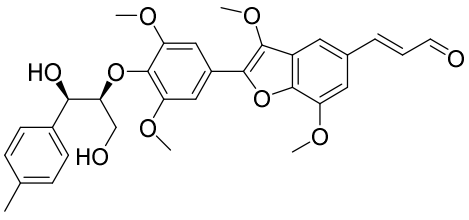

(98)

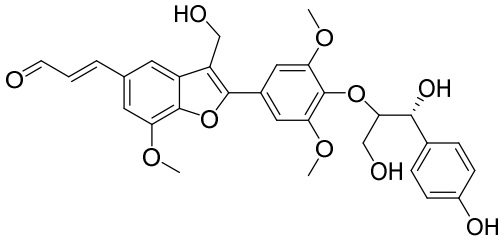

(99)

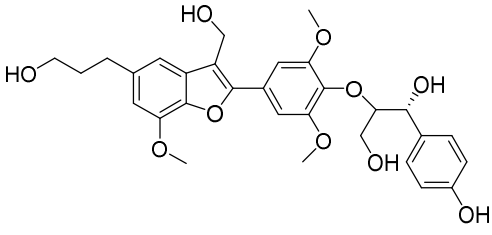

(100)

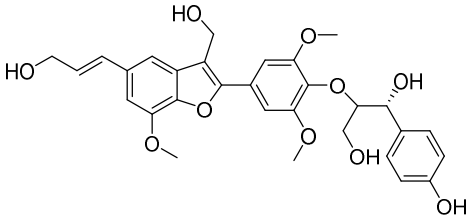

(101)

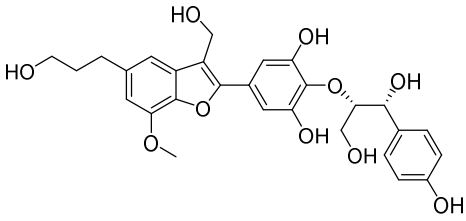

(102)

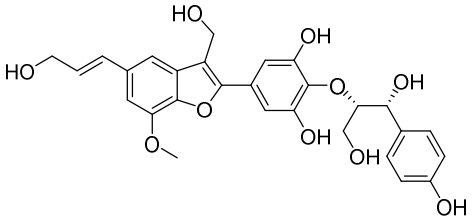

(103)

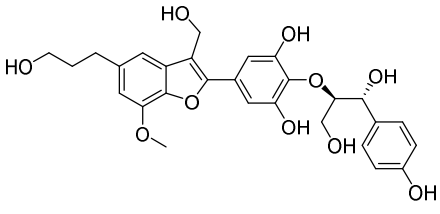

(104)

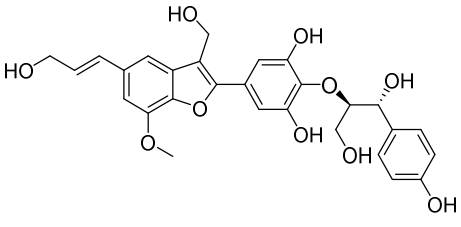

(105)

1.2.7. Summary of phytochemical constituents of Pandanus species

Table 1.1. Summary of phytochemical constituents isolated from Pandanus species together with their origins

No.	Compounds	Origin
1	Pinoresinol	*P. odoratissimus* fruits, roots; *P. tectorius* fruits
2	(+)-Syringaresinol	*P. odoratissimus* fruits;

		P. tectorius fruits
3	(+)-Medioresinol	*P. odoratissimus* fruits; *P. tectorius* fruits
4	Eudesmin	*P. odoratissimus* roots
5	Kobusin	*P. odoratissimus* roots
6	Epipinoresinol	*P. odoratissimus* roots
7	De-4′-O-methyleudesmin	*P. odoratissimus* roots
8	3,4-Bis(4-hydroxy-3-methoxy-benzyl)-tetrahydrofuran	*P. odoratissimus* roots
9	(+)-Sesamin	*P. odoratissimus* roots
10	Salicifoliol	*P. odoratissimus* roots
11	(+)-Lyoniresinol	*P. tectorius* fruits
12	(−)-Balanophonin	*P. tectorius* fruits
13	Vitexin	*P. tectorius* roots
14	Tricin	*P. tectorius* roots
15	Tangeretin	*P. tectorius* fruits
16	Sakranetin	*P. tectorius* fruits
17	Chrysin	*P. tectorius* fruits
18	Naringenin	*P. tectorius* fruits
19	5,8-Dihydroxy-7-methoxy-flavone	*P. tectorius* fruits
20	*Pandanus*in A	*P. tectorius* fruits
21	Bergapten	*P. tectorius* fruits
22	6-(6′-Hydroxy-3′,7′-dimethylocta-2′,7′-dienyl)-7-hydroxycoumarin	*P. tectorius* fruits
23	6-(6′,7′-Dihydroxy-3′,7′-dimethyloct-2′-enyl)-7-hydroxycoumarin	*P. tectorius* fruits
24	4-Hydroxy-3-(2′,3′-dihydroxy-3′-methylbutyl)-benzoic acid methyl ester	*Pandanus* sp.
25	*p*-Coumaric acid	*P. amaryllifolius* leaves
26E/26Z	*p*-Coumaroyl dimethyl maleate	*P. amaryllifolius* leaves
27E/27Z	*p*-Coumaroyl malate	*P. amaryllifolius* leaves
28E/28Z	*p*-Coumaroyl monomethyl malate	*P. amaryllifolius* leaves
29	Protocatechuic aldehyde	*P. tectorius* fruits
30	(7R,8R)-Guaiacyl glycerol	*P. tectorius* fruits
31	(Z)-4-Hydroxy-3-(4-hydroxy-3-methylbut-2-en-1-yl) benzaldehyde	*P. tectorius* fruits
32	*p*-Hydroxybenzaldehyde	*P. tectorius* fruits
33	Syringaldehyde	*P. tectorius* fruits
34	(Z)-Ferulaldehyde	*P. tectorius* fruits
35	Vanillin	*P. tectorius* fruits
36	(Z)-Sinapinaldehyde	*P. tectorius* fruits
37	trans-Ethyl caffeate	*P. tectorius* fruits
38	cis-Ethyl caffeate	*P. tectorius* fruits
39	*p*-Ethyl coumarate	*P. tectorius* fruits
40	Sinapaldehyde	*P. tectorius* fruits
41	trans-3,4-Dihydroxy cinnamaldehyde	*P. tectorius* fruits
42	Dihydroconiferyl alcohol	*P. tectorius* fruits
43	Coniferyl alcohol	*P. tectorius* fruits
44	3-Hydroxyl-1-(4-hydroxyl-3-methoxyphenyl) propane-1-one	*P. tectorius* fruits
45	Salicylaldehyde	*P. tectorius* fruits
46	3-Bis-(4-hydroxy-3-methoxyphenyl)-3-methoxypropanol	*P. tectorius* fruits
47	Tachioside	*P. tectorius* fruits
48	*p*-Hydroxycinamaldehyde	*P. tectorius* fruits
49–54	Phenolic compounds	*P. tonkinensis* roots
55	2-Acetyl-1-pyrroline	*P. amaryllifolius* leaves
56	Pandamarine	*P. amaryllifolius* leaves
57	Pandanamine	*P. amaryllifolius* leaves
58	Pandamarilactonine-A	*P. amaryllifolius* leaves/roots
59	Pandamarilactonine-B	*P. amaryllifolius* leaves/roots
60	Pandamarilactone-1	*P. amaryllifolius* leaves
61	Norpandamarilactonine-A	*P. amaryllifolius* leaves

62	Norpandamarilactonine-B	*P. amaryllifolius* leaves/roots
63	Pandamarilactonine-C	*P. amaryllifolius* leaves/roots
64	Pandamarilactonine-D	*P. amaryllifolius* leaves/roots
65	Pandamarilactonine-E	*P. amaryllifolius* roots
66	Pandamarilactonine-F	*P. amaryllifolius* roots
67	Pandamarilactonine-F-N-oxide	*P. amaryllifolius* roots
68	Pandamarilactonine-G	*P. amaryllifolius* roots
69	Pandamarilactonine-H	*P. amaryllifolius* roots
70	Epi-pandamarilactonine-H	Synthetic derivative
71	Dubiusamine-A	*P. dubius* leaves
72	Dubiusamine-B	*P. dubius* leaves
73	*Pandanus*ine A	*P. amaryllifolius* aerial parts
74	*Pandanus*ine B	*P. amaryllifolius* aerial parts
75	Pandalizine C	*P. amaryllifolius* aerial parts
76	Pandalizine D	*P. amaryllifolius* aerial parts
77	Pandalizine E	*P. amaryllifolius* aerial parts
78	Norpandamarilactonine C	*P. amaryllifolius* aerial parts
79	Norpandamarilactonine D	*P. amaryllifolius* aerial parts
80	Pandalizine A	*P. utilis* leaves
81	Pandalizine B	*P. utilis* leaves
82	N-Acetylnorpandamarilactonine A	*P. amaryllifolius* aerial parts
83	N-Acetylnorpandamarilactonine B	*P. amaryllifolius* aerial parts
84	Pandalizine A	*P. amaryllifolius* aerial parts
85	Pandalizine B	*P. amaryllifolius* aerial parts
86	Pandanmenyamine	*P. amaryllifolius* aerial parts
87	Pandamarilactones-2	*P. amaryllifolius* aerial parts
88	Pandamarilactones-3	*P. amaryllifolius* aerial parts
89	5(E)-Pandamarilactonine-32	*P. amaryllifolius* aerial parts
90	Pandalactonine	*P. amaryllifolius* aerial parts
91	Benzofuran derivative	*P. odoratissimus* roots
92	Benzofuran derivative	*P. odoratissimus* roots
93	Benzofuran derivative	*P. odoratissimus* roots
94–105	Benzofuran derivatives	*P. tectorius* roots and rhizomes

1.3. Bioactivities of natural products from *Pandanus* species

1.3.1. Antioxidant

Plants from the genus *Pandanus* have been widely studied for their antioxidant properties, which are generally attributed to their rich content of phenolic and flavonoid compounds. Extracts of *P. amaryllifolius* leaves have demonstrated significant free radical scavenging and ferric reducing activity, although the effectiveness varies depending on geographical origin and phytochemical composition [25]. Optimization of extraction conditions, such as solvent concentration, temperature, and solvent-to-sample ratio, has been shown to enhance the antioxidant activity of *P. amaryllifolius*, highlighting the importance of process parameters [26]. In *P. tectorius*, both fruit and leaf extracts exhibit strong antioxidant potential. The fruit core, particularly when extracted with ethyl acetate, has shown notable radical scavenging effects associated with higher phenolic content [27]. Similarly, leaf extracts demonstrate dose-dependent antioxidant activity across different assays, indicating broad efficacy against oxidative

processes [27]. Other members of the genus, such as *Pandanus canaranus*, also possess substantial antioxidant capacity. Solvent polarity plays an important role, with methanol and ethyl acetate extracts generally yielding stronger results than non-polar solvents [28]. In the case of *Pandanus conoideus* (red fruit), optimization using ultrasound-assisted extraction has improved phenolic recovery and enhanced antioxidant performance, while also demonstrating that extraction duration must be carefully controlled to avoid degradation of active compounds [29].

Overall, studies consistently support the antioxidant potential of *Pandanus* species, though results vary depending on species, plant part, and extraction technique. Process optimization and solvent selection are crucial for maximizing yields of bioactive compounds, reinforcing the value of *Pandanus* as a promising source of natural antioxidants.

1.3.2. Cytotoxicity

Across the genus *Pandanus*, cytotoxic, anti-cancer, and anti-tumor activities have been documented. For *P. amaryllifolius*, crude leaf extracts showed *in vitro* antiproliferative effects against breast cancer cells (MCF-7) in cell-based assays [25]. In *P. odoratissimus*, root/leaf extracts suppressed proliferation of non-small-cell lung cancer (Calu-6) cells and triggered apoptosis *in vitro*, and an aqueous extract improved survival and reduced tumor burden in an Ehrlich ascites carcinoma mouse model [30, 31]. A related species, *P. fascicularis*, likewise showed dose-dependent anti-tumor effects in the same murine model, with increased survival and reduced solid-tumor mass [32]. The red-fruit species *P. conoideus* yielded an ethyl-acetate fraction that reduced the viability of HSC-3 oral squamous carcinoma cells in a concentration- and time-dependent manner *in vitro* [33]. By contrast, fruit extracts (keys and cores) of *P. tectorius* consistently lacked cytotoxicity toward several cancer cell lines (HeLa, HepG2, MCF-7) under the conditions tested [27]; yet nanoformulation of *P. tectorius* leaf extracts as SNEDDS converted these into preparations with measurable anti-cancer activity against HeLa via apoptosis [34]. Overall, current evidence indicates that members of *Pandanus* can exert cytotoxic or anti-tumor effects *in vitro* and *in vivo*—often involving apoptosis or cell-cycle perturbations—but outcomes vary markedly with species, plant part, solvent, and formulation.

1.3.3. Anti-inflammation

Evidence from preclinical studies indicates that several *Pandanus* species exhibit anti-inflammatory activity. In *P. fascicularis*, both leaf chloroform extracts and prop-root extracts suppressed inflammation in rat paw edema models and were accompanied by antinociceptive/analgesic effects, consistent with modulation of inflammatory mediators [35, 36]. Mechanistically, the prop-root study points to flavonoids as likely contributors via inhibition of prostaglandin-synthesizing enzymes, aligning with the observed attenuation of inflammatory responses [36]. For *P. odoratissimus*, methanolic leaf extracts reduced edema in both acute (carrageenan) and chronic (formalin) rat models, and the species' traditional use in rheumatic conditions further reinforces its anti-inflammatory claim [37, 38]. Complementing these lines of evidence, *P. amaryllifolius* yields diverse alkaloids, and its ethanolic crude extract has shown anti-inflammatory activity in prior work; recent oral-biology data also highlight actions relevant to inflammatory contexts such as microbial challenge and wound repair [22, 39]. Taken together, available data indicate that *Pandanus* spp. contain bioactives—especially phenolics/flavonoids and alkaloids—that can attenuate inflammatory processes with concurrent analgesic benefits, supporting their ethnomedicinal use in inflammatory disorders.

1.3.4. Antibacterial activities

Evidence from the provided studies indicates that many *Pandanus* species possess antibacterial properties, with outcomes strongly shaped by species identity, extraction solvent, and test conditions. For *P. amaryllifolius* leaves, ethanol or water extracts often show little to no inhibition of *Staphylococcus aureus* or *Escherichia coli*, whereas ethyl acetate fractions—and ethanol/ethyl-acetate mixtures—consistently inhibit growth, underscoring the importance of extracting mid-polarity constituents [40]. *P. conoideus* ("Buah Merah") shows a similar trend: among n-hexane, methanol, water, and ethyl acetate extracts, the ethyl acetate fraction is the most active against oral pathogens, including *S. mutans*, *S. sanguinis*, and *Enterococcus faecalis*, with corroborating MIC/MBC data and evidence of synergism in combinations [41]. Bioactivity-guided fractionation further traced activity against *E. faecalis* to a flavonoid isolated from the ethyl acetate fraction, highlighting phenolic metabolites as likely antibacterial principles

[42]. In vitro studies on *P. amaryllifolius* ethanolic leaf extracts also demonstrate clear zones of inhibition against *S. aureus* and *E. coli*, with *in silico* docking supporting plausible interactions with bacterial targets [42, 43]. At the same time, under biofilm-like test conditions, a *P. conoideus* red-fruit extract failed to yield measurable MIC/MKC against *S. mutans*, suggesting delivery barriers can negate otherwise promising phytochemicals [44]. Beyond human pathogens, antibacterial benefits extend to aquaculture: methanolic *P. tectorius* leaf extract primed white-leg shrimp and improved survival following *Vibrio parahaemolyticus* challenge while up-regulating immune genes, pointing to potential as a plant-based prophylactic [45]. Collectively, these findings indicate that *Pandanus* spp. harbor antibacterial constituents—especially flavonoids and other medium-polarity compounds—whose apparent effectiveness depends on solvent, species, and biological context; further standardization and *in vivo* validation are warranted.

1.3.5. Summary of reported bioactivities of Pandanus species

Table 1.2. Summary of Pandanus species and their reported biological activities.

Species	Plant part / Extract	Reported bioactivities	Main observations / Notes
P. amaryllifolius	Leaves, crude extracts	Antioxidant	Significant free radical scavenging and ferric reducing activities; affected by extraction conditions and geographical origin
	Leaf crude extracts	Cytotoxicity / Anticancer	In vitro antiproliferative effects against MCF-7 breast cancer cells
	Ethanolic extracts and alkaloids	Anti-inflammatory	Demonstrated anti-inflammatory potential and relevance to wound healing
	Ethanol and ethyl acetate leaf extracts	Antibacterial	Activity against *Staphylococcus aureus* and *Escherichia coli*
P. canaranus	Leaf extracts	Antioxidant	Methanol and ethyl acetate extracts showed stronger activity than non-polar extracts
P. conoideus	Fruit extracts	Antioxidant	Ultrasound-assisted extraction improved phenolic recovery and antioxidant performance
	Ethyl acetate fruit fraction	Cytotoxicity	Reduced viability of HSC-3 oral carcinoma cells
	Ethyl acetate fruit extract	Antibacterial	Active against oral pathogens including *S. mutans*, *S. sanguinis*, and *E. faecalis*
	Red fruit extract	Antibacterial	No measurable MIC/MKC against *S. mutans* under biofilm-like conditions
P. fascicularis	Leaf and prop-root extracts	Antitumor	Increased survival and reduced tumor mass in murine models
	Leaf and prop-root extracts	Anti-inflammatory / Analgesic	Suppressed inflammation in rat paw edema models

P. odoratissimus	Roots and leaves	Cytotoxicity / Antitumor	Suppressed proliferation of Calu-6 cells and induced apoptosis; reduced tumor burden in vivo
	Methanolic leaf extracts	Anti-inflammatory	Reduced edema in acute and chronic inflammation models
P. tectorius	Fruits and leaves	Antioxidant	Strong antioxidant potential associated with phenolic-rich extracts
	Fruit extracts	Cytotoxicity	No significant cytotoxicity toward HeLa, HepG2, and MCF-7 cells under tested conditions
	Leaf SNEDDS formulations	Anticancer	Formulated extracts showed apoptosis-inducing effects against HeLa cells
	Methanolic leaf extract	Antibacterial / Immunostimulatory	Improved survival of shrimp challenged with *Vibrio parahaemolyticus*

1.4. General summary and scope of this thesis

Pandanus species exhibit rich phytochemical diversity spanning multiple metabolite classes, such as lignans, flavonoids, coumarins, phenolics, alkaloids, and benzofuran derivatives, documented across several taxa within the genus. Functionally, these plants demonstrate notable biological potential: consistent antioxidant activity has been reported for multiple species and plant parts, antibacterial effects have been traced to defined constituents in bioassays, and broader anti-inflammatory and anticancer claims are supported in the pharmacological literature. Collectively, the genus represents a promising source of bioactive natural products with relevance to oxidative stress, infection control, and inflammation-related conditions.

The overarching aim of this thesis is to investigate selected chemical constituents and to evaluate representative bioactivities of two *Pandanus* species, including *P. tectorius* and *P. amaryllifolius* occurring in Vietnam. To achieve this objective, the thesis is structured into six chapters that progressively integrate phytochemical analysis, bioactivity evaluation, and optimization of extraction processes, as summarized below.

Chapter 2 describes the materials, experimental procedures, and analytical techniques employed throughout this study, including plant collection and authentication, extraction and fractionation methods, chromatographic separation, spectroscopic analysis, and biological assays used for activity evaluation.

Chapter 3 presents a comprehensive phytochemical and bioactivity screening of *P. tectorius* and *P. amaryllifolius* samples. Quantitative determination of major metabolite classes is integrated with antioxidant, enzyme inhibitory, anti-inflammatory, and

cytotoxic assays, together with multivariate analysis, to identify chemical–bioactivity relationships and to guide the selection of representative materials for further investigation.

Chapter 4 focuses on the isolation, structural elucidation, and bioactivity evaluation of individual compounds from *P. tectorius* leaves. This chapter aims to identify key secondary metabolites responsible for the activities observed in the screening phase and to establish their chemical structures and biological relevance.

Chapter 5 addresses the optimization of extraction conditions and the evaluation of bioactivities of *P. tectorius* fruit extracts. By applying experimental design and process optimization, this chapter seeks to enhance the recovery of bioactive constituents and to assess the resulting extracts for their antioxidant and enzyme inhibitory potential.

Chapter 6 describes the optimization of extraction conditions and the enrichment of phenolic fractions from *P. amaryllifolius* leaves, together with the evaluation of their biological activities. This chapter aims to improve the recovery of phenolic compounds from an alkaloid-rich matrix and to clarify their contribution to the observed antioxidant and bioactive properties.

These chapters provide a coherent framework for linking phytochemical diversity to biological function in *Pandanus* species, supporting the rational discovery and development of bioactive natural products from these plants.

CHAPTER 2. MATERIALS AND METHODS

2.1. Plant materials

Species names, parts, codes, number of samples, times, and locations of *Pandanus* samples are presented in Table 2.1. These were identified by Dr. Bui Van Thanh, Institute of Biology, Vietnam Academy of Science and Technology. Voucher specimens of the plants were deposited at the Center for High Technology Research and Development, Vietnam Academy of Science and Technology.

Table 2.1. The information on the collected Pandanus samples

No.	Species	Part	Code	Number of samples	Time	Location (Coordinates)
1	*Pandanus tectorius*	Leaves	PtL 01-03	3	Feb. 2020	Thanh Oai, Ha Noi (20.912181 °N, 105.737122 °E)
			PtL 04-05	2	Mar. 2021	
			PtL 06	1	Jan. 2024	Na Hang, Tuyen Quang (22.407260 °N, 105.438909 °E)
			PtL 07	1	Aug. 2024	Quynh Luu, Nghe An (19.162208 °N, 105.730549 °E)
		Fruits	PtF 01-02	2	Feb. 2020	Thanh Oai, Ha Noi (20.912181 °N, 105.737122 °E)
			PtF 03-04	2	Mar. 2021	
			PtF 05	1	Jan. 2024	Na Hang, Tuyen Quang (22.407260 °N, 105.438909 °E)
2	*Pandanus amaryllifolius*	Leaves	Pama 01-03	3	Apr. 2021	Tam Dao, Phu Tho (21.425607 °N, 105.615562 °E)
			Pama 04	1	May. 2023	Ba Vi, Ha Noi (21.05096 °N, 105.23032 °E)
			Pama 05	1	Mar. 2024	Ba Vi, Ha Noi (21.05100 °N, 105.23031 °E)
			Pama 06	1	Jul. 2024	Ham Yen, Tuyen Quang (22.012317 °N, 105.083216°E)
Total				**18**		

a)  b) 

Figure 2.1. Leaves of a) P. tectorius and b) P. amaryllifolius

2.2. Chemicals and instruments

High-resolution mass spectra (HR-ESI-MS) were obtained with an AGILENT 6550 iFunnel Q-TOF LC/MS system (Agilent Technologies, US), while ESI-MS was measured by a Thermo LCQ Fleet system (Thermo Scientific, US). NMR spectra were recorded on a Bruker AM500 FT-NMR spectrometer with tetramethylsilane (TMS) as an internal standard. The optical rotations were read on a JASCO P-2000 digital polarimeter. Column chromatography (CC) was carried out using Diaion HP-20 resin (0.25-0.85 mm, Mitsubishi Chemical Corp., Japan), silica gel 60 (70-230 mesh, Merck, Germany), or RP-C18 resin (150 µm, YMC, Japan). HPLC analysis and prep-HPLC were conducted on a Thermo Ultimate 3000 HPLC-DAD system (Thermo Scientific, US). CD spectra were recorded on a Chirascan CD spectrometer (Applied Photophysics, Surrey, UK).

2.3. Phytochemical analysis and bioactivity assays

2.3.1. Extraction of the samples

To prepare the extract for chemical analysis and bioassays, 50 g of each sample was extracted in triplicate with 1 L of methanol in a sonication bath at 60°C. The solution was filtered and evaporated to yield the total extract.

2.3.2. Total phenolic assay

The total phenolic contents of the samples were evaluated by modifying a reported method [46]. The external calibration was done with different concentrations of gallic acid (10-400 µg/mL). The analytes were prepared by extracting (in triplicate) 2 g of the dry sample in 15 mL of methanol in a sonication bath at 60°C for 20 minutes. The

solutions were filtered, combined, and made the volume up to 50 mL. Each 100 µL of the sample or standard solution was mixed with 400 µL of Folin–Ciocalteu 10% and 500 µL of Na_2CO_3 6% and incubated for 15 min at 40 °C. Its absorbance was measured with a UV–Vis. Spectrophotometer at 750 nm. The total phenolic content was calculated as mg gallic acid equivalent (mg GAE/g) by using the gallic acid calibration curve.

2.3.3. Total flavonoid assay

The total flavonoid contents of the samples were examined using a previous method [46]. The external calibration was done with different concentrations of quercetin (10-200 µg/mL). The analytes were prepared by the same process as the total phenolic assay. Add 100 µL of $NaNO_2$ 5% to the 500 µL sample or standard solution mix at room temperature for 5 min, then add 100 µL of $AlCl_3$ 10% and 500 µL NaOH 1M to the mixture. Keep the mixture at room temperature for 15 min. Its absorbance was measured with a UV–Vis spectrophotometer at 510 nm. The total flavonoid content was calculated as mg quercetin equivalent (mg QE/g) by using the quercetin calibration curve.

2.3.4. Total alkaloid assay

The total alkaloid contents of the samples were quantified by a previous method. [47]. The total extracts of the samples were prepared by the same process for bioassay as described above. Then, 5 grams of each extract was suspended in 50 mL of water and acidified to pH 2 by HCl 1N and partitioned with EA (75 mL × 3 times). The organic phase was removed, and the water phase was basified by 1N NaOH to pH 11 and then extracted with CH_2Cl_2 (4 times × 200 mL). The combined CH_2Cl_2 extracts were evaporated under reduced pressure to give total alkaloid mixtures. Total alkaloid content was measured by the percentage in weight of the extract (%).

2.3.5. Total saponin assay

The total saponin contents (TSC) of the samples were determined by vanillin-sulphuric acid assay. [48]. 50 µL of each extract or subfraction solution was incubated with 50 µL of 8% (w/v) vanillin in ethanol and 1500 µL of sulphuric acid 72% (v/v) for 15 min at 70 °C. The standards and the reagent blank were made up with various concentrations of aescin and the solvent, respectively. Next, the samples were cooled at ambient temperature for 5 minutes. The absorbances of the standards and samples were measured against the blank at 560 nm.

2.3.6. Antioxidant assays

The antioxidant potential of the extracts was assessed using DPPH and hydroxyl radical scavenging assays, following established protocols [49, 50].

For the DPPH assay, 100 µL of each sample was mixed with 1900 µL of DPPH solution in methanol and incubated in the dark at 37°C for 20 minutes. Absorbance was measured at 517 nm, with ascorbic acid serving as the reference standard.

In the hydroxyl radical scavenging assay, a 200 µL aliquot of each test sample was added to a mixture containing 400 µL of 50 mM phosphate buffer (pH 7.8), 400 µL of 2.8 mM deoxyribose, and 400 µL of 500 µM ferrous ammonium sulfate [$Fe(NH_4)_2(SO_4)_2$]. The mixture was incubated at 37°C for 1 hour. The reaction was terminated by the addition of 1000 µL of 10% (w/v) trichloroacetic acid and 1000 µL of 1% (w/v) thiobarbituric acid. The resulting solution was then heated in a boiling water bath for 15 minutes, and absorbance was measured at 532 nm. Catechin was used as the positive control for this assay.

2.3.7. α-amylase inhibitory activity

The *α*-amylase inhibitory activity was determined using a modified version of the DNSA method [51]. The substrate was prepared by boiling 1 g of starch in 100 mL of phosphate buffer (pH 7.0) for 10 minutes and then allowed to cool to room temperature. The DNSA reagent was prepared by dissolving 12 g of sodium potassium tartrate tetrahydrate in 8 mL of 2 M NaOH and 20 mL of 96 mM 3,5-dinitrosalicylic acid solution. The extracts were initially dissolved in 10% DMSO, followed by further dilution in buffer (Na_2HPO_4/NaH_2PO_4 (0.02 M), NaCl (0.006 M), pH 6.9) to achieve various concentrations. A 200 µL aliquot of each sample solution was mixed with 200 µL of *α*-amylase solution (2 units/mL) and incubated at 37°C for 3 minutes. Subsequently, 200 µL of the starch substrate was added, and the reaction mixture was incubated at 37°C for 15 minutes. The reaction was stopped by adding 200 µL of the DNSA reagent, and the solution was boiled for 10 minutes in a water bath at 85–90°C. After cooling to room temperature, the absorbance was measured at 650 nm using a microplate reader, with acarbose serving as the positive control.

2.3.8. Cytotoxicity assay

A549 (human lung carcinoma), K562 (human lymphoblast cell), and MCF7 (human breast cancer cell) were cultured at 37 °C in RMPI1640 medium supplemented

with 10% fetal bovine serum (FBS), 100 U/mL penicillin, and 100 µg/mL streptomycin in a 5% CO_2 incubator. The viability of cells was evaluated using the 3-(4,5-dimethylthiazol-2-yl)-2,5-diphenyl tetrazolium bromide (MTT) method [52]. The cells were seeded in 96-well plates at a concentration of 1×10^5 cells/well and treated with various concentrations of essential oils (0.3, 1, 3, 10, and 30 µg/mL) and incubated in a humidified 5% CO_2 atmosphere at 37°C. After 48 h incubation, 0.5 mg/mL MTT was added to each well and incubated for another 4 h. After removing the supernatant, formazan crystals were dissolved in isopropanol, and the OD values were measured at 570 nm using a microplate reader. Camptothecin was used as a positive control.

2.3.9. NO production inhibition assay

The effects of samples on the NO production in LPS-stimulated RAW 264.7 macrophage cells, based on the Griess reaction, were examined [53]. The cells were seeded in a 96-well plate at a concentration of 0.5×10^5 cells per well and incubated in the humidified incubator at 37°C and 5% CO_2 for 22 hours. After incubation, cells were treated with the sample with concentrations from 3 to 25 µg/mL, then 0.1 mg/mL LPS (Sigma Aldrich, USA) was added after 30 minutes. The cells were incubated for the next 24 hours. Then, 100 µL of the culture supernatant was transferred to another 96-well plate and mixed with 100 µL of Griess reagent. The absorbance of the reaction solution was read at 570 nm with an iMark microplate reader (BioRad, USA). The remaining cells from the original 96-well plate were further used for the cell viability assay (MTT assay) [52]. The assay is based on the cleaving action of dehydrogenases in functioning mitochondria of living cells on the tetrazolium ring of MTT (3-(4,5-dimethylthazol 2-yl)-2,5-diphenyl tetrazolium bromide), thus estimating the viable cell number. Cardamonin, which is a well-known NO production inhibitor, was used as a positive control [52, 53].

2.3.10.Statistical analysis

The data were collected and presented as matrices by MS Excel (Microsoft, US). The statistical analysis of the data, such as Kruskal–Wallis test and Partial Least Square regression, was conducted using MS Excel and the R programming language. The Box-Behnken Design-based Response Surface Method was generated on the Design-Expert 12.0 (Stat-Ease, US).

CHAPTER 3. PHYTOCHEMICALS AND BIOACTIVITIES SCREENING OF *PANDANUS* PLANT SAMPLES

3.1. Chapter overview

This chapter presents a systematic phytochemical and bioactivity screening of selected *Pandanus* plant extracts to establish a foundation for subsequent in-depth investigations. Eighteen samples representing leaves and fruits of *Pandanus tectorius* and leaves of *Pandanus amaryllifolius* were evaluated to elucidate interspecific and organ-related differences in secondary metabolite composition. Quantitative analyses of total phenolics, flavonoids, saponins, and alkaloids were combined with non-parametric statistical testing to characterize chemical variability among sample groups. The biological potential of the extracts was further assessed through antioxidant, α-amylase inhibitory, anti-inflammatory, and cytotoxic assays. Finally, multivariate analysis using partial least squares (PLS) regression was applied to integrate chemical composition with biological responses and to clarify key structure–activity relationships. These results provide a comprehensive screening framework that supports the rational selection of representative *Pandanus* samples and bioactive metabolite classes for targeted isolation and detailed characterization in the following chapters.

3.2. Experimental

3.2.1. Extraction of the samples

To prepare the extracts for chemical analysis and bioassays, 50 g of each sample was extracted in triplicate with 1 L of methanol in a sonication bath at 60°C. The solution was filtered and evaporated to yield the total extract.

3.2.2. Analytical methods

Total phenolic, flavonoid, alkaloid, and saponin contents, antioxidant, cytotoxic, and NO production inhibitory effects of *P. tectorius* and *P. amaryllifolius* extracts were evaluated using the protocols as shown in Chapter 2.

3.3. Phytochemical investigation of the *Pandanus tectorius* and *Pandanus amaryllifolius* plants' samples

The quantitative analysis of the major phytochemical groups—including total phenolics (TPC), flavonoids (TFC), saponins (TSC), and alkaloids (TAC)—was

conducted on all eighteen *Pandanus* samples representing three distinct biological groups: leaves of *P. tectorius*, fruits of *P. tectorius*, and leaves of *P. amaryllifolius*. The complete dataset is summarized in 0, which highlights substantial variability both within and between sample categories. As shown in the table, the four phytochemical parameters exhibit characteristic concentration patterns that appear to be influenced by species identity as well as plant organ.

As shown, the total phenolic content (TPC) exhibited pronounced variation among the three investigated sample groups, namely leaves of *P. tectorius* (PtL), fruits of *P. tectorius* (PtF), and leaves of *P. amaryllifolius* (PaL). TPC values ranged from 34.62 to 127.26 mg GAE/g dry weight across all eighteen samples, indicating substantial heterogeneity associated with both species identity and plant organ. At the group level, fruits of *P. tectorius* (PtF) consistently displayed the highest TPC values, with individual samples ranging from 92.04 ± 6.97 to 127.26 ± 9.39 mg GAE/g. In contrast, leaves of *P. tectorius* (PtL) showed intermediate phenolic levels (63.14 ± 10.50 to 88.18 ± 12.58 mg GAE/g), whereas leaves of *P. amaryllifolius* (PaL) contained markedly lower amounts of phenolic compounds, with TPC values largely below 55 mg GAE/g. A general decreasing trend in TPC values from PtF to PtL and PaL was observed at the descriptive level, suggesting that both interspecific differences and organ-specific metabolic allocation may influence phenolic accumulation in two *Pandanus* species.

The non-parametric Kruskal–Wallis test confirmed that these apparent differences were statistically significant ($\chi^2 = 13.56$, df = 2, $p = 0.00114$), indicating that at least one group differed significantly from the others in terms of TPC. Subsequent pairwise comparisons using Dunn's post-hoc test with Benjamini–Hochberg correction further clarified the pattern of variation. As shown in the post-hoc results, TPC in PaL samples was significantly lower than that in PtF samples (adjusted $p = 0.0009$, ***), and also significantly lower than that in PtL samples (adjusted $p = 0.0259$, *). In contrast, no statistically significant difference was observed between PtF and PtL groups (adjusted $p = 0.1387$, ns), despite the numerically higher mean TPC values recorded for PtF. The lack of statistical significance between PtF and PtL groups can be partly attributed to the relatively high intra-group variability observed in PtL samples, as reflected by the broad range and comparatively large standard deviations reported in Table 3.1. Several PtL samples (e.g., PtL01–PtL04) exhibited TPC values approaching those of the lower-end

PtF samples, thereby reducing the overall contrast between the two *P. tectorius* organs at the statistical level. Nevertheless, the consistently elevated TPC values in fruits suggest a biological trend toward enhanced phenolic accumulation in reproductive tissues, which may be linked to protective roles against oxidative stress, microbial attack, or herbivory during fruit development. In contrast, the uniformly low TPC levels observed in *P. amaryllifolius* leaves indicate a fundamentally different phenolic metabolism compared to *P. tectorius*. This interspecific disparity may reflect differences in genetic background, ecological adaptation, or dominant secondary metabolite pathways. Notably, *P. amaryllifolius* is widely recognized for its characteristic aroma and alkaloid-rich profile rather than for phenolic abundance, a feature that is consistent with the present quantitative findings.

In contrast to the broader variability observed for total phenolics, total flavonoid content (TFC) showed a more clearly species-driven pattern across the investigated *Pandanus* samples (Table 3.1). Leaves and fruits of *P. tectorius* consistently exhibited substantially higher flavonoid levels (approximately 27–40 mg QE/g) than leaves of *P. amaryllifolius*, in which TFC remained uniformly low and did not exceed 7 mg QE/g. This pronounced quantitative separation suggests that flavonoid biosynthesis and accumulation are markedly more developed in *P. tectorius*. The Kruskal–Wallis test confirmed a significant overall difference in TFC among the three groups ($p = 0.00301$). Pairwise comparisons further demonstrated that *P. amaryllifolius* leaves differed significantly from both *P. tectorius* fruits and leaves after Benjamini–Hochberg correction (adjusted $p = 0.0066$ and 0.0073, respectively). In contrast, no statistically significant difference was detected between fruits and leaves of *P. tectorius* (adjusted $p = 0.6216$), despite the slightly higher mean values observed in the fruit samples. This result indicates that, unlike total phenolics, flavonoid accumulation in *P. tectorius* is not strongly organ-specific but rather reflects a species-level metabolic trait. The substantial overlap in TFC values between PtF and PtL samples supports this interpretation and suggests a relatively uniform distribution of flavonoids across vegetative and reproductive tissues.

Table 3.1. Quantitative levels of total phenolics (TPC), flavonoids (TFC), saponins (TSC), and alkaloids (TAC) in the extracts from leaves of P. tectorius, fruits of P. tectorius, and leaves of P. amaryllifolius.

No.	Species	Part	Code	Group	TPC (mgGAE/g)	TFC (mgQE/g)	TSC (mgAE/g)	TAC (%)
1	*P. tectorius*	Leaves	PtL01	PtL	82.86 ± 13.58	34.78 ± 5.35	29.13 ± 1.45	1.21 ± 0.25
2	*P. tectorius*	Leaves	PtL02	PtL	78.82 ± 13.53	35.81 ± 6.84	31.46 ± 3.49	1.15 ± 0.15
3	*P. tectorius*	Leaves	PtL03	PtL	88.18 ± 12.58	34.24 ± 7.14	29.19 ± 2.51	1.25 ± 0.16
4	*P. tectorius*	Leaves	PtL04	PtL	86.32 ± 13.56	33.2 ± 3.46	27.04 ± 3.46	1.27 ± 0.28
5	*P. tectorius*	Leaves	PtL05	PtL	70.41 ± 10.88	29.03 ± 4.46	24.13 ± 1.23	ND
6	*P. tectorius*	Leaves	PtL06	PtL	63.14 ± 10.5	27.65 ± 5.05	22.91 ± 2.16	ND
7	*P. tectorius*	Leaves	PtL07	PtL	115.71 ± 8.96	39.85 ± 2.13	48.93 ± 3.85	ND
8	*P. tectorius*	Fruits	PtF01	PtF	127.26 ± 9.39	36.48 ± 1.97	52.59 ± 4.8	ND
9	*P. tectorius*	Fruits	PtF02	PtF	105.68 ± 9.44	38.2 ± 2.18	47.61 ± 2.62	ND
10	*P. tectorius*	Fruits	PtF03	PtF	114.03 ± 8.32	36.37 ± 2.32	51.82 ± 1.67	ND
11	*P. tectorius*	Fruits	PtF04	PtF	93.29 ± 7.42	31.49 ± 1.77	38.83 ± 4.24	ND
12	*P. tectorius*	Fruits	PtF05	PtF	92.04 ± 6.97	31.07 ± 1.7	38.73 ± 3.02	ND
13	*P. amaryllifolius*	Leaves	Pama01	Pama	42.53 ± 5.45	5.27 ± 0.43	7.54 ± 0.69	15.11 ± 0.79
14	*P. amaryllifolius*	Leaves	Pama02	Pama	45.46 ± 5.22	6.57 ± 0.47	8.58 ± 0.58	8.68 ± 0.72
15	*P. amaryllifolius*	Leaves	Pama03	Pama	52.07 ± 4.94	6.97 ± 0.64	9.88 ± 0.75	21.76 ± 0.93
16	*P. amaryllifolius*	Leaves	Pama04	Pama	37.92 ± 8.05	4.36 ± 0.38	11.12 ± 0.75	21.14 ± 1.12
17	*P. amaryllifolius*	Leaves	Pama05	Pama	46.38 ± 7.64	5.78 ± 0.39	8.52 ± 0.96	16.57 ± 1.04
18	*P. amaryllifolius*	Leaves	Pama06	Pama	34.62 ± 4.96	6.92 ± 0.36	8.13 ± 1.01	17.01 ± 1.11

Conversely, the consistently low flavonoid content of *P. amaryllifolius* leaves reinforces the chemical distinction between the two species and highlights flavonoids as a discriminating phytochemical marker within the genus *Pandanus*.

Total saponin content (TSC) exhibited a distribution pattern that was more strongly associated with plant organ than that observed for flavonoids, while still retaining a clear species-level differentiation (Table 3.1). Saponin levels in fruits of *P. tectorius* were markedly elevated, ranging from 38.73 ± 3.02 to 52.59 ± 4.80 mg AE/g, and were consistently higher than those detected in *P. tectorius* leaves (22.91 ± 2.16 to 31.46 ± 3.49 mg AE/g). In contrast, leaves of *P. amaryllifolius* contained only minor amounts of saponins, with TSC values generally below 12 mg AE/g. Statistical analysis using the Kruskal–Wallis test confirmed a highly significant overall difference among the three sample groups ($p = 0.00096$). Dunn's post-hoc comparisons with Benjamini–Hochberg correction revealed that saponin levels in *P. amaryllifolius* leaves were significantly lower than those in both *P. tectorius* fruits (adjusted $p = 0.0007$) and leaves (adjusted $p = 0.0295$). In contrast, the difference between fruits and leaves of *P. tectorius* did not reach statistical significance (adjusted $p = 0.1117$), despite the consistently higher TSC values observed in fruit samples. The substantial overlap in TSC values between fruits and leaves within *P. tectorius* indicates that saponin biosynthesis is not exclusively fruit-specific but rather broadly distributed across organs in this species. Conversely, the uniformly low saponin content in *P. amaryllifolius* leaves further underscores the marked chemical divergence between the two species and highlights saponins as a distinguishing metabolite class within the studied *Pandanus* taxa.

In contrast to phenolics, flavonoids, and saponins, total alkaloid content (TAC) displayed a markedly distinct distribution pattern among the investigated *Pandanus* samples (Table 3.1). Alkaloids were consistently detected at substantial levels in leaves of *P. amaryllifolius*, with TAC values ranging from 8.68 ± 0.72% to 21.76 ± 0.93%. By comparison, alkaloids were largely absent or below the detection limit in fruits of *P. tectorius* and were detected only at trace levels in several leaf samples of *P. tectorius*, indicating a pronounced interspecific divergence in alkaloid accumulation. This contrasting pattern was strongly supported by statistical analysis. The Kruskal–Wallis test revealed a highly significant overall difference in TAC among the three groups ($p = 0.00103$). Dunn's post-hoc comparisons with Benjamini–Hochberg correction showed

that TAC in *P. amaryllifolius* leaves was significantly higher than in both fruits (adjusted $p = 0.0011$) and leaves (adjusted $p = 0.0115$) of *P. tectorius*. In contrast, no statistically significant difference was observed between fruits and leaves of *P. tectorius* (adjusted $p = 0.2511$), consistent with the near absence of alkaloids in both organs.

High contents of alkaloids in *P. amaryllifolius* leaves suggest that this species relies on a fundamentally different chemical defense strategy compared to *P. tectorius*, in which phenolics, flavonoids, and saponins appear to dominate the secondary metabolite profile. This divergence highlights alkaloids as a key species-specific metabolite class within the genus *Pandanus* and provides a biochemical explanation for the distinct sensory and ethnobotanical characteristics commonly attributed to *P. amaryllifolius*. Taken together, the combined analysis of TPC, TFC, TSC, and TAC reveals both shared and contrasting phytochemical patterns among the three *Pandanus* sample groups. Fruits and leaves of *P. tectorius* are characterized by consistently high levels of phenolics, flavonoids, and saponins, with only moderate organ-dependent variation and substantial overlap between vegetative and reproductive tissues. In contrast, leaves of *P. amaryllifolius* exhibit markedly lower contents of these metabolite classes, indicating a reduced reliance on phenolic- and saponin-based chemical defenses.

Overall, while organ-specific effects are evident for certain metabolite classes—particularly saponins and alkaloids—the dominant driver of phytochemical variation across the dataset appears to be species identity. These statistically supported patterns provide a robust framework for chemotaxonomic differentiation and for the rational selection of target plant materials in subsequent isolation and bioactivity studies.

3.4. Free radical scavenging and *α*-amylase inhibitory activities of the *Pandanus tectorius* and *Pandanus amaryllifolius* plants' extracts

The screening results summarized in Table 3.2 reveal marked differences in antioxidant and α-amylase inhibitory activities among the three investigated *Pandanus* sample groups. For both DPPH and hydroxyl radical scavenging assays, extracts from *P. tectorius*—including leaves and fruits—consistently exhibited stronger activities than those from *P. amaryllifolius* leaves across all tested concentrations. In particular, *P. tectorius* fruits generally showed the highest scavenging efficiencies, reaching approximately 70–76% inhibition at 50 µg/mL in the DPPH assay and comparable levels in the hydroxyl radical assay. Although these activities were lower than those of the

positive controls (ascorbic acid and catechin), which exhibited strong radical scavenging effects under the same experimental conditions, several *P. tectorius* extracts approached the activity range of these standards at higher concentrations, indicating substantial antioxidant potential for crude plant extracts. A clear dose-dependent increase in radical scavenging activity was observed for all samples, indicating a concentration-responsive antioxidant effect. However, the magnitude of this response differed substantially among groups. While *P. tectorius* extracts displayed moderate-to-strong activity even at 20 μg/mL, *P. amaryllifolius* leaf extracts showed only weak scavenging effects, rarely exceeding 50% inhibition at the higher concentration. In comparison with the positive controls, the antioxidant activity of *P. amaryllifolius* leaves remained markedly lower, suggesting a limited contribution of phenolic-type constituents to radical scavenging in this species. This pattern mirrors the quantitative phytochemical data, in which *P. tectorius* samples were characterized by significantly higher contents of phenolics and flavonoids—compound classes well known for their hydrogen-donating and free radical–quenching capacities. The hydroxyl radical scavenging assay exhibited trends similar to those of the DPPH assay, although slightly higher variability was observed among individual samples. Nevertheless, fruits of *P. tectorius* again ranked among the most active extracts, with inhibition levels at 50 μg/mL reaching values comparable to those of the flavonoid standard catechin at similar concentrations. In contrast, the consistently low hydroxyl scavenging activity of *P. amaryllifolius* leaves, which remained far below that of the positive control, further supports the notion that this species relies less on phenolic-based antioxidant defenses.

In terms of α-amylase inhibition, *P. tectorius* extracts demonstrated moderate inhibitory activity, particularly at 200 μg/mL, with several fruit and leaf samples exceeding 55–60% inhibition. While these values were lower than those observed for the positive control acarbose, which showed strong inhibition at the same concentration, the activity of *P. tectorius* extracts is notable given their crude nature. Conversely, *P. amaryllifolius* leaf extracts exhibited only weak inhibitory effects, with inhibition percentages remaining below 16% even at the highest tested concentration and far below the activity of acarbose.

Table 3.2. Screening results of radical scavenging (DPPH and hydroxyl) and α-amylase inhibitory activities of extracts from Pandanus species.

No.	Species	Part	Code	DPPH scavenging effect, %I		Hydroxyl, %I		*α*-amylase inhibition, %I	
				20 µg/mL	50 µg/mL	20 µg/mL	50 µg/mL	100 µg/mL	200 µg/mL
1	*P. tectorius*	Leaves	PtL01	29.28 ± 2.97	62.49 ± 2.08	31.24 ± 2.44	63.85 ± 6.71	19.10 ± 1.67	54.87 ± 2.12
2	*P. tectorius*	Leaves	PtL02	23.10 ± 2.08	59.90 ± 4.16	30.50 ± 3.05	61.55 ± 4.66	20.77 ± 1.85	53.98 ± 5.58
3	*P. tectorius*	Leaves	PtL03	32.40 ± 3.28	65.56 ± 3.70	25.22 ± 1.15	68.87 ± 4.67	28.16 ± 1.14	57.64 ± 2.79
4	*P. tectorius*	Leaves	PtL04	26.96 ± 2.74	76.11 ± 3.16	34.97 ± 1.92	73.41 ± 3.77	16.09 ± 0.64	41.21 ± 1.36
5	*P. tectorius*	Leaves	PtL05	21.95 ± 1.57	58.51 ± 2.24	23.37 ± 2.15	60.50 ± 3.42	16.63 ± 1.73	38.10 ± 2.83
6	*P. tectorius*	Leaves	PtL06	18.35 ± 1.01	56.12 ± 4.32	24.23 ± 2.61	55.50 ± 3.98	16.84 ± 1.04	33.87 ± 2.02
7	*P. tectorius*	Leaves	PtL07	22.79 ± 2.09	63.10 ± 2.75	22.32 ± 1.56	68.70 ± 4.47	26.94 ± 1.46	62.43 ± 6.02
8	*P. tectorius*	Fruits	PtF01	35.32 ± 2.93	76.25 ± 7.93	33.05 ± 1.37	73.51 ± 2.33	22.71 ± 1.57	63.51 ± 6.01
9	*P. tectorius*	Fruits	PtF02	23.72 ± 1.42	70.02 ± 5.36	25.42 ± 0.79	71.76 ± 6.90	27.39 ± 2.27	58.43 ± 3.24
10	*P. tectorius*	Fruits	PtF03	32.23 ± 1.21	72.68 ± 4.20	31.15 ± 1.51	72.94 ± 7.42	18.99 ± 2.02	56.82 ± 6.04
11	*P. tectorius*	Fruits	PtF04	29.57 ± 2.65	70.58 ± 5.45	35.94 ± 1.46	72.23 ± 2.98	22.66 ± 1.20	59.31 ± 3.16
12	*P. tectorius*	Fruits	PtF05	22.70 ± 1.16	68.91 ± 2.19	29.17 ± 2.46	70.78 ± 5.26	21.88 ± 2.28	58.32 ± 4.15
13	*P. amaryllifolius*	Leaves	Pama01	16.27 ± 1.71	46.07 ± 4.91	11.95 ± 0.47	32.12 ± 1.24	6.27 ± 0.20	12.78 ± 0.65
14	*P. amaryllifolius*	Leaves	Pama02	20.98 ± 1.03	46.92 ± 3.22	10.97 ± 0.77	34.00 ± 2.85	5.02 ± 0.37	13.78 ± 1.45
15	*P. amaryllifolius*	Leaves	Pama03	19.23 ± 0.77	51.41 ± 4.76	22.29 ± 1.91	46.63 ± 2.45	6.97 ± 0.56	14.87 ± 0.64
16	*P. amaryllifolius*	Leaves	Pama04	13.99 ± 1.35	37.31 ± 1.37	15.49 ± 1.18	31.60 ± 2.62	7.04 ± 0.27	15.32 ± 0.51
17	*P. amaryllifolius*	Leaves	Pama05	16.88 ± 0.71	48.73 ± 3.36	18.65 ± 0.86	42.66 ± 3.76	5.21 ± 0.21	13.51 ± 0.88
18	*P. amaryllifolius*	Leaves	Pama06	16.41 ± 0.73	33.47 ± 2.32	12.47 ± 1.18	30.37 ± 2.78	6.49 ± 0.41	13.06 ± 1.43
Control	*Ascorbic acid* *			38.49 ± 4.38	88.23 ± 6.21				
Control	*Catechin* **					32.44 ± 2.24	79.44 ± 8.97		
Control	*Acarbose***							49.31 ± 5.31	81.17 ± 5.62

Overall, the bioactivity profiles presented in Table 3.2 align closely with the phytochemical composition patterns observed for TPC, TFC, and TSC. While the activities of the crude *Pandanus* extracts are generally lower than those of purified positive controls, *P. tectorius*—particularly its fruits—emerges as a rich source of antioxidant and moderate α-amylase inhibitory constituents. In contrast, *P. amaryllifolius* leaves display comparatively limited activity in these assays. These results not only corroborate the chemical differentiation between the two species but also support the selection of *P. tectorius*—especially fruit material—as a promising candidate for further bioactivity-guided isolation and mechanistic studies.

3.5. NO production inhibitory and cytotoxic effects of the *Pandanus* plants' extracts

To further evaluate the anti-inflammatory potential and cellular safety of the investigated *Pandanus* extracts, selected representative samples were assessed for their inhibitory effects on nitric oxide (NO) production in LPS-stimulated RAW264.7 macrophages, as well as for cytotoxicity against A549, K562, and MCF7 cancer cell lines. Owing to the limited amount of extract obtained from several samples, only those available in sufficient quantity were selected for bioassays and thus considered representative of their respective sample groups.

Table 3.3. Inhibitory effects of Pandanus extracts on NO production in LPS-stimulated RAW264.7 macrophages at 30 and 100 µg/mL

Sample	Part	Conc.	NO inhibition on RAW264.7	
			%I	% cell survival
LPS		0.1		98.75 ± 1.46
Cardamonin*		2.5 µg/mL	46.40 ± 4.39	121.53 ± 5.37
		10 µg/mL	78.54 ± 1.76	109.32 ± 5.04
PtL01	Leaves	30 µg/mL	21.02 ± 1.65	111.70 ± 2.46
		100 µg/mL	59.23 ± 2.86	103.61 ± 2.44
PtF01	Fruits	30 µg/mL	28.17 ± 0.73	120.31 ± 4.70
		100 µg/mL	57.45 ± 6.66	119.81 ± 3.46
Pama01	Leaves	30 µg/mL	48.35 ± 2.56	105.83 ± 7.31
		100 µg/mL	92.91 ± 0.95	18.50 ± 4.26
Pama02	Leaves	30 µg/mL	16.06 ± 5.34	115.78 ± 1.54
		100 µg/mL	53.67 ± 1.48	122.85 ± 1.42

* Positive control

As shown in Table 3.3, all tested extracts exhibited concentration-dependent inhibition of NO production in LPS-stimulated RAW264.7 cells. Extracts from *P. tectorius* leaves (PtL01) and fruits (PtF01) displayed moderate NO inhibitory activity, with inhibition values of approximately 21–28% at 30 µg/mL, increasing to around 57–59% at 100 µg/mL. Importantly, these inhibitory effects were accompanied by high cell viability (>100%), indicating that the observed reduction in NO production was not attributable to cytotoxic effects. In contrast, *P. amaryllifolius* leaf extracts showed more divergent behavior. Pama02 exhibited moderate NO inhibition at 100 µg/mL (53.67%) while maintaining excellent cell viability (>120%), suggesting a genuine anti-inflammatory effect. Conversely, Pama01 displayed strong NO inhibition at 100 µg/mL (92.91%); however, this effect was accompanied by a dramatic decrease in cell survival (18.50%), indicating that NO suppression in this case was largely associated with cytotoxicity rather than selective inhibition of inflammatory signaling.

On the other hand, the cytotoxic activities of selected *Pandanus* extracts against A549 (lung carcinoma), K562 (chronic myelogenous leukemia), and MCF7 (breast carcinoma) cell lines are summarized in Table 3.4.

Table 3.4. Cytotoxicity of Pandanus extracts against A549, K562, and MCF7 cell lines at 25 and 100 µg/mL, expressed as percentage cell survival.

Sample	Part	Conc.	% Cell survival in cytotoxic assay		
			A549	K562	MCF7
Camptothecin*		0,25 µg/mL	71.38 ± 5.07	76.81 ± 5.09	80.28 ± 6.43
		1 µg/mL	57.73 ± 8.55	49.22 ± 5.29	57.79 ± 3.23
PtL01	Leaves	25 µg/mL	68.11 ± 1.26	68.78 ± 4.49	75.76 ± 7.55
		100 µg/mL	78.37 ± 3.70	40.54 ± 0.81	70.05 ± 2.33
PtF01	Fruits	25 ug/mL	92.13 ± 11.53	32.33 ± 2.24	86.79 ± 6.59
		100 ug/mL	71.13 ± 11.05	30.59 ± 1.15	76.33 ± 3.01
Pama01	Leaves	25 µg/mL	78.61 ± 5.21	48.46 ± 7.42	86.11 ± 5.51
		100 µg/mL	79.51 ± 0.81	36.25 ± 3.55	58.96 ± 2.23
Pama02	Leaves	25 ug/mL	94.36 ± 8.54	70.16 ± 3.11	88.93 ± 3.77
		100 ug/mL	54.63 ± 2.44	76.26 ± 3.42	71.63 ± 4.64

* Positive control

In general, most extracts exhibited weak to moderate cytotoxicity, with pronounced cell line–dependent effects. Extracts from *P. tectorius* demonstrated selective cytotoxicity toward K562 cells. Both leaf (PtL01) and fruit (PtF01) extracts reduced K562 cell viability to approximately 30–41% at 100 µg/mL, while exerting considerably weaker effects on A549 and MCF7 cells, for which cell survival generally remained above 70%. This selective sensitivity of K562 cells suggests potential activity

against hematological malignancies rather than solid tumors. *P. amaryllifolius* leaf extracts showed a more variable cytotoxic profile. Pama01 exhibited moderate cytotoxicity against K562 and MCF7 cells at 100 μg/mL, whereas Pama02 displayed relatively low cytotoxicity across all three cell lines, with the exception of A549 cells at the higher concentration. Notably, none of the extracts approached the potency of the positive control camptothecin, indicating that the observed effects are moderate in magnitude.

Taken together, the NO inhibition and cytotoxicity assays reveal that *P. tectorius* extracts combine moderate anti-inflammatory activity with acceptable cellular safety, particularly at concentrations relevant to antioxidant and enzyme inhibitory assays. In contrast, *P. amaryllifolius* extracts exhibit stronger but less selective biological effects, likely reflecting the higher alkaloid content of this species. These findings further support the notion of distinct bioactivity profiles between the two *Pandanus* species and underscore the importance of integrating phytochemical composition with functional bioassays when evaluating the therapeutic potential of plant extracts.

3.6. Multivariate correlation between chemical compositions and bioactivities of *Pandanus* plant extracts

To comprehensively elucidate the relationships between phytochemical composition and biological activities of *Pandanus* plant extracts, partial least squares (PLS) regression was employed as a multivariate analytical approach. Unlike univariate analyses, PLS enables simultaneous integration of multiple chemical variables—total phenolics (TPC), flavonoids (TFC), saponins (TSC), and alkaloids (TAC)—with diverse biological responses, including antioxidant, enzyme inhibitory, anti-inflammatory, and cytotoxic activities. The predictive performance of the PLS model was further evaluated using the coefficients of determination (R^2) and cross-validated predictability (Q^2). The overall R^2 (mean across all response variables) reached 0.7466, indicating that approximately 75% of the total variance in the bioactivity data could be explained by the four phytochemical descriptors (TPC, TFC, TSC, and TAC). This demonstrates a strong explanatory power of the model and confirms that the selected chemical variables capture most of the biological information in the dataset. The adjusted values of R^2 and Q^2 indicate that the PLS model is well-suited for predicting and interpreting the relationships between phytochemical composition and antioxidant as well as α-amylase

inhibitory activities, which showed strong and consistent correlations with the chemical variables. In contrast, the predictive performance for NO inhibition and cytotoxic activities is less reliable, mainly due to the limited sample size and the higher biological complexity of these responses. Therefore, while the model provides robust insights into chemical drivers of antioxidant and enzyme inhibitory effects, correlations involving anti-inflammatory and cytotoxic activities should be interpreted with caution.

Model performance and interpretability were evaluated by combining cross-validation (CV) results (Figure 3.1), correlation coefficients between X and Y variables, variable importance in projection (VIP) scores, and the proportion of variance explained by individual latent components. Cross-validation results (Figure 3.1) demonstrated a pronounced reduction in RMSEP values upon inclusion of the first latent component for all investigated biological activities, indicating that the dominant structure–activity relationships were captured at an early stage of model construction. For antioxidant activities (DPPH and hydroxyl radical scavenging) and α-amylase inhibition, RMSEP values reached a minimum with one component and remained stable thereafter, suggesting relatively simple and largely linear relationships between chemical composition and bioactivity. In contrast, NO inhibition and cytotoxic effects—particularly against K562 cells—required two components to achieve optimal predictive performance, reflecting greater biological and mechanistic complexity. The close overlap between CV and adjCV curves across all models indicates statistical stability and the absence of severe overfitting, despite the limited number of samples. The reliability of the model was further supported by the distribution of explained variance. The first PLS component accounted for 91.52% of the total variance in the chemical dataset, while the second component explained an additional 6.78%, together capturing more than 98% of the variance. This result indicates that phytochemical variability among the studied samples is dominated by a single major compositional gradient, with minor secondary contributions. VIP analysis showed that all four chemical variables contributed meaningfully to the model, with VIP values close to or exceeding the threshold of 1 across components, confirming that no variable was redundant and that the model retained chemical interpretability.

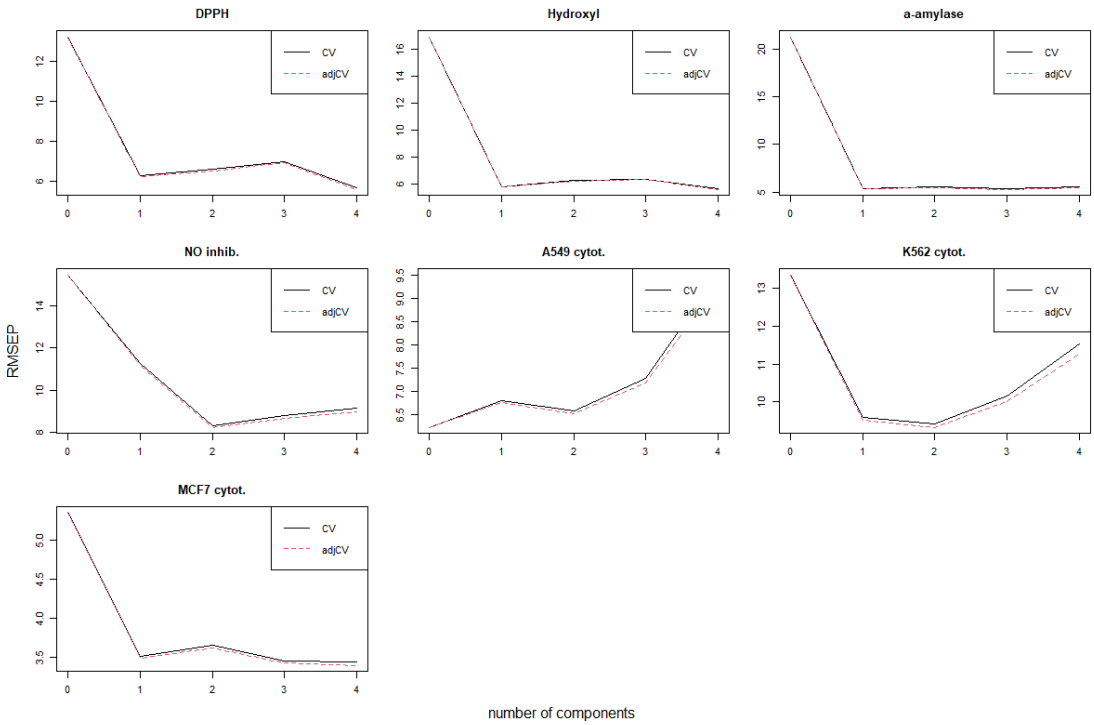

Figure 3.1. Cross-validation performance of PLS regression models used to evaluate the relationship between phytochemical composition and biological activities of Pandanus plant extracts.

Correlation analysis between chemical variables and biological responses revealed clear and biologically coherent patterns. Strong positive correlations were observed between TPC, TFC, and TSC and antioxidant activities, including DPPH and hydroxyl radical scavenging, as well as α-amylase inhibition. These relationships indicate that phenolic-, flavonoid-, and saponin-rich extracts are the primary drivers of antioxidant and enzyme inhibitory effects in *Pandanus* species. In contrast, TAC displayed strong negative correlations with these activities, highlighting an inverse relationship between alkaloid abundance and phenolic-type bioactivities at the multivariate level.

The PLS biplot (Figure 3.2) provides a clear visual representation of these relationships. Vectors corresponding to TPC, TFC, and TSC are closely aligned and oriented toward DPPH scavenging, hydroxyl scavenging, and α-amylase inhibition, indicating strong positive associations and a shared chemical basis for these activities. Their opposite orientation relative to TAC further confirms the antagonistic relationship between alkaloid-rich and phenolic-rich chemical profiles.

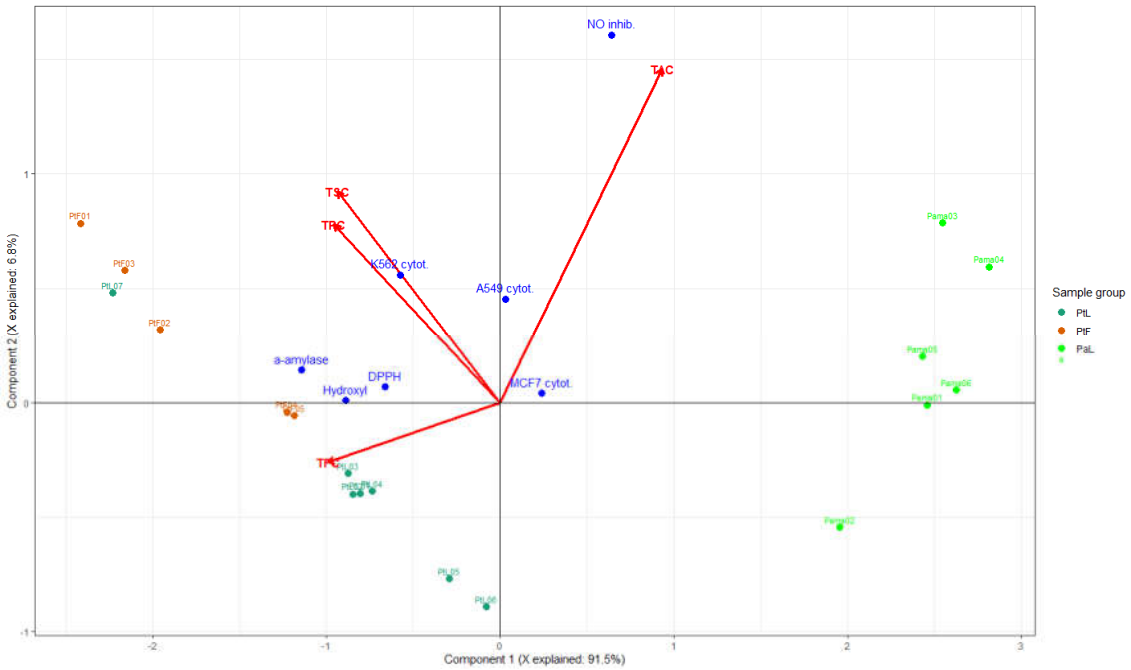

Figure 3.2. PLS biplot showing the relationships between phytochemical variables (TPC, TFC, TSC, and TAC; arrows) and biological activities (circles) of Pandanus plant extracts based on the first two latent components.

For NO inhibition and cytotoxic responses, a more complex pattern emerges. TAC is strongly oriented toward NO inhibition and cytotoxicity against MCF7 cells, indicating that alkaloids play a dominant role in these responses. However, the biplot also reveals that cytotoxicity—particularly against K562 cells—is not exclusively associated with TAC. The TPC and TSC vectors form acute angles with K562 cytotoxicity and, to a lesser extent, MCF7 cytotoxicity, indicating positive contributions of phenolic- and saponin-related constituents to these effects. This interpretation is consistent with correlation analysis, in which TPC and TSC exhibited positive correlations with K562 cytotoxicity, and with cross-validation results showing that two latent components are required to adequately model this response.

In contrast, cytotoxicity against A549 cells shows weaker and less structured associations with individual chemical variables in both the correlation matrix and the biplot, consistent with its relatively poorer predictive performance in the CV analysis. This suggests that A549 cytotoxicity may depend on additional factors not fully captured by the four global phytochemical descriptors used in the present model.

Taken together, the integration of cross-validation performance, explained variance, correlation analysis, VIP profiling, and biplot visualization demonstrates that

the constructed PLS model is both statistically robust and chemically meaningful. Antioxidant and α-amylase inhibitory activities of *Pandanus* extracts are predominantly governed by phenolic-, flavonoid-, and saponin-rich chemical profiles, whereas NO inhibition and cytotoxic effects arise from combined contributions of alkaloids and phenolic-type constituents, with variable dominance depending on the specific biological endpoint. This multivariate framework highlights the functional partitioning and partial overlap of metabolite classes within *Pandanus* species and provides a coherent interpretation of the complex chemical–bioactivity relationships observed in this study.

3.7. Chapter summary

A comprehensive screening of phytochemical composition and biological activities of *P. tectorius* and *P. amaryllifolius* extracts was conducted, revealing clear interspecific and organ-dependent patterns. Quantitative analysis demonstrated that fruits and leaves of *P. tectorius* are characterized by consistently high levels of phenolics, flavonoids, and saponins, whereas leaves of *P. amaryllifolius* contain markedly lower amounts of these metabolite classes but are distinguished by a high alkaloid content. Statistical evaluation confirmed that species identity represents the primary driver of phytochemical variation, while organ-specific effects contribute additional but secondary differentiation. Bioactivity screening showed that *P. tectorius* extracts, particularly those derived from fruits, exhibit strong antioxidant activity and moderate α-amylase inhibition, in agreement with their phenolic- and saponin-rich chemical profiles. In contrast, *P. amaryllifolius* leaf extracts displayed comparatively weaker antioxidant and enzyme inhibitory activities but showed more pronounced effects in NO inhibition and selected cytotoxic assays, reflecting the functional relevance of their alkaloid-dominated composition. Importantly, most extracts exhibited moderate activity levels and acceptable cellular safety, indicating genuine biological effects rather than nonspecific cytotoxicity. Multivariate PLS analysis further integrated these findings by demonstrating robust correlations between phytochemical composition and biological responses. Antioxidant and α-amylase inhibitory activities were primarily associated with phenolic-, flavonoid-, and saponin-rich profiles, whereas NO inhibition and cytotoxicity were governed by combined contributions of alkaloids and phenolic-type constituents, with variable dominance depending on the biological endpoint. The PLS

model was shown to be statistically stable and chemically interpretable, providing a coherent framework for understanding overlapping and distinct roles of major metabolite classes in *Pandanus* species.

Taken together, the results presented in this chapter indicate that all three investigated sample groups—*P. tectorius* leaves, *P. tectorius* fruits, and *P. amaryllifolius* leaves—represent valuable and complementary sources of bioactive natural products. While *P. tectorius* samples are particularly promising for the discovery of antioxidant and enzyme inhibitory compounds, *P. amaryllifolius* leaves offer distinct potential for alkaloid-associated anti-inflammatory and cytotoxic activities. These findings provide a solid scientific basis for the selection of representative samples and targeted metabolite classes, which will be explored in greater depth through isolation, structural elucidation, and mechanistic studies in the subsequent chapters of this thesis.

CHAPTER 4. ISOLATION, STRUCTURE ELUCIDATION, AND BIOACTIVITY EVALUATION OF COMPOUNDS FROM *PANDANUS TECTORIUS* LEAVES

4.1. Chapter overview

Two novel benzofuran derivatives, Pandanusfuran A and Pandanusfuran B, along with four known lignans, were isolated from the leaves of *Pandanus tectorius*. The structures of these compounds were comprehensively determined using advanced spectroscopic techniques, including nuclear magnetic resonance (NMR), high-resolution mass spectrometry (HRMS), and electronic circular dichroism (ECD). The absolute configurations were elucidated using Snatzke's method, a sophisticated approach exploiting induced circular dichroism (ICD) in dimolybdenum tetraacetate complexes. This combination of spectroscopic methods provided clear structural assignments, particularly distinguishing between epimers. The benzofuran derivatives isolated from *P. tectorius* added valuable chemotaxonomic markers and expanded the chemical diversity of this genus.

4.2. Samples

Leaves of *P. tectorius* were collected from Thanh Oai town, on the outskirts of Hanoi City of Vietnam, in March 2021 and identified by Dr. Bui Van Thanh, formerly of the Institute of Ecology and Biological Resources, currently the Institute of Biology, Vietnam Academy of Science and Technology. The voucher specimens were deposited at the Institute of Biology (HN00128210208) and the Center for High Technology Research and Development (NCCG 210208), Vietnam Academy of Science and Technology.

4.3. Isolation of compounds from the *Pandanus tectorius* leaves

Dried powder (3.5 kg) of *P. tectorius* leaves was extracted three times with methanol (MeOH) in a sonication bath. The combined extracts were concentrated to obtain the residue (178 g), which was suspended in water (2 L) and then successively partitioned with hexane (2 L × 3 times) and ethyl acetate (EtOAc) (2 L × 3 times) to afford the corresponding fractions, respectively. The EtOAc fraction (37.5 g) was subjected to a silica gel chromatography column (CC) with gradient mixtures of CH_2Cl_2–MeOH (1/0-0/1, v/v) to afford seven subfractions (E1- E7). The fraction E4 (689 mg) was separated using silica gel eluted with n-hexane–acetone (3/1, v/v) followed by preparative HPLC (90 min, 50-

80% MeOH in H_2O) to yield the compounds **Pt1** (5.1 mg) and **Pt2** (3.5 mg). Fraction E3 (2.68 g) was chromatographed on a silica gel CC eluted with CH_2Cl_2–acetone (10/1, v/v) to afford compound **Pt3** (24.7 mg) and compound **Pt4** (32.1 mg). Fraction E6 (3.72 g) was isolated using a YMC RP-C18 column eluted with MeOH–water (3:1, v/v) to yield compound **Pt5** (14.9 mg) and compound **Pt6** (22.3 mg).

The absolute configuration of compounds Pt1 and Pt2 was elucidated by their ECD spectra in combination with the ECD measurement of their $Mo_2(OAc)_4$ complex (Snatzke' s method). For the preparation of the complex, 0.5 mg of each compound was mixed with 1.2 mg of $Mo_2(OAc)_4$ and then dissolved in 1.5 mL of anhydrous DMSO. The ECD spectrum was measured right after dissolving the mixture in the range of 250-500 nm. After 20 minutes, the stationary ICD spectrum was used to subtract the previous ECD spectrum. The Cotton effect at 290-340 nm in the ICD spectrum was correlated to the absolute configuration of the diol moiety.

To check if these compounds might be artefacts of the extracting process in methanol, we performed an HPLC-DAD analysis on the ethanol extract of the plant material (1 g of the *P. tectorius* leaves were extracted in 25 mL of ethanol 90%, in triplicated, then combined the solution and evaporated the solvent to gain the ethanol extract). The extract was subsequently analyzed using an HPLC-DAD system (Agilent 1100) equipped with a Hypersil Gold C18 column (250 × 4.6 mm, 5 µm). Separation was performed under isocratic elution with 35% methanol over 20 min at a flow rate of 1.0 mL/min. Detection was carried out using a DAD detector set at 254 nm.

Pandanusfuran A **(Pt1)**: white amorphous powder; HR-ESI-MS: *m/z* 253.1071 $[M+H]^+$ (calc for $C_{13}H_{17}O_5$, 253.1076); $[\alpha]_D^{25}$ -32.2; CD (MeOH) λ_{max} (mdeg): 220 (+1,73), 264 (-6,66); ^{1}H NMR (DMSO-*d*$_6$, 600 MHz): see Table 4.1; ^{13}C NMR (DMSO-*d*$_6$, 150 MHz): see Table 4.1.

Pandanusfuran B **(Pt2)**: White amorphous powder; HR-ESI-MS: *m/z* 287.0697 $[M+Cl]^-$ (calc for $C_{13}H_{17}O_5Cl$, 287.0686); $[\alpha]_D^{25}$ -41.5; ^{1}H NMR (DMSO-*d*$_6$, 600 MHz): see Table 4.2; ^{13}C NMR (DMSO-*d*$_6$, 150 MHz): see Table 4.2.

Pinoresinol **(Pt3)**: Yellow oil; ESI-MS: *m/z* 359 $[M+H]^+$, *m/z* 341 $[M+H-H_2O]^+$, *m/z* 739 $[2M+Na]^+$; molecular formula: $C_{20}H_{22}O_6$ (358 g/mol); ^{1}H NMR ($CDCl_3$, 600 MHz): see Table 4.3; ^{13}C NMR ($CDCl_3$, 150 MHz): see Table 4.3.

Pinoresinol monomethyl ether **(Pt4)**: Pale yellow oil; ESI-MS: *m/z* 373 $[M+H]^+$, *m/z* 395 $[M+Na]^+$; molecular formula: $C_{21}H_{24}O_6$ (372 g/mol); ^1H NMR ($CDCl_3$, 600 MHz): see Table 4.4; ^{13}C NMR ($CDCl_3$, 150 MHz): see Table 4.4.

Arctigenin **(Pt5):** Pale yellow oil; ESI-MS: *m/z* 373 $[M+H]^+$, *m/z* 767 $[2M+Na]^+$; molecular formula: $C_{21}H_{24}O_6$ (372 g/mol); ^1H NMR ($CDCl_3$, 600 MHz): see Table 4.5; ^{13}C NMR ($CDCl_3$, 150 MHz): see Table 4.5.

Matairesinol **(Pt6):** Yellow oil; ESI-MS: *m/z* 359 $[M+H]^+$, *m/z* 739 $[2M+Na]^+$; molecular formula: $C_{20}H_{22}O_6$ (358 g/mol); ^1H NMR ($CDCl_3$, 600 MHz): see Table 4.6; ^{13}C NMR ($CDCl_3$, 125 MHz): see Table 4.6.

4.4. Structure elucidation of the isolated compounds from *Pandanus tectorius* leaves

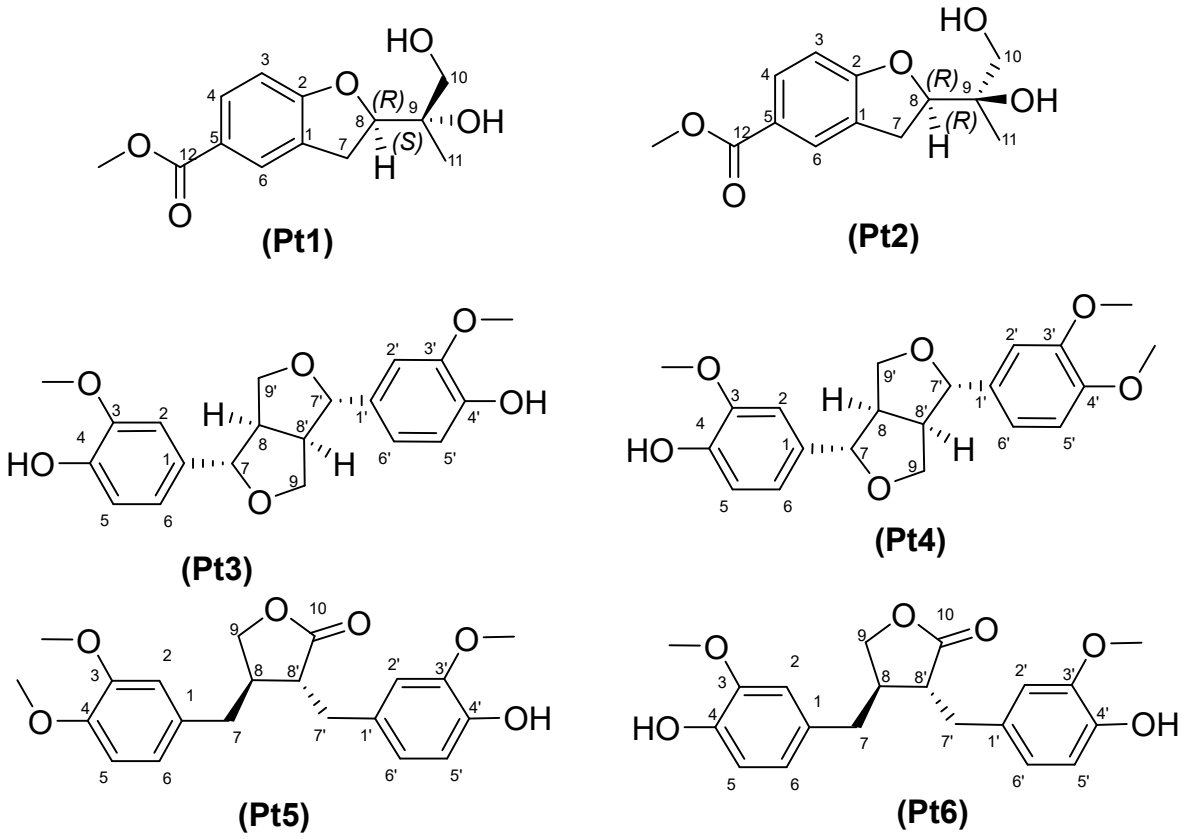

Figure 4.1. Structures of six isolated compounds from Pandanus tectorius leaves

*4.4.1. Compound Pt1: (8R, 9S)-9,10-dihydroxypropan-8-yl)-7,8-dihydrobenzofuran-5-carboxylate (***Pandanusfuran** ***A)***

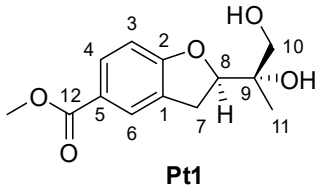

Figure 4.2. The structure of Pt1

Compound **Pt1** was isolated as a white amorphous powder that generated $[M+H]^+$ ion with the mass-to-charge ratio (*m/z*) value of 253.1071 when analyzed by HR-ESI-MS (Figure 4.3), suggesting the molecular formula $C_{13}H_{16}O_5$.

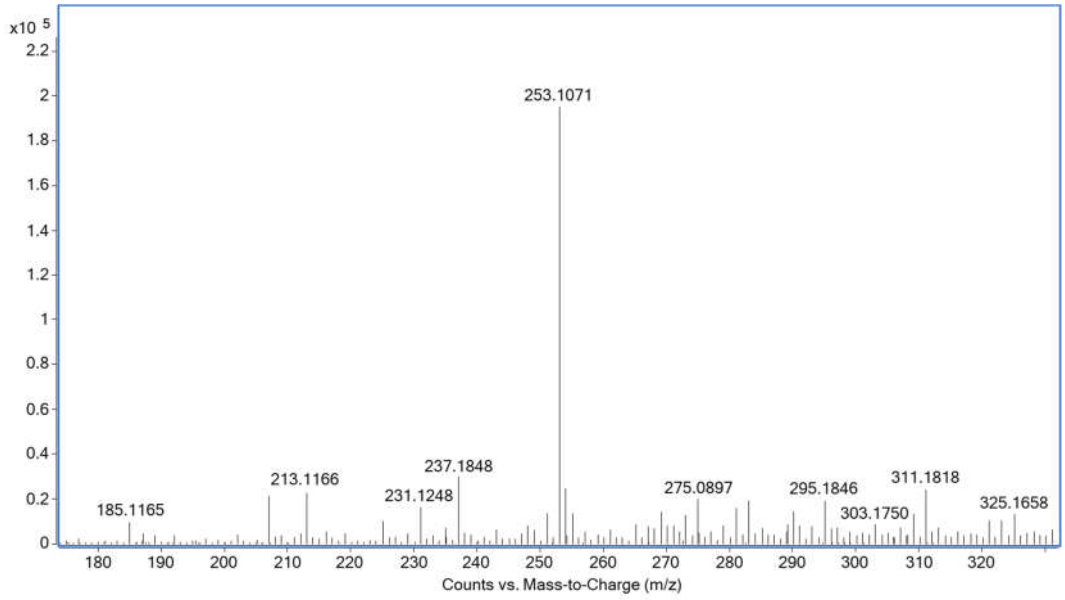

Figure 4.3. HR-ESI-MS spectrum of Pt1

^{1}H NMR spectrum of compound **Pt1** (Figure 4.4) showed the signals of three aromatic protons of an ABX system [6.79 (1H, d, *J* = 8.4 Hz, H-3), 7.73 (1H, dd, *J* = 8.4, 1.8 Hz, H-4), 7.77 (1H, d, *J* = 1.8 Hz, H-6)] which were also supported by the COSY correlation of H-3 and H-4; two pairs of methylene protons at δ_H 3.14 (1H, dd, *J* = 8.4, 16.2 Hz, H-7a), 3.25 (1H, dd, *J* = 9.6, 16.2 Hz, H-7b), 3.53 (1H, dd, *J* = 6.0, 10.2 Hz, H-10a), 3.27 (1H, dd, *J* = 5.4, 10.2 Hz, H-10b); an oxymethine sp^3 proton at δ_H 4.84 (1H, dd, *J* = 8.4, 9.6 Hz, H-8), a methyl group at δ_H 1.04 (3H, s, H-11) and a methoxy group at 3.79 (3H, s, 12-*O*-CH_3).

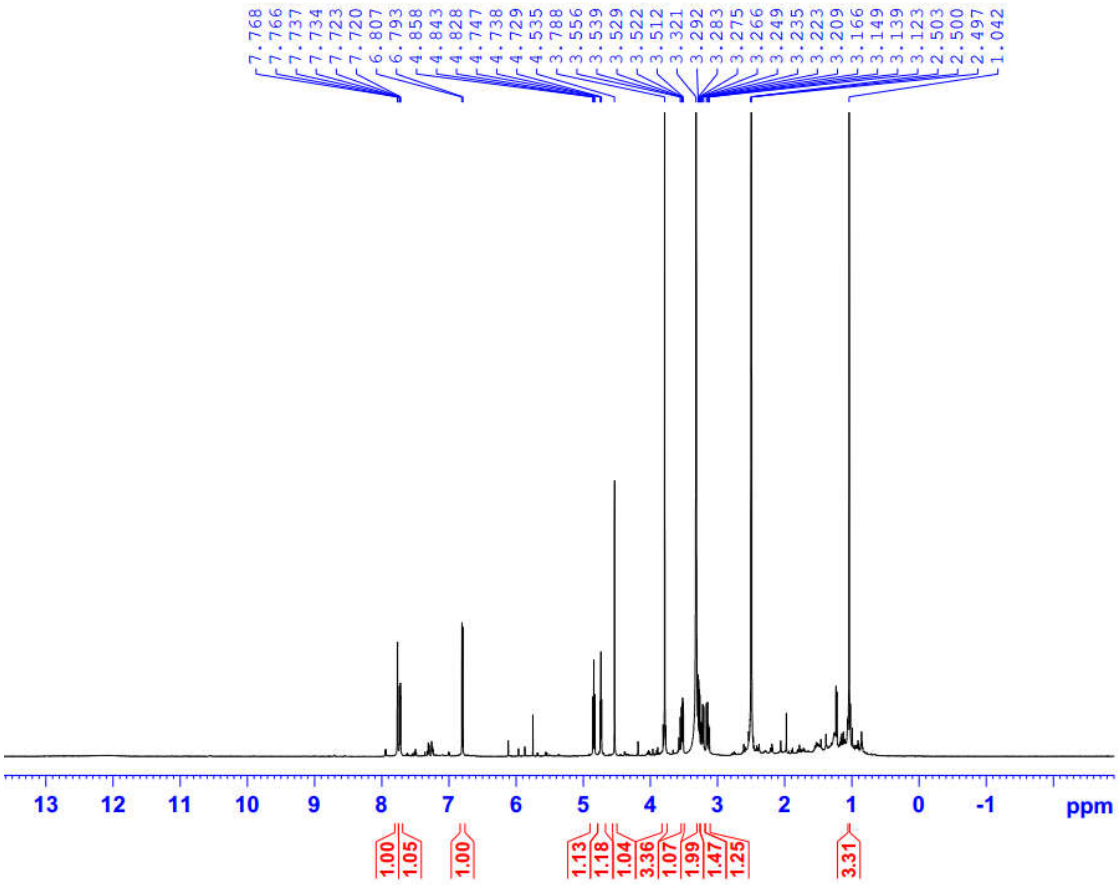

Figure 4.4. ^{1}H NMR spectrum of Pt1

^{13}C and HSQC spectra of the compound (Figure 4.5, Figure 4.6) exhibited signals of one methyl (δ_C 20.7, C-11), one methoxy (δ_C 51.7, 12-*O*-CH_3), one conjugated carbonyl (δ_C 166.0, C-12), two quaternary sp^2 [δ_C 128.6 (C-1), 121.3 (C-5)], three methines sp^2 [δ_C 130.2 (C-4), 126.0 (C-6), 108.5 (C-3)], one oxy-quaternary sp^2 (δ_C 164.0, C-2), one methylene sp^3 (δ_C 28.6, C-7), and one oxymethine sp^3 (δ_C 86.7, C-8). The HMBC spectrum showed the correlations of aromatic protons and carbons, such as H-3 (δ_H 6.79) with C-1 (δ_C 128.6), C-5 (δ_C 121.3), H-4 (δ_H 7.73) with C-2 (δ_C 164.0), C-6 (δ_C 126.0), H-6 (δ_H 7.77) with C-2 (δ_C 164.0), and C-4 (δ_C 130.2). The position of the furan ring was determined by the HMBC correlations of H-7 (δ_H 3.14 and 3.25) and H-8 (δ_H 4.84) with C-1 (δ_C 128.6) and C-2 (δ_C 164.0), and H-7 (δ_H 3.14 and 3.25) with C-6 (δ_C 126.0). The position of the dihydroxy isopropyl group was identified by the HMBC correlations of H-10 (δ_H 3.27 and 3.53) and H-11 (δ_H 1.04) with C-8 (δ_C 86.7). NMR spectra of compound **Pt1** were highly similar to those of gasphostrin D, a reported benzofuran derivative [54] (Table 4.1). However, compound **Pt1** exhibited one more methoxy group than the reported compound,

and the HMBC correlation between methoxy protons (δ_H 3.79) and C-12 (δ_C 166.0) might reveal the methylation of the carboxyl group (Figure 4.7).

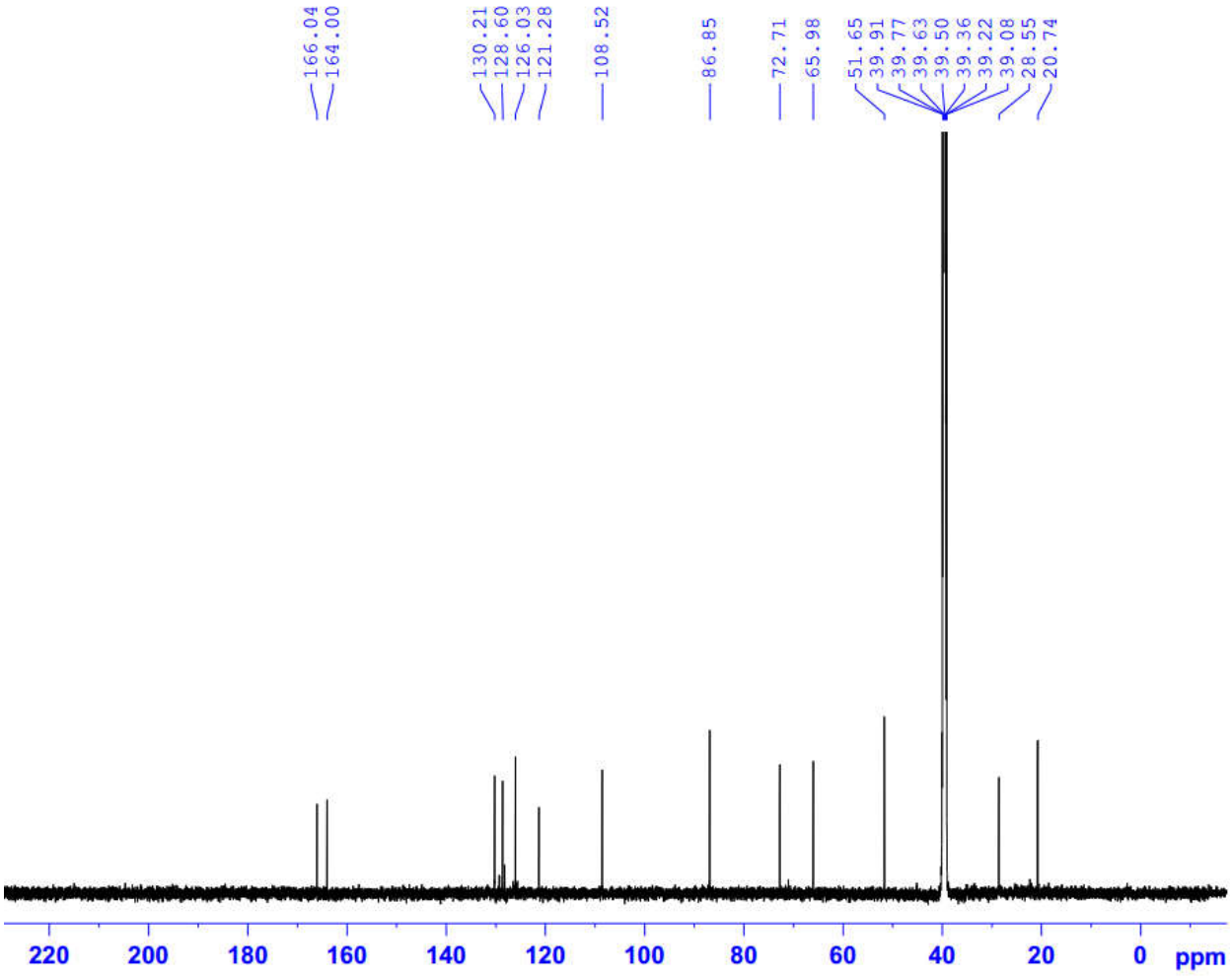

Figure 4.5. ^{13}C NMR spectrum of Pt1

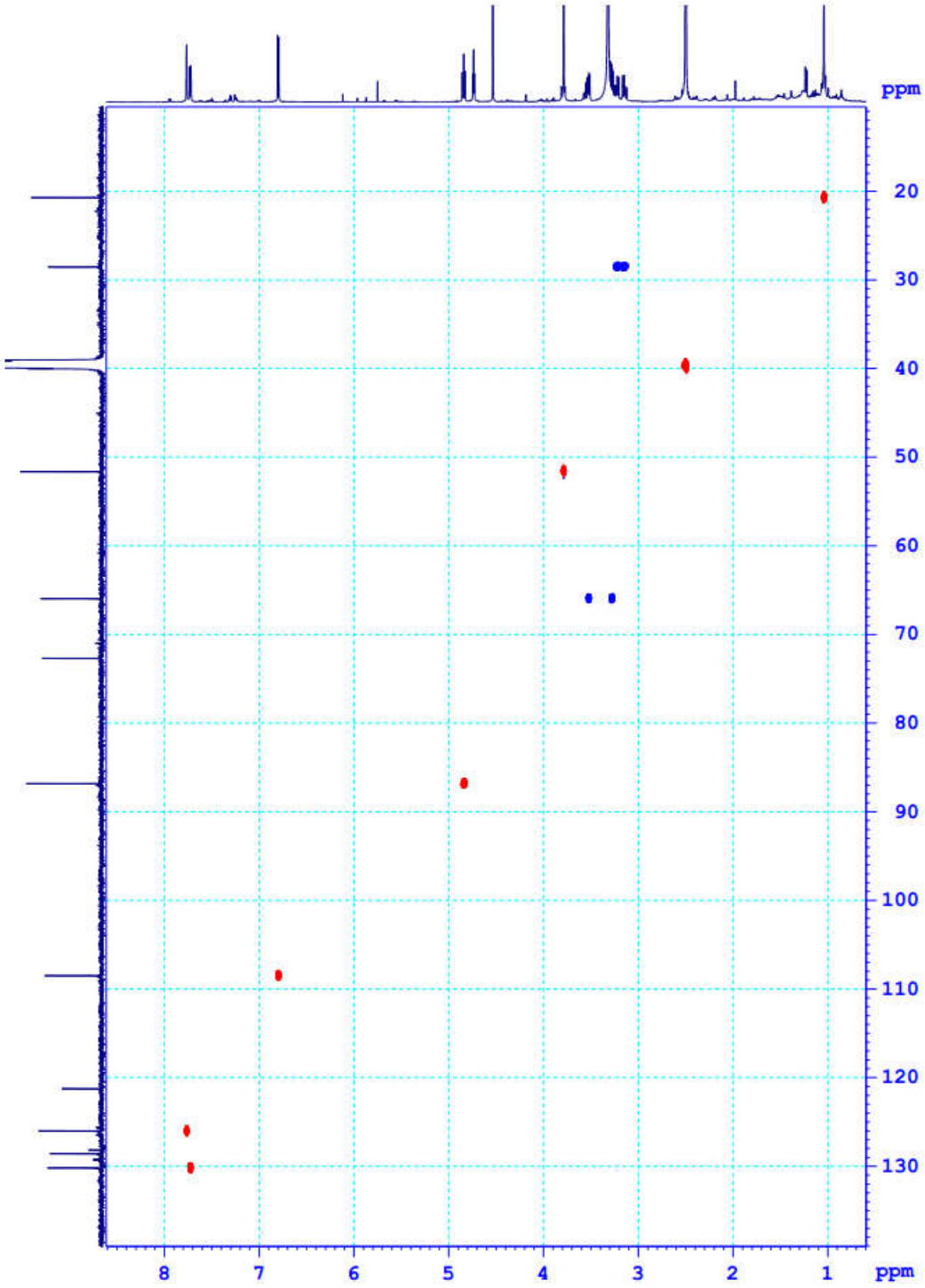

Figure 4.6. HSQC spectrum of Pt1

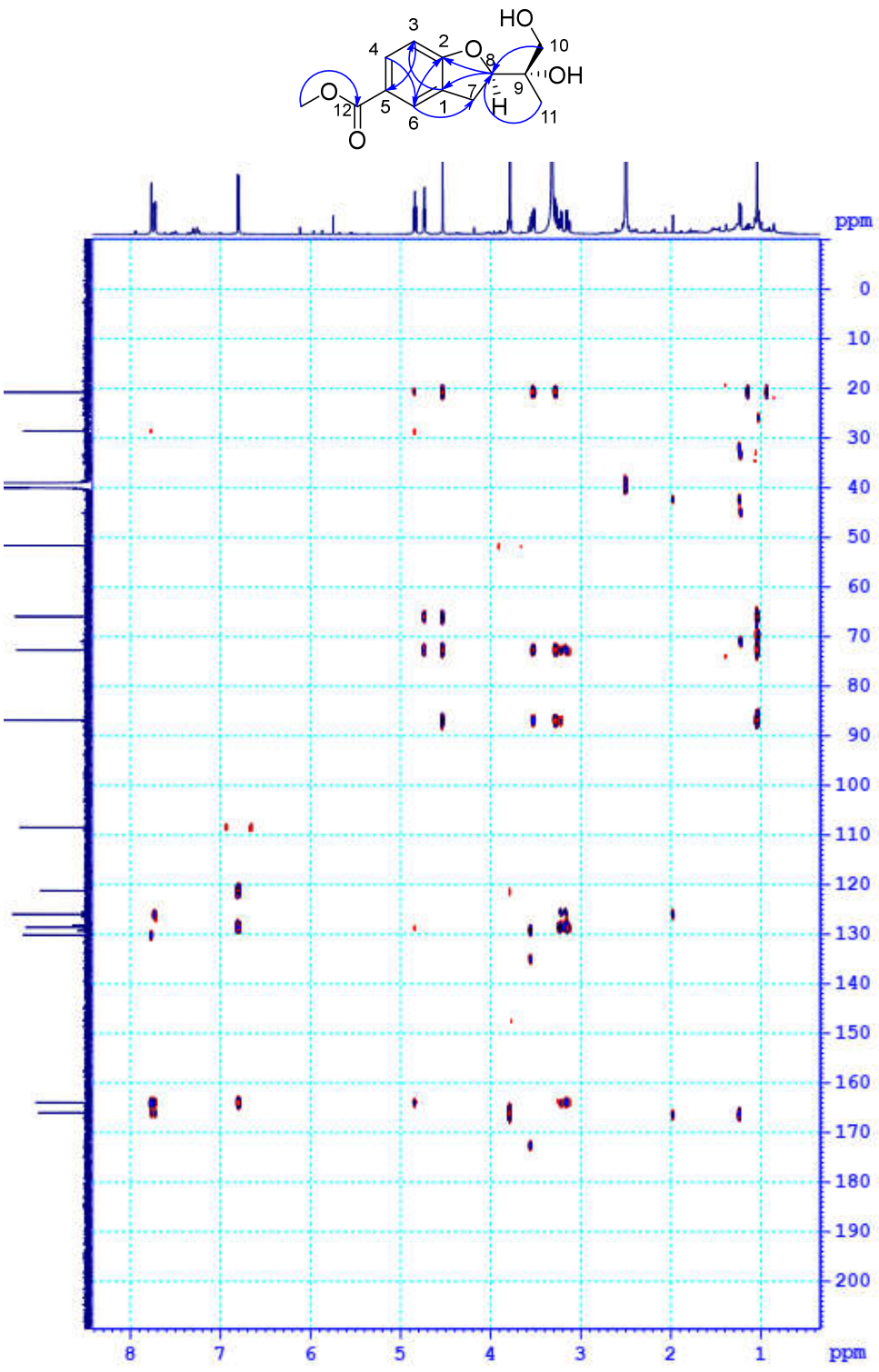

Figure 4.7. HMBC spectrum and key HMBC correlations of Pt1

Table 4.1. ^{1}H NMR and ^{13}C NMR data of Pt1 and gasphostrin D in DMSO-d_6

No.	Pt1 (DMSO-d_6)			Gasphostrin D (DMSO-d_6)	
	^{13}C (150 MHz)		^{1}H (600 MHz)	^{13}C (300 MHz)	^{1}H (75 MHz)
1	128.6	C		128.4	
2	164.0	C		163.6	
3	108.5	CH	6.79 (1H, d, *J* = 8.4 Hz)	108.4	6.79 (1H, d, *J* = 8.3 Hz)
4	130.2	CH	7.73(1H, dd, *J* = 8.4, 1.8 Hz)	130.8	7.83 (1H, dd, *J* = 8.3; 1.8 Hz)
5	121.2	C		122.6	
6	126.0	CH	7.77 (1H, d, *J* = 1.8 Hz)	126.4	7.76 (1H, d, *J* = 1.8 Hz)
7	28.6	CH_2	3.14 (1H, dd, *J* = 8.4, 16.2 Hz)	28.7	3.19, m
7			3.25 (1H, dd, *J* = 9.6, 16.2 Hz)		
8	86.7	CH	4.84 (1H, dd, *J* = 8.4, 9.6 Hz)	86.5	4.83 (1H, dd, *J* = 9.7; 8.1 Hz)
9	72.7	C		72.5	
10	66.0	CH_2	3.53 (1H, dd, *J* = 6.0, 10.2 Hz)	66.7	3.33, m
			3.27 (1H, dd, *J* = 5.4, 10.2 Hz)		
11	20.7	CH_3	1.04 (3H, s)	20.0	1.09, s
12	166.0	C		167.2	
12-*O*-Me	51.7	CH_3	3.79 (3H, s)		

The absolute configuration of C-8 of compound **Pt1** was determined by comparison of the experimental ECD spectrum to the referenced spectra [54]. The experimental ECD spectrum of compound **Pt1** (Figure 4.8) showed opposite trends of Cotton effects to gasphostrin D (8*S*, 9*R*) and was well-matched with the calculated ECD spectrum of the 8*R*, 9*R* derivative of this compound [54]. Thus, the absolute configuration of C-8 was determined as R.

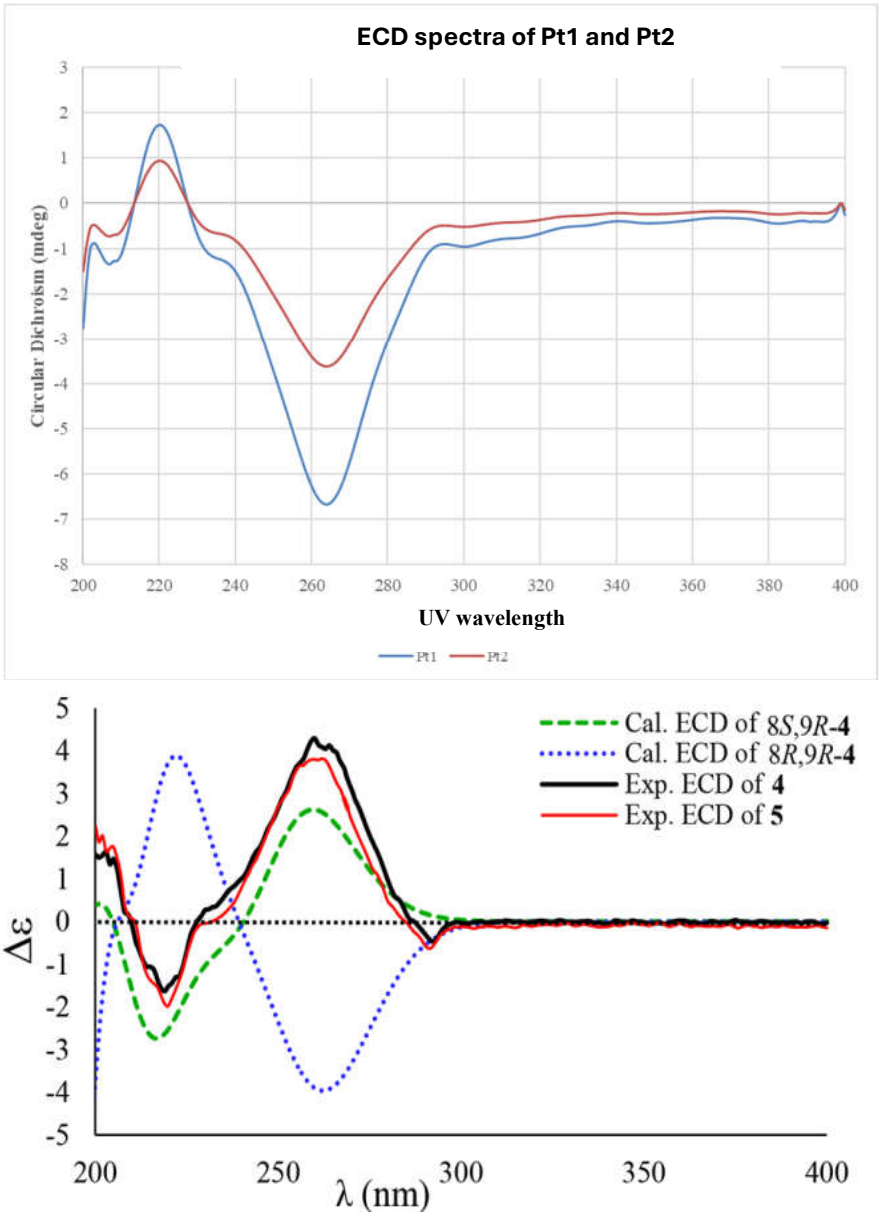

Figure 4.8. Experimental ECD spectra of Pt1 and Pt2; (b) experimental and theoretically calculated ECD spectra of 8S,9R- gasphostrin D and 8R,9R- gasphostrin D (compound 4) from the reference [54]

Besides, Snatzke's method was applied to elucidate the absolute configuration of C-9. The induced negative Cotton effect at 324 nm revealed an S configuration of C-9 (Figure 4.9).

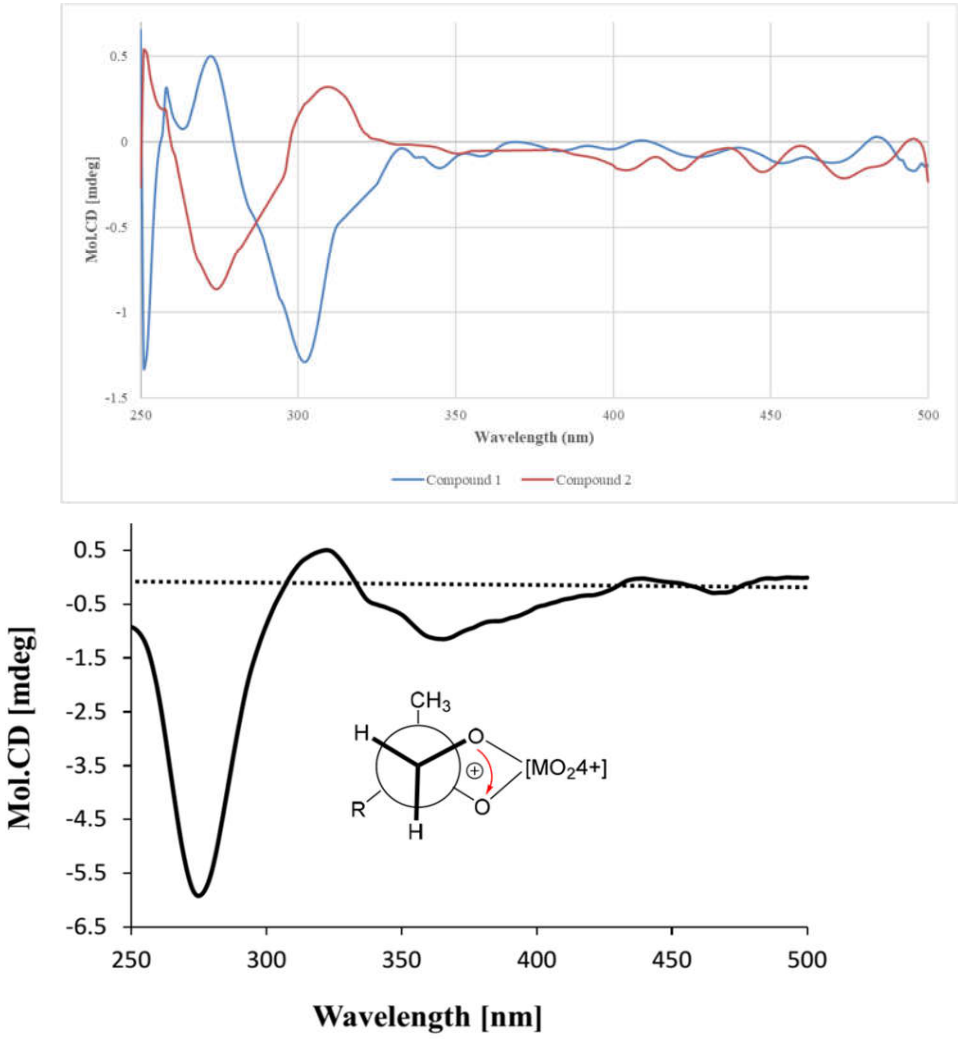

Figure 4.9. ICD spectra of the $Mo_2(OAc)_4$ complex of (a) Pt1 and Pt2 and (b) 8S,9R-gasphostrin D in DMSO from the reference [54]

Moreover, the negative optical rotation of the compound **Pt1** ($[\alpha]_D^{25}$ -32.2) was opposed to gasphostrin D ($[\alpha]_D^{25}$ +78.9) and matched to several similar 2*R*-benzofuran derivatives [55]. Significant chemical shift difference between H-10a [δ_H 3.53 (1H, dd, *J* = 5.0, 8.5 Hz)] and H-10b [δ_H 3.27 (1H, dd, *J* = 5.0, 8.5 Hz)] was in good agreement with those of (8*S*, 9*S*)-dihydrofurocoumarin and (8*S*, 9*S*)-diacetatefurocoumarin, meanwhile, the 9*R*-derivatives showed a smaller difference between chemical shifts of these two protons [56]. These indicated *S*-configuration of C-9 of compound **Pt1**.

Thus, the compound was assigned as methyl (*R*)-8-((*S*)-9,10-dihydroxypropan-8-yl)-7,8-dihydrobenzofuran-5-carboxylate, a new compound, and named Pandanusfuran A.

*4.4.2. Compound Pt2: (8R, 9R)-9,10-dihydroxypropan-8-yl)-7,8-dihydrobenzofuran-5-carboxylate (***Pandanusfuran *B)***

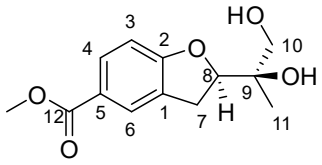

Figure 4.10. The structure of Pt2

Compound **Pt2** was isolated as a white amorphous powder. The molecular formula of compound **Pt2** was determined as $C_{13}H_{16}O_5$ by the HRESIMS (Figure 4.11) at m/z 287.0697 $[M+Cl]^-$.

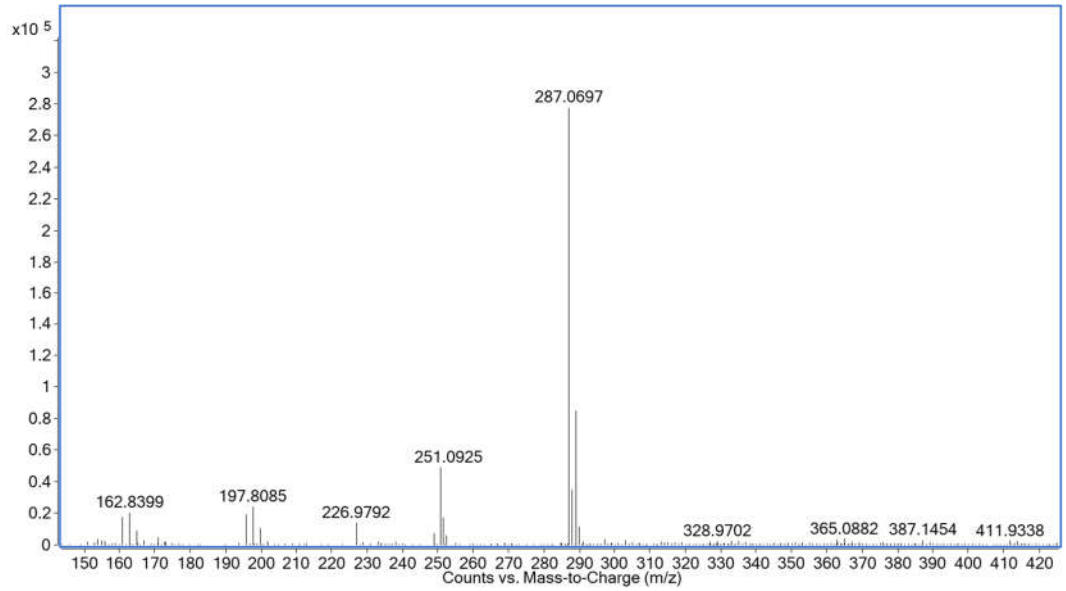

Figure 4.11. HR-ESI-MS spectrum of Pt2

^{1}H NMR spectrum of compound **Pt2** (Figure 4.12) showed the signals of three aromatic protons of an ABX system [6.81 (1H, d, J = 8.4 Hz, H-3), 7.73(1H, dd, J = 8.4, 1.8 Hz, H-4), 7.78 (1H, d, J = 1.8 Hz, H-6)]; two pairs of methylene protons at δ_H 3.13 (1H, dd, J = 9.6, 16.2 Hz, H-7a), 3.26 (1H, dd, J = 8.4, 16.2 Hz, H-7b), and 3.32 (2H, overlap, H-10); an oxymethine sp^3 proton at δ_H 4.83 (1H, dd, J= 9.6, 8.4 Hz, H-8), a methyl group at δ_H 1.04 (3H, s, H-11) and a methoxy group at 3.79 (3H, s, 12-*O*-CH_3).

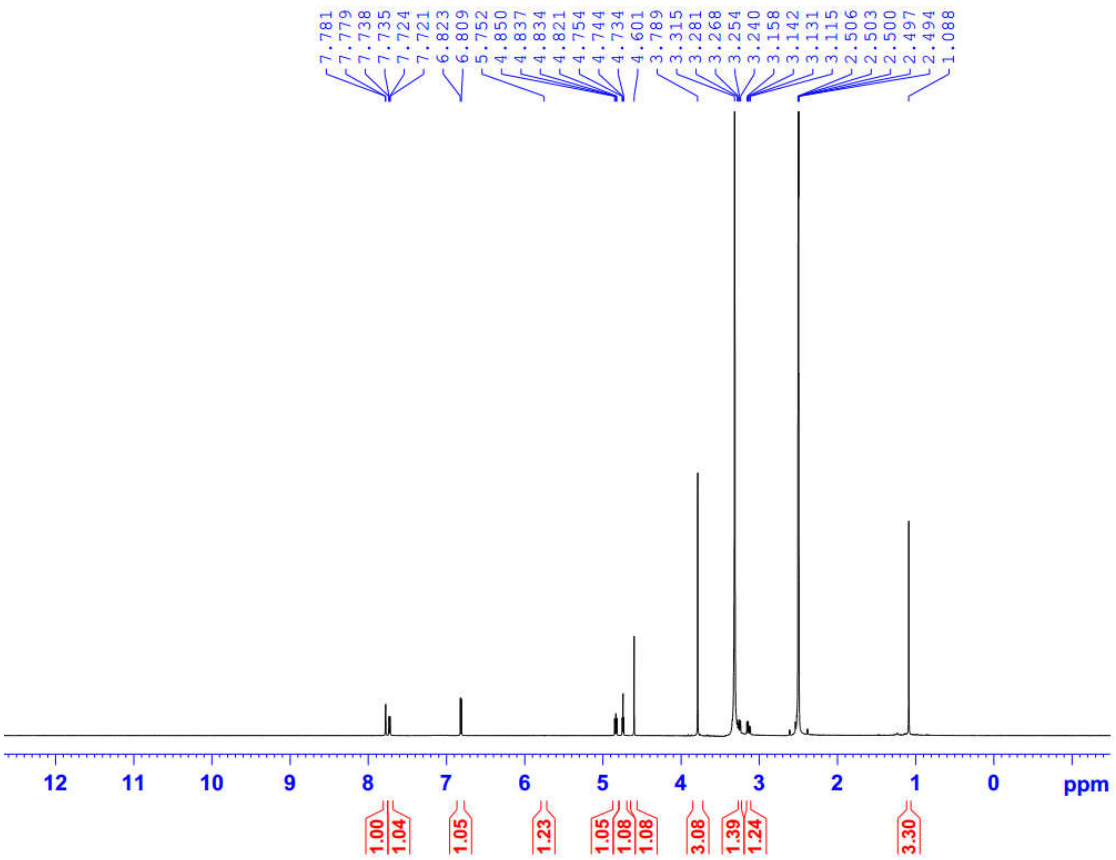

Figure 4.12. ^{1}H NMR spectrum of Pt2

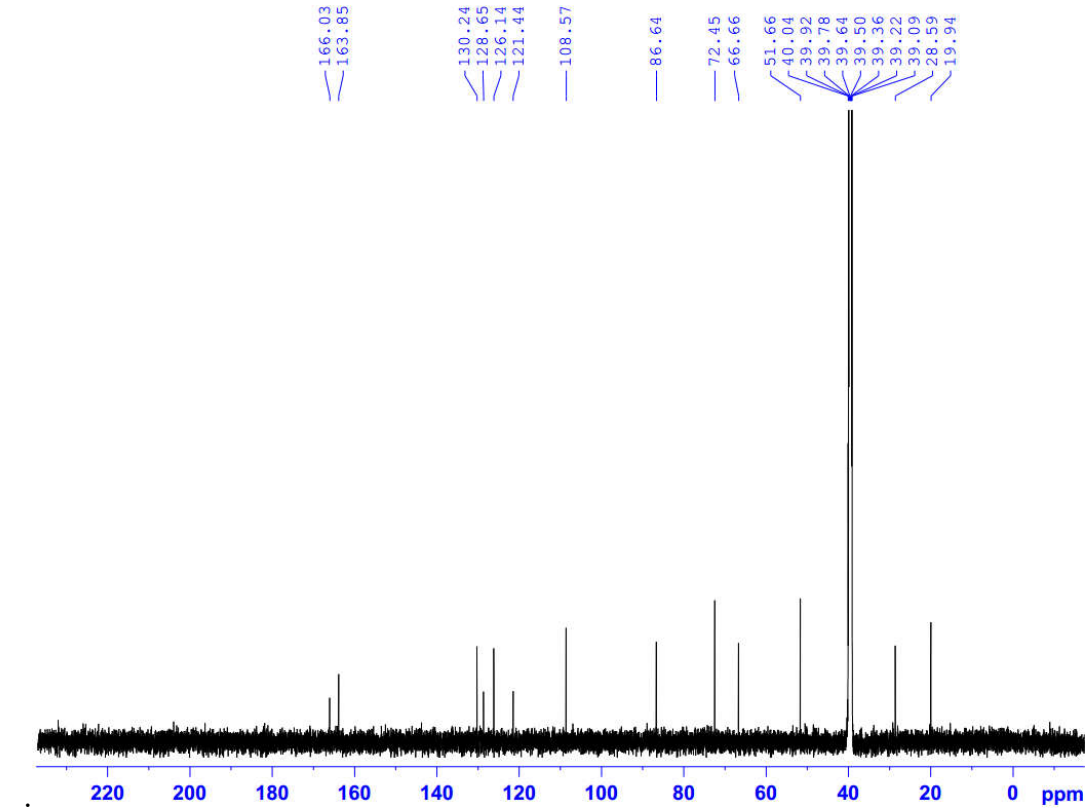

Figure 4.13. ^{13}C NMR spectrum of Pt2

^{13}C and HSQC spectra of the compound (Figure 4.13 & Figure 4.14) exhibited signals of one methyl (δ_C 19.9, C-11), one methoxy (δ_C 51.7, 12-*O*-CH_3), one conjugated carbonyl (δ_C 166.0, C-12), two quaternary sp^2 [δ_C 128.7 (C-1), 121.4 (C-5)], three methines sp^2 [δ_C 130.2 (C-4), 126.1 (C-6), 108.6 (C-3)], one oxy-quaternary sp^2 (δ_C 163.9, C-2), one methylene sp^3 (δ_C 28.6, C-7), and one oxymethine sp^3 (δ_C 86.6, C-8).

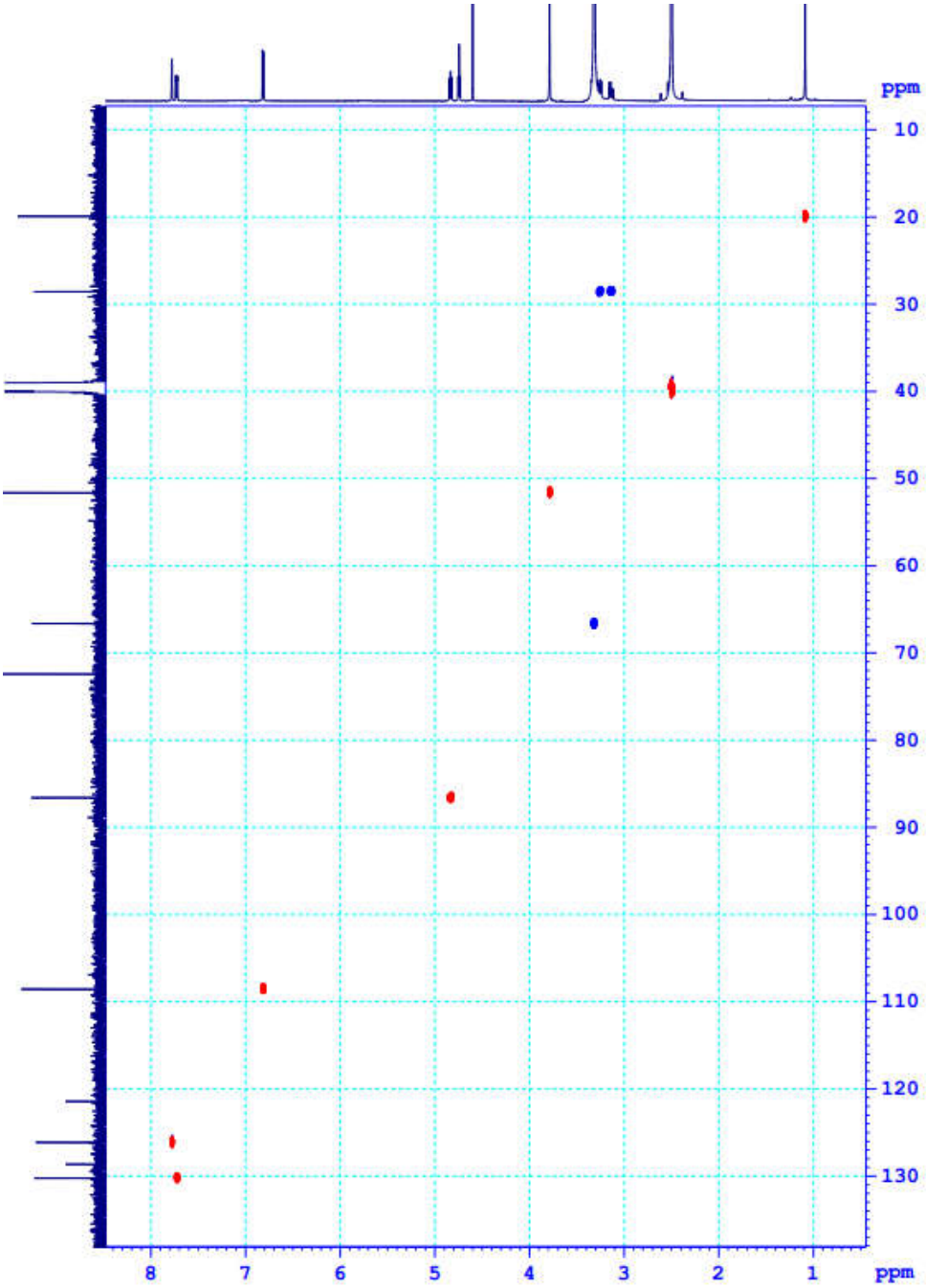

Figure 4.14. HSQC spectrum of Pt2

The HMBC spectrum (Figure 4.15) showed the correlations of H-3 (δ_H 6.81) with C-1 (δ_C 128.7), C-5 (δ_C 121.4), H-4 (δ_H 7.73) with C-2 (δ_C 163.9), C-6 (δ_C 126.1), H-6 (δ_H 7.78) with C-2 (δ_C 163.9), and C-4 (δ_C 130.2). The position of the furan ring was determined by the HMBC correlations of H-7 (δ_H 3.13 and 3.26) and H-8 (δ_H 4.83) with C-1 (δ_C 128.7) and C-2 (δ_C 163.9), and H-7 (δ_H 3.13 and 3.26) with C-6 (δ_C 126.1). The dihydroxy isopropyl group was identified by the HMBC correlations of H-10 (δ_H 3.32) and H-11 (δ_H 1.04) with C-8 (δ_C 86.6). The NMR spectra of compound **Pt2** resembled those of compound **Pt1** (Table 4.2), indicating their same planar structures.

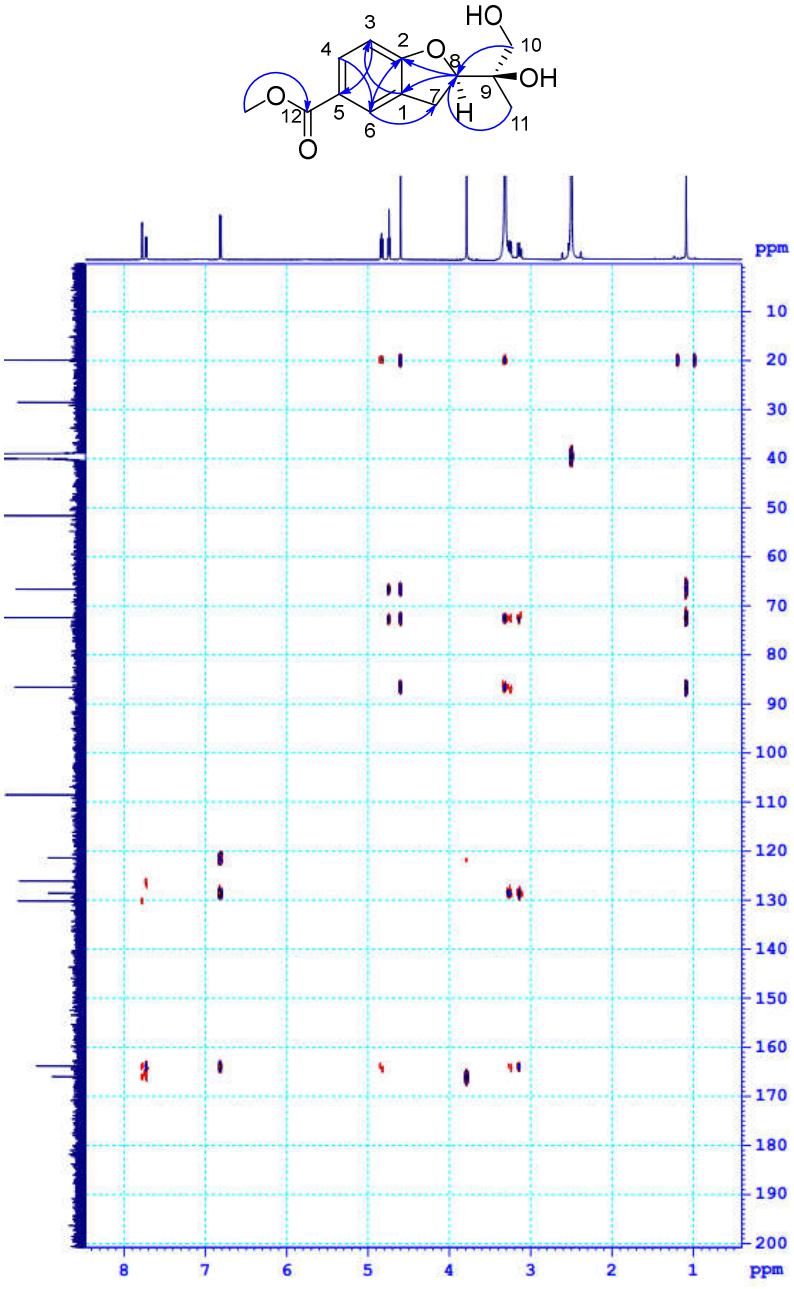

Figure 4.15. HMBC spectrum of Pt2

Significantly, compound **Pt2** displayed similar optical rotation ($[\alpha]_D^{25}$ -41.5) and ECD curves to compound **Pt1** revealed an R configuration of C-8 (Figure 4.8). Besides, Snatzke' s method was applied to elucidate the absolute configuration of C-9. The induced positive cotton effect at 324 nm reflecting the O−C−C−O torsion angle was consistent with positive helicity, which revealed an R configuration of C-9. Moreover, the overlap of H-10a and H-10b as opposed to the significant splitting in compound **Pt1,** and highly similar to the small differences of those protons in several reported 9*R*-benzofuran derivatives, such as gasphostrin D [54] or (8*S*, 9*R*)-dihydrofurocoumarin and (8*S*, 9*R*)-diacetatefurocoumarin [56]. These might reveal the R configuration of C-9. Thus, compound **Pt2** was identified as methyl (*R*)-8-((*R*)-9,10-dihydroxypropan-8-yl)-7,8-dihydrobenzofuran-5-carboxylate. Compound **Pt2** is also new and named Pandanusfuran B.

Table 4.2. ^{1}H NMR and ^{13}C NMR data of compounds Pt1 and Pt2 in DMSO-d_6

No.	Pt1 (DMSO-d_6)			Pt2 (DMSO-d_6)	
	^{13}C (150 MHz)		^{1}H (600 MHz)	^{13}C (150 MHz)	^{1}H (600 MHz)
1	128.6	C		128.4	
2	164.0	C		163.6	
3	108.5	CH	6.79 (1H, d, *J* = 8.4 Hz)	108.4	6.81 (1H, d, *J* = 8.4 Hz)
4	130.2	CH	7.73(1H, dd, *J* = 8.4, 1.8 Hz)	130.8	7.73 (1H, dd, *J* = 8.4; 1.8 Hz)
5	121.2	C		122.6	
6	126.0	CH	7.77 (1H, d, *J* = 1.8 Hz)	126.4	7.78 (1H, d, *J* = 1.8 Hz)
7	28.6	CH_2	3.14 (1H, dd, *J* = 8.4, 16.2 Hz) 3.25 (1H, dd, *J* = 9.6, 16.2 Hz)	28.7	3.19, m
8	86.7	CH	4.84 (1H, dd, *J* = 8.4, 9.6 Hz)	86.5	4.83 (1H, dd, *J* = 9.6; 8.4 Hz)
9	72.7	C		72.5	
10	66.0	CH_2	3.53 (1H, dd, *J* = 6.0, 10.2 Hz) 3.27 (1H, dd, *J* = 5.4, 10.2 Hz)	66.7	3.33, m
11	20.7	CH_3	1.04 (3H, s)	20	1.09, s
12	166.0	C		167.2	
12-*O*-Me	51.7	CH_3	3.79 (3H, s)	51.7	3.79 (3H, s)

To check if these compounds might be artefacts of the extracting process in methanol, we performed an HPLC-DAD analysis on the ethanol extract of the plant material (1 g of the *P. tectorius* leaves were extracted in 25 mL of ethanol 90%, in triplicated, then combined the solution and evaporated the solvent to gain the ethanol extract). We compared it to the chromatograms of isolated compounds under the same analysis parameter. As shown, compounds **Pt1** and **(2)** could be found in the ethanol extract (Figure 4.16), thus, they were natural products.

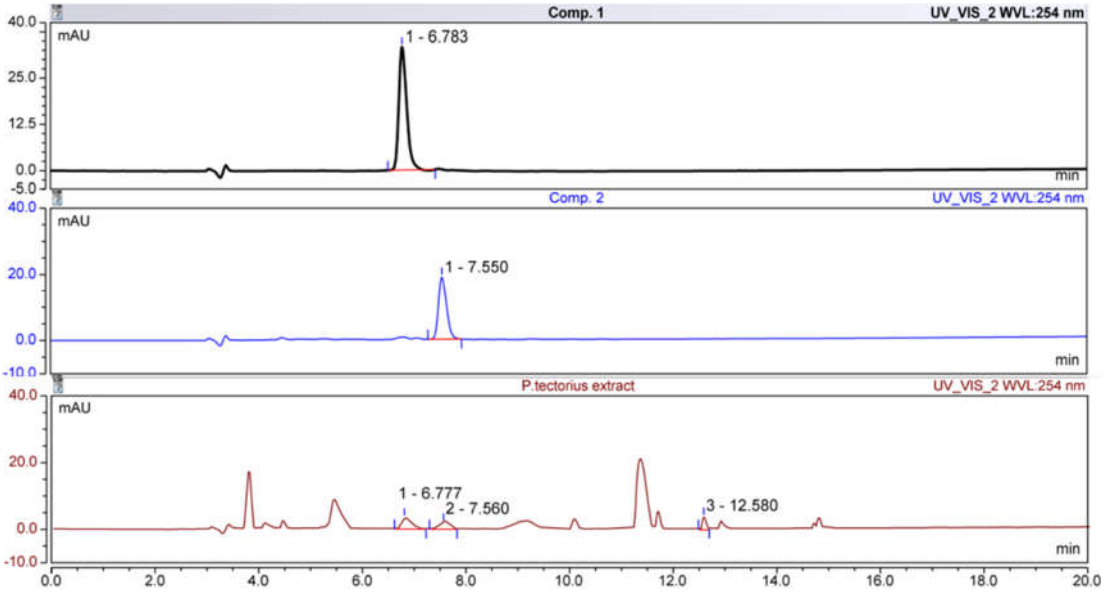

Figure 4.16. HPLC-DAD chromatogram at UV 254 nm for checking artifacts.

The upper graphs exhibit the chromatogram of the mixture of compound **Pt1** (rt 6.8 min) and compound **Pt2** (rt 7.6 min). The lower graph shows the chromatogram of *Pandanus tectorius* aerial parts ethanol extract, which is analyzed under the same condition.

4.4.3. Compound Pt3: Pinoresinol

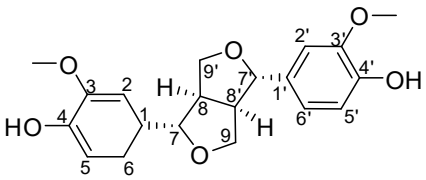

Figure 4.17. The structure of pinoresinol (Pt3)

Compound **Pt3** was obtained as a light yellow oil. The ^{1}H-NMR spectrum of **Pt3** exhibited signals of an ABX system due to three protons δ_H 6.90 (2H, d, J = 2.4 Hz, H-2, 2'), 6.83 (2H, dd, J = 8.4; 2.4 Hz, H-6, 6'), and 6.88 (2H, d, J = 8.4 Hz, H-5, 5'), an oxymethine group δ_H 4.74 (2H, d, J =4.2 Hz, H-7, 7'). Additionally, the spectrum

showed two oxymethylene signals δ_H 3.89 (2H, dd, J = 9.0; 4.2 Hz, H-9, 9') and 4.26 (2H, dd, J = 9.0; 6.6 Hz, H-9, 9'), a methine group δ_H 3.11 (2H, m, H-8, 8′), and two methoxy groups at δ_H 3.91 (3H, s) and 3.90 (3H, s). Besides, the ^{13}C-NMR and DEPT spectrum showed ten carbons, including three aromatic -CH groups δ_C 108.6 (C-2, 2′), 114.3 (C-5, 5′), 119.2 (C-6, 6′); three non-protonated carbons 133.2 (C-1, 1′), two aromatic rings directly associated with oxygen δ_C 145.3 (C-3) and 147.0 (C-4), and two methoxy groups at δ_C 56.1 Two methine signals δ_C 54.4 (C-8, 8′), an oxymethine group at δ_C 85.8 (C-7, 7′), and an oxymethylene group δ_C 71.2 (C-9, C-9′) suggested a structure of a furofuran derivative.

In addition, the molecular weight of **Pt3** was determined as 358 Da corresponding with the formula $C_{20}H_{22}O_6$ based on the ions at *m/z* 359 $[M+H]^+$, *m/z* 739 $[2M+Na]^+$, *m/z* 341 $[M-H_2O+H]^+$on the ESI-MS spectrum. The number of carbon and hydrogen in the predicted formula was twice as much as the number shown in the spectrum of **Pt3**, hence it is possibly indicated that this compound has an axially symmetric benzofuran structure, and the signals in the NMR spectrum were double shortened. The spectral data of **Pt3** resembled the data of pinoresinol in previous publications [57] so it can be identified as pinoresinol.

Table 4.3. NMR data of Pt3 and those of pinoresinol from the reference

No.	Pt3 ($CDCl_3$)			Pinoresinol ($CDCl_3$)
	^{13}C (150 MHz), δ_C		^{1}H (600 MHz), δ_H	^{13}C (125 MHz), δ_C
1, 1'	133.2	C	–	132.8
2, 2'	108.6	CH	6.90 (2H, d, J = 2.4 Hz)	108.5
3, 3'	147.0	C	–	146.7
4, 4'	145.3	C	–	145.2
5, 5'	114.3	CH	6.88 (2H, d, J = 8.4 Hz)	114.2
6, 6'	119.2	CH	6.83 (2H, dd, J = 8.4; 2.4 Hz)	118.9
7, 7'	85.8	CH	4.74 (2H, d, J = 4.2 Hz)	85.8
8, 8'	54.4	CH	3.11 (2H, m)	55.4
9, 9'	71.2	CH_2	3.89 (2H, dd, J = 9.0; 4.2 Hz); 4.26 (2H, dd, J = 9.0; 6.6 Hz)	71.6
3-OMe	56.1	CH_3	3.91 (3H, s)	55.9
3'-OMe	56.1	CH_3	3.90 (3H, s)	55.9

4.4.4. Compound Pt4: Pinoresinol monomethyl ether

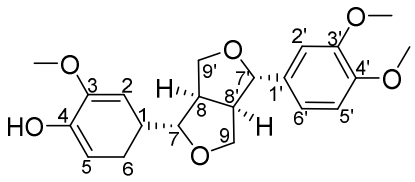

Figure 4.18. The structure of pinoresinol monomethyl ether (Pt4)

Compound **Pt4** was isolated as a yellowish-brown oil. Six proton signals in the ^{1}H-NMR spectrum δ_H 6.91 (1H, d, J = 2.4 Hz, H-2), 6.90 (1H, d, J= 2.4 Hz, H-2'), 6.90 (1H, d, J = 9.0 Hz, H-5), 6.84 (1H, d, J=9.0 Hz, H-5′), 6.87 (1H, dd, J = 9.0; 2.4 Hz, H-6′) and 6.84 (1H, dd, J = 9.0; 2.4 Hz, H-6) suggested two ABX system. Additionally, the ^{1}H-NMR spectrum showed an oxymethine group δ_H 4.76 (2H, d, J = 4.8 Hz, H-7, 7′); two oxymethylene groups δ_H 4.27 (4H, m, H-9,9'); two methine groups δ_H 3.12 (2H, m, H-8, 8′); and three methoxy groups at δ_H 3.91 (3H, s), 3.90 (3H, s), and 3.89 (3H, s).

Besides, twenty-one carbon signals including six aromatic carbons δ_C 108.6 (C-2), 109.2 (C-2′), 114.2 (C-5), 111.3(C-5′), 119.1 (C-6), 118.3 (C-6′); six non-protonated aromatic carbons δ_C 132.7 (C-1), 133.4 (C-1′); four aromatic carbons directly bonding with oxygen δ_C 148.7 (C-3), 149.6 (C-3′), 145.5 (C-4) and 146.6 (C-4′); and three methoxy groups at δ_C 56.0 were observed in the ^{13}C-NMR and DEPT spectrum. Two methine groups δ_C 54.2 (C-8, 8′), two oxymethine groups δ_C 86.0 and 85.7 (C-7, 7′), two oxymethylene groups δ_C 71.7 (C-9, C-9′) allowed the identification of two benzofuran rings.

The molecular weight of **Pt4** was 372 Da suggesting the formula was $C_{21}H_{24}O_6$ as determined from the ESI-MS spectrum at *m/z* 373 $[M+H]^+$, and *m/z* 395 $[M+Na]^+$.

It can be seen that half of the number of NMR and MS data of **Pt4** were similar to those of **Pt3**, except for an additional methoxy group. On the basis of spectral analysis and comparison with the literature [58] the structure of **Pt4** was determined to be pinoresinol monomethyl ether.

Table 4.4.Comparison of NMR data of Pt4 and pinoresinol monomethyl ether

No.	**Pt4 ($CDCl_3$)**			**Pinoresinol monomethyl ether ($CDCl_3$)**
	^{13}C (150 MHz), δ_C		**^{1}H (600 MHz) , δ_H**	**^{13}C (125 MHz) , δ_C**
1	132.7	C	–	132.9
2	108.6	CH	6.91 (1H, d, J = 2.4 Hz)	108.6
3	148.7	C	–	148.6
4	145.5	C	–	145.2
5	114.2	CH	6.90 (1H, d, J = 9.0 Hz)	114.2
6	119.1	CH	6.84 (1H, dd, J = 9.0; 2.4 Hz)	119.0

7	86.0	CH	4.76 (1H, d, *J* = 4.8 Hz)	85.8
8	54.5	CH	3.12 (1H, m)	54.1
9	71.7	CH_2	4.27 (2H , m)	71.6
1′	133.4	C	–	133.5
2′	109.2	CH	6.90 (1H, d, *J* = 2.4 Hz)	109.2
3′	149.6	C	–	149.2
4′	146.6	C	–	146.7
5′	111.3	CH	6.84 (1H, d, *J* = 9.0 Hz)	111.0
6′	118.3	CH	6.87 (1H, dd, *J* = 9.0; 2.4 Hz)	118.2
7′	85.7	CH	4.76 (1H, d, *J* = 4.8 Hz)	85.9
8′	54.5	CH	3.12 (1H, m)	54.2
9′	71.7	CH_2	4.27 (2H, m)	71.7
3-OCH_3	56.0	CH_3	3.91 (3H, s)	56.0
3′-OCH_3	56.0	CH_3	3.90 (3H, s)	56.0
4′-OCH_3	56.0	CH_3	3.88 (3H, s)	56.0

4.4.5. Compound Pt5: Arctigenin

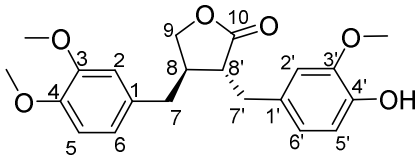

Figure 4.19. The structure of arctigenin (Pt5)

Compound **Pt5** was found as a yellowish-brown oil. The molecular weight was determined as 372 Da based on the ESI-MS spectrum at *m/z* 373 $[M+H]^+$.

Six aromatic protons of two sets of an ABX system δ_H 6.64 (1H, d, *J* = 2.4 Hz, H-2), 6.75 (1H, d, *J* = 9.6 Hz, H-5), 6.55 (1H, d, *J* = 9.6; 2.4 Hz, H-6), and δ_H 6.46 (1H, dd, *J* = 2.4 Hz, H-2′), 6.82 (1H, dd, *J* = 7.8 Hz, H-5′), 6.64 (1H, d, *J* = 7.8; 2.4 Hz, H-6′); two methine groups δ_H 2.55 (1H, m, H-8), 2.50 (1H, m, H-8′); two oxymethylene groups δ_H 4.14 (1H, dd, *J* = 9.0; 7.8 Hz, H-9a), 3.89 (1H, dd, *J* =9.0; 7.8 Hz, H-9b); two methylene groups δ_H 2.91 (2H, m, H-7), 2.94 (1H, dd, *J* = 13.8; 6.0 Hz, H-7′a), 2.90 (1H, dd, *J* = 13.8; 6.0 Hz, H-7′b); and three methoxy groups δ_H 3.81 (3H, s), 3.86 (3H, s), 3.88 (3H, s) were observed in the ^{1}H-NMR spectrum.

In addition, the ^{13}C-NMR and DEPT spectrum showed twenty-one carbon signals including six aromatic carbons δ_C 111.8 (C-2), 111.5 (C-2′), 111.3 (C-5), 114.2 (C-5′), 120.6 (C-6), 122.0 (C-6′); two non-protonated aromatic carbons δ_C 130.4 (C-1), 129.4 (C-1′); four aromatic carbons directly bonding with oxygen δ_C 149.0 (C-3), 146.7 (C-3′), 147.8 (C-4) and 144.5 (C- 4′), which contributed to the presence of two benzene rings in the structure of **Pt5**. Besides, the ^{13}C-NMR and DEPT spectrum showed signals of two methylene groups δ_C 38.1 (C-7), 34.5 (C-7′); three methoxy groups, especially, two methine groups δ_C 46.6 (C-8), 40.9 (C-8′), an oxymethylene group δ_C 71.2 (C-9),

and a carboxyl group δ_C 179.7 (C-10) revealed the presence of a lactone ring. Thus, the structure of compound **Pt5** was identified as arctigenin by comparison of its spectral data with those published [58, 59].

Table 4.5.Comparison of NMR data of Pt5 and arctigenin

Position	Pt5 ($CDCl_3$)			Arctigenin ($CDCl_3$)
	^{13}C (150 MHz), δ_C		^{1}H (600 MHz) , δ_H	^{13}C (125 MHz), δ_C
1	130.4	C	–	130.4
2	111.8	CH	6.64 (1H, d, *J* = 2.4 Hz)	111.9
3	149.0	C	–	149.3
4	147.8	C	–	147.9
5	111.3	CH	6.75 (1H, d, *J* = 9.6 Hz)	111.9
6	120.6	CH	6.55 (1H, d, *J* = 9.6; 2.4 Hz)	120.7
7	38.1	CH_2	2.91 (2H, m)	38.0
8	46.6	CH	2.55 (1H, m)	41.2
9	71.2	CH_2	4.14 (1H, dd, *J* = 9.0; 7.8 Hz); 3.89 (1H, dd, *J* = 9.0; 7.8 Hz)	71.2
10	179.7	C=O	–	178.8
1′	129.4	C	–	133.0
2′	111.5	CH	6.46 (1H, dd, *J* = 2.4 Hz)	111.9
3′	146.7	C	–	149.1
4′	144.5	C	–	145.1
5′	114.2	CH	6.82 (1H, dd, *J* = 7.8 Hz)	113.2
6′	122	CH	6.64 (1H, d, *J* = 7.8; 2.4 Hz)	121.9
7′	34.5	CH_2	2.94 (1H, dd, *J* = 13.8; 6.0 Hz); 2.90 (1H, dd, *J* = 13.8; 6.0 Hz)	34.4
8′	40.9	CH	2.50 (1H, m)	46.4
3-OCH_3	55.9	CH_3	3.81 (3H, s)	56.0
3′-OCH_3	55.8	CH_3	3.86 (3H, s)	56.0
4-OCH_3	55.8	CH_3	3.88 (3H, s)	55.9

4.4.6. Compound Pt6: Matairesinol

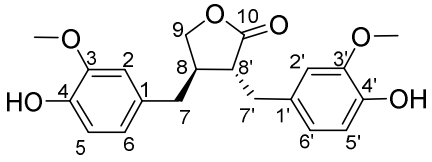

Figure 4.20. The structure of matairesinol (Pt6)

Compound **Pt6** was isolated as a yellow oil. Its molecular weight of 358 Da was assigned based on the ESI-MS spectrum at *m/z* 359 $[M+H]^+$, *m/z* 739 $[M+H]^+$.

The ^{1}H-NMR spectrum showed six protons of two sets of an ABX system δ_H 6.41 (1H, d, *J* = 2.4 Hz, H-2), 6.81 (1H, d, *J* =8.4 Hz, H-5), 6.51 (1H, dd, *J* = 8.4; 2.4 Hz,

H-6) and δ_H 6,61 (1H, dd, J = 2.4 Hz, H-2′), 6.79 (1H, dd, J =8.4 Hz, H-5′), 6.59 (1H, d, J = 8.4; 2.4 Hz, H-6′); two methine groups δ_H 2.48 (1H, m, H-8), 2.56 (1H, m, H-8′); two oxymethylene δ_H 4.16 (1H, dd, J =9.6; 7.8 Hz, H-9a), 3.89 (1H, dd, J = 9.6; 7.8 Hz, H-9b); two methylene groups δ_H 2.60 (2H, m, H-7), 2.95 (1H, dd, J = 13.8; 6.6 Hz, H-7′a) and 2.89 (1H, dd, J = 13.8; 6.6 Hz, H-7′b); and two methoxy groups δ_H 3.80 (3H, s) and 3.81 (3H, s). ^{13}C-NMR and DEPT spectra showed twenty-one carbon signals including six aromatic carbons δ_C 111.0 (C-2), 111.5 (C-2′), 114.4 (C-5), 114.1 (C-5′), 121.3 (C-6), 122.1 (C-6′); two non-protonated aromatic carbons δ_C 129.6 (C-1), 129.5 (C-1′); four aromatic carbons directly attached to oxygen 146.7 (C-3), 146.6 (C-3′), 144.6 (C-4), 144.4 (C-4′), which confirmed the presence of two benzene rings in the structure of **Pt6**. Two methine groups δ_C 41.1 (C-8), 46.6 (C-8′); an oxymethylene group δ_C 71.3 (C-9); and a carboxyl group δ_C 178.8 (C-10) suggested a lactone ring. Besides, two methylene groups δ_C 38.3 (C-7), 34.6 (C-7′), and two methoxy groups were obtained in the ^{13}C-NMR and DEPT spectra.

The spectral data of the **Pt6** compound resembled those of **Pt5** except for the absence of a methoxy group. The structure of compound **Pt6** was identified as matairesinol when compared with those reported in the literature [60].

Table 4.6. Comparison of NMR data of Pt6 and matairesinol

Position	Pt6 ($CDCl_3$)			Matairesinol ($CDCl_3$)
	^{13}C (150 MHz), δ_C		^{1}H (600 MHz) , δ_H	^{13}C (125 MHz), δ_C
1	129.6	C	–	129.7
2	111.0	CH	6.41 (1H, d, J = 2.4 Hz)	111.1
3	146.7	C	–	146.7
4	144.6	C	–	144.6
5	114.4	CH	6.81 (1H, d, J = 8.4 Hz)	114.6
6	121.3	CH	6.51 (1H, dd, J = 8.4; 2.4 Hz)	121.3
7	38.3	CH_2	2.60 (2H, m)	38.2
8	41.1	CH	2.48 (1H, m)	41.0
9	71.3	CH_2	3.89 (1H, dd, J = 9.6; 7.8 Hz); 4.16 (1H, dd, J = 9.6; 7.8 Hz)	71.4
10	178.8	C=O	–	179.1
1′	129.5	C	–	129.4
2′	111.5	CH	6.61 (1H, d, J = 2.4 Hz)	111.6
3′	146.6	C	–	146.6
4′	144.4	C	–	144.4
5′	114.1	CH	6.79 (1H, d, J = 8.4 Hz)	114.3
6′	122.1	CH	6.59 (1H, dd, J = 8.4; 2.4 Hz)	122.0
7′	34.6	CH_2	2.89 (1H, dd, J = 13.8; 6.6 Hz); 2.95 (1H, dd, J = 13.8; 6.6 Hz)	34.6

8′	46.6	CH	2.56 (1H, m)	46.5
3-OCH_3	55.9	CH_3	3.80 (3H, s)	55.7
3′-OCH_3	55.8	CH_3	3.81 (3H, s)	55.8

4.5. Bioactivities of the isolated compounds

The bioactivity evaluation of compounds isolated from the leaves of *P. tectorius* revealed diverse pharmacological potentials across different assays (Table 4.7). With respect to antioxidant activity, the lignans, including pinoresinol, pinoresinol monomethyl ether, arctigenin, and matairesinol, exhibited relatively stronger radical scavenging capacity compared to the newly identified Pandanusfurans. Their IC_{50} values in the DPPH and hydroxyl radical assays ranged between 143.5 – 155.6 µM and 165.7 –181.2 µM, respectively, which are comparable to the positive controls ascorbic acid (DPPH) and catechin (hydroxyl radical). In contrast, Pandanusfurans A and B were markedly less potent, with IC_{50} values exceeding 200 µM in both antioxidant models, suggesting only moderate activity in this category.

In terms of α-amylase inhibition, Pandanusfurans again demonstrated more favorable activity than the lignans. Pandanusfuran A and B inhibited α-amylase with IC_{50} values of 178.4 and 165.7 µM, respectively, approaching the potency of the reference inhibitor acarbose (160.1 µM). By contrast, the lignans showed considerably weaker inhibition, with IC_{50} values above 290 µM, highlighting their limited role in modulating carbohydrate-digesting enzymes.

The cytotoxic evaluation against three human cancer cell lines (A549, K562, and MCF7) indicated selective activity of the Pandanusfurans. Both Pandanusfurans A and B exhibited moderate cytotoxicity against the A549 lung carcinoma line, with IC_{50} values of 34.5 and 37.1 µM, respectively, while showing negligible effects against K562 leukemia and MCF7 breast cancer cells at concentrations up to 50 µM. None of the lignans displayed significant cytotoxicity toward any of the tested cell lines. These results suggest that the cytotoxic potential of compounds is largely restricted to the novel furan derivatives, and even then, only toward specific cancer types.

Regarding anti-inflammatory activity, none of the isolated compounds demonstrated meaningful nitric oxide (NO) inhibitory activity, with IC_{50} values above 50 µM across the board. This stands in contrast to cardamonin, which served as a positive reference and exhibited potent NO inhibition with an IC_{50} of 4.83 µM.

Table 4.7. Bioactivities of the isolated compounds from leaves of Pandanus tectorius

Code	Name	DPPH, IC_{50} (µM)	Hydroxyl, IC_{50} (µM)	α-amylase, IC_{50} (µM)	A549, IC_{50} (µM)	K562, IC_{50} (µM)	MCF7, IC_{50} (µM)	NO inhib., IC50 (µM)
Pt1	Pandanusfuran A	231.0 ± 13.2	201.5 ± 9.7	178.4 ± 12.6	34.5 ± 2.8	>50	>50	>50
Pt2	Pandanusfuran B	220.8 ± 12.2	227.3 ± 6.6	165.7 ± 10.9	37.1 ± 2.8	>50	>50	>50
Pt3	Pinoresinol	150.4 ± 5.2	165.4 ± 5.2	292.6 ± 18.7	>50	>50	>50	>50
Pt4	Pinoresinol monomethyl ether	146.6 ± 7.5	173.6 ± 6.9	310.2 ± 21.4	>50	>50	>50	>50
Pt5	Arctigenin	155.6 ± 9.2	181.2 ± 5.3	328.9 ± 25.1	>50	>50	>50	>50
Pt6	Matairesinol	143.5 ± 4.7	176.1 ± 4.2	305.4 ± 22.8	>50	>50	>50	>50
Control	Ascorbic acid	139.9 ± 12.9						
	Catechin		111.2 ± 5.4					
	Acarbose			160.1±13.5				
	Camptothecin				1.2 ± 0.2	1.9 ± 0.4	1.2 ± 0.1	
	Cardamonin							4.8 ± 0.5

4.6. Discussion

Pandanaceae includes about 750 species distributed in five genera: *Benstonea* Callmander & Buerki*, Freycinetia* Gaudichaud*, Martellidendron* Callmander & Chassot*, Pandanus* Parkinson, and *Sararanga* Hemsley [61]. *Pandanus* was the largest genus in the family, with more than 400 species [61]. Previous phytochemistry investigations on this family mostly focused on the genus *Pandanus,* while only one study on the secondary metabolites of the *Freycinetia* plant [62] and no information about the chemical constituents of the rest of the genera has been reported.

Lignans have been found in some *Pandanus* species, such as *P. tectorius* [7], *P. boninensis* [6]*,* or *P. odoratissimus* [23], but could not be found in *P. amaryllifolius*, *P. dubius*, and *P. utilis*, which alkaloids were the specific compositions [14-16, 19, 20, 22, 63]. In this study, four lignans were isolated from *P. tectorius,* including pinoresinol, pinoresinol monomethyl ether, arctigenin, and matairesinol. While pinoresinol has been discovered in some species as mentioned above, this is the first isolation of pinoresinol monomethyl ether, arctigenin, and matairesinol from a *Pandanus* plant. These findings enrich the chemical diversity of *Pandanus* species and provide evidence for further chemotaxonomic studies. Besides, other studies indicated that *P. tectorius* might contain flavonoids [9] or coumarins [7], but few previous studies reported benzofuran derivatives in this species [24]. Significantly, most of the highly similar compounds with two isolated benzofuran derivatives were isolated from microorganisms rather than from plants [54]. Therefore, the isolation of Pandanusfurans A and B from *P. tectorius* could reveal an interesting biosynthesis pathway in the plant that should be investigated further. In addition, another benzofuran racemate was previously separated from the roots of *P. odoratissimus* [23]. This may reveal a close chemotaxonomic relationship between *P. tectorius* and *P. odoratissimus*.

The compounds isolated from *P. tectorius* leaves displayed distinct biological profiles. The lignans (pinoresinol, pinoresinol monomethyl ether, arctigenin, and matairesinol) exhibited moderate antioxidant activity, but were weak in α-amylase inhibition and inactive in cytotoxicity and NO assays. In contrast, the newly identified Pandanusfurans showed weaker antioxidant effects yet demonstrated α-amylase inhibition close to that of acarbose and selective cytotoxicity against A549 cells, while

remaining inactive against K562 and MCF7. None of the isolated compounds exhibited notable NO inhibition, in contrast to cardamonin. These findings suggest that Pandanusfurans represent promising multifunctional scaffolds with moderate antioxidant, antidiabetic, and selective anticancer potential, whereas the lignans mainly contribute to antioxidant activity.

4.7. Chapter summary

This chapter reports the isolation of two new benzofuran derivatives, Pandanusfuran A (**Pt1**) and Pandanusfuran B (**Pt2**), together with four known lignans (pinoresinol, pinoresinol monomethyl ether, arctigenin, matairesinol) from leaves of *P. tectorius*. Structures were established by HR-ESI-MS and NMR spectra, meanwhile, absolute configurations of the new compounds were assigned by ECD spectra and Snatzke's method ($Mo_2(OAc)_4$-induced ECD). HPLC-DAD of the ethanol extract verified **Pt1** and **Pt2** as native constituents rather than methanolysis artefacts. The lignans showed considerable antioxidant activity, while α-amylase inhibition was stronger for the new benzofurans, which approached the value of acarbose, whereas the lignans were weak inhibitors. New benzofurans also displayed selective cytotoxicity toward A549 with minimal effects on K562/MCF7 and negligible NO inhibition. Overall, these results primarily expand the chemical profile of *Pandanus*; biologically, the new benzofurans show modest *in vitro* activities and should be regarded as preliminary scaffolds for future optimization.

CHAPTER 5. OPTIMIZATION OF THE EXTRACTION CONDITION AND BIOACTIVITIES EVALUATION OF *PANDANUS TECTORIUS* FRUITS EXTRACTS

5.1. Chapter overview

This study aimed to optimize the extraction conditions for phenolic- and saponin-enriched fractions from *Pandanus tectorius* fruits using Response Surface Methodology (RSM) based on a Box–Behnken Design (BBD), followed by an evaluation of their antioxidant and anti-inflammatory activities. Four key variables—ethanol concentration, extraction temperature, solvent-to-material ratio, and extraction time—were assessed through single-factor experiments and RSM optimization. Refined quadratic models for total phenolic content (TPC) and total saponin content (TSC) demonstrated high statistical significance and predictive accuracy. Multi-response optimization yielded seven extraction conditions, each favoring different phytochemical targets. Validation experiments confirmed the model's predictive reliability. Bioactivity assays revealed that phenolic-rich extracts exhibited potent DPPH and hydroxyl radical scavenging effects, while saponin-rich extracts showed stronger inhibition of nitric oxide (NO) production in LPS-stimulated RAW 264.7 macrophages, though high saponin content was associated with cytotoxicity. These findings demonstrate that *P. tectorius* fruit extracts can be tailored for targeted bioactivities through optimized extraction strategies, supporting their potential as natural sources of antioxidant and anti-inflammatory agents.

5.2. Experimental design

5.2.1. Samples

Fruits of *P. tectorius* were collected at Thanh Oai commune, Vietnam, in August 2021 and identified by Dr. Bui Van Thanh, Institute of Biology, Vietnam Academy of Sciences and Technology (VAST). A voucher specimen (NCCG 210213) was deposited at the Centre for High Technology Research and Development, VAST. The collected sample was cleaned, dried at 60°C in the oven, powdered, and preserved at -20 ℃ for further experiments.

5.2.2. Analytical methods

Total phenolic and saponin contents, antioxidant, and NO production inhibitory effects of *P. tectorius* fruit extracts under designed conditions were evaluated using the protocols as shown in Chapter 2.

5.2.3. Preliminary single-factor experiments

Preliminary single-factor experiments were conducted to establish the appropriate ranges for key extraction parameters, including temperature, ethanol concentration, solvent-to-material ratio, and extraction time. First, the influence of ethanol concentration on TPC and TSC was examined by performing extractions with ethanol concentrations ranging from 0% to 96%, at 60°C for 120 minutes, maintaining a constant solvent-to-material ratio of 20 mL/g. Subsequently, the effect of extraction temperature on the total phenolic content (TPC) and total saponin content (TSC) was investigated by extracting the plant material in 60% ethanol at temperatures ranging from 30°C to 100°C for 120 minutes, using a solvent-to-material ratio of 20 mL/g. Next, the effect of varying the solvent-to-material ratio was assessed by extracting the material in 60% ethanol at 60°C for 120 minutes, using ratios ranging from 5 to 50 mL/g. Finally, the impact of extraction time was evaluated by extracting the plant material in 60% ethanol at 60°C with a fixed solvent-to-material ratio of 20 mL/g for durations ranging from 60 to 360 minutes.

5.2.4. Box-Behnken Design for the Response Surface Method

To optimize the extraction conditions for phenolic enrichment from *Pandanus tectorius* fruits, response surface methodology (RSM) based on the Box–Behnken Design (BBD) was employed. The experimental design was carried out using Design-Expert software version 12.0 (Stat-Ease, Inc., Minneapolis, USA). Four independent variables were selected: extraction temperature (°C, A), ethanol concentration (%, B), solvent-to-material ratio (mL/g, C), and extraction time (minutes, D). The total phenolic content (TPC) and total saponin content (TSC) were designated as the response variables.

Based on the results of preliminary single-factor experiments, the solvent system included ethanol concentrations of 0% (distilled water), 45%, and 90%. The temperature range tested was 30–80 °C, the solvent-to-material ratios ranged from 10 to 50 mL/g, and the extraction times varied between 60 and 240 minutes. All experimental runs were

performed in triplicate, and the average value of TPC was used for subsequent statistical analysis. The coded levels of the independent variables used in the experimental design are presented in Table 5.1.

Table 5.1. Coded and actual levels of independent variables used in the Box–Behnken design

Variables	Unit	Code levels		
		-1	**0**	**1**
Temperature (A)	°C	30	55	80
Ethanol concentration (B)	%	0	45	90
Volume-to-weight ratio (C)	mL/g	10	30	50
Extraction time (D)	minutes	60	150	240

5.3. Optimization of the extraction of *Pandanus tectorius* fruits

5.3.1. The process range conditions for the extraction

To establish appropriate experimental ranges for a subsequent Box-Behnken Design (BBD) optimization, a preliminary single-factor study was conducted. This study aimed to investigate the influence of four key variables—ethanol concentration, temperature, solvent-to-material ratio, and extraction time—on the extraction efficiency of total phenolic content (TPC) and total saponin content (TSC) from the fruit of *P. tectorius*.

The influence of ethanol concentration (%EtOH) is illustrated in Figure 5.1. The TPC yield from the fruit extract increased significantly with ethanol concentration, peaking at approximately 70% before plateauing. Similarly, the TSC yield rose with increasing ethanol content, reaching its maximum at 50% EtOH before declining at higher concentrations. This suggests that a hydroethanolic solvent is more effective than pure water or ethanol for extracting compounds from *P. tectorius* fruit, likely due to the varying polarities of the target phenolics and saponins. Based on these effects, the range of 0–90% EtOH was selected as the operational range for the BBD.

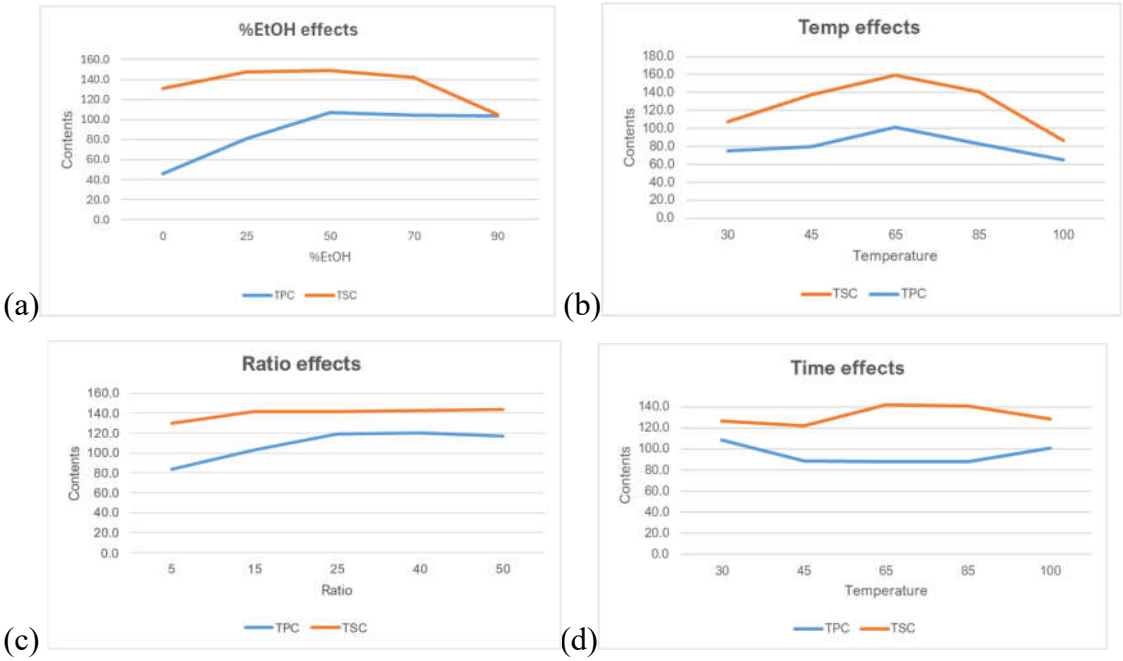

Figure 5.1. The effects of (a) ethanol concentration, (b) extracting temperature, (c) solvent-to-material ratio, and (d) extracting time on TPC and TSC of the extracts

Regarding the extraction temperature, both TPC and TSC yields initially increased with temperature, reaching their optimal values at 65°C. At temperatures higher than this, a significant decrease in the yields of both compounds was observed. The data from the table shows that at 85°C, the yields had already begun to decline from their peak. This decline is likely attributable to the degradation of thermosensitive substances within the fruit and the rapid evaporation of the ethanol. Therefore, to ensure compound stability and avoid degradation, the temperature range for the BBD was determined to be 30–80°C.

The solvent-to-material ratio demonstrated a strong positive correlation with extraction yield. A substantial increase in both TPC and TSC was observed when the ratio was increased from 5 to 25. A ratio below 10 was deemed unsuitable as the solvent volume was likely insufficient for proper wetting and extraction of the raw fruit material. While yields continued to rise slightly as the ratio increased from 25 to 50, the rate of increase diminished, indicating marginal gains. To balance extraction efficiency with solvent consumption, the working range for the ratio in the BBD was established as 10–50 mL/g.

The extraction time showed different effects on TPC and TSC. The highest TPC was achieved at a shorter duration of 60 minutes, with longer times showing no

improvement and potential degradation. Conversely, the TSC yield peaked at around 180 minutes. To accommodate the different optimal times for these two compound groups from *P. tectorius* while maintaining process efficiency, an extraction time range of 60–240 minutes was chosen as appropriate for the subsequent BBD experiments.

In conclusion, based on the single-factor experimental results, the ranges for the four independent variables were selected for the Box-Behnken Design as follows: ethanol concentration (0–90%), temperature (30–80°C), solvent-to-material ratio (10–50 mL/g), and time (60–240 min).

5.3.2. Optimal extraction conditions

5.3.2.1. TPC and TSC of the extracts in the Box-Behnken design

The RSM with BBD was applied to determine the optimal condition for the extraction of phenolic compounds from *P. tectorius* fruits. The extraction design variables effect on the TPC and TSC values are given in Table 5.2.

Table 5.2. TPC and TSC of the extracts to independent variables using Box-Behnken design

No.	A: EtOH (%)	B: Temp. (°C)	C: Ratio (mL/g)	D: Time (min)	TPC (mgGAE/g)	TSC (mgAE/g)
1	45	30	30	60	58.3	132.8
2	45	30	50	150	74.5	140.2
3	90	30	30	150	91.5	111.2
4	45	30	30	240	73.1	140.5
5	45	55	10	60	65.2	138.5
6	90	55	30	60	116.6	125.9
7	90	80	30	150	112.3	142.2
8	45	30	10	150	56.8	121.4
9	90	55	50	150	121.5	136.7
10	0	55	30	240	47.3	135.2
11	45	80	30	240	94.5	164.2
12	90	55	50	60	116.2	124.4
13	45	80	30	60	105.6	152.3
14	90	55	30	150	111.3	129.9
15	0	55	50	150	50.2	131.1
16	0	55	30	60	47.9	128.9
17	45	55	30	150	90.3	161.5
18	45	80	50	150	111.2	170.6
19	90	55	30	240	119.3	128.7
20	45	80	10	150	87.8	149.8
21	0	30	30	150	27.8	110.8

22	45	55	30	150	92.8	155.2
23	45	55	50	240	100.7	160.1
24	0	80	30	150	58.7	142.6
25	45	55	30	150	99.3	162.8
26	45	55	10	240	70.5	139.3
27	45	55	30	150	87.6	162.4
28	90	55	10	150	96.3	121.6
29	45	55	30	150	96.4	158.9
30	0	55	10	150	35.5	123.5

5.3.2.2. The optimal model for TPC enrichment

The experimental results from the Box-Behnken Design were analyzed using Analysis of Variance (ANOVA) to evaluate the effects of the process variables on the total phenolic content (TPC) yield. The statistical significance of the fitted quadratic model was checked by ANOVA. The experimental results from the Box-Behnken Design were analyzed using Analysis of Variance (ANOVA) to evaluate the effects of the process variables on the total phenolic content (TPC) yield. The ANOVA results indicate that the fitted quadratic model is highly significant, with a model F-value of 55.56 and a p-value < 0.0001, which implies that the model is highly suitable for describing the relationship between the independent variables and the TPC yield. Furthermore, the non-significant "Lack of Fit" (p = 0.4437) confirms that the model fits the experimental data well. The model's suitability is also reinforced by its strong fit statistics. The coefficient of determination (R^2) of 0.9811 indicates that 98.11% of the variability in the response could be explained by the model, while the close agreement between the Adjusted R^2 (0.9634) and Predicted R^2 (0.9172) demonstrates good predictive power. Additionally, a high Adeq Precision of 27.1472 and a low coefficient of variation (C.V. % = 6.09%) suggest an adequate signal-to-noise ratio and high experimental reliability. An analysis of the individual model terms revealed that the linear terms A (EtOH concentration), B (temperature), and C (ratio); the interaction term BD (temperature and time); and the quadratic terms A^2, B^2, and C^2 all had a significant effect on TPC yield ($p < 0.05$). The significance of the quadratic terms confirms that the relationship is non-linear. To improve and refine the model, it was proposed that non-significant interaction terms with p-values greater than 0.5, specifically AD (p = 0.6711), BC (p = 0.5854), and CD (p = 0.8905), be eliminated to produce a more concise and robust model.

Following the initial analysis, the model was refined by removing the non-significant interaction terms (AD, BC, and CD) to produce a "Reduced Quadratic model" with markedly improved statistical significance and fit. The refined model's F-value increased substantially from 55.56 to 81.79, indicating it is now even more significant in explaining the relationship between the variables and the TPC yield, while the overall model p-value remained highly significant (< 0.0001) and the Lack of Fit remained non-significant (p = 0.5396). The most notable improvements are seen in the Fit Statistics, which highlight the enhanced robustness and predictive power of this refined model. Specifically, the Adjusted R^2 increased from 0.9634 to 0.9684, and more importantly, the Predicted R^2 increased from 0.9172 to 0.9430. This significantly narrowed the gap between the two values from 0.0462 to just 0.0254, indicating that removing the "noise" from irrelevant terms has made the model more accurate and reliable for making predictions. Furthermore, the Adeq Precision increased from 27.15 to 32.49, signifying an improved signal-to-noise ratio, and the Coefficient of Variation (C.V. %) decreased from 6.09% to 5.66%, pointing to higher precision and reliability. Therefore, the model reduction process was highly successful, resulting in a more precise and robust model for the optimization of TPC extraction. The final regression equation to predict the TPC based on the actual values of the process variables is as follows:

$$TPC = -86.0066 + 1.26713A + 2.45024B + 1.35943C + 0.26148D - 0.00224AB + 0.002416AC - 0.00288BD - 0.00558A^2 - 0.01173B^2 - 0.0148C^2 - 0.00029D^2$$

Where: A = EtOH (%), B = Temperature (°C), C = Ratio (mL/g), D = Time (min)

To visualize the relationship between the independent variables and the yield of Total Phenolic Content (TPC), three-dimensional (3D) response surface plots were generated based on the model equation. These plots illustrate the interactive effects of two variables at a time on the TPC yield while the other two variables are held constant at their central point. Figure 5.2(a) displays the interactive effect of ethanol concentration (A) and temperature (B) on TPC extraction. The plot reveals a significant curved surface, indicating that TPC yield increases with both variables up to an optimal region before leveling off. The peak TPC is predicted at high ethanol concentrations (approximately 70-90%) and moderately high temperatures (approximately 70-80°C).

This demonstrates a synergistic effect where higher temperatures enhance the solvent's extraction capacity. For instance, at a constant temperature of 55°C, increasing the ethanol concentration from 0% to 90% (while other factors are held at their center points) raised the TPC yield from 47.9 mg GE/g to 111.3 mg GE/g. This trend is scientifically sound, as higher temperatures reduce solvent viscosity and increase the solubility and diffusion rate of phenolic compounds. At the same time, the appropriate ethanol concentration optimizes solvent polarity for extracting these target compounds. Figure 5.2(b) illustrates the relationship between ethanol concentration (A) and the solvent-to-material ratio (C). The response surface shows a clear positive correlation, where TPC yield consistently increases as both the ethanol concentration and the ratio are elevated. The steep incline suggests that both factors are strong drivers of extraction efficiency within the tested range. The experimental data support this, showing that at a fixed ethanol concentration of 45% and temperature of 30°C, increasing the ratio from 10 to 50 mL/g increased the TPC yield from 56.8 to 74.5 mg GE/g. This effect is primarily due to the principles of mass transfer; a larger volume of solvent (higher ratio) increases the concentration gradient between the solid material and the liquid phase, thereby promoting the diffusion of phenolic compounds into the solvent until equilibrium is approached. The interaction between temperature (B) and extraction time (D) is presented in Figure 5.2(c). The plot indicates that temperature is a more dominant factor than time in increasing TPC yield. However, a significant interaction between the two is evident. At lower temperatures (e.g., 30-40°C), extending the extraction time has a minimal effect on the TPC yield. In contrast, at higher temperatures (e.g., 80°C), a longer extraction time leads to a more substantial increase in TPC. This is supported by the data: at 80°C and 45% EtOH, the TPC yield was 111.2 mg GE/g after 150 minutes. The upward trend of the surface suggests that at elevated temperatures, which provide the necessary activation energy for extraction, a longer duration allows for more complete diffusion of solutes from the plant matrix.

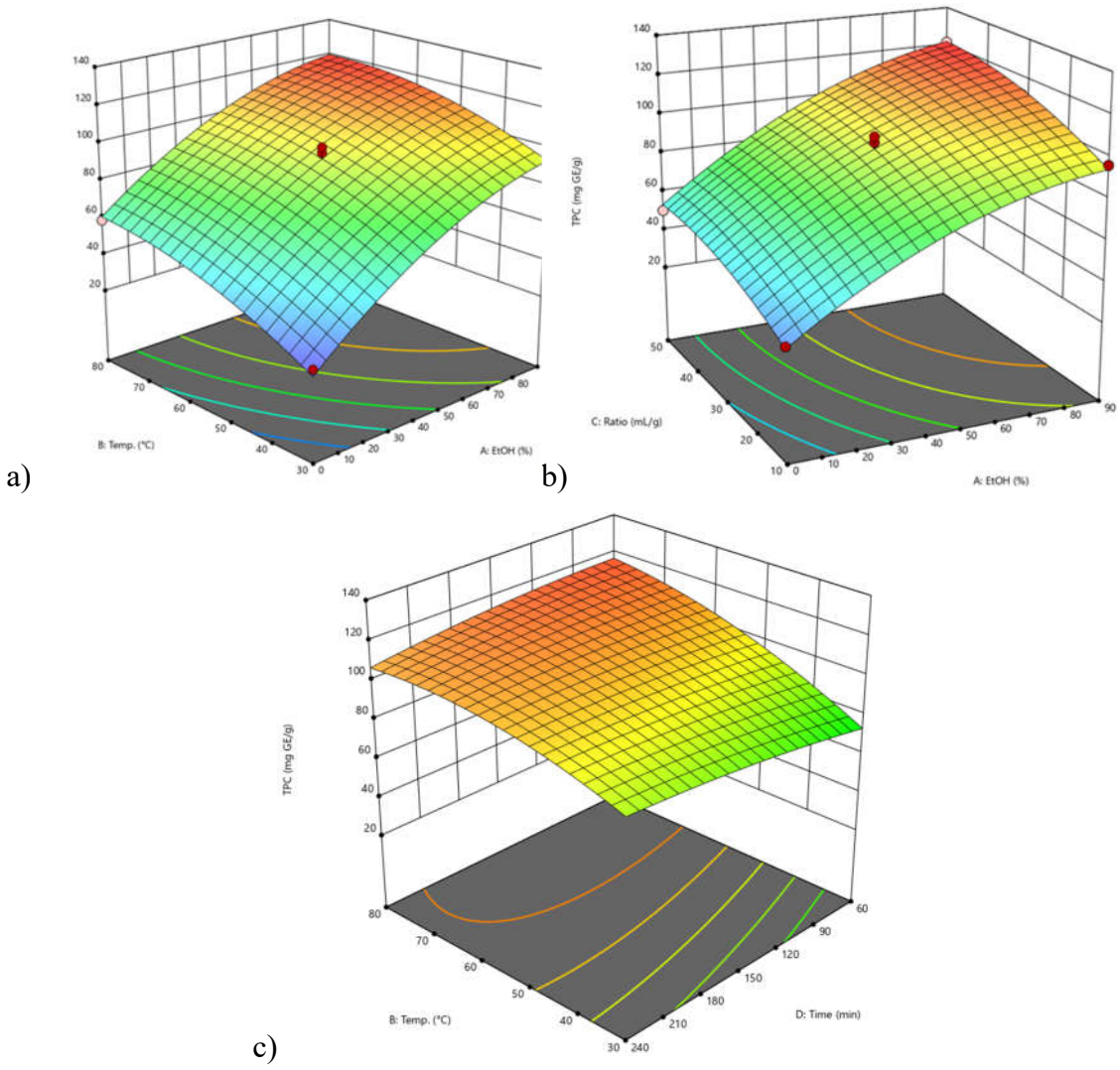

Figure 5.2. Response surfaces between (a) ethanol concentration and temperature, (b) ethanol concentration and solvent-to-material ratio, c) time and temperature to total phenolic contents of the P. tectorius fruit extracts.

5.3.2.3. The optimal model for TSC enrichment

The results from the Box-Behnken design for the total saponin content (TSC) response were analyzed using Analysis of Variance (ANOVA). The initial quadratic regression model was found to be highly significant, demonstrated by a model F-value of 42.97 and a p-value < 0.0001. Additionally, the "Lack of Fit" was not significant (p = 0.4082), indicating that there was no systematic error and the model was compatible with the experimental data. The high coefficient of determination (R^2 = 0.9757) also suggested that the model could explain 97.57% of the variability in the data. However, a more detailed analysis of the fit statistics revealed the necessity of refining the model

to improve its predictive power. Specifically, a significant discrepancy was observed between the Adjusted R^2 value of 0.953 and the Predicted R^2 value of 0.8871. This difference of 0.0659 suggests that the model was likely over-fitted, containing non-significant terms that contribute "noise." An examination of the individual p-values showed that several interaction terms, such as AB (p = 0.9123), AD (p = 0.6888), BC (p = 0.7832), and BD (p = 0.5652), had a very weak effect on the model. The presence of these terms reduces the model's ability to accurately predict new outcomes.

Therefore, to enhance its reliability and predictive capability, the model was refined by eliminating the insignificant interaction terms with a p-value greater than 0.5. This refinement process proved to be highly successful, resulting in a more robust and accurate model. The model F-value increased sharply from 42.97 to 73.17, indicating a statistically stronger model. Most importantly, the difference between the Adjusted R^2 (0.9614) and Predicted R^2 (0.932) was reduced significantly to just 0.0294. This confirms that the model was no longer over-fitted and possessed excellent predictive capability. Furthermore, other statistical indicators also improved: the Adeq Precision increased from 21.68 to 27.82, and the Coefficient of Variation (C.V. %) decreased to 2.31%, both of which confirm the enhanced strength and precision of the new model.

Based on the coefficients for the refined model, the final regression equation in terms of actual factors is:

$$TSC=30.65944+1.05281A+1.84852B+1.13388C+0.190449D+0.001958AC+0.001446CD-0.01256A^2-0.01181B^2-0.01749C^2-0.00065D^2$$

Where: A = EtOH (%), B = Temperature (°C), C = Ratio (mL/g), D = Time (min)

The response surface plots were constructed to visualize the interactive effects of the independent variables on the Total Saponin Content (TSC). These plots are crucial for understanding the complex relationships and identifying the optimal conditions for extraction. Figure 5.3(a) illustrates the combined effect of ethanol concentration (A) and temperature (B). The surface plot is distinctly dome-shaped, indicating that the TSC yield is maximized at intermediate levels of both variables. The yield increases as ethanol concentration rises from 0% and temperature increases from 30°C, reaching a peak before declining. This suggests that while a certain amount of ethanol and heat is beneficial for dissolving and extracting saponins, excessive levels can have an adverse effect. This may be due to changes in solvent properties, such as polarity, at very high

ethanol concentrations or potential solvent loss at temperatures approaching the boiling point of ethanol, which would alter the extraction conditions. The experimental data confirm this, showing that at a fixed ratio and time, the TSC yield at 45% EtOH and 80°C (170.6 mg AE/g) is significantly higher than at 90% EtOH and 80°C (152.3 mg AE/g), highlighting the existence of an optimal range. The interaction between ethanol concentration (A) and solvent-to-material ratio (C) is depicted in Figure 5.3(b). Similar to the previous plot, this response surface also shows a clear optimal region. The TSC yield increases as both the ethanol concentration and the ratio are increased, but only up to a certain point. The curvature indicates that after reaching an optimal ethanol concentration (around 40-50%) and ratio (around 30-40 mL/g), the TSC yield begins to plateau or even slightly decrease. This demonstrates the significant interactive effect between these two variables. For example, at a fixed temperature of 55°C, increasing the ratio from 10 to 50 mL/g at 45% EtOH shows a significant increase in yield (from 158.9 to 162.4 mg AE/g), underscoring the importance of an adequate solvent volume to facilitate mass transfer. Figure 5.3(c) presents the interactive effect of extraction time (D) and solvent-to-material ratio (C). The surface shows that both factors have a positive effect on the TSC yield, with the yield increasing as both time and ratio are extended. The slope is steeper for the ratio than for time, suggesting the solvent volume is a more dominant factor in this interaction. The plot shows a continuous rise towards the upper limits of both variables, with the highest TSC yields found at longer times (around 180-240 min) and higher ratios (around 40-50 mL/g). This is consistent with mass transfer principles, where a larger solvent volume and a longer contact time allow for more complete diffusion of the saponins from the plant matrix into the solvent, leading to a higher extraction yield. For instance, at 45% EtOH and 55°C, increasing the extraction time from 60 minutes to 240 minutes at a ratio of 50 mL/g resulted in an increased yield from 150.2 mg/g to 160.1 mg AE/g.

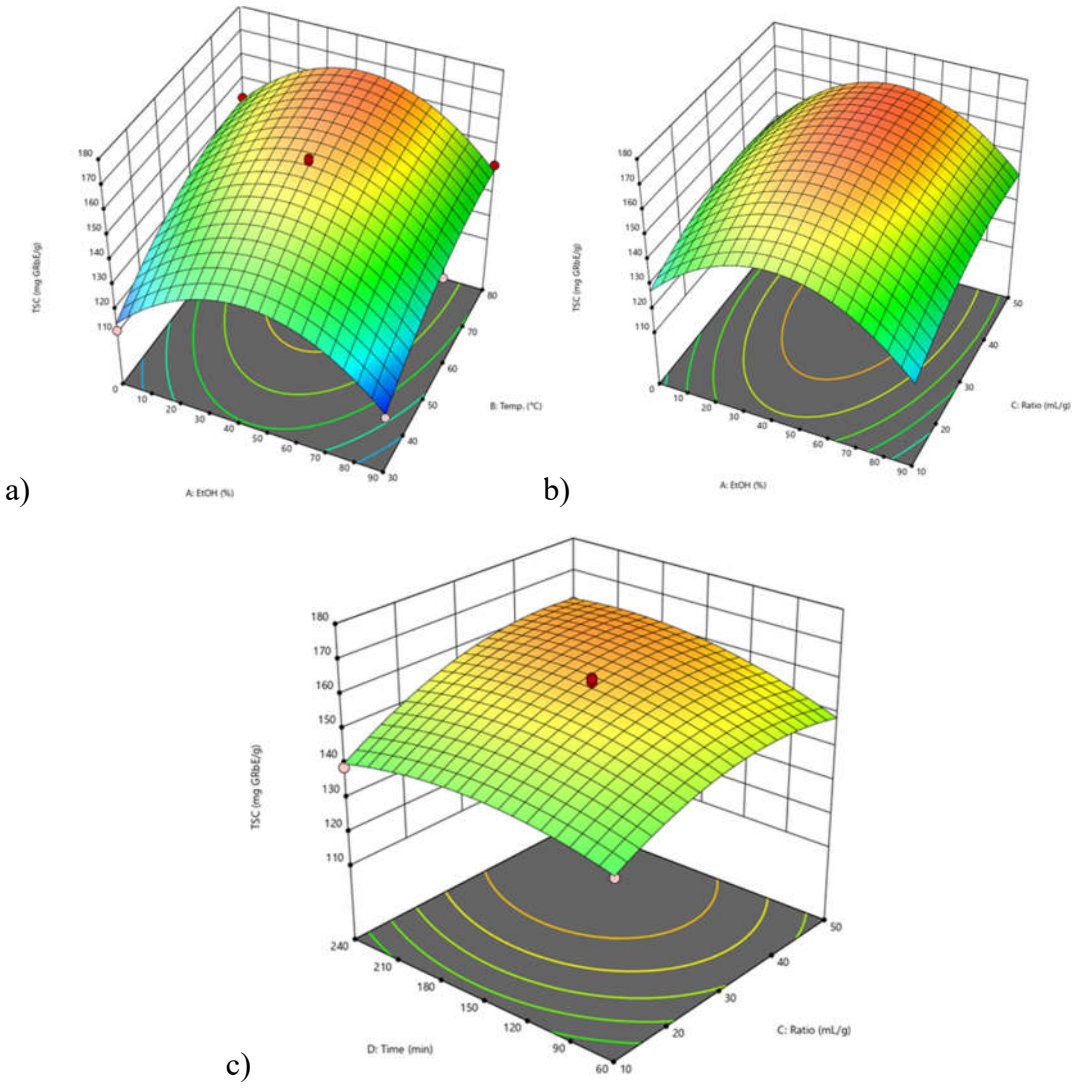

Figure 5.3. Response surfaces between (a) ethanol concentration and temperature, (b) ethanol concentration and solvent-to-material ratio, c) time and solvent-to-material ratio to total saponin contents of the P. tectorius fruit extracts.

5.3.2.4. Optimise the extraction conditions

The refined regression models for both Total Phenolic Content (TPC) and Total Saponin Content (TSC) were utilized to determine the optimal conditions for extracting phytochemicals from *P. tectorius* fruit. As the ideal conditions for maximizing TPC and TSC differ, a multi-response optimization was performed using the numerical optimization feature of the software Design-Expert. This approach allows for finding a range of ideal conditions by assigning different "Importance levels" to each response, providing flexibility based on the desired outcome.

Table 5.3. Summary of predicted optimal conditions for achieving different extraction goals, prioritizing either TPC, TSC, or a balance of both responses.

Condition	Importance level		%EtOH (%)	Temp. (°C)	Ratio (mL/g)	Time (min)
	TPC	TSC				
Opt_TPC1	5	0	90.0	80.0	48.2	104.0
Opt_TPC2	4	1	76.6	80.0	48.6	128.1
Opt_TPC3	3	2	68.9	79.1	47.2	146.4
Balance	2.5	2.5	59.3	78.3	45.5	167.0
Opt_TSC 1	2	3	55.0	78.1	44.7	175.1
Opt_TSC 2	1	4	49.1	78.1	43.6	186.0
Opt_TSC 3	0	5	45.3	78.3	42.9	193.1

Table 3 summarizes seven potential optimal solutions generated by varying the importance placed on TPC versus TSC. The results show a clear trade-off between the two responses. Conditions prioritizing TPC, designated as the 'Opt_TPC' series, consistently require a high ethanol concentration between 70-90% and a high temperature of approximately 80°C. Conversely, conditions prioritizing TSC, the 'Opt_TSC' series, favor a lower ethanol concentration around 45-55% and significantly longer extraction times exceeding 175 minutes, while the optimal temperature remains high. The 'Balance' condition represents a compromise, using intermediate parameters to achieve good, though not maximal, yields of both TPC and TSC simultaneously. This analysis provides a set of validated optimal conditions, allowing for the selection of specific extraction parameters depending on whether the desired final product is an extract rich in phenolics, saponins, or a balanced combination of both.

To confirm the validity and predictive accuracy of the developed models, a series of validation experiments was conducted. The seven sets of optimal conditions derived from the numerical optimization were slightly adjusted for practical convenience in a laboratory setting. Extractions were then performed in triplicate under these adjusted conditions. Table 5.4 presents a comparison between the TPC and TSC yields predicted by the regression models and the values obtained through these validation experiments.

The results demonstrate a strong correlation and excellent agreement between the predicted and experimental values across all seven tested conditions, affirming the reliability of the optimization process. Specifically, the experimental data closely matched the values predicted by the models. For instance, the 'Balance' condition

showed remarkable accuracy, with an experimental TPC of 114.7 ± 7.1 mg GAE/g against a prediction of 115.0 mg GAE/g. Furthermore, the analysis confirmed that the Opt_TSC3 condition, which was designed to maximize saponin content, successfully yielded the highest experimental TSC of 185.6 ± 10.6 mg AE/g and concurrently the lowest experimental TPC of 105.6 ± 8.5 mg GAE/g. This lowest TPC value showed excellent agreement with its predicted value of 103.5 mg GAE/g. While the highest experimental TSC was greater than its predicted value of 169.5 mg AE/g, the model nonetheless accurately identified the specific conditions required to achieve the maximum saponin yield.

Table 5.4. Predicted versus experimental yields (mean ± SD, n=3) of TPC (mg GAE/g) and TSC (mg AE/g) for the validation of the seven adjusted optimal extraction conditions.

Samples	EtOH (%)	Temp. (°C)	Ratio (mL/g)	Time (min)	Predict values		Experimental	
					TPC	TSC	TPC	TSC
Opt_TPC1	90	80	48	104	129.3	138.5	124.8 ± 8.8	126.1 ± 12.7
Opt_TPC2	75	80	48	130	124.2	155.2	121.1 ± 11.1	142.8 ± 16.5
Opt_TPC3	65	80	47	150	118.8	163.0	118.3 ± 6.5	151.8 ± 15.9
Balance	60	80	46	170	115.0	166.3	114.7 ± 7.1	162.4 ± 19.6
Opt_TSC1	55	80	45	175	111.7	168.0	109.7 ± 8.8	168.3 ± 15.2
Opt_TSC2	50	80	44	190	107.4	169.2	106.2 ± 11.8	178.9 ± 12.1
Opt_TSC3	45	80	43	195	103.5	169.5	105.6 ± 8.5	185.6 ± 10.6

The experimental data also validated the predicted trade-off between the two responses; conditions designed to favor TPC resulted in extracts with higher experimental TPC yields, while conditions prioritizing TSC successfully produced extracts richer in saponins. The close correspondence between the predicted and actual results validates the accuracy of the regression models. This confirms that the developed models are reliable and effective tools for navigating the design space and optimizing the extraction of both phenolic and saponin compounds from *P. tectorius* fruit.

5.4. Bioactivities of the extracts

The antioxidant activity of the seven extracts was evaluated through their ability to scavenge DPPH and hydroxyl radicals, with the results presented as IC_{50} values. The data revealed a clear correlation between antioxidant activity and the Total Phenolic

Content (TPC) of the extracts. The samples belonging to the 'Opt_TPC' series, which were optimized for high TPC, were the only ones to exhibit significant activity with IC50 values below 100 µg/mL in both assays. Among them, the 'Opt_TPC1' extract demonstrated the highest potency, with an IC_{50} value of 76.4 µg/mL for DPPH scavenging and 62.5 µg/mL for hydroxyl radical scavenging. In contrast, the saponin-optimized extracts ('Opt_TSC' series) and the 'Balance' extract showed considerably weaker activity, with IC_{50} values exceeding 100 µg/mL in most tests. While the TPC-rich extracts demonstrated notable antioxidant potential, their activity was lower than that of the pure compound positive controls. Specifically, the DPPH scavenging activity of the most potent extract ('Opt_TPC1') was less than that of ascorbic acid (IC_{50} = 27.4 µg/mL), and its hydroxyl radical scavenging activity was less than that of catechin (IC_{50} = 31.7 µg/mL). This result is expected, as crude extracts are complex mixtures, whereas the controls are highly active, pure antioxidant compounds. These findings collectively suggest that the phenolic constituents are the primary contributors to the antioxidant capacity of the *P. tectorius* extracts.

The anti-inflammatory potential of the seven optimized *P. tectorius* fruit extracts was evaluated by measuring their ability to inhibit nitric oxide (NO) production in LPS-stimulated cells (Table 5.5). A clear trend emerged regarding the extracts' potency, which was found to correlate with the saponin contents.

Table 5.5. Free-radical scavenging and NO production inhibitory effects of P. tectorius fruit extracts under optimal conditions

Samples	**DPPH (IC_{50}, µg/mL)**	**Hydroxyl (IC_{50}, µg/mL)**	**NO inhibition (IC_{50}, µg/mL)**
Opt_TPC1	76.4 ± 3.8^{a}	62.5 ± 4.1^{d}	91.3 ± 8.2^{i}
Opt_TPC2	82.1 ± 4.5^{b}	70.8 ± 5.3^{e}	85.4 ± 6.6^{j}
Opt_TPC3	89.5 ± 5.1^{b}	79.1 ± 6.2^{f}	84.2 ± 7.3^{j}
Balance	>100	95.6 ± 8.1^{g}	75.5 ± 3.9^{k}
Opt_TSC 1	>100	>100	68.8 ± 1.1^{l}
Opt_TSC 2	>100	>100	ND
Opt_TSC 3	>100	>100	ND
Ascorbic acid *	27.4 ± 1.6^{c}	-	-
Catechin **	-	31.7 ± 2.8^{h}	-
Cardamonin #			3.1 ± 0.4^{m}

*, **, # Positive control

a-m: Data are expressed as mean ± SD. Means in each column with different letters are significantly different ($p < 0.05$).

The IC_{50} values ranged from 91.3 μg/mL for the TPC-rich extract Opt_TPC1 down to 68.8 μg/mL for the saponin-rich extract Opt_TSC1, indicating that Opt_TSC1 was the most potent anti-inflammatory agent among the tested samples. As expected, all crude extracts were less potent than the pure compound positive control, cardamonin, which had an IC_{50} of 3.1 μg/mL. To ensure that the observed NO inhibition was not a result of cytotoxicity, cell survival was assessed (data not shown). The extracts from the Opt_TPC series, the Balance condition, and Opt_TSC1 all demonstrated excellent safety profiles, with cell survival rates consistently above 92%. In contrast, the Opt_TSC2 and Opt_TSC3 extracts, which contained the highest concentrations of saponins, exhibited significant cytotoxicity, causing cell survival to drop to as low as 64.3%. Consequently, the IC_{50} values for these two extracts could not be determined. This finding suggests that while saponin-rich extracts possess greater anti-inflammatory potency, very high concentrations of saponins or co-extracted compounds may induce a cytotoxic effect on the RAW264.7 cells.

5.5. Chapter summary

This study successfully optimized the extraction process of phenolic- and saponin-enriched fractions from *Pandanus tectorius* fruit using the Box–Behnken Design. The developed models demonstrated strong statistical validity and predictive power, allowing for the fine-tuning of extraction conditions based on desired phytochemical enrichment. Phenolic-rich extracts obtained under high ethanol concentration and temperature conditions exhibited strong antioxidant activity, while saponin-rich extracts, obtained under lower ethanol concentration and longer extraction times, showed superior nitric oxide inhibitory effects, albeit with potential cytotoxicity at higher doses. These results highlight the importance of process optimization in maximizing both the yield and bioactivity of natural products. Furthermore, this study provides a robust methodological framework for future valorization of *P. tectorius* as a promising source of functional ingredients in pharmaceutical or nutraceutical applications.

CHAPTER 6. OPTIMIZATION OF THE EXTRACTION CONDITION AND BIOACTIVITY EVALUATION OF THE PHENOLIC ENRICHMENT FROM *PANDANUS AMARYLLIFOLIUS* LEAVES

6.1. Chapter overview

Pandanus amaryllifolius leaf is a common food, as well as, a well-known tradition medicine. Previously, we reported the alkaloid compostions of the *Pandanus amaryllifolius* leaves [64]. Based on the chemical and bioactivity screening results, this study investigates the optimal conditions to enrich the phenolic content of the extract from *Pandanus amaryllifolius* leaves and evaluates bioactivities of this enrichment. The phenolic enrichment was prepared under optimized conditions using the Response Surface Methodology (RSM) with the Box-Behnken Design. The antioxidant properties were assessed using DPPH and hydroxyl radical scavenging assays, while the NO production inhibition was measured in LPS-stimulated RAW 264.7 macrophage cells. Results indicated that the phenolic enrichment showed potent antioxidant activity comparable to ascorbic acid and catechin, and significantly higher NO inhibition than the separated non-alkaloid and alkaloid fractions. The study also highlights the synergistic effect of phenolic and alkaloid compounds on the antioxidants and anti-inflammatory activities of the phenolic enrichment from *Pandanus amaryllifolius* leaves.

6.2. Experimental design

6.2.1. Samples

Leaves of *P. amaryllifolius* were collected at Tam Dao, Phu Tho province, Vietnam, in April 2021 and identified by Dr. Bui Van Thanh, Institute of Biology, Vietnam Academy of Sciences and Technology (VAST). A voucher specimen (NCCG 210213) was deposited at the Department of Agro-Pharmaceutical Research, Centre for High Technology Research and Development, VAST. The collected sample was cleaned, dried at 50°C in the oven, powdered, and preserved at -20 °C for further experiments.

6.2.2. Analytical methods

Total phenolic contents (TPC), antioxidant, and NO production inhibitory effects of *P. amaryllifolius* leaves extracts under designed conditions were evaluated using the protocols as mentioned in Chapter 2.

6.2.3. Preliminary single-factor experiments

Ranges of the extraction factors, such as temperature, ethanol concentration, and time, were evaluated from the following experiments. Firstly, the effect of extraction temperature on the TPC of the extracts was investigated by extracting the material in ethanol 96% at 30-80 °C for 180 minutes. Next, the impact of the ethanol concentration on the TPC values was determined by extracting the *P. amaryllifolius* leaves in ethanol 0-96% for 180 minutes at 60 °C. Lastly, the influence of extraction time on TPC was evaluated by extracting the material in ethanol 96% at 60 °C for 60-360 minutes. In each experiment, 5 g of *Pandanus amaryllifolius* leaves was extracted in 150 mL of solvent, maintaining a fixed ratio of leaf weight to solvent volume at 1:30 (g/mL).

6.2.4. Response Surface Method

The response surface method (RSM) applying the Box-Behnken Design (BBD) was utilised to design the experiments to optimise the conditions to enrich phenolics in the extract of *P. amaryllifolius* leaves. The design was conducted on the Design-Expert 12.0 software (Stat-Ease, Inc., Minneapolis, US). Extraction temperature (°C, X_1), ethanol concentration (%, X_2), and extraction time (minutes, X_3) were selected as independent factors, while total phenolic contents (TPC) were selected as the responses. From preliminary single-factor experiments, ethanol 0% (distilled water), 48%, and 96% were used as the solvents, whereas the temperature ranged from 30 ℃ to 80 ℃; meanwhile, the extraction time varied between 60 to 300 minutes. Each experiment was conducted in triplicate, and the mean of the response (TPC) was used for further calculation. The levels of the variables in the experimental design are shown in Table 6.1.

Table 6.1. Levels of the variables in Box- Behnken design

Variables	**Unit**	**Code levels**		
		-1	**0**	**1**
Temperature (X_1)	℃	30	55	80
Ethanol concentration (X_2)	%	0	48	96
Time (X_3)	minutes	60	180	300

6.3. Optimize the conditions for the enrichment of the phenolic content from *Pandanus amaryllifolius* leaves

6.3.1. The process range conditions for the extraction

The impact of temperature, ethanol concentration, and extraction time on the total phenolic content (TPC) of *Pandanus amaryllifolius* leaf extracts was systematically investigated. The data from the experimental design, summarized in Table S1 and Figure 1, reveal distinct trends associated with each parameter, leading to the identification of optimal ranges for phenolic extraction.

The TPC was positively correlated with temperature within the range of 30–80°C, with the highest TPC (95.84 mg GAE/g) observed at 70°C, and slightly decreased to 86.93 mg GAE/g at 80°C. These suggested that higher temperatures may cause degradation of phenolic compounds or excessive evaporation of ethanol. For practical purposes and to align with the experimental environment's ambient conditions, temperatures below 30°C were deemed unsuitable. These findings confirm that the temperature range for maximizing phenolic extraction should lie between 30°C and 80°C.

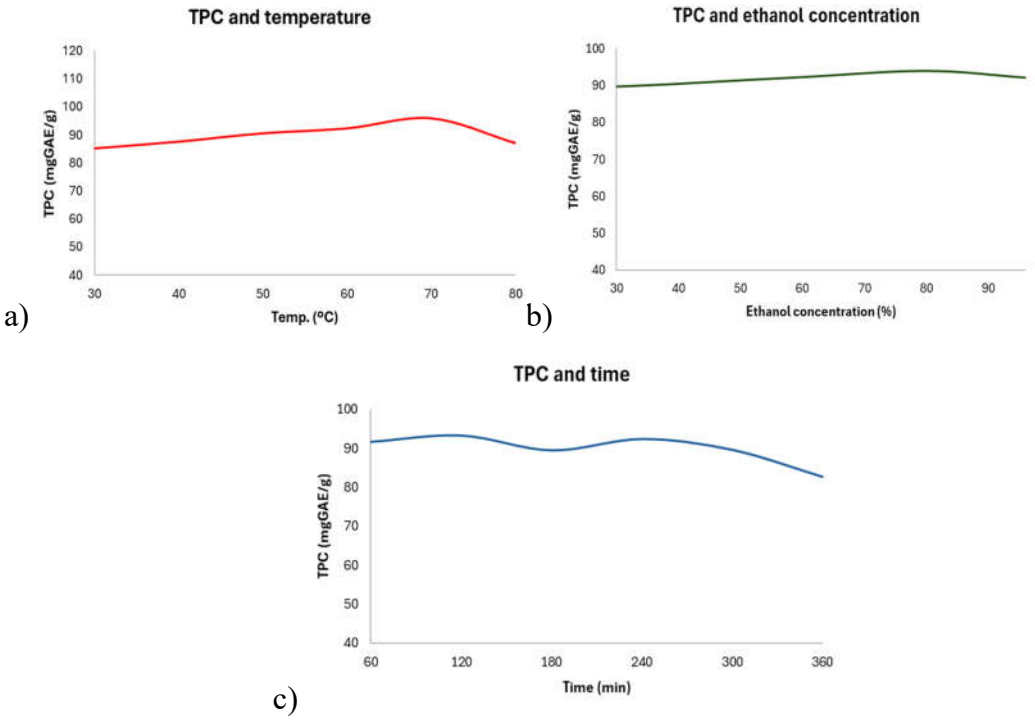

Figure 6.1. Effect of extraction temperature (a), ethanol concentration (b), and extraction time (c) on total phenolic content of extracts from P. amaryllifolius leaves

Meanwhile, the ethanol concentration influenced the TPC, with relatively small differences observed across the tested range. The TPC increased steadily with rising ethanol concentrations, from 80.38 mg GAE/g at 0% ethanol (distilled water) to 93.93 mg GAE/g at 80% ethanol, after which it slightly decreased to 92.12 mg GAE/g at 96% ethanol. While 80% ethanol yielded the highest TPC, the variations between concentrations above 40% were not substantial. This result highlights the need to optimize ethanol concentration further within the range of 0–96% to identify the precise conditions that balance extraction efficiency and solvent consumption.

The extraction time also had a noticeable impact on TPC, with values generally increasing within the range of 60 to 240 minutes. The highest TPC (93.37 mg GAE/g) was observed at 120 minutes, indicating this duration was particularly effective for phenolic extraction. While longer times, such as 240 minutes, still yielded relatively high TPC (92.46 mg GAE/g), a gradual decline was observed beyond this point, with 89.67 mg GAE/g at 300 minutes and 82.67 mg GAE/g at 360 minutes. This reduction could be attributed to the potential degradation of phenolic compounds or decreased solvent efficiency over prolonged periods. Shorter durations, such as 60 minutes, also provided a reasonably high TPC (91.73 mg GAE/g), suggesting that the extraction process reaches a significant level of efficiency early on. However, extending the time to 240 minutes ensures thorough extraction, particularly for phenolic compounds that may require more time to diffuse into the solvent. Based on these findings, the optimal time range for extraction is 60–300 minutes, providing flexibility to balance efficiency and resource consumption while minimizing the risk of phenolic degradation..

6.3.2. Optimal extraction conditions

The RSM with BBD was applied to determine the optimal condition for the extraction of phenolic compounds from *P. amaryllifolius* leaves. The extraction design variables effect on the TPC values, are given in Table 6.2.

Table 6.2. Responses of TPC of the extracts to independent variables using the Box-Behnken design

No.	Variables			TPC (mg GAE/g)	
	X_1: Temp. (°C)	**X_2: EtOH (%)**	**X_3: Time (min)**	**Experimental value**	**Predicted value**
1	55	48	180	92.66	91.10
2	55	48	180	89.57	91.10
3	30	48	300	81.15	81.66
4	30	0	180	54.97	54.92
5	55	96	60	89.43	90.09
6	55	48	180	92.9	91.10
7	55	48	180	92.24	91.10
8	80	96	180	85.71	86.05
9	30	96	180	82.74	82.90
10	55	0	300	76.74	76.27
11	55	48	180	90.51	91.10
12	80	48	60	90.7	90.28
13	55	96	300	89.95	89.59
14	55	48	180	89.93	91.10
15	55	0	60	70.21	70.76
16	55	48	180	89.55	91.10
17	30	48	60	70.57	70.10
18	80	48	300	83.17	83.73
19	80	0	180	81.43	81.38

The modified quadratic models for the estimation of polyphenol content (TPC) in terms of extracting temperature (X_1), ethanol concentration (X_2), and extracting time (X_3) are shown below:

$$TPC = -13.700711 + 2.12296X_1 + 0.956150X_2 + 0.159595X_3 - 0.007927X_1X_2 - 0.001509X_1X_3 - 0.000261X_2X_3 - 0.012019X_1^2 - 0.004918X_2^2 - 0.000149X_3^2 + 0.000032X_1X_2^2 \quad (1)$$

The analysis of variance (Table 6.3) illustrated the model F value at 90.26 with $p < 0.0001$, which implied that the model was highly significant. The lack of fit was insignificant ($p > 0.05$), indicating that the model fit the analytical results. The model, adjusted, and predicted R^2 at 0.9912, 0.9802, and 0.9437, respectively, implied that the model could be validated for use in the investigated ranges.

Table 6.3. The analysis of variance for the response surface model of the phenolic enrichment from P. amaryllifolius leaves

Source	Sum of	df	Mean	F-value	p-value	
Model	1741.539	10	174.1539	90.26363	4.05E-07	significant
A-Temp.	122.6556	1	122.6556	63.57217	4.47E-05	
B-EtOH	519.7088	1	519.7088	269.364	1.91E-07	
C-Time	12.75125	1	12.75125	6.608947	0.033087	
AB	137.945	1	137.945	71.49663	2.92E-05	
AC	81.99303	1	81.99303	42.49682	0.000184	
BC	9.030025	1	9.030025	4.680244	0.062459	
A^2	252.8046	1	252.8046	131.0281	3.07E-06	
B^2	240.5061	1	240.5061	124.6539	3.71E-06	
C^2	20.55429	1	20.55429	10.65325	0.01146	
AB^2	6.6248	1	6.6248	3.433621	0.10101	
Residual	15.43514	8	1.929392			
Lack of Fit	2.01805	2	1.009025	0.451227	0.656815	not significant
Pure Error	13.41709	6	2.236181			
Cor Total	1756.974	18				

The response surface plots of ethanol concentration – extracting temperature, ethanol concentration – extracting time, and extracting time and temperature are shown in Figure 2. As can be seen, the TPC of the *P. amaryllifolius* leaves extract increased sharply when raising the ethanol concentration from 0 to about 70% then remained stable at the higher ratio of alcohol. Meanwhile, the rise in temperature from 30 ℃ to 60 ℃ might enhance the TPC of the extract, while a higher temperature might decrease the phenolic contents due to the decomposition of some metabolites. Besides, the temperature approximating the boiling point of ethanol led to a decrease in the extraction yield due to the fast evaporation of the solvent, and a longer extraction time certainly affected the TPC values of the extract.

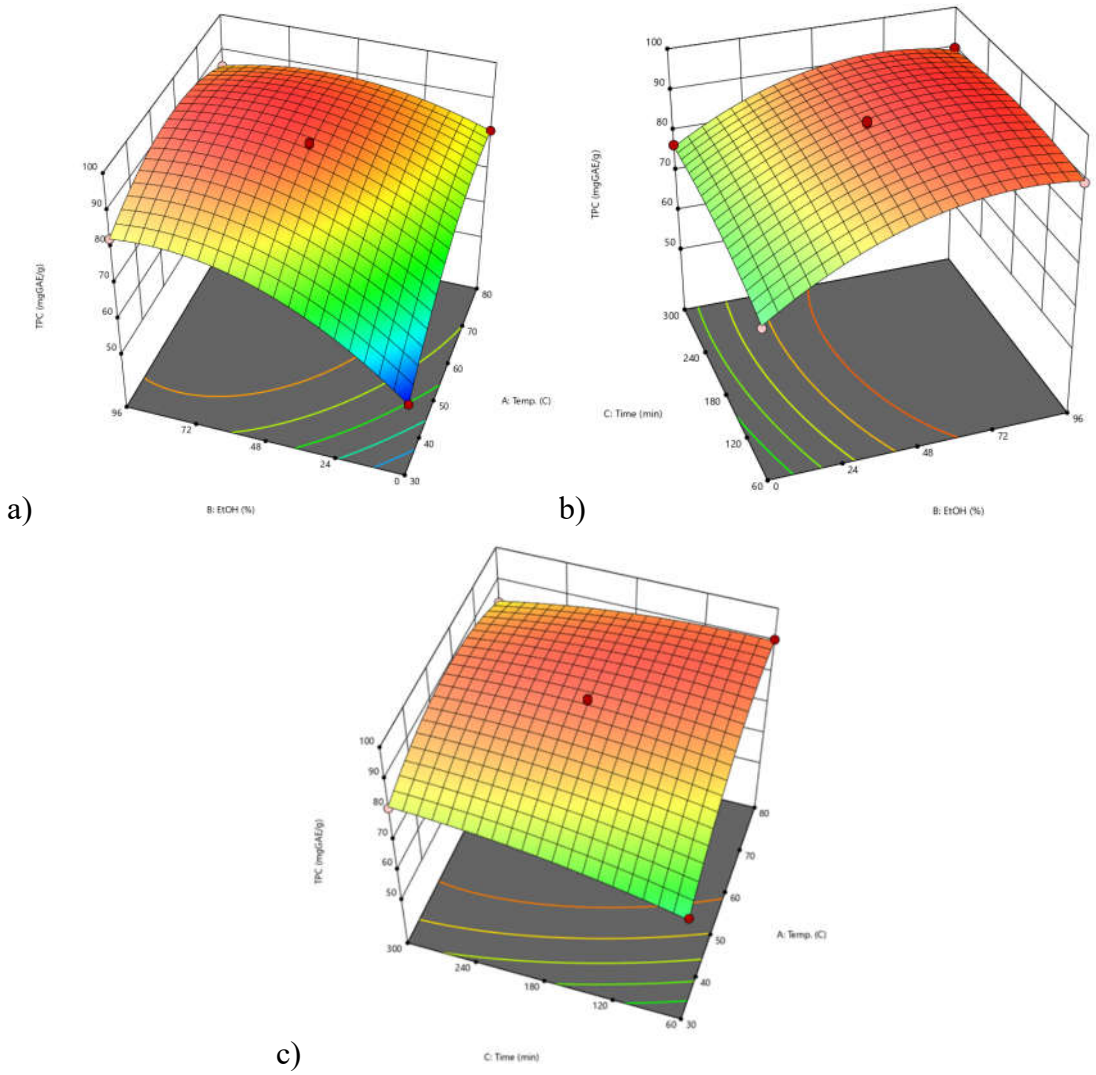

Figure 6.2. Response surfaces between (a) temperature and ethanol concentration, (b) ethanol concentration and time in response, c) time and temperature to total phenolic contents of the P. amaryllifolius extracts

From the numerical optimisation, the maximum predicted TPC of the phenolic enrichment at 93.59 mgGAE/g could be obtained under the conditions of 61.18 °C extraction temperature, 163.00 min extraction time, and 71.79% ethanol concentration. The actual condition was slightly modified at 65 °C, ethanol 70%, and an extraction time of 160 minutes. The TPC of the phenolic enrichment under the optimal condition was 105.69 mgGAE/g, which was higher than the calculated value above.

6.4. Chemical composition of the phenolic enrichment from the *P. amaryllifolius* leaves

6.4.1. Isolation of the compounds from the P. amaryllifolius leaves' phenolic enrichment

The phenolic enrichment from the optimal extraction condition was further isolated by chromatographic methods. 200 g of the enrichment was acidified with 1N HCl solution to pH 2-3 and successively partitioned with ethyl acetate (EtOAc) (2 L × 4 times). The organic layer was separated and completely evaporated to afford the non-alkaloid extract (62.4 g). The water layer, which contained alkaloids, was basified by 1N NaOH to pH 9-10 and was extracted with CH_2Cl_2 (4×2 L). The CH_2Cl_2 layers were combined to collect the alkaloid fraction (22.6 g).

The non-alkaloid extract was subjected to a Diaion HP-20 chromatography column (CC) then wash the column with water, followed by MeOH 30% and 100% to obtain M30W (4.5 g) and M100W (13.6 g) fractions, respectively. The fraction M30W was loaded on a silica gel column with gradient mixtures of CH_2Cl_2–MeOH (20/1-1/1, v/v) to afford four subfractions (W1-W4). Fraction W3 (121 mg) was separated by preparative HPLC (120 min, 30-60% MeOH in H_2O) to yield the compounds **Pam1** (5.5 mg), **Pam2** (6.5 mg), and **Pam3** (3.7 mg). Fraction W1 (105 mg) was separated by preparative HPLC (120 min, 30-60% MeOH in H_2O) to yield the compound **Pam4** (11.2 mg). Fraction W4 (127 mg) was separated by preparative HPLC (120 min, 20-70% MeOH in H_2O) to yield the compounds **Pam5** (1.1 mg), **Pam6** (3.2 mg), and **Pam7** (3.4 mg). The fraction M100W was subjected to a silica gel column eluted with gradient mixtures of CH_2Cl_2–MeOH (50/1-1/1, v/v) to afford ten subfractions (M1-M10). Fraction M6 (91.4 mg) was separated by preparative HPLC (120 min, 40-100% MeOH in H_2O) to yield the compounds **Pam8** (15.5 mg) and **Pam9** (6.8 mg). Fraction M4 (304 mg) was separated by preparative HPLC (120 min, 30-80% MeOH in H_2O) to yield the compounds **Pam10** (4.1 mg), and **Pam11** (6.6 mg). Fraction M8 (178 mg) was chromatographed on a silica gel CC eluted with CH_2Cl_2–acetone (5/1, v/v) to get compounds **Pam12** (3.1 mg) and **Pam13** (5.6 mg). Fraction M5 (90.9 mg) was separated on a silica gel CC eluted with CH_2Cl_2–methanol (9/1, v/v) to gain compound **Pam14** (5.6 mg) and **Pam15** (2.8 mg). Fraction M9 (91.8 mg) was chromatographed on a silica gel CC eluted with CH_2Cl_2–methanol (9/1, v/v) to afford compound Pam**16** (4.5 mg).

Methyl shikimate **(Pam1)**: ESI-MS: *m/z* 189 $[M+H]^+$; ^1H NMR ($CDCl_3$, 600 MHz): δ 6.61 (1H, d, *J* = 1.8 Hz, H-2), 4.24 (1H, m, H-3), 3.85 (1H, m, H-4), 3.58 (1H, m, H-5), 2.07 (1H, dd, *J* = 2.4, 18.0 Hz, H-6), 2.41 (1H, dd, J = 3.6, 18.0 Hz, H-6), 3.67 (3H, s, 7-OCH_3), 4.82 (2H, brs, 3,5-OH), 4.60 (1H, brs, 4-OH). ^{13}C NMR ($CDCl_3$, 125 MHz): δ 127.3 (C-1), 139.7 (C-2), 66.8 (C-3), 70 (C-4), 65.4 (C-5), 29.6 (C-6), 166.7 (C-7), 51.5 (7-OCH_3).

n-butyl shikimate **(Pam2)**: *m/z* 231 $[M+H]^+$; ^1H NMR ($CDCl_3$, 600 MHz): δ 6.61 (1H, t, *J* = 1.2 Hz, H-2), 4.80 (1H, brs, H-3), 3.85 (1H, m, H-4), 4.59 (1H, m, H-5), 2.62 (1H, m, H-6a), 2.13 (1H, m, H-6b), 4.08 (2H, t, *J* = 6.4 Hz, H-1'), 1.59 (2H, m, H-2'), 1.36 (2H, m, H-3'), 0.90 (3H, t, *J* = 7.2 Hz, H-4'). ^{13}C NMR ($CDCl_3$, 125 MHz): δ 127.6 (C-1), 139.4 (C-2), 65.4 (C-3), 70.1 (C-4), 66.8 (C-5), 29.6 (C-6a), 166.2 (C-7), 63.6 (C-1'), 30.2 (C-2'), 18.7 (C-3'), 13.5 (C-4').

5-*epi*-shikimate methyl **(Pam3)**: *m/z* 189 $[M+H]^+$; ^1H NMR ($CDCl_3$, 600 MHz): δ 6.57 (1H, t, *J* = 3.0 Hz, H-2), 4.63 (1H, m, H-3), 3.49 (1H, m, H-4), 3.45 (1H, m, H-5), 2.13 (1H, dd, *J* = 9.0, 18.0 Hz, H-6a), 2.61 (1H, dd, *J* = 4.8, 18.0 Hz, H-6), 3.70 (3H, s, 7-OCH_3), 5.56 (1H, brs, 3-OH), 5.14 (1H, brs, 4-OH), 3.50 (1H, brs, 5-OH),. ^{13}C NMR ($CDCl_3$, 125 MHz): δ 129.2 (C-1), 136.4 (C-2), 68.6 (C-3), 77.0 (C-4), 61.5 (C-5), 32.1 (C-6), 165.6 (C-7), 52.0 (7-OCH_3).

Pinoresinol 4-*O*-*β*-*D*-glucoside **(Pam4)**: white amorphous powder, ESI-MS: *m/z* 521 $[M+H]^+$; *m/z* 1041 $[2M+H]^+$; molecular formula: $C_{26}H_{32}O_{11}$; ^1H NMR (CD_3OD, 600 MHz): δ 7.05 (1H, d, *J* = 2.4 Hz, H-2), 7.17 (1H, d, *J* = 9.0 Hz, H-5), 6.94 (2H, dd, *J* = 9.0; 2.4 Hz, H-6,6'), 4.78 (1H, d, *J* = 4.8 Hz, H-7), 3.15 (2H, m, H-8), 3.72 (2H, dd, *J* = 9.0; 4.8 Hz, H-9a), 4.26 (2H, dd, *J* = 9.0; 2.4 Hz, H-9b), 6.97 (1H, d, *J* = 2.4 Hz, H-2'), 6.79 (1H, d, *J* = 9.0 Hz, H-5'), 6.94 (2H, dd, *J* = 9.0; 2.4 Hz, H-6'), 4.73 (1H, d, *J* = 4.5 Hz, H-7'), 3.15 (2H, m, H-8'), 3.72 (2H, dd, *J* = 9.0; 4.8 Hz, H-9'a), 4.26 (2H, dd, *J* = 9.0; 2.4 Hz, H-9'b), 3.88 (3H, s, 3-*O*-CH_3), 3.89 (3H, s, 3'-*O*- CH_3), 4.89 (1H, d, *J* = 8.4 Hz, H-1"), 3.44 (1H, m, H-2"), 3.42 (1H, m, H-3"), 3.30 (1H, m, H-4"), 3.40 (1H, m, H-5"), 3.46-3.53 (2H, m, H-6"); ^{13}C NMR (CD_3OD, 125 MHz): δ 137.5 (C-1), 111.0 (C-2), 151.0 (C-3), 147.3 (C-4), 118.1 (C-5), 119.8 (C-6), 87.4 (C-7), 55.35 (C-8), 72.7 (C-9), 133.8 (C-1'), 111.7 (C-2'), 149.1 (C-3'), 147.5 (C-4'), 116.11 (C-5'), 119.8 (C-6'), 87.1 (C-7'), 55.54 (C-8'), 72.7 (C-9'), 56.5 (3-*O*- CH_3), 56.8 (3'-*O*- CH_3), 102.9 (C-1"), 74.9 (C-2"), 77.9 (C-3"), 71.4 (C-4"), 78.2 (C-5"), 62.5 (C-6").

Vanillic acid **(Pam5)**: ESI-MS: *m/z* 169 $[M+H]^+$; ^1H NMR (CD_3OD, 600 MHz): δ 77.58 (1H, d, *J* = 2.4 Hz, H-2); 6.85 (1H, d, *J* = 9.0 Hz, H-5); 7.57 (1H, dd, *J* = 9.0, 2.4 Hz, H-6); 3.92 (3H, s, 3-OCH_3). ^{13}C NMR ($CDCl_3$, 150 MHz): δ 121.6 (C-1); 125.3 (C-2); 148.7 (C-3); 154.6 (C-4); 113.9 (C-5); 115.9 (C-6); 170.0 (C-7); 56.4 (3-OCH_3).

p-hydroxybenzaldehyde **(Pam6)**: ESI-MS: *m/z* 123 $[M+H]^+$; ^{1}H NMR (DMSO-d_6, 600 MHz): δ 6.88 (2H, d, J = 7.2 Hz, H-2,6); 7.76 (2H, d, J = 7.2 Hz, H-3,5); 9.72 (1H, s). ^{13}C NMR (DMSO-d_6, 150 MHz): δ 129.1 (C-1); 132.8 (C-2,6); 116.5 (C-3,5); 163.9 (C-4); 191.8 (C-7).

Methyl gallate **(Pam7)**: ESI-MS: *m/z* 185 $[M+H]^+$.^{1}H NMR (CD_3OD, 600 MHz): δ 7.06 (2H, s, H-2,6); 3.83 (3H, s, 7-OCH_3). ^{13}C NMR (CD_3OD, 150 MHz): δ 121.5 (C-1); 110.1 (C-2,6); 146.5 (C-3,5); 139.8 (C-4); 169.0 (C-7); 52.3 (7-OCH_3).

Pinoresinol **(Pam8)**: See compound **Pt3**.

Pinoresinol monomethyl ether **(Pam9)**: See compound **Pt4**.

Methyl 4-hydroxybenzoate **(Pam10)**: *m/z* 153 $[M+H]^+$; ^{1}H NMR (DMSO-d_6, 600 MHz): δ 7.81 (1H, d, J = 6.6 Hz, H-2,6), 6.84 (1H, d, J = 6.6 Hz, H-3,5), 3.78 (3H, s, OCH_3). ^{13}C NMR (DMSO-d_6, 125 MHz): δ 120.2 (C-1), 131.3 (C-2), 115.3 (C-3), 161.9 (C-4), 115.3 (C-5), 131.3 (C-6), 166.0 (C-7), 51.6 (7-OCH_3).

3,4-dihydroxyl benzoate methyl **(Pam11)**: *m/z* 169 $[M+H]^+$; ^{1}H NMR (DMSO-d_6, 600 MHz): δ 7.42 (1H, d, J= 1.8 Hz, H-2), 6.83 (1H, d, J= 7.8 Hz, H-5), 7.44 (1H, dd, J= 1.8, 7.8 Hz, H-6), 3.80 (3H, s, OCH_3) . ^{13}C NMR (DMSO-d_6, 125 MHz): δ 121.6 (C-1), 123.4 (C-2), 151.1 (C-3), 163.2 (C-4), 112.7 (C-5), 115 (C-6), 167.1 (C-7), 55.5 (7-OCH_3).

4-hydroxy benzoic acid **(Pam12)**: *m/z* 139 $[M+H]^+$; ^{1}H NMR (DMSO-d_6, 600 MHz): δ 7.77 (1H, d, J = 9.0 Hz, H-2,6), 6.80 (1H, d, J = 9.0 Hz, H-3,5) . ^{13}C NMR (DMSO-d_6, 125 MHz): δ 121.3 (C-1), 131.6 (C-2), 115.5 (C-3), 161.5 (C-4), 115.5 (C-5), 131.6 (C-6), 167.1 (C-7).

Methyl 4-hydroxy-3-methoxybenzoate **(Pam13)**: *m/z* 183 $[M+H]^+$; ^{1}H NMR (CD_3OD, 600 MHz): δ 7.54 (1H, d, J= 1.8 Hz, H-2,6), 6.83 (1H, d, J= 8.4 Hz, H-5), 7.54 (1H, dd, J= 8.4, 1.8 Hz, H-2,6), 3.87 (3H, s, OCH_3), 3.90 (3H, s, OCH_3). ^{13}C NMR (CD_3OD, 125 MHz): δ 121.6 (C-1), 125.2 (C-2), 149.2 (C-3), 154.4 (C-4), 113.5 (C-5), 116.3 (C-6), 168.9 (C-7), 52.3 (3-OCH_3), 56.4 (7-OCH_3).

Methyl syringate **(Pam14)**: *m/z* 213 $[M+H]^+$; ^{1}H NMR (CD_3OD, 600 MHz): δ 7.34 (2H, s, H-2,6), 3.89 (6H, s, 3,5-OCH_3), 3.89 (3H, s, 7-OCH_3). ^{13}C NMR (CD_3OD, 125 MHz): δ 121.37 (C-1), 108.1 (C-2), 148.94 (C-3), 141.94 (C-4), 148.94 (C-5), 108.1 (C-6), 168.63 (C-7), 56.8 (3,5-OCH_3), 52.5 (7-OCH_3).

Vanillin **(Pam15)**: ESI-MS: *m/z* 153 $[M+H]^+$; ^{1}H NMR (DMSO-d_6, 600 MHz): δ 7.38 (1H, d, J = 1.8 Hz, H-2); 6.96 (1H, d, J = 8.4 Hz, H-5); 7.43 (1H, dd, J = 8.4, 1.8 Hz, H-6); 9.77 (1H, s, H-7); 3.92 (3H, s, 3-OCH_3); 10.24 (1H, brs, 4-OH); ^{13}C NMR ($CDCl_3$, 150 MHz): δ 128.7 (C-1); 126.0 (C-2); 148.2 (C-3); 153.0 (C-4); 110.7 (C-5); 115.4 (C-6); 191.0 (C-7); 55.6 (3-OCH_3).

n-butyl D-galactopyranoside (**Pam16**): *m/z* 237 $[M+H]^+$; ^1H NMR ($CDCl_3$, 600 MHz): δ 4.75 (1H, d, J = 3.6 Hz, H-1), 3.78 (1H, dd, J = 3.6, 6.0 Hz, H-2), 3.73 (1H, m, H-3), 3.68 (1H, m, H-4), 3.57 (1H, m, H-5), 3.50 (2H, m, H-6), 3.42 (2H, m, H-1'), 1.59 (2H, m, H-2'), 1.40 (2H, m, H-3'), 1.40 (3H, t, J = 7.8 Hz, H-3'). ^{13}C NMR ($CDCl_3$, 125 MHz): δ 99.7 (C-1), 75.3 (C-2), 73.5 (C-3), 73.2 (C-4), 71.9 (C-5), 68.1 (C-6), 62.8 (C-1'), 32.4 (C-2'), 20.1 (C-3'), 14.1 (C-4').

6.4.2. Structure elucidation of the isolated compounds

From the non-alkaloid fraction, 16 compounds were isolated, and their structures (Figure 3) were elucidated using spectroscopy methods.

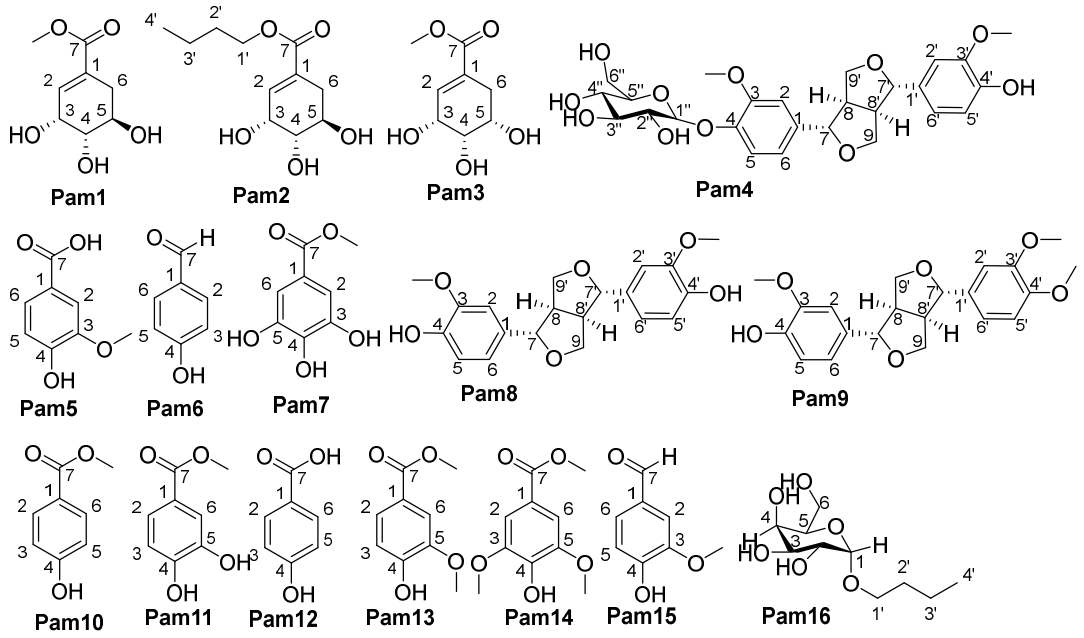

Figure 6.3. Structures of isolated compounds from the phenolic enrichments of P. amaryllifolius leaves

6.4.2.1. Compound Pam1: Methyl shikimate

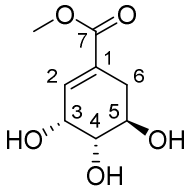

Figure 6.4. The structure of methyl shikimate (Pam1)

Compound **Pam1** was obtained as a white amorphous solid. The ESI-MS spectrum of **Pam1** showed peaks at *m/z* 189 $[M+H]^+$, allowing the determination of the molecular weight of 188 Da. The ^1H-NMR spectrum showed the signals of three oximethine sp^3 protons at δ_H 4.24 (1H, m, H-3), 3.85 (1H, m, H-4), 3.58 (1H, m, H-5), one methylene

group at δ_H 2.07 (1H, dd, J = 2.4, 18.0 Hz, H-6) and 2.41 (1H, dd, J = 3.6, 18.0 Hz, H-6), one methoxy group at δ_H 3.67 (3H, s, 7-OCH_3), an olefine proton at δ_H 6.61 (1H, d, J = 1.8 Hz, H-2), and three hydroxy protons at 4.82 (2H, brs, 3,5-OH) and 4.60 (1H, brs, 4-OH). The ^{13}C NMR spectrum showed three sp^3 oximethine signals at δ_C 66.8 (C-3), 70.0 (C-4), and 65.4 (C-5), two olefinic carbons at δ_C 127.3 (C-1) and 139.7 (C-2), and a methoxy group at 51.5 (7-OCH_3). Compound **Pam1** was determined as methyl shikimate by comparing its NMR data to the literature. [65].

6.4.2.2. Compound Pam2: n-butyl shikimate

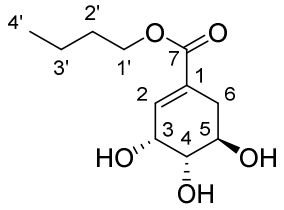

Figure 6.5. The structure of n-butyl shikimate (Pam2)

Compound **Pam2** was obtained as a white amorphous solid. The ESI-MS spectrum of **Pam2** showed peaks at *m/z* 231 $[M+H]^+$. The ^1H-NMR spectrum exhibited the signals of three oximethine sp^3 protons at δ_H 4.30 (1H, brs), 3.62 (1H, m), 3.93 (1H, m), two methylene signals at δ_H 2.62 (1H, m, H-6a), 2.13 (1H, m, H-6b), an olefine proton at δ_H 6.61 (1H, d, J = 1.2 Hz, H-2). The ^{13}C NMR spectrum showed three sp^3 oximethine signals at δ_C 65.4 (C-3), 70.1 (C-4), 66.8 (C-5), two olefine carbons at δ_C 127.6 (C-1) and 139.4 (C-2), and signals of an n-butyl fragment at δ_C 63.6 (C-1'), 30.2 (C-2'), 18.7 (C-3'), 13.5 (C-4'). Compound **Pam2** was determined as n-butyl shikimate by comparing its NMR data to the reported literature [66].

6.4.2.3. Compound Pam3: 5-epi-shikimate methyl

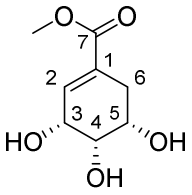

Figure 6.6. The structure of 5-epi-shikimate methyl (Pam3)

Compound **Pam3** was obtained as a white amorphous solid. The ESI-MS spectrum of **Pam3** showed peaks at *m/z* 231 $[M+H]^+$. The ^1H-NMR spectrum showed three oximethine sp^3 protons at δ_H 4.63 (1H, m, H-3), 3.49 (1H, m, H-4), 3.45 (1H, m, H-5), two signals of a methylene group at δ_H 2.13 (1H, dd, J = 9.0, 18.0 Hz, H-6a) and 2.61 (1H, dd, J = 4.8, 18.0 Hz, H-6b) , one methoxy group at δ_H 3.67 (3H, s, 7-OCH_3),an

olefine proton at δ_H 6.61 (1H, d, J = 1.8 Hz, H-2), and two hydroxy protons at 4.78 (2H, brs, 3,5-OH) and 4.58 (1H, brs, 4-OH). The ^{13}C NMR spectrum showed three sp^3 oximethine signals at δ_C 66.6 (C-3), 77.0 (C-4), and 61.5 (C-5), two olefin carbons at δ_C 129.2 (C-1) and 136.4 (C-2), and a methoxy group at 52.0 (7-OCH_3). ESI-MS and NMR data of compound **Pam3** were highly similar to those of compound **Pam1**. By comparing to the reference data, compound **Pam3** was determined as 5-*epi*-shikimate methyl [67].

6.4.2.4. Compound Pam4: Pinoresinol 4-O-β-D-glucoside

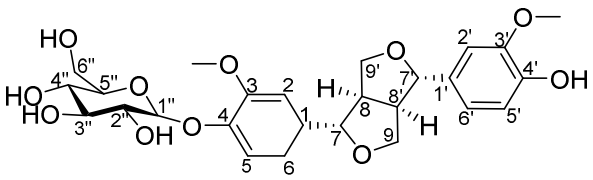

Figure 6.7. The structure of pinoresinol 4-O-β-D-glucoside (Pam4)

Compound **Pam4** was obtained as a white powder. The molecular weight of **Pam4** was 520 Da by the ESI-MS spectrum at m/z 521 $[M+H]^+$, and m/z 1041 $[2M+H]^+$.

The ^{1}H-NMR spectrum indicated two ABX systems at δ_H 7.05 (1H, d, J = 2.4 Hz, H-2), 7.17 (1H, d, J = 9.0 Hz, H-5), 6.94 (2H, dd, J = 9.0; 2.4 Hz, H-6, H-6'), 6.97 (1H, d, J = 2.4 Hz, H-2'), 6.79 (1H, d, J = 9.0 Hz, H-5'); a sugar unit identified as *β*-D-glucopyranoside based on the anomeric proton signals at δ_H 4.91 (1H, d, J = 8.4 Hz, H-1") and other signals ranging from 3.30 ppm to 3.46 ppm; two methoxy groups δ_H 3.86 (3H, s, 3'-OMe) and 3.84 (3H, s, 3-OMe); and two oxygenated methine groups δ_H 4.73 (1H, d, J = 4.8 Hz, H-7'), 4.78 (1H, d, J = 4.8 Hz, H-7).

The ^{13}C-NMR spectrum and DEPT spectrum showed twenty-six carbon signals, in which 12 carbon signals at δ_C 111.6-151.0 (6 CH, 6 C) confirmed the presence of two ABX systems. In addition to the typical signals of *β*-D-glucopyranoside at δ_C 102.9 (C-1"); 77.9 (C-3"); 74.9 (C-2"); 71.4 (C-4"); 78.2 (C-5"); 62.5 (C-6"), in the ^{13}C NMR spectrum, there were signals of two methine groups, two methylene groups attached to oxygen, respectively at δ_C 87.4 (C-7); 87.1 (C-7′); 72.7 (C-9, C-9′), and two methoxy groups at δ_C 56.8 (3'-OMe); 56.4 (3-OMe).

The spectral data of **Pam4** have many similarities with those of **Pt3**, except for an additional sugar unit, *β-D*-glucopyranoside. In conclusion, the structure of **Pam4** was

determined to be pinoresinol 4-*O-β-D*-glucopyranoside by comparison of spectral data with those reported in the literature [57].

6.4.2.5. *Compound Pam5: Vanillic acid*

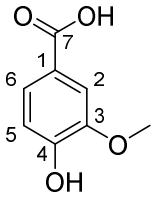

Figure 6.8. The structure of vanillic acid (Pam5)

Compound **Pam5** was obtained as a white amorphous solid. The ESI-MS spectrum exhibited a molecular ion peak at *m/z* 169 $[M+H]^+$, corresponding to a molecular weight of 168 Da. The ^{1}H NMR spectrum of **Pam5** showed signals of an aromatic ABX system at δ_H 7.58 (1H, d, J = 2.4 Hz, H-2), 6.85 (1H, d, J = 9.0 Hz, H-5), and 7.57 (1H, dd, J = 9.0, 2.4 Hz, H-6), along with a methoxy signal at δ_H 3.92 (3H, s, OCH_3). The ^{13}C NMR and DEPT spectra displayed a carboxyl carbon at δ_C 170.0 (C-7), three aromatic methine carbons at δ_C 125.3 (C-2), 113.9 (C-5), and 115.9 (C-6), two oxygenated aromatic carbons at δ_C 148.7 (C-3) and 154.6 (C-4), and a methoxy carbon at δ_C 56.4 (3-OCH_3). Based on these spectroscopic data and comparison with reference values, compound **Pam5** was identified as vanillic acid [68].

6.4.2.6. Compound Pam6: p-hydroxybenzaldehyde

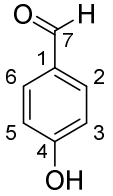

Figure 6.9. The structure of p-hydroxybenzaldehyde (Pam6)

Compound **Pam6** was obtained as a white amorphous solid with a molecular weight of 122 Da, as determined from the ion peak at m/z 123 $[M+H]^+$ in the ESI-MS spectrum. The ^{1}H NMR spectrum of compound **Pam6** showed signals corresponding to an aromatic A_2B_2 system at δ_H 6.88 (2H, d, J = 7.2 Hz, H-2,6) and 7.76 (2H, d, J = 7.2 Hz, H-3,5), together with an aldehydic proton signal at δ_H 9.72 (1H, s, H-7). The ^{13}C NMR and DEPT spectra revealed an aldehyde carbon at δ_C 191.8 (C-7), aromatic methine carbons at δ_C 132.8 (C-2,6) and 116.5 (C-3,5), and an oxygenated aromatic

carbon at δ_C 163.9 (C-4). Comparison of these spectroscopic data with literature values led to the identification of compound **Pam6** as *p*-hydroxybenzaldehyde [69].

6.4.2.7. Compound Pam7: Methyl gallate

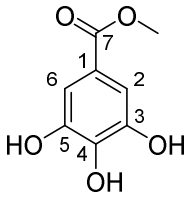

Figure 6.10. The structure of methyl gallate (Pam7)

Compound **Pam7** was obtained as a white amorphous solid. The ESI-MS spectrum displayed a molecular ion peak at m/z 185 $[M+H]^+$, corresponding to a molecular weight of 184 Da. The ^{1}H NMR spectrum of compound **Pam7** showed signals of two equivalent aromatic protons at δ_H 7.06 (2H, s, H-2,6) and a methoxy group at δ_H 3.83 (3H, s, 7-OCH_3). The ^{13}C NMR and DEPT spectra revealed aromatic methine carbons at δ_C 110.1 (C-2,6), oxygenated aromatic carbons at δ_C 146.5 (C-3,5), a quaternary oxygenated aromatic carbon at δ_C 139.8 (C-4), and a methoxy carbon at δ_C 52.3 (7-OCH_3). Comparison of these NMR data with reference values confirmed the identity of compound **Pam7** as methyl gallate [70].

6.4.2.8. Compound Pam10: methyl 4-hydroxybenzoate

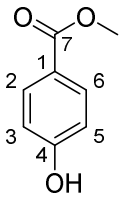

Figure 6.11. The structure of methyl 4-hydroxybenzoate (Pam10)

Compound **Pam10** was isolated as a white powder. The ESI-MS spectrum illustrated a molecular peak at *m/z* 153 $[M+H]^+$. The ^{1}H-NMR spectrum of the compound exhibited the presence of an A_2B_2 benzene moiety at δ_H 7.81 (1H, d, J = 6.6 Hz, H-2,6), 6.84 (1H, d, J = 6.6 Hz, H-3,5), and a methoxy group at δ_H 3.78 (3H, s, OCH_3). The ^{13}C NMR spectrum showed six signals of an A_2B_2 phenyl group at δ_C 120.2 (C-1), 131.3 (C-2), 115.3 (C-3), 161.9 (C-4), 115.3 (C-5), 131.3 (C-6), a carboxylate and a methoxy group at δ_C 166.0 (C-7), 51.6 (7-OCH_3), respectively. These data were highly in agreement with those of methyl 4-hydroxybenzoate in the literature [71]. Thus, compound **Pam10** could be determined as methyl 4-hydroxybenzoate.

6.4.2.9. Compound Pam11: 3,4-dihydroxyl benzoate methyl

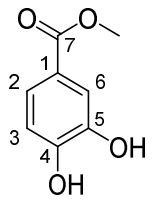

Figure 6.12. The structure of 3,4-dihydroxyl benzoate methyl (Pam11)

Compound **Pam11** illustrated a molecule peak at *m/z* 169 $[M+H]^+$ on the ESI-MS spectrum. The ^{1}H-NMR spectrum of compound **Pam11** exhibited the presence of an ABX aromatic moiety at δ_H 7.42 (1H, d, *J* = 1.8 Hz, H-2), 6.83 (1H, d, *J*= 7.8 Hz, H-5), 7.44 (1H, d, *J*= 1.8, 7.8 Hz, H-6), and a methoxy group at δ_H 3.80 (3H, s, OCH_3). The ^{13}C NMR spectrum showed six signals of an ABX dihydroxy benzene moiety at δ_C 121.6 (C-1), 123.4 (C-2), 151.1 (C-3), 163.2 (C-4), 112.7 (C-5), 115 (C-6), and a methyl carboxylate moiety at δ_C 167.1 (C-7) and 55.5 (7-OCH_3). Compound **Pam11** was identified as 3,4-dihydroxyl benzoate methyl by comparing the spectroscopy data with the reference [72].

6.4.2.10. Compound Pam12: 4-hydroxy benzoic acid

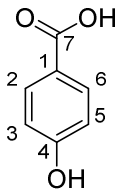

Figure 6.13. The structure of 4-hydroxy benzoic acid (Pam12)

Compound **Pam12** was isolated as a white solid. The ESI-MS spectrum showed a molecular peak at *m/z* 139 $[M+H]^+$. The ^{1}H-NMR spectrum of the compound exhibited the presence of an A_2B_2 benzene moiety at δ_H 7.77 (1H, d, *J* = 9.0 Hz, H-2,6), 6.80 (1H, d, *J* = 9.0 Hz, H-3,5), which was like **Pam10**. The ^{13}C NMR spectrum also showed six signals of an A_2B_2 phenyl group at δ_C 121.3 (C-1), 131.6 (C-2), 115.5 (C-3), 161.5 (C-4), 115.5 (C-5), 131.6 (C-6), and a carboxyl group at δ_C 167.1 (C-7). However, the NMR data of **Pam12** did not show any signals of the methoxy group, as in the spectra of **Pam10**. These were also proved via the decrease of a methyl group on the molecular weight. Thus, the compound could be determined as methyl 4-hydroxybenzoic acid [73].

6.4.2.11. Compound Pam13: methyl 4-hydroxy-3-methoxybenzoate

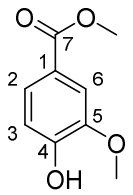

Figure 6.14. The structure of methyl 4-hydroxy-3-methoxybenzoate (Pam13)

Compound **Pam13** illustrated a molecule peak at *m/z* 183 $[M+H]^+$ on the ESI-MS spectrum. The ^{1}H-NMR spectrum of compound **Pam13** exhibited the presence of an ABX aromatic moiety at δ_H 7.42 (1H, d, *J*= 1.8 Hz, H-2), 6.83 (1H, d, *J*= 7.8 Hz, H-5), 7.44 (1H, dd, *J*= 1.8, 7.8 Hz, H-6), and two methoxy group at δ_H 3.87 (3H, s, OCH_3), 3.90 (3H, s, OCH_3). The ^{13}C NMR spectrum showed six signals of an ABX dihydroxy benzene moiety at δ_C 121.6 (C-1), 125.2 (C-2), 149.2 (C-3), 154.4 (C-4), 113.5 (C-5), 116.3 (C-6), a carboxylate group at δ_C 168.9 (C-7) and two methoxy group at δ_C 52.3 (3-OCH_3), 56.4 (7-OCH_3). These were highly similar to those of compound 5, with the addition of a methoxy group. Compound **Pam13** was identified as methyl 4-hydroxy-3-methoxybenzoate by comparing the spectroscopy data with the reference [74]

6.4.2.12. Compound Pam14: methyl syringate

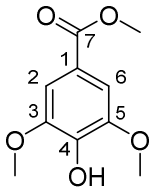

Figure 6.15. The structure of methyl syringate (Pam14)

Compound **Pam14** was obtained as a white amorphous solid. The ESI-MS spectrum of **Pam14** showed peaks at *m/z* 213 $[M+H]^+$. The ^{1}H-NMR spectrum showed signals of two meta-aromatic protons at δ_H 7.34 (2H, s, H-2,6) and three methoxy groups at δ_H 3.89 (6H, s, 3,5-OCH_3), 3.88 (3H, s, 7-OCH_3). The ^{13}C NMR spectrum illustrated six signals of a three-hydroxy aromatic moiety at δ_C 121.37 (C-1), 108.1 (C-2), 148.94 (C-3), 141.94 (C-4), 148.94 (C-5), 108.1 (C-6), a carboxylate group at δ_C 168.63 (C-7), and three methoxy groups at δ_C 56.8 (3,5-OCH_3), 52.5 (7-OCH_3). The compound was determined as methyl syringate by comparing its spectroscopy data to the previous report [75].

6.4.2.13. Compound Pam15: Vanillin

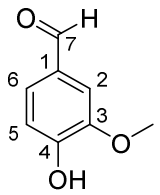

Figure 6.16. The structure of vanillin(Pam15)

Compound **Pam15** was obtained as a white amorphous solid. The ESI-MS spectrum exhibited a molecular ion peak at m/z 153 $[M+H]^+$, consistent with a molecular weight of 152 Da. The ^{1}H NMR spectrum of **Pam15** displayed characteristic signals of an aromatic ABX system at δ_H 7.38 (1H, d, J = 1.8 Hz, H-2), 6.96 (1H, d, J = 8.4 Hz, H-5), and 7.43 (1H, dd, J = 8.4, 1.8 Hz, H-6), together with a methoxy signal at δ_H 3.92 (3H, s, 3-OCH_3), a hydroxyl group signal at δH 10.24 (1H, brs, 4-OH), and an aldehydic proton signal at δ_H 9.77 (1H, s, H-7). The ^{13}C NMR and DEPT spectra showed an aldehyde carbon at δ_C 191.0 (C-7), three aromatic CH carbons at δ_C 126.0 (C-2), 110.7 (C-5), and 115.4 (C-6), two oxygenated aromatic carbons at δ_C 148.2 (C-3) and 153.0 (C-4), and a methoxy carbon at δ_C 55.6 (3-OCH_3). These spectral data suggested a benzaldehyde derivative. Comparison with reported data confirmed that compound **Pam15** was identified as vanillin [68].

6.4.2.14. Compound Pam16: n-butyl D-galactopyranoside

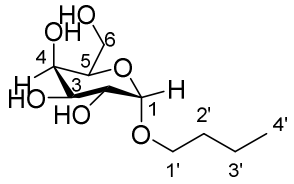

Figure 6.17. The structure of n-butyl D-galactopyranoside (Pam16)

Compound **Pam16** was obtained as a white amorphous solid. The ESI-MS spectrum of **Pam16** showed *m/z* 237 $[M+H]^+$. The ^{1}H-NMR spectrum showed the signal of an anomeric proton at δ_H 4.75 (1H, d, J= 3.6 Hz, H-1), together with four signals at δ_H 3.78 (1H, dd, J= 3.6, 6.0 Hz, H-2), 3.73 (1H, m, H-3), 3.68 (1H, m, H-4), 3.57 (1H, m, H-5), 3.50 (2H, m, H-6) of a sugar moiety, and signals of an oxidated n-butyl group at δ_H 3.42 (2H, m, H-1'), 1.59 (2H, m, H-2'), 1.40 (2H, m, H-3'), 1.40 (3H, t, J= 7.8 Hz, H-4'). The ^{13}C NMR spectrum exhibited signals of a galactose moiety at δ_C 99.7 (C-1), 75.3 (C-2), 73.5 (C-3), 73.2 (C-4), 71.9 (C-5), 68.1 (C-6), and an oxygenated n-butyl moiety at δ_C 62.8 (C-1'), 32.4 (C-2'), 20.1 (C-3'), 14.1 (C-4'). The compound was

determined as n-butyl D-galactopyranoside by comparing its NMR data to the previous study [76].

6.5. Bioactivities of extract and enrichments from the *P. amaryllifolius* leaves

Table 6.4. Free-radical scavenging effects of phenolic enrichment from P. amaryllifolius leaves

Sample	DPPH (IC_{50}, µg/mL)	Hydroxyl (IC_{50}, µg/mL)	NO inhibition (IC_{50}, µg/mL)
The phenolic enrichment	32.68 ± 2.93^{a}	40.20 ± 3.84^{e}	21.44 ± 2.61^{h}
The non-alkaloid fraction	28.75 ± 1.81^{b}	41.11 ± 3.76^{e}	57.61 ± 4.54^{i}
The alkaloid fraction	52.10 ± 4.26^{c}	82.35 ± 6.09^{f}	33.47 ± 2.92^{j}
Ascorbic acid *	24.65 ± 2.27^{d}	-	
Catechin **	-	32.27 ± 1.56^{g}	
Cardamonin#			2.98 ± 0.35^{k}

*, **, # Positive control

a-k: Data are expressed as mean ± SD. Means in each column with different letters are significantly different ($p < 0.05$).

The phenolic enrichment from *Pandanus amaryllifolius* leaves exhibited significant antioxidant and NO inhibition activities compared to both its derived alkaloid and non-alkaloid fractions, as well as the positive controls used in this study (Table 6.4). For DPPH and hydroxyl radical scavenging assays, the phenolic enrichment displayed IC_{50} values of 32.68 µg/mL and 40.20 µg/mL, respectively, which are close to the efficacy of ascorbic acid (IC_{50} of 24.65 µg/mL) and catechin (IC_{50} of 32.27 µg/mL), respectively. This suggests that the phenolic enrichment possesses potent free radical scavenging abilities, on par with well-known antioxidants. In terms of NO inhibition, the phenolic enrichment achieved an IC_{50} of 21.44 µg/mL, which, while not as potent as cardamonin (IC_{50} of 2.98 µg/mL), is markedly more effective than either the non-alkaloid fraction (57.61 µg/mL) or the alkaloid fraction (33.47 µg/mL). This indicates that while cardamonin serves as an exceptionally potent NO inhibitor, the phenolic enrichment's moderate yet significant inhibition points to a synergistic effect within the mixture, potentially due to the interplay between phenolic and alkaloid components.

The higher NO inhibition in the phenolic enrichment compared to its separated fractions suggests a synergistic interaction between phenolic and alkaloid compounds within the mixture, enhancing the NO inhibition capacity beyond what is observed in either fraction alone. Although individual compounds like cardamonin show stronger

inhibition, the phenolic enrichment still represents a balanced and effective option for reducing oxidative stress and inflammation, leveraging the combined effects of its components. This highlights the potential of using phenolic enrichment as a natural source of antioxidants and anti-inflammatory agents, with a broader range of bioactivity than isolated components.

6.6. Chapter summary

The optimized phenolic enrichment from *Pandanus amaryllifolius* leaves demonstrated substantial antioxidant and NO inhibition activities, surpassing the efficacy of its individual non-alkaloid and alkaloid fractions. The phenolic enrichment enhanced NO inhibition capacity suggests a synergistic interaction between its phenolic and alkaloid compounds, contributing to a broader range of bioactivity. While the enrichment exhibited significant antioxidant effects comparable to standard antioxidants like ascorbic acid and catechin, its NO inhibition effect, though less than cardamonin, was markedly superior to that of the isolated fractions. The phytochemical investigation of the phenolic enrichment from *P. amaryllifolius* leaves led to the isolation of 16 compounds, including 3 lignans and 9 benzoate derivatives, together with 3 shikimates and 1 glycoside. Except for 4-hydroxybenzoic acid **(Pam9)**, the other compounds were identified for the first time from the plant. These findings support the use of phenolic enrichment as a balanced and effective option for managing oxidative stress and inflammation, highlighting its potential as a multifunctional natural therapeutic agent.

CONCLUSION

This work expands the chemical and functional landscape of *Pandanus* by combining broad extract-level screening with focused isolation/characterization and process optimization. At the genus level, extract chemistries and bioactivities are highly species- and tissue-dependent: *P. tectorius* consistently emerged as a phenolic, saponin-rich, antioxidant-active taxon; *P. amaryllifolius* concentrated alkaloids with associated cytotoxicity. These comparative findings guided subsequent targeted studies and underscore the value of integrating chemical metrics with multiaxis bioassays.

From *P. tectorius* leaves, two new benzofuran epimers (Pandanusfurans A and B) and four lignans were elucidated. The lignans chiefly contributed to antioxidant capacity, whereas the benzofurans, while weaker antioxidants, approached acarbose in α-amylase inhibition and showed selective cytotoxicity toward A549 with little effect on K562, MCF7, and negligible NO inhibition. Given these modest yet multifaceted activities, the benzofurans are best viewed as preliminary scaffolds for further optimization rather than as immediate leads.

Process engineering of *P. tectorius* fruits demonstrated that extract composition and bioactivity can be predictably tuned. TPC-oriented conditions (higher ethanol, 80 °C) produced stronger radical-scavenging, whereas TSC-oriented conditions (lower ethanol, extended times) enhanced NO inhibition but at the highest saponin levels could introduce cytotoxicity in RAW 264.7 cells. The validated multi-response windows provide practical guidance for producing phenolic-rich, saponin-rich, or balanced extracts depending on intended use, while also highlighting safety considerations for highly saponin-enriched fractions.

For *P. amaryllifolius*, the optimized phenolic enrichment achieved antioxidant performance comparable to standard references and stronger NO suppression than separated fractions, consistent with synergistic contributions from phenolics and alkaloids. The accompanying compositional work catalogued multiple shikimate-derived and simple phenolic constituents, as well as a lignan glycoside, providing a basis for future standardization and quality control.

Overall, the thesis (i) delineates species-level chemical–bioactivity patterns across *Pandanus*, (ii) contributes two new benzofurans, and (iii) establishes statistically

validated extraction windows that reconcile yield, composition, bioactivity, and safety. Limitations include the largely in-vitro nature of activity data and the moderate potencies observed for many samples/isolates. Future work should prioritize structure–activity optimization of the benzofurans, *in vivo* efficacy and toxicity studies for phenolic- and saponin-enriched extracts (with attention to saponin-related cytotoxicity at higher doses), targeted standardization protocols for fruits or leaves preparations, and biosynthetic or chemotaxonomic investigations linking norisoprenoids to aroma and ecological function in *Pandanus*.

LIST OF THE PUBLICATIONS

A. SCIE journals

1) Do Hoang Giang et al. (2025) Optimization of the extraction conditions and evaluation of bioactivities of the phenolic enrichment from *Pandanus amaryllifolius* leaves. *Journal of Analytical Methods in Chemistry*, 2025, art.ID. 5256388.

2) Do Hoang Giang et al. (2025) Pandanusfuran A and B: two new benzofuran epimers from *Pandanus tectorius* leaves. *Journal of Chemistry*, 2025, art.ID. 5587982.

3) Do Hoang Giang et al. (2025) Optimization of Phenolic- and Saponin-Enriched Extraction from *Pandanus tectorius* Fruit Using Box–Behnken Design and Evaluation of Their Bioactivities. *Journal of Analytical Methods in Chemistry*, 2025, art.ID. 5539843.

B. Other international journals

4) Do Hoang Giang et al. (2025) Total phenolic and saponin content and α-amylase inhibition of marketed *Pandanus tectorius* fruits and leaves. *International Journal of Engineering Research and Development,* 21(9), pp. 90-95.

C. Vietnamese journals

5) Do Hoang Giang et al. (2024) Shikimate esters, megastigmane and glycoside from leaves of *Pandanus amaryllifolius*. *Journal of Tropical Science and Engineering*, 35(09-2024), pp. 82–88.

6) Do Hoang Giang et al. (2025) Phenolics from fruits of *Pandanus tectorius*. *HaUI Journal of Science and Technology*, 61(5B), pp. 92–96.

7) Do Hoang Giang et al. (2025) Phenolics from leaves of *Pandanus amaryllifolius*. *Journal of Tropical Science and Engineering*, 38(06-2025), pp. 122–127.

REFERENCES

1. Lim TK, "*Pandanus tectorius*," *Edible Medicinal And Non-Medicinal Plants: Volume 4, Fruits*, Ed., pp. 136-146, Springer Netherlands, Dordrecht, 2012.

2. Ho PH, *Plants of Vietnam*, Tre Publisher, Hanoi, 2003.

3. Loi DT, *Medicinal plants and remedies in Vietnam*, Y Hoc Publisher, Hanoi, 2004.

4. Do Huy Bich DQT, Bui Xuan Chuong, Nguyen Thuong Dong, Do Trung Dam, Pham Van Hien, Vu Ngoc Lo, Pham Duy Mai, Pham Kim Man, Doan Thi Nhu, Nguyen Tap,Tran Toan, *Medicinal plants and animals in Vietnam*, Science and Technology Publisher, 2006.

5. Cuong NM, Son NT, Van DT, Tram NCT, Thao DT, Su PQ, Thuan ND, "Isolation of natural products from fruits of *Pandanus odoratissimus* L.," *Vietnam Journal of Chemistry*, 53, 4, 432-435, 2015.

6. Inada A, Ikeda Y, Murata H, Inatomi Y, Nakanishi T, Bhattacharyya K, Kar T, Bocelli G, Cantoni A, "Unusual cyclolanostanes from leaves of *Pandanus boninensis*," *Phytochemistry*, 66, 23, 2729-2733, 2005.

7. Nguyen TP, Le TD, Minh PN, Dat BT, Pham NKT, Do TML, Nguyen DT, Mai TD, "A new dihydrofurocoumarin from the fruits of *Pandanus tectorius* Parkinson ex Du Roi," *Natural Product Research*, 30, 21, 2389-2395, 2016.

8. Hoa LTC, "Chemical compositions and bioactivities of *Pandanus tectorius* Parkinson. ex Du Roi leaves in Loc Binh, Phu Loc town, Thua Thien Hue province," Ed., Hanoi University of Education, Hanoi, 2013.

9. Zhang X, Guo P, Sun G, Chen S, Yang M, Fu N, Wu H, Xu X, "Phenolic compounds and flavonoids from the fruits of *Pandanus tectorius* Soland," *Journal of Medicinal Plants Research*, 6, 13, 2622-2626, 2012.

10. Suzuki R, Kan S, Sugita Y, Shirataki Y, "*p*-Coumaroyl Malate Derivatives of the *Pandanus amaryllifolius* Leaf and Their Isomerization," *Chemical and Pharmaceutical Bulletin*, 65, 12, 1191-1194, 2017.

11. Tri MD, Dung LT, An NH, Dat BT, "Chemical constituents of *Pandanus tectorius* Sol. fruits," *Natural Products Conference 3rd*, Ed., Ho Chi Minh City, 2012.

12. Mai DT, Le TD, Nguyen TP, Phan NM, Nguyen HA, Nguyen TTP, Tran LQ, "A new aldehyde compound from the fruit of *Pandanus tectorius* Parkinson ex Du Roi," *Natural Product Research*, 29, 15, 1437-1441, 2015.

13. Trang DTH, Trang PT, Phuong DM, Anh DH, Anh NQ, Van Kiem P, Viet PH, "The chemical composition from the fruits of *Pandanus* tonkinensis, their NO production inhibitory and lipid peroxidation inhibitory activities," *Vietnam Journal of Chemistry*, 61, S1, 1-7, 2023.

14. Byrne L, Bill G, Pang W, Vandes RB, Ramirez UC, White A, "The X-Ray Crystal-Structure of (+/-)-Pandamarine, the Major Alkaloid of *Pandanus amaryllifolius*," *Australian Journal of Chemistry*, 45, 11, 1903-1908, 1992.

15. Takayama H, Ichikawa T, Kitajima M, Nonato MG, Aimi N, "Isolation and Characterization of Two New Alkaloids, Norpandamarilactonine-A and -B, from

Pandanus amaryllifolius by Spectroscopic and Synthetic Methods," *Journal of Natural Products*, 64, 9, 1224-1225, 2001.

16. Takayama H, Ichikawa T, Kitajima M, Aimi N, Lopez D, Nonato MG, "A new alkaloid, pandanamine; finding of an anticipated biogenetic intermediate in *Pandanus amaryllifolius* Roxb," *Tetrahedron Letters*, 42, 16, 2995-2996, 2001.

17. Takayama H, Ichikawa T, Kitajima M, Nonato MG, Aimi N, "Isolation and Structure Elucidation of Two New Alkaloids, Pandamarilactonine-C and -D, from *Pandanus amaryllifolius* and Revision of Relative Stereochemistry of Pandamarilactonine-A and -B by Total Synthesis," *Chemical and Pharmaceutical Bulletin*, 50, 9, 1303-1304, 2002.

18. Tan MA, Kitajima M, Kogure N, Nonato MG, Takayama H, "Isolation of Pandamarilactonine-H from the Roots of *Pandanus amaryllifolius* and Synthesis of epi-Pandamarilactonine-H," *Journal of Natural Products*, 73, 8, 1453-1455, 2010.

19. Tan MA, Kitajima M, Kogure N, Nonato MG, Takayama H, "Isolation and total syntheses of two new alkaloids, dubiusamines-A, and -B, from *Pandanus dubius*," *Tetrahedron*, 66, 18, 3353-3359, 2010.

20. Cheng Y-B, Hu H-C, Tsai Y-C, Chen S-L, El-Shazly M, Nonato MG, Wu Y-C, Chang F-R, "Isolation and absolute configuration determination of alkaloids from *Pandanus amaryllifolius*," *Tetrahedron*, 73, 25, 3423-3429, 2017.

21. Cheng Y-B, Tsai Y-H, Lo I-W, Haung C-C, Tsai Y-C, Beerhues L, El-Shazly M, Hou M-F, Yuan S-S, Wu C-C, Chang F-R, Wu Y-C, "Pandalisines A and B, novel indolizidine alkaloids from the leaves of *Pandanus utilis*," *Bioorganic & Medicinal Chemistry Letters*, 25, 19, 4333-4336, 2015.

22. Tsai Y-C, Yu M-L, El-Shazly M, Beerhues L, Cheng Y-B, Chen L-C, Hwang T-L, Chen H-F, Chung Y-M, Hou M-F, Wu Y-C, Chang F-R, "Alkaloids from *Pandanus amaryllifolius*: Isolation and Their Plausible Biosynthetic Formation," *Journal of Natural Products*, 78, 10, 2346-2354, 2015.

23. Jong T-T, Chau S-W, "Antioxidative Activities of constituents Isolated from *Pandanus* odoratissimus," *Phytochemistry*, 49, 7, 2145-2148, 1998.

24. Huang Y, Chen J, Liu Z, Peng L, Qiao W, Li W, Guo D-a, "Pantelignans A-F, benzofuran sesquineolignan racemates from the roots and rhizomes of *Pandanus tectorius*: isolation, chiral resolution, and configurational assignment," *Journal of Molecular Structure*, 1338, art.ID. 142322, 2025.

25. Ghasemzadeh A, Jaafar HZE, "Profiling of phenolic compounds and their antioxidant and anticancer activities in pandan (*Pandanus amaryllifolius* Roxb.) extracts from different locations of Malaysia," *BMC Complementary and Alternative Medicine*, 13, 1, 341, 2013.

26. Ghasemzadeh A, Jaafar HZE, "Optimization of Reflux Conditions for Total Flavonoid and Total Phenolic Extraction and Enhanced Antioxidant Capacity in Pandan (*Pandanus amaryllifolius* Roxb.) Using Response Surface Methodology," *The Scientific World Journal*, 2014, 1, art.ID. 523120, 2014.

27. Andriani Y, Ramli NM, Syamsumir DF, Kassim MNI, Jaafar J, Aziz NA, Marlina L, Musa NS, Mohamad H, "Phytochemical analysis, antioxidant, antibacterial and

cytotoxicity properties of keys and cores part of *Pandanus tectorius* fruits," *Arabian Journal of Chemistry*, 12, 8, 3555-3564, 2019.

28. Balamurugan V, Raja K, Selvakumar S, Vasanth K, "Phytochemical screening, antioxidant, anti-diabetic and cytotoxic activity of leaves of *Pandanus* canaranus Warb," *Materials Today: Proceedings*, 48, 322-329, 2022.

29. Susanti EP, Rohman A, Setyaningsih W, "Dual Response Optimization of Ultrasound-Assisted Oil Extraction from Red Fruit (*Pandanus* conoideus): Recovery and Total Phenolic Compounds," *Agronomy*, 12, 2, art. ID. 523, 2022.

30. Raja GG, Vargheseb HS, Kotagiric S, Swamy V, "Evaluation of anti-cancer potential of aqueous extract of *Pandanus odoratissimus* (Y.Kimura) Hatus. forma ferreus, by in vivo ascitic tumor model in swiss albino mice," *Pharmacognosy Journal*, 6, 1, 57-62, 2014.

31. Raj GG, Varghese HS, Kotagiri S, Vrushabendra Swamy BM, Swamy A, Pathan RK, "Anticancer Studies of Aqueous Extract of Roots and Leaves of *Pandanus* Odoratissimus f. ferreus (Y. Kimura) Hatus: An In Vitro Approach," *Journal of Traditional and Complementary Medicine*, 4, 4, 279-284, 2014.

32. Nuringtyas TR, Pratama Y, Wahyuono S, Moeljopawiro S, "Cytotoxicity of Buah Merah (*Pandanus conoideus* Lamk.) Extract on Breast Cancer Cell Line (T47D)," *Indonesian Journal of Biotechnology*, 19, 1, 71-78, 2014.

33. Rahmawati DY, Anggraini W, Djamil MS, "Cytotoxicity of Red Fruit Ethyl Acetate Extract (*Pandanus* conoideus Lam.) on Squamous Cell Carcinoma Cell Line (HSC-3)," *Scientific Dental Journal*, 5, 1, 42-46, 2021.

34. Kholieqoh AH, Kassim MNI, Sifzizul T, Muhammad T, Anam K, Sung YY, Amir H, Praja HN, Andriani Y, "SNEDDS to improve the bioactivities of *Pandanus tectorius* leaves: Optimization, antioxidant, and anticancer activities via apoptosis induction in human cervical cancer cell line," *Journal of Applied Pharmaceutical Science*, 14, 10, 175-189, 2024.

35. Rajeswari J, Kesavan K, Jayakar B, "Phytochemical and pharmacological evaluation of prop roots of *Pandanus* fascicularis Lam," *Asian Pacific Journal of Tropical Medicine*, 4, 8, 649-653, 2011.

36. Panda P, Panda DP, Panda PK, Nayak SS, "Antinociceptive and anti-inflammatory activities of *Pandanus* fascicularis Lamk. leaves in animal models," *Oriental pharmacy and experimental medicine*, 7, 5, 485-493, 2008.

37. Adkar PP, Bhaskar VH, "*Pandanus* odoratissimus (Kewda): A Review on Ethnopharmacology, Phytochemistry, and Nutritional Aspects," *Advances in Pharmacological and Pharmaceutical Sciences*, 2014, 1, art. ID. 120895, 2014.

38. Londonkar R, Kamble A, Reddy VC, "Anti-Inflammatory Activity of *Pandanus* odoratissimus Extract," *International Journal of Pharmacology*, 6, 3, 311-314, 2010.

39. Wilairat M, Rotpenpian N, "*Pandanus amaryllifolius* ethanolic extract promotes oral gingival fibroblast healing and inhibits Porphyromonas gingivalis: An in-vitro study," *Journal of Oral Biology and Craniofacial Research*, 15, 5, 919-924, 2025.

40. Mardiyaningsih A, Aini R, "Development of *Pandanus amaryllifolius* Roxb Leaves Extract as Antibacterial Agent," *Pharmaciana*, 4, 2, 185-192, 2014.

41. Damayanti L, Evaangelina IA, Laviana A, Herdiyati Y, Kurnia D, "Antibacterial Activity of Buah Merah (*Pandanus conoideus* Lam.) Against Bacterial Oral Pathogen of *Streptococcus sanguinis* ATCC10556, *Streptococcus mutans* ATCC 25175, and *Enterococcus faecalis* ATCC 29212: An *in Vitro* Study," *The Open Dentistry Journal*, 14, 113-119, 2020.

42. Herdiyati Y, Atmaja HE, Satari MH, Kurnia D, "Potential Antibacterial Flavonoid from Buah Merah (*Pandanus conodieus* Lam.) Against Pathogenic Oral Bacteria of Enterococcus faecalis ATCC 29212," *The Open Dentistry Journal*, 14, 433-439, 2020.

43. Wahyuni DK, Nuha GA, Atere TG, Kharisma VD, Tari VS, Rahmawati CT, Murtadlo AAA, Syukriya AJ, Wacharasindu S, Prasongsuk S, Purnobasuki H, "Antimicrobial potentials of *Pandanus amaryllifolius* Roxb.: Phytochemical profiling, antioxidant, and molecular docking studies," *PLOS ONE*, 19, 8, e0305348, 2024.

44. Sutarto POM, Naliani S, Vinna Kurniawati Sugiaman, Wibisono JAV, "Antibacterial effectiveness of red fruit extract (*Pandanus conoideus* Lam) against S.mutans as an acrylic resin based denture cleaner," *Makassar Dental Journal*, 12, 1, 43-48, 2023.

45. Anirudhan A, Iryani MTM, Andriani Y, Sorgeloos P, Tan MP, Wong LL, Mok WJ, Ming W, Yantao L, Lau CC, Sung YY, "The effects of *Pandanus tectorius* leaf extract on the resistance of White-leg shrimp Penaeus vannamei towards pathogenic Vibrio parahaemolyticus," *Fish and Shellfish Immunology Reports*, 4, 100101, 2023.

46. Fattahi S, Zabihi E, Abedian Z, Pourbagher R, Motevalizadeh Ardekani A, Mostafazadeh A, Akhavan-Niaki H, "Total Phenolic and Flavonoid Contents of Aqueous Extract of Stinging Nettle and In Vitro Antiproliferative Effect on Hela and BT-474 Cell Lines," *International Journal of Molecular and Cellular Medicine*, 3, 2, 102-107, 2014.

47. Vietnam Ministry of Health, *Vietnamese Pharmacopoeia V*, Medical Publishing House, Ha Noi, Vietnam, 2017.

48. Le AV, Parks SE, Nguyen MH, Roach PD, "Improving the Vanillin-Sulphuric Acid Method for Quantifying Total Saponins," *Technologies*, 6, 3, art.ID. 84, 2018.

49. Brand-Williams W, Cuvelier ME, Berset C, "Use of a free radical method to evaluate antioxidant activity," *LWT - Food Science and Technology*, 28, 1, 25-30, 1995.

50. Thuong PT, Su ND, Ngoc TM, Hung TM, Dang NH, Thuan ND, Bae KH, Oh WK, "Antioxidant activity and principles of Vietnam bitter tea *Ilex kudingcha*," *Food Chemistry*, 113, 1, 139-145, 2009.

51. Sudha P, Zinjarde SS, Bhargava SY, Kumar AR, "Potent α-amylase inhibitory activity of Indian Ayurvedic medicinal plants," *BMC Complementary and Alternative Medicine*, 11, 1, 5, 2011.

52. Trang DT, Hoang TKV, Nguyen TTM, Van Cuong P, Dang NH, Dang HD, Nguyen Quang T, Dat NT, "Essential Oils of Lemongrass (Cymbopogon citratus Stapf) Induces Apoptosis and Cell Cycle Arrest in A549 Lung Cancer Cells," *BioMed Research International*, 2020, 1, art.ID. 5924856, 2020.

53. Phuong TTT, Dang NH, Anh NTH, Giang DH, Dat NT, "A New Megastigmane Glycoside and Other Constituents from *Amomum muricarpum* Elmer," *Records of Natural Products*, 17, 1, 184-188, 2023.

54. Niu S, Liu QM, Xia JM, Xie CL, Luo ZH, Shao ZZ, Liu GM, Yang XW, "Polyketides from the Deep-Sea-Derived Fungus *Graphostroma* sp. MCCC 3A00421 Showed Potent Antifood Allergic Activities," *Journal of Agricultural and Food Chemistry*, 66, 6, 1369-1376, 2018.

55. M. RT, G. RC, N. PJ, "Synthesis and absolute configuration of the four possible stereoisomers of prandiol," *Tetrahedron: Asymmetry*, 13, 11, 1147-1152, 2002.

56. Ricardo TM, Raúl CG, Santos S, Norma F, Pedro JN, "Isolation, Total Synthesis, and Relative Stereochemistry of a Dihydrofurocoumarin from *Dorstenia contrajerva*," *Journal of Natural Products*, 61, 10, 1216-1220, 1998.

57. Casabuono A, Pomillo A, "Lignans and a stilbene from *Festuca argentina*," *Phytochemistry*, 35, 2, 479-483, 1994.

58. Roy SC, Rana KK, Guin C, "Short and Stereoselective Total Synthesis of Furano Lignans (±)-Dihydrosesamin, (±)-Lariciresinol Dimethyl Ether, (±)-Acuminatin Methyl Ether, (±)-Sanshodiol Methyl Ether, (±)-Lariciresinol, (±)-Acuminatin, and (±)-Lariciresinol Monomethyl Ether and Furofuran Lignans (±)-Sesamin, (±)-Eudesmin, (±)-Piperitol Methyl Ether, (±)-Pinoresinol, (±)-Piperitol, and (±)-Pinoresinol Monomethyl Ether by Radical Cyclization of Epoxides Using a Transition-Metal Radical Source," *The Journal of Organic Chemistry*, 67, 10, 3242-3248, 2002.

59. Yang M, Xu X, Xie C, Xie Z, Huang J, Yang D, "Separation and Purification of Arctiin, Arctigenin, Matairesinol, and Lappaol F from *Fructus arctii* by High-Speed Counter-Current Chromatography," *Separation Science and Technology*, 48, 11, 1738-1744, 2013.

60. Urones JG, De Pascual Teresa J, Marcos S, Martín D, "Ent-isolariciresinol in *Reseda suffruticosa*," *Phytochemistry*, 26, 5, 1540-1541, 1987.

61. Callmander MW, Booth TJ, Beentje H, Buerki S, "Update on the systematics of Benstonea (Pandanaceae): When a visionary taxonomist foresees phylogenetic relationships," *Phytotaxa*, 112, 2, 57-60, 2013.

62. Inada A, Morimoto C, Yoshikawa T, Inatomi Y, Murata H, "24-Ethyl,24-methyl-29-nor-lanostanes from Leaves of *Freycinetia formosana*," *Chemical and Pharmaceutical Bulletin*, 57, 11, 1303-1304, 2009.

63. Laluces HMC, Nakayama A, Nonato MG, Cruz TEd, Tan MA, "Antimicrobial alkaloids from the leaves of *Pandanus amaryllifolius*," *Journal of Applied Pharmaceutical Science*, 5, 10, 151-153, 2015.

64. Doncheva T, Kostova N, Toshkovska R, Philipov S, Vu N, Nguyen D, Nguyen T, Do G, Dang H, "Alkaloids from *Pandanus amaryllifolius* and *Pandanus tectorius* from Vietnam and Their Anti-inflammatory Properties," *Proceedings of the Bulgarian Academy of Sciences*, 75, 6, 812-820, 2022.

65. Huang J, Chen F-E, "An Efficient Synthesis of a Potential (−)-Reserpine Intermediate from (−)-Shikimic Acid of the Chiral Pool," *Helvetica*, 90, 7, 1366-1372, 2007.

66. Chen J, Chen J-J, Yang L-Q, Hua L, Gao K, "Labdane Diterpenoids and Shikimic Acid Derivatives from *Araucaria cunninghamii*," *Planta Med*, 77, 05, 485-488, 2011.

67. Campbell MM, Kaye AD, Sainsbury M, Yavarzadeh R, "Brief syntheses of (±)-methyl shikimate, (±)-methyl epishikimate and structural variants," *Tetrahedron*, 40, 13, 2461-2470, 1984.

68. Challice JS, Loeffler RST, Williams AH, "Structure of calleryanin and its benzylic esters from Pyrus and Prunus," *Phytochemistry*, 19, 11, 2435-2437, 1980.

69. Magano J, Chen MH, Clark JD, Nussbaumer T, "2-(Diethylamino)ethanethiol, a New Reagent for the Odorless Deprotection of Aromatic Methyl Ethers," *The Journal of Organic Chemistry*, 71, 18, 7103-7105, 2006.

70. Subramanian R, Chandra M, Yogapriya S, Aravindh S, Ponmurugan K, "Isolation of Methyl Gallate from Mango Twigs and its Anti-biofilm Activity," *Journal of Biologically Active Products from Nature*, 6, 5-6, 383-392, 2016.

71. Liu S, Sun C, Ha Y, Ma M, Wang N, Zhou Y, Zhang Z, "Novel antibacterial alkaloids from the Mariana Trench-derived actinomycete Streptomyces sp. SY2255," *Tetrahedron Letters*, 137, 154935, 2024.

72. Degotte G, Pendeville H, Di Chio C, Ettari R, Pirotte B, Frédérich M, Francotte P, "Dimeric polyphenols to pave the way for new antimalarial drugs," *RSC Medicinal Chemistry*, 14, 4, 715-733, 2023.

73. Lin Z, Fang Y, Huang A, Chen L, Guo S, Chen J, "Chemical constituents from Sedum aizoon and their hemostatic activity," *Pharmaceutical Biology*, 52, 11, 1429-1434, 2014.

74. Xia Z, Khaled O, Mouriès-Mansuy V, Ollivier C, Fensterbank L, "Dual Photoredox/Gold Catalysis Arylative Cyclization of o-Alkynylphenols with Aryldiazonium Salts: A Flexible Synthesis of Benzofurans," *The Journal of Organic Chemistry*, 81, 16, 7182-7190, 2016.

75. Ha TTT, Dung NT, Trung KH, Tai BH, Kiem PV, "Phytochemical constituents from the rhizomes of *Kaempferia parviflora* Wall. ex Baker and their acetylcholinesterase inhibitory activity," *Natural Product Research*, 38, 6, 994-1001, 2024.

76. Wang Y, Renault L, Guégan J-P, Benvegnu T, "Direct Conversion of Agarose into Alkyl Mono- and Disaccharide Surfactants Based on 3,6-Anhydro L- and D-Galactose Units," *Chemistry Select*, 6, 3, 389-395, 2021.

APPENDIX

Supplementary tables

Table S1. Kruskal-Wallis test with Benjamini–Hochberg FDR-adjusted p-values for differences in TPC, TFC, TSC, TAC contents of Pandanus tectorius leaves, Pandanus tectorius fruits, and Pandanus amaryllifolius leaves extracts.

variable	n	statistic	df	p	dunn_pairs	dunn_min_padj
TPC	18	13.56090226	2	**0.00114**	3	0.000886114

Dunn post-hoc (BH) for TPC

variable	group1	group2	n1	n2	statistic	p	p.adj
TPC	PaL	PtF	6	5	3.619326116	0.000295371	**0.0009**
TPC	PaL	PtL	6	7	2.380881048	0.017271288	**0.0259**
TPC	PtF	PtL	5	7	-1.480702942	0.13868575	0.1387

variable	n	statistic	df	p	dunn_pairs	dunn_min_padj
TFC	18	11.61203008	2	**0.00301**	3	0.006584747

Dunn post-hoc (BH) for TFC

variable	group1	group2	n1	n2	statistic	p	p.adj
TFC	PaL	PtF	6	5	3.062506713	0.002194916	**0.0066**
TFC	PaL	PtL	6	7	2.813768511	0.004896447	**0.0073**
TFC	PtF	PtL	5	7	-0.493567647	0.621611554	0.6216

variable	n	statistic	df	p	dunn_pairs	dunn_min_padj
TSC	18	13.89774436	2	**0.00096**	3	0.00069643

Dunn post-hoc (BH) for TSC

variable	group1	group2	n1	n2	statistic	p	p.adj
TSC	PaL	PtF	6	5	3.681194938	0.000232143	**0.0007**
TSC	PaL	PtL	6	7	2.332782441	0.019659567	**0.0295**
TSC	PtF	PtL	5	7	-1.590384642	0.11174813	0.1117

variable	n	statistic	df	p	dunn_pairs	dunn_min_padj
TAC	18	13.76464891	2	**0.00103**	3	0.001109969

variable	group1	group2	n1	n2	statistic	p	p.adj
TAC	PaL	PtF	6	5	-3.560613164	0.00036999	**0.0011**
TAC	PaL	PtL	6	7	-2.667464337	0.0076426	**0.0115**
TAC	PtF	PtL	5	7	1.147689541	0.25109675	0.2511

Table S2. R^2 values, Q^2 values, variables correlation, VIP score, and % variance by components of the PLSR for chemical components and bioactivities of Pandanus tectorius leaves, Pandanus tectorius fruits, and Pandanus amaryllifolius leaves extracts

Overall model performance

Metric	Value
Mean R^2 (train)	0.7466
Mean Q^2 (CV)	0.3262

Adjusted

Response	R^2 (train)	Q^2 (CV)
DPPH	0.892	0.795
Hydroxyl	0.928	0.873
α-Amylase	0.951	0.924
NO inhibition	0.83	0.61
A549 cytotoxicity	0.188	−1.618
K562 cytotoxicity	0.69	0.165
MCF7 cytotoxicity	0.746	0.535

correlation_XY							
	DPPH	**Hydroxyl**	***α*-amylase**	**NO inhib.**	**A549 cytot.**	**K562 cytot.**	**MCF7 cytot.**
TPC	0.9076	0.9237	0.9362	-0.6136	0.0205	0.7822	-0.7526
TFC	0.8712	0.9431	0.9608	-0.7683	-0.1641	0.7711	-0.7281
TSC	0.8497	0.8888	0.9366	-0.5872	0.0045	0.7916	-0.7893
TAC	-0.8269	-0.8614	-0.8743	0.8852	0.1964	-0.6223	0.7757

VIP score				
Components	**Comp 1**	**Comp 2**	**Comp 3**	**Comp 4**
VIP score	0.9891	1.0072	0.9799	1.0232

% Variance by components				
Components	**Comp 1**	**Comp 2**	**Comp 3**	**Comp 4**
Individual Variance	91.52	6.78	1.16	0.54
Cumulative Variance	91.52	98.30	99.46	100.00

NMR SPECTRA OF THE ISOLATED COMPOUNDS

Pt1-DMSO-1H

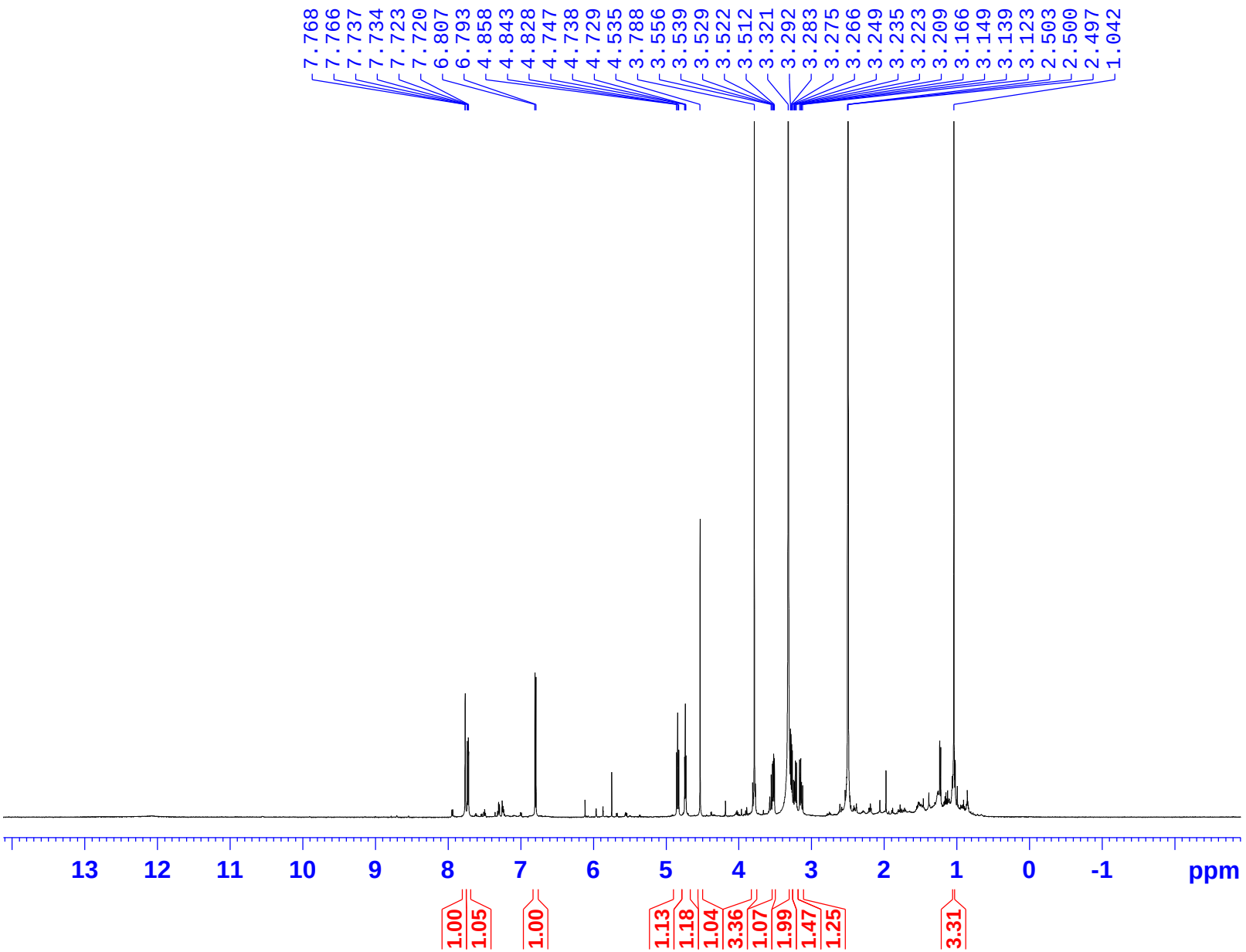
7.768
7.766
7.737
7.734
7.723
7.720
6.807
6.793
4.858
4.843
4.828
4.747
4.738
4.729
4.535
3.788
3.556
3.539
3.529
3.522
3.512
3.321
3.292
3.283
3.275
3.266
3.249
3.235
3.223
3.209
3.166
3.149
3.139
3.123
2.503
2.500
2.497
1.042
13
12
11
10
9
8
7
6
5
4
3
2
1
0
-1
ppm
1.00
1.05
1.00
1.13
1.18
1.04
3.36
1.07
1.99
1.47
1.25
3.31

Pt1-DMSO-1H

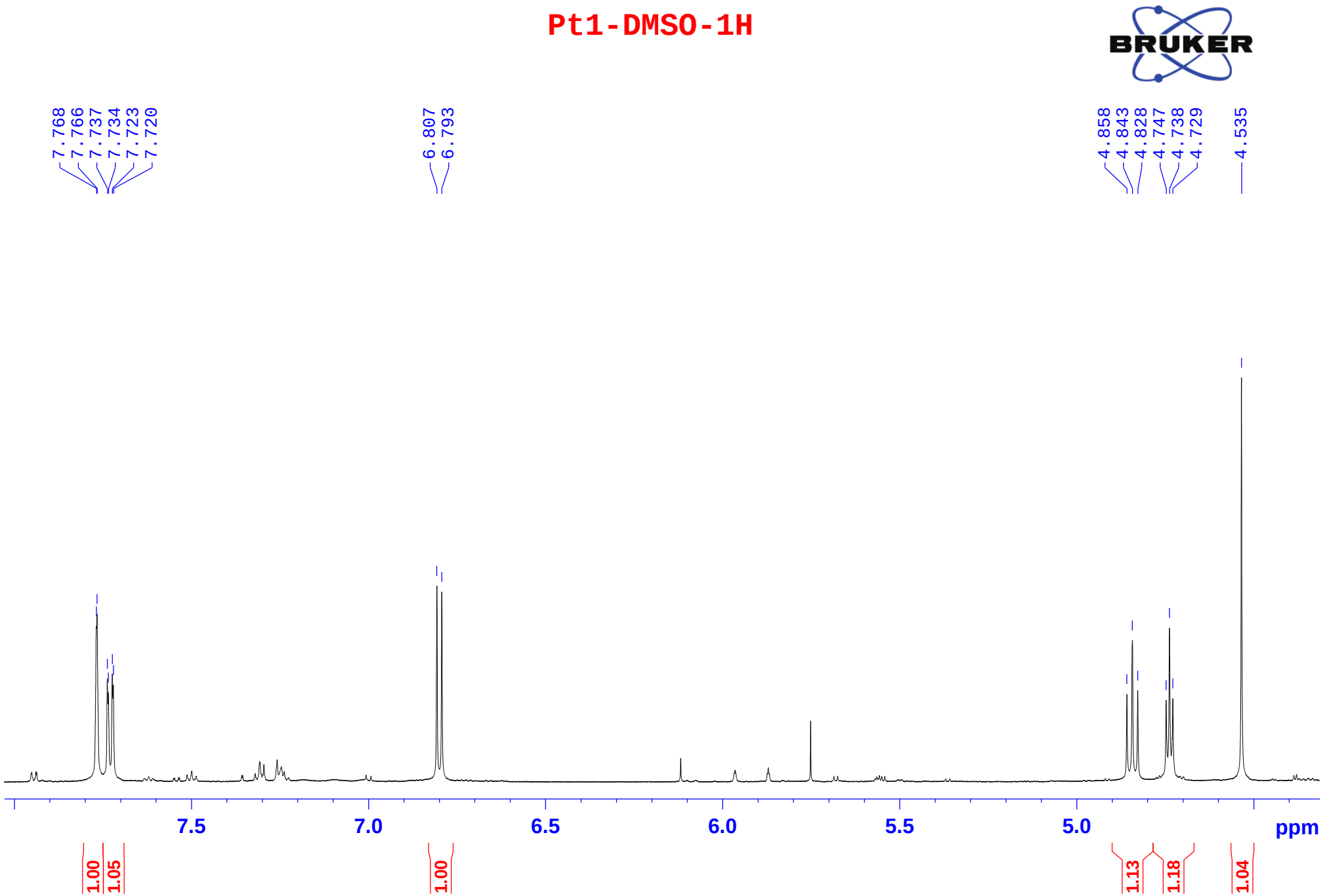
7.768
7.766
7.737
7.734
7.723
7.720
6.807
6.793
4.858
4.843
4.828
4.747
4.738
4.729
4.535
7.5
7.0
6.5
6.0
5.5
5.0
ppm
1.00
1.05
1.00
1.13
1.18
1.04

Pt1-DMSO-1H

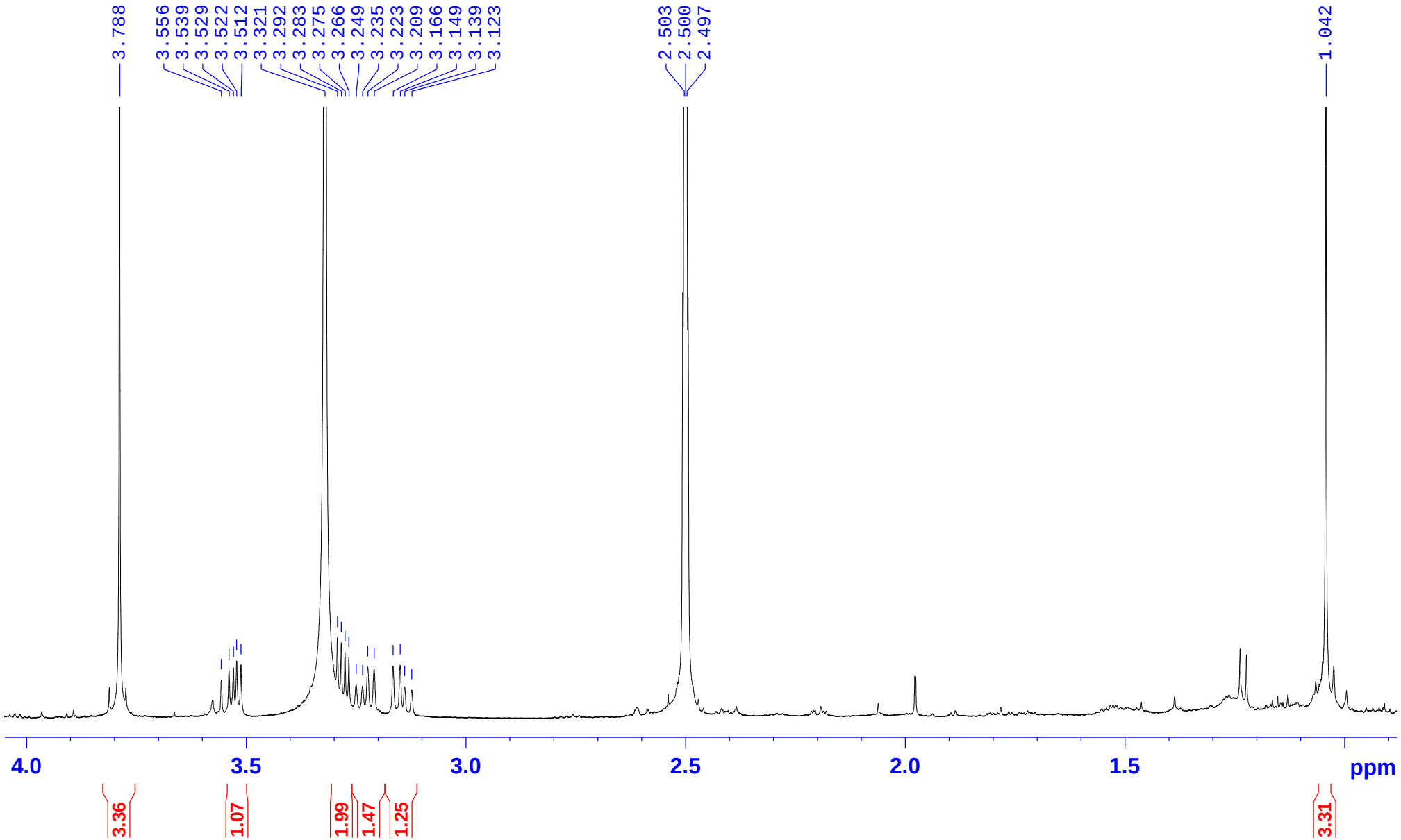
3.788
3.556
3.539
3.529
3.522
3.512
3.321
3.292
3.283
3.275
3.266
3.249
3.235
3.223
3.209
3.166
3.149
3.139
3.123
2.503
2.500
2.497
1.042
4.0
3.5
3.0
2.5
2.0
1.5
ppm
3.36
1.07
1.99
1.47
1.25
3.31

Pt1-DMSO-C13CPD

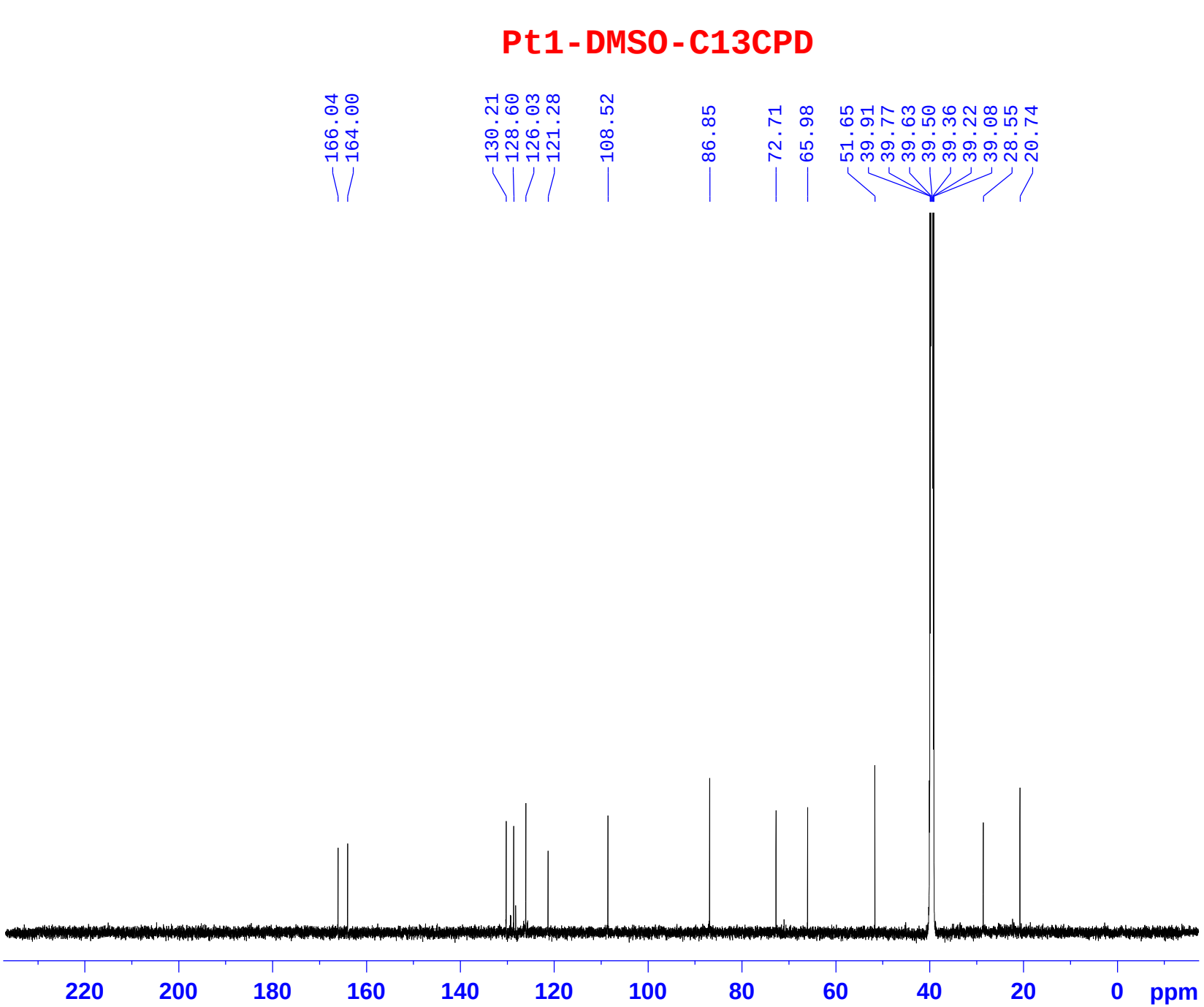

Pt1-DMSO-C13CPD

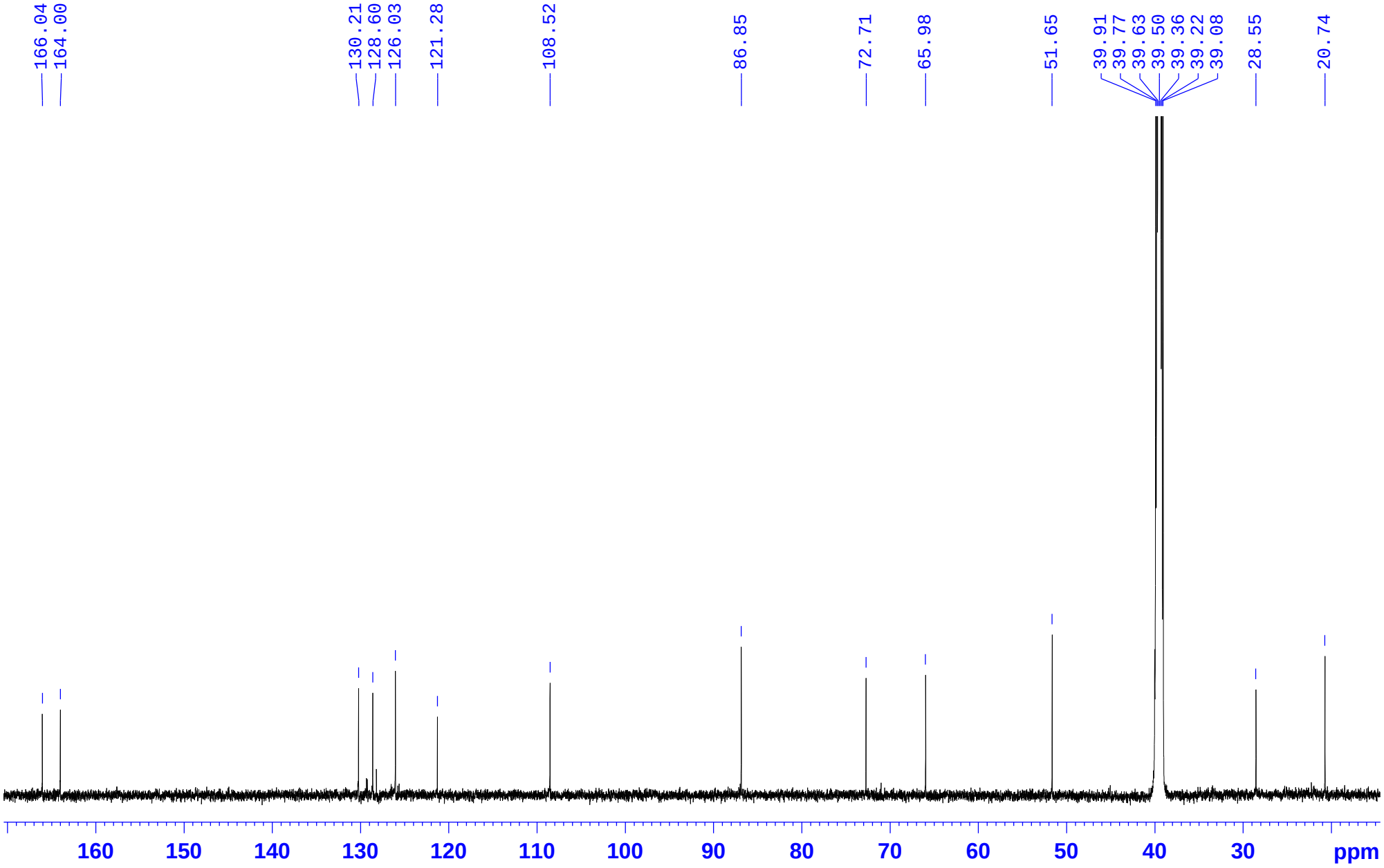

Pt1-DMSO-COSYGP

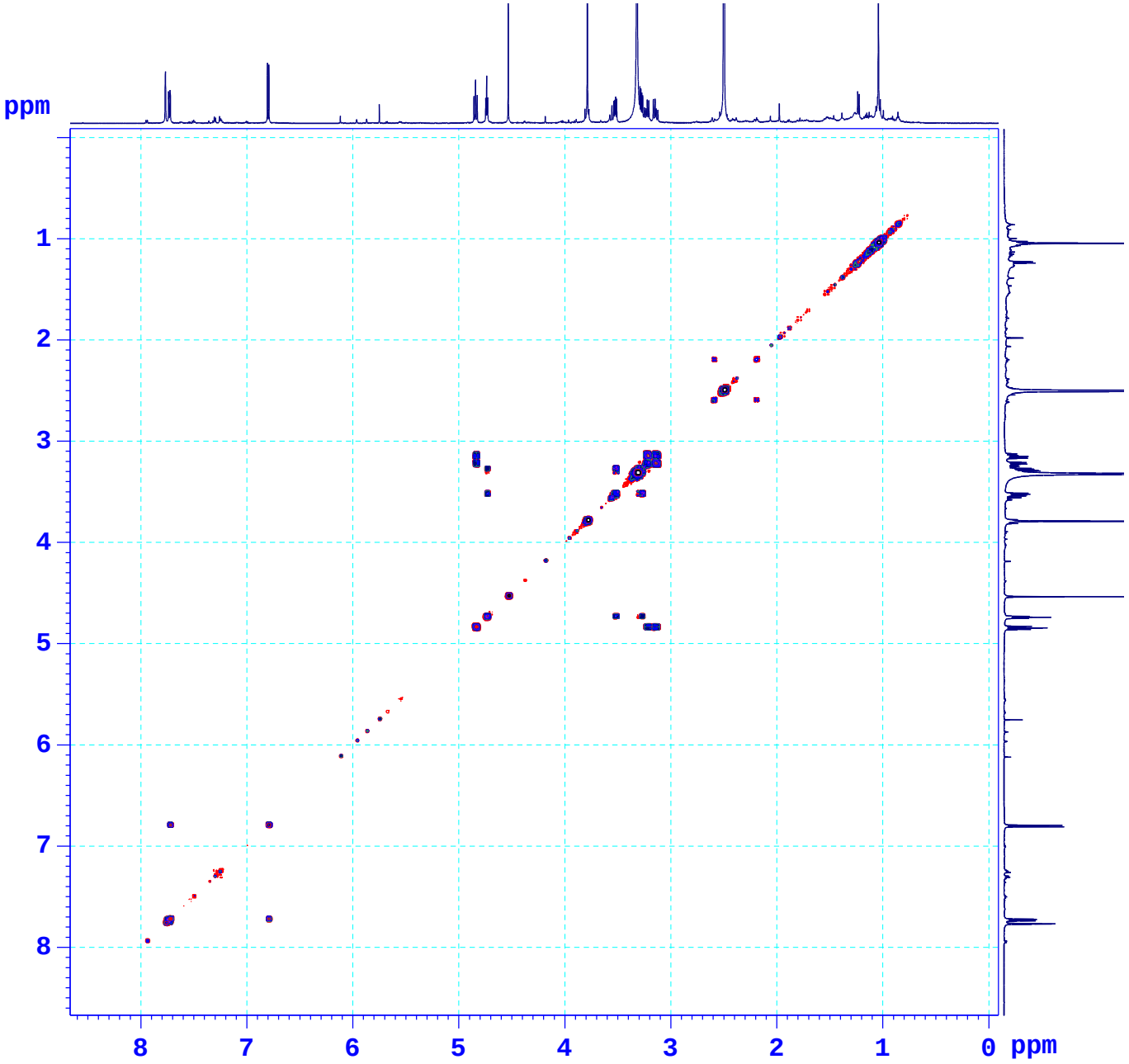

Pt1-DMSO-COSYGP

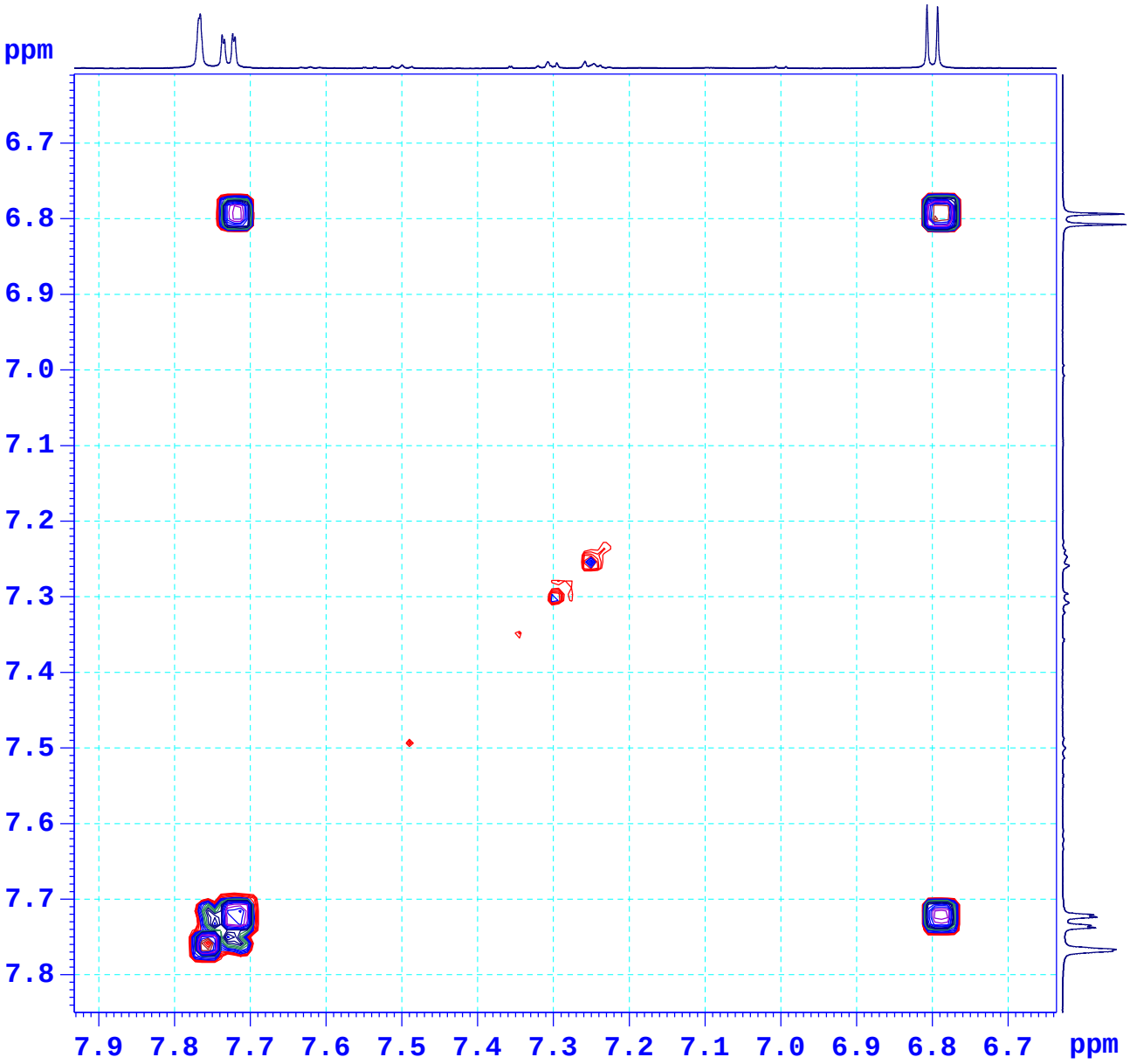

Pt1-DMSO-COSYGP

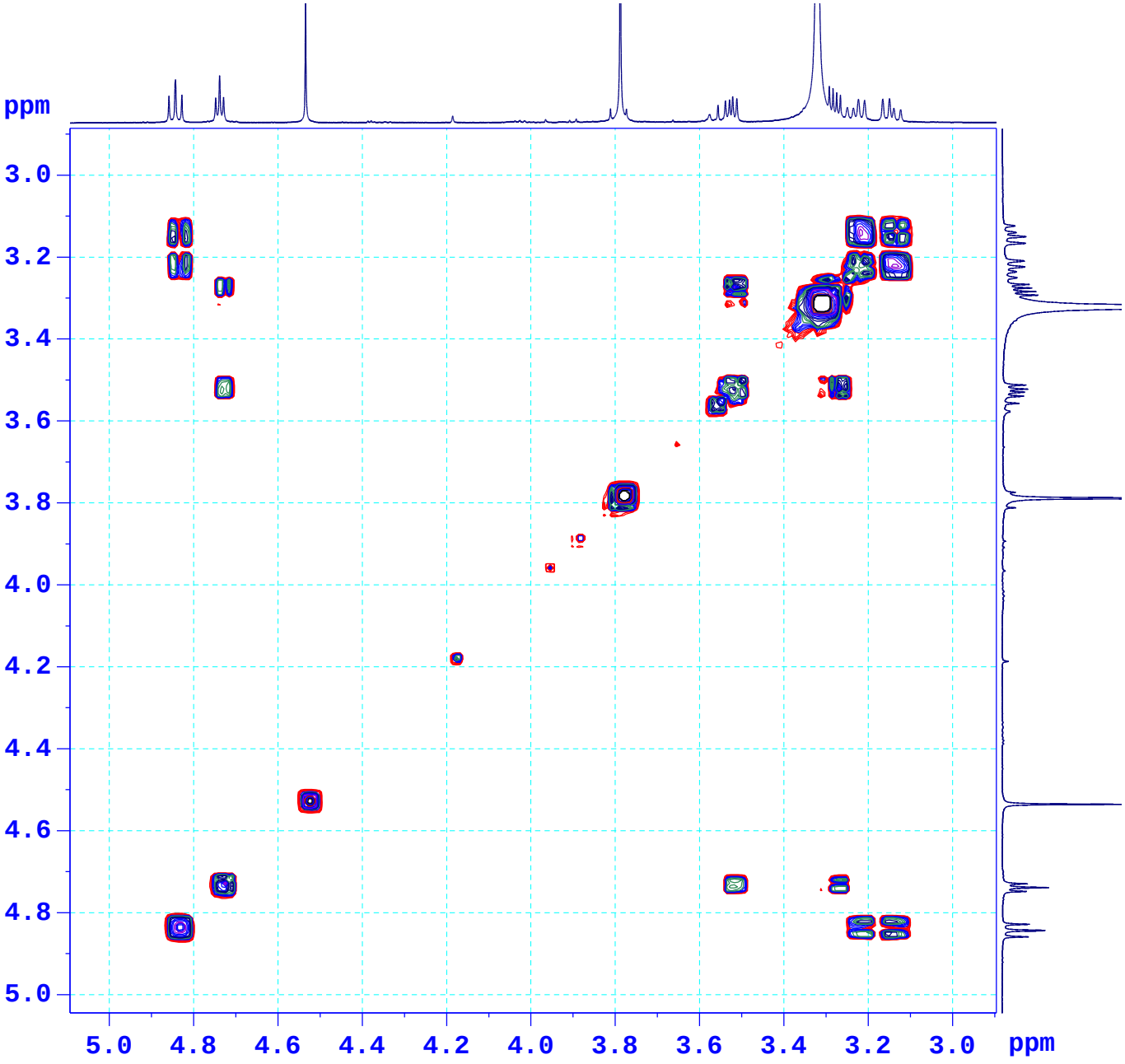

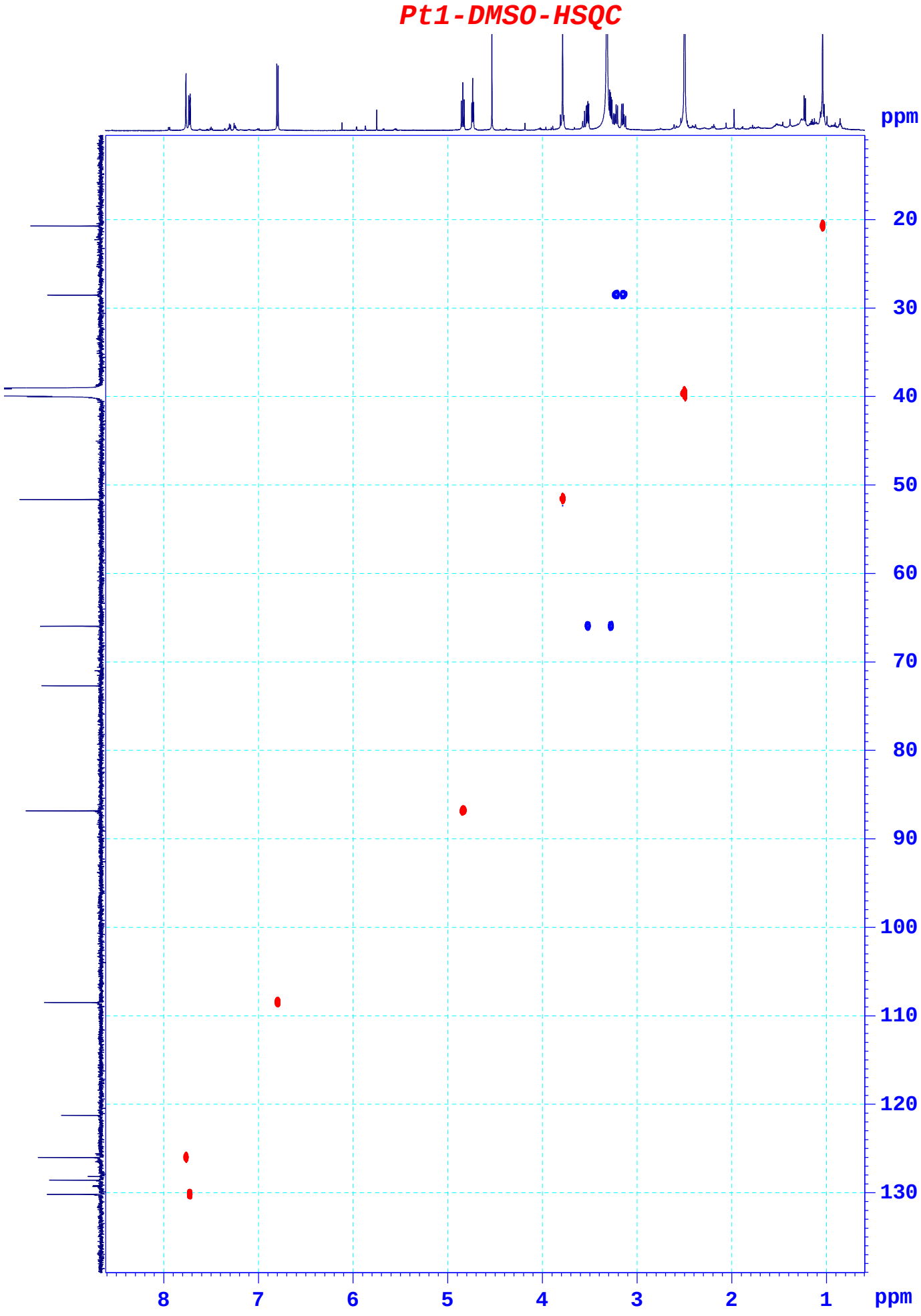
Pt1-DMSO-HSQC
ppm
20
30
40
50
60
70
80
90
100
110
120
130
8
7
6
5
4
3
2
1
ppm

Pt1-DMSO-HSQC

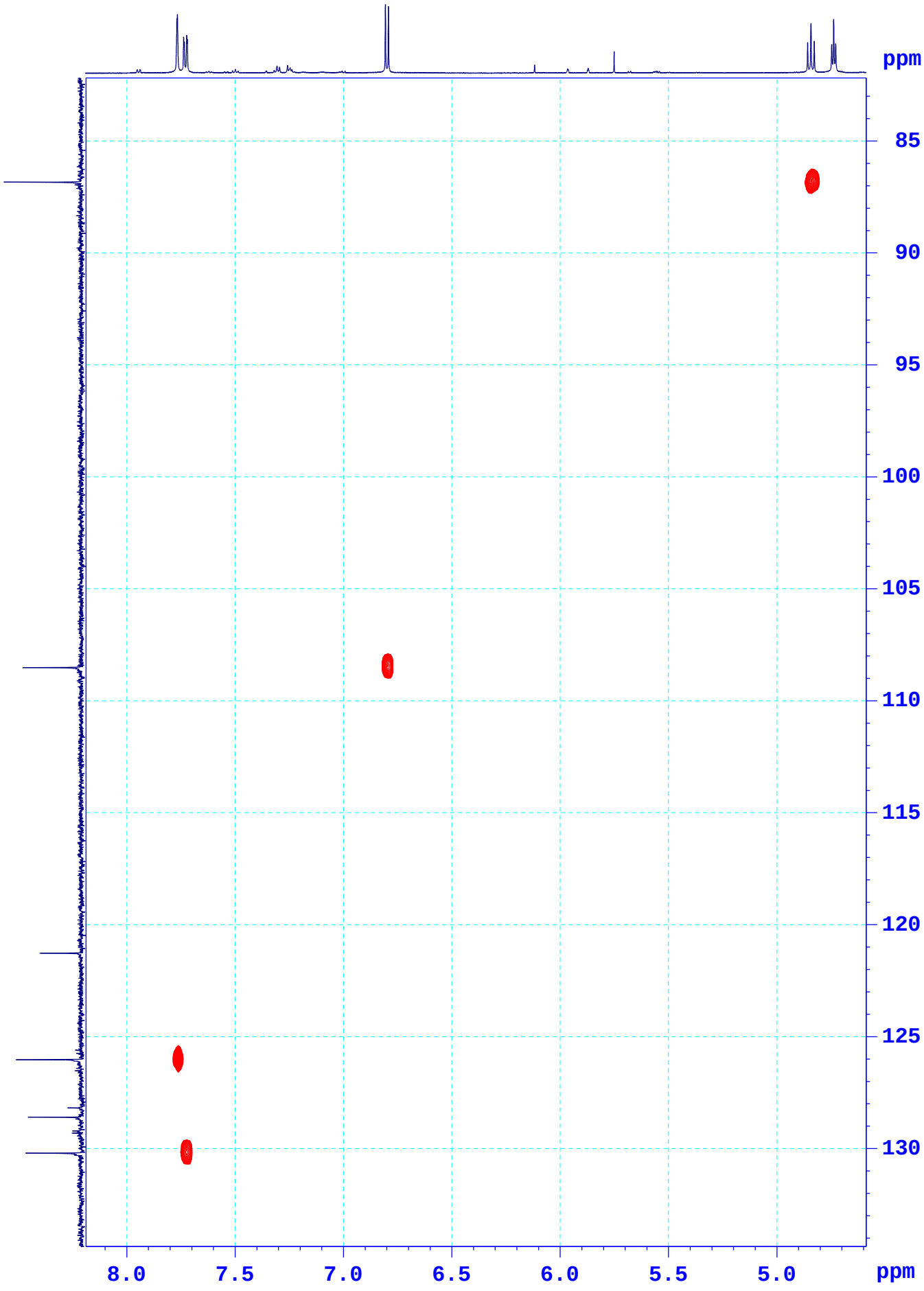

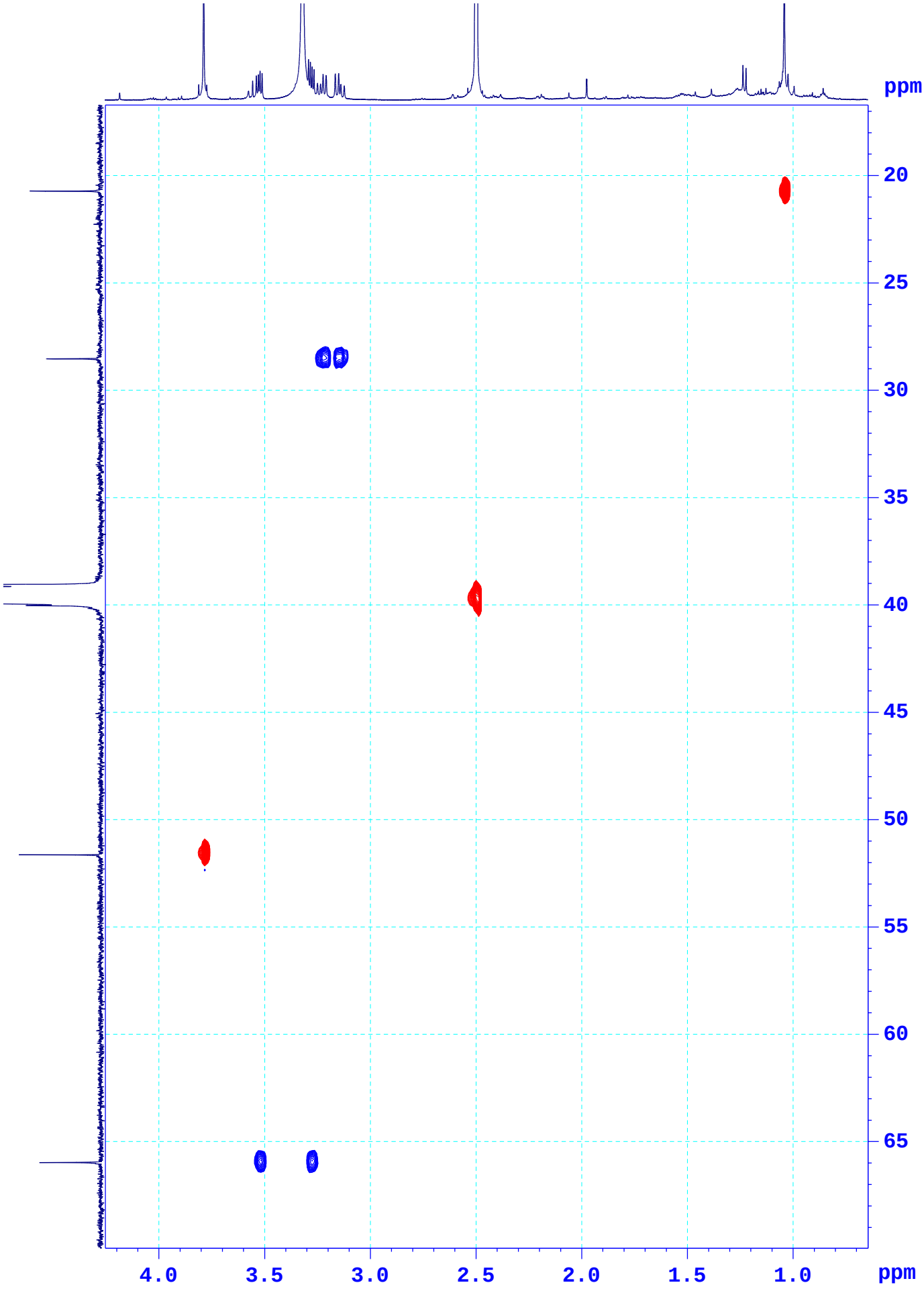
Pt1-DMSO-HSQC
ppm
20
25
30
35
40
45
50
55
60
65
4.0
3.5
3.0
2.5
2.0
1.5
1.0
ppm

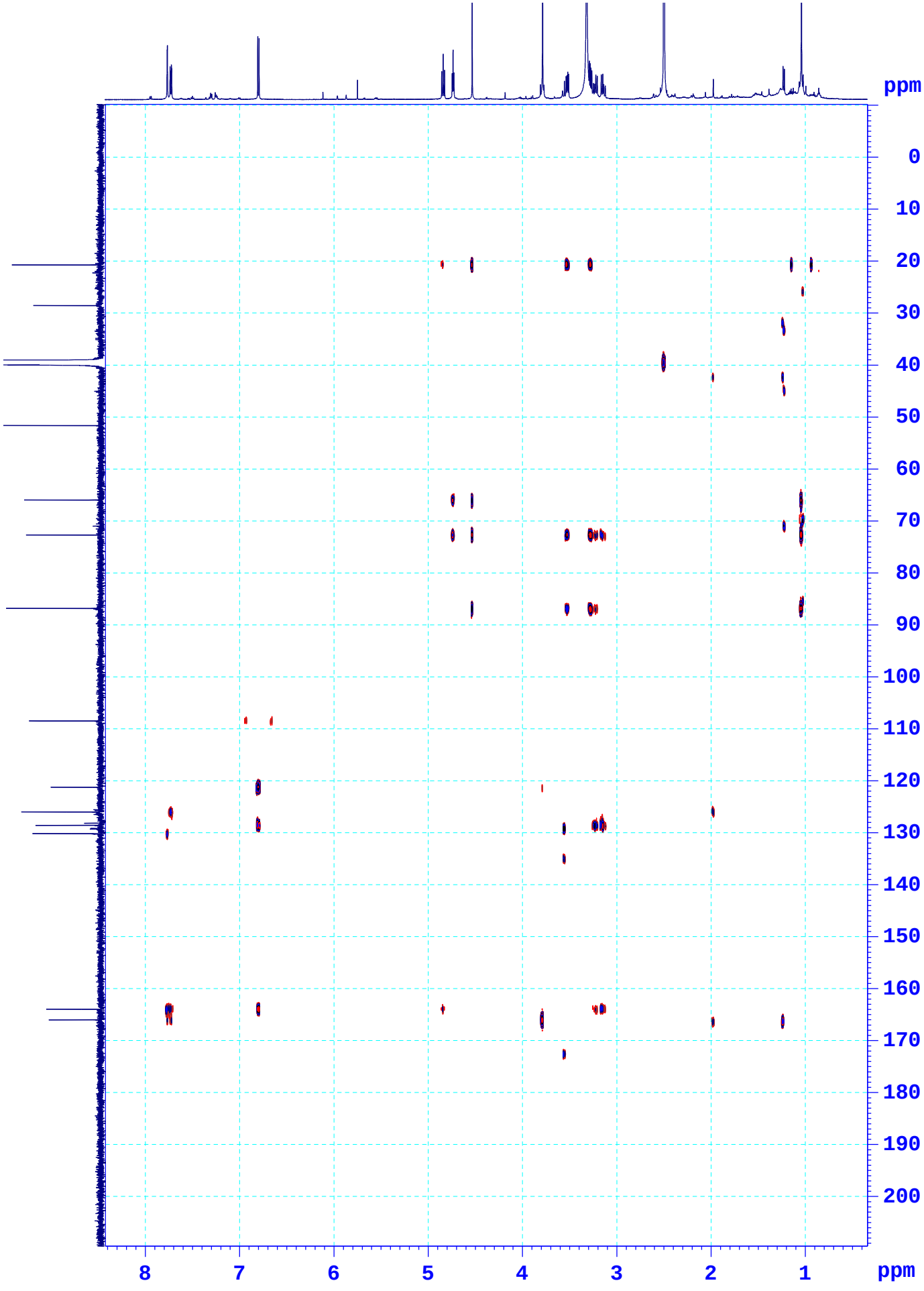
Pt1-DMSO-HMBC
ppm
0
10
20
30
40
50
60
70
80
90
100
110
120
130
140
150
160
170
180
190
200
8
7
6
5
4
3
2
1
ppm

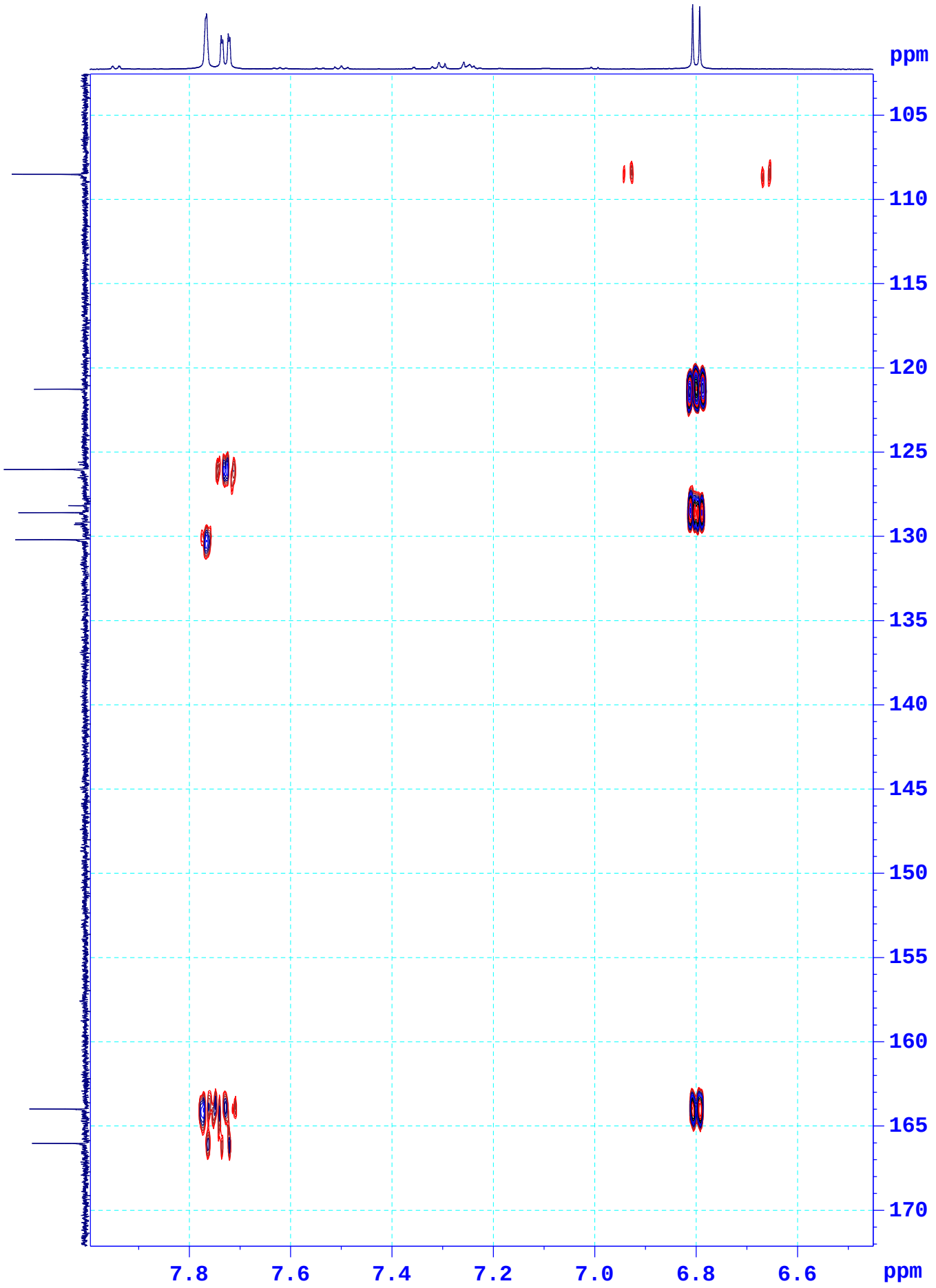
Pt1-DMSO-HMBC
ppm
105
110
115
120
125
130
135
140
145
150
155
160
165
170
7.8
7.6
7.4
7.2
7.0
6.8
6.6
ppm

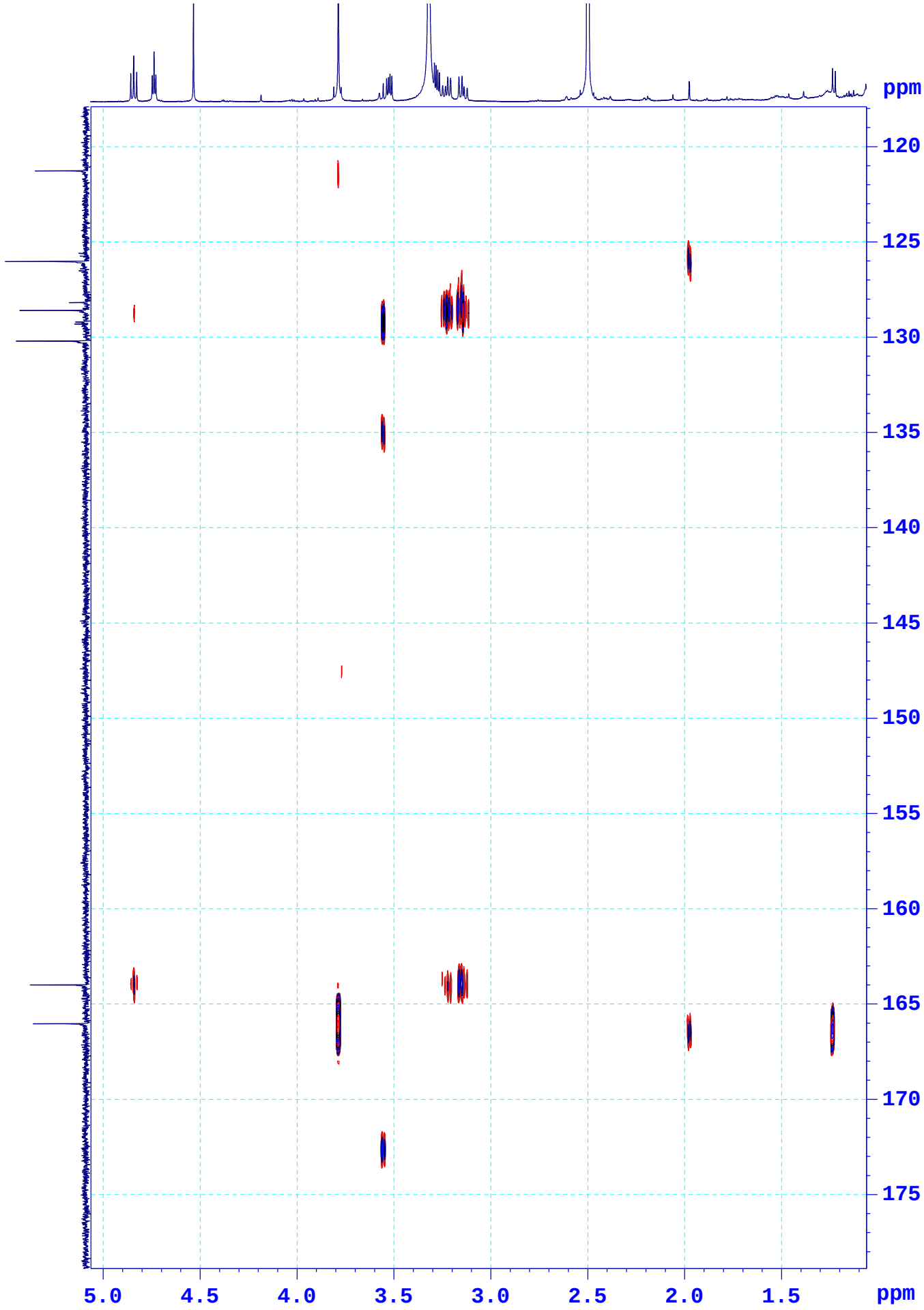
Pt1-DMSO-HMBC
ppm
120
125
130
135
140
145
150
155
160
165
170
175
5.0
4.5
4.0
3.5
3.0
2.5
2.0
1.5
ppm

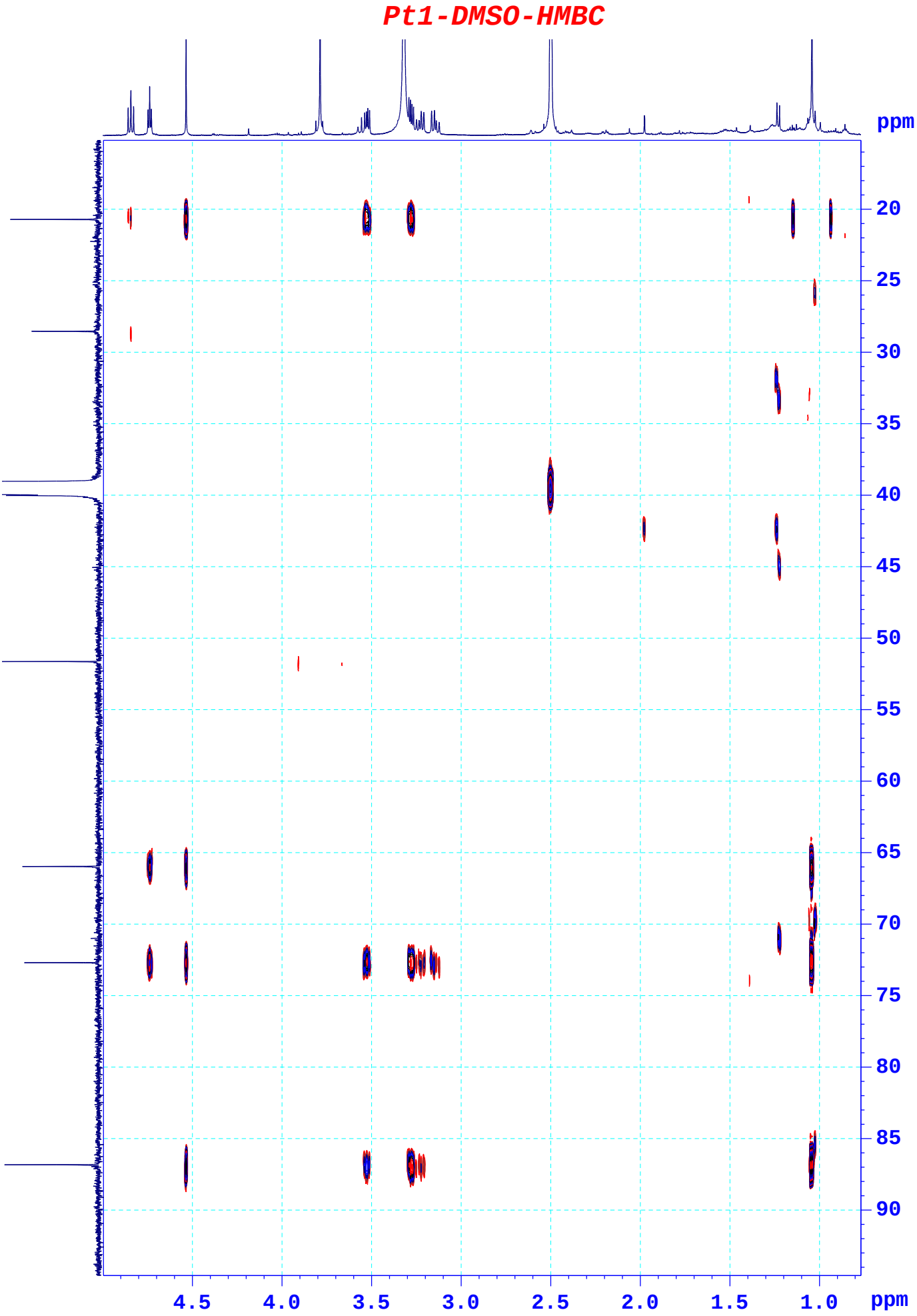
Pt1-DMSO-HMBC
ppm
20
25
30
35
40
45
50
55
60
65
70
75
80
85
90
4.5
4.0
3.5
3.0
2.5
2.0
1.5
1.0
ppm

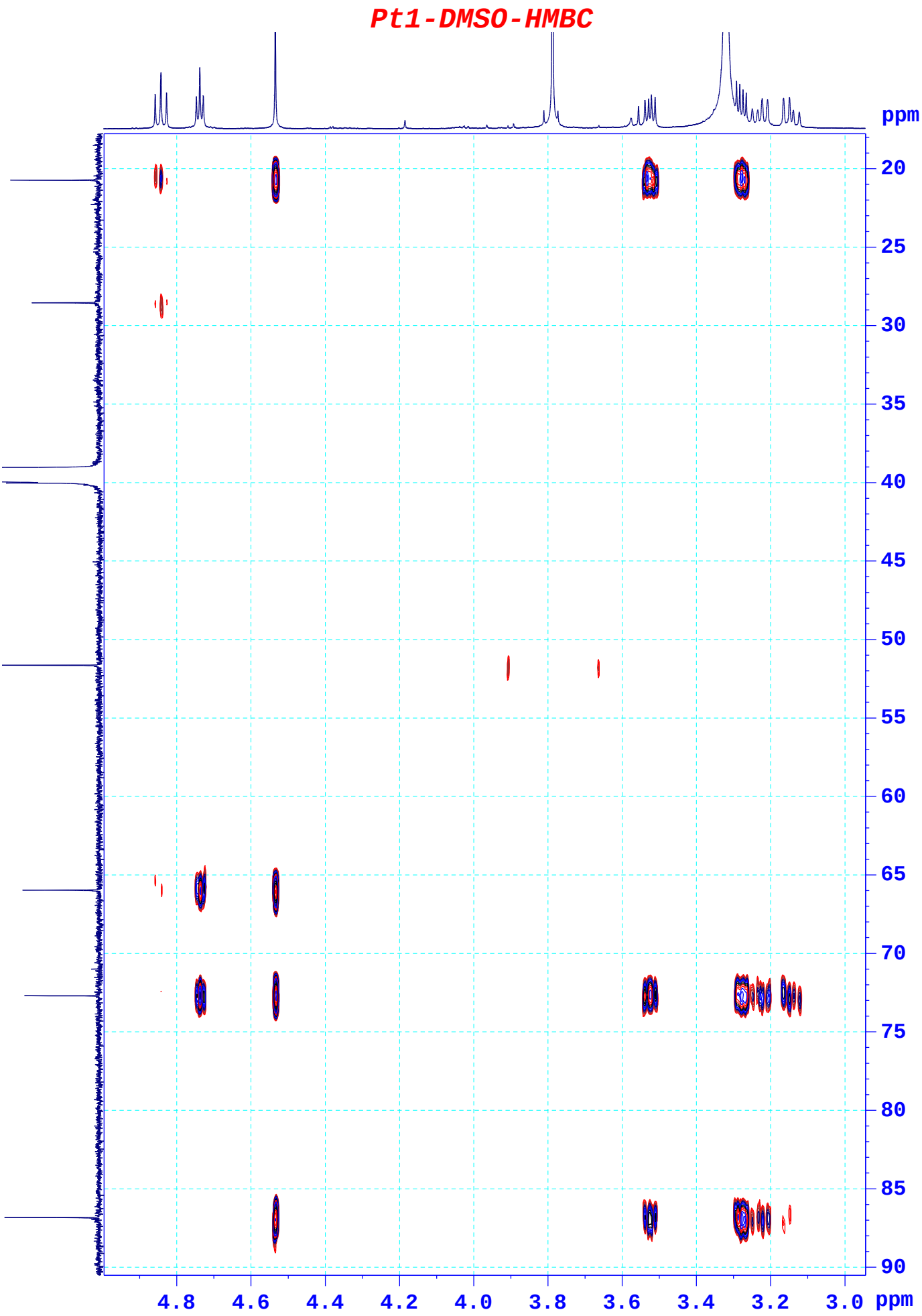
Pt1-DMSO-HMBC
ppm
20
25
30
35
40
45
50
55
60
65
70
75
80
85
90
4.8
4.6
4.4
4.2
4.0
3.8
3.6
3.4
3.2
3.0
ppm

Pt2-DMSO-1H

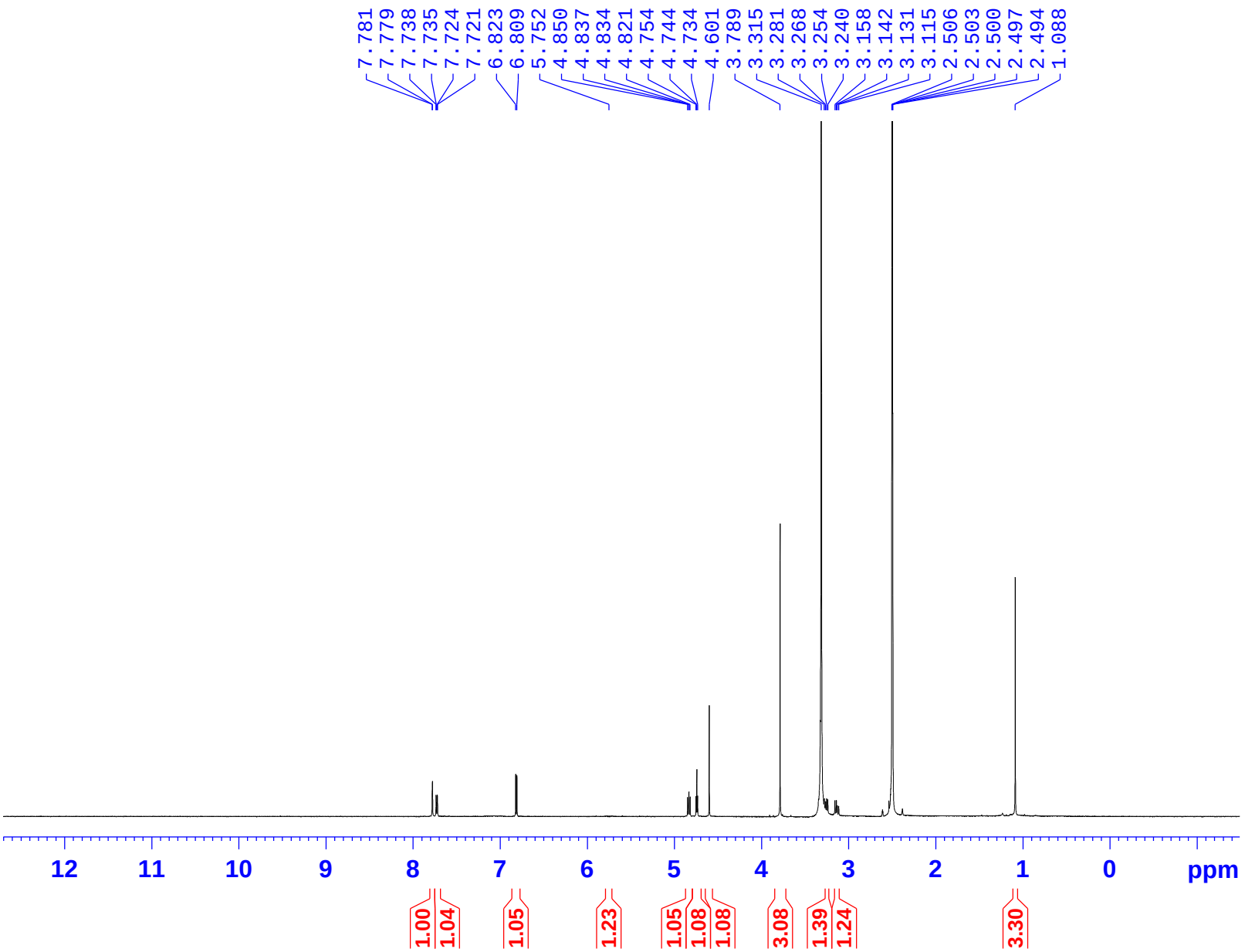
7.781
7.779
7.738
7.735
7.724
7.721
6.823
6.809
5.752
4.850
4.837
4.834
4.821
4.754
4.744
4.734
4.601
3.789
3.315
3.281
3.268
3.254
3.240
3.158
3.142
3.131
3.115
2.506
2.503
2.500
2.497
2.494
1.088
12
11
10
9
8
7
6
5
4
3
2
1
0
ppm
1.00
1.04
1.05
1.23
1.05
1.08
1.08
3.08
1.39
1.24
3.30

Pt2-DMSO-1H

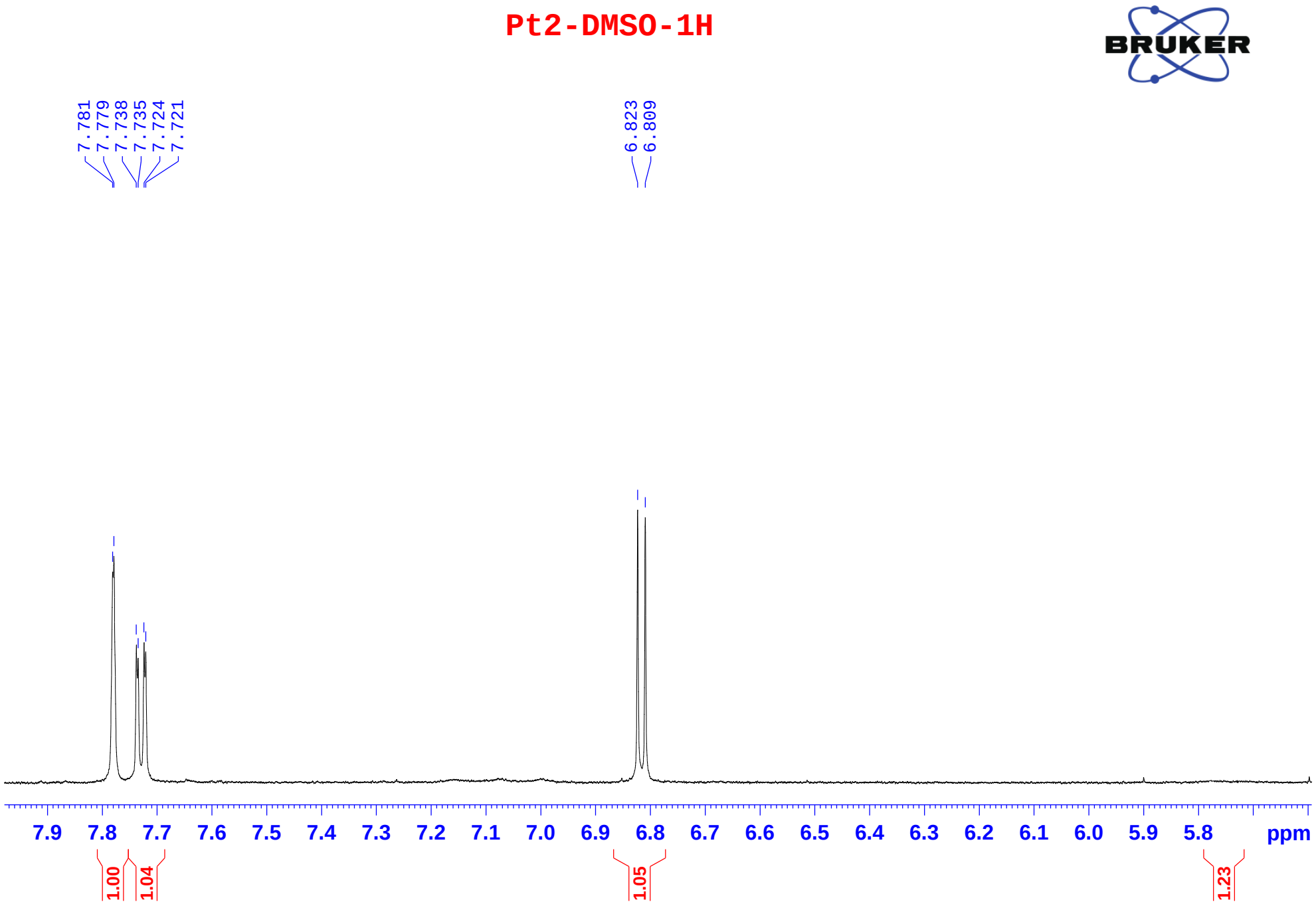
7.781
7.779
7.738
7.735
7.724
7.721
6.823
6.809
7.9 7.8 7.7 7.6 7.5 7.4 7.3 7.2 7.1 7.0 6.9 6.8 6.7 6.6 6.5 6.4 6.3 6.2 6.1 6.0 5.9 5.8 ppm
1.00
1.04
1.05
1.23

Pt2-DMSO-1H

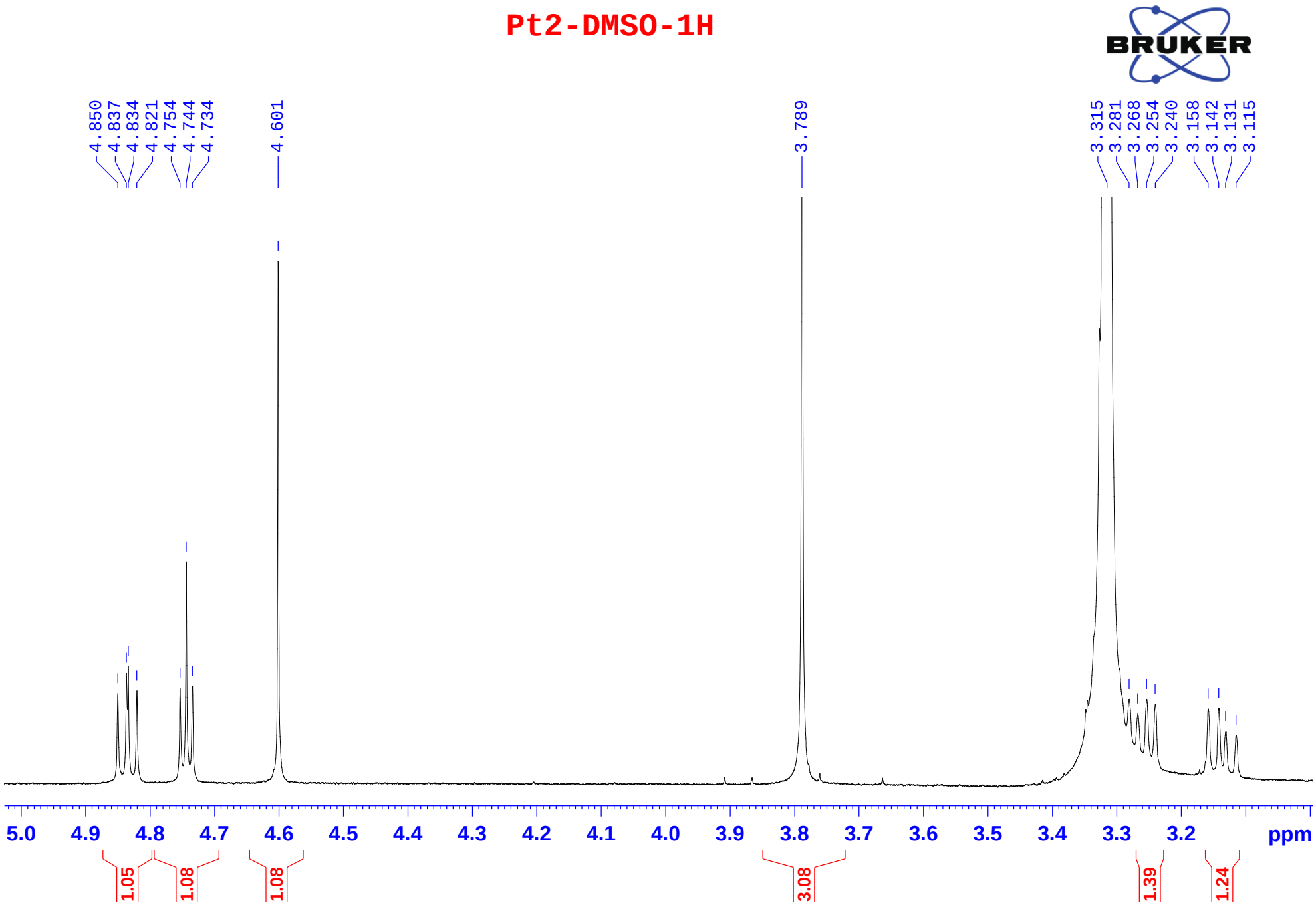
4.850
4.837
4.834
4.821
4.754
4.744
4.734
4.601
3.789
3.315
3.281
3.268
3.254
3.240
3.158
3.142
3.131
3.115
5.0
4.9
4.8
4.7
4.6
4.5
4.4
4.3
4.2
4.1
4.0
3.9
3.8
3.7
3.6
3.5
3.4
3.3
3.2
ppm
1.05
1.08
1.08
3.08
1.39
1.24

Pt2-DMSO-C13CPD

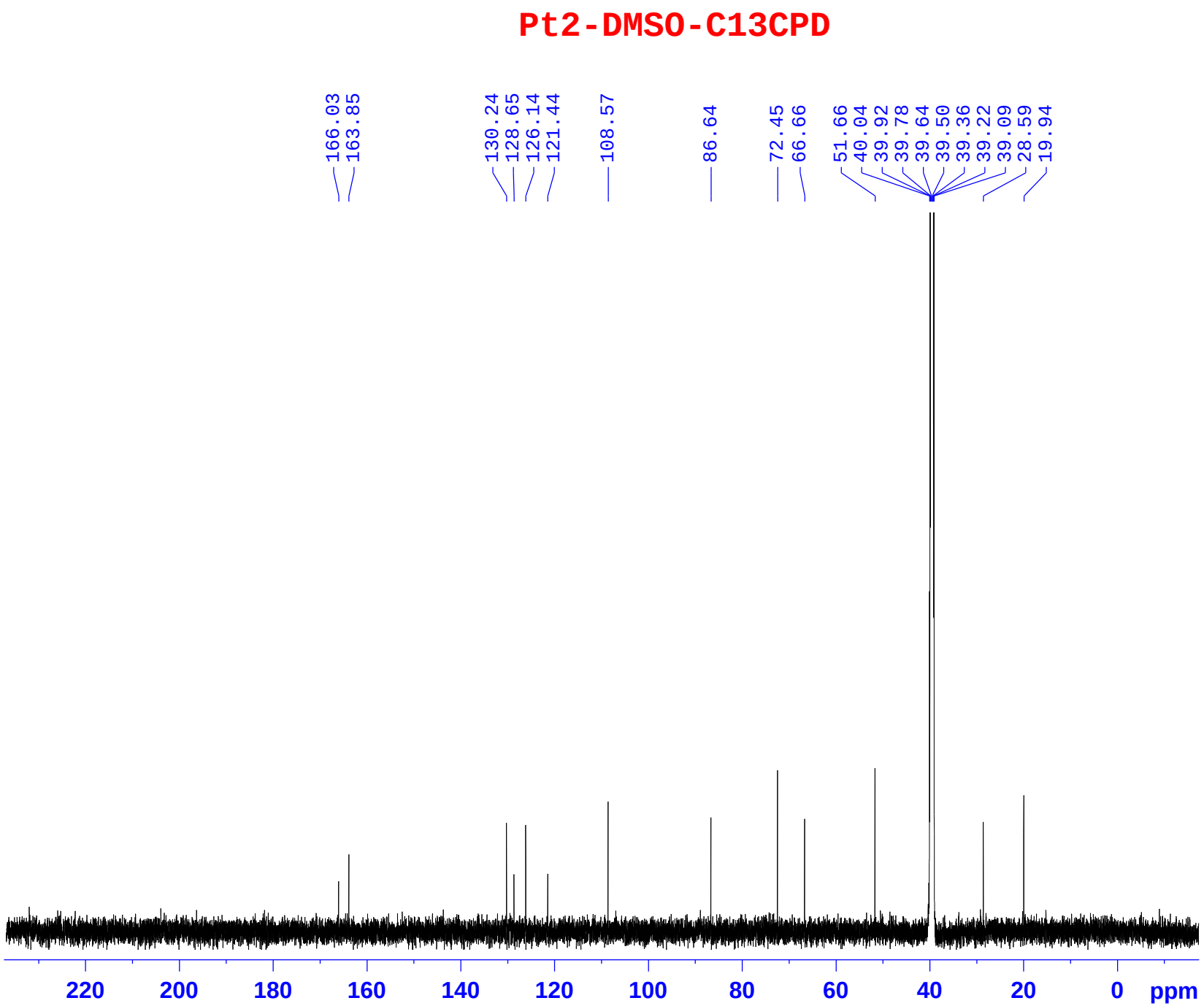

Pt2-DMSO-C13CPD

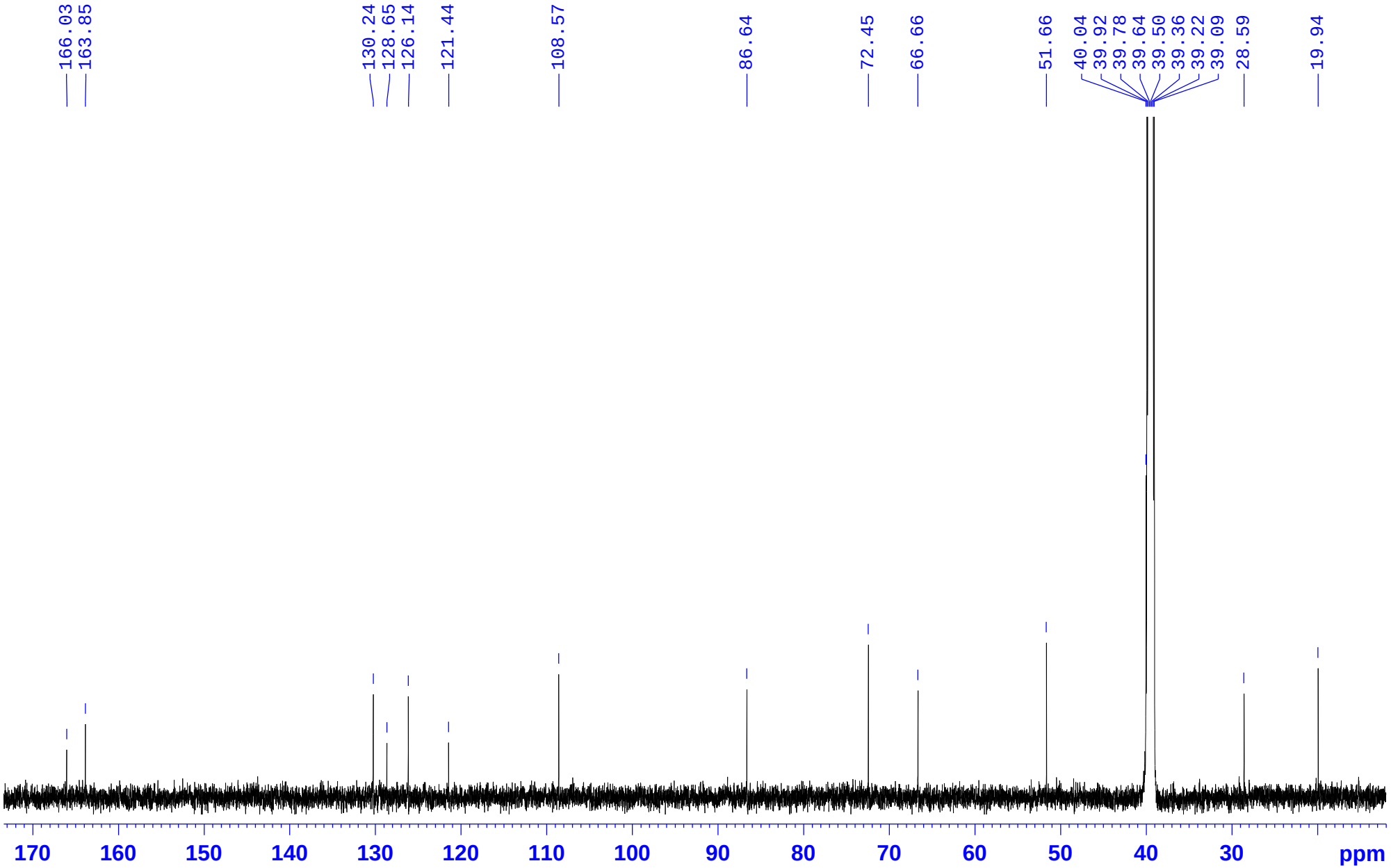

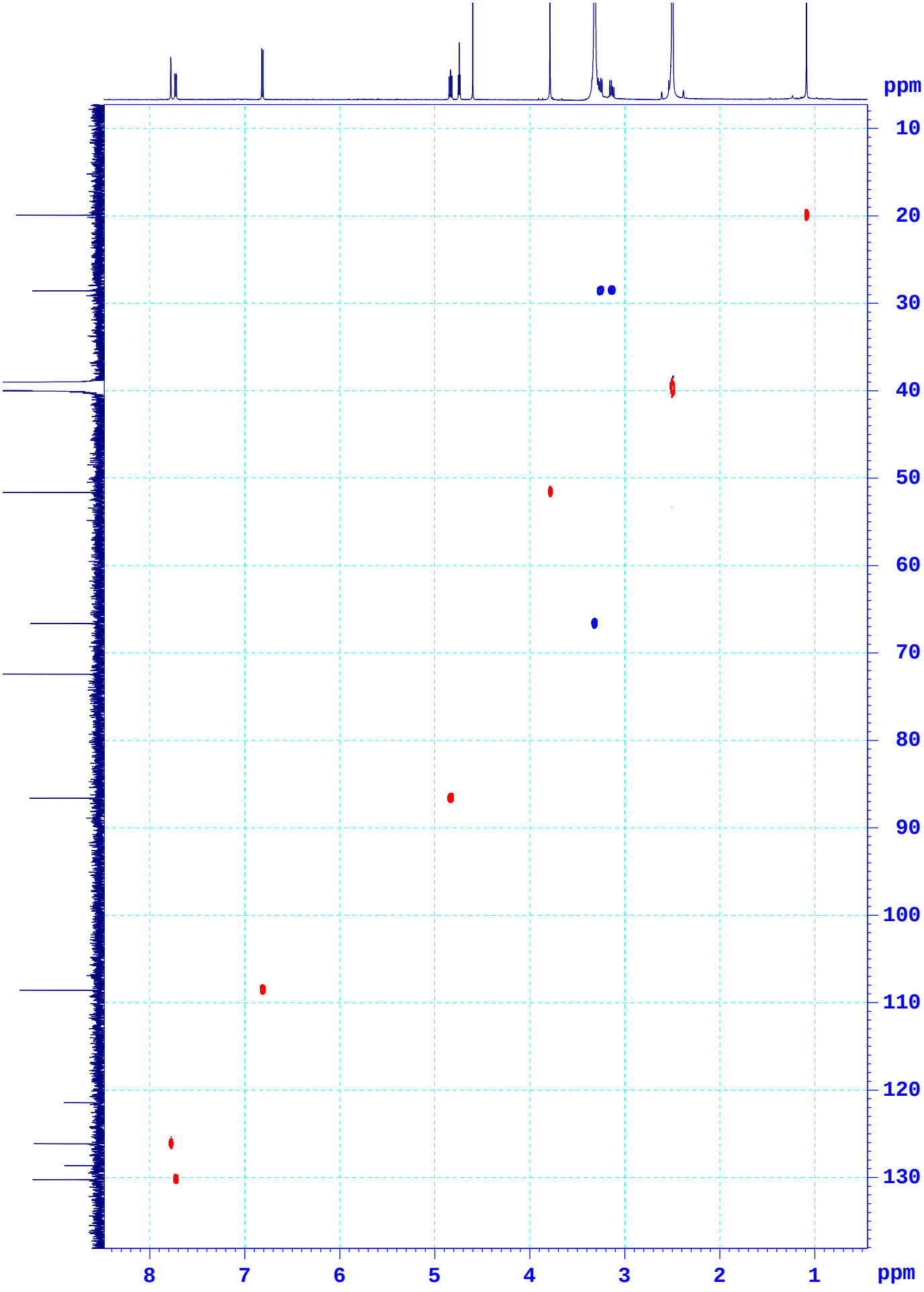
Pt2-DMSO-HSQC
ppm
10
20
30
40
50
60
70
80
90
100
110
120
130
8
7
6
5
4
3
2
1
ppm

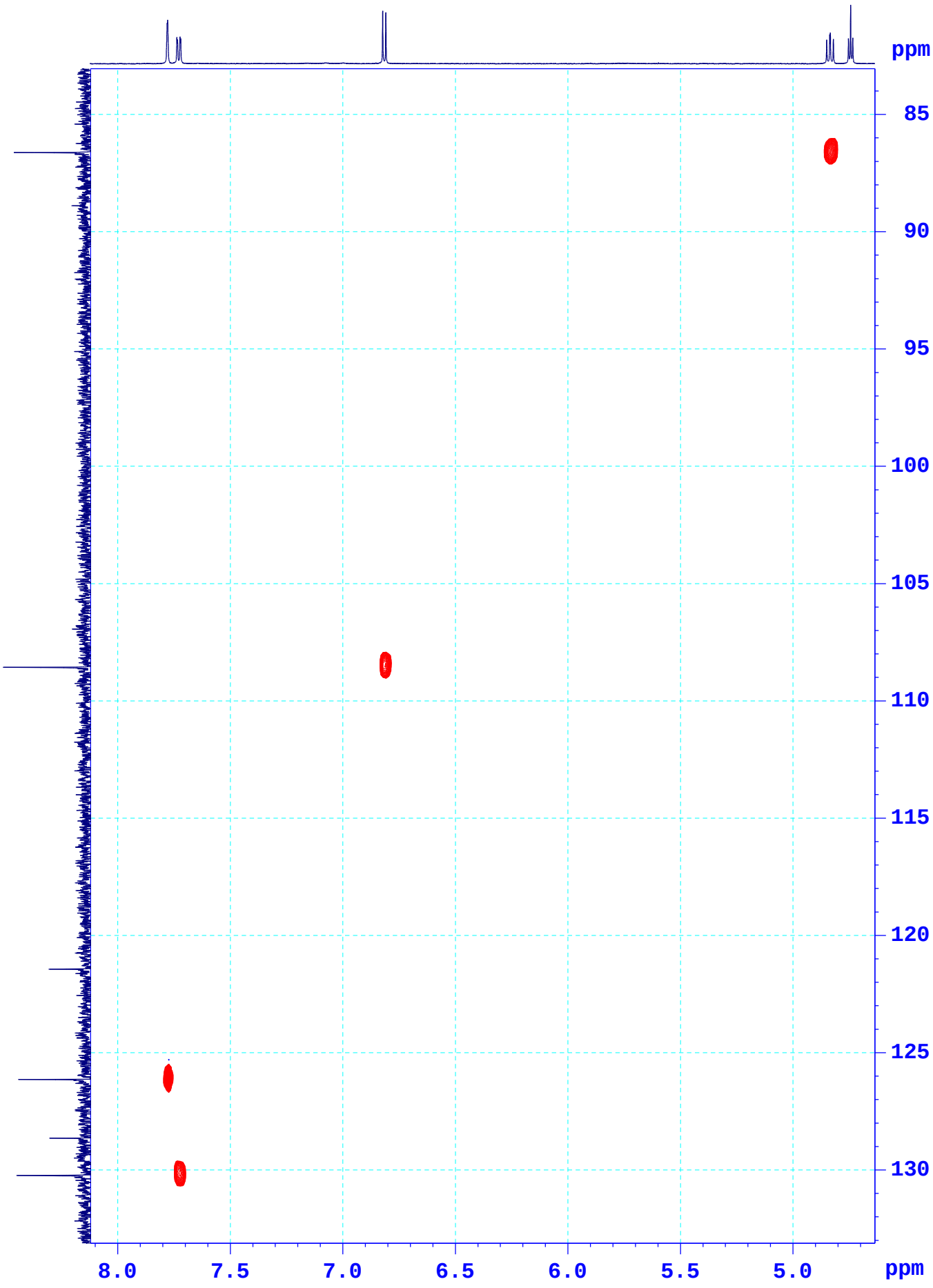
Pt2-DMSO-HSQC
ppm
85
90
95
100
105
110
115
120
125
130
8.0
7.5
7.0
6.5
6.0
5.5
5.0
ppm

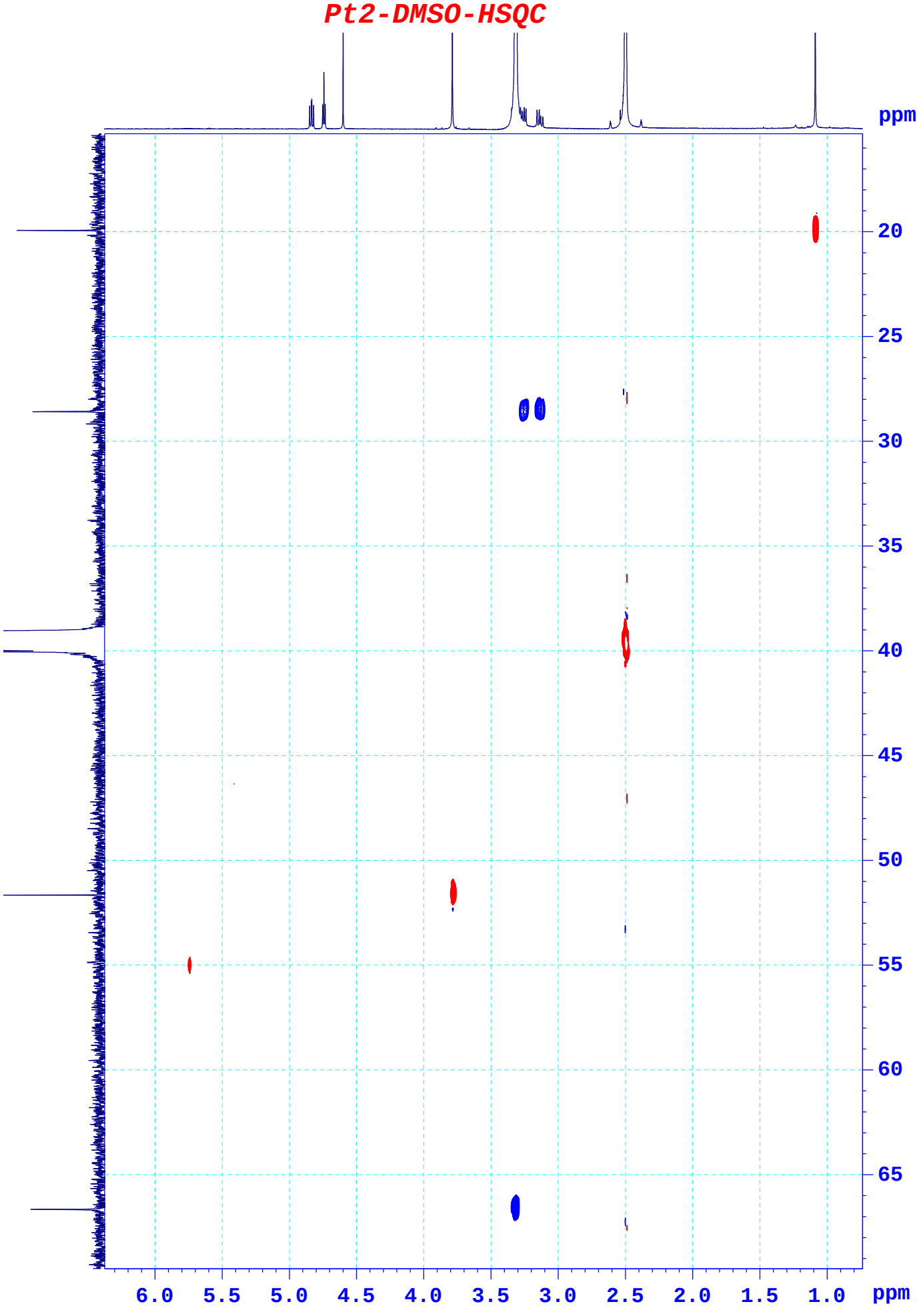
Pt2-DMSO-HSQC
ppm
20
25
30
35
40
45
50
55
60
65
6.0
5.5
5.0
4.5
4.0
3.5
3.0
2.5
2.0
1.5
1.0
ppm

Pt2-DMSO-COSYGP

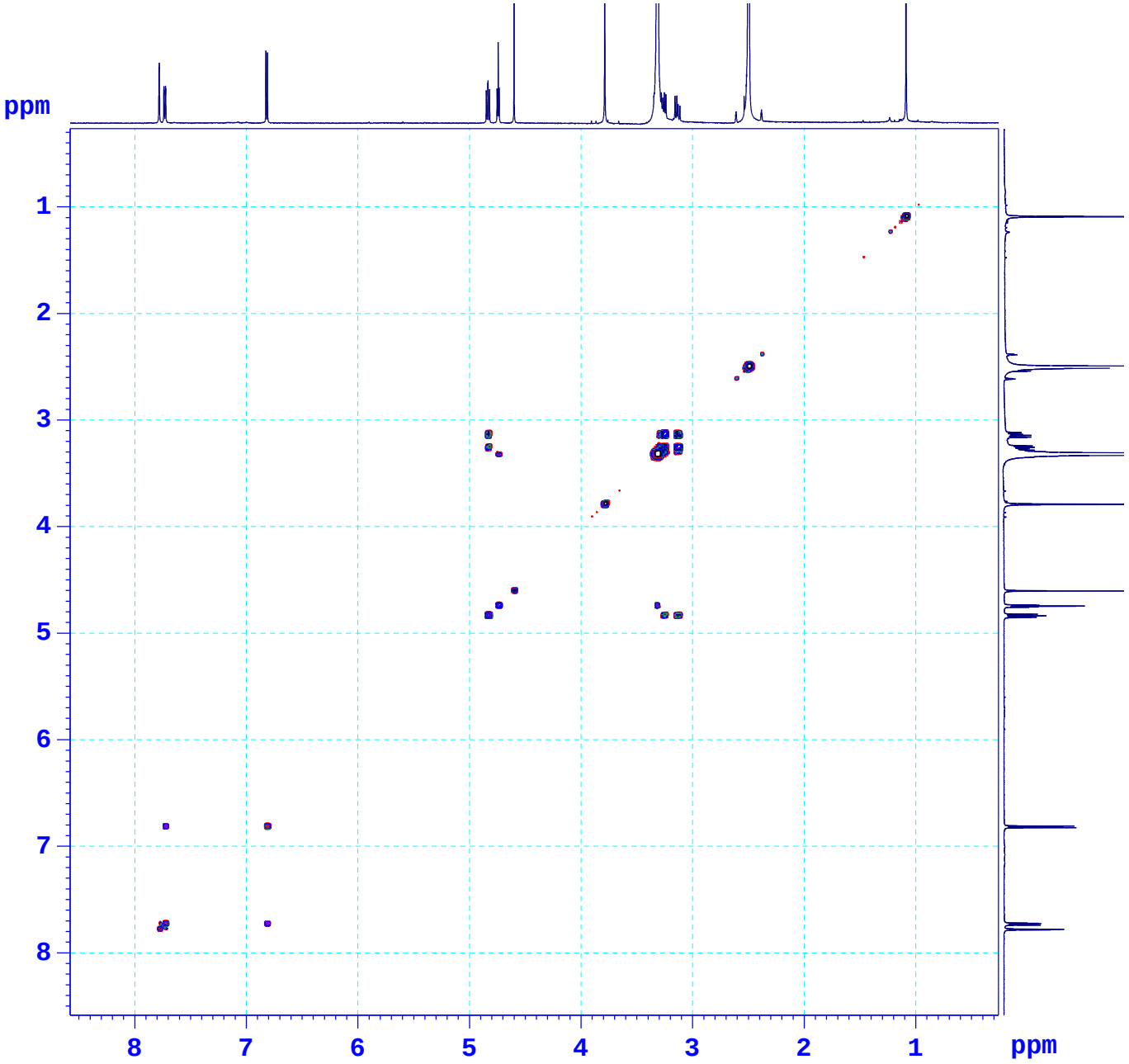

Pt2-DMSO-COSYGP

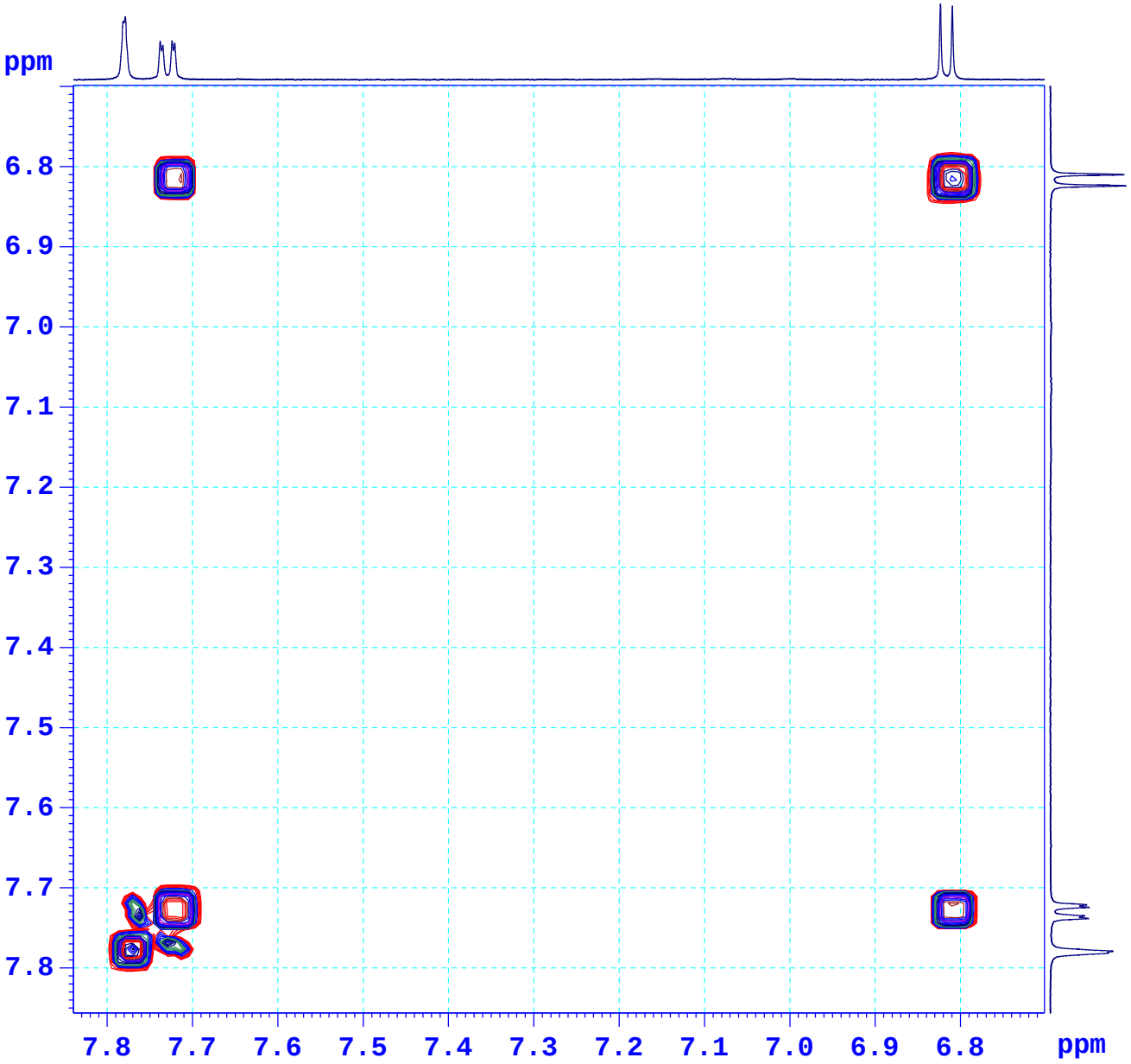

Pt2-DMSO-COSYGP

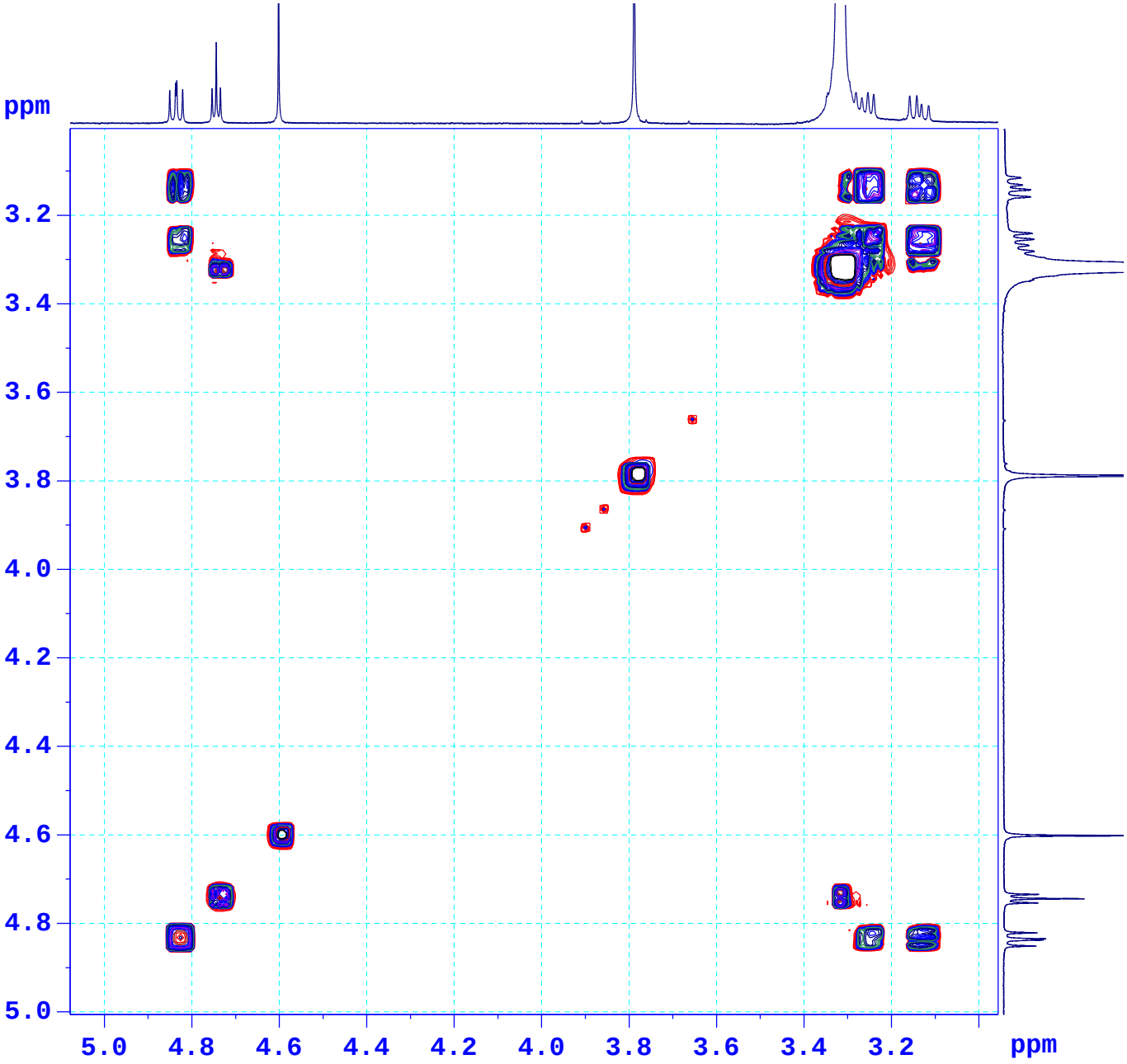

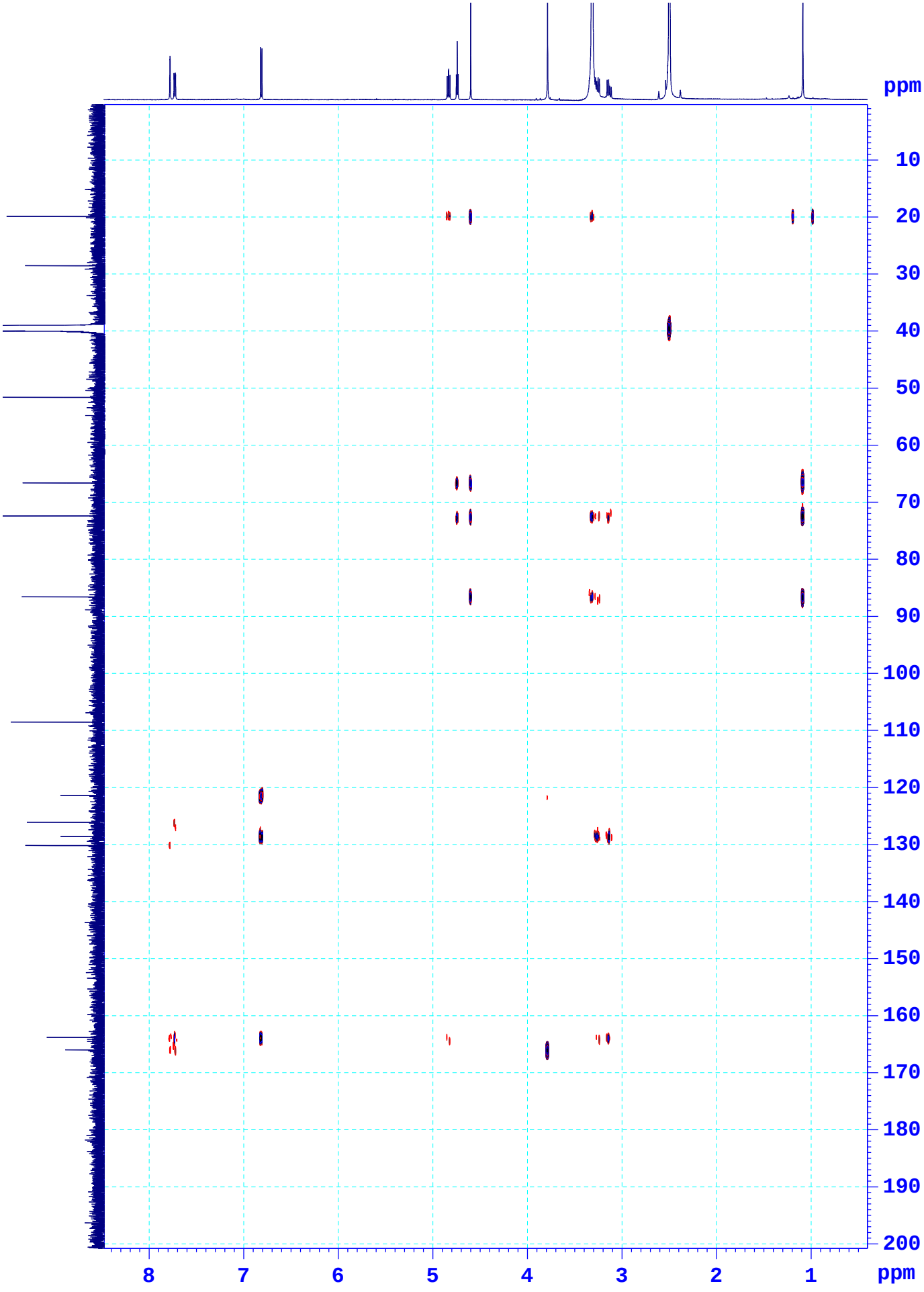
Pt2-DMSO-HMBC
ppm
10
20
30
40
50
60
70
80
90
100
110
120
130
140
150
160
170
180
190
200
8
7
6
5
4
3
2
1
ppm

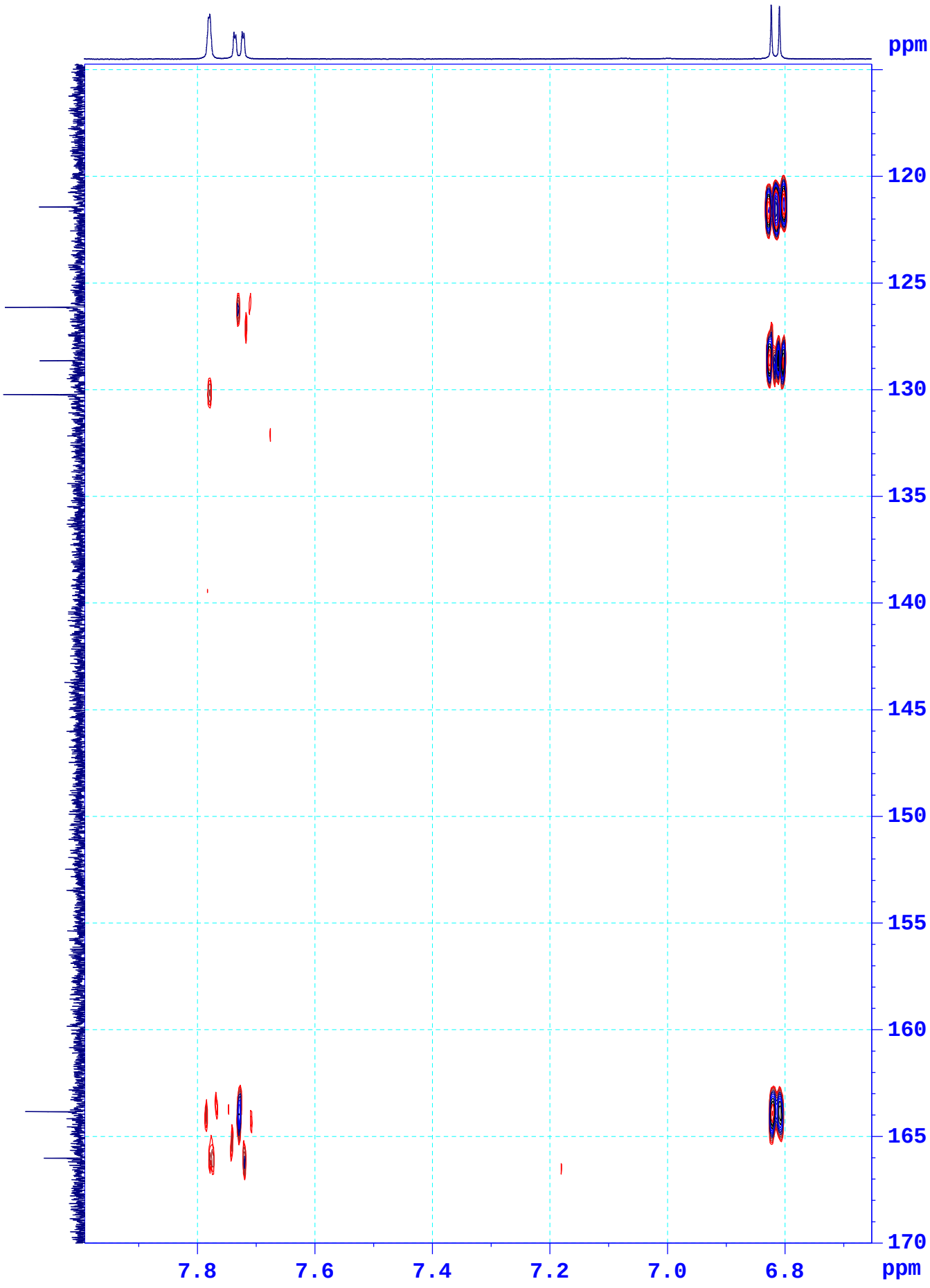
Pt2-DMSO-HMBC
ppm
120
125
130
135
140
145
150
155
160
165
170
7.8
7.6
7.4
7.2
7.0
6.8
ppm

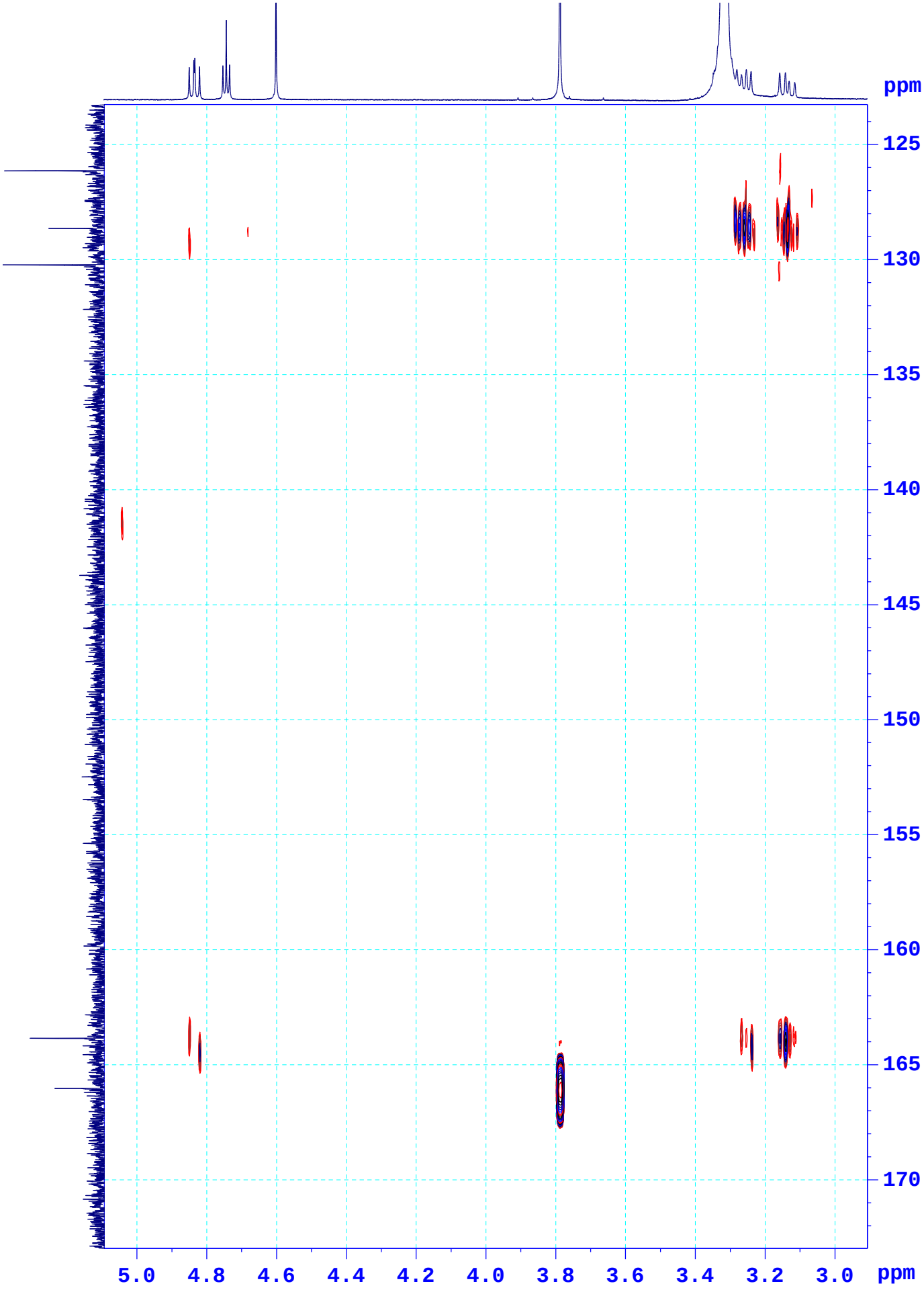
Pt2-DMSO-HMBC
ppm
125
130
135
140
145
150
155
160
165
170
5.0
4.8
4.6
4.4
4.2
4.0
3.8
3.6
3.4
3.2
3.0
ppm

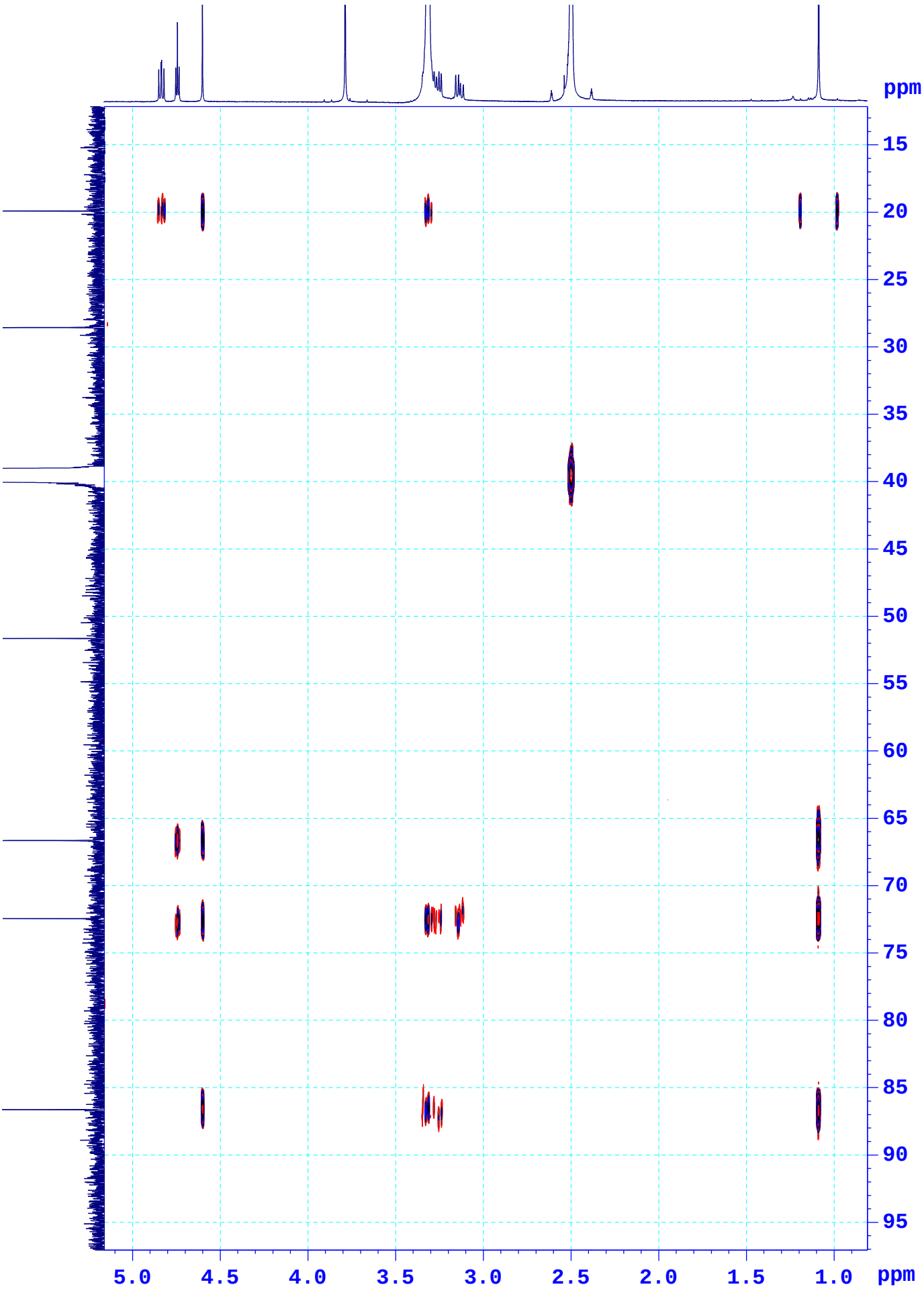
Pt2-DMSO-HMBC
ppm
15
20
25
30
35
40
45
50
55
60
65
70
75
80
85
90
95
5.0
4.5
4.0
3.5
3.0
2.5
2.0
1.5
1.0
ppm

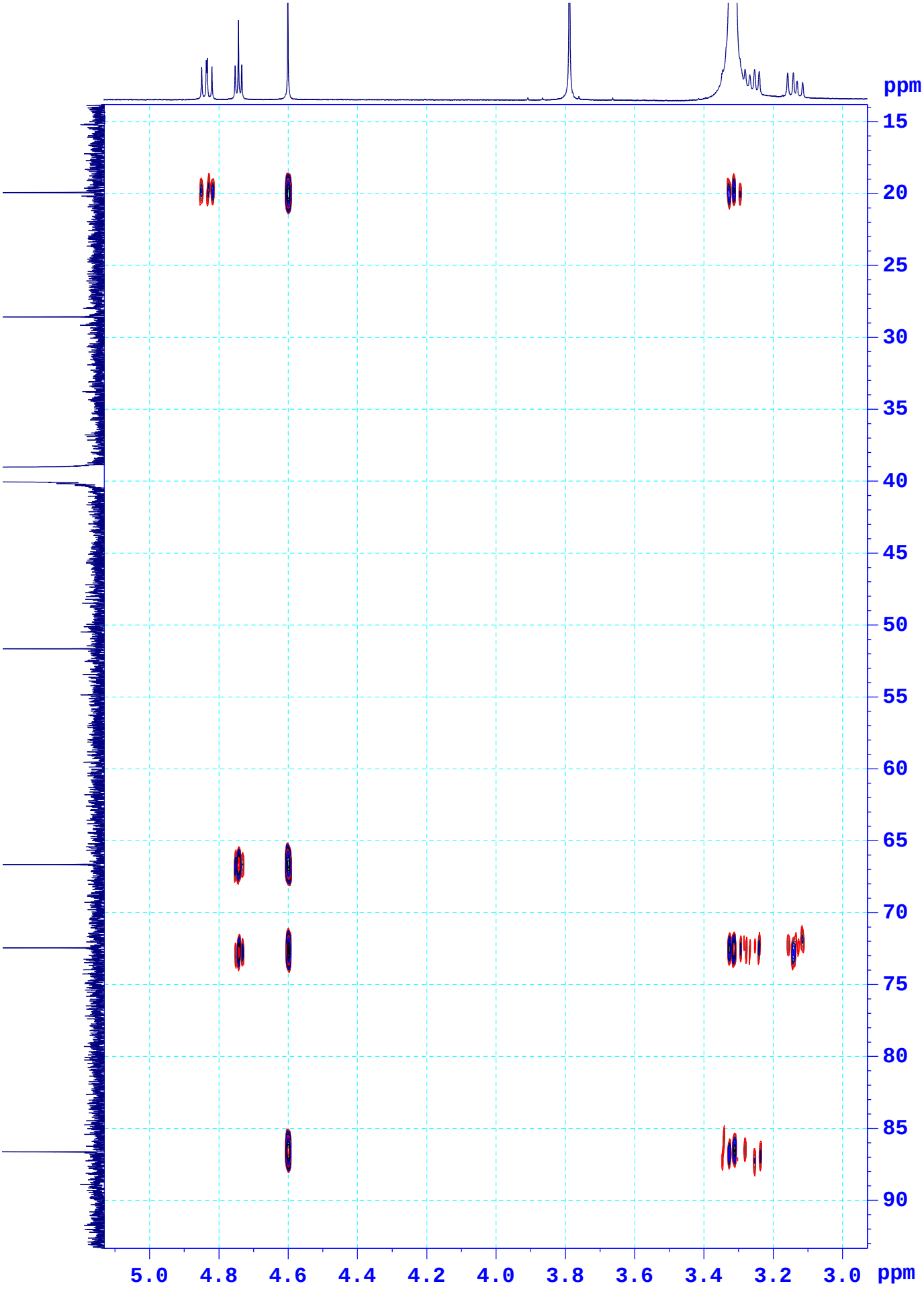
Pt2-DMSO-HMBC
ppm
15
20
25
30
35
40
45
50
55
60
65
70
75
80
85
90
5.0
4.8
4.6
4.4
4.2
4.0
3.8
3.6
3.4
3.2
3.0
ppm

PAM1-DMSO-1H

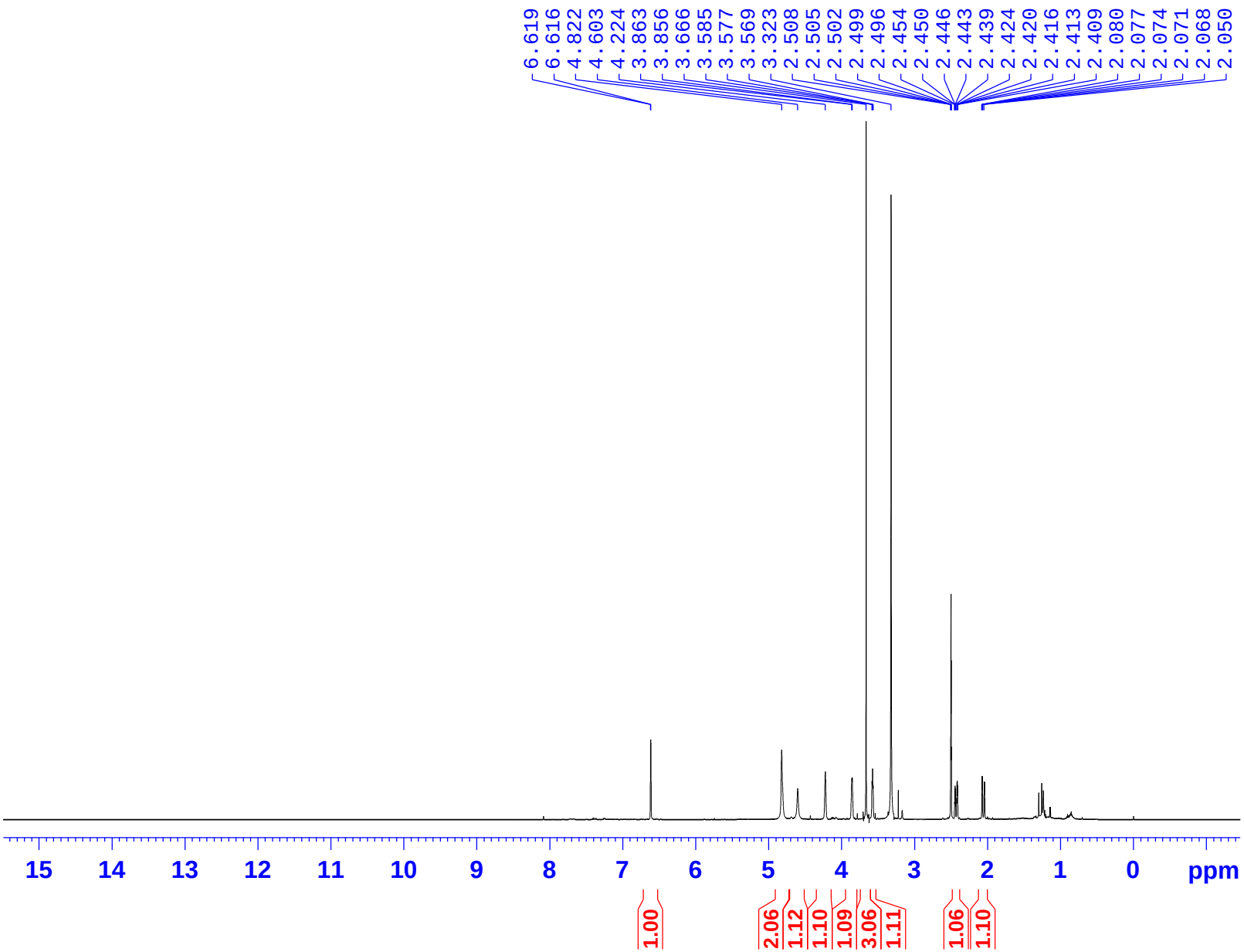
6.619
6.616
4.822
4.603
4.224
3.863
3.856
3.666
3.585
3.577
3.569
3.323
2.508
2.505
2.502
2.499
2.496
2.454
2.450
2.446
2.443
2.439
2.424
2.420
2.416
2.413
2.409
2.080
2.077
2.074
2.071
2.068
2.050
15
14
13
12
11
10
9
8
7
6
5
4
3
2
1
0
ppm
1.00
2.06
1.12
1.10
1.09
3.06
1.11
1.06
1.10

PAM1-DMSO-C13CPD

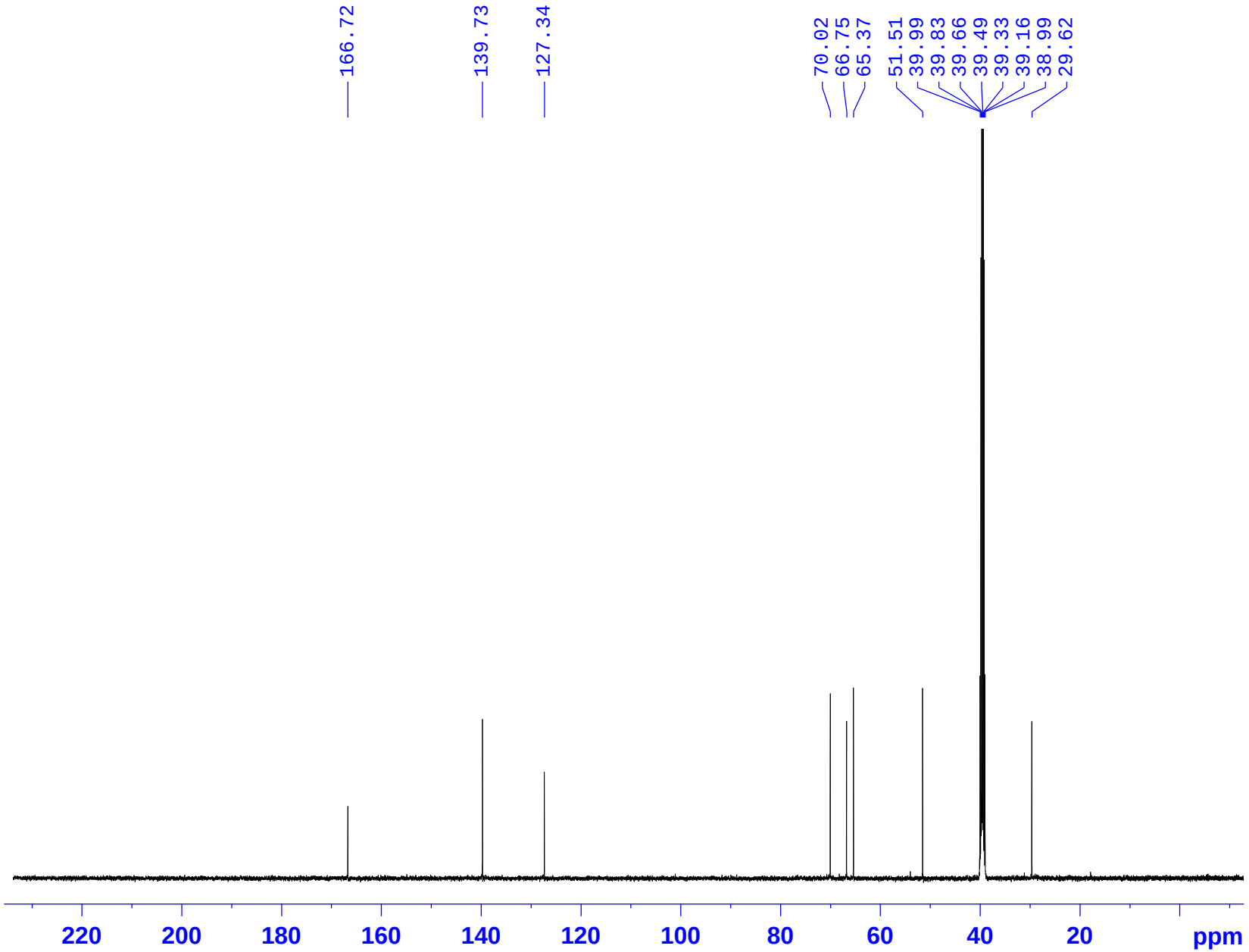

PAM2-DMSO-1H

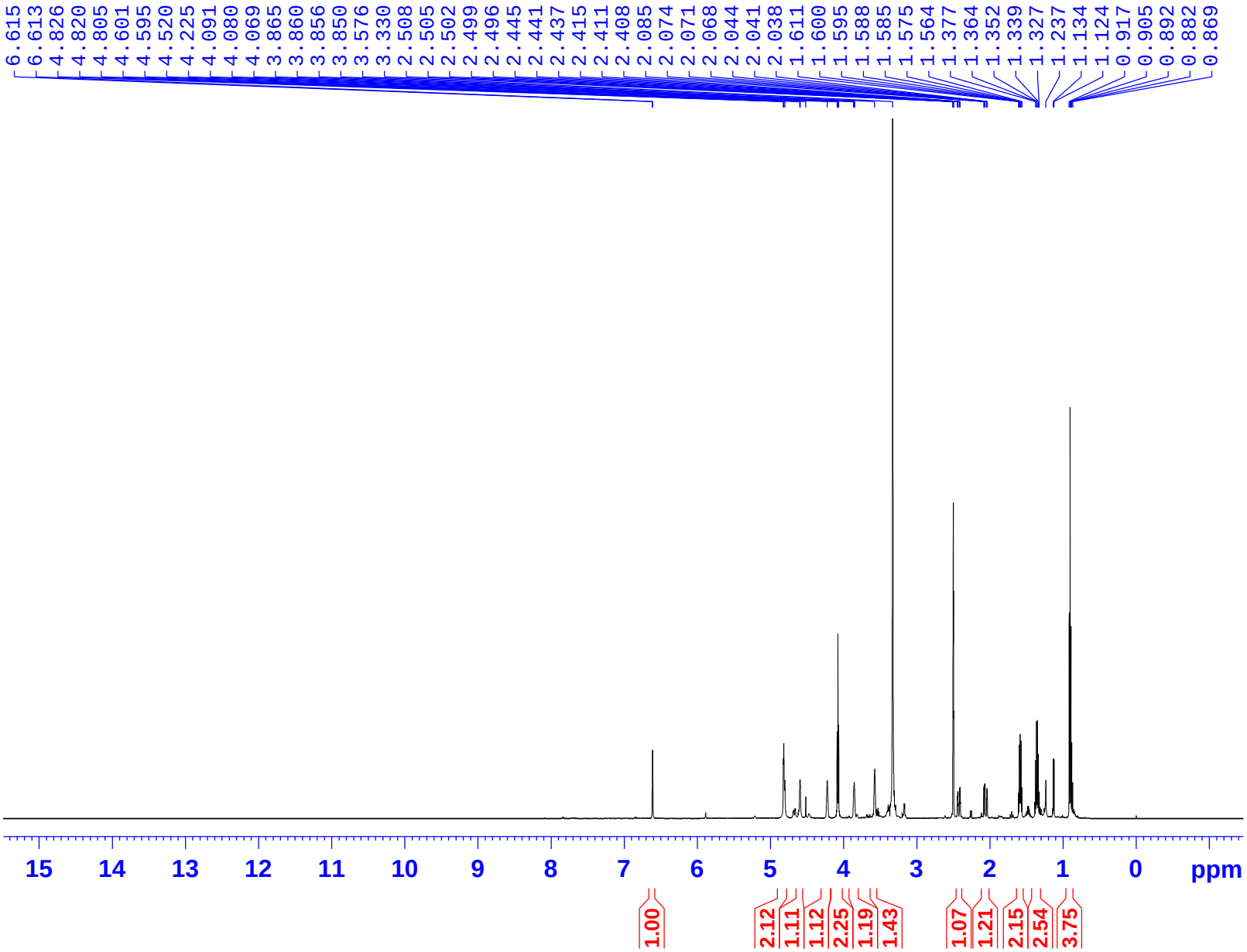
6.615
6.613
4.826
4.820
4.805
4.601
4.595
4.520
4.225
4.091
4.080
4.069
3.865
3.860
3.856
3.850
3.576
3.330
2.508
2.505
2.502
2.499
2.496
2.445
2.441
2.437
2.415
2.411
2.408
2.085
2.074
2.071
2.068
2.044
2.041
2.038
1.611
1.600
1.595
1.588
1.585
1.575
1.564
1.377
1.364
1.352
1.339
1.327
1.237
1.134
1.124
0.917
0.905
0.892
0.882
0.869
15
14
13
12
11
10
9
8
7
6
5
4
3
2
1
0
ppm
1.00
2.12
1.11
1.12
2.25
1.19
1.43
1.07
1.21
2.15
2.54
3.75

PAM2-DMSO-C13CPD

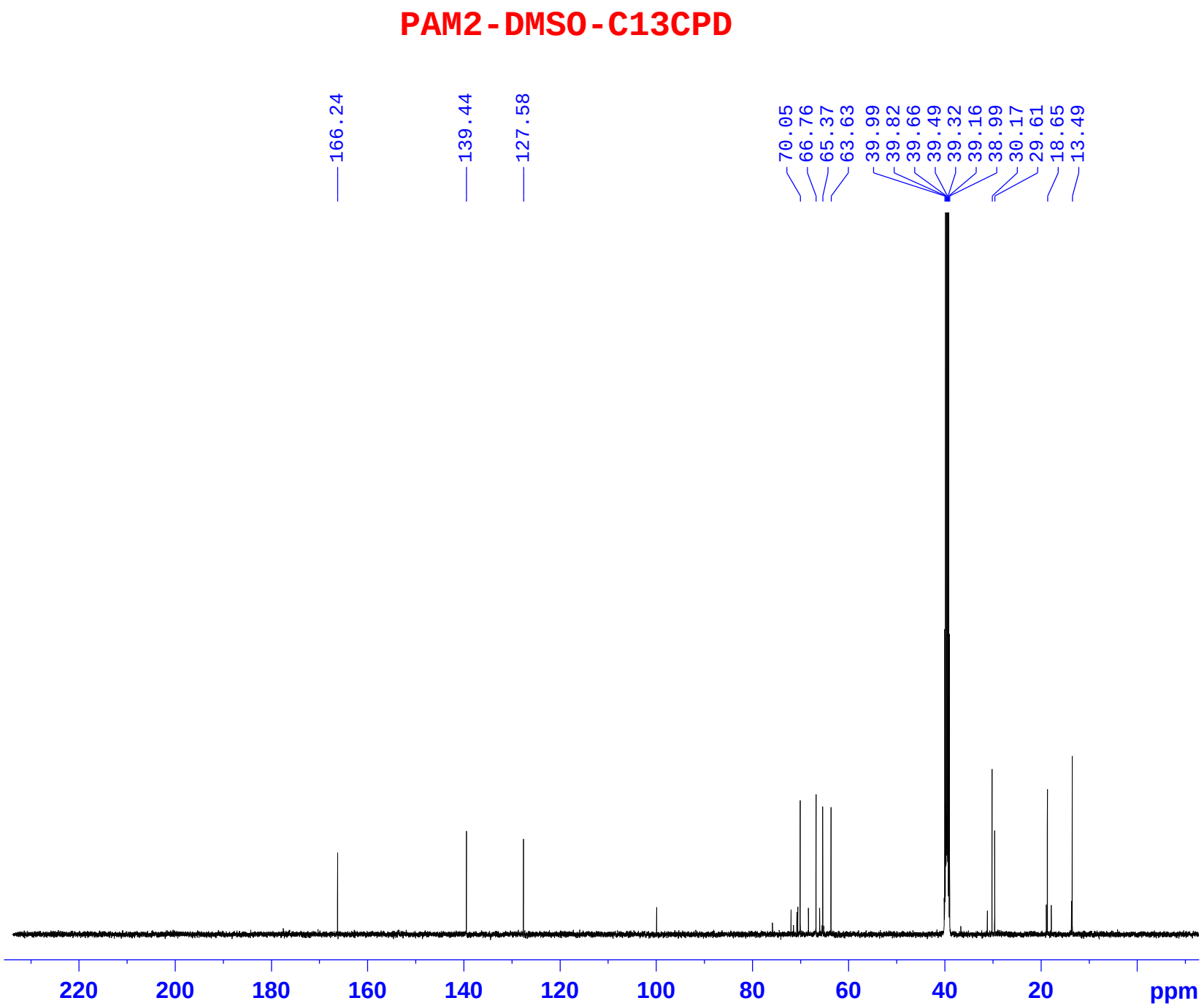

PAM3-DMSO-1H

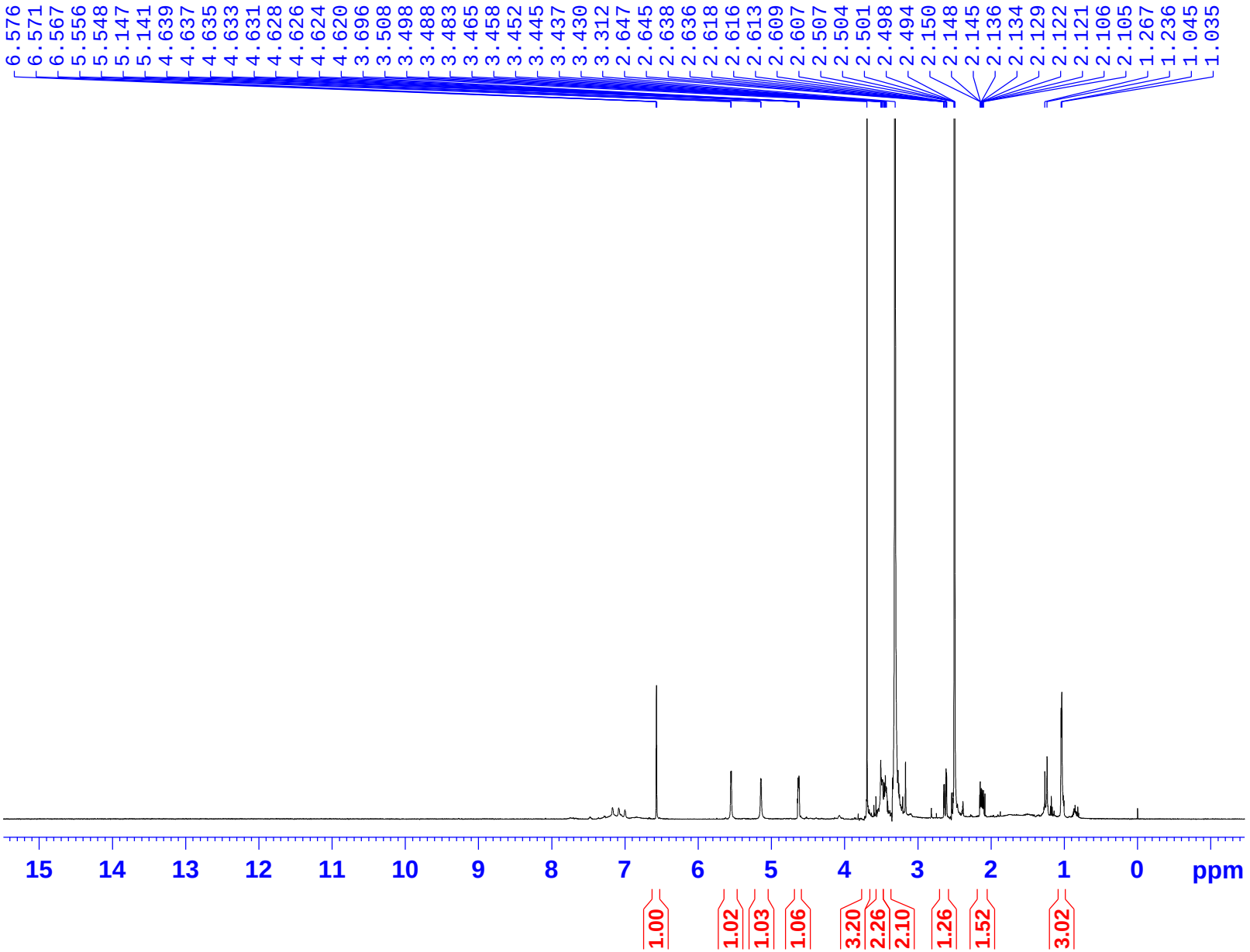
6.576
6.571
6.567
6.556
6.548
5.147
5.141
4.639
4.637
4.635
4.633
4.631
4.628
4.626
4.624
4.620
3.696
3.508
3.498
3.488
3.483
3.465
3.458
3.452
3.445
3.437
3.430
3.312
2.647
2.645
2.638
2.636
2.618
2.616
2.613
2.609
2.607
2.507
2.504
2.501
2.498
2.494
2.150
2.148
2.145
2.136
2.134
2.129
2.122
2.121
2.106
2.105
1.267
1.236
1.045
1.035
15
14
13
12
11
10
9
8
7
6
5
4
3
2
1
0
ppm
1.00
1.02
1.03
1.06
3.20
2.26
2.10
1.26
1.52
3.02

PAM3-DMSO-C13CPD

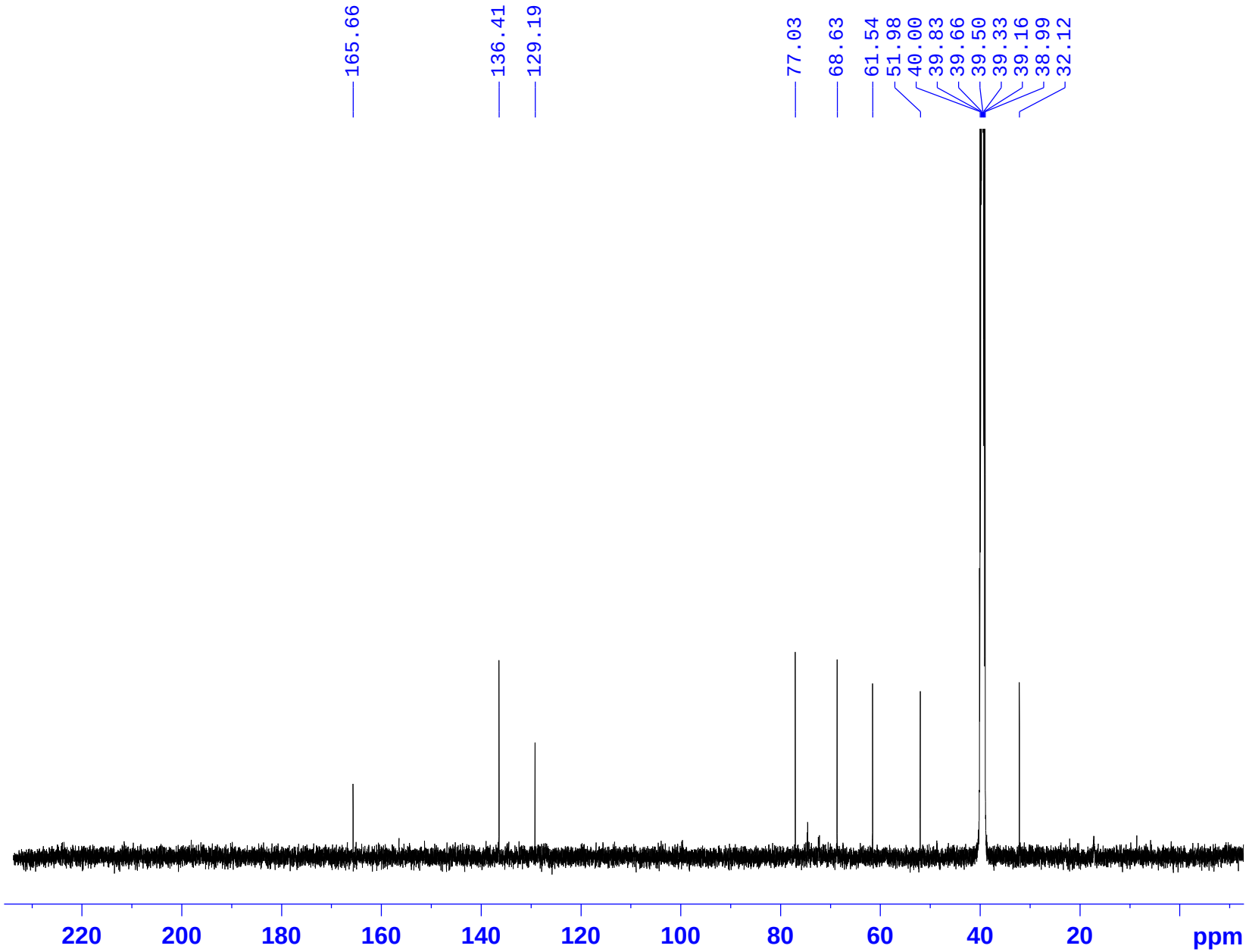

PAM5-MeOD-1H

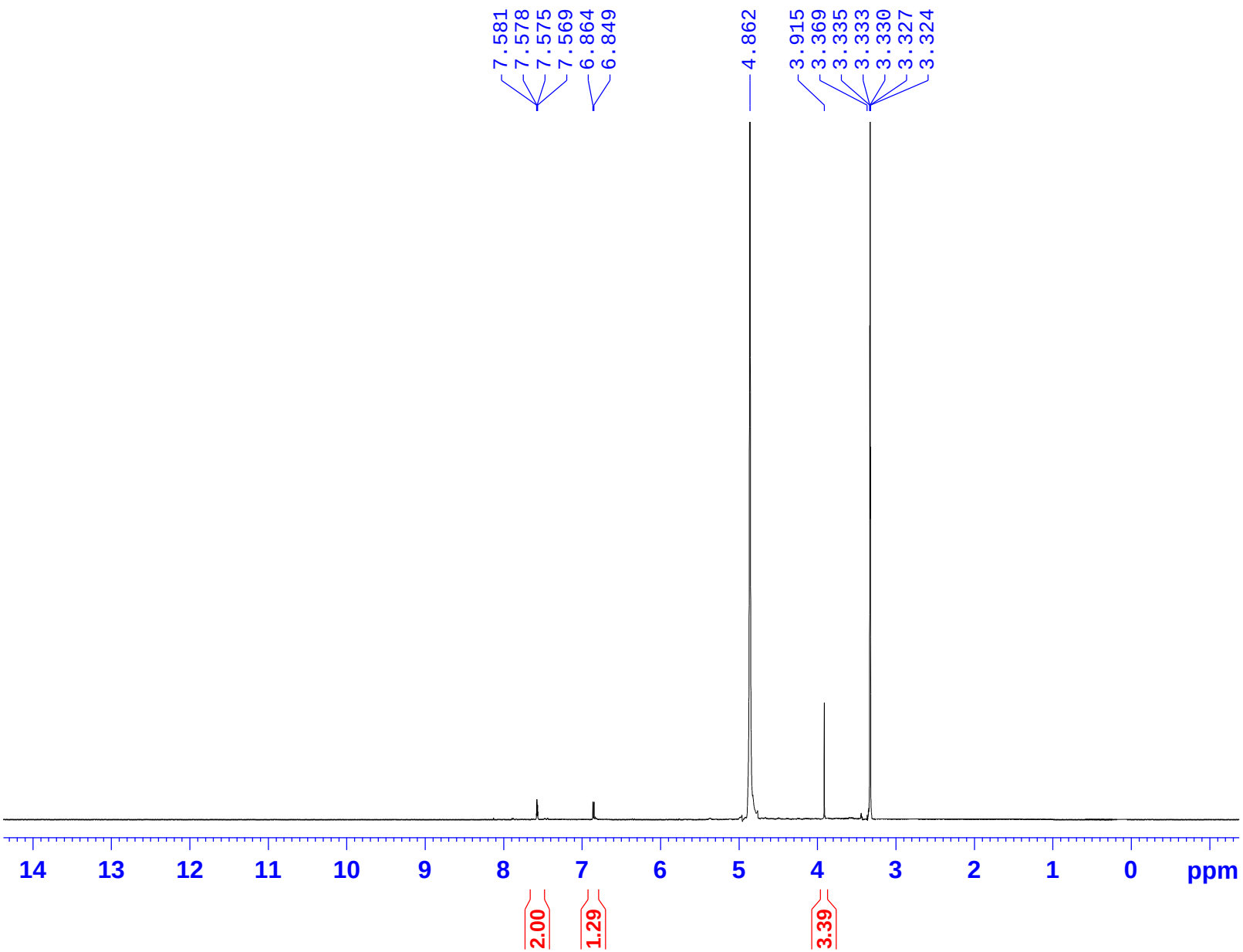
7.581
7.578
7.575
7.569
6.864
6.849
4.862
3.915
3.369
3.335
3.333
3.330
3.327
3.324
14
13
12
11
10
9
8
7
6
5
4
3
2
1
0
ppm
2.00
1.29
3.39

PAM5-MeOD-C13CPD

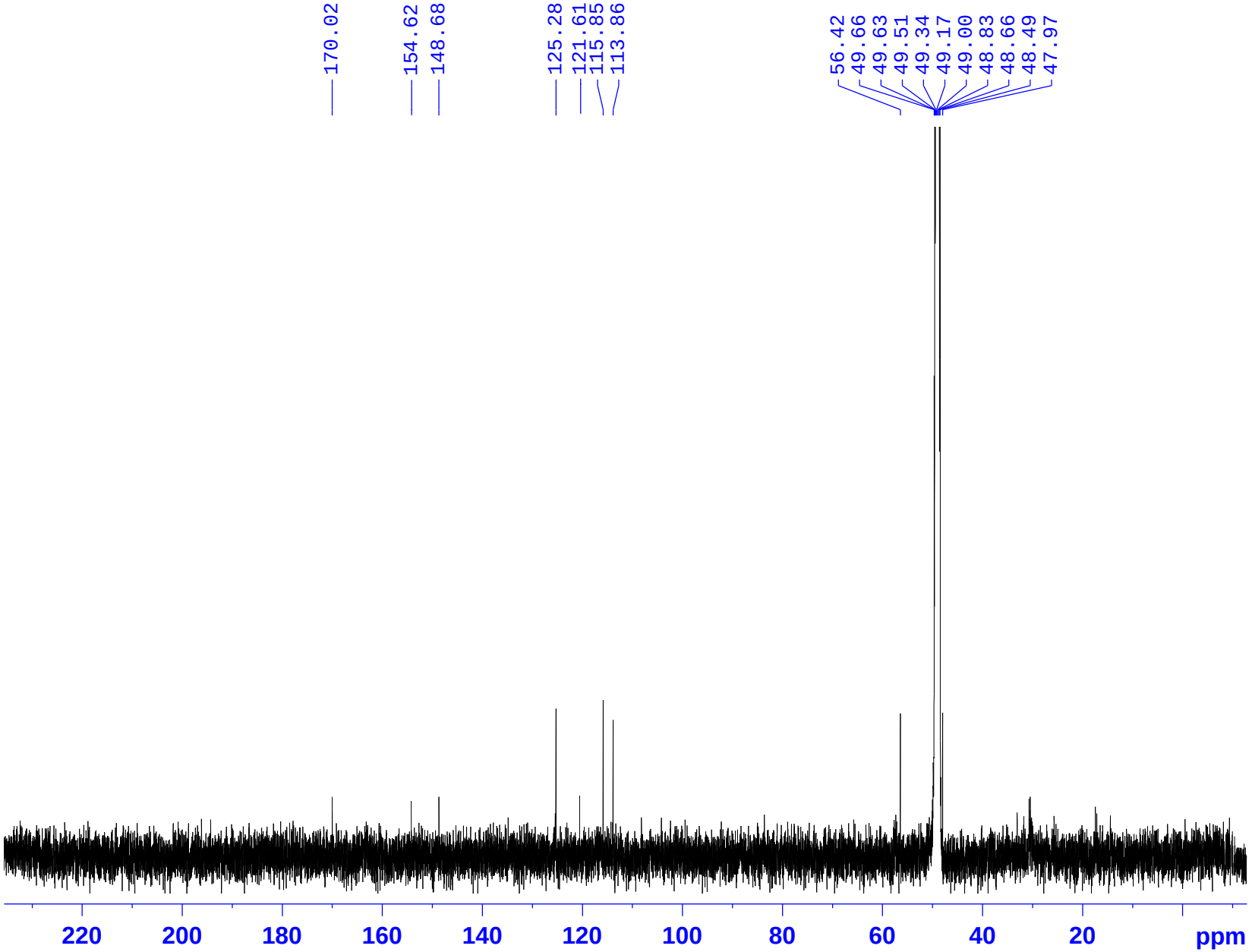

PAM6-MeOD-1H

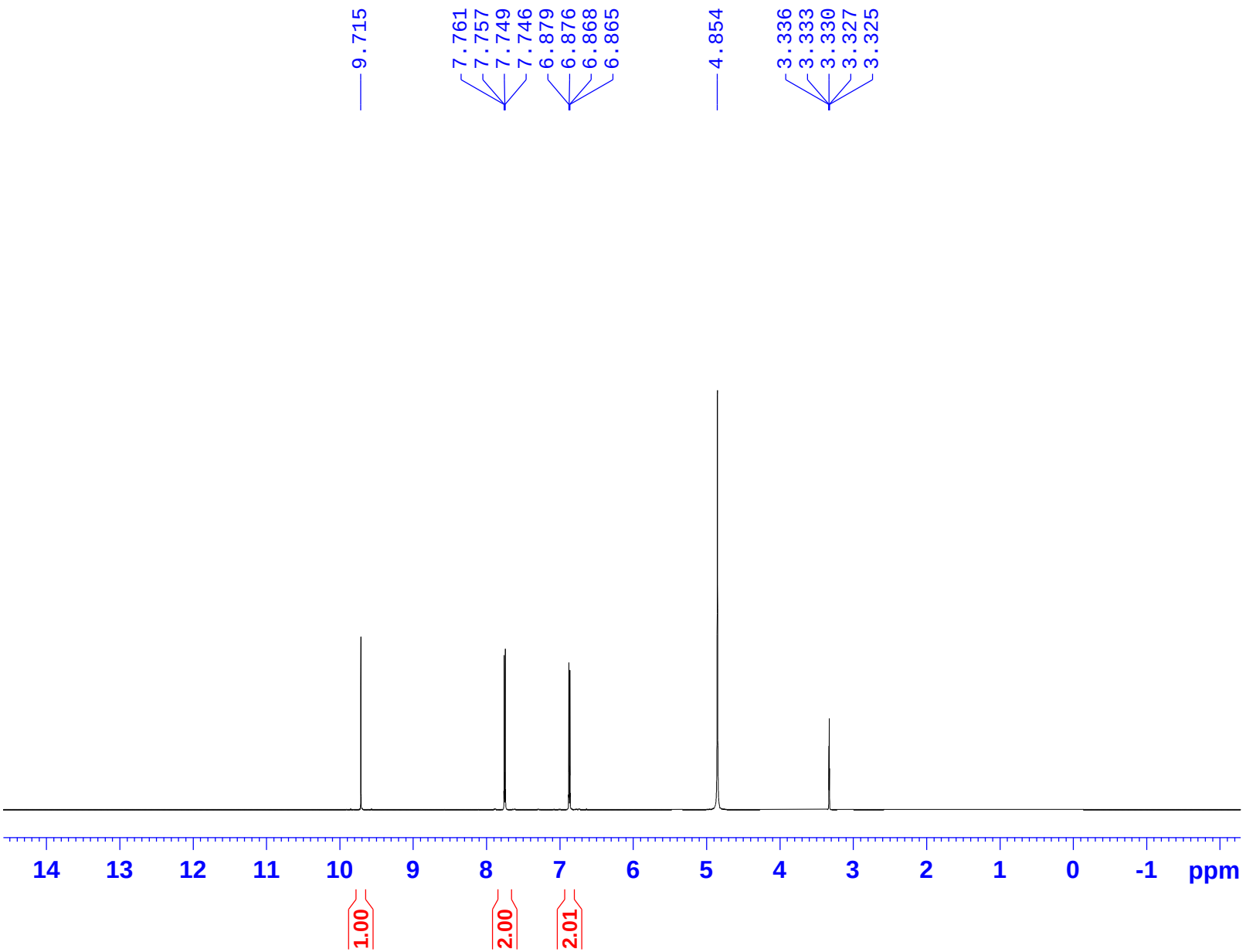
9.715
7.761
7.757
7.749
7.746
6.879
6.876
6.868
6.865
4.854
3.336
3.333
3.330
3.327
3.325
14
13
12
11
10
9
8
7
6
5
4
3
2
1
0
-1
ppm
1.00
2.00
2.01

PAM6-MeOD-1H

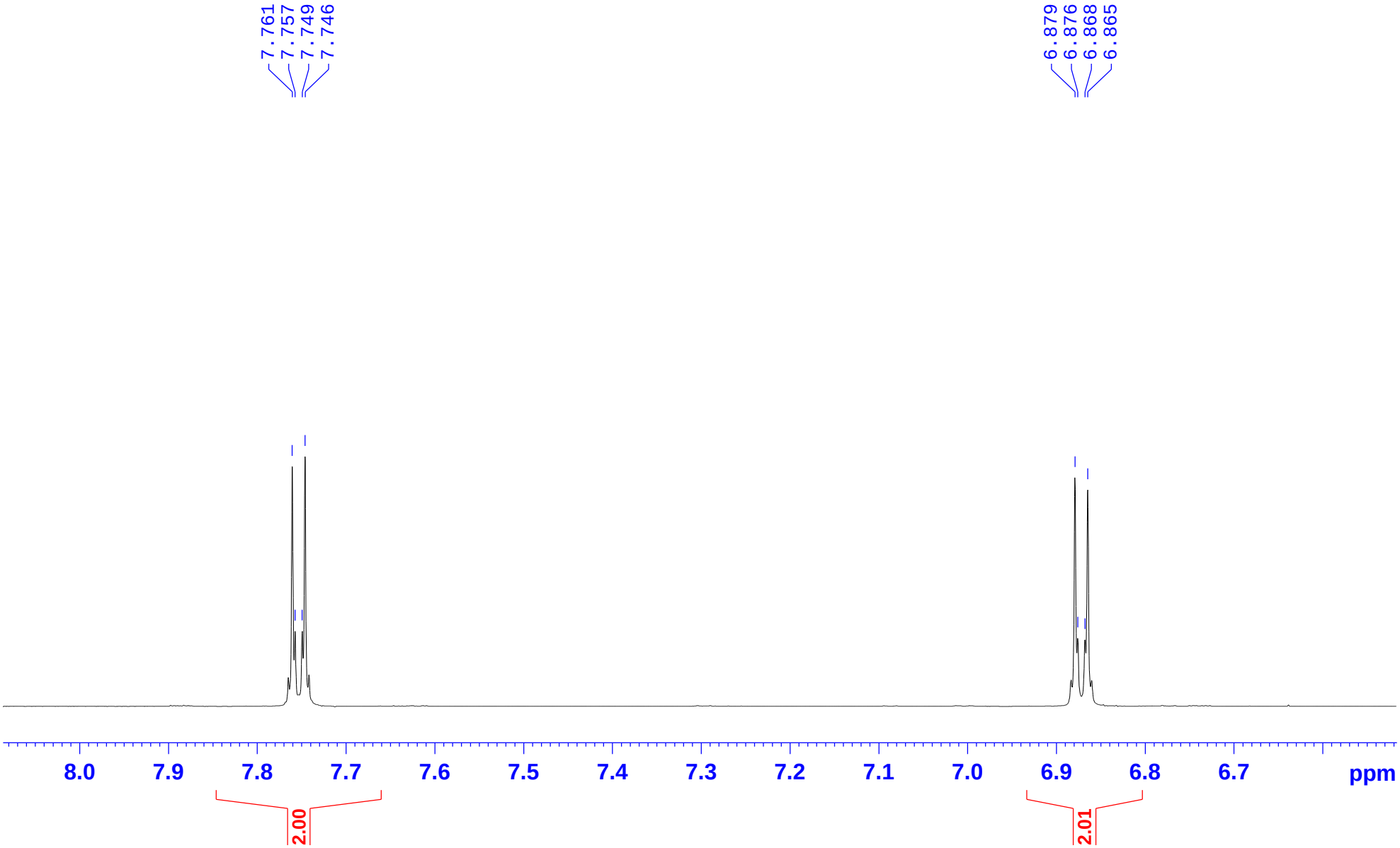
7.761
7.757
7.749
7.746
6.879
6.876
6.868
6.865
8.0
7.9
7.8
7.7
7.6
7.5
7.4
7.3
7.2
7.1
7.0
6.9
6.8
6.7
ppm
2.00
2.01

PAM7-MeOD-1H

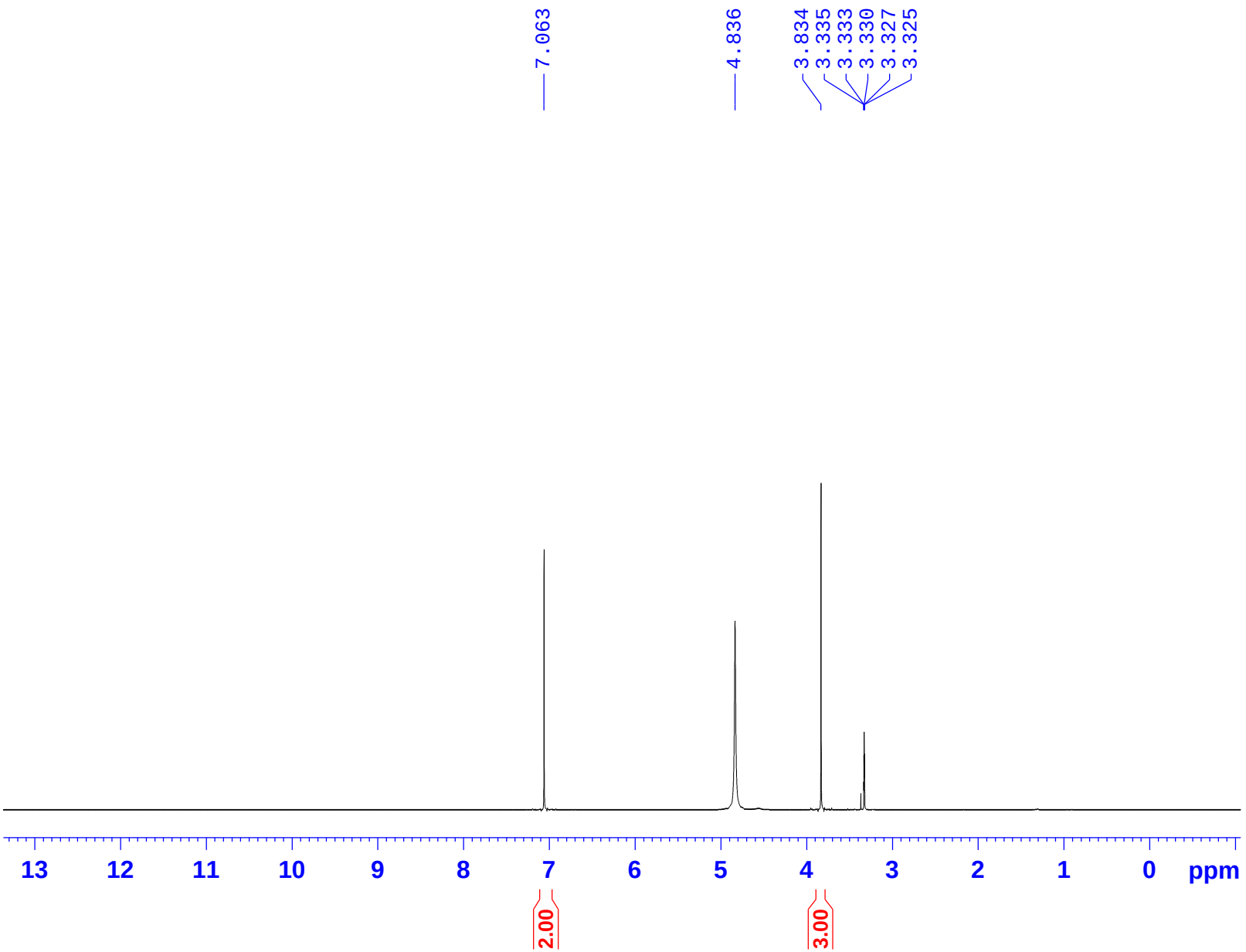
7.063
4.836
3.834
3.335
3.333
3.330
3.327
3.325
13
12
11
10
9
8
7
6
5
4
3
2
1
0
ppm
2.00
3.00

PAM7-MeOD-C13CPD

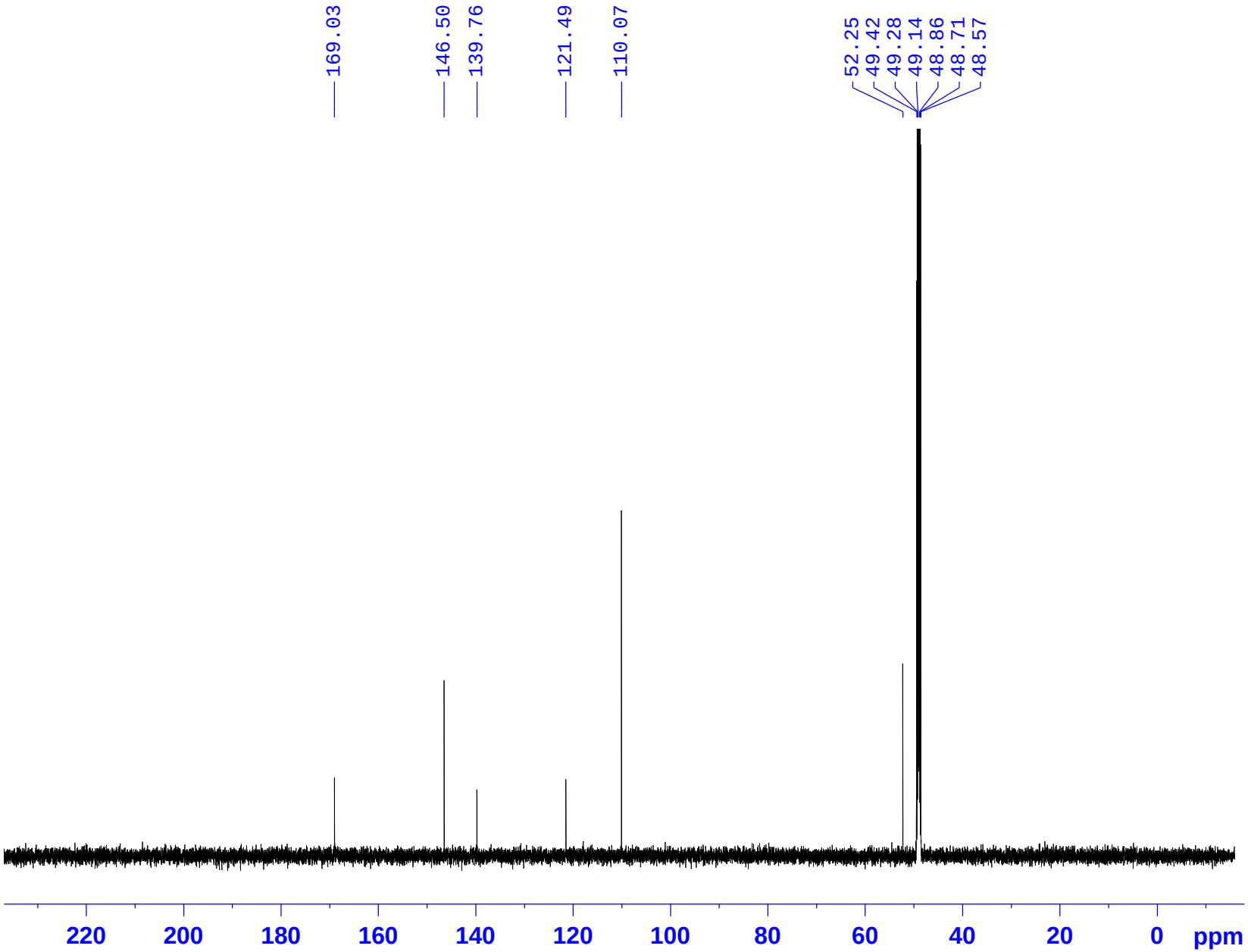

PAM10-DMSO-1H

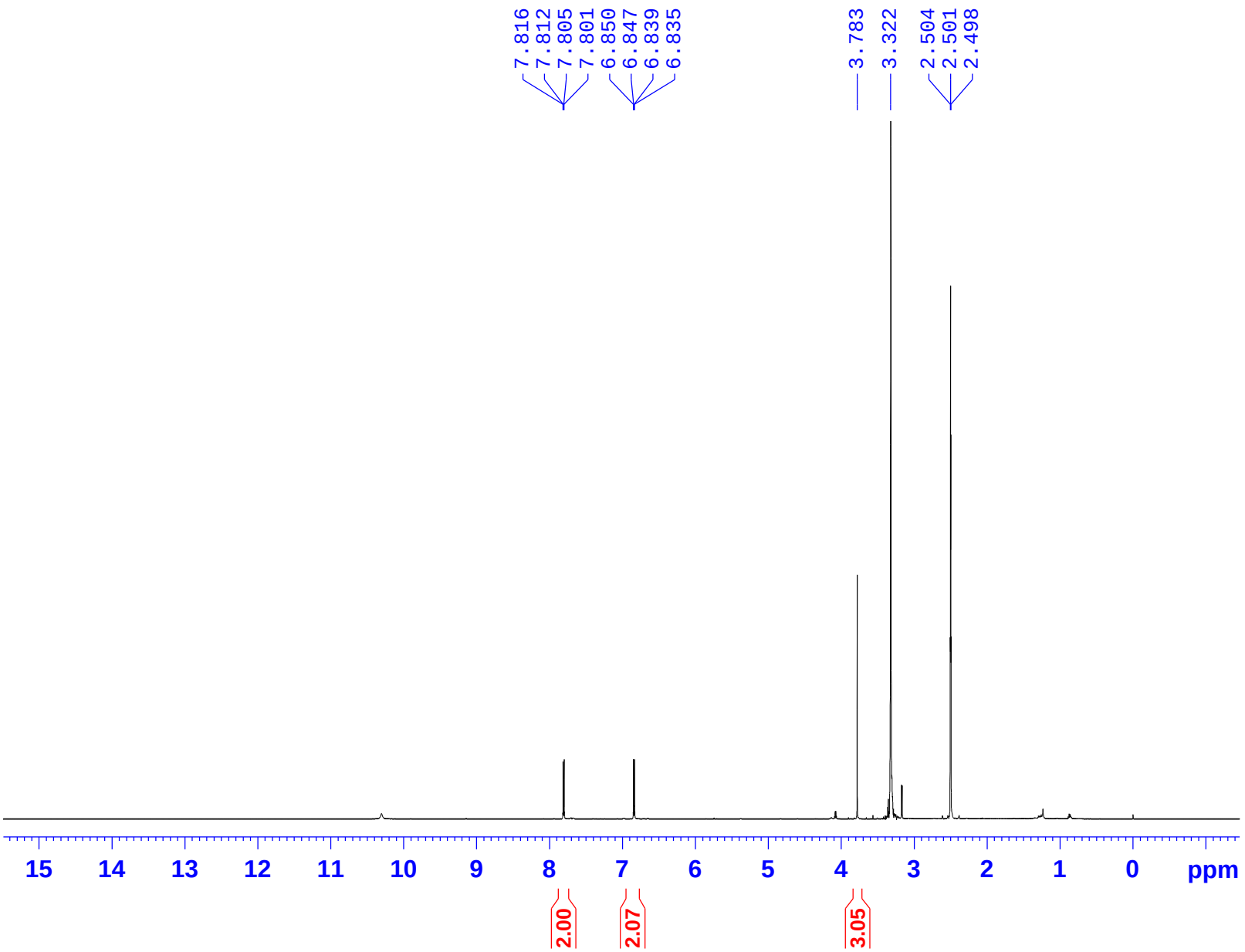

PAM10-DMSO-C13CPD

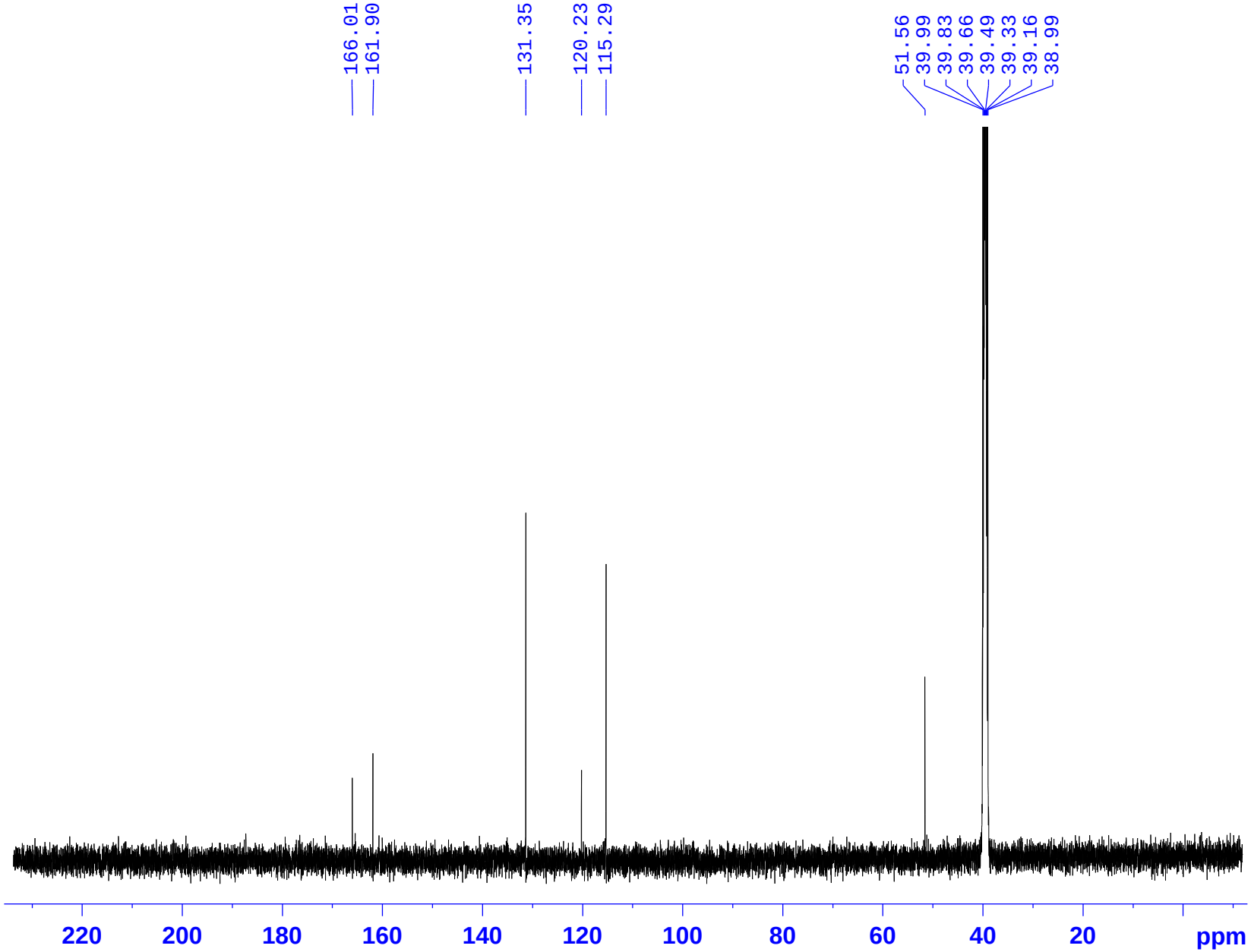

PAM11-DMSO-1H

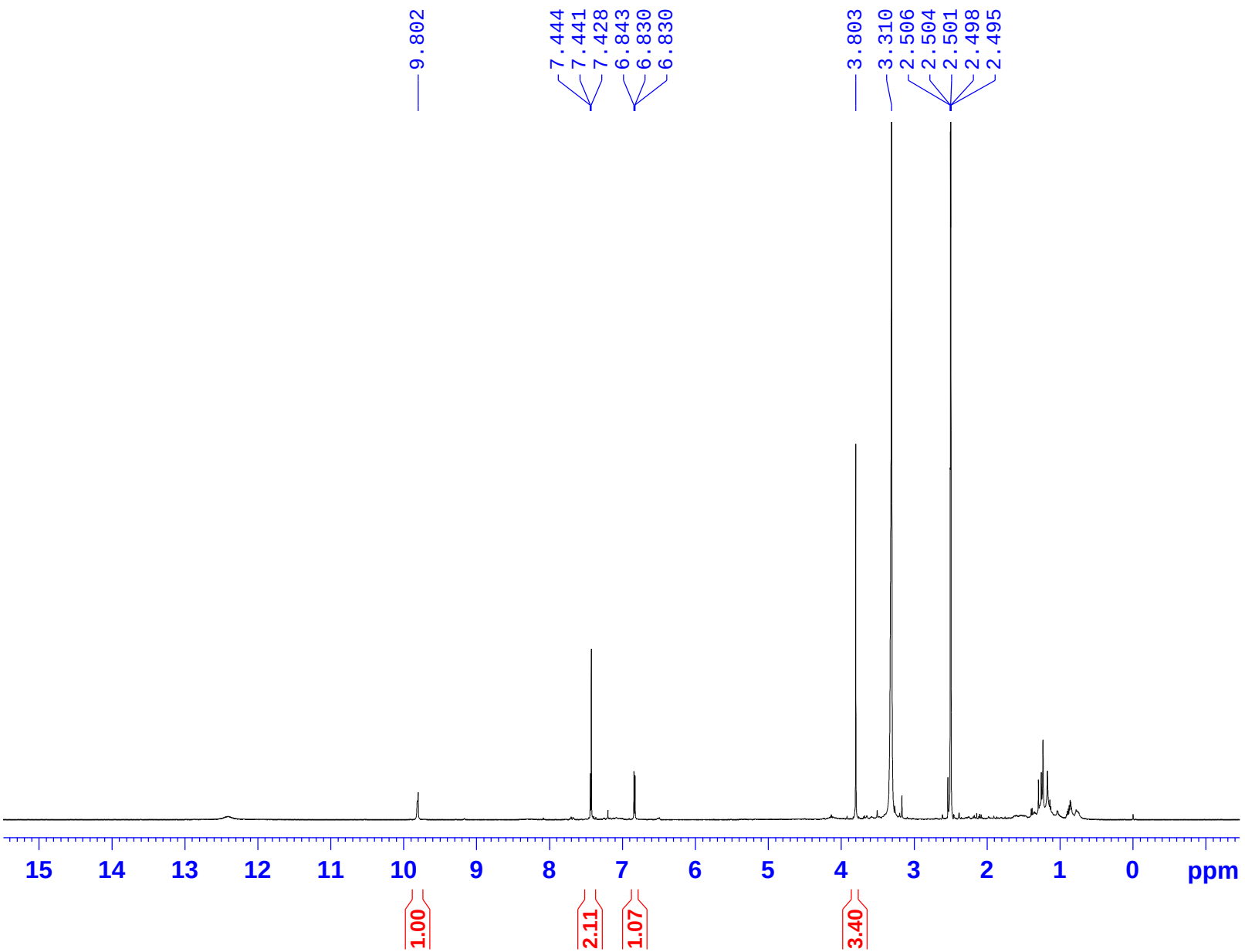

PAM11-DMSO-C13CPD

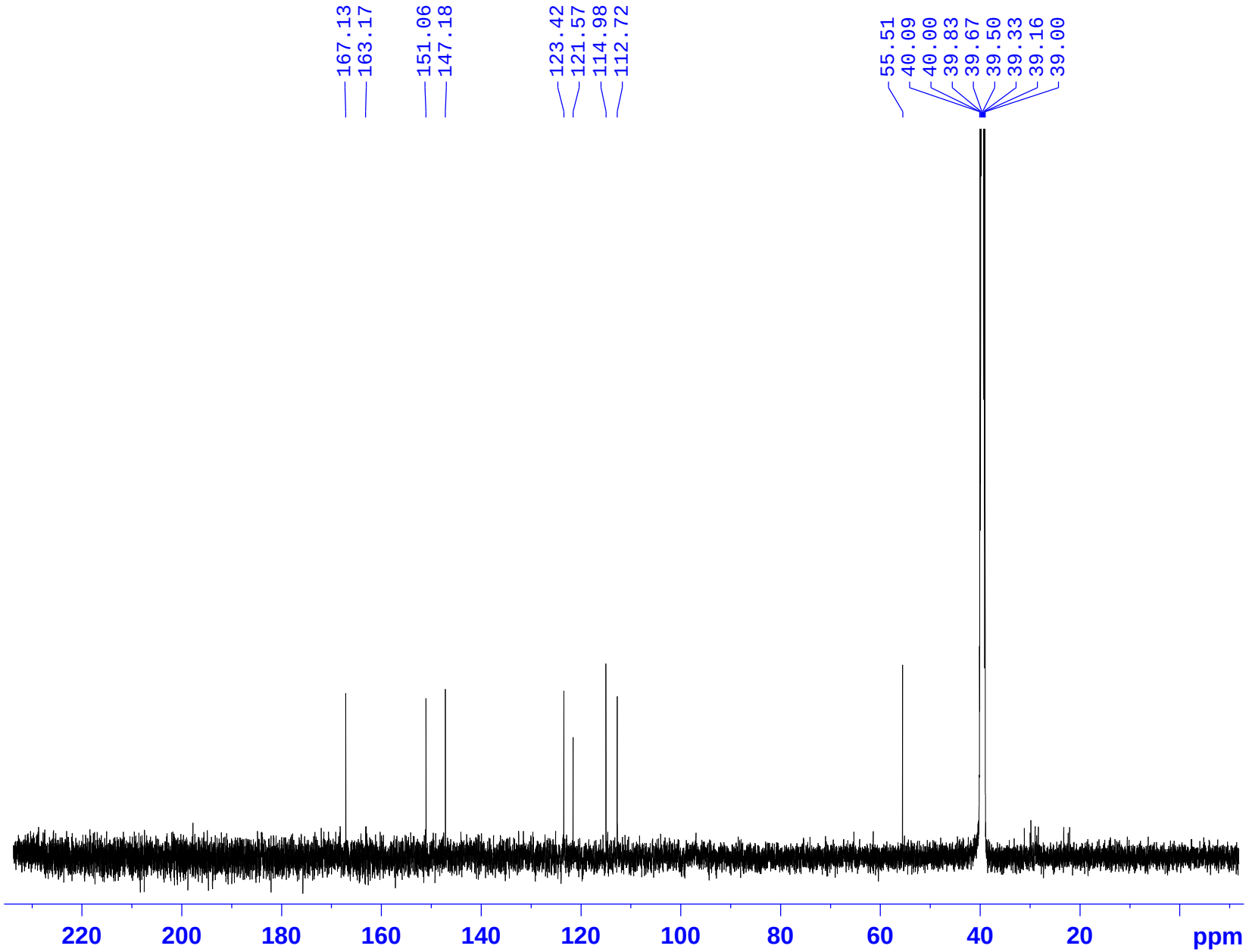

PAM12-DMSO-1H

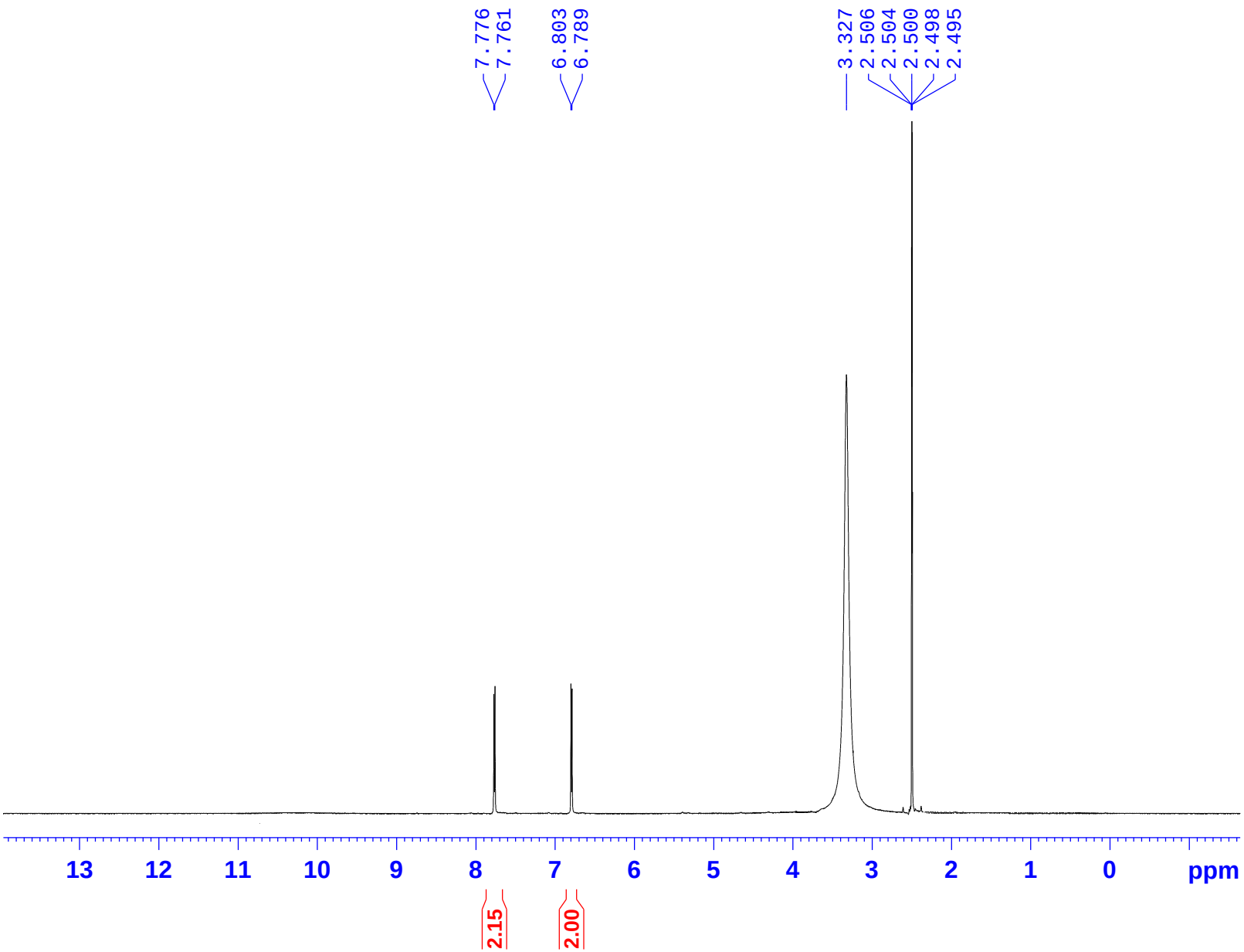

PAM12-DMSO-C13CPD

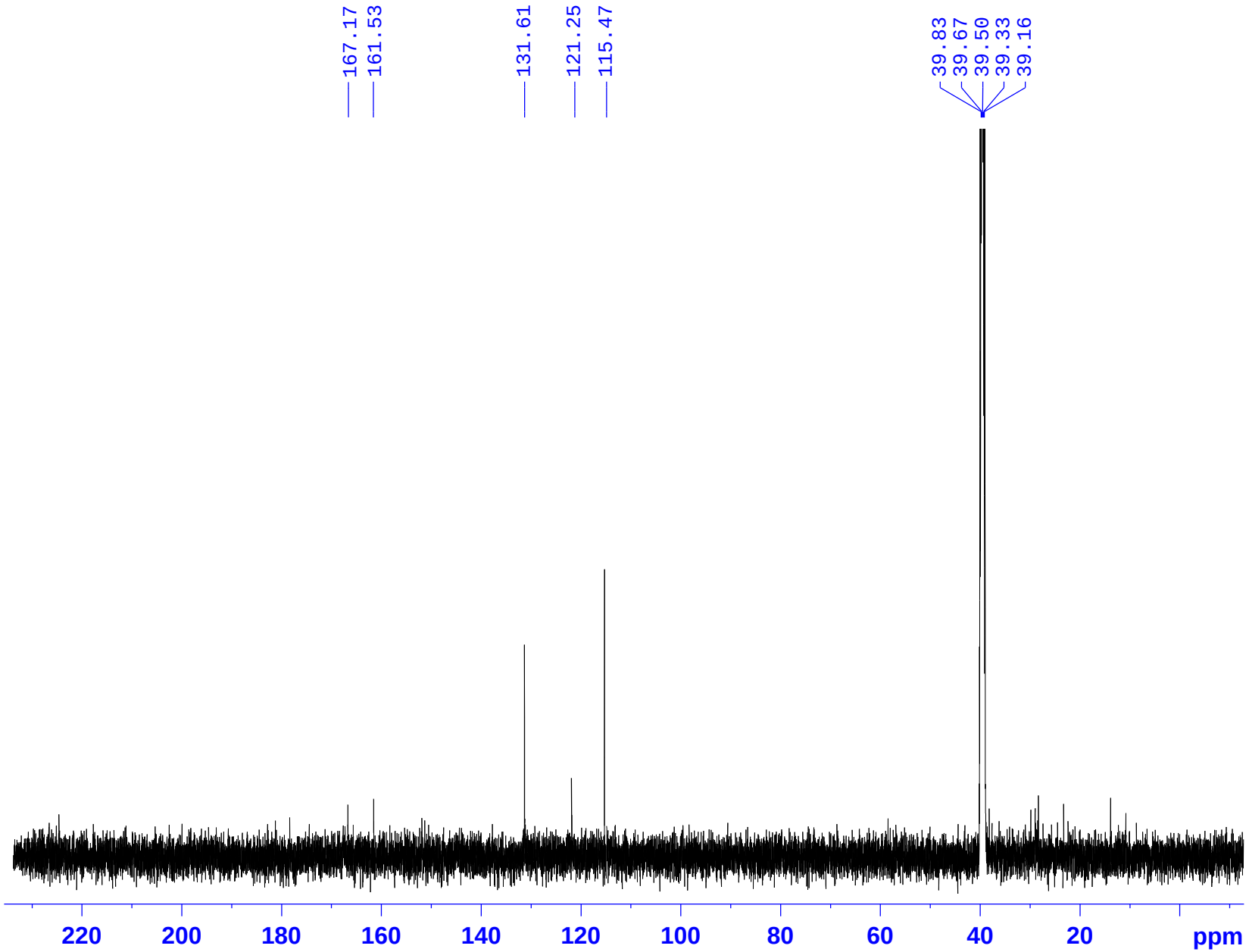

PAM13-MeOD-1H

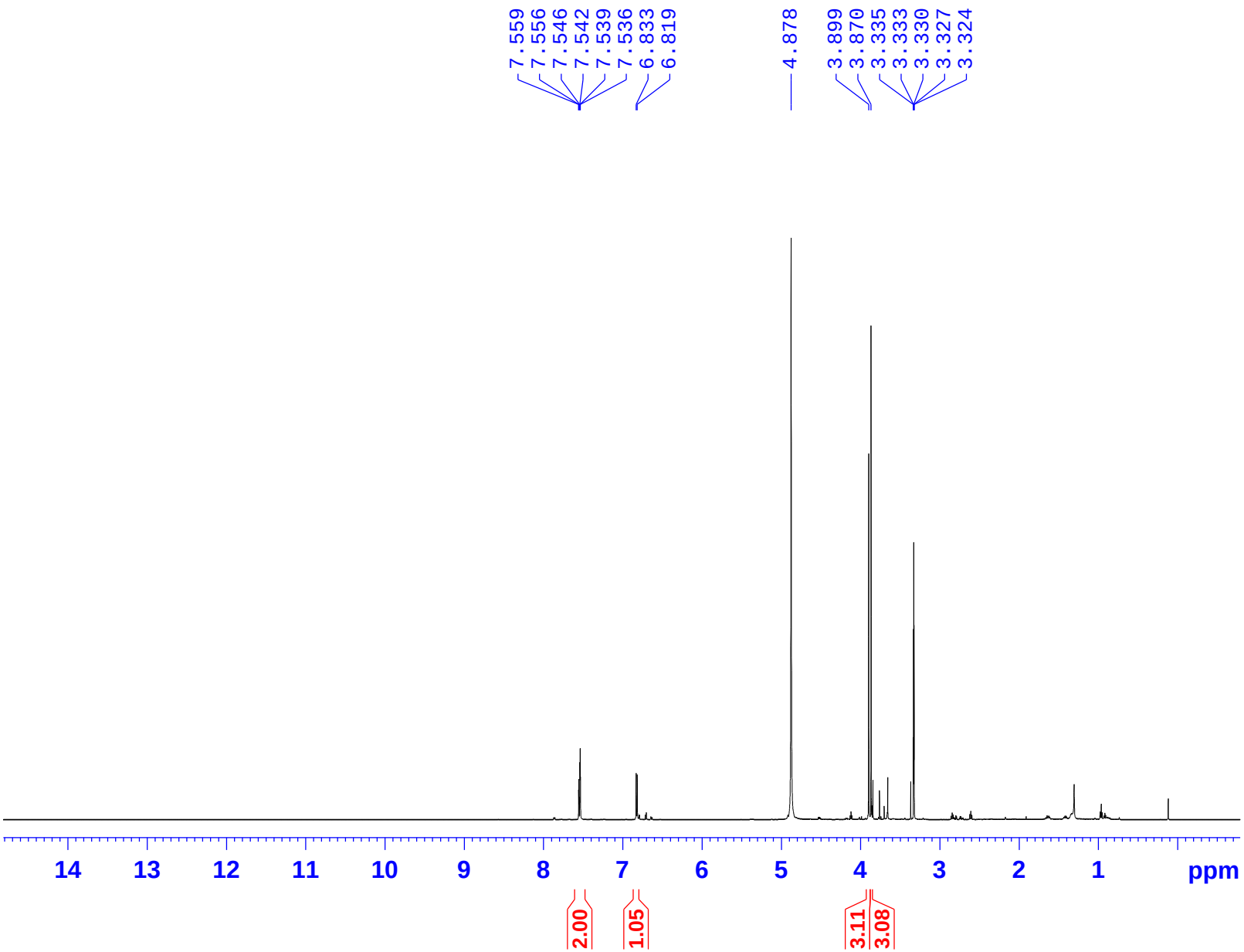

PAM13-MeOD-C13CPD

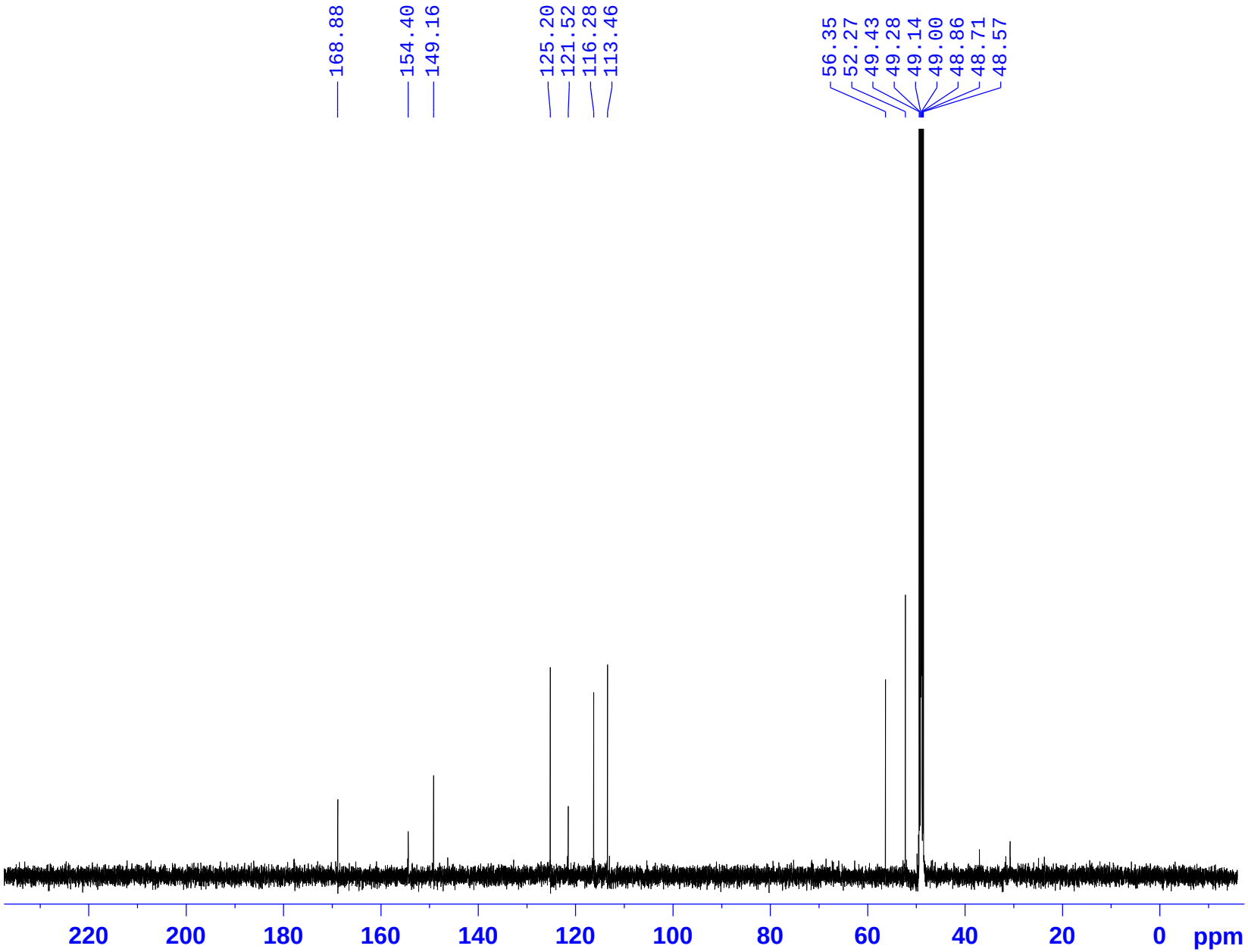

PAM14-MeOD-1H

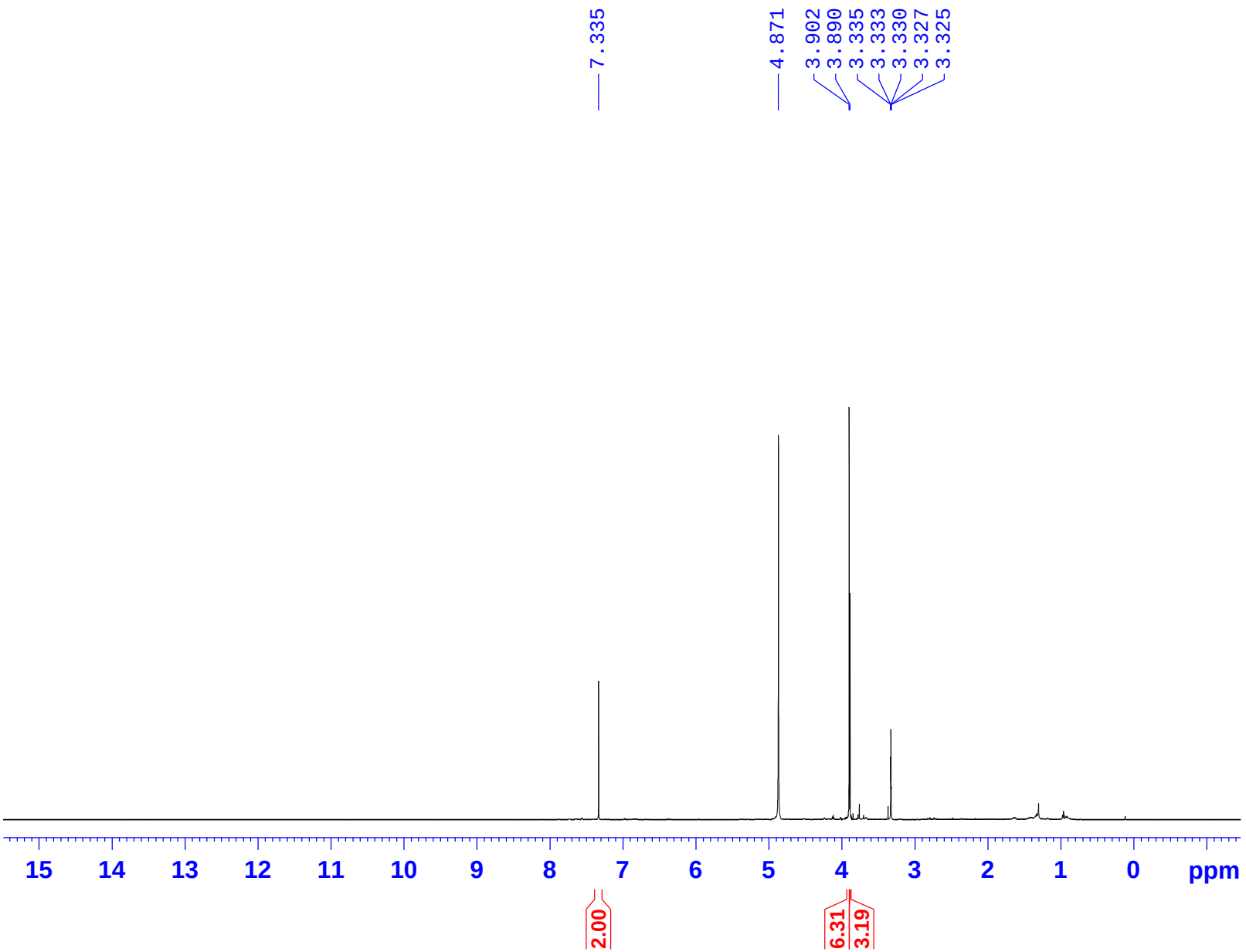

PAM14-MeOD-C13CPD

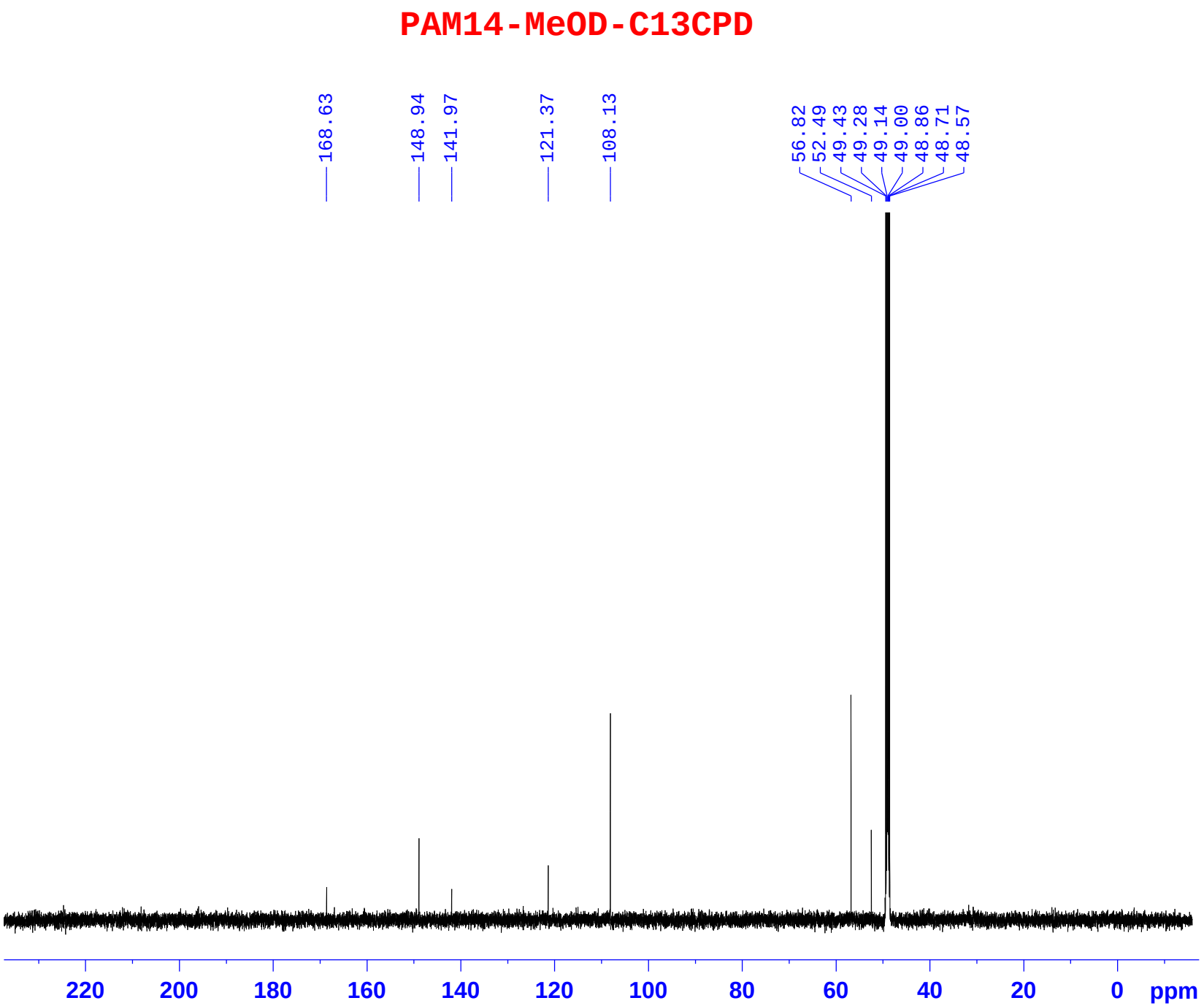

PAM15-DMSO-1H

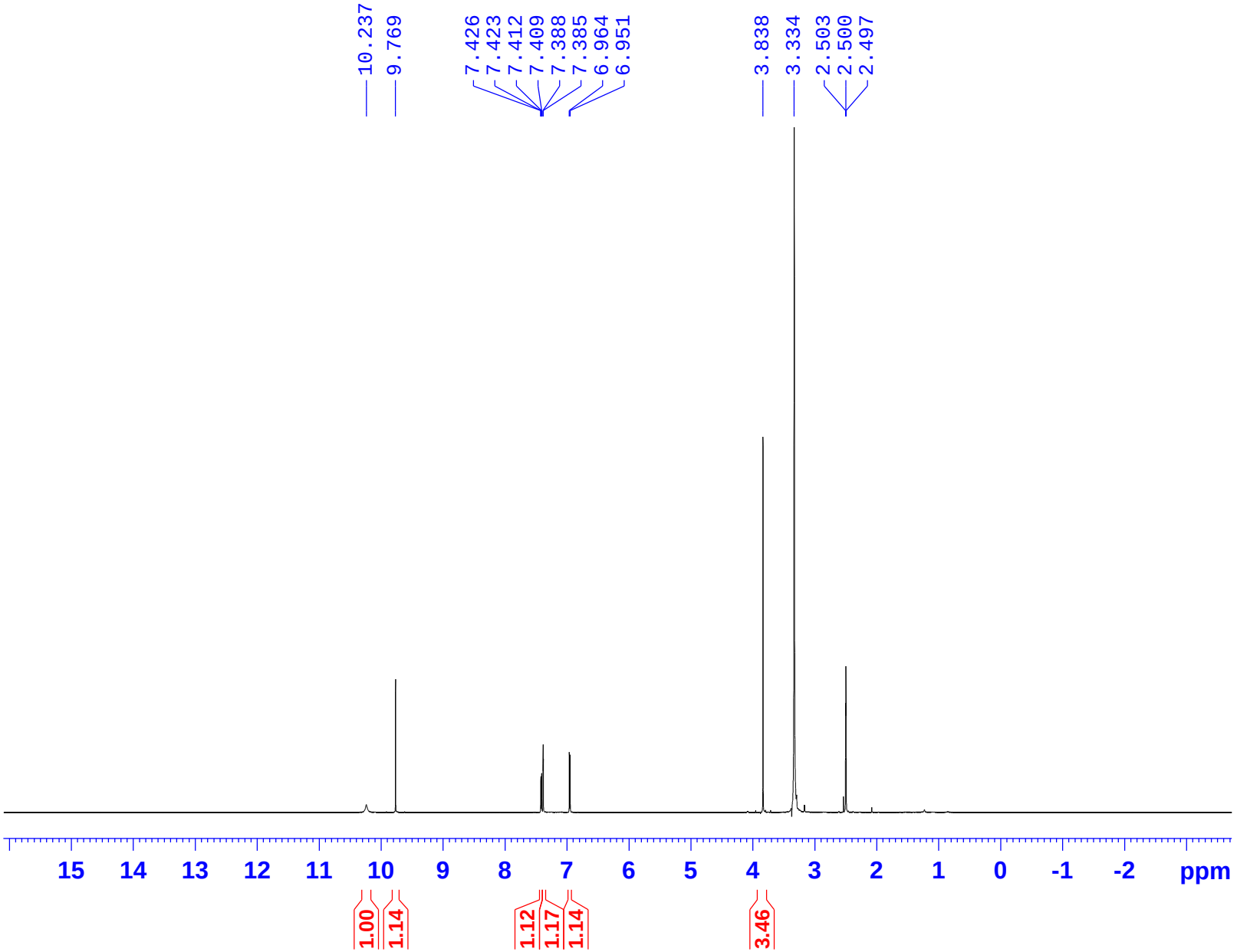

PAM15-DMSO-C13CPD

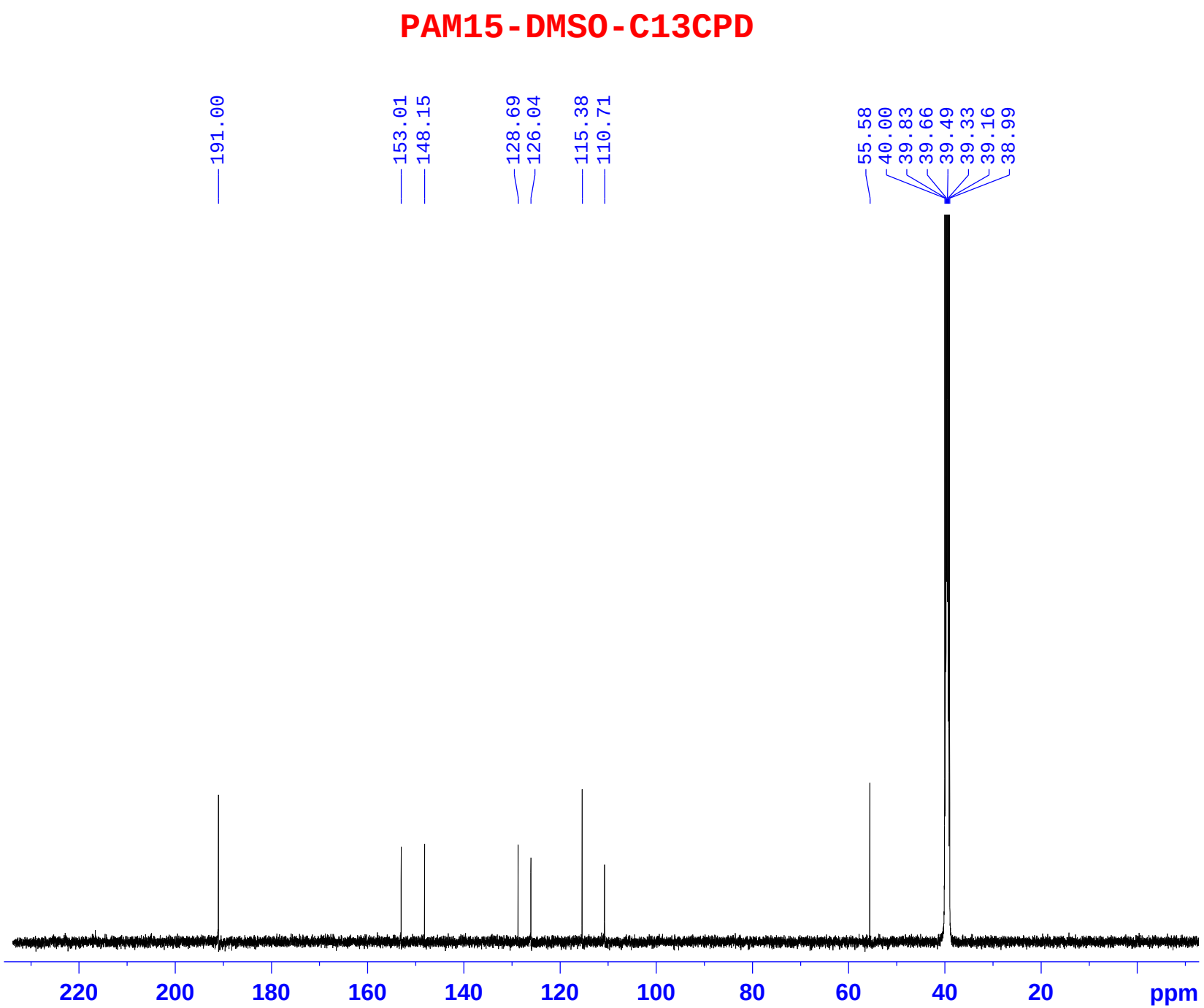

PAM16-Acetone-1H

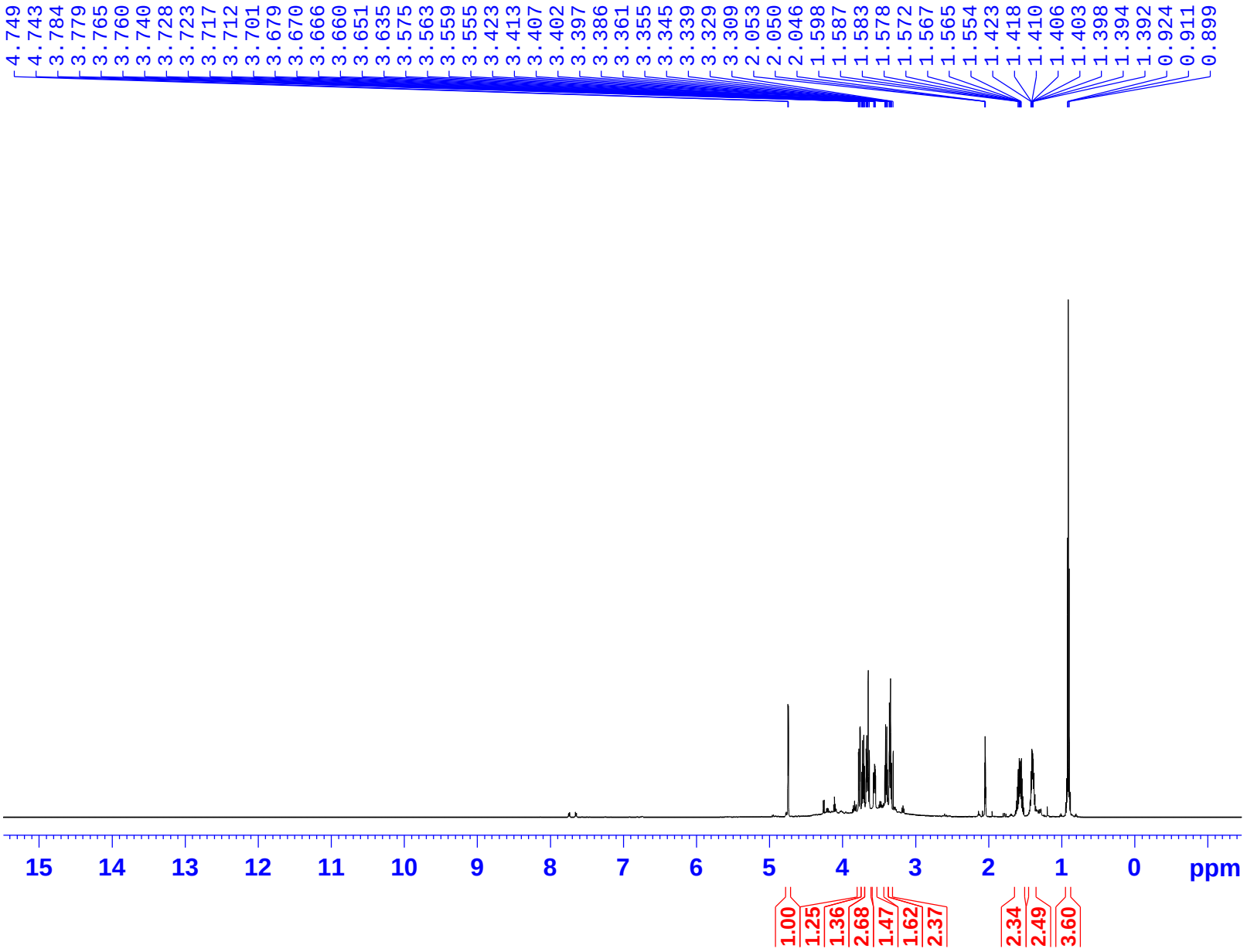

PAM16-Acetone-C13CPD

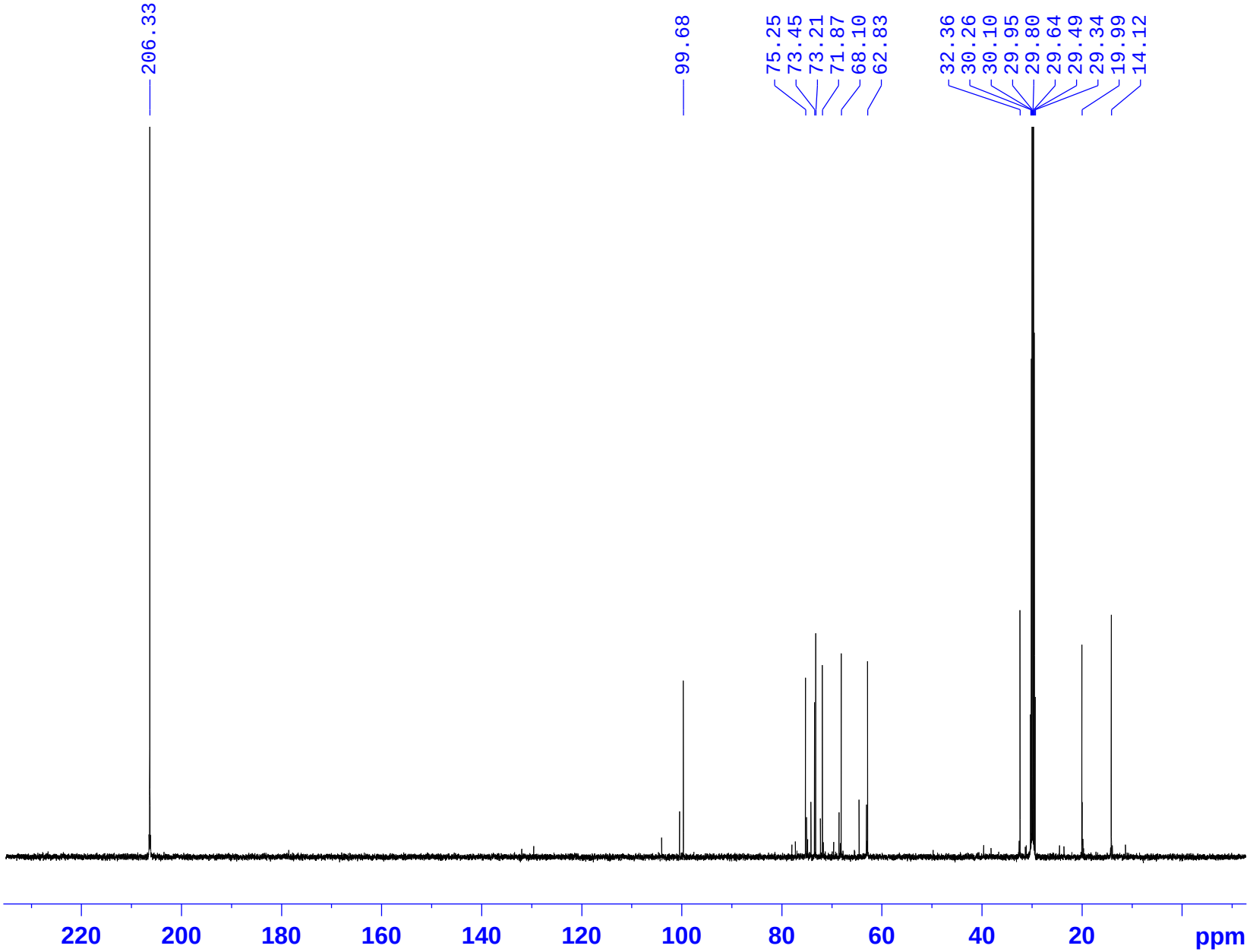

PLANT IDENTIFICATION CERTIFICATES

VIỆN HÀN LÂM
KHOA HỌC VÀ CÔNG NGHỆ VN
VIỆN SINH THÁI VÀ
TÀI NGUYÊN SINH VẬT

CỘNG HOÀ XÃ HỘI CHỦ NGHĨA VIỆT NAM
Độc lập - Tự do - Hạnh phúc

Hà Nội, ngày 18 tháng 08 năm 2020

PHIẾU XÁC ĐỊNH TÊN KHOA HỌC

I. Thông tin mẫu gửi

- Đơn vị/ Người gửi mẫu: Đỗ Hoàng Giang
- Địa chỉ: Trung tâm Nghiên cứu và Chuyển giao Công nghệ
- Ký hiệu mẫu: NCCG 200105, NCCG 200106, NCCG 200107.
- Tình trạng mẫu: Mẫu tiêu bản khô.
- Số lượng tiêu bản: 03.
- Nơi lấy mẫu: huyện Thanh Oai, Hà Nội
- Thời gian lấy mẫu: 02/2020 Thời gian gửi mẫu: 18/06/2020

II. Người và phương pháp xác định

- Người xác định: TS. Bùi Văn Thanh
- Đơn vị: Phòng Thực vật dân tộc học, Viện Sinh thái và Tài nguyên sinh vật
- Phương pháp xác định:

+ Xác định mẫu vật dựa trên phương pháp hình thái so sánh.

+ Các tài liệu sử dụng chính: Cây cỏ Việt Nam (tập 3), Danh lục thực vật Việt Nam (tập 3), http://www.theplantlist.org/

III. Kết quả xác định

- Ký hiệu mẫu: NCCG 200105, NCCG 200106, NCCG 200107.
- Tên Khoa học: *Pandanus tectorius* Parkinson ex Du Roi.
- Họ thực vật: Pandanaceae

(Kết quả xác định tên khoa học chỉ có giá trị đối với mẫu được gửi đến và được lưu tại phòng Thực vật dân tộc học)

Người xác định

TS. Bùi Văn Thanh

VIỆN TRƯỞNG

VIỆN HÀN LÂM KHOA HỌC VÀ CÔNG NGHỆ VIỆT NAM
VIỆN SINH THÁI VÀ TÀI NGUYÊN SINH VẬT

Nguyễn Văn Sinh

VIỆN HÀN LÂM
KHOA HỌC VÀ CÔNG NGHỆ VN
VIỆN SINH THÁI VÀ
TÀI NGUYÊN SINH VẬT

CỘNG HOÀ XÃ HỘI CHỦ NGHĨA VIỆT NAM
Độc lập - Tự do - Hạnh phúc

Hà Nội, ngày 13 tháng 09 năm 2021

PHIẾU XÁC ĐỊNH TÊN KHOA HỌC

I. Thông tin mẫu gửi

- Đơn vị/ Người gửi mẫu: Đỗ Hoàng Giang
- Địa chỉ: Trung tâm Nghiên cứu và Chuyển giao Công nghệ
- Ký hiệu mẫu: NCCG 210207, NCCG 210208
- Tình trạng mẫu: Mẫu tiêu bản khô.
- Số lượng tiêu bản: 02.
- Nơi lấy mẫu: huyện Thanh Oai, Hà Nội
- Thời gian lấy mẫu: 03/2021 Thời gian gửi mẫu: 17/08/2021

II. Người và phương pháp xác định

- Người xác định: TS. Bùi Văn Thanh
- Đơn vị: Phòng Thực vật dân tộc học, Viện Sinh thái và Tài nguyên sinh vật
- Phương pháp xác định:

+ Xác định mẫu vật dựa trên phương pháp hình thái so sánh.

+ Các tài liệu sử dụng chính: Cây cỏ Việt Nam (tập 3), Danh lục thực vật Việt Nam (tập 3), http://www.theplantlist.org/

III. Kết quả xác định

- Ký hiệu mẫu: NCCG 210207, NCCG 210208
- Tên Khoa học: *Pandanus tectorius* Parkinson ex Du Roi.
- Họ thực vật: Pandanaceae

(Kết quả xác định tên khoa học chỉ có giá trị đối với mẫu được gửi đến và được lưu tại phòng Thực vật dân tộc học)

Người xác định

TS. Bùi Văn Thanh

VIỆN TRƯỞNG

VIỆN HÀN LÂM KHOA HỌC VÀ CÔNG NGHỆ VIỆT NAM
VIỆN SINH THÁI VÀ TÀI NGUYÊN SINH VẬT

Nguyễn Văn Sinh

VIỆN HÀN LÂM
KHOA HỌC VÀ CÔNG NGHỆ VN
VIỆN SINH THÁI VÀ TÀI NGUYÊN SINH VẬT

CỘNG HOÀ XÃ HỘI CHỦ NGHĨA VIỆT NAM
Độc lập - Tự do - Hạnh phúc

Hà Nội, ngày 22 tháng 09 năm 2021

PHIẾU XÁC ĐỊNH TÊN KHOA HỌC

I. Thông tin mẫu gửi

- Đơn vị/ Người gửi mẫu: Đỗ Hoàng Giang
- Địa chỉ: Trung tâm Nghiên cứu và Chuyển giao Công nghệ
- Ký hiệu mẫu: NCCG 210213, NCCG 210214, NCCG 210215
- Tình trạng mẫu: Mẫu tiêu bản khô.
- Số lượng tiêu bản: 03.
- Nơi lấy mẫu: Tam Đảo, Vĩnh Phúc
- Thời gian lấy mẫu: 04/2021 Thời gian gửi mẫu: 25/08/2021

II. Người và phương pháp xác định

- Người xác định: TS. Bùi Văn Thanh
- Đơn vị: Phòng Thực vật dân tộc học, Viện Sinh thái và Tài nguyên sinh vật
- Phương pháp xác định:

+ Xác định mẫu vật dựa trên phương pháp hình thái so sánh.

+ Các tài liệu sử dụng chính: Cây cỏ Việt Nam (tập 3), Danh lục thực vật Việt Nam (tập 3), http://www.theplantlist.org/

III. Kết quả xác định

- Ký hiệu mẫu: NCCG 210213, NCCG 210214, NCCG 210215
- Tên Khoa học: *Pandanus amaryllifolius* Roxb.
- Họ thực vật: Pandanaceae

(Kết quả xác định tên khoa học chỉ có giá trị đối với mẫu được gửi đến và được lưu tại phòng Thực vật dân tộc học)

Người xác định

TS. Bùi Văn Thanh

VIỆN TRƯỞNG

VIỆN HÀN LÂM KHOA HỌC VÀ CÔNG NGHỆ VIỆT NAM
VIỆN SINH THÁI VÀ TÀI NGUYÊN SINH VẬT

Nguyễn Văn Sinh

PUBLICATIONS

LIST OF THE PUBLICATIONS

A. SCIE journals

1) Do Hoang Giang et al. (2025) Optimization of the extraction conditions and evaluation of bioactivities of the phenolic enrichment from *Pandanus amaryllifolius* leaves. *Journal of Analytical Methods in Chemistry*, 2025, art.ID. 5256388.

2) Do Hoang Giang et al. (2025) Pandanusfuran A and B: two new benzofuran epimers from *Pandanus tectorius* leaves. *Journal of Chemistry*, 2025, art.ID. 5587982.

3) Do Hoang Giang et al. (2025) Optimization of Phenolic- and Saponin-Enriched Extraction from *Pandanus tectorius* Fruit Using Box–Behnken Design and Evaluation of Their Bioactivities. *Journal of Analytical Methods in Chemistry*, 2025, art.ID. 5539843.

B. Other international journals

4) Do Hoang Giang et al. (2025) Total phenolic and saponin content and α-amylase inhibition of marketed *Pandanus tectorius* fruits and leaves. *International Journal of Engineering Research and Development*, 21(9), pp. 90-95.

C. Vietnamese journals

5) Do Hoang Giang et al. (2024) Shikimate esters, megastigmane and glycoside from leaves of *Pandanus amaryllifolius*. *Journal of Tropical Science and Engineering*, 35(09-2024), pp. 82–88.

6) Do Hoang Giang et al. (2025) Phenolics from fruits of *Pandanus tectorius*. *HaUI Journal of Science and Technology*, 61(5B), pp. 92–96.

7) Do Hoang Giang et al. (2025) Phenolics from leaves of *Pandanus amaryllifolius*. *Journal of Tropical Science and Engineering*, 38(06-2025), pp. 122–127.

PUBLICATIONS IN SCIE JOURNALS

Wiley
Journal of Analytical Methods in Chemistry
Volume 2025, Article ID 5256388, 10 pages
https://doi.org/10.1155/jamc/5256388

WILEY

Research Article

Optimization of the Extraction Conditions and Evaluation of Bioactivities of the Phenolic Enrichment From *Pandanus amaryllifolius* Leaves

Do Hoang Giang,[1,2] **Bui Thi Nhat Le**,[2] **Nguyen Thi Thu Minh**,[2] **Nguyen Thi Thu Thuy**,[3] **Nguyen Hai Dang**,[1] **Hoang Le Tuan Anh**,[2] **Nguyen Ngoc Tung**,[2] **and Nguyen Tien Dat**[2]

[1]*University of Science and Technology of Hanoi, Vietnam Academy of Science and Technology (VAST), 18-Hoang Quoc Viet, Cau Giay, Hanoi 10000, Vietnam*
[2]*Center for High Technology Research and Development, VAST, 18-Hoang Quoc Viet, Cau Giay, Hanoi 10000, Vietnam*
[3]*Joint Vietnam-Russia Tropical Science and Technology Research Center, Nguyen Van Huyen, Cau Giay, Hanoi 10000, Vietnam*

Correspondence should be addressed to Nguyen Tien Dat; ngtiend@gmail.com

Received 5 November 2024; Accepted 29 March 2025

Academic Editor: Larisa Lvova

This study investigates the optimal conditions to enrich the phenolic content of the extract from *Pandanus amaryllifolius* leaves and evaluates the bioactivities of this enrichment. The phenolic enrichment was prepared under optimized conditions using the response surface methodology (RSM) with the Box–Behnken design. The antioxidant properties were assessed using DPPH and hydroxyl radical scavenging assays, while the NO production inhibition was measured in LPS-stimulated RAW 264.7 macrophage cells. Results indicated that the phenolic enrichment showed potent antioxidant activity comparable to ascorbic acid and catechin and significantly higher NO inhibition than the separated nonalkaloid and alkaloid fractions. The study also highlights the synergistic effect of phenolic and alkaloid compounds on the antioxidants and anti-inflammatory activities of the phenolic enrichment from *Pandanus amaryllifolius* leaves.

Keywords: antioxidant; Box–Behnken; *Pandanus amaryllifolius*; phenolic

1. Introduction

Pandanus amaryllifolius Roxb is an evergreen tree with fragrantly scented leaves. The plant is cultivated for its leaves in gardens in Vietnam, Indonesia, Malaysia, Thailand, New Guinea, Sri Lanka, and the Philippines [1, 2]. Phytochemical studies reported that alkaloids were the major secondary metabolites in *P. amaryllifolius* with considerable anti-inflammatory and anticancer effects [2–6]. Besides, flavonoids, coumaroyl malate, and coumarin derivatives, together with terpenoids and other organic compounds, were determined from leaves of *P. amaryllifolius* [7–12]. While these findings highlight the diverse chemical profile of *P. amaryllifolius*, detailed quantitative data on the composition of these compounds remain limited and warrant further investigation. Furthermore, variations in the reported antioxidant effects of alkaloids across studies have raised questions about the consistency of these results [9–11]. Antioxidants, particularly those derived from plant sources, play a crucial role in mitigating oxidative stress, which is linked to various chronic diseases such as cancer, cardiovascular diseases, and neurodegenerative disorders. Plant-based antioxidants offer advantages over synthetic counterparts due to their biocompatibility, lower toxicity, and additional bioactive properties. In this context, the optimization of extraction processes becomes essential to maximize the yield and efficacy of phytoconstituents.

Conventional extraction methods often suffer from limitations such as low selectivity, high solvent consumption, and extended processing times [13]. To overcome these challenges, the response surface methodology (RSM) with the Box–Behnken design (BBD) was employed for optimizing the extraction of bioactive products from natural sources [14]. The BBD was chosen for its efficiency in evaluating interactions among variables with fewer experimental runs than traditional methods [13, 14]. Parameters such as solvent concentration, extraction time, and temperature were systematically optimized to enrich the phenolic content, significantly improving the extraction yield.

Previously, we investigated alkaloids from the aerial part of *P. amaryllifolius* from Vietnam and evaluated their anti-inflammatory activity [15]. In the current study, we continuously determined and elucidated the structures of phenolics from the nonalkaloid fraction of the samples. The extracting process was optimized to enrich the phenolic content using the RSM with BBD. Moreover, the antioxidant and NO production inhibitory effects of the fractions and compounds were investigated.

2. Materials and Methods

2.1. Plant Materials. Leaves of *P. amaryllifolius* were collected at Tam Dao, Vinh Phuc Province, Vietnam, in April 2021 and identified by Dr. Bui Van Thanh, Institute of Ecology and Biological Resources, Vietnam Academy of Sciences and Technology (VAST). A voucher specimen (NCCG 210213) was deposited at the Department of Agro-Pharmaceutical Research, Center for High Technology Research and Development, VAST. The collected sample was cleaned, dried at 50°C in the oven, powdered, and preserved at −20°C for further experiments.

2.2. General. ESI-MS was measured by a Thermo LCQ Fleet system. NMR spectra were recorded on a Bruker AVANCE NEO 600-MHz spectrometer with tetramethylsilane (TMS) as an internal standard. Column chromatography (CC) was carried out using Diaion HP-20 resin (0.25–0.85 mm, Mitsubishi Chemical Corp., Japan), silica gel 60 (70–230 mesh, Merck, Germany), or RP-C18 resin (150 μm, YMC, Japan). HPLC analysis and prep-HPLC were conducted on a Thermo Ultimate 3000 HPLC-DAD and an Agilent 1100 system. The extraction was processed in a shaking water bath (Daihan Scientific).

2.3. Total Phenolic Assay. The total phenolic contents (TPC) of the samples were evaluated by the Folin–Ciocalteu method [16]. In brief, 0.1 mL of each solution of *P. amaryllifolius* leaves' extract was mixed with 0.9 mL of Folin–Ciocalteu 10% and 1.0 mL of Na_2CO_3 6% solution. Next, the mixture was incubated at 40°C for 15 min, and then the absorbance was measured at 760 nm. Gallic acid, which was processed under the same condition, was used as the standard compound for the calibration curve of the measurement.

2.4. Preliminary Single-Factor Experiments. Ranges of the extraction factors, such as temperature, ethanol concentration, and time, were evaluated from the following experiments. Firstly, the effect of extraction temperature on the TPC of the extracts was investigated by extracting the material in ethanol 96% at 30°C–80°C for 180 min. Next, the impact of the ethanol concentration on the TPC values was determined by extracting the *P. amaryllifolius* leaves in ethanol 0%–96% for 180 min at 60°C. Lastly, the influence of extraction time on TPC was evaluated by extracting the material in ethanol 96% at 60°C for 60–360 min. In each experiment, 5 g of *P. amaryllifolius* leaves was extracted in 150 mL of solvent, maintaining a fixed ratio of leaf weight to solvent volume at 1:30 (g/mL).

2.5. RSM. The RSM applying the BBD was utilized to design the experiments to optimize the condition to enrich phenolics into the extract of *P. amaryllifolius* leaves. The design was conducted on the Design-Expert 12.0 software (Stat-Ease, Inc., Minneapolis, US). Extraction temperature (°C, X_1), ethanol concentration (%, X_2), and extraction time (minute, X_3) were selected as independent factors, while TPCs were selected as the responses. From preliminary single-factor experiments, ethanol 0% (distilled water), 48%, and 96% were used as the solvents, whereas the temperature ranged from 30°C to 80°C; meanwhile, the extraction time varied between 60 and 300 min. Each experiment was conducted in triplicate and the mean of the response (TPC) was used for further calculation. The levels of the variables in the experimental design are shown in Table 1.

2.6. Extraction and Isolation. The phenolic enrichment from the optimal extracting condition was further isolated by chromatographic methods. 200 g of the enrichment was acidified with 1 N HCl solution to pH 2–3 and successively partitioned with ethyl acetate (EtOAc) (2 L × 4 times). The organic layer was separated and completely evaporated to afford nonalkaloid extract (62.4 g). The water layer which contained alkaloids was basified by 1 N NaOH to pH 9–10 and was extracted with CH_2Cl_2 (4 × 2 L). The CH_2Cl_2 layers were combined to collect the alkaloid fraction (22.6 g). The alkaloid fraction was analyzed and compared to the reported compounds in our in-house library [15] using the HPLC-DAD system to identify its composition.

The nonalkaloid extract was subjected to a Diaion HP-20 CC and then the column was washed with water, followed by MeOH 30% and 100% to obtain M30W (4.5 g) and M100W (13.6 g) fractions, respectively. The fraction M30W was loaded on a silica gel column with gradient mixtures of CH_2Cl_2–MeOH (20/1-1/1, v/v) to afford four subfractions (W1–W4). Fraction W1 (105 mg) was separated by preparative HPLC (120 min, 30%–60% MeOH in H_2O) to yield the compound **Pam1** (11.2 mg). The fraction M100W was subjected to a silica gel column eluted with gradient mixtures of CH_2Cl_2–MeOH (50/1-1/1, v/v) to afford 10 subfractions (M1–M10). Fraction M6 (91 mg) was separated by preparative HPLC (120 min, 40%–100% MeOH in H_2O) to yield the compounds **Pam2** (15.5 mg) and **Pam3** (6.8 mg).

Table 1: Levels of the variables in Box–Behnken design.

Variables	Unit	Code levels		
		−1	0	1
Temperature (X_1)	°C	30	55	80
Ethanol concentration (X_2)	%	0	48	96
Time (X_3)	minutes	60	180	300

Fraction M4 (304 mg) was separated by preparative HPLC (120 min, 30%–80% MeOH in H_2O) to yield the compounds **Pam4** (4.1 mg) and **Pam5** (6.6 mg). Fraction M8 (178 mg) was chromatographed on a silica gel CC eluted with CH_2Cl_2–acetone (5/1, v/v) to afford compounds **Pam6** (3.1 mg) and **Pam7** (5.6 mg). Fraction M5 (91 mg) was chromatographed on a silica gel CC eluted with CH_2Cl_2–methanol (9/1, v/v) to afford compound **Pam8** (5.6 mg).

Pinoresinol 4-*O*-*β*-*D*-glucoside **(Pam1)**: white amorphous powder, ESI-MS: *m/z* 521 $[M+H]^+$; *m/z* 1041 $[2M+H]^+$; molecular formula: C26H32O11; ^{1}H NMR (CD_3OD, 500 MHz): δ 7.05 (1H, d, J = 2.0 Hz, H-2), 7.17 (1H, d, J = 8.5 Hz, H-5), 6.94 (2H, dd, J = 8.5; 2.0 Hz, H-6), 4.78 (1H, d, J = 4.5 Hz, H-7), 3.15 (2H, m, H-8), 3.72 (2H, dd, J = 9.0; 4.5 Hz, H-9a), 4.26 (2H, dd, J = 9.0; 2.0 Hz, H-9b), 6.97 (1H, d, J = 2.0 Hz, H-2′), 6.79 (1H, d, J = 8.5 Hz, H-5′), 6.94 (2H, dd, J = 8.5; 2.0 Hz, H-6′), 4.73 (1H, d, J = 4.5 Hz, H-7′), 3.15 (2H, m, H-8′), 3.72 (2H, dd, J = 9.0; 4.5 Hz, H-9′a), 4.26 (2H, dd, J = 9.0; 2.0 Hz, H-9′b), 3.88 (3H, s, 3-*O*-CH_3), 3.89 (3H, s, 3′-*O*-CH_3), 4.89 (1H, d, J = 7.5 Hz, H-1″), 3.44 (1H, m, H-2″), 3.42 (1H, m, H-3″), 3.30 (1H, m, H-4″), 3.40 (1H, m, H-5″), 3.46–3.53 (2H, m, H-6″); ^{13}C NMR (CD_3OD, 125 MHz): δ 137.5 (C-1), 111.0 (C-2), 151.0 (C-3), 147.3 (C-4), 118.1 (C-5), 119.8 (C-6), 87.4 (C-7), 55.35 (C-8), 72.7 (C-9), 133.8 (C-1′), 111.7 (C-2′), 149.1 (C-3′), 147.5 (C-4′), 116.11 (C-5′), 119.8 (C-6′), 87.1 (C-7′), 55.54 (C-8′), 72.7 (C-9′), 56.5 (3-*O*-CH_3), 56.8 (3′-*O*-CH_3), 102.9 (C-1″), 74.9 (C-2″), 77.9 (C-3″), 71.4 (C-4″), 78.2 (C-5″), 62.5 (C-6″).

Pinoresinol **(Pam2)**: Yellow oil; ESI-MS: *m/z* 359 $[M+H]^+$, *m/z* 341 $[M+H\text{-}H_2O]^+$, *m/z* 739 $[2M+Na]^+$; molecular formula: $C_{20}H_{22}O_6$ (358 g/mol); ^{1}H NMR ($CDCl_3$, 500 MHz): δ 7.0 (2H, brs, H-2, 2′), 6.89 (2H, d, J = 8.0 Hz, H-5, 5′), 6.82 (2H, dd, J = 8.0; 2.0 Hz, H-6, 6′), 4.73 (2H, d, J = 4.0 Hz, H-7, 7′), 3.11 (2H, m, H-8, 8′), 3.88 (2H, dd, J = 9.0; 4.0 Hz, H-9, 9′), 4.26 (2H. dd. J = 9.0; 6.5 Hz, H-9, 9′), 3.91 (3H, s, 3-*O*-CH_3), 3.89 (3H, s, 3′-*O*-CH_3); ^{13}C NMR ($CDCl_3$, 125 MHz): δ 133.1 (C-1, 1′), 108.8 (C-2, 2′), 146.9 (C-3, 3′), 145.4 (C-4, 4′), 114.4 (C-5, 5′), 119.1 (C-6, 6′), 86.0 (C-7, 7′), 54.3 (C-8, 8′), 71.6 (C-9, 9′), 56.1 (3-*O*-CH_3), 56.1 (3′-*O*-CH_3).

Pinoresinol monomethyl ether **(Pam3)**: pale yellow oil; ESI-MS: *m/z* 373 $[M+H]^+$, *m/z* 395 $[M+Na]^+$; molecular formula: $C_{21}H_{24}O_6$ (372 g/mol); ^{1}H NMR ($CDCl_3$, 500 MHz): δ 6.90 (1H, d, J = 2.0 Hz, H-2), 6.89 (1H, d, J = 9.0 Hz, H-5), 6.83 (1H, dd, J = 9.0; 2.0 Hz, H-6), 4.75 (1H, d, J = 4.5 Hz, H-7), 3.31 (1H, m, H-8), 4.25 (2H, m, H-9), 6.90 (1H, dd, J = 6.5; 1.5 Hz, H-2′), 6.85 (1H, d, J = 9.0 Hz, H-5′), 6.87 (1H, dd, J = 9.0, 2.0 Hz, H-6′), 4.75 (1H, d, J = 4.5 Hz, H-7′), 3.31 (1H, m, H-8′), 3.87 (2H, m, H-9′), 3.89 (3H, s, 3-*O*-CH_3), 3.90 (3H, s, 3′-*O*-CH_3), 3.91 (3H, s, 4′-*O*-CH_3),; ^{13}C NMR ($CDCl_3$, 125 MHz): δ 132.9 (C-1), 108.7 (C-2), 148.7 (C-3), 145.3 (C-4), 114.3 (C-5), 119 (C-6), 85.8 (C-7), 54.2 (C-8), 71.7 (C-9), 133.6 (C-1′), 109.3 (C-2′), 149.3 (C-3′), 146.8 (C-4′), 111.1 (C-5′), 118.3 (C-6′), 85.8 (C-7′), 54.2 (C-8′), 71.7 (C-9′), 56.0 (3-*O*-CH_3), 56.0 (3′-*O*-CH3), 56.0 (4′-*O*-CH_3).

Methyl 4-hydroxybenzoate **(Pam4)**: *m/z* 153 $[M+H]^+$; ^{1}H NMR (DMSO-d_6, 600 MHz): δ 7.81 (1H, d, J = 6.6 Hz, H-2,6), 6.84 (1H, d, J = 6.6 Hz, H-3,5), 3.78 (3H, s, OCH_3). ^{13}C NMR (DMSO-d_6, 125 MHz): δ 120.2 (C-1), 131.3 (C-2), 115.3 (C-3), 161.9 (C-4), 115.3 (C-5), 131.3 (C-6), 166.0 (C-7), 51.6 (7-OCH_3).

3,4-Dihydroxyl benzoate methyl **(Pam5)**: *m/z* 169 $[M+H]^+$; ^{1}H NMR (DMSO-d_6, 600 MHz): δ 7.42 (1H, d, J = 1.8 Hz, H-2), 6.83 (1H, d, J = 7.8 Hz, H-5), 7.44 (1H, dd, J = 1.8, 7.8 Hz, H-6), 3.80 (3H, s, OCH_3). ^{13}C NMR (DMSO-d_6, 125 MHz): δ 121.6 (C-1), 123.4 (C-2), 151.1 (C-3), 163.2 (C-4), 112.7 (C-5), 115 (C-6), 167.1 (C-7), 55.5 (7-OCH_3).

4-Hydroxy benzoic acid **(Pam6)**: *m/z* 139 $[M+H]^+$; ^{1}H NMR (DMSO-d_6, 600 MHz): δ 7.77 (1H, d, J = 9.0 Hz, H-2,6), 6.80 (1H, d, J = 9.0 Hz, H-3,5). ^{13}C NMR (DMSO-d_6, 125 MHz): δ 121.3 (C-1), 131.6 (C-2), 115.5 (C-3), 161.5 (C-4), 115.5 (C-5), 131.6 (C-6), 167.1 (C-7).

Methyl 4-hydroxy-3-methoxybenzoate **(Pam7)**: *m/z* 183 $[M+H]^+$; ^{1}H NMR (CD_3OD, 600 MHz): δ 7.54 (1H, d, J = 1.8 Hz, H-2,6), 6.83 (1H, d, J = 8.4 Hz, H-5), 7.54 (1H, dd, J = 8.4, 1.8 Hz, H-2,6), 3.87 (3H, s, OCH_3), 3.90 (3H, s, OCH_3). ^{13}C NMR (CD_3OD, 125 MHz): δ 121.6 (C-1), 125.2 (C-2), 149.2 (C-3), 154.4 (C-4), 113.5 (C-5), 116.3 (C-6), 168.9 (C-7), 52.3 (3-OCH_3), 56.4 (7-OCH_3).

Methyl syringate **(Pam8)**: *m/z* 213 $[M+H]^+$; ^{1}H NMR (CD_3OD, 600 MHz): δ 7.34 (2H, s, H-2,6), 3.89 (6H, s, 3,5-OCH_3), 3.89 (3H, s, 7-OCH_3). ^{13}C NMR (CD_3OD, 125 MHz): δ 121.37 (C-1), 108.1 (C-2), 148.94 (C-3), 141.94 (C-4), 148.94 (C-5), 108.1 (C-6), 168.63 (C-7), 56.8 (3,5-OCH_3), 52.5 (7-OCH_3).

2.7. Antioxidant and NO Production Inhibition Assay. The antioxidant activities of the phenolic enrichment were evaluated by DPPH and hydroxyl radicals scavenging assays using previously established methods [17, 18]. For DPPH free radical scavenging effect, 100 µL of each sample was combined with 1900 µL of DPPH in methanol and incubated in the dark at 37°C for 20 min. The absorbance was then measured at 517 nm, with ascorbic acid as the positive control. For the hydroxyl radicals scavenging assay, 200 µL aliquot of the test sample was combined with 400 µL of 50 mM phosphate buffer (pH 7.8), 400 µL of 2.8 mM deoxyribose, and 400 µL of 500 µM $Fe(NH_4)_2(SO_4)_2$ and then incubated at 37°C for 1 h. The reaction was stopped by adding 1000 µL of 10% (w/v) trichloroacetic acid and 1000 µL of 1% (w/v) thiobarbituric acid, followed by heating the mixture in a water bath at boiling temperature for 15 min. The absorbance of the resulting solution was read at 532 nm, using catechin as a positive control.

The impact of samples on NO production in LPS-stimulated RAW 264.7 macrophage cells was assessed using the Griess reaction [19]. Cells were seeded in 96-well

plates at a density of 0.5×10^5 cells per well and incubated in a humidified chamber at 37°C with 5% CO_2 for 22 h. After incubation, samples at concentrations ranging from 3 to 25 μg/mL were added, followed by the addition of 0.1 mg/mL LPS (Sigma-Aldrich, USA) after 30 min. The cells were then incubated for an additional 24 h. Subsequently, 100 μL of the culture supernatant was transferred to a new 96-well plate and combined with 100 μL of the Griess reagent. The absorbance of the reaction mixture was measured at 570 nm using an iMark microplate reader (Bio-Rad, USA). The remaining cells in the original 96-well plate were used for the 3-(4,5-dimethylthiazol-2-yl)-2,5-diphenyltetrazolium bromide (MTT) assay to evaluate cell viability, based on the reduction of MTT by mitochondrial dehydrogenases in viable cells, thus estimating the number of live cells. Cardamonin, a known NO production inhibitor, was used as a positive control.

3. Results and Discussion

3.1. The Process Range Conditions for the Extraction. The impact of temperature, ethanol concentration, and extraction time on the TPC of *P. amaryllifolius* leaf extracts was systematically investigated. The data from the experimental design, summarized in Table S1 and Figure 1, reveal distinct trends associated with each parameter, leading to the identification of optimal ranges for phenolic extraction.

The TPC was positively correlated with temperature within the range of 30°C–80°C, with the highest TPC (95.84 mg GAE/g) observed at 70°C, and slightly decreased to 86.93 mg GAE/g at 80°C. These suggested that higher temperatures may cause degradation of phenolic compounds or excessive evaporation of ethanol. For practical purposes and to align with the experimental environment's ambient conditions, temperatures below 30°C were deemed unsuitable. These findings confirm that the temperature range for maximizing phenolic extraction should lie between 30°C and 80°C.

Meanwhile, the ethanol concentration influenced the TPC, with relatively small differences observed across the tested range. The TPC increased steadily with rising ethanol concentrations, from 80.38 mg GAE/g at 0% ethanol (distilled water) to 93.93 mg GAE/g at 80% ethanol, after which it slightly decreased to 92.12 mg GAE/g at 96% ethanol. While 80% ethanol yielded the highest TPC, the variations between concentrations above 40% were not substantial. This result highlights the need to optimize ethanol concentration further within the range of 0%–96% to identify the precise conditions that balance extraction efficiency and solvent consumption.

The extraction time also had a noticeable impact on TPC, with values generally increasing within the range of 60–240 min. The highest TPC (93.37 mg GAE/g) was observed at 120 min, indicating this duration was particularly effective for phenolic extraction. While longer times, such as 240 min, still yielded relatively high TPC (92.46 mg GAE/g), a gradual decline was observed beyond this point, with 89.67 mg GAE/g at 300 min and 82.67 mg GAE/g at 360 min. This reduction could be attributed to the potential degradation of phenolic compounds or decreased solvent efficiency over prolonged periods. Shorter durations, such as 60 min, also provided a reasonably high TPC (91.73 mg GAE/g), suggesting that the extraction process reaches a significant level of efficiency early on. However, extending the time to 240 min ensures thorough extraction, particularly for phenolic compounds that may require more time to diffuse into the solvent. Based on these findings, the optimal time range for extraction is 60–300 min, providing flexibility to balance efficiency and resource consumption while minimizing the risk of phenolic degradation.

3.2. Optimizing the Extracting Condition to Prepare the Phenolic Enrichment From P. amaryllifolius Leaves. The RSM with BBD was applied to determine the optimal condition for the extraction of phenolic from *P. amaryllifolius* leaves. The extraction design variables' effect on the TPC values is given in Table 2.

The modified quadratic models for the estimation of polyphenol content (TPC) in terms of extracting temperature (X_1), ethanol concentration (X_2), and extracting time (X_3) are shown below:

$$\begin{aligned}\mathrm{TPC} = {} & -13.700711 + 2.12296X_1 + 0.956150X_2 + 0.159595X_3 - 0.007927X_1X_2 - 0.001509X_1X_3 - 0.000261X_2X_3 \\ & - 0.012019X_1^2 - 0.004918X_2^2 - 0.000149X_3^2 + 0.000032X_1X_2^2.\end{aligned} \tag{1}$$

The analysis of variance illustrated the model F value at 90.26 with $p < 0.0001$ which implied that the model was highly significant. The lack of fit was insignificant ($p > 0.05$), indicating that the model fit the analytical results. The model, adjusted, and predicted R^2 at 0.9912, 0.9802, and 0.9437, respectively, implied that the model could be validated for use in the investigated ranges. The response surface plots of ethanol concentration–extracting temperature, ethanol concentration–extracting time, and extracting time–temperature are shown in Figure 2.

As can be seen, the TPC of the *P. amaryllifolius* leaves extract increased sharply when raising the ethanol concentration from 0 to about 70% and then kept stably at the higher ratio of the alcohol. Meanwhile, the rise in temperature from 30°C to 60°C might enhance the TPC of the extract, while a higher temperature might decrease the phenolic contents due to the decomposition of some metabolites. Besides, the temperature approximated the boiling point of ethanol led to a decrease in the extraction yield due to the fast evaporation of the solvent and a longer extraction

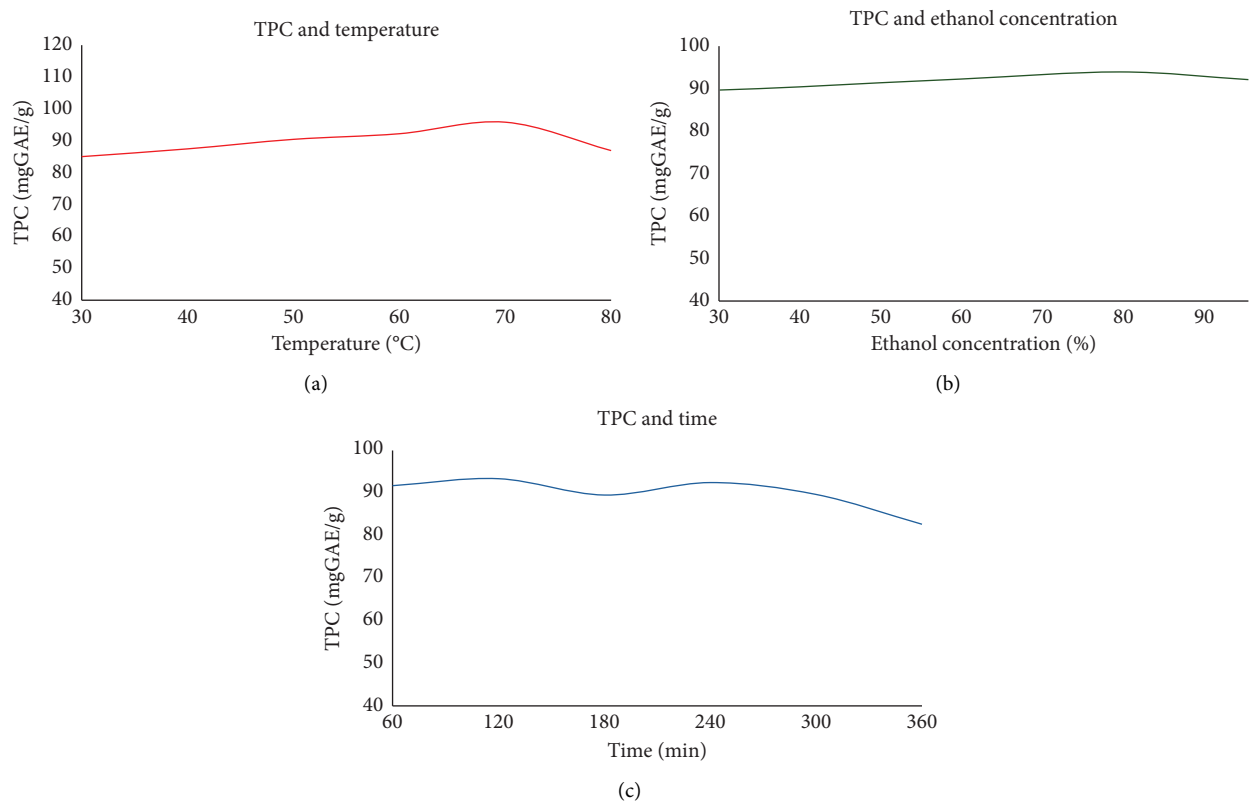

Figure 1: Effect of extraction temperature (a), ethanol concentration (b), and extraction time (c) on total phenolic content of extracts from *P. amaryllifolius* leaves.

Table 2: Responses of TPC of the extracts to independent variables using Box–Behnken design.

No.	Variables			TPC (mg GAE/g)	
	X_1: Temp. (°C)	X_2: EtOH (%)	X_3: Time (min)	Experimental value	Predicted value
1	55	48	180	92.66	91.10
2	55	48	180	89.57	91.10
3	30	48	300	81.15	81.66
4	30	0	180	54.97	54.92
5	55	96	60	89.43	90.09
6	55	48	180	92.9	91.10
7	55	48	180	92.24	91.10
8	80	96	180	85.71	86.05
9	30	96	180	82.74	82.90
10	55	0	300	76.74	76.27
11	55	48	180	90.51	91.10
12	80	48	60	90.7	90.28
13	55	96	300	89.95	89.59
14	55	48	180	89.93	91.10
15	55	0	60	70.21	70.76
16	55	48	180	89.55	91.10
17	30	48	60	70.57	70.10
18	80	48	300	83.17	83.73
19	80	0	180	81.43	81.38

time also affected certainly the TPC values of the extract. From the numerical optimization, the maximum predicted TPC of the phenolic enrichment at 93.59 mgGAE/g could be obtained under the conditions of 61.18°C extraction temperature, 163.00-min extraction time, and 71.79% ethanol concentration. The actual condition was slightly modified at 65°C, ethanol 70%, and an extraction time of 160 min. The TPC of the phenolic enrichment under the optimal condition was 105.69 mgGAE/g, which was higher than the calculated value above.

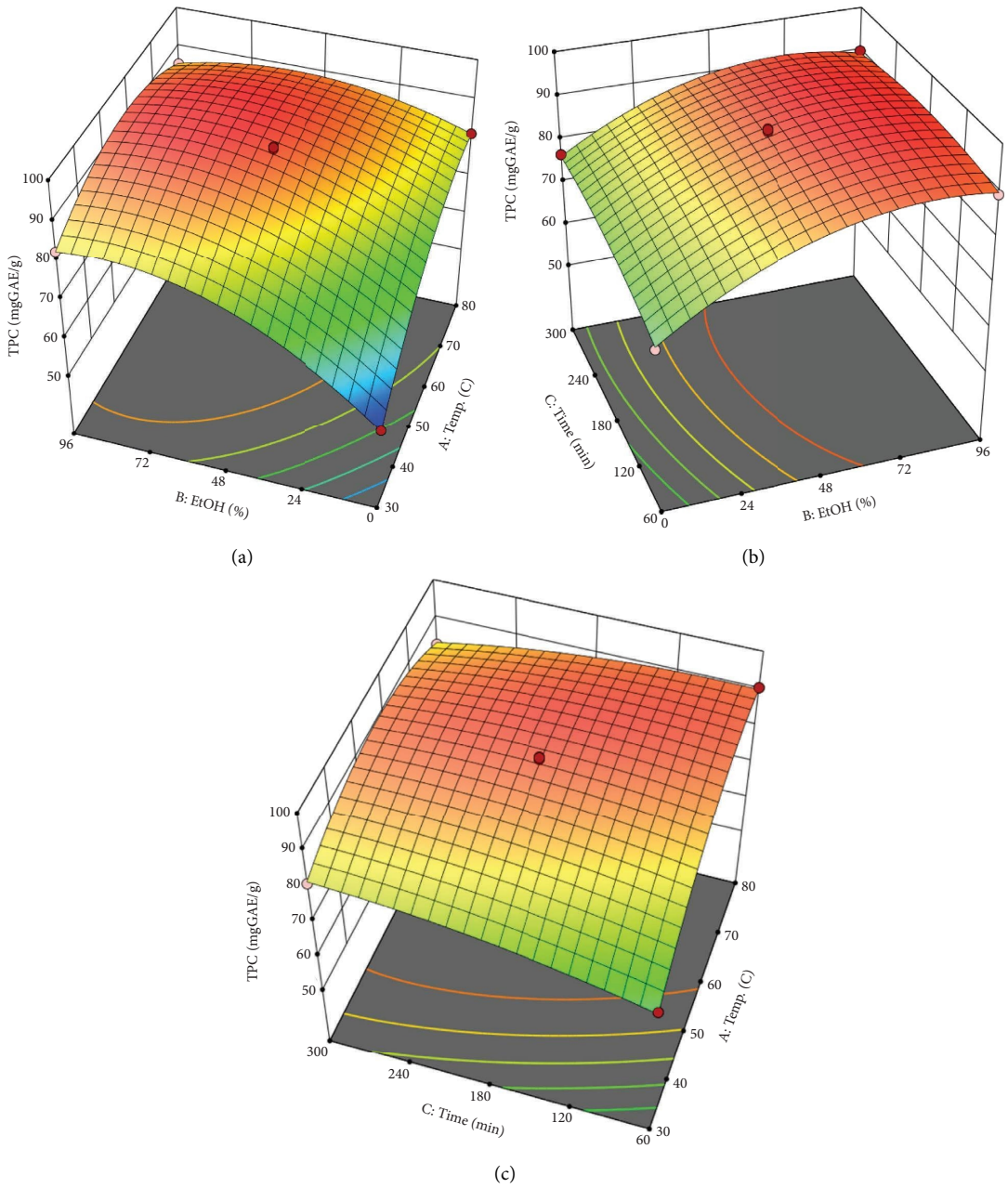

Figure 2: Response surfaces between (a) temperature and ethanol concentration, (b) ethanol concentration and time in response, and (c) time and temperature to total phenolic contents of the *P. amaryllifolius* extracts.

3.3. Chemical Composition of the Phenolic Enrichment From the P. amaryllifolius Leaves. The phenolic enrichment was further isolated for the determination of its chemical composition. The alkaloid fraction was analyzed in comparison with the reference compounds as reported in [15] using the HPLC-DAD method. The analytical data identified pandalizine A, pandalizine B, pandamarilactione B, pandamarilactone-1, pandamarilactione G, and dubiusamine A in the alkaloids fraction. This result indicated that a certain amount of alkaloids still presented in the contents and may affect to the bioactivities of the phenolic enrichment from the *P. amaryllifolius* leaves.

Meanwhile, from the nonalkaloid fraction, eight phenolics were isolated and their structures (Figure 3) were elucidated using spectroscopy methods.

Compound **Pam1** was obtained as a white powder. The molecular weight of **Pam1** was 520 Da by the ESI-MS spectrum (Figure S1) at *m/z* 521 $[M+H]^+$ and *m/z* 1041 $[2M+H]^+$. The ^{1}H-NMR spectrum (Figure S2) indicated two ABX systems at δ_H 7.05 (1H, d, $J = 2.0$ Hz, H- 2), 7.17 (1H, d, $J = 8.5$ Hz, H-5), 6.94 (2H, dd, $J = 8.5$; 2.0 Hz, H-6, H-6′), 6.97 (1H, d, $J = 2.0$ Hz, H-2′), 6.79 (1H, d, $J = 8.5$ Hz, H-5′); a sugar unit identified as *β-D*-glucopyranoside based on the anomeric proton signals at δ_H 4.91 (1H, d, $J = 7.5$ Hz,

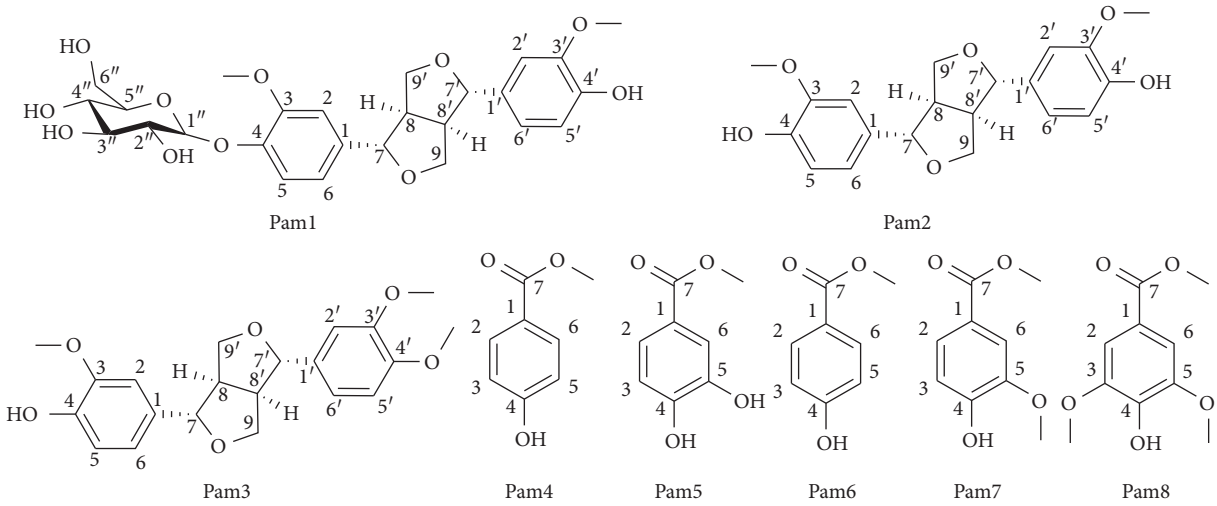

Figure 3: Structures of isolated compounds from the phenolic enrichments of *P. amaryllifolius* leaves.

H-1″) and other signals ranging from 3.30 ppm to 3.46 ppm; two methoxy groups δ_H 3.86 (3H, s, 3′-OMe) and 3.84 (3H, s, 3-OMe); and two oxygenated methine groups δ_H 4.73 (1H, d, $J = 4.5$ Hz, H-7′), 4.78 (1H, d, $J = 4.5$ Hz, H-7). The ^{13}C-NMR and DEPT spectra showed 26 carbon signals of which 12 carbon signals at δ_C 111.6–151.0 (6 CH, 6 C) confirmed the presence of two ABX systems. In addition to the typical signals of *β*-D-glucopyranoside at δ_C 102.9 (C-1″); 77.9 (C-3″); 74.9 (C-2″); 71.4 (C-4″); 78.2 (C-5″); 62.5 (C-6″), in the ^{13}C NMR spectrum (Figure S3), there were signals of two methine groups, two methylene groups attached to oxygen, respectively, at δ_C 87.4 (C-7); 87.1 (C-7′); 72.7 (C-9, C-9′), and two methoxy groups at δ_C 56.8 (3′-OMe); 56.4 (3-OMe). The structure of **Pam1** was determined to be pinoresinol 4-*O*-*β*-*D*-glucopyranoside by comparison of spectral data with those reported in the literature [20].

Compound **Pam2** was obtained as a light yellow oil. The ^{1}H-NMR spectrum of **Pam2** (Figure S5) exhibited signals of an ABX system due to three protons δ_H 7.00 (2H, s, H-2, 2′); 6.82 (2H, d, $J = 8.5$ Hz, H-6, 6′), and δ_H 6.89 (2H, d, $J = 8.0$ Hz, H-5, 5′), an oxymethine group δ_H 4.73 (2H, d, $J = 4.0$ Hz, H-7, 7′). Additionally, the spectrum showed two oxymethylene signals δ_H 3.88 (2H, dd, $J = 9.0$; 4.0 Hz, H-9a, 9′a) and 4.26 (2H, dd, $J = 9.0$; 6.5 Hz, H-9b, 9′b), a methine group δ_H 3.05 (2H, m, H-8, 8′), and two methoxy groups at δ_H 3.91 (3H, s) and 3.89 (3H, s). Besides, the ^{13}C-NMR and DEPT spectrum (Figure S6) showed 10 carbons, including three aromatic -CH groups δ_C 108.8 (C-2, 2′), 114.4 (C-5, 5′), and 119.4 (C-6, 6′), three nonprotonated carbons 133.1 (C-1, 1′), two aromatic rings directly associated with oxygen δ_C 145.4 (C-3) and 146.9 (C-4), and two methoxy groups at δ_C 56.1 Two methine signals δ_C 54.3 (C-8, 8′), an oxymethine group at δ_C 86.0 (C-7, 7′), and an oxymethylene group δ_C 71.6 (C-9, C-9′) suggested a structure of a benzofuran derivative. In addition, the molecular weight of **Pam2** was determined as 358 Da corresponding with the formula $C_{20}H_{22}O_6$ based on the ions at *m/z* 359 $[M + H]^+$, *m/z* 739 $[2M + Na]^+$, *m/z* 341 $[M\text{-}H_2O + H]^+$on the ESI-MS spectrum (Figure S4). The number of carbon and hydrogen in the predicted formula was twice as much as the number shown in the spectrum of **Pam2**; hence, it is possibly indicated that this compound has an axially symmetric benzofuran structure and the signals in the NMR spectrum were double shorted. The spectral data of **Pam2** resembled the data of pinoresinol in previous publications [20], so it can be identified as pinoresinol.

Compound **Pam3** was isolated as a yellowish-brown oil. The molecular weight of **Pam3** was 372 Da suggesting the formula was $C_{21}H_{24}O_6$ as determined from the ESI-MS spectrum (Figure S7) at *m/z* 373 $[M + H]^+$, and *m/z* 395 $[M + Na]^+$. Six proton signals in the ^{1}H-NMR spectrum (Figure S8) δ_H 6.91 (1H, s, H-2′), 6.90 (1H, s, H-2), 6.89 (1H, d, $J = 9.0$ Hz, H-5), 6.85 (1H, d, $J = 9.0$ Hz, H-5′), 6.87 (1H, dd, $J = 9.0$; 2.0 Hz, H-6′), and 6.83 (1H, dd, $J = 9.0$; 2.0 Hz) suggested an ABX system. Additionally, the ^{1}H-NMR spectrum showed an oxymethine group δ_H 4.73 (2H, d, $J = 4.0$ Hz, H-7, 7′); two oxymethylene groups δ_H 4.25 (2H, m, H-9), and 3.87 (2H, m, H-9′); two methine groups δ_H 3.31 (2H, m, H-8, 8′); and three methoxy groups at δ_H 3.91 (3H, s), 3.90 (3H, s), and 3.89 (3H, s). Besides, 21 carbon signals including six aromatic carbons δ_C 108.7 (C-2), 109.3 (C-2′), 114.3 (C-5), 111.1(C-5′), 119.0 (C-6), and 118.3 (C-6′); six nonprotonated aromatic carbons δ_C 133.6 (C-1), 132.9 (C-1′); four aromatic carbons directly bonding with oxygen δ_C 148.7 (C-3), 149.3 (C-3′), 145.3 (C-4), and 146.8 (C-4′); and three methoxy groups at δ_C 56.0 were observed in the ^{13}C-NMR and DEPT spectrum (Figure S9). Two methine groups δ_C 54.2 (C- 8, 8′), two oxymethine groups δ_C 85.8 and 85.9 (C-7, 7′), two oxymethylene groups δ_C 71.7 (C-9, C-9′) allowed the identification of two benzofuran rings. It can be seen that half of the number of NMR and MS data of **Pam3** were similar to those of **Pam2**, except for an additional methoxy group. Based on spectral analysis and comparison with the literature [21], the structure of **Pam3** was determined to be pinoresinol monomethyl ether.

Table 3: Free radical scavenging effects of phenolic enrichment from *P. amaryllifolius* leaves.

Sample	DPPH (IC_{50}, μg/mL)	Hydroxyl (IC_{50}, μg/mL)	NO inhibition (IC_{50}, μg/mL)
The phenolic enrichment	32.68 ± 2.93^{a}	40.20 ± 3.84^{e}	21.44 ± 2.61^{h}
The nonalkaloid fraction	28.75 ± 1.81^{b}	41.11 ± 3.76^{e}	57.61 ± 4.54^{i}
The alkaloid fraction	52.10 ± 4.26^{c}	82.35 ± 6.09^{f}	33.47 ± 2.92^{j}
Ascorbic acid*	24.65 ± 2.27^{d}	—	
Catechin**	—	32.27 ± 1.56^{g}	
Cardamonin#			2.98 ± 0.35^{k}

*,**,#Positive control.
[a–k]Data are expressed as mean ± SD. Means in each column with different letters are significantly different ($p < 0.05$).

The rest of the compounds, including methyl 4-hydroxybenzoate **(Pam4)**, 3,4-dihydroxyl benzoate methyl **(Pam5)**, 4-hydroxy benzoic acid **(Pam6)**, methyl 4-hydroxy-3-methoxybenzoate **(Pam7)**, and methyl syringate **(Pam8)** were identified by comparing their NMR (Figure S10–S24) data to those of reported studies [22–26]. Previously, flavonoids, coumaroyl malate, coumarin derivatives, and some other phenolics have been investigated from *P. amaryllifolius* leaves [2, 8, 9]. In the current study, the phytochemical investigation of the phenolic enrichment from *P. amaryllifolius* leaves led to the isolation of 8 compounds, including 3 lignans and 5 benzoate derivatives, whereas, except for 4-hydroxy benzoic acid **(Pam6)**, the other phenolics were identified for the first time from the plant.

3.4. Antioxidant and NO Production Inhibition of the Phenolic Enrichment. The isolated lignans, such as pinoresinol 4-*O*-*β*-*D*-glucopyranoside (**Pam1**), pinoresinol (**Pam2**), and pinoresinol monomethyl ether (**Pam3**) have been proven as significant antioxidant compounds [27–29], while other *p*-hydroxybenzoic derivatives also had considerable free-radical scavenging effects [30, 31]. In this study, the phenolic enrichment of *P. amaryllifolius* leaves, which contained these compounds, was evaluated for its antioxidant activity via DPPH and hydroxy free radical scavenging effects (Table 3). Besides, the NO production inhibition of the phenolic enrichment was evaluated and compared with those of the alkaloid and nonalkaloid fractions.

The phenolic enrichment from *P. amaryllifolius* leaves exhibited significant antioxidant and NO inhibition activities compared to both its derived alkaloid and nonalkaloid fractions as well as the positive controls used in this study. For DPPH and hydroxyl radical scavenging assays, the phenolic enrichment displayed IC_{50} values of 32.68 and 40.20 μg/mL, respectively, which are close to the efficacy of ascorbic acid (IC_{50} of 24.65 μg/mL) and catechin (IC_{50} of 32.27 μg/mL), respectively. This suggests that the phenolic enrichment possesses potent free radical scavenging abilities, on par with well-known antioxidants. In terms of NO inhibition, the phenolic enrichment achieved an IC_{50} of 21.44 μg/mL, which, while not as potent as cardamonin (IC_{50} of 2.98 μg/mL), is markedly more effective than either the nonalkaloid fraction (57.61 μg/mL) or the alkaloid fraction (33.47 μg/mL). This indicates that while cardamonin serves as an exceptionally potent NO inhibitor, the phenolic enrichment's moderate yet significant inhibition points to a synergistic effect within the mixture, potentially due to the interplay between phenolic and alkaloid components.

The higher NO inhibition in the phenolic enrichment compared to its separated fractions suggests a synergistic interaction between phenolic and alkaloid compounds within the mixture, enhancing the NO inhibition capacity beyond what is observed in either fraction alone. Although individual compounds like cardamonin show stronger inhibition, the phenolic enrichment still represents a balanced and effective option for reducing oxidative stress and inflammation, leveraging the combined effects of its components. This highlights the potential of using phenolic enrichment as a natural source of antioxidants and anti-inflammatory agents, with a broader range of bioactivity than isolated components.

4. Conclusion

The optimized phenolic enrichment from *P. amaryllifolius* leaves demonstrated substantial antioxidant and NO inhibition activities, surpassing the efficacy of its individual nonalkaloid and alkaloid fractions. The phenolic enrichment enhanced NO inhibition capacity suggests a synergistic interaction between its phenolic and alkaloid compounds, contributing to a broader range of bioactivity. While the enrichment exhibited significant antioxidant effects comparable to standard antioxidants like ascorbic acid and catechin, its NO inhibition effect, though less than cardamonin, was markedly superior to that of the isolated fractions. These findings support the use of phenolic enrichment as a balanced and effective option for managing oxidative stress and inflammation, highlighting its potential as a multifunctional natural therapeutic agent.

Data Availability Statement

The data that support the findings of this study are available from the corresponding author upon reasonable request.

Conflicts of Interest

The authors declare no conflicts of interest.

Funding

This study was funded by the Vietnam Academy of Science and Technology (VAST) under the grant number NCXS

01.02/23-25 and the Center for High Technology Research and Development.

Acknowledgments

This research was supported by the Vietnam Academy of Science and Technology (VAST) under the grant number NCXS 01.02/23-25 and the Center for High Technology Research and Development.

Supporting Information

Additional supporting information can be found online in the Supporting Information section. *(Supporting Information)*

Detailed NMR data of the isolated compounds.

References

[1] W. Routray and K. Rayaguru, "Chemical Constituents and Post-Harvest Prospects of *Pandanus amaryllifolius* Leaves: A Review," *Food Reviews International* 26, no. 3 (2010): 230–245, https://doi.org/10.1080/87559129.2010.484114.

[2] W. Wang, Z. Ren, S. Zheng, et al., "Botany, Phytochemistry, Pharmacology, and Applications of *Pandanus amaryllifolius* Roxb.: A Review," *Fitoterapia* 177 (2024): 106144, https://doi.org/10.1016/j.fitote.2024.106144.

[3] Y.-C. Tsai, M.-L. Yu, M. El-Shazly, et al., "Alkaloids From *Pandanus amaryllifolius*: Isolation and Their Plausible Biosynthetic Formation," *Journal of Natural Products* 78, no. 10 (2015): 2346–2354, https://doi.org/10.1021/acs.jnatprod.5b00252.

[4] Y.-B. Cheng, H.-C. Hu, Y.-C. Tsai, et al., "Isolation and Absolute Configuration Determination of Alkaloids From *Pandanus amaryllifolius*," *Tetrahedron* 73, no. 25 (2017): 3423–3429, https://doi.org/10.1016/j.tet.2017.05.002.

[5] H. Takayama, T. Ichikawa, M. Kitajima, M. Nonato, and N. Aimi, "Isolation and Characterization of Two New Alkaloids, Norpandamarilactonine-A and-B, From *Pandanus amaryllifolius* by Spectroscopic and Synthetic Methods," *Journal of Natural Products* 64, no. 9 (2001): 1224–1225, https://doi.org/10.1021/np010213h.

[6] M. A. Tan, M. Kitajima, N. Kogure, M. G. Nonato, and H. Takayama, "Isolation of Pandamarilactonine-H From the Roots of *Pandanus amaryllifolius* and Synthesis of Epi-Pandamarilactonine-H," *Journal of Natural Products* 73, no. 8 (2010): 1453–1455, https://doi.org/10.1021/np1003998.

[7] V. Cheetangdee and S. Chaiseri, "Free Amino Acid and Reducing Sugar Composition of Pandan (*Pandanus amaryllifolius*) Leaves," *Kasetsart Journal* 40 (2006): 67–74.

[8] R. Suzuki, S. Kan, Y. Sugita, and Y. Shirataki, "*p*-Coumaroyl Malate Derivatives of the *Pandanus amaryllifolius* Leaf and Their Isomerization," *Chemical and Pharmaceutical Bulletin* 65, no. 12 (2017): 1191–1194, https://doi.org/10.1248/cpb.c17-00604.

[9] A. Ghasemzadeh and H. Z. E. Jaafar, "Profiling of Phenolic Compounds and Their Antioxidant and Anticancer Activities in Pandan (*Pandanus amaryllifolius* Roxb.) Extracts from Different Locations of Malaysia," *BMC Complementary and Alternative Medicine* 13, no. 1 (2013): 341, https://doi.org/10.1186/1472-6882-13-341.

[10] N. T. C. Quyen, N. T. N. Quyen, L. T. H. Nhan, and T. Q. Toan, "Antioxidant Activity, Total Phenolics and Flavonoids Contents of *Pandanus amaryllifolius* (Roxb.)," *IOP Conference Series: Materials Science and Engineering* 991, no. 1 (2020): 012019, https://doi.org/10.1088/1757-899x/991/1/012019.

[11] A. Ghasemzadeh and H. Z. E. Jaafar, "Optimization of Reflux Conditions for Total Flavonoid and Total Phenolic Extraction and Enhanced Antioxidant Capacity in Pandan (*Pandanus amaryllifolius* Roxb.) Using Response Surface Methodology," *The Scientific World Journal* 2014, no. 1 (2014): 1–10, https://doi.org/10.1155/2014/523120.

[12] B. L. Lee, J. Su, and C. N. Ong, "Monomeric C18 Chromatographic Method for the Liquid Chromatographic Determination of Lipophilic Antioxidants in Plants," *Journal of Chromatography A* 1048, no. 2 (2004): 263–267, https://doi.org/10.1016/j.chroma.2004.07.057.

[13] A. Weremfo, S. Abassah-Oppong, F. Adulley, K. Dabie, and S. Seidu-Larry, "Response Surface Methodology as a Tool to Optimize the Extraction of Bioactive Compounds From Plant Sources," *Journal of the Science of Food and Agriculture* 103, no. 1 (2023): 26–36, https://doi.org/10.1002/jsfa.12121.

[14] M. A. Bezerra, R. E. Santelli, E. P. Oliveira, L. S. Villar, and L. A. Escaleira, "Response Surface Methodology (RSM) as a Tool for Optimization in Analytical Chemistry," *Talanta* 76, no. 5 (2008): 965–977, https://doi.org/10.1016/j.talanta.2008.05.019.

[15] T. Doncheva, N. Kostova, R. Toshkovska, et al., "Alkaloids from *Pandanus amaryllifolius* and *Pandanus tectorius* from Vietnam and Their Anti-inflammatory Properties," *Comptes Rendus de l'Academie Bulgare des Sciences* 75, no. 6 (2022): 812–820, https://doi.org/10.7546/crabs.2022.06.04.

[16] S. Fattahi, E. Zabihi, Z. Abedian, et al., "Total Phenolic and Flavonoid Contents of Aqueous Extract of Stinging Nettle and *In Vitro* Antiproliferative Effect on Hela and BT-474 Cell Lines," *International Journal of Molecular and Cellular Medicine* 3, no. 2 (2014): 102–107.

[17] W. Brand-Williams, M. E. Cuvelier, and C. Berset, "Use of a Free Radical Method to Evaluate Antioxidant Activity," *LWT-Food Science and Technology* 28, no. 1 (1995): 25–30, https://doi.org/10.1016/s0023-6438(95)80008-5.

[18] P. T. Thuong, N. D. Su, T. M. Ngoc, et al., "Antioxidant Activity and Principles of Vietnam Bitter Tea *Ilex kudingcha*," *Food Chemistry* 113, no. 1 (2009): 139–145, https://doi.org/10.1016/j.foodchem.2008.07.041.

[19] N. H. Dang, L. T. V. Anh, and N. T. Dat, "Anti-Inflammatory Effects of Essential Oils of Amomum Aromaticum Fruits in Lipopolysaccharide-Stimulated RAW264," *Cells* 2020, no. 1 (2020): 8831187.

[20] A. C. Casabuono and A. B. Pomillo, "Lignans and a Stilbene From *Festuca argentina*," *Phytochemistry* 35, no. 2 (1994): 479–483, https://doi.org/10.1016/s0031-9422(00)94786-1.

[21] S. C. Roy, K. K. Rana, and C. Guin, "Short and Stereoselective Total Synthesis of Furano Lignans (±)-Dihydrosesamin, (±)-Lariciresinol Dimethyl Ether, (±)-Acuminatin Methyl Ether, (±)-Sanshodiol Methyl Ether, (±)-Lariciresinol, (±)-Acuminatin, and (±)-Lariciresinol Monomethyl Ether and Furofuran Lignans (±)-Sesamin, (±)-Eudesmin, (±)-Piperitol Methyl Ether, (±)-Pinoresinol, (±)-Piperitol, and (±)-Pinoresinol Monomethyl Ether by Radical Cyclization of Epoxides Using a Transition-Metal Radical Source," *Journal of Organic Chemistry* 67, no. 10 (2002): 3242–3248, https://doi.org/10.1021/jo010857u.

[22] S. Liu, C. Sun, Y. Ha, et al., "Novel Antibacterial Alkaloids From the Mariana Trench-Derived Actinomycete *Streptomyces* sp. SY2255," *Tetrahedron Letters* 137 (2024): 154935, https://doi.org/10.1016/j.tetlet.2024.154935.

[23] G. Degotte, H. Pendeville, C. Di Chio, et al., "Dimeric Polyphenols to Pave the Way for New Antimalarial Drugs,"

RSC Medicinal Chemistry 14, no. 4 (2023): 715–733, https://doi.org/10.1039/d2md00392a.

[24] Z. Lin, Y. Fang, A. Huang, L. Chen, S. Guo, and J. Chen, "Chemical Constituents From Sedum Aizoon and Their Hemostatic Activity," *Pharmaceutical Biology* 52, no. 11 (2014): 1429–1434, https://doi.org/10.3109/13880209.2014.895019.

[25] Z. Xia, O. Khaled, V. Mouriès-Mansuy, C. Ollivier, and L. Fensterbank, "Dual Photoredox/Gold Catalysis Arylative Cyclization of O-Alkynylphenols With Aryldiazonium Salts: A Flexible Synthesis of Benzofurans," *Journal of Organic Chemistry* 81, no. 16 (2016): 7182–7190, https://doi.org/10.1021/acs.joc.6b01060.

[26] T. T. T. Ha, N. T. Dung, K. H. Trung, B. H. Tai, and P. V. Kiem, "Phytochemical Constituents From the Rhizomes of Kaempferia Parviflora Wall. Ex Baker and Their Acetylcholinesterase Inhibitory Activity," *Natural Product Research* 38, no. 6 (2024): 994–1001, https://doi.org/10.1080/14786419.2023.2210738.

[27] C.-C. Chen, H.-Y. Chen, M.-S. Shiao, Y.-L. Lin, Y.-H. Kuo, and J.-C. Ou, "Inhibition of Low Density Lipoprotein Oxidation by Tetrahydrofurofuran Lignans From Forsythia Suspensa and Magnolia Coco," *Planta Medica* 65, no. 8 (1999): 709–711, https://doi.org/10.1055/s-1999-14093.

[28] J. Deng, W. Cheng, and G. Yang, "A Novel Antioxidant Activity Index (AAU) for Natural Products Using the DPPH Assay," *Food Chemistry* 125, no. 4 (2011): 1430–1435, https://doi.org/10.1016/j.foodchem.2010.10.031.

[29] F. S. Youssef, M. L. Ashour, H. A. El-Beshbishy, A. Ahmed Hamza, A. N. B. Singab, and M. Wink, "Pinoresinol-4-O-β-D-glucopyranoside: A Lignan From Prunes (Prunus Domestica) Attenuates Oxidative Stress, Hyperglycaemia and Hepatic Toxicity In Vitro and In Vivo," *Journal of Pharmacy and Pharmacology* 72, no. 12 (2020): 1830–1839, https://doi.org/10.1111/jphp.13358.

[30] R. S. Das, A. Kumar, A. V. Wankhade, and S. A. Mandavgane, "Antioxidant Analysis of Ultra-Fast Selectively Recovered 4-Hydroxy Benzoic Acid From Fruits and Vegetable Peel Waste Using Graphene Oxide Based Molecularly Imprinted Composite," *Food Chemistry* 376 (2022): 131926, https://doi.org/10.1016/j.foodchem.2021.131926.

[31] R. Manuja, S. Sachdeva, A. Jain, and J. Chaudhary, "A Comprehensive Review on Biological Activities of P-Hydroxy Benzoic Acid and Its Derivatives" (2013).

Wiley
Journal of Chemistry
Volume 2025, Article ID 5587982, 7 pages
https://doi.org/10.1155/joch/5587982

WILEY

Research Article

Pandanusfuran A and B: Two New Benzofuran Epimers From *Pandanus tectorius* Leaves

Do Hoang Giang,[1,2] **Nguyen Hai Dang**,[1] **Nguyen Thu Uyen**,[2] **Nguyen Thi Thuy Hang**,[3] **Nguyen Thi Thu Thuy**,[4] **Cao Thanh Hai**,[5] **Hoang Le Tuan Anh**,[2] **Nguyen Ngoc Tung**,[2] **and Nguyen Tien Dat**[2]

[1]*University of Science and Technology of Hanoi, Vietnam Academy of Science and Technology, Hanoi, Vietnam*
[2]*Center for High Technology Research and Development, Vietnam Academy of Science and Technology, Hanoi, Vietnam*
[3]*Institute of Chemistry, Vietnam Academy of Science and Technology, Hanoi, Vietnam*
[4]*Department of Pharmacy, Joint Vietnam-Russia Tropical Science and Technology Research Center, Hanoi, Vietnam*
[5]*Thai Nguyen University of Sciences, Thai Nguyen University, Thai Nguyen, Thai Nguyen Province, Vietnam*

Correspondence should be addressed to Nguyen Tien Dat; ngtiend@gmail.com

Received 22 July 2025; Revised 5 October 2025; Accepted 13 November 2025

Academic Editor: Munmun Bardhan

From the leaves of *Pandanus tectorius*, we isolated two new benzofuran epimers—Pandanusfuran A (**1**) and Pandanusfuran B (**2**)—together with four known lignans (pinoresinol (**3**), pinoresinol monomethyl ether (**4**), arctigenin (**5**), and matairesinol (**6**)). Structures and absolute configurations were established by an orthogonal validation strategy combining HR-ESI-MS, 1D/2D NMR (600 MHz), ECD, and Snatzke's $Mo_2(OAc)_4$-induced CD method, with diagnostic Cotton effects supporting configuration assignments at C-8/C-9. To exclude methanol-derived artifacts, the natural occurrence of 1–2 was confirmed by HPLC-DAD detection in an independently prepared ethanol extract under identical chromatographic conditions. Isolation yields were as follows: **1** (5.1 mg), **2** (3.5 mg), **3** (24.7 mg), **4** (32.1 mg), **5** (14.9 mg), and **6** (22.3 mg) from 3.5 kg of dried leaves. Spectroscopic signatures (chemical shifts, coupling patterns, HRMS formulae, and ECD/ICD profiles) were concordant across instruments and repeat scans, and the diagnostic ICD signals for the $Mo_2(OAc)_4$ complexes of Pandanusfuran A and B were reproduced under the same conditions, collectively evidencing reproducibility of the structural results. In an NO-production assay in LPS-stimulated RAW264.7 cells (with MTT viability as the control and cardamonin as a positive control), 1-2 showed weak activity ($IC_{50} > 50\ \mu M$). These findings constitute the first report of benzofuran derivatives from *P. tectorius* and enrich the chemotaxonomic landscape of the genus.

Keywords: benzofuran; ECD; lignan; *Pandanus tectorius*; Snatzke's method

1. Introduction

Pandanus tectorius Parkinson ex Du Roi is a robust, hardy plant which is widely distributed in tropical, subtropical, and warm temperate regions of Southeast Asia and the Pacific [1]. *P. tectorius* fruits have been used as food in several Pacific islands [1]. The roots were used for the treatment of nephropathy, hepatitis, hypertension, and diabetes [2, 3]. Previous studies indicated that lignans, flavonoids, coumarins, and other phenolic derivatives were the major secondary metabolites of *P. tectorius* plants and some other species of the *Pandanus* genus as well [4–9].

Previous phytochemical investigations have revealed that benzofuran derivatives were relatively uncommon secondary metabolites within the *Pandanus* genus. Most prior studies on *Pandanus* species have focused primarily on lignans, flavonoids, and other phenolic constituents, while benzofuran scaffolds have been rarely reported [10].

Recently, a new series of benzofurans was identified from *P. tectorius* [11], suggesting that this chemical class, although previously overlooked, may represent a minor yet characteristic metabolite group in the genus. This study reports the isolation of two new benzofuran epimers from *P. tectorius*, which may serve as significant chemotaxonomic markers for the species. The absolute configurations of these compounds were determined using electronic circular dichroism (ECD) analysis combined with Snatzke's method—an established empirical approach for assigning the absolute configuration of optically active acyclic 1,2-diols [12, 13]. This approach exploits the induced circular dichroism (ICD) of dimolybdenum tetraacetate ($Mo_2(OAc)_4$) complexes formed upon addition to the diol sample. The resulting conformationally constrained molybdate ester generates a characteristic Cotton effect around 305 nm, whose sign directly correlates with the O-C-C-O torsional angle, thereby allowing configuration assignment of the diol. A key advantage of this method is its procedural simplicity: The diol is simply mixed with $Mo_2(OAc)_4$ in dimethyl sulfoxide (DMSO) at room temperature, and CD spectra can be readily acquired. Furthermore, this method has proven reliable across various structural and steric conditions, demonstrating utility even in cases of low chemical and optical purity, making it exceptionally versatile in synthetic organic chemistry [12]. Determining the absolute configurations of the two epimeric benzofurans is of particular significance, as even slight stereochemical differences can lead to substantial variations in their physicochemical characteristics and biological activities. Therefore, elucidation of the absolute configurations of these epimers provides valuable insight into their structure–activity relationships and enhances the chemical understanding of *Pandanus*-derived metabolites.

2. Materials and Methods

2.1. Plant Materials. Leaves of *P. tectorius* were collected from Thanh Oai town, on the outskirts of Hanoi City of Vietnam, in March 2021, and identified by Dr. Bui Van Thanh, Institute of Biology, Vietnam Academy of Science and Technology. The voucher specimens were deposited at the Institute of Biology (HN00128210208) and the Center for High Technology Research and Development (NCCG 210208), Vietnam Academy of Science and Technology.

2.2. Extraction and Isolation. Dried powder (3.5 kg) of *P. tectorius* leaves was extracted with 20 L (in triplicate) of methanol (MeOH) in a sonication bath. The combined extracts were evaporated to remove the solvent and obtain the crude residue (178 g). Then, the residue was suspended in 2 L of water and then successively partitioned with hexane (2 L × 3 times) and acetate ethyl (EtOAc) (2 L × 3 times) to afford the corresponding fractions, respectively. The EtOAc fraction (37.5 g) was loaded onto a silica gel chromatography column (CC) eluted by mixtures of CH_2Cl_2 and MeOH (100/0–0/100, v/v) to afford seven subfractions (E1–E7). The fraction E4 (689 mg) was isolated on a silica gel CC eluted with *n*-hexane–acetone (3/1, v/v) followed by preparative HPLC (90 min, 50%–80% MeOH in H_2O) to yield the compounds (**1**) (5.1 mg) and (**2**) (3.5 mg). Fraction E3 (2.68 g) was chromatographed on a silica gel CC eluted with CH_2Cl_2–acetone (10/1, v/v) to afford compound (**3**) (24.7 mg) and compound (**4**) (32.1 mg). Fraction E6 (3.72 g) was isolated using a YMC RP-C18 column eluted with MeOH–water (3 : 1, v/v) to yield compound (**5**) (14.9 mg) and compound (**6**) (22.3 mg). Structures of the isolated compounds are shown in Figure 1.

Pandanusfuran A (**1**): white amorphous powder; HR-ESI-MS: *m/z* 253.1071 $[M+H]^+$(calc for $C_{13}H_{17}O_5$, 253.1076); $[\alpha]_D^{25}$ −32.2; CD (MeOH) λ_{max} (mdge): 220 (+1.73), 264 (−6.66); ^{1}H NMR (DMSO-d_6, 600 MHz): δ 6.79 (1H, d, *J* = 8.4 Hz, H-3), 7.73(1H, dd, *J* = 8.4, 1.8 Hz, H-4), 7.77 (1H, d, *J* = 1.8 Hz, H-6), 3.14 (1H, dd, *J* = 8.4, 16.2 Hz, H-7a), 3.25 (1H, dd, *J* = 9.6, 16.2 Hz, H-7b), 4.84 (1H, dd, *J* = 8.4, 9.6 Hz, H-8), 3.53 (1H, dd, *J* = 6.0, 10.2 Hz, H-10a), 3.27 (1H, dd, *J* = 5.4, 10.2 Hz, H-10b), 1.04 (3H, s, H-11), 3.79 (3H, s, 12-O-Me); ^{13}C NMR (DMSO-d_6, 150 MHz): δ 128.6 (C-1), 164.0 (C-2), 108.5 (C-3), 130.2 (C-4), 121.3 (C-5), 126.0 (C-6), 28.6 (C-7), 86.7 (C-8), 72.7 (C-9), 66.0 (C-10), 20.7 (C-11), 166.0 (C-12), 51.7 (12-O-Me). Purity 98.7% (by HPLC).

Pandanusfuran B (**2**): white amorphous powder; HR-ESI-MS: *m/z* 287.0697 $[M+Cl]^-$ (calc for $C_{13}H_{17}O_5$, 287.0686); $[\alpha]_D^{25}$ −41.5; ^{1}H NMR (DMSO-d_6, 600 MHz): δ 6.81 (1H, d, *J* = 8.4 Hz, H-3), 7.73(1H, dd, *J* = 8.4, 1.8 Hz, H-4), 7.78 (1H, d, *J* = 1.8 Hz, H-6), 3.13 (1H, dd, *J* = 9.6, 16.2 Hz, H-7a), 3.26 (1H, dd, *J* = 8.4, 16.2 Hz, H-7b), 4.83 (1H, dd, *J* = 9.6, 8.4 Hz, H-8), 3.32 (2H, overlap, H-10), 1.04 (3H, s, H-11), 3.79 (3H, s, 12-O-Me); ^{13}C NMR (DMSO-d_6, 150 MHz): δ 128.7 (C-1), 163.9 (C-2), 108.6 (C-3), 130.2 (C-4), 121.4 (C-5), 126.1 (C-6), 28.6 (C-7), 86.6 (C-8), 72.5 (C-9), 66.7 (C-10), 19.9 (C-11), 166.0 (C-12), 51.7 (12-O-Me). Purity 97.3% (by HPLC).

*2.3. Preparation of $Mo_2(OAc)_4$ Complex of the Compounds (**1**) and (**2**) for ECD (Snatzke's Method).* Compounds (**1**) and (**2**) were each reacted with $Mo_2(OAc)_4$ in anhydrous DMSO, and ECD spectra were recorded from 250 to 500 nm immediately after mixing. After 20 min, the stable ICD spectrum was obtained, and the Cotton effect at 290–340 nm was used to determine the diol's absolute configuration.

2.4. NO Production Inhibition Assay. RAW 264.7 macrophages were treated with samples (3–25 μg/mL) and stimulated by LPS. NO production was quantified using the Griess reaction, and cell viability was checked via the MTT assay [14]. Cardamonin served as the positive control.

3. Results and Discussion

3.1. Structural Elucidation of the Isolated Compounds. Compound (**1**) was isolated as a white amorphous powder that generated $[M+H]^+$ ion with the mass-to-charge ratio (*m/z*) value of 253.1071 on HRESIMS, suggesting the molecular formula $C_{13}H_{16}O_5$. ^{1}H NMR spectrum of compound (**1**) performed the signals of three aromatic protons of an ABX system [6.79 (1H, d, *J* = 8.4 Hz, H-3), 7.73 (1H, dd,

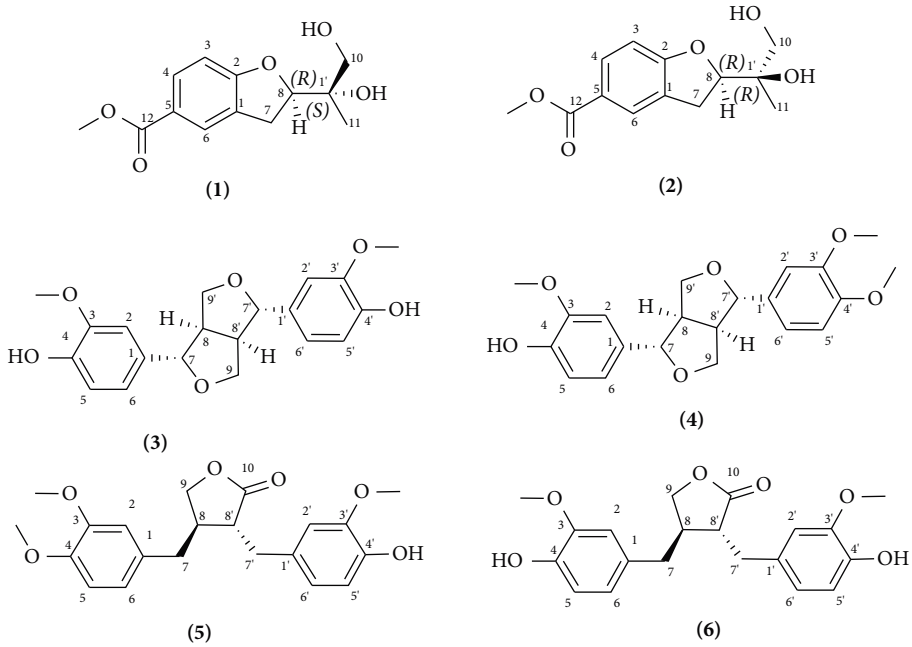

Figure 1: Structures of six isolated compounds.

J = 8.4, 1.8 Hz, H-4), 7.77 (1H, d, J = 1.8 Hz, H-6)] which were also confirmed by the COSY correlation of H-3 and H-4; four methylene protons at δ_H 3.14 (1H, dd, J = 8.4, 16.2 Hz, H-7a), 3.25 (1H, dd, J = 9.6, 16.2 Hz, H-7b), 3.53 (1H, dd, J = 6.0, 10.2 Hz, H-10a), 3.27 (1H, dd, J = 5.4, 10.2 Hz, H-10b); an oxymethine sp^3 proton at δ_H 4.84 (1H, dd, J = 8.4, 9.6 Hz, H-8); a methyl group at δ_H 1.04 (3H, s, H-11); and a methoxy group at 3.79 (3H, s, 12-O-CH_3). The ^{13}C and HSQC spectra showed signals of one methyl (δ_C 20.7, C-11), one methoxy (δ_C 51.7, 12-O-CH_3), one conjugated carbonyl (δ_C 166.0, C-12), two quaternary sp^2 [δ_C 128.6 (C-1), 121.3 (C-5)], three methines sp^2 [δ_C 130.2 (C-4), 126.0 (C-6), 108.5 (C-3)], one oxy-quaternary sp^2 (δ_C 164.0, C-2), one methylene sp^2 (δ_C 28.6, C-7), and one oxymethine sp^3 (δ_C 86.7, C-8). The HMBC spectrum showed the correlations of aromatic protons and carbons, such as H-3 (δ_H 6.79) with C-1 (δ_C 128.6) and C-5 (δ_C 121.3), H-4 (δ_H 7.73) with C-2 (δ_C 164.0) and C-6 (δ_C 126.0), and H-6 (δ_H 7.77) with C-2 (δ_C 164.0) and C-4 (δ_C 130.2). The position of the furan ring was determined by the HMBC correlations of H-7 (δ_H 3.14 and 3.25) and H-8 (δ_H 4.84) with C-1 (δ_C 128.6) and C-2 (δ_C 164.0), and H-7 (δ_H 3.14 and 3.25) with C-6 (δ_C 126.0). The position of the dihydroxy isopropyl group was identified by the HMBC correlations of H-10 (δ_H 3.27 and 3.53) and H-11 (δ_H 1.04) with C-8 (δ_C 86.7). NMR spectra of compound (**1**) were highly similar to those of gasphostrin D, a reported benzofuran derivative [15] (Table S1). However, compound (**1**) exhibited one more methoxy group than the reported compound, and the HMBC correlation between methoxy protons (δ_H 3.79) and C-12 (δ_C 166.0) might reveal the methylation of the carboxyl group.

Compound (**2**) was isolated as a white amorphous powder. The molecular formula of compound (**2**) was determined as $C_{13}H_{16}O_5$ by the HR-ESI-MS at m/z 287.0697 $[M + Cl]^-$. The ^1H NMR spectrum of compound (**2**) showed the signals of three aromatic protons of an ABX system [6.81 (1H, d, J = 8.4 Hz, H-3), 7.73 (1H, dd, J = 8.4, 1.8 Hz, H-4), 7.78 (1H, d, J = 1.8 Hz, H-6)]; two pairs of methylene protons at δ_H 3.13 (1H, dd, J = 9.6, 16.2 Hz, H-7a), 3.26 (1H, dd, J = 8.4, 16.2 Hz, H-7b), and 3.32 (2H, overlap, H-10); an oxymethine sp^3 proton at δ_H 4.83 (1H, dd, J = 9.6, 8.4 Hz, H-8); a methyl group at δ_H 1.04 (3H, s, H-11); and a methoxy group at 3.79 (3H, s, 12-O-CH_3). ^{13}C and HSQC spectra of the compound exhibited signals of one methyl (δ_C 19.9, C-11), one methoxy (δ_C 51.7, 12-O-CH_3), one conjugated carbonyl (δ_C 166.0, C-12), two quaternary sp^2 [δ_C 128.7 (C-1), 121.4 (C-5)], three methines sp^2 [δ_C 130.2 (C-4), 126.1 (C-6), 108.6 (C-3)], one oxy-quaternary sp^2 (δ_C 163.9, C-2), one methylene sp^2 (δ_C 28.6, C-7), and one oxymethine sp^3 (δ_C 86.6, C-8). The HMBC spectrum showed the correlations of H-3 (δ_H 6.81) with C-1 (δ_C 128.7) and C-5 (δ_C 121.4), H-4 (δ_H 7.73) with C-2 (δ_C 163.9) and C-6 (δ_C 126.1), and H-6 (δ_H 7.78) with C-2 (δ_C 163.9) and C-4 (δ_C 130.2) (Figure 2). The position of the furan ring was determined by the HMBC correlations of H-7 (δ_H 3.13 and 3.26) and H-8 (δ_H 4.83) with C-1 (δ_C 128.7) and C-2 (δ_C 163.9), and H-7 (δ_H 3.13 and 3.26) with C-6 (δ_C 126.1). The dihydroxy isopropyl group was identified by the HMBC correlations of H-10 (δ_H 3.32) and H-11 (δ_H 1.04) with C-8 (δ_C 86.6). The NMR spectra of compound (**2**) resembled those of compound (**1**) (Table S1), indicating their same planar structures.

The C-8 absolute configurations of both compounds were determined by comparison of the experimental ECD spectra to the referenced spectra [15]. The ECD spectra of the compounds (Figure 3) showed opposite trends of Cotton effects to gasphostrin D (8*S*, 9*R*) and was well matched with the calculated ECD spectrum of the (8*R*, 9*R*) derivative [15]. Moreover, the negative optical rotation of the compounds

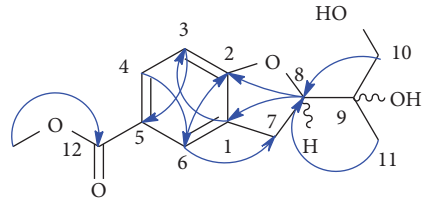

Figure 2: Key HMBC correlations of compounds (**1**) and (**2**).

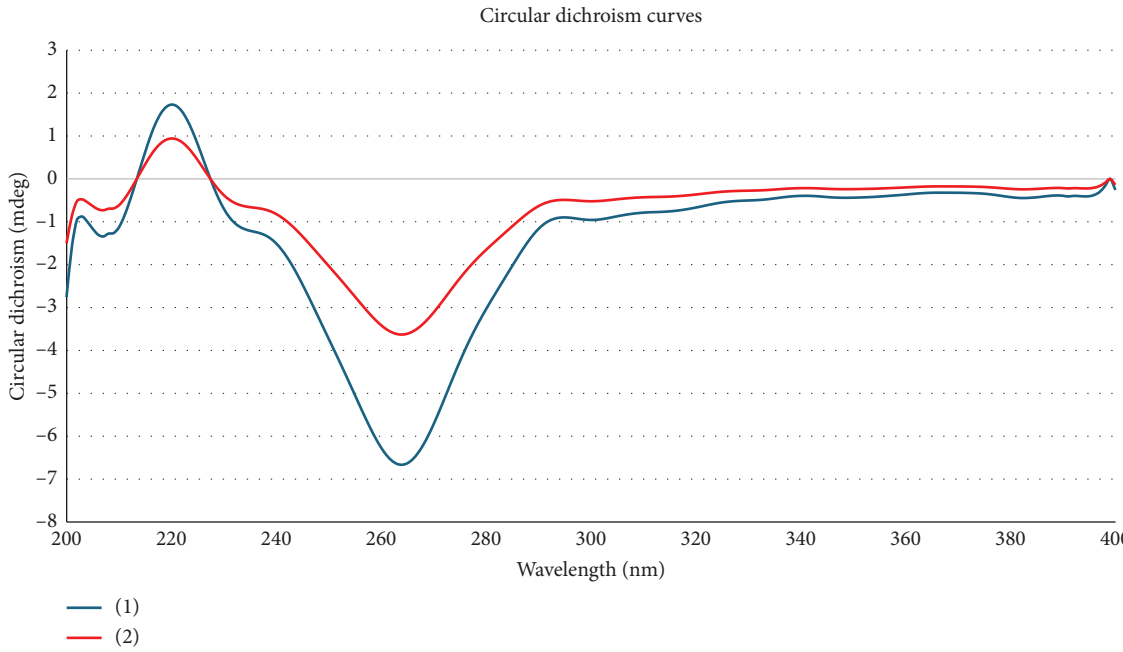

Figure 3: ECD spectra of compound (**1**) (blue) and compound (**2**) (red).

(**1**) ($[\alpha]_D^{25} - 32.2$) and (**2**) ($[\alpha]_D^{25} - 41.5$) was opposed to gasphostrin D ($[\alpha]_D^{25} + 78.9$) and matched to several similar 8*R*-benzofuran derivatives [16]. Thus, the absolute configuration of C-8 in compounds (**1**) and (**2**) was elucidated as *R*.

Snatzke's method was applied to elucidate the C-9 absolute configuration in the structures of these two isolated compounds. The induced negative Cotton effects at 290–320 nm (Figure 4), which was in contrast to those of gasphostrin D (8*S*, 9*R*) [15], revealed the 9*S* configuration of (**1**). The observed positive Cotton effect at about 324 nm, indicative of the O-C-C-O torsion angle, corresponded to a right-handed (positive) helicity, consistent with that reported for gasphostrin D (8*S*, 9*R*) [15], indicated the 9*R* configuration of (**2**). Besides, significant chemical shift difference between H-10a [δ_H 3.53 (1H, dd, $J = 5.0$, 8.5 Hz)] and H-10b [δ_H 3.27 (1H, dd, $J = 5.0$, 8.5 Hz)] of (**1**) was in good agreement with those of (8*S*, 9*S*)-dihydrofurocoumarin and (8*S*, 9*S*)-diacetatefurocoumarin, whereas the overlap of H-10 protons of the compound (**2**) was similar to the smaller difference between the chemical shifts of these two protons in the 9*R*-derivatives [17]. Therefore, compound (**1**) was assigned as methyl (*R*)-8-((*S*)-9,10-dihydroxypropan-8-yl)-7,8-dihydrobenzofuran-5-carboxylate, namely, Pandanusfuran A. Meanwhile, compound (**2**) was identified as methyl (*R*)-8-((*R*)-9,10-dihydroxypropan-8-yl)-7,8-dihydrobenzofuran-5-carboxylate, namely, Pandanusfuran B. These are two new isolated benzofurans from *P. tectorius*.

To check if these compounds might be artifacts of the extracting process in methanol, we performed an HPLC-DAD analysis on the ethanol extract of the plant material and compared it to the chromatograms of isolated compounds under the same parameters. As shown, compounds (**1**) and (**2**) could be found in the ethanol extract (Figure S13), and thus, they were natural products.

NO production inhibitory effects of the two new compounds were evaluated. These compounds exhibited weak NO production inhibition with $IC_{50} > 50$ μM in comparison to cardamonin, the positive control.

Compounds (**3**–**6**) were identified as four lignans, including pinoresinol (**3**), pinoresinol monomethyl ether (**4**), arctigenin (**5**), and matairesinol (**6**), by comparing their NMR data to the previous report [18, 19]. Therefore, six compounds were isolated from the leaves of *P. tectorius*, including two new benzofuran derivatives and four known lignans.

4. Discussion

Pandanaceae includes about 700 species with five genera: *Benstonea* Callmander & Buerki, *Freycinetia* Gaudichaud,

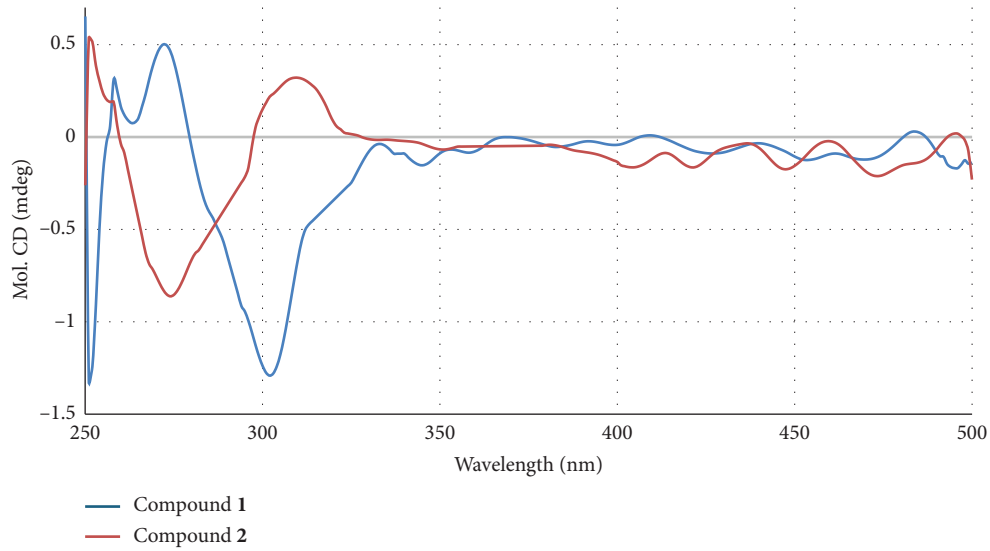

FIGURE 4: ICD spectra of the $Mo_2(AcO)_4$ complex of (**1**) and (**2**).

Martellidendron Callmander & Chassot, *Pandanus* Parkinson, and *Sararanga* Hemsley [20]. *Pandanus* was the largest genus, with more than 400 species [20]. Previous phytochemistry investigations on this family mostly focused on the genus *Pandanus*, while only one study on the secondary metabolites of the *Freycinetia* plant [21] and no information about the chemical constituents of the rest of the genera have been reported.

Lignans have been investigated in several *Pandanus* species, including *P. tectorius* [7], *P. boninensis* [4], or *P. odoratissimus* [10], but could not be found in *P. amaryllifolius*, *P. dubius*, and *P. utilis*, which alkaloids were the specific compositions [22–28]. In this study, four lignans were isolated from *P. tectorius*, including pinoresinol, phillygenin, arctigenin, and matairesinol. While pinoresinol has been discovered in some species as mentioned above, this is the first isolation of phillygenin, arctigenin, and matairesinol from a *Pandanus* plant. These results broaden the known chemical spectrum of *Pandanus* species and offer valuable insights for future chemotaxonomic investigations. Besides, other studies indicated that *P. tectorius* might contain flavonoids [5] or coumarins [7], only one study reported benzofuran derivatives in this species [11]. Significantly, most of the highly similar compounds with two isolated benzofuran derivatives were isolated from microorganisms [15, 29] rather than from plants. Therefore, the isolation of Pandanusfuran A and Pandanusfuran B from *P. tectorius* could reveal an interesting biosynthesis pathway in the plant that should be investigated further. In addition, another benzofuran racemate was previously separated from the roots of *P. odoratissimus* [10]. This may reveal a close chemotaxonomic relationship between *P. tectorius* and *P. odoratissimus*. Moreover, benzofuran derivatives are also known for their pharmacological significance, forming the core structures of several valuable therapeutic agents such as amiodarone, dronedarone, and griseofulvin. Thus, the discovery of these benzofuran epimers from *P. tectorius* not only expands the phytochemical profile of the genus but also suggests potential pharmacological relevance worthy of further investigation.

5. Conclusion

The current study reports the isolation of two unprecedented benzofuran derivatives, Pandanusfuran A and B, from *Pandanus tectorius* leaves. Additionally, four known lignans—pinoresinol, pinoresinol monomethyl ether, arctigenin, and matairesinol—were also isolated and identified. Employing state-of-the-art analytical techniques such as NMR, HRMS, ECD, and Snatzke's method, we accurately determined the chemical structures and absolute configurations of these compounds. Furthermore, the discovery of benzofuran derivatives alongside these lignans enriches the phytochemical profile of the *Pandanus* genus, offering significant implications for future chemotaxonomic and biosynthetic studies.

Data Availability Statement

The data that support the findings of this study are available in the supporting information of this article.

Conflicts of Interest

The authors declare no conflicts of interest.

Funding

This research was supported by the Vietnam Academy of Science and Technology (VAST) under the grant number NCXS 01.02/23-25.

Acknowledgments

This research was supported by the Vietnam Academy of Science and Technology (VAST) under grant number NCXS 01.02/23-25. We are also grateful for the support of the

Top-tier Research Group Phytomedicine at the University of Science and Technology of Hanoi, VAST.

Supporting Information

Additional supporting information can be found online in the Supporting Information section. *(Supporting Information)*

Detailed NMR data of the new compounds and additional supporting information can be found online in the Supporting Information section.

References

[1] T. K. Lim, "*Pandanus tectorius*," in *Edible Medicinal and Non-Medicinal Plants: Volume 4, Fruits*, ed. T. K. Lim (Dordrecht: Springer, 2012), 136–146.

[2] V. V. Chi, *Dictionary of Vietnamese Medicinal Plants* (Medicine Publisher, 2012).

[3] D. T. Loi, *Medicinal Plants in Vietnam* (Medicine Publisher, 2004).

[4] A. Inada, Y. Ikeda, H. Murata, et al., "Unusual Cyclolanostanes From Leaves of *Pandanus boninensis*," *Phytochemistry* 66, no. 23 (2005): 2729–2733, https://doi.org/10.1016/j.phytochem.2005.08.019.

[5] X. Zhang, P. Guo, G. Sun, et al., "Phenolic Compounds and Flavonoids From the Fruits of *Pandanus tectorius* Soland," *Journal of Medicinal Plants Research* 6, no. 13 (2012): 2622–2626, https://doi.org/10.5897/jmpr11.1424.

[6] D. T. Mai, T. D. Le, T. P. Nguyen, et al., "A New Aldehyde Compound From the Fruit of *Pandanus tectorius* Parkinson ex du Roi," *Natural Product Research* 29, no. 15 (2015): 1437–1441, https://doi.org/10.1080/14786419.2014.1003929.

[7] T. P. Nguyen, T. D. Le, P. N. Minh, et al., "A New Dihydrofurocoumarin From the Fruits of *Pandanus tectorius* Parkinson ex du Roi," *Natural Product Research* 30, no. 21 (2016): 2389–2395, https://doi.org/10.1080/14786419.2016.1188095.

[8] N. S. Musa, N. M. Ramli, J. Saidin, and Y. Andriani, "Antioxidant and Cytotoxicity Properties of Ethyl Acetate Fractions of *Pandanus tectorius* Fruit Against HeLa Cell Lines," *ALOTROP Jurnal Pendidikan dan Ilmu Kimia* 1, no. 2 (2017): 106–112.

[9] R. Suzuki, S. Kan, Y. Sugita, and Y. Shirataki, "p-Coumaroyl Malate Derivatives of the *Pandanus amaryllifolius* Leaf and Their Isomerization," *Chemical & Pharmaceutical Bulletin* 65, no. 12 (2017): 1191–1194, https://doi.org/10.1248/cpb.c17-00604.

[10] T.-T. Jong and S.-W. Chau, "Antioxidative Activities of Constituents Isolated From *Pandanus* odoratissimus," *Phytochemistry* 49, no. 7 (1998): 2145–2148, https://doi.org/10.1016/s0031-9422(98)00390-2.

[11] Y. Huang, J. Chen, Z. Liu, et al., "Benzofuran Sesquineolignan Racemates From the Roots and Rhizomes of *Pandanus tectorius*: Isolation, Chiral Resolution, and Configurational Assignment," *Journal of Molecular Structure* 1338 (2025): 142322, https://doi.org/10.1016/j.molstruc.2025.142322.

[12] L. Di Bari, G. Pescitelli, C. Pratelli, D. Pini, and P. Salvadori, "Determination of Absolute Configuration of Acyclic 1,2-Diols With $Mo_2(OAc)_4$. 1. Snatzke's Method Revisited," *Journal of Organic Chemistry* 66, no. 14 (2001): 4819–4825, https://doi.org/10.1021/jo010136v.

[13] J. Frelek, N. Ikekawa, S. Takatsuto, and G. Snatzke, "Application of $[Mo_2(OAc)_4]$ for Determination of Absolute Configuration of Brassinosteroid Vic-Diols by Circular Dichroism," *Chirality* 9, no. 56 (1997): 578–582, https://doi.org/10.1002/(sici)1520-636x(1997)9:5/6%3A578::aid-chir27%3E3.3.co;2-k.

[14] D. H. Giang, T. T. T. Phuong, N. H. Dang, N. T. Hong Anh, and D. Nguyen Tien, "A New Megastigmane Glycoside and Other Constituents From *Amomum muricarpum* Elmer," *Records of Natural Products* 17, no. 1 (2022): 184–188, https://doi.org/10.25135/rnp.333.2203.2395.

[15] S. Niu, Q. Liu, J. M. Xia, et al., "Polyketides From the Deep-Sea-Derived Fungus *Graphostroma* Sp. MCCC 3A00421 Showed Potent Antifood Allergic Activities," *Journal of Agricultural and Food Chemistry* 66, no. 6 (2018): 1369–1376, https://doi.org/10.1021/acs.jafc.7b04383.

[16] R. Tovar-Miranda, R. Cortés-García, and P. Joseph-Nathan, "Synthesis and Absolute Configuration of the Four Possible Stereoisomers of Prandiol," *Tetrahedron: Asymmetry* 13, no. 11 (2002): 1147–1152, https://doi.org/10.1016/s0957-4166(02)00267-7.

[17] R. Tovar-Miranda, R. Cortés-García, N. F. Santos-Sánchez, and P. Joseph-Nathan, "Isolation, Total Synthesis, and Relative Stereochemistry of a Dihydrofurocoumarin From *Dorstenia contrajerva*," *Journal of Natural Products* 61, no. 10 (1998): 1216–1220, https://doi.org/10.1021/np9801209.

[18] M. M. A. Rahman, P. M. Dewick, D. E. Jackson, and J. A. Lucas, "Lignans of *Forsythia intermedia*," *Phytochemistry* 29, no. 6 (1990): 1971–1980, https://doi.org/10.1016/0031-9422(90)85050-p.

[19] D. H. Giang, B. T. N. Le, N. T. T. Minh, et al., "Optimization of the Extraction Conditions and Evaluation of Bioactivities of the Phenolic Enrichment From *Pandanus* amaryllifolius Leaves," *Journal of Analytical Methods in Chemistry* 2025 (10, 2025): 5256388, https://doi.org/10.1155/jamc/5256388.

[20] M. W. Callmander, T. J. Booth, H. Beentje, and S. Buerki, "Update on the Systematics of Benstonea (Pandanaceae): When a Visionary Taxonomist Foresees Phylogenetic Relationships," *Phytotaxa* 112, no. 2 (2013): 57–60, https://doi.org/10.11646/phytotaxa.112.2.4.

[21] A. Inada, C. Morimoto, T. Yoshikawa, Y. Inatomi, and H. Murata, "24-Ethyl, 24-Methyl-29-nor-Lanostanes From Leaves of *Freycinetia formosana*," *Chemical and Pharmaceutical Bulletin* 57, no. 11 (2009): 1303–1304, https://doi.org/10.1248/cpb.57.1303.

[22] L. T. Byrne, B. Q. Guevara, W. C. Patalinghug, B. V. Recio, C. R. Ualat, and A. H. White, "The X-Ray Crystal-Structure of (+/−)-Pandamarine, the Major Alkaloid of *Pandanus amaryllifolius*," *Australian Journal of Chemistry* 45, no. 11 (1992): 1903–1908, https://doi.org/10.1071/ch9921903.

[23] H. Takayama, T. Ichikawa, M. Kitajima, N. Aimi, D. Lopez, and M. G. Nonato, "A New Alkaloid, Pandanamine; Finding of an Anticipated Biogenetic Intermediate in *Pandanus amaryllifolius* Roxb," *Tetrahedron Letters* 42, no. 16 (2001): 2995–2996, https://doi.org/10.1016/s0040-4039(01)00339-2.

[24] H. Takayama, T. Ichikawa, M. Kitajima, M. G. Nonato, and N. Aimi, "Isolation and Characterization of Two New Alkaloids, Norpandamarilactonine-A and B, From *Pandanus amaryllifolius* by Spectroscopic and Synthetic Methods," *Journal of Natural Products* 64, no. 9 (2001): 1224–1225, https://doi.org/10.1021/np010213h.

[25] H. M. C. Laluces, A. Nakayama, M. G. Nonato, T. E. d. Cruz, and M. A. Tan, "Antimicrobial Alkaloids From the Leaves of *Pandanus amaryllifolius*," *Journal of Applied Pharmaceutical Science* 5, no. 10 (2015): 151–153, https://doi.org/10.7324/japs.2015.501026.

[26] Y.-B. Cheng, H.-C. Hu, Y.-C. Tsai, et al., "Isolation and Absolute Configuration Determination of Alkaloids From

Pandanus amaryllifolius," *Tetrahedron* 73, no. 25 (2017): 3423–3429, https://doi.org/10.1016/j.tet.2017.05.002.

[27] M. A. Tan, M. Kitajima, N. Kogure, M. G. Nonato, and H. Takayama, "Isolation and Total Syntheses of Two New Alkaloids, Dubiusamines-A, and B, From *Pandanus dubius*," *Tetrahedron* 66, no. 18 (2010): 3353–3359, https://doi.org/10.1016/j.tet.2010.02.073.

[28] Y.-B. Cheng, Y.-H. Tsai, I. W. Lo, et al., "Pandalisines A and B, Novel Indolizidine Alkaloids From the Leaves of *Pandanus utilis*," *Bioorganic & Medicinal Chemistry Letters* 25, no. 19 (2015): 4333–4336, https://doi.org/10.1016/j.bmcl.2015.07.041.

[29] C. Prompanya, T. Dethoup, L. Gales, et al., "New Polyketides and New Benzoic Acid Derivatives From the Marine Sponge-Associated Fungus *Neosartorya quadricincta* KUFA 0081," *Marine Drugs* 14, no. 7 (2016): 134, https://doi.org/10.3390/md14070134.

Wiley
Journal of Analytical Methods in Chemistry
Volume 2025, Article ID 5539843, 12 pages
https://doi.org/10.1155/jamc/5539843

WILEY

Research Article

Optimization of Phenolic- and Saponin-Enriched Extraction From *Pandanus tectorius* Fruit Using Box–Behnken Design and Evaluation of Their Bioactivities

Do Hoang Giang,[1,2] **Nguyen Hai Dang**,[1] **Tran Thi Thu Phuong**,[1] **Le Thanh Huong**,[1] **Nguyen Thu Uyen**,[2] **Nguyen Thi Luyen**,[2] **Nguyen Thi Thu Thuy**,[3] **Hoang Le Tuan Anh**,[2] **Nguyen Ngoc Tung**,[2] **and Nguyen Tien Dat**[2]

[1]*University of Science and Technology of Hanoi, Vietnam Academy of Science and Technology, Hanoi 10000, Vietnam*
[2]*Center for High Technology Research and Development, Vietnam Academy of Science and Technology, Hanoi 10000, Vietnam*
[3]*Department of Pharmacy, Joint Vietnam-Russia Tropical Science and Technology Research Center, Hanoi 10000, Vietnam*

Correspondence should be addressed to Nguyen Tien Dat; ngtiend@gmail.com

Received 11 July 2025; Revised 7 October 2025; Accepted 31 October 2025

Academic Editor: Ricardo Jorgensen Cassella

Pandanus tectorius fruits are a promising but underutilized source of bioactive constituents. We optimized extraction conditions for phenolic- and saponin-enriched fractions using Box–Behnken/response surface methodology across ethanol concentration, temperature, solvent-to-material ratio, and time and then evaluated antioxidant and anti-inflammatory activities. Total phenolic content (TPC; Folin–Ciocalteu, 760 nm) and total saponin content (TSC; vanillin–sulfuric acid, 560 nm) served as responses for model fitting ($R^2 > 0.96$), validation, and multiresponse optimization that yielded seven distinct optimums targeting different extract profiles. Phenolic-rich extracts showed potent DPPH and hydroxyl radical scavenging, whereas saponin-rich extracts more strongly inhibited LPS-induced nitric oxide in RAW 264.7 cells; excessive saponin enrichment, however, coincided with cytotoxicity. These results demonstrate that tuned extraction can deliver purpose-built extracts for antioxidant or anti-inflammatory applications, supporting the valorization of *P. tectorius* as a natural source for functional and nutraceutical ingredients.

Keywords: anti-inflammation; antioxidant; Box–Behnken; multiresponse optimization; *Pandanus tectorius*; response surface method

1. Introduction

The genus *Pandanus* (family Pandanaceae) comprises approximately 700–750 species predominantly distributed across tropical and subtropical regions of the Paleotropics, extending from West Africa to the Pacific Islands [1, 2]. Members of this genus are morphologically distinctive, characterized by spiral phyllotaxy, long, narrow leaves, and prominent aerial prop roots that aid in anchorage and adaptation to coastal or sandy habitats [1]. Ecologically, *Pandanus* species contribute significantly to shoreline stabilization and serve as key components in tropical forest ecosystems. Culturally, they hold economic and ethnobotanical value, with their leaves widely used in traditional crafts (e.g., mats, baskets, and roofing materials) and, in some regions, as aromatic ingredients in culinary practices [1, 2].

Pandanus tectorius Parkinson ex Du Roi, a member of the Pandanaceae family, is widely distributed throughout tropical and subtropical coastal regions of Asia and the Pacific. It has long been used in traditional medicine for the treatment of ailments such as hypertension, diabetes, urinary tract infections, and inflammation. Recent phytochemical investigations have revealed that this species is

a rich source of structurally diverse secondary metabolites with notable biological activities. Key compound classes identified include phenolic acids and aldehydes (e.g., p-coumaric acid, ferulic acid, vanillin, and syringaldehyde), flavonoids (e.g., vitexin, tricin, chrysin, and sakuranetin), and various lignans such as pinoresinol, syringaresinol, medioresinol, eudesmin, and sesamin, which have been isolated from fruits, roots, and leaves [3–8]. Coumarins, including bergapten and several prenylated derivatives, have also been detected, along with one benzofuran compound and multiple volatile constituents such as geranyl acetate and ethyl cinnamate identified by GC-MS analysis [4, 7, 8]. Furthermore, several miscellaneous compounds such as 5-hydroxymethylfurfural, methylsuccinic acid, long-chain fatty alcohol esters, and sugar derivatives were also reported [6, 9–12].

A growing body of evidence has demonstrated that *P. tectorius* possesses a wide range of biological activities, including antioxidant, cytotoxic, antimicrobial, and antidiabetic effects. Among the phytoconstituents, phenolic compounds stand out as the most studied and bioactive group. Several in vitro assays, such as DPPH, ABTS, and hydroxyl radical scavenging tests, have confirmed the strong antioxidant capacity of both crude extracts and phenolic-enriched fractions, especially those obtained using ethyl acetate or methanol [7–10, 13]. These effects are attributed to abundant phenolic aldehydes and acids, flavonoids, and lignans found in fruits and leaves. For instance, caffeoylquinic acid derivatives from *P. tectorius* have shown lipid-lowering effects in hyperlipidemic hamsters via modulation of PPARα and AMPK signaling pathways [14]. Moreover, phenolic constituents were reported to protect Schwann cells from oxidative stress through activation of the Nrf2/Keap1 antioxidant response pathway [15]. Antidiabetic potential has also been widely explored through α-glucosidase inhibition assays. Multiple phenolic compounds—including aromatic aldehydes, coumarins, and flavonoids—exhibited strong inhibitory activity and promising hypoglycemic effects [6, 9, 10]. In addition, extracts of *P. tectorius* have demonstrated selective cytotoxicity against various human cancer cell lines such as A549, MCF-7, and HeLa, with dose-dependent inhibition of cell viability [8, 16, 17]. Furthermore, antimicrobial activity has been observed in both polar and semipolar extracts, effective against a range of gram-positive and gram-negative bacteria [7]. Recent developments also explored the use of *P. tectorius* fruit extract in nanoparticle formulations for potential therapeutic applications in metabolic disorders [16].

Despite extensive research on phenolics, the saponins of *P. tectorius* remain largely underexplored. Saponins in *Pandanus* species are expected to comprise triterpenoid and steroidal frameworks, consistent with related genera, and have been associated with membrane-active, hemolytic, and immunomodulatory properties relevant to inflammation. Preliminary studies in *P. tectorius* and allied species have suggested that saponin-containing fractions contribute to anti-inflammatory or cytoprotective effects, yet systematic enrichment, quantification, and modeling remain limited [15]. This knowledge gap highlights the need for targeted extraction and comparative evaluation of both phenolic and saponin constituents to better understand their relative contributions to bioactivity.

Because extraction efficiency is determined by complex interactions among solvent polarity, temperature-driven mass transfer and degradation kinetics, solvent-to-material ratio, and extraction time, the traditional one-factor-at-a-time approach is inadequate for identifying true optima. Response surface methodology (RSM), particularly the Box–Behnken design (BBD), enables quantitative assessment of main, interaction, and curvature effects while reducing experimental runs and improving predictive accuracy. Therefore, the present study employed RSM/BBD to optimize the extraction of phenolic- and saponin-enriched fractions from *P. tectorius* fruits, aiming to maximize both yield and bioactivity through multiresponse optimization.

2. Materials and Methods

2.1. Plant Materials. Fruits of *P. tectorius* were collected at Thanh Oai Province, Vietnam, in August 2021 and identified by Dr. Bui Van Thanh, Institute of Biology, Vietnam Academy of Sciences and Technology (VAST). A voucher specimen (NCCG 210213) was deposited at the Center for High Technology Research and Development, VAST. The collected sample was cleaned, dried at 60°C in the oven to under 10% moisture, milled, sieved to < 1 mm to improve batch homogeneity and mass transfer reproducibility prior to extraction, and preserved at −20°C for further experiments.

2.2. General. The solvents, such as ethanol (EtOH), water, DMSO, and necessary inorganic chemicals, were purchased from Daihan Scientific, Korea; meanwhile, other chemicals were supplied by Merck, Germany. The extraction was processed in a shaking water bath with the support of a stirrer (Daihan Scientific, Korea).

2.3. Determination of Total Phenolic Content (TPC). The TPCs of the samples were determined using the Folin–Ciocalteu assay [18]. The characteristic blue chromophore also provided qualitative confirmation of phenolics in the samples. Standard solutions of gallic acid at various concentrations were prepared for calibration. Sample extracts were dissolved in methanol at defined concentrations. A volume of 100 μL from each sample or standard solution was combined with 900 μL of 10% Folin–Ciocalteu reagent and 1000 μL of 6% sodium carbonate (Na_2CO_3). The resulting mixture was incubated at 40°C for 15 min. Absorbance was measured at 760 nm using a UV–visible spectrophotometer. The TPC was quantified based on the gallic acid standard curve and expressed as milligrams of gallic acid equivalents per gram of sample (mg GAE/g).

2.4. Determination of Total Saponin Content (TSC). The TSC of the samples was assessed using the vanillin–sulfuric acid method [19]. The characteristic reddish (vanillin–H_2SO_4)

chromophore also indicated qualitative confirmation of saponins in the samples. For this procedure, 100 μL of each extract was mixed with 100 μL of 8% (w/v) vanillin in EtOH and 2800 μL of 80% (v/v) sulfuric acid. The mixture was incubated at 70°C for 15 min. Solutions of the reference compound (aescin) and reagent blanks (with solvent) were also prepared. After incubation, the mixtures were allowed to cool at room temperature for 5 min, and absorbance was recorded at 560 nm against the blank.

2.5. Preliminary Single-Factor Experiments. Preliminary single-factor experiments were conducted to establish the appropriate ranges for key extraction parameters, including temperature, EtOH concentration, solvent-to-material ratio, and extraction time. First, the influence of EtOH concentration on TPC and TSC was examined by performing extractions with EtOH concentrations ranging from 0% to 90%, at 60°C for 120 min, maintaining a constant solvent-to-material ratio of 20 mL/g. Subsequently, the effect of extraction temperature on the TPC and TSC was investigated by extracting the plant material in 60% EtOH at temperatures ranging from 30°C to 100°C for 120 min, using a solvent-to-material ratio of 20 mL/g. Next, the effect of varying the solvent-to-material ratio was assessed by extracting the material in 60% EtOH at 60°C for 120 min, using ratios ranging from 5 to 50 mL/g. Finally, the impact of extraction time was evaluated by extracting the plant material in 60% EtOH at 60°C with a fixed solvent-to-material ratio of 20 mL/g for durations ranging from 60 to 360 min.

2.6. Response Surface Method. To optimize the extraction conditions for phenolic enrichment from *P. tectorius* fruits, RSM based on the BBD was employed. The experimental design was carried out using Design-Expert software version 12.0 (Stat-Ease, Inc., Minneapolis, USA). Four independent variables were selected: extraction temperature (°C, A), EtOH concentration (%, B), solvent-to-material ratio (mL/g, C), and extraction time (minutes, D). The TPC and TSC were designated as the response variables.

Based on the results of preliminary single-factor experiments, the solvent system included EtOH concentrations of 0% (distilled water), 45%, and 90%. The temperature range tested was 30°C–80°C, the solvent-to-material ratios ranged from 10 to 50 mL/g, and the extraction times varied between 60 and 240 min. All experimental runs were performed in triplicate, and the average value of TPC was used for subsequent statistical analysis. The coded levels of the independent variables used in the experimental design are presented in Table 1.

2.7. Antioxidant Assay. The antioxidant potential of the phenolic-enriched extracts was assessed using DPPH and hydroxyl radical scavenging assays, following established protocols [20, 21].

For the DPPH assay, 100 μL of each sample was mixed with 1900 μL of DPPH solution in methanol and incubated in the dark at 37°C for 20 min. Absorbance was measured at 517 nm, with ascorbic acid serving as the reference standard.

Table 1: Coded and actual levels of independent variables used in the Box–Behnken design.

Variables	Unit	Code levels		
		−1	0	1
Temperature (A)	°C	30	55	80
Ethanol concentration (B)	%	0	45	90
Volume-to-weight ratio (C)	mL/g	10	30	50
Extraction time (D)	min	60	150	240

In the hydroxyl radical scavenging assay, a 200 μL aliquot of each test sample was added to a mixture containing 400 μL of 50 mM phosphate buffer (pH 7.8), 400 μL of 2.8 mM deoxyribose, and 400 μL of 500 μM ferrous ammonium sulfate [$Fe(NH_4)_2(SO_4)_2$]. The mixture was incubated at 37°C for 1 h. The reaction was terminated by the addition of 1000 μL of 10% (w/v) trichloroacetic acid and 1000 μL of 1% (w/v) thiobarbituric acid. The resulting solution was then heated in a boiling water bath for 15 min, and absorbance was measured at 532 nm. Catechin was used as the positive control for this assay.

2.8. Nitric Oxide (NO) Production Inhibition Assay. The inhibitory effect of the samples on NO production in lipopolysaccharide (LPS)-stimulated RAW 264.7 macrophages was evaluated using the Griess reagent method [22]. Cells were seeded in 96-well plates at a density of 0.5×10^5 cells per well and incubated at 37°C in a humidified atmosphere containing 5% CO_2 for 22 h. Following this incubation, samples at concentrations ranging from 3 to 25 μg/mL were added to the wells. After 30 min, 0.1 mg/mL of LPS (Sigma-Aldrich, USA) was introduced to stimulate NO production, and the cells were further incubated for 24 h. After treatment, 100 μL of the culture supernatant was transferred to a new 96-well plate and mixed with an equal volume of Griess reagent. The absorbance was measured at 570 nm using an iMark microplate reader (Bio-Rad, USA). To assess cell viability, the remaining cells in the original plate were subjected to the MTT assay. This assay measures mitochondrial dehydrogenase activity in viable cells through the reduction of MTT (3-(4,5-dimethylthiazol-2-yl)-2,5-diphenyl tetrazolium bromide), providing an estimate of living cell numbers [23]. Cardamonin, a known inhibitor of NO production, served as the positive control.

2.9. Statistical Analysis. All RSM computations were conducted in Design-Expert v12.0. Model adequacy was evaluated by analysis of variance (ANOVA) (model F, p), lack of fit, coefficients of determination (R^2, adjusted R^2, and predicted R^2), Adeq Precision, and coefficient of variation (CV). Data are reported as mean ± SD of triplicate runs.

3. Results and Discussion

3.1. The Process Range Conditions for the Extraction. To establish appropriate experimental ranges for a subsequent BBD optimization, a preliminary single-factor study was conducted. This study aimed to investigate the influence of four

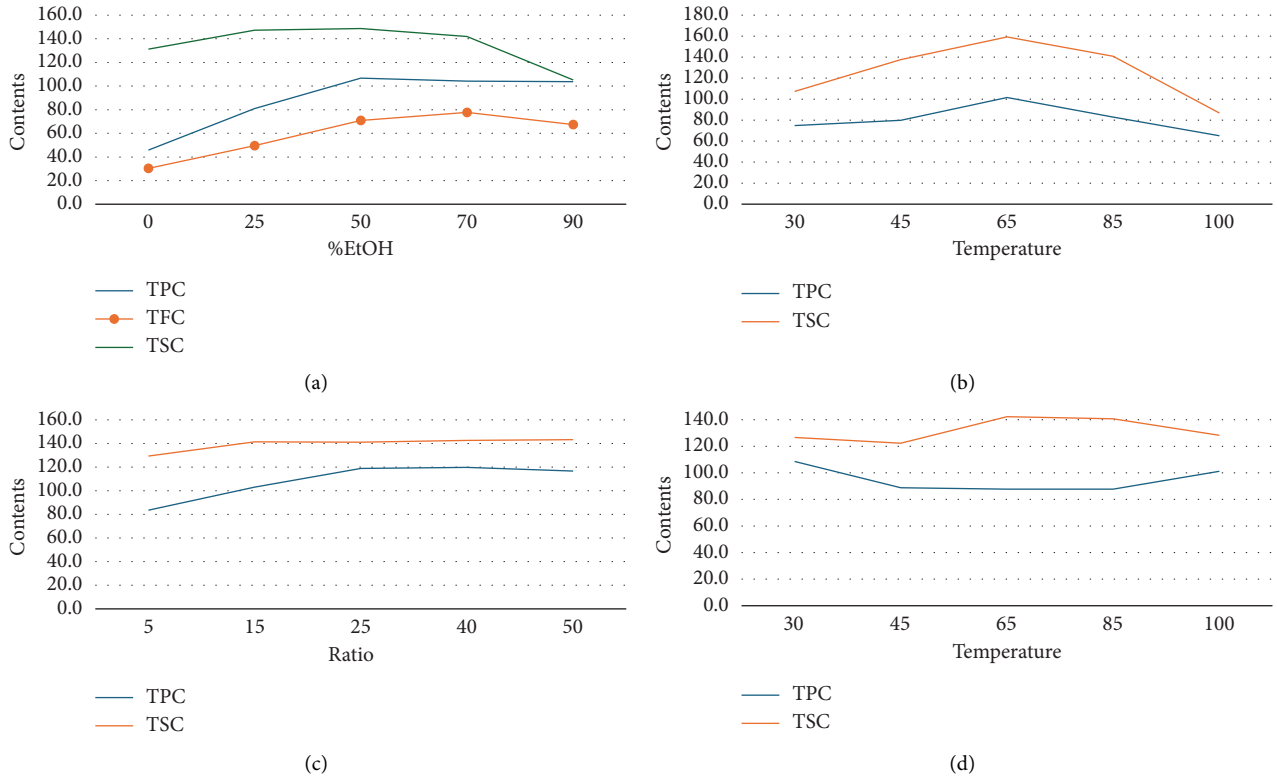

FIGURE 1: The effects of (a) ethanol concentration, (b) extracting temperature, (c) solvent-to-material ratio, and (d) extracting time on TPC and TSC of the extracts.

key variables—ethanol concentration, temperature, solvent-to-material ratio, and extraction time—on the extraction efficiency of TPC and TSC from the fruit of *P. tectorius*.

The influence of EtOH concentration (%EtOH) is illustrated in Figure 1(a). The TPC yield from the fruit extract increased significantly with EtOH concentration, peaking at approximately 70% before plateauing. Similarly, the TSC yield rose with increasing EtOH content, reaching its maximum at 50% EtOH before declining at higher concentrations. This suggests that a hydroethanolic solvent is more effective than pure water or EtOH for extracting compounds from *P. tectorius* fruit, likely due to the varying polarities of the target phenolics and saponins. Based on these effects, the range of 0%–90% EtOH was selected as the operational range for the BBD.

Regarding the extraction temperature, both TPC and TSC yields initially increased with temperature, reaching their optimal values at 65°C. At temperatures higher than this, a significant decrease in the yields of both compounds was observed. The data from the table show that at 85°C, the yields had already begun to decline from their peak. This decline is likely attributable to the degradation of thermosensitive substances within the fruit and the rapid evaporation of the EtOH. Therefore, to ensure compound stability and avoid degradation, the temperature range for the BBD was determined to be 30°C–80°C.

The solvent-to-material ratio demonstrated a strong positive correlation with extraction yield. A substantial increase in both TPC and TSC was observed when the ratio was increased from 5 to 25. A ratio below 10 was deemed unsuitable as the solvent volume was likely insufficient for proper wetting and extraction of the raw fruit material. Although yields continued to rise slightly as the ratio increased from 25 to 50, the rate of increase diminished, indicating marginal gains. To balance extraction efficiency with solvent consumption, the working range for the ratio in the BBD was established as 10–50 mL/g.

The extraction time showed different effects on TPC and TSC. The highest TPC was achieved at a shorter duration of 60 min, with longer times showing no improvement and potential degradation. Conversely, the TSC yield peaked at around 180 min. To accommodate the different optimal times for these two compound groups from *P. tectorius* while maintaining process efficiency, an extraction time range of 60–240 min was chosen as appropriate for the subsequent BBD experiments.

In conclusion, based on the single-factor experimental results, the ranges for the four independent variables were selected for the BBD as follows: EtOH concentration (0%–90%), temperature (30°C–80°C), solvent-to-material ratio (10–50 mL/g), and time (60–240 min).

3.2. Optimize the Extraction Conditions Using BBD. The RSM with BBD was applied to determine the optimal condition for the extraction of phenolic compounds from *P. tectorius* fruits. The extraction design variable effects on the TPC and TSC values are given in Table 2.

Table 2: TPC and TSC of the extracts to independent variables using the Box–Behnken design.

No.	A: EtOH (%)	B: Temp. (°C)	C: Ratio (mL/g)	D: Time (min)	TPC (mgGAE/g)	TSC (mgAE/g)
1	45	30	30	60	58.3	132.8
2	45	30	50	150	74.5	140.2
3	90	30	30	150	91.5	111.2
4	45	30	30	240	73.1	140.5
5	45	55	10	60	65.2	138.5
6	90	55	30	60	116.6	125.9
7	90	80	30	150	112.3	142.2
8	45	30	10	150	56.8	121.4
9	90	55	50	150	121.5	136.7
10	0	55	30	240	47.3	135.2
11	45	80	30	240	94.5	164.2
12	90	55	50	60	116.2	124.4
13	45	80	30	60	105.6	152.3
14	90	55	30	150	111.3	129.9
15	0	55	50	150	50.2	131.1
16	0	55	30	60	47.9	128.9
17	45	55	30	150	90.3	161.5
18	45	80	50	150	111.2	170.6
19	90	55	30	240	119.3	128.7
20	45	80	10	150	87.8	149.8
21	0	30	30	150	27.8	110.8
22	45	55	30	150	92.8	155.2
23	45	55	50	240	100.7	160.1
24	0	80	30	150	58.7	142.6
25	45	55	30	150	99.3	162.8
26	45	55	10	240	70.5	139.3
27	45	55	30	150	87.6	162.4
28	90	55	10	150	96.3	121.6
29	45	55	30	150	96.4	158.9
30	0	55	10	150	35.5	123.5

3.3. The Optimal Model for TPC Enrichment. The experimental results from the BBD were analyzed using ANOVA to evaluate the effects of the process variables on the TPC yield. The statistical significance of the fitted quadratic model was checked by ANOVA. The experimental results from the BBD were analyzed using ANOVA to evaluate the effects of the process variables on the TPC yield. The ANOVA results indicate that the fitted quadratic model is highly significant, with a model F-value of 55.56 and a p value < 0.0001, which implies that the model is highly suitable for describing the relationship between the independent variables and the TPC yield. Furthermore, the nonsignificant "lack of fit" ($p = 0.4437$) confirms that the model fits the experimental data well. The model's suitability is also reinforced by its strong fit statistics. The coefficient of determination (R^2) of 0.9811 indicates that 98.11% of the variability in the response could be explained by the model, whereas the close agreement between the adjusted R^2 (0.9634) and predicted R^2 (0.9172) demonstrates good predictive power. Additionally, a high Adeq Precision of 27.1472 and a low CV % of 6.09% suggest an adequate signal-to-noise ratio and high experimental reliability. An analysis of the individual model terms revealed that the linear terms A (EtOH concentration), B (temperature), and C (ratio); the interaction term BD (temperature and time); and the quadratic terms A^2, B^2, and C^2 all had a significant effect on TPC yield ($p < 0.05$). The significance of the quadratic terms confirms that the relationship is nonlinear. To improve and refine the model, it was proposed that nonsignificant interaction terms with p values greater than 0.5, specifically AD ($p = 0.6711$), BC ($p = 0.5854$), and CD ($p = 0.8905$), be eliminated to produce a more concise and robust model.

Following the initial analysis, the model was refined by removing the nonsignificant interaction terms (AD, BC, and CD) to produce a "reduced quadratic model" with markedly improved statistical significance and fit. The refined model's F-value increased substantially from 55.56 to 81.79, indicating it is now even more significant in explaining the relationship between the variables and the TPC yield, whereas the overall model p value remained highly significant (< 0.0001) and the lack of fit remained nonsignificant ($p = 0.5396$). The most notable improvements are seen in the fit statistics, which highlight the enhanced robustness and predictive power of this refined model. In particular, the adjusted R^2 increased from 0.9634 to 0.9684, and more importantly, the predicted R^2 increased from 0.9172 to 0.9430. This significantly narrowed the gap between the two values from 0.0462 to just 0.0254, indicating that removing the "noise" from irrelevant terms has made the model more accurate and reliable for making predictions. Furthermore, the Adeq Precision increased from 27.15 to 32.49, signifying an improved signal-to-noise ratio, and the CV % decreased

from 6.09% to 5.66%, pointing to higher precision and reliability. Therefore, the model reduction process was highly successful, resulting in a more precise and robust model for the optimization of TPC extraction. The final regression equation to predict the TPC based on the actual values of the process variables is as follows:

$$\begin{aligned}\mathrm{TPC} = &-86.0066 + 1.26713\mathrm{A} + 2.45024\mathrm{B} + 1.35943\mathrm{C} + 0.26148\mathrm{D} - 0.00224\mathrm{AB} \\ &+ 0.002416\mathrm{AC} - 0.00288\mathrm{BD} - 0.00558\mathrm{A}^2 - 0.01173\mathrm{B}^2 - 0.0148\mathrm{C}^2 - 0.00029\mathrm{D}^2,\end{aligned} \tag{1}$$

where A = EtOH (%), B = temperature (°C), C = ratio (mL/g), and D = time (min).

To visualize the relationship between the independent variables and the yield of TPC, three-dimensional (3D) response surface plots were generated based on the model equation. These plots illustrate the interactive effects of two variables at a time on the TPC yield, whereas the other two variables are held constant at their central point. Figure 2(a) displays the interactive effect of EtOH concentration (A) and temperature (B) on TPC extraction. The plot reveals a significant curved surface, indicating that TPC yield increases with both variables up to an optimal region before leveling off. The peak TPC is predicted at high EtOH concentrations (approximately 70%–90%) and moderately high temperatures (approximately 70°C–80°C). This demonstrates a synergistic effect where higher temperatures enhance the solvent's extraction capacity. For instance, at a constant temperature of 55°C, increasing the EtOH concentration from 0% to 90% (whereas other factors are held at their center points) raised the TPC yield from 47.9 mg GE/g to 111.3 mg GE/g. This trend is scientifically sound, as higher temperatures reduce solvent viscosity and increase the solubility and diffusion rate of phenolic compounds. At the same time, the appropriate EtOH concentration optimizes solvent polarity for extracting these target compounds. Figure 2(b) illustrates the relationship between EtOH concentration (A) and the solvent-to-material ratio (C). The response surface shows a clear positive correlation, where TPC yield consistently increases as both the EtOH concentration and the ratio are elevated. The steep incline suggests that both factors are strong drivers of extraction efficiency within the tested range. The experimental data support this, showing that at a fixed EtOH concentration of 45% and temperature of 30°C, increasing the ratio from 10 to 50 mL/g increased the TPC yield from 56.8 to 74.5 mg GE/g. This effect is primarily due to the principles of mass transfer; a larger volume of solvent (higher ratio) increases the concentration gradient between the solid material and the liquid phase, thereby promoting the diffusion of phenolic compounds into the solvent until equilibrium is approached.

The interaction between temperature (B) and extraction time (D) is presented in Figure 2(c). The plot indicates that temperature is a more dominant factor than time in increasing TPC yield. However, a significant interaction between the two is evident. At lower temperatures (e.g., 30°C–40°C), extending the extraction time has a minimal effect on the TPC yield. In contrast, at higher temperatures (e.g., 80°C), a longer extraction time leads to a more substantial increase in TPC. This is supported by the data: At 80°C and 45% EtOH, the TPC yield was 111.2 mg GE/g after 150 min. The upward trend of the surface suggests that at elevated temperatures, which provide the necessary activation energy for extraction, a longer duration allows for more complete diffusion of solutes from the plant matrix.

3.4. The Optimal Model for TSC Enrichment. The results from the BBD for the TSC response were analyzed using ANOVA. The initial quadratic regression model was found to be highly significant, demonstrated by a model F-value of 42.97 and a p value < 0.0001. Additionally, the "lack of fit" was not significant ($p = 0.4082$), indicating that there was no systematic error and the model was compatible with the experimental data. The high coefficient of determination ($R^2 = 0.9757$) also suggested that the model could explain 97.57% of the variability in the data. However, a more detailed analysis of the fit statistics revealed the necessity of refining the model to improve its predictive power. Specifically, a significant discrepancy was observed between the adjusted R^2 value of 0.953 and the predicted R^2 value of 0.8871. This difference of 0.0659 suggests that the model was likely overfitted, containing nonsignificant terms that contribute "noise." An examination of the individual p values showed that several interaction terms, such as AB ($p = 0.9123$), AD ($p = 0.6888$), BC ($p = 0.7832$), and BD ($p = 0.5652$), had a very weak effect on the model. The presence of these terms reduces the model's ability to accurately predict new outcomes.

Therefore, to enhance its reliability and predictive capability, the model was refined by eliminating the insignificant interaction terms with a p value greater than 0.5. This refinement process proved to be highly successful, resulting in a more robust and accurate model. The model F-value increased sharply from 42.97 to 73.17, indicating a statistically stronger model. Most importantly, the difference between the adjusted R^2 (0.9614) and the predicted R^2 (0.932) was reduced significantly to just 0.0294. This confirms that the model was no longer overfitted and possessed excellent predictive capability. Furthermore, other statistical indicators also improved: The Adeq Precision increased from 21.68 to 27.82 and the CV % decreased to 2.31%, both of which confirm the enhanced strength and precision of the new model.

Based on the coefficients for the refined model, the final regression equation in terms of actual factors is

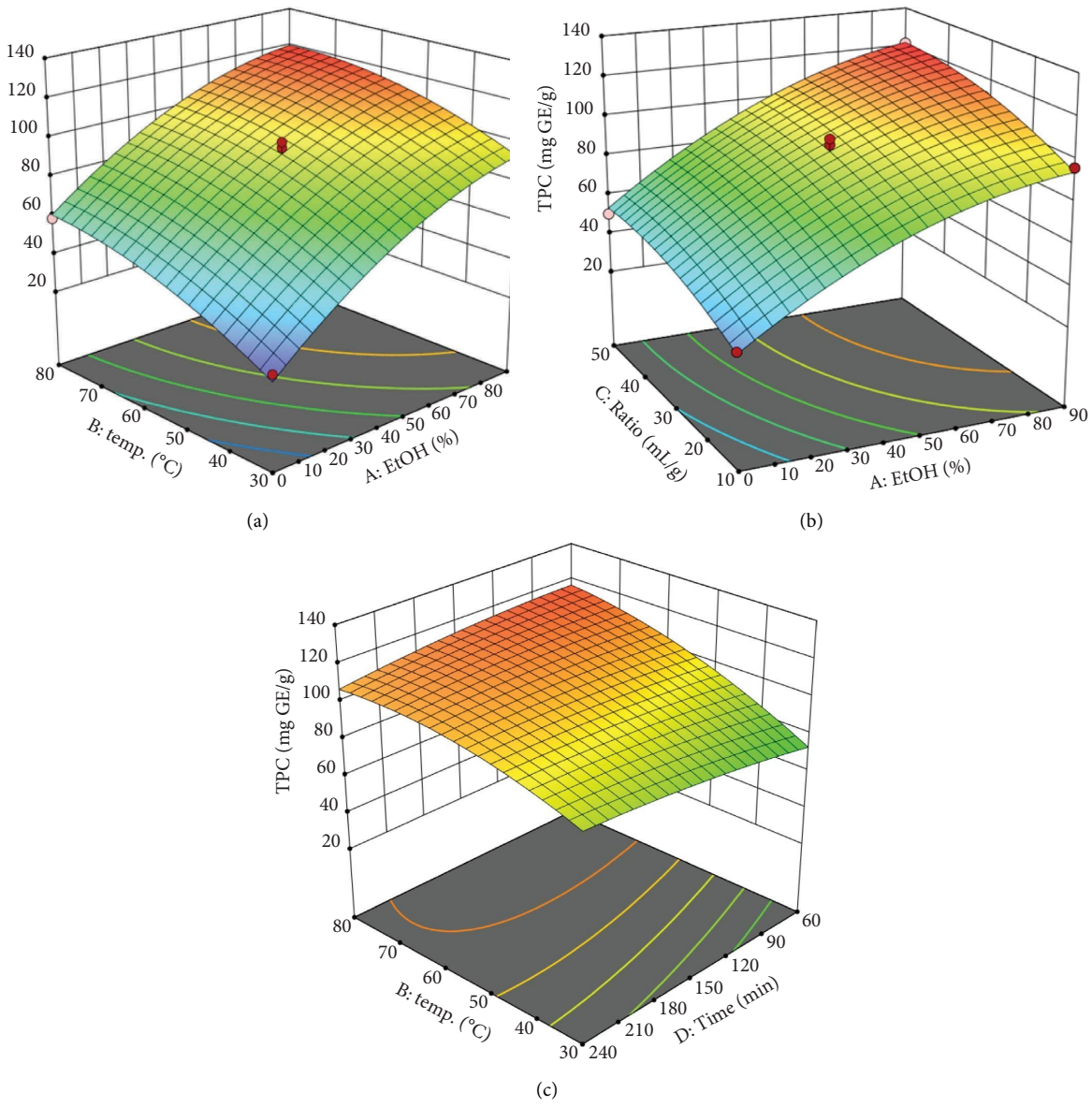

FIGURE 2: Response surfaces between (a) ethanol concentration and temperature, (b) ethanol concentration and solvent-to-material ratio, and (c) time and temperature to total phenolic contents of the *P. tectorius* fruit extracts.

$$\begin{aligned} TSC = & 30.65944 + 1.05281A + 1.84852B + 1.13388C + 0.190449D + 0.001958AC \\ & + 0.001446CD\_0.01256A^2 - 0.01181B^{2-}0.01749C^2 - 0.00065D^2, \end{aligned} \tag{2}$$

where A = EtOH (%), B = temperature (°C), C = ratio (mL/g), and D = time (min).

The response surface plots were constructed to visualize the interactive effects of the independent variables on the TSC. These plots are crucial for understanding the complex relationships and identifying the optimal conditions for extraction. Figure 3(a) illustrates the combined effect of EtOH concentration (A) and temperature (B). The surface plot is distinctly dome-shaped, indicating that the TSC yield is maximized at intermediate levels of both variables. The yield increases as EtOH concentration rises from 0% and temperature increases from 30°C, reaching a peak before declining. This suggests that although a certain amount of EtOH and heat is beneficial for dissolving and extracting saponins, excessive levels can have an adverse effect. This may be due to changes in solvent properties, such as polarity, at very high EtOH

concentrations or potential solvent loss at temperatures approaching the boiling point of EtOH, which would alter the extraction conditions. The experimental data confirm this, showing that at a fixed ratio and time, the TSC yield at 45% EtOH and 80°C (170.6 mg AE/g) is significantly higher than at 90% EtOH and 80°C (152.3 mg AE/g), highlighting the existence of an optimal range. The interaction between EtOH concentration (A) and solvent-to-material ratio (C) is depicted in Figure 3(b). Similar to the previous plot, this response surface also shows a clear optimal region. The TSC yield increases as both the EtOH concentration and the ratio are increased, but only up to a certain point. The curvature indicates that after reaching an optimal EtOH concentration (around 40%–50%) and ratio (around 30–40 mL/g), the TSC yield begins to plateau or even slightly decrease. This demonstrates the significant interactive effect between these two variables. For example, at a fixed temperature of 55°C, increasing the ratio from 10 to 50 mL/g at 45% EtOH shows a significant increase in yield (from 158.9 to 162.4 mg AE/g), underscoring the importance of an adequate solvent volume to facilitate mass transfer.

Figure 3(c) presents the interactive effect of extraction time (D) and solvent-to-material ratio (C). The surface shows that both factors have a positive effect on the TSC yield, with the yield increasing as both time and ratio are extended. The slope is steeper for the ratio than for time, suggesting the solvent volume is a more dominant factor in this interaction. The plot shows a continuous rise toward the upper limits of both variables, with the highest TSC yields found at longer times (around 180–240 min) and higher ratios (around 40–50 mL/g). This is consistent with mass transfer principles, where a larger solvent volume and a longer contact time allow for more complete diffusion of the saponins from the plant matrix into the solvent, leading to a higher extraction yield. For instance, at 45% EtOH and 55°C, increasing the extraction time from 60 min to 240 min at a ratio of 50 mL/g resulted in an increased yield from 150.2 mg/g to 160.1 mg AE/g.

The extraction time exerted contrasting effects on phenolic and saponin recovery due to their distinct physicochemical properties. Phenolic compounds, being relatively small and highly soluble in aqueous ethanolic media, reach diffusion equilibrium rapidly, and prolonged heating may promote oxidative degradation or polymerization. In contrast, saponins are amphiphilic glycosides with bulky triterpenoid or steroidal aglycones, which require extended contact time for complete solvent penetration and micellar solubilization. Consequently, phenolic yield tends to plateau or slightly decline with time, whereas saponin yield continues to increase until reaching its own saturation point.

3.5. Optimize the Extraction Conditions. The refined regression models for both TPC and TSC were utilized to determine the optimal conditions for extracting phytochemicals from *P. tectorius* fruit. As the ideal conditions for maximizing TPC and TSC differ, a multiresponse optimization was performed using the numerical optimization feature of the software Design-Expert. This approach allows for finding a range of ideal conditions by assigning different "importance levels" to each response, providing flexibility based on the desired outcome.

Table 3 summarizes seven potential optimal solutions generated by varying the importance placed on TPC versus TSC. The results show a clear trade-off between the two responses. Conditions prioritizing TPC, designated as the "Opt_TPC" series, consistently require a high EtOH concentration between 70% and 90% and a high temperature of approximately 80°C. Conversely, conditions prioritizing TSC, the "Opt_TSC" series, favor a lower EtOH concentration around 45%–55% and significantly longer extraction times exceeding 175 min, whereas the optimal temperature remains high. The "balance" condition represents a compromise, using intermediate parameters to achieve good, though not maximal, yields of both TPC and TSC simultaneously. This analysis provides a set of validated optimal conditions, allowing for the selection of specific extraction parameters depending on whether the desired final product is an extract rich in phenolics, saponins, or a balanced combination of both.

To confirm the validity and predictive accuracy of the developed models, a series of validation experiments was conducted. The seven sets of optimal conditions derived from the numerical optimization were slightly adjusted for practical convenience in a laboratory setting. Extractions were then performed in triplicate under these adjusted conditions. Table 4 presents a comparison between the TPC and TSC yields predicted by the regression models and the values obtained through these validation experiments.

The results demonstrate a strong correlation and excellent agreement between the predicted and experimental values across all seven tested conditions, affirming the reliability of the optimization process. In particular, the experimental data closely matched the values predicted by the models. For instance, the "balance" condition showed remarkable accuracy, with an experimental TPC of 114.7 ± 7.1 mg GAE/g against a prediction of 115.0 mg GAE/g. Furthermore, the analysis confirmed that the Opt_TSC3 condition, which was designed to maximize saponin content, successfully yielded the highest experimental TSC of 185.6 ± 10.6 mg AE/g and concurrently the lowest experimental TPC of 105.6 ± 8.5 mg GAE/g. This lowest TPC value showed excellent agreement with its predicted value of 103.5 mg GAE/g. Although the highest experimental TSC was greater than its predicted value of 169.5 mg AE/g, the model nonetheless accurately identified the specific conditions required to achieve the maximum saponin yield.

The experimental data also validated the predicted trade-off between the two responses; conditions designed to favor TPC resulted in extracts with higher experimental TPC yields, whereas conditions prioritizing TSC successfully produced extracts richer in saponins. The close correspondence between the predicted and actual results validates the accuracy of the regression models. This confirms that the developed models are reliable and effective tools for navigating the design space and optimizing the extraction of both phenolic and saponin compounds from *P. tectorius* fruit.

3.6. Bioactivities of the Extracts

3.6.1. Antioxidant and NO Production Inhibitory Effect. The antioxidant activity of the seven extracts was evaluated through their ability to scavenge DPPH and hydroxyl radicals,

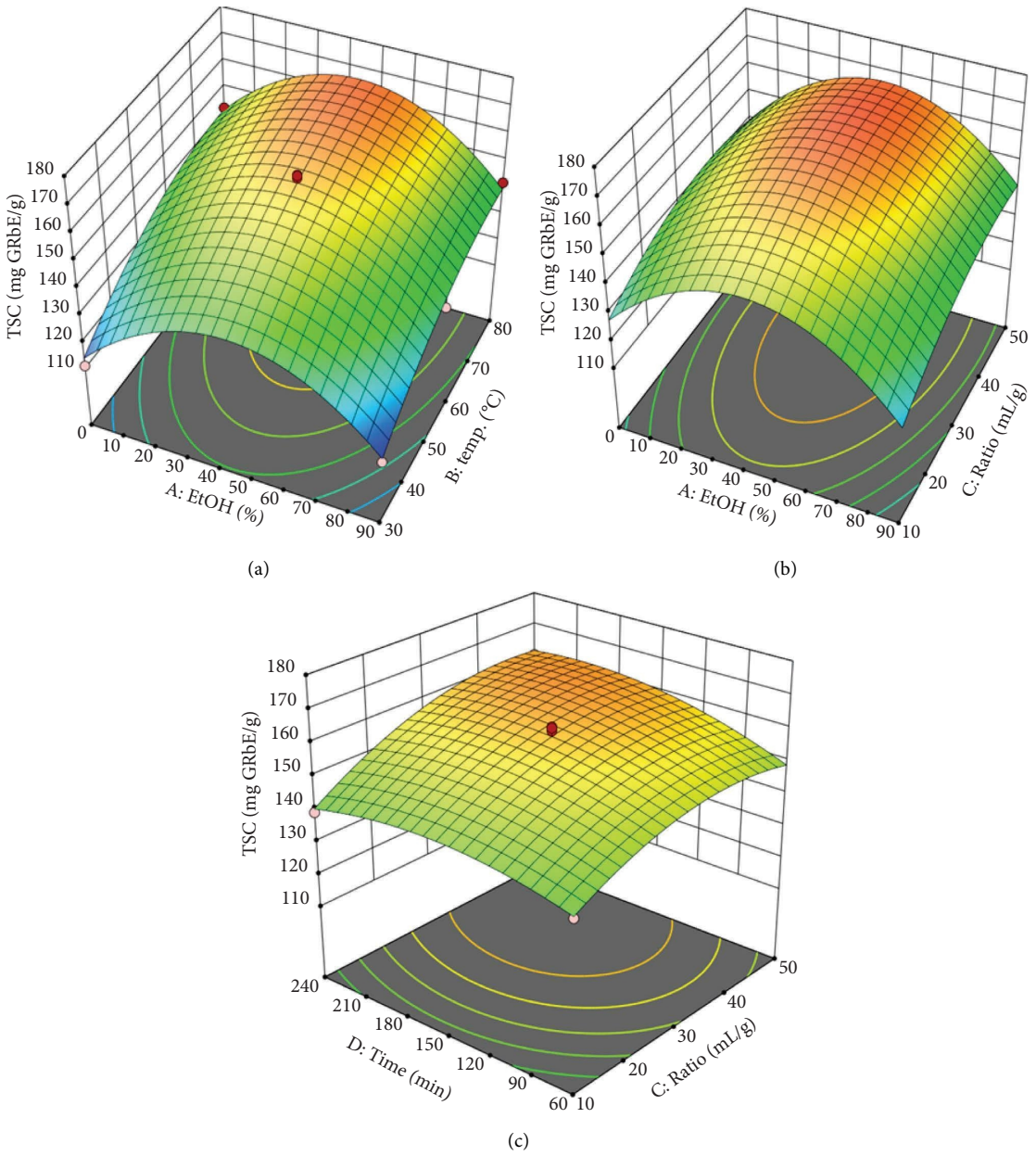

Figure 3: Response surfaces between (a) ethanol concentration and temperature, (b) ethanol concentration and solvent-to-material ratio, and (c) time and solvent-to-material ratio to total saponin contents of the *P. tectorius* fruit extracts.

Table 3: Summary of predicted optimal conditions for achieving different extraction goals, prioritizing either TPC, TSC, or a balance of both responses.

Condition	Importance level		%EtOH (%)	Temp. (°C)	Ratio (mL/g)	Time (min)
	TPC	TSC				
Opt_TPC1	5	0	90.0	80.0	48.2	104.0
Opt_TPC2	4	1	76.6	80.0	48.6	128.1
Opt_TPC3	3	2	68.9	79.1	47.2	146.4
Balance	2.5	2.5	59.3	78.3	45.5	167.0
Opt_TSC 1	2	3	55.0	78.1	44.7	175.1
Opt_TSC 2	1	4	49.1	78.1	43.6	186.0
Opt_TSC 3	0	5	45.3	78.3	42.9	193.1

Table 4: Predicted versus experimental yields (mean ± SD, $n = 3$) of TPC (mg GAE/g) and TSC (mg AE/g) for the validation of the seven adjusted optimal extraction conditions.

Samples	EtOH (%)	Temp. (°C)	Ratio (mL/g)	Time (min)	Predict values		Experimental	
					TPC	TSC	TPC	TSC
Opt_TPC1	90	80	48	104	129.3	138.5	124.8 ± 8.8	126.1 ± 12.7
Opt_TPC2	75	80	48	130	124.2	155.2	121.1 ± 11.1	142.8 ± 16.5
Opt_TPC3	65	80	47	150	118.8	163.0	118.3 ± 6.5	151.8 ± 15.9
Balance	60	80	46	170	115.0	166.3	114.7 ± 7.1	162.4 ± 19.6
Opt_TSC1	55	80	45	175	111.7	168.0	109.7 ± 8.8	168.3 ± 15.2
Opt_TSC2	50	80	44	190	107.4	169.2	106.2 ± 11.8	178.9 ± 12.1
Opt_TSC3	45	80	43	195	103.5	169.5	105.6 ± 8.5	185.6 ± 10.6

Table 5: Free-radical scavenging and NO production inhibitory effects of *P. tectorius* fruit extracts under optimal conditions.

Samples	DPPH (IC_{50}, μg/mL)	Hydroxyl (IC_{50}, μg/mL)	NO inhibition (IC_{50}, μg/mL)
Opt_TPC1	76.4 ± 3.8^{a}	62.5 ± 4.1^{d}	91.3 ± 8.2^{i}
Opt_TPC2	82.1 ± 4.5^{b}	70.8 ± 5.3^{e}	85.4 ± 6.6^{j}
Opt_TPC3	89.5 ± 5.1^{b}	79.1 ± 6.2^{f}	84.2 ± 7.3^{j}
Balance	> 100	95.6 ± 8.1^{g}	75.5 ± 3.9^{k}
Opt_TSC 1	> 100	> 100	68.8 ± 1.1^{l}
Opt_TSC 2	> 100	> 100	ND
Opt_TSC 3	> 100	> 100	ND
Ascorbic acid*	27.4 ± 1.6^{c}	—	—
Catechin**	—	31.7 ± 2.8^{h}	—
Cardamonin#			3.1 ± 0.4^{m}

*,**,#Positive control.

a–mData are expressed as mean ± SD. Means in each column with different letters are significantly different ($p < 0.05$).

with the results presented as IC_{50} values. The data revealed a clear correlation between antioxidant activity and the TPC of the extracts. The samples belonging to the "Opt_TPC" series, which were optimized for high TPC, were the only ones to exhibit significant activity with IC_{50} values below 100 μg/mL in both assays. Among them, the "Opt_TPC1" extract demonstrated the highest potency, with an IC_{50} value of 76.4 μg/mL for DPPH scavenging and 62.5 μg/mL for hydroxyl radical scavenging. In contrast, the saponin-optimized extracts ("Opt_TSC" series) and the "balance" extract showed considerably weaker activity, with IC_{50} values exceeding 100 μg/mL in most tests. Although the TPC-rich extracts demonstrated notable antioxidant potential, their activity was lower than that of the pure compound positive controls. Specifically, the DPPH scavenging activity of the most potent extract ("Opt_TPC1") was less than that of ascorbic acid ($IC_{50} = 27.4$ μg/mL), and its hydroxyl radical scavenging activity was less than that of catechin ($IC_{50} = 31.7$ μg/mL). This result is expected, as crude extracts are complex mixtures, whereas the controls are highly active, pure antioxidant compounds. These findings collectively suggest that the phenolic constituents are the primary contributors to the antioxidant capacity of the *P. tectorius* extracts.

The anti-inflammatory potential of the seven optimized *P. tectorius* fruit extracts was evaluated by measuring their ability to inhibit NO production in LPS-stimulated cells (Table 5). A clear trend emerged regarding the extracts' potency, which was found to correlate with the saponin contents.

The IC_{50} values ranged from 91.3 μg/mL for the TPC-rich extract Opt_TPC1 down to 68.8 μg/mL for the saponin-rich extract Opt_TSC1, indicating that Opt_TSC1 was the most potent anti-inflammatory agent among the tested samples. As expected, all crude extracts were less potent than the pure compound positive control, cardamonin, which had an IC_{50} of 3.1 μg/mL. To ensure that the observed NO inhibition was not a result of cytotoxicity, cell survival was assessed (Table S1). The extracts from the Opt_TPC series, the balance condition, and Opt_TSC1 all demonstrated excellent safety profiles, with cell survival rates consistently above 92%. In contrast, the Opt_TSC2 and Opt_TSC3 extracts, which contained the highest concentrations of saponins, exhibited significant cytotoxicity, causing cell survival to drop to as low as 64.3%. Consequently, the IC_{50} values for these two extracts could not be determined. This finding suggests that although saponin-rich extracts possess greater anti-inflammatory potency, very high concentrations of saponins or coextracted compounds may induce a cytotoxic effect on the RAW 264.7 cells. Phenolic compounds exert antioxidant effects mainly through electron or hydrogen donation and stabilization of resulting phenoxyl radicals, as well as through transition-metal chelation (Fe^{2+}/Cu^{2+}) that limits Fenton-type radical formation [24, 25]. In contrast, saponins are amphiphilic glycosides whose aglycone cores and membrane-active properties modulate inflammatory signaling and suppress LPS-induced NO production via iNOS/NF-κB downregulation, while stabilizing cellular membranes [26]. These class-specific properties explain why TPC-enriched extracts excel in antioxidant assays, whereas TSC-enriched extracts more effectively inhibit NO production. Among the optimized conditions, Opt_TPC1 and Opt_TSC1 displayed the highest

bioactivities within their groups. The 90% EtOH and moderate extraction time (104 min) in Opt_TPC1 favored recovery of midpolarity flavonoids and aldehydes with strong redox capacity, accounting for its lower IC_{50} values despite similar TPC yields to Opt_TPC2–3. Conversely, Opt_TSC1 (55% EtOH, 175 min) likely promoted the extraction of moderately polar triterpenoid saponins with stronger membrane-modulating activity, whereas higher water content in Opt_TSC2–3 may have diluted or degraded active aglycones. Overall, the superior potency of these extracts reflects not only quantitative yield but also qualitative compositional shifts controlled by solvent polarity and extraction kinetics, underscoring the need to balance concentration and selectivity in RSM optimization.

The optimized phenolic- and saponin-enriched extracts of *P. tectorius* thus exhibit distinct functional profiles with promising industrial relevance. Phenolic-rich extracts could serve as natural antioxidants in food and nutraceutical products, whereas saponin-rich extracts, showing anti-inflammatory and mild surfactant properties, may be applicable in cosmetic or pharmaceutical formulations. Further work on scale-up, stability, and formulation compatibility would support their practical use.

4. Conclusion

This study successfully optimized the extraction conditions for phenolic- and saponin-rich fractions from *P. tectorius* fruits using RSM based on a BBD. The developed quadratic models exhibited excellent statistical reliability, with coefficients of determination (R^2) exceeding 0.98 for both TPC and TSC responses, confirming the adequacy of the fitted models. Under the validated optimal conditions, the experimental yields reached 124.8 ± 8.8 mg GAE/g for total phenolics and 168.3 ± 15.2 mg AE/g for total saponins, closely matching the predicted values. The optimized phenolic extract (Opt_TPC1) demonstrated potent antioxidant effects with DPPH and hydroxyl radical IC_{50} values of 76.4 and 62.5 μg/mL, respectively, whereas the saponin-rich extract (Opt_TSC1) showed considerable anti-inflammatory activity with an IC_{50} of 68.8 μg/mL for NO inhibition. These results highlight the compositional and functional complementarity between phenolic and saponin fractions and support the potential of *P. tectorius* fruit as a renewable source of bioactive ingredients. Nevertheless, the cytotoxicity observed in extracts with excessive saponin content indicates a need for further refinement. Future studies should focus on isolating individual active compounds, improving extract selectivity, and conducting comprehensive safety assessments to ensure both efficacy and biocompatibility in prospective food, cosmetic, and pharmaceutical applications.

Data Availability Statement

The data supporting the findings of this study are included in this published article and its supporting information files.

Conflicts of Interest

The authors declare no conflicts of interest.

Funding

This study was funded by the Vietnam Academy of Science and Technology (VAST) under the Grant Number NCXS 01.02/23-25.

Acknowledgments

This research was supported by the Vietnam Academy of Science and Technology (VAST) under Grant Number NCXS 01.02/23-25. We are also grateful for the support of the Toptier Research Group Phytomedicine at the University of Science and Technology of Hanoi, VAST.

Supporting Information

Additional supporting information can be found online in the Supporting Information section. *(Supporting Information)*

Table S1. NO inhibition screening data.

References

[1] T. Gallaher, M. W. Callmander, S. Buerki, and S. C. Keeley, "A Long Distance Dispersal Hypothesis for the Pandanaceae and the Origins of the *Pandanus tectorius* Complex," *Molecular Phylogenetics and Evolution* 83 (2015): 20–32, https://doi.org/10.1016/j.ympev.2014.11.002.

[2] M. A. Tan, M. G. Nonato, N. Kogure, M. Kitajima, and H. Takayama, "Secondary Metabolites from *Pandanus* simplex," *Biochemical Systematics and Ecology* 40 (2012): 4–5, https://doi.org/10.1016/j.bse.2011.09.001.

[3] X. Zhang, H. Wu, C. Wu, et al., "Two New Phenolic Compounds from the Fruits of *Pandanus tectorius* Soland," *Records of Natural Products* 7, no. 4 (2013): 359–362.

[4] Y. Huang, J. Chen, Z. Liu, et al., "Benzofuran Sesquineolignan Racemates from the Roots and Rhizomes of Pandanus Tectorius: Isolation, Chiral Resolution, and Configurational Assignment," *Journal of Molecular Structure* 1338 (2025).

[5] C. Wu, X. Zhang, X. Zhang, et al., "The Caffeoylquinic acid-rich *Pandanus tectorius* Fruit Extract Increases Insulin Sensitivity and Regulates Hepatic Glucose and Lipid Metabolism in Diabetic db/db Mice," *The Journal of Nutritional Biochemistry* 25, no. 4 (2014): 412–419, https://doi.org/10.1016/j.jnutbio.2013.12.002.

[6] M. A. Tan, H. Takayama, N. Aimi, M. Kitajima, S. G. Franzblau, and M. G. Nonato, "Antitubercular Triterpenes and Phytosterols from *Pandanus tectorius* Soland. Var. Laevis," *Journal of Natural Medicines* 62, no. 2 (2008): 232–235, https://doi.org/10.1007/s11418-007-0218-8.

[7] P. Sahakitpichan, N. Chimnoi, W. Thamniyom, S. Ruchirawat, and T. Kanchanapoom, "Aromatic Rutinosides from the Aerial Roots of *Pandanus tectorius*," *Phytochemistry Letters* 37 (2020): 47–50, https://doi.org/10.1016/j.phytol.2020.04.008.

[8] Y. Andriani, N. M. Ramli, D. F. Syamsumir, et al., "Phytochemical Analysis, Antioxidant, Antibacterial and Cytotoxicity Properties of Keys and Cores Part of *Pandanus tectorius* Fruits," *Arabian Journal of Chemistry* 12, no. 8 (2019): 3555–3564, https://doi.org/10.1016/j.arabjc.2015.11.003.

[9] D. T. Mai, T. D. Le, T. P. Nguyen, et al., "A New Aldehyde Compound from the Fruit of *Pandanus Tectorius* Parkinson Ex Du Roi," *Natural Product Research* 29, no. 15 (2015): 1437–1441, https://doi.org/10.1080/14786419.2014.1003929.

[10] T. P. Nguyen, T. D. Le, P. N. Minh, et al., "A New Dihydrofurocoumarin from the Fruits of *Pandanus Tectorius* Parkinson Ex Du Roi," *Natural Product Research* 30, no. 21 (2016): 2389–2395, https://doi.org/10.1080/14786419.2016.1188095.

[11] Z.-y. Zhu and P.-z. Zhang, "A New Lignan from *Pandanus tectorius*," *Natural Product Research* 36, no. 21 (2022): 5553–5558, https://doi.org/10.1080/14786419.2021.2021201.

[12] X. Zhang, P. Guo, G. Sun, et al., "Phenolic Compounds and Flavonoids from the Fruits of *Pandanus tectorius* Soland," *Journal of Medicinal Plants Research* 6, no. 13 (2012): 2622–2626, https://doi.org/10.5897/jmpr11.1424.

[13] C. Cheng, S. C. Park, and S. S. Giri, "Effect of *Pandanus tectorius* Extract as Food Additive on Oxidative Stress, Immune Status, and Disease Resistance in Cyprinus carpio," *Fish & Shellfish Immunology* 120 (2022): 287–294, https://doi.org/10.1016/j.fsi.2021.12.004.

[14] X. Zhang, C. Wu, H. Wu, et al., "Anti-Hyperlipidemic Effects and Potential Mechanisms of Action of the Caffeoylquinic Acid-Rich *Pandanus tectorius* Fruit Extract in Hamsters Fed a High Fat-Diet," *PLoS One* 8, no. 4 (2013): e61922, https://doi.org/10.1371/journal.pone.0061922.

[15] S. Sundus, K. Hira, N. Sohail, et al., "Protective Role of *Pandanus Tectorius* Parkinson Ex Du Roi in Diabetes, Hyperlipidemia, Liver and Kidney Dysfunction in Alloxan Diabetic Rats," *Clinical Phytoscience* 7, no. 1 (2021): 48, https://doi.org/10.1186/s40816-021-00279-z.

[16] J.-G. Zhang, C. Jin-Ping, W. Yu-Xia, G. Jia-Liang, L. Yu-Qing, and C. Wang, "*Pandanus tectorius* Fruits Attenuated Cell Injury and Oxidative Stress in High glucose-induced Schwann Cells by Activating Nrf2/Keap1 Signaling Pathway," *Journal of Asian Natural Products Research*, 1–17.

[17] P. Ppsk, M. Asmidar, Y. Andriani, P. Norouzitallab, Y. Y. Sung, and K. Baruah, "Evaluating the Protective Immunological Effects of *Pandanus tectorius* Leaf Extract Against Pathogenic *Vibrio campbellii* Using Gnotobiotic Brine Shrimp Model System," *Aquaculture Research* 2025, no. 1 (2025): https://doi.org/10.1155/are/8215825.

[18] S. Fattahi, E. Zabihi, Z. Abedian, et al., "Total Phenolic and Flavonoid Contents of Aqueous Extract of Stinging Nettle and *in Vitro* Antiproliferative Effect on Hela and BT-474 Cell Lines," *International Journal of Molecular and Cellular Medicine* 3, no. 2 (2014): 102–107.

[19] A. V Le, S. E Parks, M. H Nguyen, and P. D Roach, "Improving the Vanillin-Sulphuric Acid Method for Quantifying Total Saponins," *Technologies* 6, no. 3 (2018): 84, https://doi.org/10.3390/technologies6030084.

[20] W. Brand-Williams, M. E. Cuvelier, and C. Berset, "Use of a Free Radical Method to Evaluate Antioxidant Activity," *LWT-Food Science and Technology* 28, no. 1 (1995): 25–30, https://doi.org/10.1016/s0023-6438(95)80008-5.

[21] P. T. Thuong, N. D. Su, T. M. Ngoc, et al., "Antioxidant Activity and Principles of Vietnam Bitter Tea *Ilex Kudingcha*," *Food Chemistry* 113, no. 1 (2009): 139–145, https://doi.org/10.1016/j.foodchem.2008.07.041.

[22] N. H. Dang, L. T. V. Anh, and N. T. Dat, "Anti-Inflammatory Effects of Essential Oils of *Amomum aromaticum* Fruits in Lipopolysaccharide-Stimulated RAW264.7 Cells," *Journal of Food Quality* 2020, no. 1 (2020): 1–5, https://doi.org/10.1155/2020/8831187.

[23] T. Mosmann, "Rapid Colorimetric Assay for Cellular Growth and Survival: Application to Proliferation and Cytotoxicity Assays," *Journal of Immunological Methods* 65, no. 1-2 (1983): 55–63, https://doi.org/10.1016/0022-1759(83)90303-4.

[24] R. Ksouri, H. Falleh, W. Megdiche, et al., "Antioxidant and Antimicrobial Activities of the Edible Medicinal Halophyte Tamarix gallica L. and Related Polyphenolic Constituents," *Food and Chemical Toxicology* 47, no. 8 (2009): 2083–2091, https://doi.org/10.1016/j.fct.2009.05.040.

[25] Z. Lomozová, M. Hrubša, P. F. Conte, et al., "The Effect of Flavonoids on the Reduction of Cupric Ions, the copper-driven Fenton Reaction and copper-triggered Haemolysis," *Food Chemistry* 394 (2022): https://doi.org/10.1016/j.foodchem.2022.133461.

[26] S. Fordos, S. Amin, N. Abid, et al., "Saponins: Advances in Extraction Techniques, Functional Properties, and Industrial Applications," *Applied Food Research* 5, no. 2 (2025): https://doi.org/10.1016/j.afres.2025.101146.

PUBLICATIONS IN OTHER INTERNATIONAL JOURNALS

International Journal of Engineering Research and Development
e- ISSN: 2278-067X, p-ISSN: 2278-800X, www.ijerd.com
Volume 21, Issue 9 (September 2025), PP 90-95

Total phenolic and saponin content and α-amylase inhibition of marketed *Pandanus tectorius* fruits and leaves

Do Hoang Giang[1,2], Nguyen Hai Dang[1], Nguyen Tien Dat[2]
[1]*University of Science and Technology of Hanoi, Vietnam Academy of Science and Technology, Hanoi, Vietnam*
[2]*Center for High Technology Research and Development, Vietnam Academy of Science and Technology, Hanoi, Vietnam.*
*Corresponding Author:*Do Hoang Giang

ABSTRACT:
Pandanus tectorius is widely marketed in Vietnam as crude herbal material and tea, yet comparative data on its phytochemical quality and α-amylase inhibition remain limited. In this study, thirteen fruit and nine leaf samples were purchased from local markets and e-commerce sources and extracted with 90% ethanol. Total phenolic content (TPC) and total saponin content (TSC) were determined by Folin–Ciocalteu and vanillin–sulfuric acid assays, while α-amylase inhibition was evaluated using a modified DNSA method. Results were expressed on both a sample basis (mg/g dry material) and an extract basis (mg/g extract). Extraction yields were higher in leaves (11.51–14.51%) than in fruits (9.59–11.94%). On a sample basis, fruits and leaves contained comparable levels of TPC (12.17 vs 12.99 mg GAE/g; p = 0.187) and TSC (5.63 vs 5.31 mg AE/g; p = 0.214). On an extract basis, fruit extracts were significantly more enriched, with TPC of 115.43 vs 99.38 mg GAE/g extract (p = 0.002) and TSC of 53.42 vs 40.73 mg AE/g extract (p < 0.0001). The α-amylase inhibitory activity was moderate, with IC_{50} values ranging from 130.48 to 200.45 µg/mL (fruits 163.77 µg/mL, leaves 171.49 µg/mL), compared with 88.96 µg/mL for acarbose. Correlation analysis revealed a strong negative relationship between TPC and IC_{50} ($r = -0.842$, $R^2 = 0.709$), while TSC correlated only weakly ($r = -0.319$, $R^2 = 0.102$). These results indicate that phenolic compounds are the main contributors to the inhibitory activity and that fruit extracts represent a more concentrated source of bioactive metabolites suitable for functional food or nutraceutical applications.
Keywords*: Pandanus tectorius, phenolic, saponin, α-amylase*

Date of Submission: 02-09-2025 Date of acceptance: 11-09-2025

I. INTRODUCTION

The genus *Pandanus* (family Pandanaceae) comprises approximately 700–750 species predominantly distributed across tropical and subtropical regions of the Paleotropics, ranging from West Africa to the Pacific Islands [1, 2].Members of this genus are morphologically distinctive, with spiral phyllotaxy, long, narrow leaves, and aerial prop roots that facilitate adaptation to sandy or coastal habitats. Ecologically, *Pandanus* species play an important role in shoreline stabilization and tropical forest ecosystems, while culturally they possess considerable economic and ethnobotanical value. Their leaves are widely used for weaving mats, baskets, and roofing materials, and in some regions as aromatic culinary ingredients [1, 2].*Pandanus tectorius* Parkinson ex Du Roi is a widely distributed species occurring in tropical and subtropical coastal regions from South Asia to the Pacific Islands, and in Vietnam, it is commonly found from the northern midland areas to the coastal regions of Khanh Hoa [3]. Traditionally, this plant has been employed in folk medicine for the treatment of various ailments. Its roots have been used for edema, dysuria, and kidney stones, and externally for bone fractures and hemorrhoids, while its leaves, characterized by a sweet taste and cooling properties, are applied to reduce fever and treat colds. Young shoots have also been reported to support the treatment of kidney stones and pediatric convulsions [4-6].Beyond medicinal uses, *P. tectorius* holds ecological significance in mangrove and coastal ecosystems.

Phytochemical studies have demonstrated that *P. tectorius* is a rich source of structurally diverse secondary metabolites. International and regional investigations have identified multiple compound classes, including phenolic acids and aldehydes (e.g., p-coumaric acid, ferulic acid, vanillin, syringaldehyde), flavonoids (e.g., vitexin, tricin, chrysin, sakuranetin, naringenin), and lignans such as pinoresinol, syringaresinol, medioresinol, lyoniresinol, and balanophonin[7-12]. Coumarins, benzofuran derivatives, and volatile

constituents such as geranyl acetate and ethyl cinnamate have also been reported [8, 11, 12]. In addition, other miscellaneous compounds, including long-chain fatty alcohol esters, methylsuccinic acid, sugar derivatives, and 5-hydroxymethylfurfural, have been documented [10, 13-16].These phytoconstituents underpin a broad spectrum of biological activities. Extracts and isolated compounds from *P. tectorius* have demonstrated strong antioxidant, anti-inflammatory, antimicrobial, cytotoxic, and antidiabetic properties. In particular, phenolic-rich extracts exhibit potent radical scavenging capacity in DPPH, ABTS, and hydroxyl radical assays [11-14, 17], protective effects against oxidative stress in Schwann cells through the Nrf2/Keap1 pathway [18], lipid-lowering effects via PPARα and AMPK signaling [19], and α-glucosidase inhibitory activity contributing to hypoglycemic potential [10, 13, 14]. Cytotoxicity against several cancer cell lines, including A549, MCF-7, and HeLa, has also been documented [12, 15, 20]. Moreover, antimicrobial effects against gram-positive and gram-negative bacteria have been reported [11]. Recent studies have further highlighted the potential of *P. tectorius* fruit extracts in nanoparticle formulations for therapeutic applications in metabolic disorders [15].

In Vietnam, the fruits and leaves of *P.tectorius* are widely available on the market, either as raw materials or in packaged tea bags. Beyond their use in traditional medicine, they are also consumed as a common food product. The present study investigates the levels of major classes of secondary metabolites, including phenolics and saponins, and evaluates the *α*-amylase inhibitory activity of marketed fruits and leaves of *P. tectorius* in Vietnam, thereby contributing to quality assessment and further exploration of the biomedical potential of this species.

II. MATERIAL AND METHODS

2.1. Materials

Nine dried leaf samples and thirteen dried fruit samples of *P.tectorius* were purchased from herbal markets in Hanoi, Vietnam, or through e-commerce platforms. Common solvents such as ethanol, DMSO, and inorganic salts were obtained from Daihan Scientific (South Korea), while reference standards and other chemicals were supplied by Merck (Germany).

2.2. Extracts preparation

To prepare the extract for chemical analysis and bioassays, 50 g of each sample was powdered, then extracted in triplicate with 1 L of ethanol 90% in a sonication bath at 70°C. The solution was filtered and evaporated to yield the total extract.

2.3. Total phenolic assay

Total phenolic content (TPC) was determined using the Folin–Ciocalteu method with gallic acid as the standard [21].Absorbance was measured at 760 nm, and results were expressed as mg gallic acid equivalents per gram of dry sample (mg GAE/g).

2.4. Total saponin assay

The total saponin content (TSC) of the samples was assessed using the vanillin–sulfuric acid method[22]. For this procedure, 100 µL of each extract was mixed with 100 µL of 8% (w/v) vanillin in ethanol and 2800 µL of 80% (v/v) sulfuric acid. The mixture was incubated at 70°C for 15 minutes. Solutions of the reference compound(aescin) and reagent blanks (with solvent) were also prepared. After incubation, the mixtures were allowed to cool at room temperature for 5 minutes, and absorbance was recorded at 560 nm against the blank.

2.5. *α*-amylase inhibition assay

α-amylase inhibition was evaluated using a modified DNSA method [23].Reaction mixtures containing sample extracts and *α*-amylase were incubated with starch substrate, and the reaction was terminated with DNSA reagent. Absorbance was measured at 650 nm, with acarbose as the positive control.

III. RESULTSAND DISCUSSION

3.1. Phytochemical contents of the *P. tectorius*fruits and leaves

The extraction yields of *P. tectorius* ranged from 9.59% to 11.94% in fruits and from 11.51% to 14.51% in leaves, indicating that leaves generally provided higher extraction efficiency than fruits. In contrast, the distribution of secondary metabolites showed distinct patterns.

The total phenolic content (TPC) of fruits varied between 9.38 and 14.31 mg GAE/g sample, while the figures for the leaves ranged from 11.27 to 16.03 mg GAE/g sample.For total saponin content (TSC), fruits displayed higher values, ranging from 4.61 to 6.54 mg AE/g sample, compared to leaves, which contained 4.52–5.93 mg AE/g sample.

Table 1: Extraction yields, total phenolic (TPC) and saponin (TSC) contents of the *P. tectorius*samples

No.	Code	Part	Extraction yield	TPC (mg GAE/g)		TSC (mgAE/g)	
				Sample	Extract	Sample	Extract
1	F01	Fruits	9.78%	11.38 ± 1.34	116.32 ± 13.66	5.47 ± 0.57	55.96 ± 5.82
2	F02	Fruits	9.77%	11.17 ± 1.11	114.34 ± 11.38	5.63 ± 0.64	57.64 ± 6.51
3	F03	Fruits	11.51%	12.73 ± 1.56	110.62 ± 13.54	5.16 ± 0.59	44.82 ± 5.17
4	F04	Fruits	9.59%	12.15 ± 1.30	126.67 ± 13.51	4.61 ± 0.48	48.07 ± 5.02
5	F05	Fruits	10.15%	12.28 ± 1.46	120.97 ± 14.42	4.82 ± 0.52	47.45 ± 5.09
6	F06	Fruits	11.09%	11.02 ± 0.90	99.34 ± 8.08	6.41 ± 0.81	57.81 ± 7.27
7	F07	Fruits	11.00%	12.64 ± 1.38	114.92 ± 12.58	5.86 ± 0.74	53.27 ± 6.77
8	F08	Fruits	9.75%	11.26 ± 0.97	115.51 ± 9.90	4.94 ± 0.50	50.70 ± 5.14
9	F09	Fruits	10.00%	9.38 ± 1.13	93.75 ± 11.31	5.94 ± 0.58	59.43 ± 5.81
10	F10	Fruits	11.35%	14.31 ± 1.78	126.09 ± 15.69	6.38 ± 0.69	56.24 ± 6.05
11	F11	Fruits	11.94%	13.82 ± 1.44	115.74 ± 12.03	6.54 ± 0.55	54.78 ± 4.63
12	F12	Fruits	10.01%	12.66 ± 1.25	126.44 ± 12.54	6.06 ± 0.67	60.49 ± 6.65
13	F13	Fruits	11.17%	13.40 ± 1.45	119.93 ± 13.0	5.34 ± 0.64	47.85 ± 5.71
14	L01	Leaves	12.67%	11.27 ± 1.39	88.94 ± 10.99	4.52 ± 0.47	35.67 ± 3.73
15	L02	Leaves	14.51%	12.57 ± 1.46	86.63 ± 10.09	5.29 ± 0.52	36.45 ± 3.60
16	L03	Leaves	13.00%	12.38 ± 1.01	95.25 ± 7.78	5.53 ± 0.59	42.52 ± 4.51
17	L04	Leaves	14.15%	16.03 ± 1.60	113.31 ± 11.31	5.57 ± 0.55	39.34 ± 3.86
18	L05	Leaves	14.04%	12.15 ± 1.14	86.54 ± 8.11	5.43 ± 0.53	38.70 ± 3.76
19	L06	Leaves	12.18%	13.38 ± 1.72	109.84 ± 14.09	5.65 ± 0.66	46.41 ± 5.39
20	L07	Leaves	13.21%	14.39 ± 1.34	108.95 ± 10.17	4.75 ± 0.52	35.99 ± 3.96
21	L08	Leaves	11.51%	11.80 ± 1.46	102.55 ± 12.73	5.14 ± 0.44	44.66 ± 3.84
22	L09	Leaves	12.66%	12.96 ± 1.22	102.37 ± 9.60	5.93 ± 0.75	46.87 ± 5.96

The corresponding boxplot (Figure 1) confirmed this trend, showing that fruits had higher median saponin levels and a more clustered distribution, suggesting greater stability in saponin accumulation relative to leaves.Boxplot analysis highlighted that fruits exhibited relatively consistent TPC values, whereas leaves showed broader variability, with some samples reaching comparatively higher phenolic concentrations.

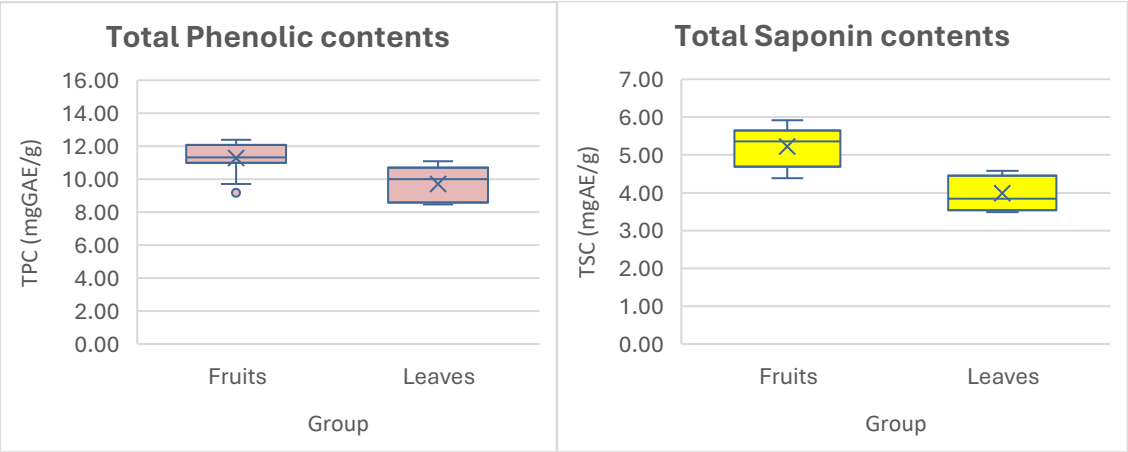

Figure 1: Boxplots of the TPC (left) and TSC (right) of the *P. tectorius*samples

To statistically evaluate these observations, permutation tests were conducted on sample-based values. The mean TPC did not differ significantly between fruits (12.17 mg GAE/g) and leaves (12.99 mg GAE/g) (mean difference = −0.82 mg GAE/g; $p = 0.187$). Similarly, the mean TSC values of fruits (5.63 mg AE/g) and leaves (5.31 mg AE/g) were not significantly different (mean difference = +0.32 mg AE/g; $p = 0.214$). These findings are consistent with the overlapping distributions shown in the boxplots, indicating that although fruits tended to accumulate more saponins and leaves occasionally exhibited higher phenolic levels, such differences were not statistically robust.

The phenolic content of *Pandanus tectorius* extracts showed a clear difference between plant parts. Fruit extracts contained between 93.75 and 126.67 mg GAE/g extract, with a mean of 115.43 mg GAE/g extract, whereas leaf extracts ranged from 86.63 to 113.31 mg GAE/g extract, with a lower mean of 99.38 mg GAE/g extract. The boxplot (Figure 2) illustrates this separation, with fruits displaying higher median values and a narrower interquartile range, suggesting more consistent phenolic enrichment compared to leaves. A permutation test confirmed the statistical significance of this difference (mean difference = +16.06 mg GAE/g extract; $p = 0.002$), indicating that fruit extracts are consistently richer in phenolic compounds.A similar pattern

was observed for saponins. Fruit extracts displayed concentrations between 44.82 and 60.49 mg AE/g extract, with a mean of 53.42 mg AE/g extract, while leaf extracts contained 35.67–46.87 mg AE/g extract, averaging 40.73 mg AE/g extract.

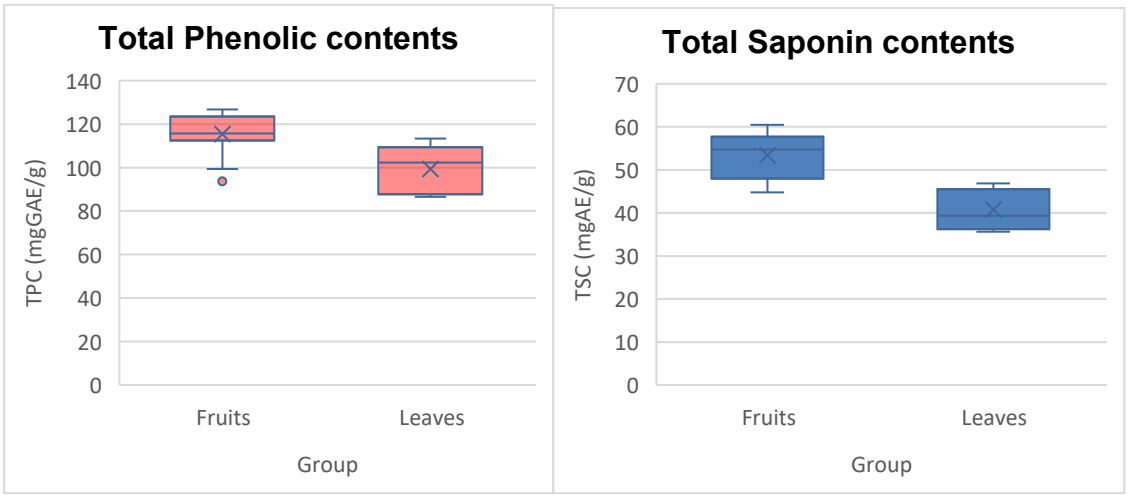

Figure 2: Boxplots of the TPC (left) and TSC (right) of the *P. tectorius*fruit and leaf extracts

The boxplot also highlights this divergence, with fruit extracts showing higher medians and tighter distributions compared to the broader and lower range of leaves. The difference in saponin content between plant parts was even more pronounced than that observed for phenolics, with a mean difference of +12.69 mg AE/g extract, which was highly significant according to permutation testing ($p < 0.0001$).Together, these results clearly demonstrate that while both fruits and leaves yield ethanol-soluble phenolics and saponins, fruit extracts consistently exhibit higher concentrations and more uniform distributions of these metabolites, as evidenced by both boxplot visualization and robust statistical testing.

3.2. *α*-amylase inhibitory effect of the extracts from the *P. tectorius* fruits and leaves

The α-amylase inhibitory activity of *P. tectorius* extracts, expressed as IC_{50} values (µg/mL), varied considerably among samples (Table 2). For fruit extracts, IC_{50} values ranged from 130.48 ± 10.51 µg/mL (F12) to 200.45 ± 26.01 µg/mL (F09), with an overall mean of approximately 162 µg/mL. Leaf extracts displayed a similar variability, ranging from 146.38 ± 12.25 µg/mL (L06) to 198.90 ± 22.32 µg/mL (L02), with a mean of about 171 µg/mL. These results indicate that both fruits and leaves possess moderate α-amylase inhibitory potential, though the activity was not uniform across all samples. When compared to the positive control acarbose (IC_{50} = 88.96 ± 9.69 µg/mL), all extracts were less potent, requiring approximately 1.5–2 times higher concentrations to achieve 50% enzyme inhibition.

Table 2: *α*-amylase inhibitory effect of the *P. tectorius*extracts

No.	Code	Part	*α*-amylase
1	F01	Fruits	158.24 ± 12.74
2	F02	Fruits	159.94 ± 14.45
3	F03	Fruits	186.32 ± 17.12
4	F04	Fruits	148.01 ± 12.12
5	F05	Fruits	160.85 ± 18.3
6	F06	Fruits	191.09 ± 17.67
7	F07	Fruits	165.07 ± 20.92
8	F08	Fruits	167.56 ± 16.15
9	F09	Fruits	200.45 ± 26.01
10	F10	Fruits	137.38 ± 15.54
11	F11	Fruits	161.16 ± 14.29
12	F12	Fruits	130.48 ± 10.51
13	F13	Fruits	162.44 ± 18.33
14	L01	Leaves	195.81 ± 25.09
15	L02	Leaves	198.9 ± 22.32
16	L03	Leaves	176.53 ± 18.86
17	L04	Leaves	148.87 ± 14.22
18	L05	Leaves	196.34 ± 19.66
19	L06	Leaves	146.38 ± 12.25

20	L07	Leaves	160.52 ± 15.33
21	L08	Leaves	161.21 ± 15.96
22	L09	Leaves	158.85 ± 13.11
Acarbose	Positive control		88.96 ± 9.69

Nevertheless, several fruit samples (notably F10 and F12) exhibited relatively strong inhibition (IC_{50} at 130–140 µg/mL), approaching the activity of acarbose. The observed variability among extracts likely reflects differences in the abundance and composition of phenolic and saponin constituents, which are known contributors to α-amylase inhibition. Overall, both fruit and leaf extracts of *P. tectorius* demonstrated promising α-amylase inhibitory activity, with fruits generally showing slightly stronger effects than leaves, although the differences were not as pronounced as those observed in metabolite concentrations. These findings support the potential role of *P. tectorius* as a natural source of α-amylase inhibitors, relevant for the management of postprandial hyperglycemia

3.3. Discussion

The correlation analysis revealed distinct relationships between metabolite levels and α-amylase inhibitory activity. A strong negative correlation was observed between total phenolic content (TPC) and IC_{50} values (Pearson's r = −0.842, R^2 = 0.709), indicating that extracts richer in phenolics required markedly lower concentrations to achieve 50% enzyme inhibition. This strong inverse association, also illustrated in the scatter plot (Figure 3a), highlights the central role of phenolic compounds as key contributors to α-amylase inhibition in *P. tectorius*. In particular, fruit samples such as F10 and F12, which exhibited the highest TPC levels, also showed the lowest IC_{50} values, approaching the potency of the positive control acarbose.In contrast, total saponin content (TSC) displayed only a weak negative correlation with IC_{50} (r = −0.319, R^2 = 0.102). Although higher TSC was generally associated with somewhat lower IC_{50} values, the relationship was inconsistent across samples, as reflected in the scattered distribution of data points in the TSC–IC_{50} plot (Figure 3b). This suggests that while saponins may contribute to α-amylase inhibition, their effect is minor compared to phenolic constituents.

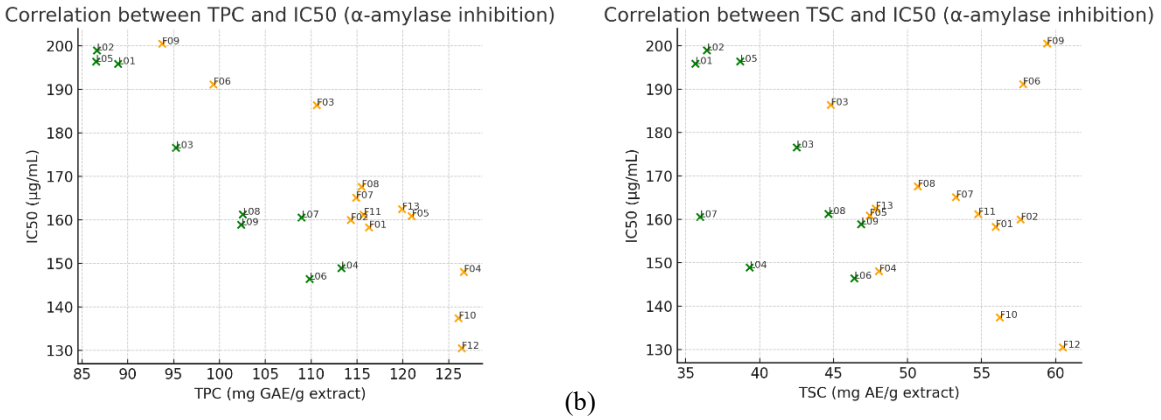

(a) (b)

Figure 2: Correlation between*α*-amylase inhibitory activity and the TPC (a) and TSC (b) of the *P. tectorius*fruit and leaf extracts

Previous studies have demonstrated that phenolic compounds inhibit α-amylase activity primarily through direct interactions with the enzyme's active site[24]. The hydroxyl groups of phenolics can form hydrogen bonds with catalytic residues, while their aromatic rings participate in hydrophobic and π–π stacking interactions, thereby reducing substrate access and catalytic efficiency[25]. This mechanism is consistent with the strong negative correlation observed between TPC and IC_{50} in the present study, suggesting that phenolic enrichment in *P. tectorius* extracts directly enhances inhibitory potency. In contrast, the weaker relationship between TSC and IC_{50} implies that saponins may act through indirect mechanisms, such as modulating membrane permeability or protein conformations, but are less effective in directly blocking *α*-amylase activity[26].Collectively, these findings highlight the importance of phenolic constituents as the principal bioactive agents responsible for *α*-amylase inhibition in *P. tectorius*. This provides a biochemical rationale for the potential application of fruit extracts, which are phenolic-rich, in the development of functional foods or phytopharmaceuticals aimed at managing postprandial hyperglycemia and related metabolic disorders.

IV. CONCLUSION

This study shows that fruits and leaves of *P. tectorius* provide similar levels of phenolics and saponins on a raw material basis, but fruit extracts are significantly richer in these metabolites when expressed per gram of ethanol extract. Phenolic content exhibited a strong negative correlation with α-amylase IC_{50} values, confirming its predominant role in the inhibitory effect, while saponins had a minor contribution. Although both plant parts have potential as herbal resources, fruit extracts appear to be superior candidates for the development of standardized phytopharmaceutical or nutraceutical products targeting postprandial hyperglycemia.

REFERENCES

[1]. Gallaher, T., Callmander, M. W., Buerki, S., Keeley, S. C. (2015). A long-distance dispersal hypothesis for the Pandanaceae and the origins of the *Pandanus tectorius* complex. *Molecular Phylogenetics and Evolution, 83*, 20-32.

[2]. Tan, M. A., Nonato, M. G., Kogure, N., Kitajima, M., Takayama, H. (2012). Secondary metabolites from *Pandanus* simplex. *Biochemical Systematics and Ecology, 40*, 4-5.

[3]. Lim, T. K., *Pandanus tectorius*. In *Edible Medicinal And Non-Medicinal Plants: Volume 4, Fruits*, Springer Netherlands: Dordrecht, 2012; pp 136-146.

[4]. Do Huy Bich, Dam Quang Trung., Bui Xuan Chuong, Nguyen Thuong Dong, Do Trung Dam, Pham Van Hien,Vu Ngoc Lo, Pham Duy Mai, Pham Kim Man, Doan Thi Nhu, Nguyen Tap, Tran Toan, *Medicinal plants and animals in Vietnam*. NXB Khoa học và Kỹ thuật: 2006.

[5]. Pham Hoang Ho, *Plants in Vietnam*. Tre Publisher: Ha Noi, 2003.

[6]. Do Tat Loi, *Medicinal Plants in Vietnam*. NXB Y học: 2004.

[7]. Zhang, X., Wu, H., Wu, C., Guo, P., Xu, X., Yang, M. (2013). Pandanusphenol A and B: Two New Phenolic Compounds from the Fruits of *Pandanus tectorius* Soland. *Records of Natural Products, 7* (4), 359-362.

[8]. Huang, Y., Chen, J., Liu, Z., Peng, L., Qiao, W., Li, W., Guo, D.-a. (2025). Pantelignans A-F, benzofuran sesquineolignan racemates from the roots and rhizomes of *Pandanus tectorius*: isolation, chiral resolution, and configurational assignment. *Journal of Molecular Structure, 1338*, 142322.

[9]. Wu, C., Zhang, X., Zhang, X., Luan, H., Sun, G., Sun, X., Wang, X., Guo, P., Xu, X. (2014). The caffeoylquinic acid-rich *Pandanus tectorius* fruit extract increases insulin sensitivity and regulates hepatic glucose and lipid metabolism in diabetic db/db mice. *The Journal of Nutritional Biochemistry, 25* (4), 412-419.

[10]. Tan, M. A., Takayama, H., Aimi, N., Kitajima, M., Franzblau, S. G., Nonato, M. G. (2008). Antitubercular triterpenes and phytosterols from *Pandanus tectorius* Soland. var. laevis. *Journal of Natural Medicines, 62* (2), 232-235.

[11]. Sahakitpichan, P., Chimnoi, N., Thamniyom, W., Ruchirawat, S., Kanchanapoom, T. (2020). Aromatic rutinosides from the aerial roots of *Pandanus tectorius*. *Phytochemistry Letters, 37*, 47-50.

[12]. Andriani, Y., Ramli, N. M., Syamsumir, D. F., Kassim, M. N. I., Jaafar, J., Aziz, N. A., Marlina, L., Musa, N. S., Mohamad, H. (2019). Phytochemical analysis, antioxidant, antibacterial and cytotoxicity properties of keys and cores part of *Pandanus tectorius* fruits. *Arabian Journal of Chemistry, 12*.

[13]. Mai, D. T., Dung, L. T., Phat, N. T., Minh, P. N., An, N. H., Phuc, N. T. T., and Tran, L. Q. (2015). A new aldehyde compound from the fruit of *Pandanus tectorius* Parkinson ex Du Roi. *Natural Product Research, 29* (15), 1437-1441.

[14]. Nguyen, T. P., Dung, L. T., Nhat, M. P., Trong, D. B., Tuyen, P. N. K., Lien, D. T. M., Tuyen, N. D., and Mai, T. D. (2016). A new dihydrofurocoumarin from the fruits of *Pandanus tectorius* Parkinson ex Du Roi. *Natural Product Research, 30* (21), 2389-2395.

[15]. Zhu, Z.-y., and Zhang, P.-z. (2022). A new lignan from *Pandanus tectorius*. *Natural Product Research, 36* (21), 5553-5558.

[16]. Zhang, X., Guo, P., Sun, G., Chen, S., Yang, M., Fu, N., Wu, H., Xu, X. (2012). Phenolic compounds and flavonoids from the fruits of *Pandanus tectorius* Soland. *Journal of Medicinal Plants Research, 6* (13), 2622-2626.

[17]. Cheng, C., Park, S. C., Giri, S. S. (2022). Effect of *Pandanus tectorius* extract as food additive on oxidative stress, immune status, and disease resistance in Cyprinus carpio. *Fish & Shellfish Immunology, 120*, 287-294.

[18]. Sundus, S., Hira, K., Sohail, N., Habiba, Tariq, A., Ara, J., Sultana, V., Ehteshamul-Haque, S. (2021). Protective role of *Pandanus tectorius* Parkinson ex Du Roi in diabetes, hyperlipidemia, liver and kidney dysfunction in alloxan diabetic rats. *Clinical Phytoscience, 7* (1), 48.

[19]. Zhang, X., Wu, C., Wu, H., Sheng, L., Su, Y., Zhang, X., Luan, H., Sun, G., Sun, X., Tian, Y., Ji, Y., Guo, P., Xu, X. (2013). Anti-Hyperlipidemic Effects and Potential Mechanisms of Action of the Caffeoylquinic Acid-Rich *Pandanus tectorius* Fruit Extract in Hamsters Fed a High Fat-Diet. *PLOS ONE, 8* (4), e61922.

[20]. Ppsk, P., Asmidar, M., Andriani, Y., Norouzitallab, P., Sung, Y. Y., Baruah, K. (2025). Evaluating the Protective Immunological Effects of *Pandanus tectorius* Leaf Extract Against Pathogenic *Vibrio campbellii* Using Gnotobiotic Brine Shrimp Model System. *Aquaculture Research, 2025* (1), 8215825.

[21]. Fattahi, S., Zabihi, E., Abedian, Z., Pourbagher, R., Motevalizadeh Ardekani, A., Mostafazadeh, A., Akhavan-Niaki, H. (2014). Total Phenolic and Flavonoid Contents of Aqueous Extract of Stinging Nettle and *in vitro* Antiproliferative Effect on Hela and BT-474 Cell Lines. *International Journal of Molecular and Cellular Medicine, 3* (2), 102-7.

[22]. Anh, V. L., Sophie, E. P., Minh, H. N., Paul, D. R. (2018). Improving the Vanillin-Sulphuric Acid Method for Quantifying Total Saponins. *Technologies, 6* (3), 84.

[23]. Sudha, P., Zinjarde, S. S., Bhargava, S. Y., Kumar, A. R. (2011). Potent α-amylase inhibitory activity of Indian Ayurvedic medicinal plants. *BMC Complementary and Alternative Medicine, 11* (1), 5.

[24]. Xiang, Y., Xiang, M., Mao, Y., Huang, L., He, Q., Dong, Y. (2025). Insights into structure-antioxidant activity relationships of polyphenol-phospholipid complexes: The effect of hydrogen bonds formed by phenolic hydroxyl groups. *Food Chemistry, 485*, 144471.

[25]. Rente, D., Paiva, A., Duarte, A. R. (2021). The Role of Hydrogen Bond Donor on the Extraction of Phenolic Compounds from Natural Matrices Using Deep Eutectic Systems. *26* (8), 2336.

[26]. Hanh, T. T. H., Dang, N. H., Dat, N. T. (2016). α-Amylase and α-Glucosidase Inhibitory Saponins from Polyscias fruticosa Leaves. *2016* (1), 2082946.

PUBLICATIONS IN VIETNAMESES JOURNALS

MỘT SỐ HỢP CHẤT SHIKIMATE ESTER, MEGASTIGMANE VÀ GLYCOSIDE TỪ LÁ DỨA THƠM (*PANDANUS AMARYLLIFOLIUS*)

ĐỖ HOÀNG GIANG [1, 2], BÙI THỊ NHẬT LỆ [2], NGUYỄN HẢI ĐĂNG [1], NGUYỄN THỊ THU THUỶ [3], NGÔ THỊ THUÝ NGÂN [4], HOÀNG LÊ TUẤN ANH [2], NGUYỄN NGỌC TÙNG [2], NGUYỄN TIẾN ĐẠT [2]

1. ĐẶT VẤN ĐỀ

Dứa thơm (*Pandanus amaryllifolius* Roxb) là một loại cây thường xanh với lá có mùi thơm. Cây có thân thẳng, cao 2 - 4,5 mét và đường kính 15 cm [1, 2]. Cụm hoa cái chưa được biết đến, nhưng nó tạo ra hoa đực trong những trường hợp cực kỳ hiếm. Lá được sử dụng rộng rãi làm hương liệu trên khắp Đông Nam Á. Cây được trồng để lấy lá ở Việt Nam, Indonesia, Malaysia, Thái Lan, New Guinea, Sri Lanka và Philippines [1-3]. Ở Việt Nam, lá dứa thơm thường được sử dụng làm thực phẩm, tạo mùi hương cho các món ăn hoặc sử dụng làm trà giải khát. Các nghiên cứu trước đây về thành phần hoá học trên loài cây này chủ yếu tập trung vào các hợp chất alkaloid [4, 5] trong khi rất hiếm công bố về các thành phần khác. Nghiên cứu này giới thiệu kết quả phân lập và xác định cấu trúc của ba hợp chất shikimate ester là methyl shikimate (**1**), *n*-butyl shikimate (**2**), methyl 5-epi-shikimate (**3**), cùng với một hợp chất megastigmane là vomifoliol (**4**) và một hợp chất glycoside *n*-butyl *D*-galactopyranoside (**5**) từ lá dứa thơm.

2. PHƯƠNG PHÁP NGHIÊN CỨU VÀ THỰC NGHIỆM

2.1. Mẫu nghiên cứu

Phần lá của cây dứa thơm (*P. amaryllifolius*) được thu hái tại Tam Đảo, Vĩnh Phúc vào tháng 04 năm 2021 và được giám định bởi TS. Bùi Văn Thanh, Viện Sinh thái và Tài nguyên Sinh vật. Mẫu tiêu bản được lưu trữ tại Trung tâm Nghiên cứu Nông dược, Trung tâm Nghiên cứu và Phát triển Công nghệ cao, Viện Hàn lâm Khoa học và Công nghệ Việt Nam.

2.2. Vật liệu và phương pháp nghiên cứu

Sắc ký lớp mỏng được thực hiện trên bản mỏng tráng sẵn TLC Silica gel 60 F_{254} (Merck). Sắc kí cột được thực hiện với các vật liệu hấp phụ Silica gel 60 có kích thước hạt 0,040-0,063 mm (240-430 mesh ASTM) (Merck, CHLB Đức); LiChroprep® RP-18 (0,040-0,063 mm) (Merck, CHLB Đức); Diaion HP-20 (Merck, CHLB Đức). Sắc ký điều chế được tiến hành trên hệ thống sắc ký lỏng hiệu năng cao Thermo Ultimate 3000 kết nối với detector DAD cùng loại, sử dụng cột YMC ODS-A 250x10 mm, 5 µm. Phổ cộng hưởng từ hạt nhân được đo trên máy Brucker Avance 600 MHz (chất chuẩn nội là Tetramethylsilane - TMS) tại Viện Hóa học, Viện Hàn lâm Khoa học và Công nghệ Việt Nam. Phổ ESI-MS được đo trên thiết bị Thermo LCQ Fleet LC/MS tại Trung tâm Nghiên cứu và Phát triển Công nghệ cao, Viện Hàn lâm Khoa học và Công nghệ Việt Nam. Độ quay cực được đo trên thiết bị JASCO P-2000 polarimeter, tại Viện Hóa sinh biển, Viện Hàn lâm Khoa học và Công nghệ Việt Nam.

http://doi.org/10.58334/vrtc.jtst.n35.09

2.3. Phân lập các chất

Phần lá của loài *P. amaryllifolius* được rửa sạch bằng nước máy, sau đó cắt nhỏ và sấy khô ở 45-55^{o}C. Mẫu sau khi sấy khô được nghiền nhỏ thành bột (1,3 kg) và chiết với 20 L methanol trong bể siêu âm ở 30-40^{o}C trong vòng 30 phút (lặp lại 4 lần). Sau đó, phần dịch lọc được tách ra, còn phần bã được chiết thêm ba lần theo cùng phương pháp. Toàn bộ dịch chiết được gom lại, cất loại hoàn toàn dung môi thu được cặn chiết tổng (129 g) sau đó hoà lại trong nước cất, rồi được acid hoá với dung dịch HCl 1N đến pH = 3 và chiết phân lớp với ethyl acetate (EA) (2L x 3 lần). Pha hữu cơ được tách riêng và cất loại dung môi để thu được phân đoạn không chứa alkaloid (PamNA, 24,6 g). Phần dịch nước được kiềm hóa bằng NaOH 1N tới pH = 9 rồi chiết phân bố với CH_2Cl_2 (4L x 3 lần), tách riêng phần hữu cơ và cất loại dung môi để thu được phân đoạn alkaloid (PamA, 1,8 g).

Phân đoạn PamNA (24,6 g) được hấp phụ hoàn toàn lên cột sắc ký Diaion HP-20, rửa với nước cất, giải hấp lần lượt với methanol 30% và 100% thu được các phân đoạn M30W (3,2 g) và M100W (8,1 g). Phân đoạn M30W được tách trên cột sắc ký silica gel với gradient dung môi CH_2Cl_2-MeOH (20/1-1/1, v/v) thu được bốn phân đoạn W1-W4. Phân đoạn W3 (121 mg) được phân tách trên sắc ký lỏng hiệu năng cao điều chế HPLC (120 min, 20-70% MeOH trong nước, 4 mL/phút) thu được các hợp chất **1** (5,5 mg), **2** (6,5 mg), và **3** (3,7 mg). Phân đoạn M100W được tách trên cột sắc ký silica gel với gradient dung môi CH_2Cl_2-MeOH (50/1-1/1, v/v) thu được mười phân đoạn M1-M10. Phân đoạn M5 (91,0 mg) được phân tách trên cột sắc ký silica gel với hệ dung môi rửa giải CH_2Cl_2-MeOH (9/1, v/v) thu được hai hợp chất **4** (3,2 mg) và **5** (4,5 mg).

Methyl shikimate (1): ESI-MS: *m/z* 189 $[M+H]^+$; ^{1}H NMR ($CDCl_3$, 600 MHz): δ_H 6,61 (1H; d; *J* = 1,8 Hz, H-2); 4,24 (1H, m, H-3); 3,85 (1H, m, H-4); 3,58 (1H, m, H-5); 2,07 (1H, dd, *J* = 2,4; 18,0 Hz, H-6); 2,41 (1H, dd, *J* = 3,6; 18,0 Hz; H-6); 3,67 (3H, s, 7-OCH_3); 4,82 (2H, brs, 3,5-OH); 4,60 (1H, brs, 4-OH). ^{13}C NMR ($CDCl_3$, 150 MHz): δ_C 127,3 (C-1); 139,7 (C-2); 66,8 (C-3); 70,0 (C-4); 65,4 (C-5); 29,6 (C-6); 166,7 (C-7); 51,5 (7-OCH_3).

***n*-butyl shikimate (2)**: ESI-MS: *m/z* 231 $[M+H]^+$; ^{1}H NMR ($CDCl_3$, 600 MHz): δ_H 6,61 (1H, t, *J* = 1,2 Hz, H-2); 4,80 (1H, brs, H-3); 3,85 (1H, m, H-4); 4,59 (1H, m, H-5); 2,62 (1H, m, H-6a); 2,13 (1H, m, H-6b); 4,08 (2H, t, *J* = 6,4 Hz, H-1'); 1,59 (2H, m, H-2'); 1,36 (2H, m, H-3'); 0,90 (3H, t, *J* = 7,2 Hz, H-4'). ^{13}C NMR ($CDCl_3$, 150 MHz): δ_C 127,6 (C-1); 139,4 (C-2); 65,4 (C-3); 70,1 (C-4); 66,8 (C-5); 29,6 (C-6a); 166,2 (C-7); 63,6 (C-1'); 30,2 (C-2'); 18,7 (C-3'); 13,5 (C-4').

Methyl 5-epi-shikimate (3): ESI-MS: *m/z* 189 $[M+H]^+$; ^{1}H NMR ($CDCl_3$, 600 MHz): δ_H 6,57 (1H, t, *J* = 3,0 Hz, H-2); 4,63 (1H, m, H-3); 3,49 (1H, m, H-4); 3,45 (1H, m, H-5); 2,13 (1H, dd, *J* = 9,0; 18,0 Hz, H-6a); 2,61 (1H, dd, *J* = 4,8; 18,0 Hz, H-6); 3,70 (3H, s, 7-OCH_3); 5,56 (1H, brs, 3-OH); 5,14 (1H, brs, 4-OH); 3,50 (1H, brs, 5-OH). ^{13}C NMR ($CDCl_3$, 150 MHz): δ_C 129,2 (C-1); 136,4 (C-2); 68,6 (C-3); 77,0 (C-4); 61,5 (C-5); 32,1 (C-6); 165,6 (C-7); 52,0 (7-OCH_3).

Vomifoliol (4): ESI-MS: *m/z* 225 $[M+H]^+$, *m/z* 207 $[M-H_2O+H]^+$, *m/z* 471 $[2M+Na]^+$; $[\alpha]_D^{25}$ +28,2 (*c* = 0,25, MeOH); ^{1}H NMR (CD_3OD, 600 MHz): δ_H 2,51 (1H, d, *J* = 17,0 Hz, H-2a); 2,20 (1H, d, *J* = 17,0 Hz, H-2b); 5,90 (1H, brs, H-4); 5,80 (1H, dd, *J* = 1,5; 15,0 Hz, H-7); 5,84 (1H, m, H-8); 4,39 (1H, m, H-9); 1,26 (3H, d, *J* =6,5 Hz, H-10); 1,03 (3H, s, H-11); 1,06 (3H, s, H-12); 1,93 (3H, s, H-13); ^{13}C NMR (CD_3OD, 150 MHz): δ_C 50,7 (C-2); 201,2 (C-3); 127,1 (C-4); 167,4 (C-5); 79,9 (C-6); 130,1 (C-7); 136,9 (C-8); 68,7 (C-9); 23,8 (C-10); 24,4 (C-11); 23,4 (C-12); 19,5 (C-13).

***n*-Butyl *D*-galactopyranoside** (**5**): ESI-MS: *m/z* 237 $[M+H]^+$; ^{1}H NMR ($CDCl_3$, 600 MHz): δ_H 4,75 (1H, d, *J* = 3,6 Hz, H-1); 3,78 (1H, dd, *J* = 3,6; 6,0 Hz, H-2); 3,73 (1H, m, H-3); 3,68 (1H, m, H-4); 3,57 (1H, m, H-5); 3,50 (2H, m, H-6); 3,42 (2H, m, H-1'); 1,59 (2H, m, H-2'); 1,40 (2H, m, H-3'); 1,40 (3H, t, *J* = 7,8 Hz, H-3'). ^{13}C NMR ($CDCl_3$, 150 MHz): δ_C 99,7 (C-1); 75,3 (C-2); 73,5 (C-3); 73,2 (C-4); 71,9 (C-5); 68,1 (C-6); 62,8 (C-1'); 32,4 (C-2'); 20,1 (C-3'); 14,1 (C-4').

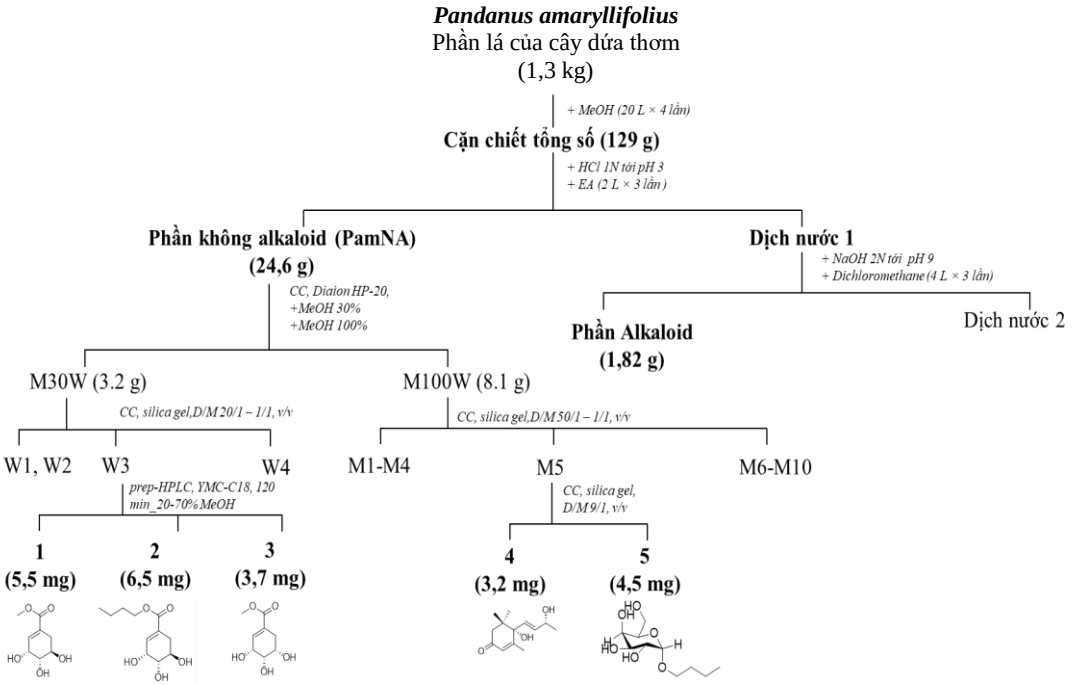

Hình 1. Sơ đồ phân lập các hợp chất

3. KẾT QUẢ VÀ THẢO LUẬN

Hợp chất **1** thu được dưới dạng chất rắn vô định hình màu trắng. Phổ ESI-MS xuất hiện tín hiệu *m/z* 189 $[M+H]^+$ cho phép xác định khối lượng phân tử 188 Da của hợp chất. Phổ ^{1}H-NMR của hợp chất **1** xuất hiện tín hiệu của ba proton oximethine sp^3 tại δ_H 4,24 (1H, m, H-3), 3,85 (1H, m, H-4), 3,58 (1H, m, H-5), một nhóm methylene tại δ_H 2,07 (1H, dd, *J* = 2,4, 18,0 Hz, H-6) và 2,41 (1H, dd, *J* = 3,6, 18,0 Hz, H-6), một nhóm methoxy tại δ_H 3,67 (3H, s, 7-OCH_3), một proton

olefine tại δ_H 6,61 (1H, d, J = 1,8 Hz, H-2), và ba hydroxy proton tại 4,82 (2H, brs, 3,5-OH) và 4,60 (1H, brs, 4-OH). Phổ ^{13}C NMR xuất hiện ba tín hiệu sp^3 oximethine tại δ_C 66,8 (C-3), 70,0 (C-4), và 65,4 (C-5), hai carbon olefine tại δ_C 127,3 (C-1) và 139,7 (C-2), một tín hiệu carbon carbonyl tại δ_C 166,7 (C-7) và một nhóm methoxy tại 51,5 (7-OCH_3). Hợp chất **1** được xác định là methyl shikimate qua so sánh các dữ liệu phổ MS và NMR nói trên với tài liệu tham khảo [6].

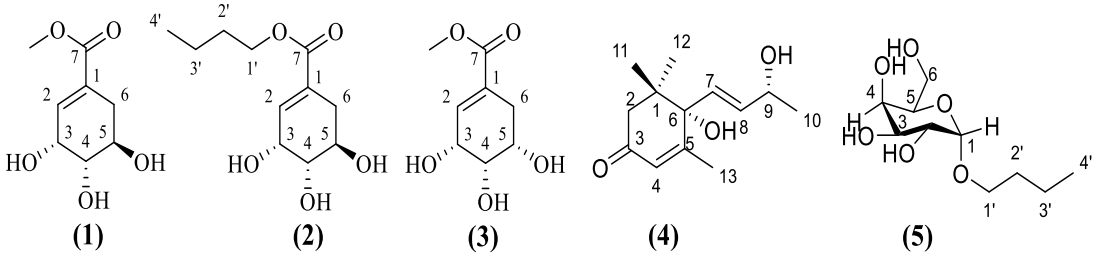

Hình 2. Cấu trúc hoá học của các hợp chất **1-5**

Hợp chất **2** thu được dưới dạng chất rắn vô định hình màu trắng. Phổ ESI-MS xuất hiện tín hiệu m/z 231[M+H]$^+$ cho phép xác định khối lượng phân tử 230 Da của **2**. Phổ ^{1}H-NMR của hợp chất **2** xuất hiện ba tín hiệu proton oximethine sp^3 tại δ_H 4,80 (1H, brs, H-3), 3,85 (1H, m, H-4), 4,59 (1H, m, H-5), hai tín hiệu methylene tại δ_H 2,62 (1H, m, H-6a), 2,13 (1H, m, H-6b), một proton olefine tại δ_H 6,61 (1H, d, J = 1,2 Hz, H-2) và bốn tín hiệu của một nhóm *n*-butylate tại δ_H 4,08 (2H, t, J = 6,4 Hz, H-1'), 1,59 (2H, m, H-2'), 1,36 (2H, m, H-3'), 0,90 (3H, t, J = 7,2 Hz, H-4'). Phổ ^{13}C NMR xuất hiện các tín hiệu oximethine sp^3 carbon tại δ_C 65,4 (C-3), 70,1 (C-4), 66,8 (C-5), hai olefine carbon tại δ_C 127,6 (C-1) và 139,4 (C-2), một tín hiệu carbon carbonyl tại δ_C 166,2 (C-7) và các tín hiệu của một gốc *n*-butyl tại 63,6 (C-1'), 30,2 (C-2'), 18,7 (C-3'), 13,5 (C-4'). Từ các dữ liệu trên, kết hợp với các dữ liệu tham khảo, hợp chất **2** được xác định là *n*-butyl shikimate [7].

Hợp chất **3** thu được dưới dạng chất rắn vô định hình màu trắng. Khối lượng phân tử của **3** được xác định là 188 Da thông qua tín hiệu m/z 189 [M+H]$^+$ trên phổ ESI-MS. Phổ ^{1}H-NMR của hợp chất **3** xuất hiện tín hiệu của ba proton oximethine sp^3 tại δ_H 4,63 (1H, m, H-3), 3,49 (1H, m, H-4), 3,45 (1H, m, H-5), một nhóm methylene tại δ_H 2,13 (1H, dd, J = 9,0; 18,0 Hz, H-6) và 2,41 (1H, dd, J = 4,8, 18,0 Hz, H-6), một nhóm methoxy tại δ_H 3,70 (3H, s, 7-OCH_3), một proton olefine tại δ_H 6,57 (1H, d, J = 3,0 Hz, H-2), và ba hydroxy proton tại 3,50 (2H, brs, 5-OH), 5,14 (1H, brs, 4-OH) và 5,56 (1H, brs, 3-OH). Phổ ^{13}C NMR xuất hiện ba tín hiệu carbon sp^3 oximethine tại δ_C 66,6 (C-3), 77,0 (C-4), và 61,5 (C-5), hai carbon olefine tại δ_C 129,2 (C-1) và 136,4 (C-2), một tín hiệu carbon carbonyl tại δ_C 165,6 (C-7), và một nhóm methoxy tại 52,0 (7-OCH_3). Dữ liệu phổ của hợp chất **3** cho thấy nhiều nét tương đồng với hợp chất **1**, tuy nhiên, có giảm đi khá rõ nét về độ chuyển dịch hoá học trên phổ ^{13}C và ^{1}H NMR ở vị trí C-5 (61,5 ppm và 3,45 ppm so với 65,4 ppm và 3,58 ppm của **1**). Từ các dữ liệu này kết hợp so sánh với các tài liệu tham khảo, có thể xác định đây là 5-epi-shikimate methyl [8].

Hợp chất **4** thu được dưới dạng chất dầu trong suốt. Trên phổ khối lượng ESI-MS của **4** xuất hiện pic ion phân tử tại *m/z* 225 $[M+H]^+$, cùng tín hiệu của các ion *m/z* 207 $[M-H_2O+H]^+$ và *m/z* 471 $[2M+Na]^+$ cho phép xác định khối lượng phân tử 224 Da. Trên phổ ^{1}H NMR của **4** xuất hiện tín hiệu của 4 nhóm methyl tại δ_H 1,26 (3H, d, J = 6,5 Hz, H-10), 1,03 (3H, s, H-11), 1,06 (3H, s, H-12) và 1,93 (3H, s, H-13). Ngoài ra trên phổ ^{1}H NMR còn cho thấy sự xuất hiện của ba proton olefine tại δ_H 5,90 (1H, brs, H-5), 5,84 (1H, m, H-8); 5,80 (1H, dd, J = 1,5; 15,0 Hz, H-7). Tín hiệu của hai proton methylene được xác định tại δ_H 2,20 (1H, d, J = 17,0 Hz, H_a-3) và 2,51 (1H, d, J = 17,0 Hz, H_b-3), trong khi tín hiệu proton oximethine được xác định tại δ_H 4,39 (1H, m, H-9). Phổ ^{13}C NMR xuất hiện tín hiệu của 13 nguyên tử carbon, trong đó có một nhóm carbonyl cộng hưởng tại δ_C 201,2 (C-4), 4 tín hiệu carbon vùng trường thấp tại 127,1 - 167,4 gợi ý sự tồn tại của hai nối đôi C=C. Ngoài ra, tín hiệu của 4 carbon methyl cũng được xác định tại δ_C 23,8 (C-10), 24,4 (C-11), 23,4 (C-12), 19,5 (C-13), tín hiệu carbon methylene được xác định tại δ_C 50,7 (C-3) và 2 tín hiệu carbon carbinol tại δ_C 79,9 (C-6), 68,7 (C-9). Dữ liệu phổ NMR của hợp chất **4** phù hợp với thông tin đã công bố về hợp chất vomifoliol, kết hợp với thông tin về trị số $[\alpha]_D^{25}$ +28,2 cho phép xác định **4** là 6*S*,9*R*-vomifoliol [9, 10].

Hợp chất **5** thu được dưới dạng chất rắn màu trắng. Phổ ESI-MS của **5** xuất hiện tín hiệu *m/z* 237 $[M+H]^+$. Phổ ^{1}H-NMR xuất hiện tín hiệu của một anomeric proton tại δ_H 4,75 (1H, d, J = 3,6 Hz, H-1), cùng bốn tín hiệu proton oxymethine tại δ_H 3,78 (1H, dd, J = 3,6; 6,0 Hz, H-2), 3,73 (1H, m, H-3), 3,68 (1H, m, H-4), 3,57 (1H, m, H-5), 3,50 (2H, m, H-6) chứng minh cấu trúc của một tiểu phân đường, cùng tín hiệu của một nhóm *n*-butyl oxy hoá tại δ_H 3,42 (2H, m, H-1'), 1,59 (2H, m, H-2'), 1,40 (2H, m, H-3'), 1,40 (3H, t, J = 7,8 Hz, H-4'). Phổ ^{13}C NMR xuất hiện tín hiệu của một tiểu phân galactose tại δ_C 99,7 (C-1), 75,3 (C-2), 73,5 (C-3), 73,2 (C-4), 71,9 (C-5), 68,1 (C-6), cùng tín hiệu của một nhóm *n*-butyl tại δ_C 62,8 (C-1'), 32,4 (C-2'), 20,1 (C-3'), 14,1 (C-4'). Các dữ liệu phổ nói trên, kết hợp với dữ liệu tham khảo [11], cho phép xác định hợp chất **5** là *n*-butyl *D*-galactopyranoside.

Các nghiên cứu trước đây trên đối tượng lá dứa thơm đã phân lập rất nhiều hợp chất alkaloid với nhiều hoạt tính sinh học đáng chú ý [4, 5, 12, 13]. Nghiên cứu này là lần đầu tiên các ester của shikimic acid, một hợp chất megastigmane và một hợp chất glycoside được phân lập và xác định cấu trúc từ lá dứa thơm *P. amaryllifolius*. Việc phát hiện các hợp chất shikimate ester cũng gợi ý về sự tồn tại của chu trình shikimic trong quá trình bán tổng hợp các hợp chất chuyển hoá thứ cấp trong cây dứa thơm. Những nghiên cứu sâu hơn cần được tiến hành để làm rõ những phát hiện mới này.

4. KẾT LUẬN

Từ phần lá của cây dứa thơm *P. amaryllifolius*, năm hợp chất gồm một hợp chất megastigmane, một hợp chất glycoside cùng với ba hợp chất shikimate ester đã được phân lập. Đây là lần đầu tiên, các hợp chất này được tìm thấy trong thành phần hoá học của lá dứa thơm. Những nghiên cứu sâu hơn về các hợp chất không phải alkaloid trong cây dứa thơm cần được tiến hành để làm rõ tính đa dạng về thành phần hoá học và hoạt tính sinh học của loài thực vật này.

Lời cảm ơn : *Nghiên cứu này được thực hiện với sự hỗ trợ của Viện Hàn lâm Khoa học và Công nghệ Việt Nam trong khuôn khổ nhiệm vụ "Phát triển nhóm nghiên cứu xuất sắc hạng I về ứng dụng các phương pháp phân tích hiện đại trong nghiên cứu chất lượng và an toàn thực phẩm", mã số: NCXS01.02/23-25.*

TÀI LIỆU THAM KHẢO

1. Đỗ Tất Lợi, *Những cây thuốc và vị thuốc Việt Nam*, NXB Y học, Hà Nội, 2004.
2. Phạm Hoàng Hộ, *Cây cỏ Việt Nam*, NXB Trẻ, Hà Nội, 2003.
3. Đỗ Huy Bích, Đặng Quang Trung, Bùi Xuân Chương, Nguyễn Thượng Dong, Đỗ Trung Đàm, Phạm Văn Hiển,Vũ Ngọc Lộ, Phạm Duy Mai, Phạm Kim Mẫn, Đoàn Thị Như, Nguyễn Tập, Trần Toàn, *Cây thuốc và động vật làm thuốc ở Việt Nam*, NXB Khoa học và Kỹ thuật, Hà Nội, 2006.
4. Takayama H., Ichikawa T., Kitajima M., Nonato M. G., Aimi N., D. L., G. N. M., *A new alkaloid, pandanamine; finding of an anticipated biogenetic intermediate in Pandanus amaryllifolius Roxb*, Tetrahedron Letters, 2001, **42**(16):995-2996. DOI:10.1016/S0040-4039(01)00339-2
5. Takayama H., Ichikawa T., Kitajima M., Nonato M. G., Aimi N., *Isolation and structure elucidation of two new alkaloids, pandamarilactonine-C and -D, from pandanus amaryllifolius and revision of relative stereochemistry of pandamarilactonine-A and -B by total synthesis*, Chemical and Pharmaceutical Bulletin, 2002, **50**(9):1303-1304.
6. Huang J., Chen F.-E., *An efficient synthesis of a potential (-)reserpine intermediate from (-)shikimic acid of the chiral pool*, Helvetica, 2007, **90**(7):1366-1372. DOI:10.1002/hlca.200790138
7. Chen J., Chen J.-J., Yang L.-Q., Hua L., Gao K., *Labdane diterpenoids and shikimic acid derivatives from araucaria cunninghamii*, Planta. Med., 2011, **77**(5):485-488. DOI: 10.1055/s-0030-1250570
8. Campbell M. M., Kaye A. D., Sainsbury M., Yavarzadeh R., *Brief synthesis of (±)-methyl shikimate, (±)-methyl epishikimate and structural variants*, Tetrahedron, 1984, **40**(13):2461-2470. DOI 10.1016/s0040-4020(01)83498-0
9. Hammami S., Jannet H. B., Bergaoui A., Ciavatta L., Cimino G., Mighri Z., *Isolation and structure elucidation of a flavanone, a flavanone glycoside and vomifoliol from echiochilon fruticosum growing in Tunisia*, Molecules, 2004, **9**(7):602-608. DOI: 10.3390/90700602
10. Dinh N. T., Do T. M., Ngo X. L., Thi H. T., Thi H. N., Thi H. M. V., Thi N. M. N., Vu T. K. O., *Chemical constituents from ethyl acetate extract of the leaves of Rourea harmandiana Pierre*, Vietnam Journal of Science, Technology and Engineering, 2020, **62**(2):30-33. DOI:10.31276/VJSTE.62(2).30-33

11. Wang Y., Renault L., Guégan J.-P., Benvegnu T., *Direct conversion of agarose into alkyl mono- and disaccharide surfactants based on 3,6-anhydro L- and D-galactose units*, Chemistry Select, 2021, **6**(3):389-395.

12. Takayama H., Ichikawa T., Kitajima M., Nonato M. G., Aimi N., *Isolation and characterization of two new alkaloids, norpandamarilactonine-A and -B, from pandanus amaryllifolius by spectroscopic and synthetic methods*, Journal of Natural Products, 2001, **64**(9):1224-1225. DOI:10.1002/slct.202004542

13. Tan M. A., Kitajima M., Kogure N., Nonato M. G., Takayama H., *Isolation of pandamarilactonine-H from the roots of pandanus amaryllifolius and synthesis of epi-pandamarilactonine-H*, Journal of Natural Products, 2010, **73**(8):1453-1455. DOI: 10.1021/np1003998

SUMMARY

SHIKIMATE ESTERS, MEGASTIGMANE AND GLYCOSIDE FROM LEAVES OF *PANDANUS AMARYLLIFOLIUS*

Phytochemical investigation of the leaves of *Pandanus amaryllifolius* led to the isolation of three shikimate esters including methyl shikimate (**1**), *n*-butyl shikimate (**2**), and 5-epi-shikimate methyl (**3**), together with vomifoliol (**4**), a megastigmane, and *n*-butyl *D*-galactopyranoside (**5**)-a glycoside. Structures of the isolated compounds were elucidated by spectroscopy data.

Keywords: *Pandanus, Pandanus amaryllifolius, shikimate ester, megastigmane, vomifoliol, D-galactopyranoside.*

Nhận bài ngày 02 tháng 7 năm 2024
Phản biện xong ngày 27 tháng 8 năm 2024
Hoàn thiện ngày 15 tháng 9 năm 2024

(1) Đại học Khoa học và Công nghệ Hà Nội, Viện Hàn lâm Khoa học và Công nghệ Việt Nam

(2) Trung tâm Nghiên cứu và Phát triển Công nghệ cao, Viện Hàn lâm Khoa học và Công nghệ Việt Nam

(3) Trung tâm Nhiệt đới Việt - Nga

(4) Trường Đại học Y Dược - Đại học Thái Nguyên

Liên hệ: ***Đỗ Hoàng Giang***

Đại học Khoa học và Công nghệ Hà Nội, Viện Hàn lâm Khoa học và Công nghệ Việt Nam

Điện thoại: 0975335463; Email: giangdh.91@gmail.com

MỘT SỐ HỢP CHẤT PHENOLIC TỪ QUẢ DỨA DẠI (*PANDANUS TECTORIUS*)

PHENOLICS FROM FRUITS OF *PANDANUS TECTORIUS*

Đỗ Hoàng Giang[1,2], Nguyễn Hải Đăng[1], Nguyễn Thu Uyên[2], Bùi Thị Nhật Lệ[2], Hoàng Thuỳ Dương[2], Lưu Hải Nhi[2], Nguyễn Thị Luyến[2], Hoàng Lê Tuấn Anh[2], Nguyễn Ngọc Tùng[2], Nguyễn Thị Thu Thuỷ[3], Ngô Thị Thuý Ngân[4], Nguyễn Tiến Đạt[2,*]

DOI: http://doi.org/10.57001/huih5804.2025.152

TÓM TẮT

Từ quả dứa dại (*Pandanus tectorius*), hai hợp chất lignan và hai dẫn xuất benzoate là matairesinol (**1**), arctigenin (**2**), methyl 4-hydroxybenzoate (**3**) và methyl syringate (**4**) đã được phân lập. Các hợp chất được phân lập bằng các phương pháp sắc ký cột truyền thống kết hợp với phương pháp điều chế hiện đại trên hệ thống sắc ký lỏng hiệu năng cao. Cấu trúc của các hợp chất được xác định dựa trên các dữ liệu phổ cộng hưởng từ hạt nhân (NMR) và khối phổ (MS). Kết quả của nghiên cứu này góp phần làm rõ hơn về thành phần hoá học của loài dứa dại, làm cơ sở cho những nghiên cứu chuyên sâu hơn về hoạt tính sinh học và ứng dụng của quả dứa dại trong lĩnh vực y dược, thực phẩm.

Từ khóa: *Dứa dại, matairesinol, arctigenin, lignan, phenolic.*

ABSTRACT

From the fruit of *Pandanus tectorius*, two lignan compounds and two benzoate derivatives - matairesinol **(1)**, arctigenin **(2)**, methyl 4-hydroxybenzoate **(3)**, and methyl syringate **(4)** were isolated. The compounds were separated using traditional column chromatography methods combined with modern preparative techniques on a high-performance liquid chromatography (HPLC) system. Their structures were determined based on nuclear magnetic resonance (NMR) and mass spectrometry (MS) data. The results of this study contribute to a better understanding of the chemical composition of *Pandanus tectorius*, providing a foundation for further in-depth research on its biological activities and potential applications in pharmaceuticals and food industries.

***Keywords*:** *Pandanus tectorius, matairesinol, arctigenin, lignan, phenolic.*

[1]Trường Đại học Khoa học và Công nghệ Hà Nội, Viện Hàn lâm Khoa học và Công nghệ Việt Nam

[2]Trung tâm Nghiên cứu và Phát triển Công nghệ cao, Viện Hàn lâm Khoa học và Công nghệ Việt Nam

[3]Trung tâm Nhiệt đới Việt - Nga

[4]Trường Đại học Y Dược - Đại học Thái Nguyên

[*]Email: ntdat@chtd.vast.vn

Ngày nhận bài: 22/02/2025

Ngày nhận bài sửa sau phản biện: 17/5/2025

Ngày chấp nhận đăng: 28/5/2025

1. GIỚI THIỆU

Dứa dại (*Pandanus tectorius* Parkinson ex Du Roi) là một loài thực vật phổ biến tại các khu vực rừng nhiệt đới, rừng ngập mặn và vùng đất ven biển, phân bố rộng rãi từ Nam Á đến các đảo thuộc Thái Bình Dương [1]. Ở Việt Nam, loài cây này thường xuất hiện tại nhiều địa phương, từ trung du và miền núi phía Bắc đến vùng duyên hải Khánh Hòa [2]. Trong y học dân gian, rễ cây dứa dại được sử dụng để trị các bệnh như phù thũng, tiểu buốt, tiểu rắt, sỏi thận hoặc dùng ngoài để chữa gãy xương, trĩ lòi [3, 4]. Lá của cây có vị ngọt, tính mát, giúp giải nhiệt và thường được dùng để chữa cảm, sốt. Ngoài ra, đọt non cũng được

ghi nhận có tác dụng hỗ trợ điều trị sỏi thận và kinh phong ở trẻ em [2-4]. Về mặt hóa học, các nghiên cứu quốc tế đã xác định nhiều nhóm hợp chất trong *P. tectorius*, bao gồm flavonoid, lignan, coumarin, và các dẫn xuất của axit benzoic [5-7]. Một số nghiên cứu về thành phần hóa học của lá và quả cây dứa dại đã phát hiện một số hợp chất lignan như pinoresinol, syringaresinol, medioresinol, lyoniresinol và balanophonin [5, 7] hoặc một số flavonoid như tangeretin, sakranetin, chrysin, naringenin [8]. Các thành phần hoá học từ cây dứa dại đã thể hiện một số hoạt tính sinh học đáng chú ý như chống oxi hoá, kháng viêm, gây độc tế bào ung thư…

Trong nghiên cứu hiện tại, chúng tôi trình bày kết quả phân lập và xác định cấu trúc của bốn hợp chất phenolic bao gồm matairesinol, arctigenin, methyl 4-hydroxybenzoate và methyl syringate từ quả dứa dại *P. tectorius*, trong đó hai hợp chất lignan cùng với hợp chất methyl syringate lần đầu tiên được phát hiện từ loài thực vật này.

2. PHƯƠNG PHÁP NGHIÊN CỨU VÀ THỰC NGHIỆM

2.1. Mẫu nghiên cứu

Phần quả của cây dứa dại *P. tectorius* được thu hái tại xã Cao Viên, huyện Thanh Oai, thành phố Hà Nội vào tháng 03 năm 2021 và được giám định bởi TS. Bùi Văn Thanh, viện Sinh thái và Tài nguyên Sinh vật. Mẫu tiêu bản (mã số NCCG 200107) được lưu trữ tại Trung tâm Nghiên cứu Nông dược, Trung tâm Nghiên cứu và Phát triển Công nghệ cao, Viện Hàn lâm Khoa học và Công nghệ Việt Nam.

2.2. Vật liệu và phương pháp nghiên cứu

Sắc kí cột được thực hiện với các vật liệu hấp phụ Silica gel 60 có kích thước hạt 0,040 - 0,063mm (240 - 430 mesh ASTM) (Merck, CHLB Đức); LiChroprep® RP-18 (0,040 - 0,063mm) (Merck, CHLB Đức); Diaion HP-20 (Merck, CHLB Đức). Sắc ký lớp mỏng được thực hiện trên bản mỏng tráng sẵn TLC Silica gel 60 F_{254} (Merck). Sắc ký điều chế được tiến hành trên hệ thống sắc ký lỏng hiệu năng cao Thermo Ultimate 3000 kết nối với detector DAD cùng loại, sử dụng cột YMC ODS-A 250x10mm, 5µm. Phổ cộng hưởng từ hạt nhân được đo trên máy Brucker Avance 600 MHz (chất chuẩn nội là Tetramethylsilane - TMS) tại Viện Hóa học, Viện Hàn lâm Khoa học và Công nghệ Việt Nam. Phổ ESI-MS được đo trên thiết bị Thermo LCQ Fleet LC/MS tại Trung tâm Nghiên cứu và Phát triển Công nghệ cao, Viện Hàn lâm Khoa học và Công nghệ Việt Nam.

2.3. Phân lập các chất

Phần quả cây dứa dại *P. tectorius* (21kg) được rửa sạch bằng nước, sau đó cắt nhỏ và sấy khô ở 45 - 55°C. Mẫu sau khi sấy khô được nghiền nhỏ thành bột (2,9kg) và chiết với 20L methanol trong bể siêu âm ở 30 - 40°C trong vòng 60 phút (lặp lại 4 lần). Toàn bộ dịch chiết được gom lại, cất loại hoàn toàn dung môi thu được cặn chiết tổng (154g). Cặn chiết này được phân tán trong 3L nước và chiết phân bố lần lượt với n-hexane (3L × 3 lần) và ethyl acetate (3L × 3 lần), thu lại từng pha hữu cơ rồi cất loại dung môi để thu được phân đoạn hexan (31,2g) và phân đoạn ethyl acetate (40,7g). Phần nước được cất loại hết dung môi hữu cơ rồi hấp phụ trên cột sắc ký Diaion HP-20, sau đó rửa bằng nước cất trước khi giải hấp lần lượt bằng methanol 50% và methanol 100% thu được phân đoạn M50 (7,5g) và M100 (11,4g).

Phân đoạn ethyl acetate được phân tách trên cột sắc ký silica gel với hệ dung môi rửa giải CH_2Cl_2 - MeOH (100/0 - 0/100, v/v) thu được chín phân đoạn E1-E9. Phân đoạn E7 (1,47g) được phân tách trên cột sắc ký silica gel với hệ dung môi rửa giải CH_2Cl_2 - methanol (9/1, v/v) thu được hợp chất **1** (6,7mg). Phân đoạn E5 được phân tách trên cột sắc ký silicagel với hệ dung môi rửa giải CH_2Cl_2 - acetone (3/1, v/v) sau đó tinh chế lại sản phẩm trên hệ thống sắc ký điều chế với gradient dung môi methanol - nước (1/2 - 4/1, v/v), tốc độ dòng 4mL/phút, thu được hợp chất **2** (7,9mg).

Phân đoạn M100 được phân tách trên cột sắc ký silica gel với hệ dung môi rửa giải CH_2Cl_2 - MeOH (30/1 - 0/100, v/v) thu được sáu phân đoạn M1-M6. Phân đoạn M5 (547mg) phân tách trên cột sắc ký RP-18 với hệ dung môi methanol - nước (2/1, v/v) thu được hai hợp chất **3** (3,6mg) và **4** (5,9mg).

Matairesinol (1): $[\alpha]_D^{25}$ = -22,4° (*c* 0,9 , MeOH); ESI-MS: *m/z* 359 $[M+H]^+$; ^{1}H NMR ($CDCl_3$, 500MHz): *δ* 6,41 (1H; d; *J* = 2,0Hz; H-2); 6,81 (1H; d; *J* = 8,0Hz; H-5); 6,51 (1H; dd; *J* =8,0; 2,0Hz; H-6); 2,53-2,63 (2H; m; H-7); 2,48 (1H; m; H-8); 3,89 (1H; dd; *J* = 9,0; 7,0Hz; H-9a); 4,16 (1H; dd; *J* = 9,0; 7,0Hz; H-9b); 6,61 (1H; d; *J* = 2,0Hz; H-2'); 6,79 (1H; d; *J* = 8,0Hz; H-5'); 6,59 (1H; dd; *J* =8,0; 2,0Hz; H-6'); 2,89 (1H; dd; *J* = 14,0; 6,0Hz ; H-7'a); 2,95 (1H; dd; *J* = 14,0; 6,0Hz; H-7'b); 2,56 (1H; m; H-8'); 3,81 (3H; s; 3-*O*-CH_3); 3,81 (3H; s; 3'-*O*-CH_3); ^{13}C NMR ($CDCl_3$; 125MHz): *δ* 129,6 (C-1); 111 (C-2); 146,7 (C-3); 144,6 (C-4); 114,4 (C-5); 121,3 (C-6); 38,3 (C-7); 41 (C-8); 71,3 (C-9); 178,8 (C-10); 129,5 (C-1'); 111,5 (C-2'); 146,6 (C-3'); 144,4 (C-4'); 114,1 (C-5'); 122,1 (C-6'); 34,6 (C-7'); 46,6 (C-8'); 55,9 (3-*O*-CH_3); 55,8 (3'-*O*-CH_3).

Arctigenin (2): $[\alpha]_D^{25}$ = -16,8° (*c* 0,8 , MeOH); ESI-MS: *m/z* 373 $[M+H]^+$; ^{1}H NMR ($CDCl_3$, 500MHz): *δ* 6,64 (1H; d; *J* =1,5Hz; H-2); 6,75 (1H; d; *J* = 8,0Hz; H-5); 6,55 (1H; d; *J* =

8,0; 1,5Hz; H-6); 2,91 (1H; m; H-7); 2,55 (1H; m; H-8); 4,14 (1H; dd; *J* = 9,0; 7,5Hz; H-9a); 3,89 (1H; dd; *J* = 9,0; 7,5Hz; H-9b); 6,46 (1H; dd; *J* = 2,0Hz; H-2'); 6,82 (1H; dd; *J* = 8,0Hz; H-5'); 6,64 (1H; d; *J* = 8,0; 2,0Hz; H-6'); 2,94 (1H; dd; *J* = 14,0; 5,5Hz; H-7'a); 2,90 (1H; dd; *J* = 14,0; 6,5Hz; H-7'b); 2,50 (1H; m; H-8'); 3,88 (3H; m; 3-*O*-CH_3); 3,88 (3H; m; 3'-*O*-CH_3); 3,88 (3H; m; 4-*O*-CH_3); ^{13}C NMR ($CDCl_3$; 125MHz): *δ* 130,4 (C-1); 111,8 (C-2); 149 (C-3); 147,8 (C-4); 111,3 (C-5); 120,6 (C-6); 38,1 (C-7); 46,6 (C-8); 71,2 (C-9); 179,7 (C-10); 129,4 (C-1'); 111,5 (C-2'); 146,7 (C-3'); 144,5 (C-4'); 114,2 (C-5'); 122,0 (C-6'); 34,5 (C-7'); 40,9 (C-8'); 55,9 (3-*O*-CH_3); 55,8 (3'-*O*-CH_3); 55,8 (4-*O*-CH_3).

Methyl 4-hydroxybenzoate (3): ESI-MS: *m/z* 153 $[M+H]^+$; ^{1}H NMR ($CDCl_3$; 600 MHz): *δ* 7,81 (1H; d; *J* = 6,6Hz; H-2;6); 6,84 (1H; d; *J* = 6,6Hz; H-3,5); 3,78 (3H; s; 7-*O*-CH_3), ^{13}C NMR ($CDCl_3$; 125MHz): *δ* 120,2 (C-1); 131,3 (C-2); 115,3 (C-3,5); 161,9 (C-4); 131,3 (C-6); 166,0 (C-7); 51,6 (7-*O*-CH_3).

Methyl syringate (4): ESI-MS: *m/z* 213 $[M+H]^+$; ^{1}H NMR ($CDCl_3$; 600MHz): *δ* 7,34 (2H; s; H-2,6); 3,88 (6H; s; 3,5-*O*-CH_3); 3,89 (3H; s; 7-*O*-CH_3), ^{13}C NMR ($CDCl_3$; 125MHz): *δ* 121,37 (C-1); 108,1 (C-2); 148,9 (C-3,5); 141,94 (C-4); 108,1 (C-6); 168,6 (C-7); 56,8 (3,5-*O*-CH_3); 52,5 (7-*O*-CH_3).

3. KẾT QUẢ VÀ THẢO LUẬN

Hợp chất **1** thu dưới dạng dầu màu vàng. Khối lượng phân tử của **1** được xác định là 358 Da dựa vào sự xuất hiện tín hiệu ion phân tử $[M+H]^+$ *ở m/z* 359 trên phổ ESI-MS. Trên phổ ^{1}H NMR xuất hiện sáu tín hiệu của hai hệ vòng thơm ABX tại δ_H 6,41 (1H, d, *J* = 2,0Hz, H-2), 6,81 (1H, d, *J* = 8,0Hz, H-5), 6,51 (1H, d, *J* = 8,0; 1,5Hz, H-6) và δ_H 6,61 (1H, dd, *J* = 2,0Hz, H-2′), 6,79 (1H, dd, *J* = 8,0Hz, H-5′), 6,59 (1H, d, *J* = 8,0; 2,0Hz, H-6′); hai tín hiệu methine δ_H 2,48 (1H, m, H-8), 2,56 (1H, m, H-8′); hai tín hiệu proton của nhóm oxymethylene tại δ_H 4,16 (1H, dd, *J* = 9,5; 7,5Hz, H-9a), 3,89 (1H, dd, *J* = 9,5; 7,5Hz, H-9b) cùng tín hiệu của hai nhóm methylene khác tại δ_H 2,60 (2H, m, H-7), 2,95 (1H, dd, *J* = 14,0; 5,5Hz, H-7′a) và 2,89 (1H, dd, *J* = 14,0; 6,5Hz, H-7′b); và tín hiệu của hai nhóm methoxy δ_H 3,80 (3H, s) và 3,81 (3H, s). Trên phổ ^{13}C NMR và phổ DEPT xuất hiện tín hiệu của 21 nguyên tử carbon bao gồm 6 nhóm -CH thuộc vòng thơm δ_C 111,0 (C-2), 111,5 (C-2′), 114,4 (C-5), 114,1 (C-5′), 121,3 (C-6), 122,1 (C-6′), 6 tín hiệu carbon thơm không liên kết với hydro bao gồm δ_C 129,6 (C-1), 129,5 (C-1′) và bốn tín hiệu carbon vòng thơm liên kết trực tiếp với oxy δ_C 146,7 (C-3), 146,6 (C-3′), 144,6 (C-4) và 144,4 (C-4′). Các tín hiệu này một lần nữa khẳng định sự xuất hiện của hai vòng thơm trong cấu trúc của **1**. Sự xuất hiện của hai tín hiệu methine δ_C 41,0 (C-8), 46,6 (C-8′), một tín hiệu oxymethylene δ_C 71,3 (C-9), và một tín hiệu nhóm carboxyl tại δ_C 178,8 (C-10) trên phổ ^{13}C NMR và phổ DEPT gợi ý về sự xuất hiện của một vòng lactone. Ngoài ra, trên phổ ^{13}C NMR và phổ DEPT của **1** còn có tín hiệu của hai nhóm methylene δ_C 38,3 (C-7), 34,6 (C-7′) và hai nhóm methoxy tại δ_C 55,9 (3-*O*-CH_3); 55,8 (3'-*O*-CH_3). Dữ liệu phổ của hợp chất **1** trùng khớp với dữ liệu phổ đã công bố của matairesinol [9], trong đó, cấu hình (-) được xác định thông qua sự tương đồng về trị số $[\alpha]_D^{25}$ = -22,4º với hợp chất tương tự trong tài liệu tham khảo. Do đó có thể xác định **1** là matairesinol [10].

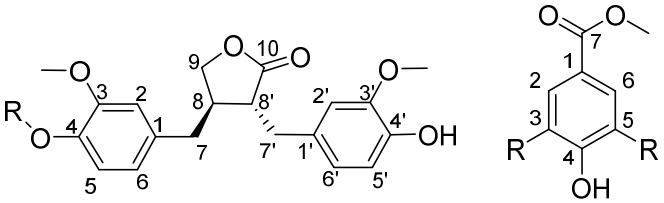

Hình 1. Cấu trúc hoá học của các hợp chất **1-4**

Hợp chất **2** thu dưới dạng dầu màu vàng nâu. Khối lượng phân tử của **2** được xác định là 372 Da dựa vào sự xuất hiện pic ion giả phân tử $[M+H]^+$ *ở m/z* 373 trên phổ ESI-MS. Trên phổ ^{1}H NMR xuất hiện sáu tín hiệu của hai hệ vòng thơm ABX tại δ_H 6,64 (1H, d, *J* = 1,5Hz, H-2), 6,75 (1H, d, *J* = 8,0Hz, H-5), 6,55 (1H, d, *J* = 8,0; 1,5Hz, H-6) và δ_H 6,46 (1H, dd, *J* = 2,0Hz, H-2′), 6,82 (1H, dd, *J* = 8,0Hz, H-5′), 6,64 (1H, d, *J* = 8,0; 2,0Hz, H-6′); hai tín hiệu methine δ_H 2,55 (1H, m, H-8), 2,50 (1H, m, H-8′); hai tín hiệu proton của nhóm oxymethylene tại δ_H 4,14 (1H, dd, *J* =9,0; 7,5Hz, H-9a), 3,89 (1H, dd, *J* = 9,0; 7,5Hz, H-9b) cùng tín hiệu của hai nhóm methylene khác tại δ_H 2,91 (2H, m, H-7), 2,94 (1H, dd, *J* = 14,0; 5,5Hz, H-7′a) và 2,90 (1H, dd, *J* = 14,0; 6,5Hz, H-7′b); và tín hiệu của ba nhóm methoxy δ_H 3,81 (3H, s), 3,86 (3H, s) và 3,88 (3H, s). Trên phổ ^{13}C NMR và phổ DEPT xuất hiện tín hiệu của 21 nguyên tử carbon bao gồm 6 nhóm -CH thuộc vòng thơm δ_C 111,8 (C-2), 111,5 (C-2′), 111,3 (C-5), 114,2 (C-5′), 120,6 (C-6), 122,0 (C-6′), 6 tín hiệu carbon thơm không liên kết với hydro bao gồm δ_C 130,4 (C-1), 129,4 (C-1′) và bốn tín hiệu carbon vòng thơm liên kết trực tiếp với oxy δ_C 149,0 (C-3), 146,7 (C-3′), 147,8 (C-4) và 144,5 (C-4′), hai nhóm methylene δ_C 38,1 (C-7), 34,5 (C-7′) và ba nhóm methoxy tại δ_C 55,9 (3-*O*-CH_3); 55,8 (3'-*O*-CH_3); 55,8 (4-*O*-CH_3). Sự xuất hiện của hai tín hiệu methine δ_C 46,6 (C-8), 40,9 (C-8′), một tín hiệu oxymethylene δ_C 71,2 (C-9), và một tín hiệu nhóm carboxyl tại δ_C 179,7 (C-10) gợi ý về sự xuất hiện của một vòng lactone. Có thể thấy, dữ liệu phổ của hợp chất **2** có sự tương đồng rất lớn với hợp chất **1** nhưng có thêm một

tín hiệu methoxy. Từ các dữ liệu trên, kết hợp với các dữ liệu tham khảo [11], hợp chất **2** được xác định là arctigenin. Cấu hình (-) được xác định thông qua sự tương đồng về trị số $[\alpha]_D^{25}$ = -16,8° với hợp chất tương tự trong tài liệu tham khảo [10].

Hợp chất **3** thu được dưới dạng chất rắn vô định hình màu trắng. Khối lượng phân tử của **3** được xác định là 152 Da thông qua tín hiệu *m/z* 153 $[M+H]^+$ trên phổ ESI-MS. Phổ ^{1}H-NMR của hợp chất **3** xuất hiện các tín hiệu proton của hệ vòng thơm A_2B_2 tại δ_H 7,81 (1H; d; *J* = 6,6Hz; H-2;6) và 6,84 (1H; d; *J* = 6,6Hz; H-3;5) cùng tín hiệu của một nhóm methoxy tại 3,78 (3H; s; 7-*O*-CH_3). Trên phổ ^{13}C NMR và DEPT của hợp chất **3** xuất hiện tín hiệu của sáu carbon vòng thơm hệ A_2B_2 tại δ_C cùng tín hiệu của một nhóm carboxyl tại δ_C 166,0 (C-7) và một tín hiệu methoxy tại δ_C 51,6 (7-*O*-CH_3). So sánh dữ liệu phổ của **3** với tài liệu tham khảo [12], có thể xác định đây là hợp chất methyl 4-hydroxybenzoate.

Hợp chất **4** thu được dưới dạng chất rắn màu trắng. Trên phổ khối lượng ESI-MS của **4** xuất hiện pic ion phân tử tại *m/z* 213 $[M+H]^+$ cho phép xác định khối lượng phân tử 212 Da của hợp chất. Trên phổ ^{1}H NMR của **4** xuất hiện tín hiệu của hai proton đối xứng nhau ở vị trí meta tại δ_H 7,34 (2H; s; H-2,6) cùng với tín hiệu của ba nhóm methoxy tại δ_H 3,89 (6H; s; 3,5-*O*-CH_3) và 3,88 (3H; s; 7-*O*-CH_3). Phổ ^{13}C NMR và DEPT xuất hiện tín hiệu của sáu carbon vòng thơm tại δ_C 121,37 (C-1); 108,1 (C-2); 148,9 (C-3,5); 141,94 (C-4); 108,1 (C-6), một tín hiệu carboxyl tại δ_C 168,6 (C-7) và ba tín hiệu methoxy tại δ_C 56,8 (3,5-*O*-CH_3); 52,5 (7-*O*-CH_3). Dữ liệu phổ của hợp chất **4** có sự tương đồng khá lớn với hợp chất **3**, nhưng có sự thay đổi ở hai vị trí carbon vòng thơm liên kết với oxy tại δ_C 148,9 (C-3,5) tương ứng với sự có mặt của hai nhóm methoxy tại δ_C 56,8 (3,5-*O*-CH_3). Từ các dữ liệu trên, kết hợp với dữ liệu tham khảo [13], có thể kết luận hợp chất 4 là methyl syringate.

Từ phần quả của cây dứa dại *P. tectorius*, bốn hợp chất đã được phân lập bao gồm matairesinol (**1**), arctigenin (**2**), methyl 4-hydroxybenzoate (**3**) và methyl syringate (**4**). Ngoại trừ hợp chất **3**, các hợp chất còn lại đều được phát hiện lần đầu tiên trong thành phần hoá học của loài *P. tectorius*. Các nghiên cứu trước đây chỉ ra rằng, cao chiết từ các bộ phận trên mặt đất của loài dứa dại *P. tectorius* thể hiện nhiều hoạt tính sinh học quý như chống oxi hoá, kháng khuẩn, gây độc tế bào ung thư [14-17]. Những phát hiện mới trong nghiên cứu này góp phần làm sáng tỏ nguồn gốc các hoạt tính sinh học kể trên của loài *P. tectorius* và cho thấy đây vẫn là một đối tượng nghiên cứu đầy tiềm năng để tìm kiếm các chất có hoạt tính sinh học.

4. KẾT LUẬN

Nghiên cứu về thành phần hoá học của quả dứa dại (*P. tectorius*) đã phát hiện bốn hợp chất phenolic, bao gồm hai hợp chất lignan là matairesinol và arctigenin, cùng hai hợp chất benzoate là methyl 4-hydroxybenzoate và methyl syringate. Trong số đó, các hợp chất matairesinol, arctigenin và methyl syringate lần đầu tiên được phát hiện từ loài dứa dại (*P. tectorius*). Kết quả của nghiên cứu cho thấy tiềm năng rất lớn trong việc khai thác và sử dụng quả dứa dại trong đời sống và trong y học, góp phần tạo ra các chế phẩm có ích, phục vụ và chăm sóc sức khoẻ của con người.

LỜI CẢM ƠN

Chúng tôi xin chân thành cảm ơn Viện Hàn lâm Khoa học và Công nghệ Việt Nam đã tạo điều kiện và hỗ trợ kinh phí để thực hiện công trình này thông qua nhiệm vụ nhiệm vụ *"Phát triển nhóm nghiên cứu xuất sắc hạng I về ứng dụng các phương pháp phân tích hiện đại trong nghiên cứu chất lượng và an toàn thực phẩm"*, mã số: NCXS01.02/23-25.

TÀI LIỆU THAM KHẢO

[1]. Lim T.K., "*Pandanus tectorius*," in *Edible Medicinal And Non-Medicinal Plants: Volume 4, Fruits*, Springer Netherlands: Dordrecht, pp 136-146, 2012.

[2]. Đỗ Huy Bích, Đặng Quang Trung, Bùi Xuân Chương, Nguyễn Thượng Dong, Đỗ Trung Đàm, Phạm Văn Hiển,Vũ Ngọc Lộ, Phạm Duy Mai, Phạm Kim Mẫn, Đoàn Thị Như, Nguyễn Tập, Trần Toàn, *Cây thuốc và động vật làm thuốc ở Việt Nam*. NXB Khoa học và Kỹ thuật, 2006.

[3]. Phạm Hoàng Hộ, *Cây cỏ Việt Nam*. NXB Trẻ, Hà Nội, 2003.

[4]. Đỗ Tất Lợi, *Những cây thuốc và vị thuốc Việt Nam*. NXB Y học, Hà Nội, 2004.

[5]. Nguyen T.P., Le T.D., Minh P.N., Dat B.T., Pham N.K.T., Do T.M.L., Nguyen D.T., Mai T.D., "A new dihydrofurocoumarin from the fruits of Pandanus tectorius Parkinson ex Du Roi.," *Nat. Prod. Res.*, 30 (21), 2389-2395, 2016.

[6]. Suzuki R., Kan S., Sugita Y., Shirataki Y., "p-Coumaroyl Malate Derivatives of the Pandanus amaryllifolius Leaf and Their Isomerization," *Chem. Pharm. Bull.*, 65 (12), 1191-1194, 2017.

[7]. Mai D.T., Le T.D., Nguyen T.P., Phan N.M., Nguyen H.A., Nguyen T.T.P., Tran L.Q., "A new aldehyde compound from the fruit of Pandanus tectorius Parkinson ex Du Roi," *Nat. Prod. Res.*, 29 (15), 1437-1441, 2015.

[8]. Zhang X., Guo P., Sun G., Chen S., Yang M., Fu N.j., Wu H., Xu X.d., "Phenolic compounds and flavonoids from the fruits of Pandanus tectorius Soland," *J. Med. Plants Res.*, 6 (13), 2622-2626, 2012.

[9]. Umezawa T., David L.B., Lewis N.G., "Formation of lignans (-)-secoisolariciresinol and (-)-matairesinol with Forsythia intermedia cell-free extracts," *J. Biol. Chem.*, 266 (16), 102-107, 1991.

[10]. Fischer J., Reynolds A.J., Sharp L.A., Sherburn M.S., "Radical Carboxyarylation Approach to Lignans. Total Synthesis of (−)-Arctigenin, (−)-Matairesinol, and Related Natural Products," *Organic Letters*, 6 (9), 1345-1348, 2004.

[11]. Yang M., Xu X., Xie C., Xie Z., Huang J., Yang D., "Separation and Purification of Arctiin, Arctigenin, Matairesinol, and Lappaol F from Fructus arctii by High-Speed Counter-Current Chromatography," *Sep. Sci. Technol.*, 48 (11), 1738-1744, 2013.

[12]. Liu S., Sun C., Ha Y., Ma M., Wang N., Zhou Y., Zhang Z., "Novel antibacterial alkaloids from the Mariana Trench-derived actinomycete Streptomyces sp. SY2255," *Tetrahedron Lett.,* 137, 154935, 2024.

[13]. Ha T.T.T., Dung N.T., Trung K.H., Tai B.H., Kiem P.V., "Phytochemical constituents from the rhizomes of Kaempferia parviflora Wall. ex Baker and their acetylcholinesterase inhibitory activity," *Nat. Prod. Res.,* 38 (6), 994-1001, 2024.

[14]. Andriani Y., Ramli N.M., Syamsumir D.F., Kassim M.N.I., Jaafar J., Aziz N.A., Marlina L., Musa N.S., Mohamad H., "Phytochemical analysis, antioxidant, antibacterial and cytotoxicity properties of keys and cores part of Pandanus tectorius fruits," *Arab. J. Chem.,* 12 (8), 3555-3564, 2019.

[15]. Musa N.S., Ramli N.M., Saidin J., Andriani Y., "Antioxidant and cytotoxicity properties of ethyl acetate fractions of Pandanus tectorius fruit against HeLa cell lines," *Alotrop J. Pendidik. Ilmu Kim.,* 1 (2), 106-112, 2017.

[16]. Andriani Y., Pangestika I., Oksal E., Amir H.M.H., Sifzizul T., Muhammad T., Wahid M.E., "Anti-atherosclerosis potency of Pandanus tectorius fruit rich by trangeretin and ethyl trans-caffeate, and their cytotoxicity against HepG2 cell line," *IOP Conf. Ser.: Mater. Sci. Eng.*, 509, 012155, 2019.

[17]. Oksal E., Pangestika I., Sifzizul T., Muhammad T., Mohamad H., Amir H., Kassim M.N.I., Andriani Y., "In vitro and in vivo studies of nanoparticles of chitosan-Pandanus tectorius fruit extract as new alternative treatment for hypercholesterolemia via Scavenger Receptor Class B type 1 pathway," *Saudi Pharm. J.,* 28 (10), 1263-1275, 2020.

AUTHORS INFORION

Do Hoang Giang[1,2], Nguyen Hai Dang[1], Nguyen Thu Uyen[2], Bui Thi Nhat Le[2], Hoang Thuy Duong[2], Luu Hai Nhi[2], Nguyen Thi Luyen[2], Hoang Le Tuan Anh[2], Nguyen Ngoc Tung[2], Nguyen Thi Thu Thuy[3], Ngo Thi Thuy Ngan[4], Nguyen Tien Dat[2]

[1]University of Science and Technology of Hanoi, Vietnam Academy of Science and Technology, Vietnam

[2]Center for High Technology Research and Development, Vietnam Academy of Science and Technology, Vietnam

[3]Joint Vietnam - Russia Tropical Science and Technology Research Center, Vietnam

[4]Thai Nguyen University of Medicine and Pharmacy - Thai Nguyen University, Vietnam

MỘT SỐ HỢP CHẤT PHENOLIC TỪ LÁ DỨA THƠM (*PANDANUS AMARYLLIFOLIUS*)

ĐỖ HOÀNG GIANG[1,2], BÙI THỊ NHẬT LỆ[2], LƯU HẢI NHI[2], HOÀNG THUỲ DƯƠNG[2] NGUYỄN HẢI ĐĂNG[1], NGUYỄN THỊ THU THUỶ[3], NGÔ THỊ THUÝ NGÂN[4], HOÀNG LÊ TUẤN ANH[2], NGUYỄN NGỌC TÙNG[2], NGUYỄN TIẾN ĐẠT[2]

[1] Đại học Khoa học và Công nghệ Hà Nội, Viện Hàn lâm Khoa học và Công nghệ Việt Nam

[2] Trung tâm Nghiên cứu và Phát triển Công nghệ cao, Viện Hàn lâm Khoa học và Công nghệ Việt Nam

[3] Trung tâm Nhiệt đới Việt - Nga

[4] Trường Đại học Y Dược, Đại học Thái Nguyên

** Tác giả liên hệ: - Nguyễn Tiến Đạt*

- Địa chỉ: Trung tâm Nghiên cứu và Phát triển công nghệ cao, Viện Hàn lâm Khoa học và Công nghệ Việt Nam, số 18 Hoàng Quốc Việt, Cầu Giấy, Hà Nội

- Số điện thoại: 0936401456; Email: ntdat@chtd.vast.vn

- Điểm nổi bật:

- ✓ Lần đầu tiên, bốn hợp chất phenolic gồm vanillin, vanillic acid, *p*-hydroxybenzaldehyde và methyl gallate được phát hiện từ lá dứa thơm (*Pandanus amaryllifolius*).
- ✓ Các hợp chất được phân lập bằng các phương pháp sắc ký và xác định cấu trúc bằng các phương pháp phổ hiện đại.

- Tóm tắt : Bằng các phương pháp sắc ký, bốn hợp chất phenolic bao gồm vanillin (**1**), vanillic acid (**2**), *p*-hydroxybenzaldehyde (**3**) và methyl gallate (**4**) được phân lập từ lá dứa thơm (*Pandanus amaryllifolius*). Cấu trúc của các hợp chất được xác định dựa vào các dữ liệu phổ cộng hưởng từ hạt nhân (NMR) và khối phổ (MS). Đây là lần đầu tiên, các hợp chất này được phát hiện từ loài dứa thơm (*Pandanus amaryllifolius*).

- Từ khoá: *Pandanus, dứa thơm, phenolic, vanillin, methyl gallate.*

1. ĐẶT VẤN ĐỀ

Dứa thơm (*Pandanus amaryllifolius* Roxb) là một loại cây mọc phổ biến tại các quốc gia nhiệt đới và cận nhiệt đới [1, 2]. Ở Việt Nam, lá dứa thơm thường được sử dụng làm thực phẩm, hương liệu, trà nhờ mùi thơm đặc trưng và vị thanh mát. Trong y học cổ truyền, lá dứa còn được dùng để làm dịu đau khớp, giảm đường huyết và hỗ trợ hệ tiêu hóa [1-3]. Các nghiên cứu trước đây về thành phần hoá học cho thấy lá dứa thơm chứa nhiều các alkaloid khung pandamarilactone, pandanamine, pandanusine [4-6]. Các thành phần hoá học của lá dứa thơm thể hiện nhiều hoạt tính sinh học quý như chống oxi hoá [7], kháng khuẩn [8], gây độc tế bào ung thư [9]… Các nghiên cứu trên lá dứa thơm chủ yếu tập trung vào thành phần các alkaloid, trong khi không có nhiều nghiên cứu về các nhóm hợp chất khác được công bố [10]. Trong một nghiên cứu gần đây, chúng tôi đã phân lập được một số hợp chất shikimate ester, megastigmane và glycoside từ lá dứa thơm [11]. Trong nghiên cứu này, chúng tôi trình bày kết quả phân lập và xác định cấu trúc của bốn hợp chất phenolic từ cặn chiết không alkaloid của lá dứa thơm gồm vanillin, vanillic acid, *p*-hydroxybenzaldehyde và methyl gallate.

http://doi.org/vrtc.jtst.n38.11

2. PHƯƠNG PHÁP NGHIÊN CỨU VÀ THỰC NGHIỆM

2.1. Mẫu nghiên cứu

Phần lá của cây dứa thơm (*P. amaryllifolius*) được thu hái tại Tam Đảo, Vĩnh Phúc vào tháng 04 năm 2021 và được giám định bởi TS. Bùi Văn Thanh, Viện Sinh thái và Tài nguyên sinh vật. Mẫu tiêu bản được lưu trữ tại Trung tâm Nghiên cứu Nông dược, Trung tâm Nghiên cứu và Phát triển Công nghệ cao, Viện Hàn lâm Khoa học và Công nghệ Việt Nam.

2.2. Vật liệu và phương pháp nghiên cứu

Sắc ký lớp mỏng được thực hiện trên bản mỏng tráng sẵn TLC Silica gel 60 F_{254} (Merck). Sắc ký cột được thực hiện với các vật liệu hấp phụ Silica gel 60 có kích thước hạt 0,040-0,063 mm (240-430 mesh ASTM) (Merck, CHLB Đức); LiChroprep® RP-18 (0,040-0,063 mm) (Merck, CHLB Đức); Diaion HP-20 (Merck, CHLB Đức). Phổ cộng hưởng từ hạt nhân được đo trên máy Brucker Avance 600 MHz (chất chuẩn nội là Tetramethylsilane - TMS) tại Viện Hóa học, Viện Hàn lâm Khoa học và Công nghệ Việt Nam. Phổ ESI-MS được đo trên thiết bị Thermo LCQ Fleet LC/MS tại Trung tâm Nghiên cứu và Phát triển Công nghệ cao, Viện Hàn lâm Khoa học và Công nghệ Việt Nam.

2.3. Phân lập các chất

Phần lá của loài *P. amaryllifolius* được xử lý và chiết xuất bằng phương pháp acid-base để tách riêng phần cặn chiết chứa alkaloid và phần cặn chiết không chứa alkaloid (PamNA) như đã trình bày trong công bố trước [11]. Phân đoạn PamNA (24,6 g) được phân tách trên cột sắc ký Diaion HP-20, với dung môi giải hấp lần lượt là với nước cất, methanol 30% và 100% thu được các phân đoạn M30W (3,2 g) và M100W (8,1 g). Phân đoạn M100W được tách trên cột sắc ký silica gel với gradient dung môi CH_2Cl_2-MeOH (50/1-1/1, v/v) thu được mười phân đoạn M1-M10. Phân đoạn M6 (55,6 mg) được phân tách trên cột sắc ký silica gel với hệ dung môi rửa giải CH_2Cl_2-MeOH (20/1, v/v) thu được hợp chất **1** (2,8 mg). Phân đoạn M7 (158,5 mg) được phân tách trên cột sắc ký RP-C18 với hệ dung môi rửa giải MeOH-H_2O (2/1, v/v) thu được hai hợp chất **2** (1,1 mg) và **3** (3,2 mg). Phân đoạn M9 (202,5 mg) được phân tách trên cột sắc ký silica gel với hệ dung môi rửa giải EA-MeOH (10/1, v/v) thu được hợp chất **4** (3,4 mg).

Vanillin (1): ESI-MS: *m/z* 153 $[M+H]^+$; ^{1}H NMR (DMSO-d_6, 600 MHz): δ_H 7,38 (1H, d, J = 1,8 Hz, H-2); 6,96 (1H, d, J = 8,4 Hz, H-5); 7,43 (1H, dd, J = 8,4; 1,8 Hz, H-6); 9,77 (1H, s, H-7); 3,92 (3H, s, 3-OCH_3); 10,24 (1H, brs, 4-OH); ^{13}C NMR ($CDCl_3$, 150 MHz): δ_C 128,7 (C-1); 126,0 (C-2); 148,2 (C-3); 153,0 (C-4); 110,7 (C-5); 115,4 (C-6); 191,0 (C-7); 55,6 (3-OCH_3).

Vanillic acid (2): ESI-MS: *m/z* 169 $[M+H]^+$; ^{1}H NMR (CD_3OD, 600 MHz): δ_H 7,58 (1H, d, J = 2,4 Hz, H-2); 6,85 (1H, d, J = 9,0 Hz, H-5); 7,57 (1H, dd, J = 9,0; 2,4 Hz, H-6); 3,92 (3H, s, 3-OCH_3). ^{13}C NMR ($CDCl_3$, 150 MHz): δ_C 121,6 (C-1); 125,3 (C-2); 148,7 (C-3); 154,6 (C-4); 113,9 (C-5); 115,9 (C-6); 170,0 (C-7); 56,4 (3-OCH_3).

***p*-hydroxybenzaldehyde (3)**: ESI-MS: *m/z* 123 $[M+H]^+$; ^{1}H NMR (DMSO-d_6, 600 MHz): δ_H 6,88 (2H, d, J = 7,2 Hz, H-2, 6); 7,76 (2H, d, J = 7,2 Hz, H-3, 5); 9,72 (1H, s).

^{13}C NMR (DMSO-d_6, 150 MHz): δ_C 129,1 (C-1); 132,8 (C-2, 6); 116,5 (C-3, 5); 163,9 (C-4); 191,8 (C-7).

Methyl gallate (4): ESI-MS: *m/z* 185 $[M+H]^+$.^{1}H NMR (CD_3OD, 600 MHz): δ_H 7,06 (2H, s, H-2, 6); 3,83 (3H, s, 7-OCH_3). ^{13}C NMR (CD_3OD, 150 MHz): δ_C 121,5 (C-1); 110,1 (C-2, 6); 146,5 (C-3, 5); 139,8 (C-4); 169,0 (C-7); 52,3 (7-OCH_3).

3. KẾT QUẢ VÀ THẢO LUẬN

Hợp chất **1** thu được dưới dạng chất rắn vô định hình màu trắng. Phổ ESI-MS xuất hiện tín hiệu *m/z* 153 $[M+H]^+$ cho phép xác định khối lượng phân tử của hợp chất là 152 Da. Phổ ^{1}H-NMR của **1** xuất hiện tín hiệu của các proton thuộc hệ vòng thơm ABX tại δ_H 7,38(1H, d, *J* = 1,8 Hz, H-2); 6,96 (1H, d, *J* = 8,4 Hz, H-5); 7,43 (1H, dd, *J* = 8,4; 1,8 Hz, H-6), một tín hiệu methoxy tại δ_H 3,92 (3H, s, 3-OCH_3), một tín hiệu nhóm hydroxy tại δ_H 10,24 (1H, brs, 4-OH) và một tín hiệu proton thuộc nhóm aldehyde tại δ_H 9,77 (1H, s, H-7). Phổ ^{13}C NMR và DEPT xuất hiện tín hiệu carbon aldehyde tại δ_C 191,0 (C-7), ba tín hiệu nhóm CH thuộc vòng thơm tại δ_C 126,0 (C-2), 110,7 (C-5) và 115,4 (C-6), hai tín hiệu carbon vòng thơm liên kết với oxy tại δ_C 148,2 (C-3); 153,0 (C-4) và một nhóm methoxy tại 55,6 (3-OCH_3). Các dữ liệu phổ nói trên cho phép dự đoán cấu trúc của một dẫn xuất benzaldehyde. So sánh các dữ liệu này với tài liệu tham khảo, có thể xác định hợp chất **1** là vanillin [12].

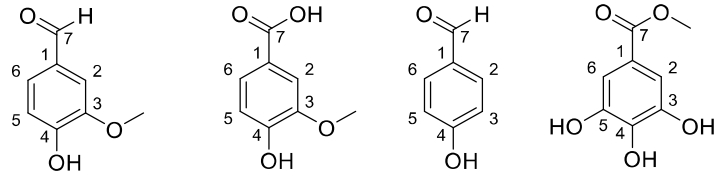

Hình 1. Cấu trúc hoá học của các hợp chất **1-4**

Hợp chất **2** thu được dưới dạng chất rắn vô định hình màu trắng. Phổ ESI-MS xuất hiện tín hiệu *m/z* 169 $[M+H]^+$ cho phép xác định khối lượng phân tử 168 Da của **2**. Phổ ^{1}H-NMR của **2** xuất hiện tín hiệu của các proton thuộc hệ vòng thơm ABX tại δ_H 7,58 (1H, d, *J* = 2,4 Hz, H-2); 6,85 (1H, d, *J* = 9,0 Hz, H-5); 7,57 (1H, dd, *J* = 9,0; 2,4 Hz, H-6), một tín hiệu methoxy tại δ_H 3,92 (3H, s, OCH_3). Phổ ^{13}C NMR và DEPT xuất hiện tín hiệu nhóm carboxyl tại δ_C 170,0 (C-7), ba tín hiệu nhóm methine vòng thơm tại δ_C 125,3 (C-2), 113,9 (C-5), 115,9 (C-6), hai tín hiệu carbon vòng thơm liên kết với oxy tại δ_C 148,7 (C-3), 154,6 (C-4) và một nhóm methoxy tại 56,4 (3-OCH_3). Dữ liệu phổ của hợp chất 2 hầu như tương đồng với hợp chất **1** ngoại trừ sự khác biệt giữa tín hiệu nhóm carboxyl ở hợp chất 2 so với nhóm aldehyde ở hợp chất **1**. Điều này được khẳng định thông qua chênh lệch 16 Da trong khối lượng phân tử giữa hai hợp chất. Từ các dữ liệu trên, kết hợp với các dữ liệu tham khảo, xác định hợp chất **2** là vanillic acid [12].

Hợp chất **3** thu được dưới dạng chất rắn vô định hình màu trắng với khối lượng phân tử 122 Da thông qua tín hiệu *m/z* 123 $[M+H]^+$ trên phổ ESI-MS. Phổ ^{1}H-NMR của hợp chất **3** xuất hiện tín hiệu của bốn proton thuộc hệ vòng thơm A_2B_2 tại δ_H 6,88 (2H, d,

J = 7,2 Hz, H-2, 6); 7,76 (2H, d, J = 7,2 Hz, H-3, 5) và một tín hiệu proton thuộc nhóm aldehyde tại δ_H 9,72 (1H, s, H-7). Phổ ^{13}C NMR và DEPT xuất hiện tín hiệu carbon aldehyde tại δ_C 191,8 (C-7), các tín hiệu nhóm methine trong vòng thơm tại δ_C 132,8 (C-2, 6); 116,5 (C-3, 5) và một tín hiệu carbon vòng thơm liên kết trực tiếp với oxy tại δ_C 163,9 (C-4). So sánh dữ liệu phổ trên với tài liệu tham khảo, có thể xác định hợp chất **3** là *p*-hydroxybenzaldehyde [13]

Hợp chất **4** thu được dưới dạng chất rắn vô định hình màu trắng. Phổ ESI-MS xuất hiện tín hiệu *m/z* 185 $[M+H]^+$ cho phép xác định khối lượng phân tử của hợp chất là 184 Da. Trên phổ ^{1}H NMR của **4** xuất hiện tín hiệu của hai proton thơm đối xứng nhau tại δ_H 7,06 (2H, s, H-2, 6) và một nhóm methoxy tại δ_H 3,83 (3H, s, 7-OCH_3). Phổ ^{13}C NMR và DEPT xuất hiện tín hiệu của carbon methine vòng thơm tại δ_C 110,1 (C-2, 6), tín hiệu của hai carbon thơm liên kết với oxy đối xứng nhau tại δ_C 146,5 (C-3, 5), và một carbon thơm liên kết với oxy tại δ_C139,8 (C-4) và một nhóm methoxy tại δ_C 52,3 (7-OCH_3). So sánh dữ liệu phổ NMR của hợp chất **4** với tài liệu tham khảo cho phép xác định đây là hợp chất methyl gallate [14].

Như vậy, từ cặn chiết không chứa alkaloid từ lá dứa thơm (*P. amaryllifolius*) chúng tôi đã phân lập được bốn hợp chất phenolic. Các nghiên cứu trước đây tập trung chủ yếu vào thành phần alkaloid của lá dứa thơm [4, 5, 15, 16]. Bên cạnh đó, một số hợp chất phenolic như *p*-hydroxybenzoic acid, gallic acid, ferulic acid, coumaric acid… cũng từng được phát hiện từ rễ và lá của loài *P. amaryllifolius* [9]. Mặc dù vậy, công bố này là lần đầu tiên phát hiện bốn hợp chất gồm vanillin (**1**), vanillic acid (**2**), *p*-hydroxybenzaldehyde (**3**), methyl gallate (**4**) từ lá dứa thơm (*P. amaryllifolius*). Các hợp chất này đã được chứng minh là có hoạt tính thu dọn nhiều loại gốc tự do như DPPH, ABTS, OH… [17, 18] hoặc hoạt tính kháng khuẩn [19], kháng virus [20]… Phát hiện này góp phần làm giàu thêm các thông tin về thành phần hoá học của loài thực vật này, đồng thời cho thấy tiềm năng lớn về khả năng chống gốc tự do, chống oxi hoá và nhiều hoạt tính sinh học khác của lá dứa thơm.

4. KẾT LUẬN

Từ phần lá của cây dứa thơm *P. amaryllifolius,* bốn hợp chất phenolic là vanillin (**1**), vanillic acid (**2**), *p*-hydroxybenzaldehyde (**3**), methyl gallate (**4**) đã được phân lập. Đây là lần đầu tiên các hợp chất này được tìm thấy trong thành phần hoá học của lá dứa thơm. Kết quả của nghiên cứu này góp phần làm sáng tỏ thêm về thành phần của lá dứa thơm, làm cơ sở cho các nghiên cứu sâu hơn về tác dụng của loại nguyên liệu thực phẩm này đối với sức khoẻ con người.

Lời cảm ơn: *Nghiên cứu này được thực hiện với sự hỗ trợ của Viện Hàn lâm Khoa học và Công nghệ Việt Nam trong khuôn khổ nhiệm vụ "Phát triển nhóm nghiên cứu xuất sắc hạng I về ứng dụng các phương pháp phân tích hiện đại trong nghiên cứu chất lượng và an toàn thực phẩm", mã số: NCXS01.02/23-25.*

Tuyên bố về đóng góp của các tác giả: *Đỗ Hoàng Giang, Nguyễn Thị Thu Thuỷ: Xây dựng tổng quan, soạn bản thảo bài báo. Nguyễn Tiến Đạt: Rà soát và chịu trách nhiệm nội dung bài báo. Ngô Thị Thuý Ngân, Nguyễn Hải Đăng: Thu thập mẫu nghiên cứu. Hoàng Thuỳ Dương: Xử lý mẫu sau khi thu thập. Lưu Hải Nhi: Chiết xuất mẫu. Bùi*

Thị Nhật Lệ: Phân lập các hợp chất bằng các phương pháp sắc ký. Nguyễn Ngọc Tùng, Hoàng Lê Tuấn Anh: Giải cấu trúc của các hợp chất đã phân lập.

TÀI LIỆU THAM KHẢO

1. Đỗ Tất Lợi, *Những cây thuốc và vị thuốc Việt Nam*. NXB Y học, Hà Nội, 2004, tr. 904.
2. Phạm Hoàng Hộ, *Cây cỏ Việt Nam*. NXB Trẻ, Hà Nội, 2003, tr. 134.
3. Đỗ Huy Bích et al., *Cây thuốc và động vật làm thuốc ở Việt Nam*. NXB Khoa học và Kỹ thuật, Hà Nội, 2006, tr. 355.
4. H. Takayama, T. Ichikawa, M. Kitajima, M. G. Nonato and N. Aimi, *A new alkaloid, pandanamine; finding of an anticipated biogenetic intermediate in Pandanus amaryllifolius Roxb*, Tetrahedron Letters, Vol. 42, No. 16, pp: 2995-2996, 2001.
5. H. Takayama, T. Ichikawa, M. Kitajima, M. G. Nonato and N. Aimi, *Isolation and Structure elucidation of two new alkaloids, Pandamarilactonine-C and -D, from Pandanus amaryllifolius and revision of relative stereochemistry of Pandamarilactonine-A and -B by total synthesis*, Chemical and Pharmaceutical Bulletin, Vol. 50, No. 9, pp: 1303-1304, 2002.
6. A. N. H. Azhar, N. A. Amran, S. Yusup and M. H. Mohd Yusoff, *Ultrasonic extraction of 2-Acetyl-1-Pyrroline (2AP) from Pandanus amaryllifolius Roxb. using ethanol as solvent*, Molecules, Vol. 27, No. 15, pp: 4906, 2022.
7. N. S. Musa, N. M. Ramli, J. Saidin and Y. Andriani, *Antioxidant and cytotoxicity properties of ethyl acetate fractions of Pandanus tectorius fruit against HeLa cell lines*, ALOTROP Jurnal Pendidikan dan Ilmu Kimia, 2017, Vol. 1, No. 2, pp:106-112, 2017.
8. N. Asyikin Md Zaki, S. Abd Hashib, U. Kalthum Ibrahim and P. Ani Narisa Ahmad Bakhtiar, *Total phenolic content and antioxidant activity of Pandanus amaryllifolius by soaking and microwave-assisted extraction*, IOP Conference Series: Materials Science and Engineering, Vol. 778, No. 1, pp: 012155, 2020.
9. A. Ghasemzadeh, H. Z. E. Jaafar, *Profiling of phenolic compounds and their antioxidant and anticancer activities in pandan (Pandanus amaryllifolius Roxb.) extracts from different locations of Malaysia*, BMC Complementary and Alternative Medicine, Vol. 13, No. 1, pp: 341, 2013.
10. W. Wang et al., *Botany, phytochemistry, pharmacology, and applications of Pandanus amaryllifolius Roxb.: A review*, Fitoterapia, Vol 177, pp: 106144, 2024.
11. Đỗ Hoàng Giang et al., *Một số hợp chất shikimate ester, megastigmane và glycoside từ lá dứa thơm (Pandanus amaryllifolius)*, Tạp chí Khoa học và Công nghệ Nhiệt đới, 2024, Vol 35, No. 9, pp: 82-88, 2024.
12. J. S. Challice, R. S. T. Loeffler and A. H. Williams, *Structure of calleryanin and its benzylic esters from Pyrus and Prunus*, Phytochemistry, Vol. 19, No. 11, pp: 2435-2437, 1980.

13. J. Magano, M. H. Chen, J. D. Clark and T. Nussbaumer, *2-(Diethylamino) ethanethiol, a new reagent for the odorless deprotection of aromatic methyl ethers*, The Journal of Organic Chemistry, Vol. 71, No. 18, pp: 7103-7105, 2006.
14. R. Subramanian, M. Chandra, S. Yogapriya, S. Aravindh and K. Ponmurugan, *Isolation of methyl gallate from mango twigs and its anti-biofilm activity*, Journal of Biologically Active Products from Nature, Vol. 6, No. 5-6, pp: 383-392, 2016.
15. H. Takayama, T. Ichikawa, M. Kitajima, M. G. Nonato and N. Aimi, *Isolation and characterization of two new alkaloids, norpandamarilactonine-A and -B, from Pandanus amaryllifolius by spectroscopic and synthetic methods*, Journal of Natural Products, Vol. 64, No. 9, pp: 1224-1225, 2001.
16. M. A. Tan, M. Kitajima, N. Kogure, M. G. Nonato and H. Takayama, *Isolation of Pandamarilactonine-H from the Roots of Pandanus amaryllifolius and synthesis of epi-Pandamarilactonine-H*, Journal of Natural Products, Vol. 73, No. 8, pp: 1453-1455, 2010.
17. A. Tai, T. Sawano, F. Yazama and H. Ito, *Evaluation of antioxidant activity of vanillin by using multiple antioxidant assays*, Biochimica et Biophysica Acta (BBA) - General Subjects, Vol. 1810, No. 2, pp: 170-177, 2011.
18. A. Tai, T. Sawano and H. Ito, *Antioxidative properties of vanillic acid esters in multiple antioxidant assays*, Bioscience, Biotechnology, and Biochemistry, Vol. 76, No. 2, pp: 314-318, 2012.
19. O. Flores-Maldonado, J. Dávila-Aviña, G.M. González, M. A. Becerril-García and A.L. Ríos-López, *Antibacterial activity of gallic acid and methyl gallate against emerging non-fermenting bacilli*, Folia Microbiologica, 2024, Online ahead of print.
20. C. R. Wang, R. Zhou, T. B. Ng, J. H. Wong, W. T. Qiao and F. Liu, *First report on isolation of methyl gallate with antioxidant, anti-HIV-1 and HIV-1 enzyme inhibitory activities from a mushroom (Pholiota adiposa)*, Environmental Toxicology and Pharmacology, Vol 37, No 2, pp: 626-637, 2014.

ABSTRACT

PHENOLICS FROM LEAVES OF *PANDANUS AMARYLLIFOLIUS*

Four phenolic compounds such as vanillin (**1**), vanillic acid (**2**), *p*-hydroxybenzaldehyde (**3**), and methyl gallate (**4**) were isolated from leaves of *Pandanus amaryllifolius*, using chromatographic methods. Structures of the isolated compounds were elucidated by spectroscopic data, such as NMR and MS. These four compounds were determined for the first time from the species *Pandanus amaryllifolius.*

Keywords: *Pandanus, Pandanus amaryllifolius, phenolic, vanillin, methyl gallate*

Nhận bài ngày 13 tháng 12 năm 2024
Phản biện xong ngày 17 tháng 02 năm 2025
Hoàn thiện ngày 19 tháng 02 năm 2025

SUPPLEMENTARY DOCUMENTS

VIỆN HÀN LÂM
KHOA HỌC VÀ CÔNG NGHỆ VN
TRƯỜNG ĐẠI HỌC KHOA HỌC VÀ CÔNG NGHỆ HÀ NỘI

Số: 1238/QĐ-ĐHKHCN

CỘNG HÒA XÃ HỘI CHỦ NGHĨA VIỆT NAM
Độc lập - Tự do - Hạnh phúc

Hà Nội, ngày 10 tháng 12 năm 2025

QUYẾT ĐỊNH
Về việc thay đổi tên đề tài luận án tiến sĩ của nghiên cứu sinh Đỗ Hoàng Giang

HIỆU TRƯỞNG
TRƯỜNG ĐẠI HỌC KHOA HỌC VÀ CÔNG NGHỆ HÀ NỘI

Căn cứ Quyết định số 2067/QĐ-TTg ngày 09/12/2009 của Thủ tướng Chính phủ về việc thành lập Trường Đại học Khoa học và Công nghệ Hà Nội (ĐHKHCNHN);

Căn cứ Quyết định số 2557/QĐ-TTg ngày 30/12/2016 của Thủ tướng Chính phủ về việc ban hành Quy chế Tổ chức và Hoạt động của Trường ĐHKHCNHN;

Căn cứ Quyết định số 307/QĐ-ĐHKHCN ngày 04/04/2025 của Hiệu trưởng Trường ĐHKHCNHN về việc ban hành Quy chế đào tạo trình độ tiến sĩ của Trường ĐHKHCNHN;

Căn cứ Quyết định số 1070/QĐ-ĐHKHCN ngày 24/10/2022 về việc công nhận đề tài luận án và người hướng dẫn của nghiên cứu sinh Đỗ Hoàng Giang;

Căn cứ Biên bản họp Hội đồng đánh giá luận án cấp cơ sở đối với nghiên cứu sinh Đỗ Hoàng Giang;

Căn cứ Đơn đề nghị về việc điều chỉnh tên đề tài của nghiên cứu sinh Đỗ Hoàng Giang và tập thể người hướng dẫn;

Xét đề nghị của Trưởng phòng Quản lý đào tạo.

QUYẾT ĐỊNH:

Điều 1. Thay đổi tên đề tài luận án Tiến sĩ của nghiên cứu sinh (NCS) Đỗ Hoàng Giang với các thông tin như sau:

Họ và tên: **Đỗ Hoàng Giang**

Mã NCS: D22.PMAB.004

Ngày sinh: 12/07/1991

Ngành: Công nghệ Sinh học nông, y, dược

Tên đề tài theo Quyết định công nhận NCS: Study on phytochemical constituents and bioactivities of natural products from Pandanus species in Vietnam/ Nghiên cứu thành phần hóa học và hoạt tính sinh học của một số loài thuộc chi Pandanus tại Việt Nam.

Tên đề tài mới: Phytochemical constituents and bioactivities of Pandanus tectorius and Pandanus amaryllifolius/ *Nghiên cứu thành phần hóa học và hoạt tính sinh học của loài dứa dại (Pandanus tectorius) và loài dứa thơm (Pandanus amaryllifolius).*

Tập thể cán bộ hướng dẫn và thời gian đào tạo không thay đổi.

Điều 2. Trưởng khoa Khoa học Sự sống, Trưởng phòng Quản lý đào tạo, Trưởng phòng Bảo đảm chất lượng và Khảo thí, Chánh văn phòng, cán bộ hướng dẫn, NCS Đỗ Hoàng Giang và các bộ phận có liên quan chịu trách nhiệm thi hành Quyết định này./.

Nơi nhận:
- Như Điều 2;
- HT;
- Các PHT;
- Lưu: VT, KHSS, QLĐT.L3

HIỆU TRƯỞNG CHÍNH

TRƯỜNG ĐẠI HỌC KHOA HỌC VÀ CÔNG NGHỆ HÀ NỘI

Jean-Marc Lavest

VIETNAM ACADEMY
OF SCIENCE AND TECHNOLOGY
UNIVERSITY OF SCIENCE AND TECHNOLOGY OF HANOI

No. 1238/QĐ-ĐHKHCN

SOCIALIST REPUBLIC OF VIETNAM
Independence - Freedom - Happiness

Hanoi, December 10 ,2025

DECISION
On the approval of the amendment to the thesis title of PhD student Do Hoang Giang
RECTOR OF UNIVERSITY OF SCIENCE AND TECHNOLOGY OF HANOI

Pursuant to Decision No. 2067/QĐ-TTg dated December 9, 2009 of the Prime Minister on the establishment of University of Science and Technology in Hanoi (USTH);

Pursuant to Decision No. 2557/QĐ-TTg dated December 30, 2016 of the Prime Minister on the Regulations on the organization and operation of USTH;

Pursuant to Decision No. 307/QĐ-ĐHKHCN dated April 04, 2025 of the Rector of USTH on issuing the Regulation of doctoral training;

Pursuant to Decision No. 1070/QĐ-ĐHKHCN dated October 24, 2022 of the Rector of USTH on the recognition of the thesis title and thesis supervisors for PhD student Do Hoang Giang;

Pursuant to the Report of the internal Jury for PhD student Do Hoang Giang;

Pursuant to the request for amendment of the PhD thesis title submitted by PhD student Do Hoang Giang and his supervisors;

At the proposal of the Director of the Department of Academic Affairs.

DECIDES

Article 1. To amend the PhD thesis title of PhD student Do Hoang Giang as follows:

Full name: **Do Hoang Giang**

PhD Student ID: D22.PMAB.004

Date of birth: 12/07/1991

Program: Pharmacological, Medical and Agronomical Biotechnology

Thesis title as stated in the recognition decision: Study on phytochemical constituents and bioactivities of natural products from Pandanus species in Vietnam.

New thesis title: Phytochemical constituents and bioactivities of Pandanus tectorius and Pandanus amaryllifolius.

Supervisors and training duration remain unchanged.

Article 2. The Director of the Department of Life Sciences, the Director of the Department of Academic Affairs, the Director of the Department of Quality Assurance and Examination, the Director of the Administration, the PhD supervisors and PhD student Do Hoang Giang shall be responsible for the implementation of this Decision./.

Recipients:
- As Article 3;
- Rector;
- Vice-Rectors;
- Archive: Admin, LS, DAA.L3

PRINCIPAL RECTOR
(Signed and sealed)
Jean-Marc Lavest

VIỆN HÀN LÂM
KHOA HỌC VÀ CÔNG NGHỆ VN
TRƯỜNG ĐẠI HỌC KHOA HỌC VÀ CÔNG NGHỆ HÀ NỘI

Số: 65 /QĐ-ĐHKHCN

CỘNG HÒA XÃ HỘI CHỦ NGHĨA VIỆT NAM
Độc lập – Tự do – Hạnh phúc

Hà Nội, ngày 29 tháng 01 năm 2026

QUYẾT ĐỊNH
Về việc thành lập Hội đồng đánh giá luận án Tiến sĩ cấp trường đối với nghiên cứu sinh Đỗ Hoàng Giang

HIỆU TRƯỞNG
TRƯỜNG ĐẠI HỌC KHOA HỌC VÀ CÔNG NGHỆ HÀ NỘI

Căn cứ Quyết định số 2067/QĐ-TTg ngày 09/12/2009 của Thủ tướng Chính phủ về việc thành lập Trường Đại học Khoa học và Công nghệ Hà Nội (ĐHKHCNHN);

Căn cứ Quyết định số 2557/QĐ-TTg ngày 30/12/2016 của Thủ tướng Chính phủ về việc ban hành Quy chế tổ chức và hoạt động của Trường ĐHKHCNHN;

Căn cứ Quyết định số 307/QĐ-ĐHKHCN ngày 04/04/2025 của Hiệu trưởng Trường ĐHKHCNHN về việc ban hành Quy chế đào tạo trình độ tiến sĩ;

Căn cứ Quyết định số 1070/QĐ-ĐHKHCN ngày 24/10/2022 của Hiệu trưởng Trường ĐHKHCNHN về việc công nhận nghiên cứu sinh Đỗ Hoàng Giang, tên đề tài và người hướng dẫn luận án tiến sĩ;

Căn cứ Quyết định số 1009/QĐ-ĐHKHCN ngày 10/10/2025 của Hiệu trưởng Trường ĐHKHCNHN về việc thành lập Hội đồng đánh giá luận án tiến sĩ cấp cơ sở đối với nghiên cứu sinh Đỗ Hoàng Giang;

Căn cứ Biên bản họp Hội đồng đánh giá luận án tiến sĩ cấp cơ sở đối với nghiên cứu sinh Đỗ Hoàng Giang ngày 24/10/2025;

Căn cứ Quyết định số 1238/QĐ-ĐHKHCN ngày 10/12/2025 của Hiệu trưởng Trường ĐHKHCNHN về việc công nhận thay đổi tên đề tài luận án tiến sĩ của nghiên cứu sinh Đỗ Hoàng Giang;

Xét đề nghị của Trưởng phòng Quản lý đào tạo.

QUYẾT ĐỊNH:

Điều 1. Thành lập Hội đồng đánh giá luận án Tiến sĩ cấp trường đối với nghiên cứu sinh Đỗ Hoàng Giang, mã số nghiên cứu sinh D22.PMAB.004, ngành Công nghệ Sinh học nông, y, dược.

Tên đề tài luận án: Phytochemical constituents and bioactivities of Pandanus tectorius and Pandanus amaryllifolius.

Danh sách thành viên hội đồng tại Phụ lục kèm theo Quyết định này.

Điều 2. Hội đồng có trách nhiệm tổ chức đánh giá luận án Tiến sĩ của Nghiên cứu sinh theo quy chế đào tạo hiện hành và tự giải thể sau khi hoàn thành nhiệm vụ.

Điều 3. Trưởng phòng Quản lý đào tạo, Trưởng khoa Khoa học Sự sống, Chánh văn phòng, Trưởng phòng Bảo đảm chất lượng và Khảo thí, Trưởng phòng Kế toán – Tài chính và các thành viên có tên tại Điều 1 chịu trách nhiệm thi hành quyết định này./.

Nơi nhận:
- Như Điều 3;
- HT;
- Các PHT;
- Lưu: VT, KTTC, KHSS, QLĐT.L5.

HIỆU TRƯỞNG CHÍNH

TRƯỜNG ĐẠI HỌC KHOA HỌC VÀ CÔNG NGHỆ HÀ NỘI

Jean-Marc Lavest

DANH SÁCH HỘI ĐỒNG ĐÁNH GIÁ LUẬN ÁN TIẾN SĨ CẤP TRƯỜNG
ĐỐI VỚI NGHIÊN CỨU SINH ĐỖ HOÀNG GIANG

(Kèm theo Quyết định số 65 /QĐ-ĐHKHCN ngày 29 / 01 /2026)

STT	Thành viên Hội đồng	Nơi công tác	Chức danh Hội đồng
1	GS.TS. Nguyễn Văn Hùng	Viện Hóa học, Viện Hàn lâm Khoa học và Công nghệ Việt Nam	Chủ tịch
2	GS.TS. Marie- Genevieve Dijoux- Franca	Trường Đại học Lyon 1, Pháp	Phản biện
3	PGS.TS. Vũ Đức Lợi	Học viện Y- dược học Cổ truyền Việt Nam	Phản biện
4	PGS.TS. Lê Nguyễn Thành	Viện Dược liệu	Phản biện
5	PGS.TS. Nguyễn Phi Hùng	Viện Hóa học, Viện Hàn lâm Khoa học và Công nghệ Việt Nam	Ủy viên
6	TS. Phạm Hoàng Nam	Trường ĐHKHCNHN, Viện Hàn lâm Khoa học và Công nghệ Việt Nam	Ủy viên
7	TS. Nguyễn Hữu Nghị	Trường ĐHKHCNHN, Viện Hàn lâm Khoa học và Công nghệ Việt Nam	Ủy viên, Thư ký

Danh sách gồm 07 thành viên./.

UNIVERSITY OF SCIENCE & TECHNOLOGY OF HANOI
UNIVERSITE DES SCIENCES ET DES TECHNOLOGIES DE HANOI
TRƯỜNG ĐẠI HỌC KHOA HỌC & CÔNG NGHỆ HÀ NỘI

PhD Thesis Examination Jury
Jury Report

Time: From 2:00 PM- 5:00 PM, April 24, 2026
Location: Meeting Room 402, USTH Building

I. JURY MEMBERS:

No.	Members	Institutions	Position in the jury
1	Prof.Dr. Nguyen Van Hung	Institute of Chemistry, Vietnam Academy of Science and Technology	Chairman
2	Prof.Dr. Marie- Genevieve Dijoux- Franca	University of Lyon 1, France	Reviewer
3	Assoc.Prof. Vu Duc Loi	Viet Nam University of Traditional Medicine	Reviewer
4	Assoc.Prof. Le Nguyen Thanh	National Institute Medicinal Materials	Reviewer
5	Assoc.Prof. Nguyen Phi Hung	Institute of Chemistry, Vietnam Academy of Science and Technology	Member
6	Dr. Pham Hoang Nam	USTH, Vietnam Academy of Science and Technology	Member
7	Dr. Nguyen Huu Nghi	USTH, Vietnam Academy of Science and Technology	Member, Secretary

II. PHD STUDENT:

Full name	**Do Hoang Giang**
Student ID	D22.PMAB.004
Program	Pharmacological, Medical and Agronomical Biotechnology
Thesis title	Phytochemical constituents and bioactivities of Pandanus tectorius and Pandanus amaryllifolius/ *Nghiên cứu thành phần hóa học và hoạt tính sinh học của loài dứa dại (Pandanus tectorius) và loài dứa thơm (Pandanus amaryllifolius).*
Supervisor	Assoc. Prof. Nguyen Tien Dat, Center for Research and Technology Transfer, Vietnam Academy of Science and Technology
Co-supervisor	Assoc. Prof. Nguyen Hai Dang, USTH

III. JURY COMMENTS:

1. Assoc. Prof. DIJOUX-FRANCA Marie G - reviewer

- Well presented, extraction, identification, fully detected with strong NMR spectra. The candidate has rich academic achievements from CV.
- The optimization experiment is interesting
- What is the global context of this study, what is objectives of the study, the two species? Is there any global context for the product from the extract?
- The two new compounds identified from this study. Do you think that methyl ester could be affected by the extraction solvent since the author used methanol for extraction.
- What do you think, how to complete the study considering the location, season, and environmental conditions?

2. Assoc. Prof. Dr. Le Nguyen Thanh- reviewer

- The thesis is logically structured to progress from broad screening to targeted isolation, then to process optimization. The optimization studies have direct implications for developing standardized extracts for nutraceutical or pharmaceutical applications
- PhD student have used comprehensive analytical methods combination of colorimetric assays (TPC, TFC, TSC, TAC), chromatographic isolation (column chromatography, preparative HPLC), and advanced spectroscopic techniques (NMR, HR-MS, ECD). The use of ECD and Snatzke's $Mo_2(OAc)_4$-induced ECD method for determining absolute configurations of the new benzofuran epimers represents modern practice in natural product chemistry.
- The thesis appears to be well-organized into chapters and has already resulted in multiple publications, which is a strong indicator of quality. Consistent chapter format: Each chapter begins with an overview and ends with a summary, aiding readability

The introduction mentions traditional uses for kidney stones and edema. Your bioassays focused on antioxidant, anti-inflammatory, and cytotoxic activities. How do these relate to the traditional indications ?

Why did not evaluate the biological activity of isolated compound from *P. amaryllifolius?*

3. Assoc. Prof. Vu Duc Loi- reviewer

+ The introduction should include a more comprehensive overview of the genus, covering botanical characteristics, chemical constituents, and biological activities.

+ The methodology section should further clarify the quantitative methods used for different compounds groups. If any methods are self-developed, proper method validation should be carried out before they are applied.

+ In the bioactivity section, IC_{50} values should be presented more comprehensively. In addition, the study would be more logical if fraction screening is performed first, followed by chemical investigation of the most active fraction.

+ An initial screening across several *Pandanus species* within the genus, and then select the two most promising ones for more in-depth investigation.

+ The conclusions should be closely aligned with the stated objectives of the thesis and should clearly distinguish the results obtained for each species, in terms of chemical composition and biological activity.

+ A separate section on recommendations

+ The reference list should be updated by reducing the number of references published before 2010.

Two Questions for the candidate as follows:

1. Why did the author not investigate all plant parts (leaves, fruits, roots, aerial parts) as described in the introduction for other species in the genus?

2. For the proposed synergism in *P. amaryllifolius*, what specific phenolic-alkaloid interactions were hypothesized, and why was no further fractionation performed to confirm this?

4. Assoc. Prof. Dr. Nguyen Phi Hung- Jury member

1. Please Provide:

- Picture or the image of the two plants/plant materials
- The information describing about these plant materials into the Result part or Appendix

2. In the Quantitative analysis:

- Table 3.1, in page 27: The author should check again the value present for TPC, TFC, and TAC (in %). Because the result showed very high value unit in % for the TAC (total alkaloid content) over 21,76% as calculated for the dry weight. The author should clarify whether the calculation is based on the original dry sample or the extract.

3. In the bioactivity test:

- Page 32, Table 3.3: The author should give a discussion why there is a significant difference in biological activity between the two test samples Pama-1 and Pama-2.
- Table 3.4: The value should be presented as % Inhibition rather than % cell survival.

4. Chapter 4: Isolation of compounds from Pandanus tectorius leaves

- Need provide the detail HPLC chromatographic condition, such as HPLC model, column, mobile phase (solvent system), flowrate in mL, UV scanning, and also the retention time of each compound.
- In other hand, the isolation of every compounds should also be described in detail.
- Table 4.1: need to revise the NMR data for compound Graphostrin D
- Table 4.2: need to provide the 1H and 13C NMR data for the methoxy moiety of the new compound Pt2.

5. The Appendix needs providing:

+ NMR spectroscopic data of all isolated compounds;
+ MS spectral data of two new compounds PT1 and Pt2;
+ The HPLC chromatographic profile and its condition;
+ The hard copies of all publications belong to this thesis.

Questions

Optimize fruit extraction but chemical constituents is investigated from leaf.

In the case of compounds Pt1 and Pt2, can you explain why the C value and also the proton value of the methoxy (-OCH3) group attached to the acetyl group appeared (resonated) at around 51.27 ppm and 3,79 ppm (the more up field)?

Usually, for an OCH3 group attached to a phenyl, so the C value often appeared at around 55 – 60 ppm, the proton value often appeared at around 3.8 – 4.1 ppm.

5. Dr. Pham Hoang Nam- Jury member

The topic is of relevance to natural product chemistry, plant-based drug discovery, and functional food development.

The methodological framework is well-constructed and appropriate for the stated objectives

The thesis is written in clear, generally accurate scientific English. The candidate demonstrates command of the relevant technical vocabulary in natural product chemistry and pharmacognosy

The fact that all major findings have been independently peer-reviewed and published prior to the defense is a strong indicator of the overall scientific rigor of the work

The candidate demonstrates a solid general scientific background in natural product chemistry, pharmacognosy, and analytical methodology

Written English is at an acceptable academic standard throughout the thesis. Based on the written work, the candidate shows a clear understanding of the research field and is capable of conducting and communicating independent doctoral-level research.

Questions

1. explicitly connect the poor PLSR predictive performance for A549 cytotoxicity to the compound-specific findings of Chapter 4; and

2. discuss the absence of individual saponin characterization as a limitation and outline it as a concrete priority for future work

3. How about the stability of the compounds during further food processing.

6. Dr. Nguyen Huu Nghi- Jury member

Table 3.1. Quantitative levels of TPC, TFC, TSC, TAC. The candidate has quantified bioactive compounds in leaves and fruits of *P. tectorius* and *P. amaryllifolius*. However, the method regarding sampling is confusing. TPC and TFC were measured by taking dried sample powders. The TAC was measured based on the extract (no information about the dried or wet extract). TSC was measured by 50 microliter extract. An explanation of the units for each measurement is necessary.

Table 4.7. The values of DPPH, hydroxyl, and alpha amylase assays were different from those in table 3.1. However, the method is the same. You should make it consistently.

The optimization design in Table 5.1, regarding temperature at 80°C is not reasonable since ethanol is evaporated at 78°C

Some author names in references are wrong and not consistent; check the hard copy of the manuscript

Discussion on extraction and biological activities in the manuscript is quite limited.

Questions

1. Why did you try to approach saponins in these plants since the literature review did not mention saponin as a common compound of these species?
2. What would be the future formulation of health products that you suggest from these herbs?

7. Prof. Dr. Nguyen Van Hung – Jury chairman

Can you summarize why did you chose the two species for your study?

- The study and investigation to discover the bioactive compounds from Plants is the impressive interest of the scientists in high-ranking research institutes in the field of Phytochemisty over the World

- In the Abstract and Introduction of the Thesis , PhD student has very effectively summarized and clarified the objectives and obtained results of the PhD Research Work
- The PHD student has applied an integrated workflow combining plant collection and authentication from multiple locations in Vietnam, solvent extraction and fractionation, quantitative determination of major phytochemical groups, Bioactivities are evaluated in vitro, and structure elucidation are performed using advanced spectroscopic techniques

In the PhD Thesis have been obtained

- From P. tectorius leaves, two new benzofuran epimers (Pandanusfuran A and B) and four known lignans are isolated and investigated biological activities
- Optimization of P. tectorius fruit extraction identifies seven validated conditions balancing TPC and TSC. Under these conditions, Phenolic-enriched extracts show superior antioxidant activity, while saponin-enriched extracts demonstrate stronger NO inhibition, with increased cytotoxicity observed at very high saponin levels.
- For P. amaryllifolius leaves, the phenolic enrichment exhibits potent antioxidant activity (IC_{50} values close to those of ascorbic acid and catechin) and enhanced NO inhibition via phenolic-alkaloid synergism. Sixteen compounds are isolated, including shikimate derivatives, simple phenolics, and a lignan glycoside
- These findings suggest that Pandanusfurans represent promising multifunctional scaffolds with moderate antioxidant, antidiabetic, and selective anticancer potential, whereas the lignans mainly contribute to antioxidant activity
- Structure: The thesis is logically structured with six chapters progressing from introduction and methodology to screening, compound isolation, extraction optimization, and conclusion.
- References: The reference list consisted of 105 entries, diverse (including books, journal articles,and theses), and relevant. Citations are used appropriately to support major statements

IV. CONCLUSION:

☑ The title of the thesis is appropriate for the program of Pharmacological, Medical and Agronomical Biotechnology (Code: 9420201).

☑ The thesis does not overlap with any previously published works or theses.

☐ The main scientific conclusions, new findings, and contributions of the thesis are as follows:

- From *P. tectorius* leaves, two new benzofuran epimers (Pandanusfurans A and B) and four lignans were elucidated. The lignans contributed to antioxidant capacity, whereas the benzofurans, showed weaker antioxidant activity but exhibited α-amylase inhibition and showed selective cytotoxicity toward A549.
- This study successfully optimized the extraction process of phenolic- and saponin enriched fractions from *Pandanus tectorius* fruit using the Box–Behnken Design. Phenolic-rich extracts obtained under high ethanol concentration and temperature conditions exhibited strong antioxidant activity.
- Saponin-rich extracts obtained under lower ethanol concentration and longer extraction times, showed good nitric oxide inhibitory effects, albeit with potential cytotoxicity at higher doses
- The phytochemical investigation of the phenolic enrichment from *P. amaryllifolius* leaves led to the isolation of 16 compounds, including 3 lignans and 9 benzoate derivatives, together with 3 shikimates and 1 glycoside. Except for 4-hydroxybenzoic acid, the other compounds were identified for the first time from the plant.
- The optimized phenolic enrichment from *Pandanus amaryllifolius* leaves demonstrated substantial antioxidant and NO inhibition activities, surpassing the efficacy of its individual non-alkaloid and alkaloid fractions.
- Contribution on Chemistry : expanding the phytochemical knowledge of the genus.
- Chemotaxonomic insights: The clear differentiation between species based on metabolite profiles (phenolics/saponins in *P. tectorius* vs. alkaloids in *P. amaryllifolius*) provides valuable chemotaxonomic markers.

☐ Agree to award the PhD diploma to the candidate.

☑ Agree to award the PhD diploma to the candidate after revision.

☐ The thesis is not qualified for the PhD diploma. A second jury could be considered.

V. SIGNATURES:

Chairman	**Secretary**
Prof.Dr. Nguyen Van Hung	**Dr. Nguyen Huu Nghi**

UNIVERSITY OF SCIENCE & TECHNOLOGY OF HANOI
UNIVERSITE DES SCIENCES ET DES TECHNOLOGIES DE HANOI
TRƯỜNG ĐẠI HỌC KHOA HỌC & CÔNG NGHỆ HÀ NỘI

USTH
VIETNAM FRANCE UNIVERSITY

Examination Jury for PhD thesis
Jury Member's Assessment Remarks

PhD Student	
Full name	Do Hoang Giang
Program	Pharmacological, Medical and Agronomical Biotechnology
PhD ID	D22.PMAB.004
PhD thesis	
Title	Phytochemical constituents and bioactivities of Pandanus tectorius and Pandanus amaryllifolius/ *Nghiên cứu thành phần hóa học và hoạt tính sinh học của loài dứa dại (Pandanus tectorius) và loài dứa thơm (Pandanus amaryllifolius).*
Supervisor	Assoc. Prof. Nguyen Tien Dat, Center for Research and Technology Transfer, Vietnam Academy of Science and Technology
Co-supervisor	Assoc. Prof. Nguyen Hai Dang, USTH
Jury Member	
Full name	Nguyen Van Hung
Title	Professor of Chemistry
Institution	Institute of Chemistry – VAST
Contact (Email/SMS)	gsnguyenvanhunghn@gmail.com
Role (Chairman/ Reviewer/ Member)	Chairman
Technical comments (e.g. on the thesis topic, research methodology, finding, discussion, thesis structure, wording, references, etc). Please note that the reviewers can fill this part as "please refer to my review report" and/or with additional comments on the revised manuscript and/ or on the presentation made by the candidate	

PhD Thesis Research Topic: The study and investigation to discover the bioactive compounds from Plants is the impressive interest of the scientists in high-ranking research institutes in the field of Phytochemisty over the World.
The PhD Thesis Work is to investigate two species, Pandanus tectorius and Pandanus amaryllifolius, belonging to the genus Pandanus. The genus is large, comprising approximately 750 species worldwide, with 17 species reported in Vietnam.

From the Genus Pandanus species have been isolated many bioactive, potentially used for the pharmaceutical industry. Therefore, for the first time, conducting
a study on the chemical constituents and biological activities of these two species in Vietnamese Flora is highly impressive and appropriated.

In the Abstract and Introduction of the Thesis, PhD student has very effectively summarized and clarified the objectives and obtained results of the PhD Research Work. In This way, he has emphasized the reasons why the Execution of the research topic is urgently needed.

Research Methodology:
+ The PHD student has applied an integrated workflow combining plant collection and authentication from multiple locations in Vietnam, solvent extraction and fractionation (maceration, liquid–liquid partitioning, column chromatography), and quantitative determination of major phytochemical groups. He has found : total phenolics (TPC), flavonoids (TFC), alkaloids (TAC), and saponins (TSC)).
+ Bioactivities are evaluated in vitro, including antioxidant activity (DPPH and hydroxyl radical scavenging), α-amylase inhibition, cytotoxicity against A549, K562, and MCF7 cell lines, and nitric oxide (NO) production inhibition in LPS-stimulated RAW 264.7 cells.
+ Structure elucidation are performed using advanced spectroscopic techniques (HR-ESI-MS, $^{1}H/^{13}C$ NMR, HSQC, HMBC, COSY, DEPT, ECD, and Snatzke's $Mo_2(OAc)_4$-induced ECD), with artifact verification via HPLC-DAD..
Findings: In the PhD Thesis have been obtained :
+ Comparative screening reveals distinct phytochemical and bioactivity profiles between the two species: P. tectorius (leaves and fruits) is rich in phenolics, flavonoids, and saponins and shows superior antioxidant activity; whereas P. amaryllifolius (leaves) contains high levels of alkaloids and exhibits notable cytotoxicity and anti-inflammatory effects.
+ From P. tectorius leaves, two new benzofuran epimers (Pandanusfuran A and B) and four known lignans are isolated. The lignans exhibit stronger radical-scavenging activity, whereas the benzofurans
display α-amylase inhibition comparable to acarbose and selective cytotoxicity toward A549 cells.
+ Optimization of P. tectorius fruit extraction identifies seven validated conditions balancing TPC and TSC. Under these conditions, Phenolic-enriched extracts show superior antioxidant activity, while saponin-enriched extracts demonstrate stronger NO inhibition, with increased cytotoxicity observed at very high saponin levels.
+ For P. amaryllifolius leaves, the phenolic enrichment exhibits potent antioxidant activity (IC_{50} values close to those of ascorbic acid and catechin) and enhanced NO inhibition via phenolic-alkaloid synergism. Sixteen compounds are isolated, including shikimate derivatives, simple phenolics, and a lignan glycoside.
Discussion: andanaceae family includes about 750 species distributed in five genera: *Benstonea* Callmander & Buerki, *Freycinetia* Gaudichaud, *Martellidendron* Callmander & Chassot, *Pandanus* Parkinson, and *Sararanga* Hemsley [61]. *Pandanus* was the largest genus in the family, with more than 400 species [61]. Previous phytochemistry investigations on

this family mostly focused on the genus *Pandanus,* while only one study on the secondary metabolites of the *Freycinetia* plant [62] and no information about the chemical constituents of the rest of the genera has been reported.

The compounds isolated from *P. tectorius* leaves displayed distinct biological profiles. The lignans (pinoresinol, pinoresinol monomethyl ether, arctigenin, and matairesinol) exhibited moderate antioxidant activity, but were weak in α-amylase inhibition and inactive in cytotoxicity and NO assays. In contrast, the newly identified Pandanusfurans showed weaker antioxidant effects yet demonstrated α-amylase inhibition close to that of acarbose and selective cytotoxicity against A549 cells, while 65
remaining inactive against K562 and MCF7. None of the isolated compounds exhibited notable NO inhibition, in contrast to cardamonin. These findings suggest that Pandanusfurans represent promising multifunctional scaffolds with moderate antioxidant, antidiabetic, and selective anticancer potential, whereas the lignans mainly contribute to antioxidant activity

Thesis structure and presentation:

+ Structure: The thesis is logically structured with six chapters progressing from introduction and methodology to screening, compound isolation, extraction optimization, and conclusion. It includes English and Vietnamese abstracts, acknowledgements, lists of abbreviations/tables/figures,publications, and references. Clear chapter overviews and summaries support readability and continuity.

+ Writing style: The writing is formal, accurate, and academic, with consistent use of scientific terminology. Although some repetition appears in the abstracts and summaries. **In overall terms**: The presentation is coherent, and experimental data are effectively integrated with figures and tables.

+ Wording: The wording is generally accurate, but there are minor issues such as inconsistent hyphenation (e.g., "nitric-oxide" vs. "nitric oxide") and some awkward phrases (e.g., "attendant cytotoxic effects"). The Vietnamese abstract is well translated.

+ References: The reference list consisted of 105 entries, diverse (including books, journal articles,and theses), and relevant. It includes both classic and recent sources (up to 2025) and is generally well formatted, and the Vietnamese Pharmacopoeia is included for local context.Citations are usedappropriately to support major statements.

+ The work integrates multidisciplinary approaches of phytochemistry, biotechnology, and statistics, providing a holistic understanding of chemical-bioactivity relationships.

+ The PhD Thesis Research Work results are published on 7 papers, including 3 SCIE-indexed publications), demonstrating scientific impact and originality

Questions:

1 .Why has the PhD student chosen two species of Pandanus tectorius and Pandanus amaryllifolius as the objects for his PhD research Topic ?

2.Why did the author not investigate another parts of these plants?

Comment on the candidate ability (e.g. general scientific background, understanding on the research field and research topic, presentation skill, English level, etc)
In my opinion, The Ph D student Đỗ Hoàng Giang expresses a solid fundamental scientific knowledge of background, presentation skills and has demonstrated competence in phytochemical isolation, structure elucidation, bioassay techniques, and statistical optimization (excellent skill in conducting experiments and analyzing the obtained data). His high English level of advanced writing is highly appreciated.

Conclusions (indicates whether the manuscript is accepted in the current form or accepted after minor/ major revisions; and whether the candidate deserves the USTH PhD degree)

The PhD Thesis presents substantial original research meets all the requirements for a PhD degree in Pharmacological, Medical, and Agronomical Biotechnology.

The PhD Research work has already resulted in 07 peer-reviewed publications, confirming its scientific high quality.

With minor revisions it would meet the standards of a PhD thesis in the research field.

The PhD Thesis is Completely satisfied all conditions for the PhD defense and PhD student Đồ Hoàng giang will have obtained **Doctor of Philosophy in Chemistry**.

☐ **Accept the manuscript in the current form.**

X Accept the manuscript with minor/ major revisions.

☐ **The manuscript is not qualified to for the PhD degree.**

....., 2026

Jury Member's signature

Professor Nguyễn Văn Hùng

=

UNIVERSITY OF SCIENCE & TECHNOLOGY OF HANOI
UNIVERSITE DES SCIENCES ET DES TECHNOLOGIES DE HANOI
TRƯỜNG ĐẠI HỌC KHOA HỌC & CÔNG NGHỆ HÀ NỘI

Examination Jury for PhD thesis

Reviewer's Report

PhD Student	
Full name	Do Hoang Giang
Program/ Department	PMAB/ Life Sciences
Student ID number	D22.PMAB.004
PhD thesis	
Title	Phytochemical constituents and bioactivities of Pandanus tectorius and Pandanus amaryllifolius
Supervisor	Assoc. Prof. Nguyen Tien Dat, Center for Research and Technology Transfer, Vietnam Academy of Science and Technology
Co-supervisor	Assoc. Prof. Nguyen Hai Dang, USTH
Reviewer	
Full name	Pr. Marie Geneviève DIJOUX-FRANCA
Title	Assoc. Prof. DIJOUX-FRANCA Marie G.,
Institution	Lab Microbial Ecology (UMR 5557 CNRS/UCBL Lyon1), University LYON1
Contact (Email/SMS)	marie.dijoux-franca@univ-lyon1.fr
Technical comments (e.g. on the research topic, methodology, finding, discussion, thesis structure, wording, references etc)	

The work of Ms. DO Hoang Giang's thesis is devoted to the study of the components of two specie of Pandanus in Vietnam. The work's objectives are twofold: firstly, to list the compounds present in these plants and, secondly, to assess their potential benefits on health.

The study is presented in six different parts:

- **Part 1.** provides a review of the literature on Pandanus genus. Secondary metabolites in different chemical classes such as phenols, coumarins, flavonoids, lignans and alkaloids are described. Bioactivities are also reported for different *Pandanus* species and for leaves and fruits extracts: antioxidant, anti-inflammatory, antimicrobial, antitumor.
Based on these data, the choice was made to work on two species: *P. tectorius* (leaves and fruits) and *P. amaryllifolius* (leaves).

- **Part 2.** outlines the materials and methodologies employed in the study, including analytical technics, fractionation methods, structural identification methods and biological assays.

- **Part 3.** presents the phytochemical screening and bioactivities of leaves and fruits extracts from the two species of *Pandanus*.
Quantitative analyses of mains classes of metabolites are presented, and guided the selection of the material for further investigation.

- **Part 4.** describes the results on isolation using CC chromatography and structural characterization of pure compounds from leaves of *P. tectorius*. Complete structures were established using 1D and 2D-NMR experiments, MS, and circular dichroism (CD) technics. The description of the structure determination method is detailed and easy to follow. Six compounds were isolated and identified.
A potential link between the key compounds and the activities of the extracts is proposed.

- **Part 5. and Part 6.** deal with the optimization of extraction processes, evaluation of bioactivities for *P. tectorius* fruit extracts and *P. amaryllifolius* leaves.
In these two chapters Mrs Do Hoang Giang uses an alternative method for extraction processes optimization.
Part 6 is completed by the isolation and identification of phenolic compounds obtained from an optimized extract.
With the work, she has thus gained new expertise in optimizing analytical methods applied to natural substances.

Upon reviewing the manuscript, we observe that Mrs Do Hoang Giang was able to employ standard techniques for the extraction, purification, characterization, and in vitro evaluation of the biological activities of natural compounds such as polyphenols and alkaloids. In doing so, she has acquired significant expertise in phytochemistry and the search for bioactive natural compounds.

She also worked on optimizing the extraction conditions for certain compounds that appear to be linked to the demonstrated biological activities. In doing so, she demonstrated the necessary rigor in selecting parameters and the value of these in silico methods.

The manuscript is well-structured, well-written, making it easier for the reviewer to read. The subjects, the context, as well as the approach followed are clearly presented and documented.

Questions/ Suggestions/ Request of Revisions
- The choice of *Pandanus* genus for the study is not clear as it is said that in this family, some species are already well described. What is the broader context? - Explain more the reason why the optimization of extraction protocol is done: is it for further developing a marketed product based on these extracts? Or? - P21- : Traditional uses of *P. amaryllifolius* are not described. Why? For example, see ref: Review article ISSN:23194820 Biman Bhuyan and Richa Sonowal. 2021. An overview of *Pandanus amaryllifolius* Roxb.Exlindl. and its potential impact on health. *Current Trends in Pharmaceutical Research*, 8(1), 2582-4783 It seems that *P. amaryllifolius* is not used in traditional medicine in Vietnam. Is this the reason? - At the end of part 1.2. Add a table with compounds isolated from the two species on which the thesis is based and the bioactivities describes for each of them - In part 1.3. a table would be useful to summarize all the specie and the bioactivities that have been described.
Conclusions (whether the work is suitable/ could be suitable after revisions for presenting to obtain the USTH PhD degree?)
The subject of this thesis is part of a comprehensive study of the plant with a view to understanding its use in traditional medicine. Specifically, it aims to describe its chemical composition and correlate it with biological activities that may or may not confirm the plant's medicinal use. The work is suitable for presenting to obtain PhD degree.
☐ **Recommended for defense at the PhD Thesis Examination Jury in the current form.** ☒ **Recommend for defense at the PhD Thesis Examination Jury with minor revisions.** ☐ **Not recommended for defense at the PhD Thesis Examination Jury.**
01/04/2026 **Reviewer's signature**   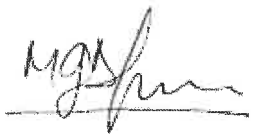   **Pr Marie-Geneviève Dijoux-Franca**

UNIVERSITY OF SCIENCE & TECHNOLOGY OF HANOI
UNIVERSITE DES SCIENCES ET DES TECHNOLOGIES DE HANOI
TRƯỜNG ĐẠI HỌC KHOA HỌC & CÔNG NGHỆ HÀ NỘI

Examination Jury for PhD thesis
Reviewer's Report

PhD Student	
Full name	Do Hoang Giang
Program/ Department	PMAB/ Life Sciences
Student ID number	D22.PMAB.004
PhD thesis	
Title	Phytochemical constituents and bioactivities of Pandanus tectorius and Pandanus amaryllifolius
Supervisor	Assoc. Prof. Nguyen Tien Dat, Center for Research and Technology Transfer, Vietnam Academy of Science and Technology
Co-supervisor	Assoc. Prof. Nguyen Hai Dang, USTH
Reviewer	
Full name	Vu Duc Loi
Title	Associate Professor, PhD Director, Tue Tinh Institute of Traditional Medicine and Pharmacy
Institution	Viet Nam University of Traditional Medicine
Contact (Email/SMS)	ducloi82@gmail.com

Technical comments (e.g. on the research topic, methodology, finding, discussion, thesis structure, wording, references etc)

Research Topic: Phytochemical Constituents and Bioactivities of Pandanus tectorius and Pandanus amaryllifolius

The thesis investigates two species, Pandanus tectorius and Pandanus amaryllifolius, belonging to the genus Pandanus. The genus is large, comprising approximately 750 species worldwide, with 17 species

reported in Vietnam. Pandanus species have important applications in the pharmaceutical and medical fields, yet remain insufficiently studied, particularly for the two selected species. Therefore, conducting a study on the chemical constituents and biological activities of these two species is highly appropriate.

Research Methodology:

+ The thesis applies an integrated workflow combining plant collection and authentication from multiple locations in Vietnam, solvent extraction and fractionation (maceration, liquid–liquid partitioning, column chromatography), and quantitative determination of major phytochemical groups (total phenolics (TPC), flavonoids (TFC), alkaloids (TAC), and saponins (TSC)).
+ Bioactivities are evaluated in vitro, including antioxidant activity (DPPH and hydroxyl radical scavenging), α-amylase inhibition, cytotoxicity against A549, K562, and MCF7 cell lines, and nitric oxide (NO) production inhibition in LPS-stimulated RAW 264.7 cells.
+ Compound isolation and structure elucidation are performed using advanced spectroscopic techniques (HR-ESI-MS, $^{1}H/^{13}C$ NMR, HSQC, HMBC, COSY, DEPT, ECD, and Snatzke's $Mo_2(OAc)_4$-induced ECD), with artifact verification via HPLC-DAD.
+ Extraction optimization is conducted using Response Surface Methodology (RSM) with Box–Behnken Design (BBD), supported by single-factor experiments, ANOVA model validation, and multi-response desirability functions.
+ Statistical tools include PLS regression for multivariate correlations and GraphPad Prism for data analysis.

Findings:

+ Comparative screening reveals distinct phytochemical and bioactivity profiles between the two species: P. tectorius (leaves and fruits) is rich in phenolics, flavonoids, and saponins and shows superior antioxidant activity; whereas P. amaryllifolius (leaves) contains high levels of alkaloids and exhibits notable cytotoxicity and anti-inflammatory effects.
+ From P. tectorius leaves, two new benzofuran epimers (Pandanusfuran A and B) and four known lignans are isolated. The lignans exhibit stronger radical-scavenging activity, whereas the benzofurans display α-amylase inhibition comparable to acarbose and selective cytotoxicity toward A549 cells.
+ Optimization of P. tectorius fruit extraction identifies seven validated conditions balancing TPC and TSC. Under these conditions, Phenolic-enriched extracts show superior antioxidant activity, while saponin-enriched extracts demonstrate stronger NO inhibition, with increased cytotoxicity observed at very high saponin levels.
+ For P. amaryllifolius leaves, the phenolic enrichment exhibits potent antioxidant activity (IC_{50} values close to those of ascorbic acid and catechin) and enhanced NO inhibition via phenolic-alkaloid synergism. Sixteen compounds are isolated, including shikimate derivatives, simple phenolics, and a lignan glycoside.

Discussion:

+ The discussion effectively links the findings to the literature, explaining species/organ differences (e.g., alkaloid accumulation in P. amaryllifolius associated with cytotoxicity), potential bioactivity mechanisms (e.g., selective effects of benzofurans related to structural features), and the trade-offs observed in extraction optimization for practical applications.
+ The thesis also addresses limitations such as the in vitro nature of the study and the moderate potency of certain samples, and proposes future directions including in vivo studies, structure-activity relationship investigation, and standardization.
+ The novelty of the study is emphasized, with web searches confirming Pandanusfurans A/B as new compounds (published in 2025).

Thesis structure and presentation:

+ Structure: The thesis is logically structured with six chapters progressing from introduction and methodology to screening, compound isolation, extraction optimization, and conclusion. It includes

English and Vietnamese abstracts, acknowledgements, lists of abbreviations/tables/figures, publications, and references. Clear chapter overviews and summaries support readability and continuity.

+ Writing style: The writing is formal, accurate, and academic, with consistent use of scientific terminology. Although some repetition appears in the abstracts and summaries, the overall presentation remains coherent, and experimental data are effectively integrated with figures and tables.

+ Wording: The wording is generally accurate, but there are minor issues such as inconsistent hyphenation (e.g., "nitric-oxide" vs. "nitric oxide") and some awkward phrases (e.g., "attendant cytotoxic effects"). The Vietnamese abstract is well translated.

+ References: The reference list is extensive (105 entries), diverse (including books, journal articles, and theses), and relevant. It includes both classic and recent sources (up to 2025) and is generally well formatted, and the Vietnamese Pharmacopoeia is included for local context. Citations are used appropriately to support major statements.

Questions/ Suggestions/ Request of Revisions

Advantages of the thesis:

+ The thesis identifies novel compounds (Pandanusfurans A and B, confirmed as new via web search) and first-in-genus megastigmanes, contributing to the phytochemical knowledge of the genus Pandanus.

+ The optimization study provides robust and practical extraction protocols for obtaining fractions enriched in specific metabolite classes and tuned for bioactivities, with potential industrial applicability.

+ The work integrates multidisciplinary approaches (phytochemistry, biotechnology, and statistics), providing a holistic understanding of chemical-bioactivity relationships.

+ The thesis is supported by a strong publication record (7 papers, including 3 SCIE-indexed publications), demonstrating scientific impact and originality.

Limitations of the thesis:

1. ***Presentation and structure:***

- Regarding the overall presentation, the thesis should consider reducing the number of separate chapters. It could be reorganized into fewer major chapters, for example:
  - ✓ Chapter 1: Introduction/Literature review
  - ✓ Chapter 2: Materials and Methods
  - ✓ Chapter 3: Results
  - ✓ Chapter 4: Discussion, Conclusions, and Recommendations

2. ***Chapter 1 (General Introduction)***

- The introduction should be expanded to include a general overview of the genus, including botanical characteristics, chemical constituents, and biological activities. After that, a more in-depth review should be provided for the two studied species, focusing on their botanical aspects, chemistry, and biological activities.
- *Summary of research content:* In the summary section of the thesis, additional information should be included regarding what has been studied on the two target species so far and what results have been obtained in previous studies. This would help identify the existing research gaps, clarify which aspects still require further investigation, and justify the necessity of the present thesis.

3. ***Chapter 2 (Materials and Methods):***

- It is recommended to add more detailed information on sample collection, including harvesting methods, harvesting time/season, sample processing, and storage conditions.
- Information on reference standards used in quantitative assays should be provided (manufacturer, batch number, expiry date, etc.).
- The thesis should clarify why, although the introduction refers to studies on various plant parts in other species (roots, fruits, leaves, aerial parts), the present study examines only leaves and fruits of P. tectorius and only leaves of P. amaryllifolius.
- *Quantification methods:* The quantification methods for each metabolite group should be clarified, including the analytical principles, detailed procedures, test samples, and reference standards. If the methods are self-developed, appropriate method validation must be conducted prior to application. Linear calibration curves should also be provided.
- The methodology is detailed and reproducible; however, it lacks specific discussion of plant authentication methods (e.g., molecular identification) and does not address seasonal/environmental variability.

4. ***Chapter 3 (Phytochemicals and bioactivities screening of Pandanus plant samples)***

- Background and methodological content should be moved to the general introduction and general methods section, rather than repeated in Chapter 3. Bioactivity result tables should include IC_{50} values.

5. ***Chapter 4 (Isolation, structure elucidation, and bioactivity evaluation of compounds from Pandanus tectorius leaves)***

- The thesis should consider presenting IC_{50} values of different solvent fractions (e.g., n-hexane, ethyl acetate, and aqueous fractions) prior to focusing on the chemical investigation of the most active fraction. After isolation of compounds from this fraction, their bioactivities should be evaluated to confirm their contributions to the observed effects. This approach would improve the logical flow of the study.

6. ***Chapter 5 (Optimization of the extraction condition and bioactivities evaluation of Pandanus tectorius fruits extracts)***

- Chapter 5 has similar issues to Chapter 4; therefore, the same revisions are recommended.

In addition, Chapters 3 and 4 should be merged and consolidated to improve coherence and overall structure.

Additional limitations

- Results: The thesis presents extensive data with tables and figures, but some bioactivity values (e.g., IC_{50}) are moderate compared with standards, and replicates are not consistently reported for all assays.
- Discussion: The correlations are insightful; however, the discussion underplays the possibility of artifacts in isolation despite HPLC verification and does not include broader ecological implications.
- Conclusions: The conclusions summarize well and propose future directions, but do not address the economic feasibility of the optimization process.

7. ***References***

- Some references published before 2010 should be reduced where appropriate, and replaced with more recent publications to ensure that the literature review reflects current research developments.

8. ***Appendices***

- The appendices should include calibration curves for quantitative assays and validation data for the quantification methods.

Questions and Discussions:

1. Why did the author not investigate all plant parts (leaves, fruits, roots, aerial parts) as described in the introduction for other species in the genus?
2. How do the absolute configurations of Pandanusfurans A/B influence their selective cytotoxicity against A549 cells? Were computational docking studies considered?
3. In the fruit optimization study, why were seven conditions presented instead of a single multi-objective optimum, and how do these conditions perform in scaled-up extractions?
4. For the proposed synergism in P. amaryllifolius, what specific phenolic-alkaloid interactions were hypothesized, and why was no further fractionation performed to confirm this?

Conclusions (whether the work is suitable/ could be suitable after revisions for presenting to obtain the USTH PhD degree?)

The thesis demonstrates originality, methodological rigor, and relevance to pharmacological biotechnology. The work is supported by publications and includes novel findings. The thesis meets the requirements for a doctoral degree. I fully support its approval and recommend that the candidate (should) be awarded the doctoral degree in accordance with current regulations from USTH, after revising the dissertation according to the reviewer comments.

☐ **Recommended for defense at the PhD Thesis Examination Jury in the current form.**

☑ **Recommend for defense at the PhD Thesis Examination Jury with minor/ major revisions.**

☐ **Not recommended for defense at the PhD Thesis Examination Jury.**

Ha Noi, 13/02/ 2026

Reviewer's signature

Vu Duc Loi

End of the document

UNIVERSITY OF SCIENCE & TECHNOLOGY OF HANOI
UNIVERSITE DES SCIENCES ET DES TECHNOLOGIES DE HANOI
TRƯỜNG ĐẠI HỌC KHOA HỌC & CÔNG NGHỆ HÀ NỘI

VIETNAM FRANCE UNIVERSITY

Examination Jury for PhD thesis

Reviewer's Report

PhD Student	
Full name	Do Hoang Giang
Program/ Department	PMAB/ Life Sciences
Student ID number	D22.PMAB.004
PhD thesis	
Title	Phytochemical constituents and bioactivities of Pandanus tectorius and Pandanus amaryllifolius
Supervisor	Assoc. Prof. Nguyen Tien Dat, Center for Research and Technology Transfer, Vietnam Academy of Science and Technology
Co-supervisor	Assoc. Prof. Nguyen Hai Dang, USTH
Reviewer	
Full name	Le Nguyen Thanh
Title	Assoc. Prof.
Institution	National Institute of Medicinal Materials
Contact (Email/SMS)	Lethanh7676@gmail.com. Tel. 0983882573
Technical comments (e.g. on the research topic, methodology, finding, discussion, thesis structure, wording, references etc)	

The dissertation of PhD student Do Hoang Giang "Phytochemical constituents and bioactivities of Pandanus tectorius and Pandanus amaryllifolius" presents a comprehensive phytochemical investigation of two *Pandanus* species (*P. tectorius* and *P. amaryllifolius*) collected in Vietnam, combined with bioactivity screening and process optimization studies. The work comprises of extract screening, isolation and structural elucidation of secondary metabolites, response surface methodology optimization of extraction conditions, and evaluation of antioxidant, cytotoxic, anti-inflammatory, and enzyme inhibitory activities.

Research topic: The *Pandanus* genus encompasses a diverse group of tropical plants, among that about 17 species in the genus were determined In Vietnam. The genus is known for diverse secondary metabolites, yet comprehensive comparative studies remain limited.. The thesis has a clear objectives. The study addresses two under-investigated *Pandanus* species with traditional medicinal uses in Vietnam and Southeast Asia.

The thesis is logically structured to progress from broad screening to targeted isolation, then to process optimization. The optimization studies have direct implications for developing standardized extracts for nutraceutical or pharmaceutical applications

Methodology:

PhD student have used comprehensive analytical methods combination of colorimetric assays (TPC, TFC, TSC, TAC), chromatographic isolation (column chromatography, preparative HPLC), and advanced spectroscopic techniques (NMR, HR-MS, ECD). The use of ECD and Snatzke's Mo□(OAc)□-induced ECD method for determining absolute configurations of the new benzofuran epimers represents modern practice in natural product chemistry..

Findings:

From *P. tectorius* leaves, two new benzofuran epimers (Pandanusfurans A and B) and four lignans were elucidated. The lignans contributed to antioxidant capacity, whereas the benzofurans, showed weaker antioxidant activity but exhibited α-amylase inhibition and showed selective cytotoxicity toward A549.

This study successfully optimized the extraction process of phenolic- and saponin enriched fractions from *Pandanus tectorius* fruit using the Box–Behnken Design. Phenolic-rich extracts obtained under high ethanol concentration and temperature conditions exhibited strong antioxidant activity.

Saponin-rich extracts obtained under lower ethanol concentration and longer extraction times, showed good nitric oxide inhibitory effects, albeit with potential cytotoxicity at higher doses

The phytochemical investigation of the phenolic enrichment from *P. amaryllifolius* leaves led to the isolation of 16 compounds, including 3 lignans and 9 benzoate derivatives, together with 3 shikimates and 1 glycoside. Except for 4-hydroxybenzoic acid, the other compounds were identified for the first time from the plant.

The optimized phenolic enrichment from *Pandanus amaryllifolius* leaves demonstrated substantial antioxidant and NO inhibition activities, surpassing the efficacy of its individual non-alkaloid and alkaloid fractions.

Contribution on Chemistry : expanding the phytochemical knowledge of the genus.

Chemotaxonomic insights: The clear differentiation between species based on metabolite profiles (phenolics/saponins in *P. tectorius* vs. alkaloids in *P. amaryllifolius*) provides valuable chemotaxonomic markers.

The results of this work have been published in 07 publications including 03 SCIE papers (*Journal of Analytical Methods in Chemistry* 02, and *Journal of Chemistry* 01; 01 **international journals** and 03 domestic journal The articles have good quality.

Thesis Structure: This is a 103 page thesis including

Chapter 1. General Introduction (18 pages),

Chapter 2. Materials and Methods (5 pages),

Chapter 3. PHYTOCHEMICALS AND BIOACTIVITIES SCREENING OF *PANDANUS* PLANT SAMPLES (16 pages),

Chapter 4. ISOLATION, STRUCTURE ELUCIDATION, AND BIOACTIVITY EVALUATION OF COMPOUNDS FROM *PANDANUS TECTORIUS* LEAVES (26 pages).

CHAPTER 5. OPTIMIZATION OF THE EXTRACTION CONDITION AND BIOACTIVITIES EVALUATION OF *PANDANUS TECTORIUS* FRUITS EXTRACTS (16 pages).

CHAPTER 6. OPTIMIZATION OF THE EXTRACTION CONDITION AND BIOACTIVITY EVALUATION OF THE PHENOLIC ENRICHMENT FROM *PANDANUS AMARYLLIFOLIUS* LEAVES (20 pages). CONCLUSION (2 pages)

Thesis contains 21 tables, 42 figures

The thesis appears to be well-organized into chapters and has already resulted in multiple publications, which is a strong indicator of quality. Consistent chapter format: Each chapter begins with an overview and ends with a summary, aiding readability

The dissertation has 79 references cover the relevant literature on *Pandanus* phytochemistry and bioactivity, including recent work (2025 citations). References include reputable journals in natural product chemistry, pharmacognosy, and analytical chemistry

The English is generally clear and understandable, with a formal academic tone appropriate for a doctoral thesis. However, there are numerous grammatical errors, typographical issues, and awkward phrasings that require correction.

Questions/ Suggestions/ Request of Revisions

List of Figures: A comprehensive list of figures (beyond the Table of Contents) would aid navigation.

Abbreviations list: Page 15 has a partial list, but many abbreviations used later (e.g., BBD, RSM, TPC, TFC, etc.) are not included.

Chapter 1. The chemical structure of isolated compoudns from *Pandanus* genus should be arranged, page 7,9, 13, 14.

The biological activity like antidiabtic effect should be added (moved from chemical part to biological part)

Chapter 3. Correct the structure numbers in Figure 4.1

Correct the name of compound Pt1 and Pt2: 8R, 9S or 8R, 9R

Page 57, 58. Pinoresinol is furofurane lignan

Chapter 6. The NMR data of isolated compound can be presented iu table, consistent with chapter 4.

Conclusion: paragraph 1: should remove P. odoratissimus nad P. tonkinensis

Reference 54 and 66: These appear to be the same paper (Niu et al. 2018 on Graphostroma sp.).

Reference 63: Byrne et al. 1992 appears to duplicate **Reference 14**.

Add the NMR, MS spectra of known compounds in SI

Quenstion: The introduction mentions traditional uses for kidney stones and edema. Your bioassays focused on antioxidant, anti-inflammatory, and cytotoxic activities. How do these relate to the traditional indications ?

Why did not evaluate the biological activity of isolated compound from *P. amaryllifolius ?*

Conclusions (whether the work is suitable/ could be suitable after revisions for presenting to obtain the USTH PhD degree?)

The thesis presents substantial original research meeting the requirements for a PhD degree in Pharmacological, Medical, and Agronomical Biotechnology.

The candidate has demonstrated competence in phytochemical isolation, structure elucidation, bioassay techniques, and statistical optimization. The work has already resulted in 07 peer-reviewed publications, attesting to its scientific quality.

With minor revisions it would meet the standards of a PhD thesis in the research field.

The work is suitable for presenting to obtain the USTH PhD degree

☐ **Recommended for defense at the PhD Thesis Examination Jury in the current form.**

☒ **Recommend for defense at the PhD Thesis Examination Jury with minor/ major revisions.**

☐ **Not recommended for defense at the PhD Thesis Examination Jury.**

Hanoi, 10th, March, 2026

Reviewer's signature

Lê Nguyễn Thành

UNIVERSITY OF SCIENCE & TECHNOLOGY OF HANOI
UNIVERSITE DES SCIENCES ET DES TECHNOLOGIES DE HANOI
TRƯỜNG ĐẠI HỌC KHOA HỌC & CÔNG NGHỆ HÀ NỘI

Examination Jury for PhD thesis
Jury Member's Assessment Form

PhD Student	
Full name	Do Hoang Giang
Program	Pharmacological, Medical and Agronomical Biotechnology
PhD ID	D22.PMAB.004
PhD thesis	
Title	Phytochemical constituents and bioactivities of Pandanus tectorius and Pandanus amaryllifolius/ *Nghiên cứu thành phần hóa học và hoạt tính sinh học của loài dứa dại (Pandanus tectorius) và loài dứa thơm (Pandanus amaryllifolius).*
Supervisor	Assoc. Prof. Nguyen Tien Dat, Center for Research and Technology Transfer, Vietnam Academy of Science and Technology
Co-supervisor	Assoc. Prof. Nguyen Hai Dang, USTH
Jury Member	
Full name	Nguyen Phi Hung
Title	Assoc. Prof. Dr.
Institution	Institute of Chemistry
Contact (Email/SMS)	nguyenphihung@ich.vast.vn
Role (Chairman/ Reviewer/ Member)	Member
Technical comments (e.g. on the thesis topic, research methodology, finding, discussion, thesis structure, wording, references, etc). Please note that the reviewers can fill this part as "please refer to my review report" and/or with additional comments on the revised manuscript and/ or on the presentation made by the candidate	

Comments to the author (PhD candidate):

1. Please Provide:

- Picture or the image of the two plants/plant materials
- The information describing about these plant materials into the Result part or Appendix

2. In the Quantitative analysis:

- Table 3.1, in page 27: The author should check again the value present for TPC, TFC, and TAC (in %). Because the result showed very high value unit in % for the TAC (total alkaloid content) over 21,76% as calculated for the dry weight. The author should clarify whether the calculation is based on the original dry sample or the extract.

3. In the bioactivity test:

- Page 32, Table 3.3: The author should give a discussion why there is a significant difference in biological activity between the two test samples Pama-1 and Pama-2.

- Table 3.4: The value should be presented as % Inhibition rather than % cell survival.

4. Chapter 4: Isolation of compounds from Pandanus tectorius leaves

- Need provide the detail HPLC chromatographic condition, such as HPLC model, column, mobile phase (solvent system), flowrate in mL, UV scanning, and also the retention time of each compound.

- In other hand, the isolation of every compounds should also be described in detail.

- Table 4.1: need to revise the NMR data for compound Graphostrin D

- Table 4.2: need to provide the 1H and 13C NMR data for the methoxy moiety of the new compound Pt2.

5. The Appendix needs providing:

+ NMR spectroscopic data of all isolated compounds;

+ MS spectral data of two new compounds PT1 and Pt2;

+ The HPLC chromatographic profile and its condition;

+ The hard copies of all publications belong to this thesis.

Comment on the candidate ability (e.g. general scientific background, understanding on the research field and research topic, presentation skill, English level, etc)

Some questions to the author:

1. In the case of compounds Pt1 and Pt2, can you explain why the C value and also the proton value of the methoxy (-OCH_3) group attached to the acetyl group appeared (resonated) at around 51.27 ppm and 3,79 ppm (the more up field)?
   Usually, for an OCH_3 group attached to a phenyl, so the C value often appeared at around 55 – 60 ppm, the proton value often appeared at around 3.8 – 4.1 ppm.
2. Does the Pandanus amaryllifolius (lá nếp/ lá dứa thơm in Vietnamese) has the fruit?
3. Why did the author choose to study on the optimization of the extract condition of the P. tectorius fruit, but not its leaves?
   Because, the author studied the chemical composition of the leaves, but not the fruits. So, what is the purpose of the above study?

Conclusions (indicates whether the manuscript is accepted in the current form or accepted after minor/ major revisions; and whether the candidate deserves the USTH PhD degree)

- **I Accept the thesis After all the comments to the author are addressed.**

☐ **Accept the manuscript in the current form.**

☒ **Accept the manuscript with minor/ major revisions.**

☐ **The manuscript is not qualified to for the PhD degree.**

Hanoi, March 23rd, 2026

Jury Member's signature

Nguyen Phi Hung

UNIVERSITY OF SCIENCE & TECHNOLOGY OF HANOI
UNIVERSITE DES SCIENCES ET DES TECHNOLOGIES DE HANOI
TRƯỜNG ĐẠI HỌC KHOA HỌC & CÔNG NGHỆ HÀ NỘI

Examination Jury for PhD thesis
Jury Member's Assessment Form

PhD Student	
Full name	Do Hoang Giang
Program	Pharmacological, Medical and Agronomical Biotechnology
PhD ID	D22.PMAB.004
PhD thesis	
Title	Phytochemical constituents and bioactivities of Pandanus tectorius and Pandanus amaryllifolius/ *Nghiên cứu thành phần hóa học và hoạt tính sinh học của loài dứa dại (Pandanus tectorius) và loài dứa thơm (Pandanus amaryllifolius).*
Supervisor	Assoc. Prof. Nguyen Tien Dat, Center for Research and Technology Transfer, Vietnam Academy of Science and Technology
Co-supervisor	Assoc. Prof. Nguyen Hai Dang, USTH
Jury Member	
Full name	Pham Hoang Nam
Title	PhD
Institution	USTH
Contact (Email/SMS)	0916073217/pham-hoang.nam@usth.edu.vn
Role (Chairman/ Reviewer/ Member)	Member
Technical comments (e.g. on the thesis topic, research methodology, finding, discussion, thesis structure, wording, references, etc). Please note that the reviewers can fill this part as "please refer to my review report" and/or with additional comments on the revised manuscript and/ or on the presentation made by the candidate	

- Thesis topic:

The thesis investigates the phytochemistry and bioactivities of two *Pandanus* species, *P. tectorius* (screw pine) and *P. amaryllifolius* (pandan), which are ecologically widespread and ethnobotanically significant plants in Vietnam and throughout the Indo-Pacific region. The research addresses a genuine knowledge gap in the genus-level chemical diversity of *Pandanus*, a group that, despite its extensive traditional use, remains incompletely characterized at the metabolite level. The scope is appropriately bounded, combining comparative extract-level screening with targeted isolation and process-level optimization, reflecting a well-planned multi-phase research strategy. The topic is of relevance to natural product chemistry, plant-based drug discovery, and functional food development.

- Research methodology:

The methodological framework is well-constructed and appropriate for the stated objectives. Plant materials were collected across multiple time points and locations, authenticated by a taxonomic specialist, and voucher specimens were properly deposited. The bioassay panel is comprehensive, covering antioxidant (DPPH, hydroxyl), enzyme inhibitory (α-amylase), cytotoxic (A549, K562, MCF7), and anti-inflammatory (NO/RAW 264.7) endpoints. Structural characterization of new compounds employed state-of-the-art instrumentation (HR-ESI-MS, 2D NMR at 500/600 MHz, HPLC-DAD, CD spectrometry), and absolute configuration was assigned using two complementary approaches (ECD comparison with reference spectra and Snatzke's $Mo_2(OAc)_4$-induced CD), providing a robust stereochemical basis. The RSM-BBD optimization studies in Chapters 5 and 6 are statistically rigorous, with well-fitted models and appropriate validation.

Two methodological points are worth noting for further consideration.

The PLSR model in Chapter 3 performs well for antioxidant and α-amylase inhibitory endpoints (Q^2 = 0.795 - 0.924), and the candidate appropriately acknowledges that the weaker predictive performance for cytotoxic activities reflects limited sample size and greater biological complexity rather than a modelling failure. It would, however, strengthen the overall coherence of the thesis to explicitly connect this observation to the findings of Chapter 4: the selective A549 cytotoxicity of Pandanusfurans A and B (IC_{50} ~35 μM) while all lignans remain inactive is precisely the kind of compound-specific driver that bulk phytochemical descriptors cannot capture-and making this link explicit would turn a limitation into a meaningful cross-chapter insight.

Regarding the saponin characterization, the thesis relies throughout on total saponin content expressed as diosgenin equivalents, without isolation or identification of individual saponin constituents. Given that saponin-enriched fractions from *P. tectorius* fruits showed both the strongest NO inhibitory activity and dose-dependent cytotoxicity at higher concentrations- observations that the candidate rightly flags as important-future work targeting the isolation and structural characterization of the dominant saponin species would be a natural and valuable extension of this research.

- Writing:

The thesis is written in clear, generally accurate scientific English. The candidate demonstrates command of the relevant technical vocabulary in natural product chemistry and pharmacognosy. Minor issues include occasional redundancy between chapter overview and results sections, and a few instances of non-idiomatic phrasing that do not impede comprehension. The abstract (both English and Vietnamese versions) is concise and representative of the thesis content.

- References

The reference list comprises more than 70 citations, predominantly from international peer-reviewed journals. The literature coverage is appropriate and up to date for the field. Citations are applied correctly and consistently throughout the text.

- Scientific quality:

The scientific quality of the thesis is further confirmed by the candidate's publication record. Three SCIE-indexed articles published as first author in 2025 directly correspond to the core research chapters: Pandanusfurans A and B in *Journal of Chemistry*, and the two extraction optimization studies in *Journal of Analytical Methods in Chemistry*. One additional article in an international journal (*International Journal of Engineering Research and Development*, 2025) reports on α-amylase inhibition of marketed *P. tectorius* samples. Three Vietnamese article on shikimate esters and megastigmanes from *P. amaryllifolius* (*Journal of Tropical Science and Engineering*, 2024), phenolics from *P. tectorius* fruits (*HaUI Journal of Science and Technology*, 2025), and phenolics from *P. amaryllifolius* leaves (*Journal of Tropical Science and Engineering*, 2025) further complement the portfolio. The fact that all major findings have been independently peer-reviewed and published prior to the defense is a strong indicator of the overall scientific rigor of the work.

Comment on the candidate ability (e.g. general scientific background, understanding on the research field and research topic, presentation skill, English level, etc)

The candidate demonstrates a solid general scientific background in natural product chemistry, pharmacognosy, and analytical methodology, as evidenced by the coherent research design, appropriate selection of analytical tools, and rigorous execution of multi-step isolation and characterization work. The ability to critically assess the limitations of the PLSR model and acknowledge the moderate potency of many isolates reflects scientific maturity and intellectual honesty. Written English is at an acceptable academic standard throughout the thesis. Based on the written work, the candidate shows a clear understanding of the research field and is capable of conducting and communicating independent doctoral-level research.

Conclusions (indicates whether the manuscript is accepted in the current form or accepted after minor/ major revisions; and whether the candidate deserves the USTH PhD degree)

The thesis makes a genuine and well-documented contribution to the phytochemistry of the genus *Pandanus*, through the discovery and full structural characterization of two new benzofuran natural products, the first report of megastigmanes in the genus, and the establishment of statistically validated multi-response extraction protocols for both species. All major findings have been independently peer-reviewed and published prior to the defense. The manuscript is recommended for **acceptance with minor revisions**, primarily to: (i) explicitly connect the poor PLSR predictive performance for A549 cytotoxicity to the compound-specific findings of Chapter 4; and (ii) discuss the absence of individual saponin characterization as a limitation and outline it as a concrete priority for future work. **The candidate is deserving of the USTH PhD degree**.

☐ **Accept the manuscript in the current form.**

× **Accept the manuscript with minor/ major revisions.**

☐ **The manuscript is not qualified to for the PhD degree.**

Hanoi 26th March, 2026

Jury Member's signature

Pham Hoang Nam

End of the document

UNIVERSITY OF SCIENCE & TECHNOLOGY OF HANOI
UNIVERSITE DES SCIENCES ET DES TECHNOLOGIES DE HANOI
TRƯỜNG ĐẠI HỌC KHOA HỌC & CÔNG NGHỆ HÀ NỘI

Examination Jury for PhD thesis
Jury Member's Assessment Form

PhD Student	
Full name	Do Hoang Giang
Program	Pharmacological, Medical and Agronomical Biotechnology
PhD ID	D22.PMAB.004
PhD thesis	
Title	Phytochemical constituents and bioactivities of Pandanus tectorius and Pandanus amaryllifolius/ *Nghiên cứu thành phần hóa học và hoạt tính sinh học của loài dứa dại (Pandanus tectorius) và loài dứa thơm (Pandanus amaryllifolius).*
Supervisor	Assoc. Prof. Nguyen Tien Dat, Center for Research and Technology Transfer, Vietnam Academy of Science and Technology
Co-supervisor	Assoc. Prof. Nguyen Hai Dang, USTH
Jury Member	
Full name	Nguyen Huu Nghi
Title	PhD
Institution	USTH
Contact (Email/SMS)	0982425406/nguyen-huu.nghi@usth.edu.vn
Role (Chairman/ Reviewer/ Member)	Member
Technical comments (e.g. on the thesis topic, research methodology, finding, discussion, thesis structure, wording, references, etc). Please note that the reviewers can fill this part as "please refer to my review report" and/or with additional comments on the revised manuscript and/ or on the presentation made by the candidate	

- Thesis topic:

The thesis manuscript presents a comprehensive investigation into the phytochemicals and bioactivities of *Pandanus tectorius* and *Pandanus amaryllifolius*. The present work also isolate and determine some chemicals in the two species. From the chemical constituent information, the research tried to optimize extraction process for P. tectorius fruit and P. amaryllifolius leaves and investigate bioactivity of phenolic and saponin enrichment extract. The research topic is scientifically relevant aligned with chemical identification, extraction and biological property investigation.

- Research methodology:

The research methods are comprehensive and technically appropriate. The author has used advanced techniques such as HR-ESI-MS, NMR, ECD for chemical identification, Box-Behnken design for optimization study, cell model (A549, K562, MCF7) as well as in vitro DPPH, hydroxyl, alpha amylase inhibition test.

Findings and discussions

The thesis presents substantial and well-structured results. The findings provide a scientific basis to get insight into chemical constituents and biological properties as well as provide optimal for extraction of bioactive compounds from the herbs. The data are extensive and generally well presented through figures, tables. The results demonstrate originality and contribute new knowledge to the field

- Writing:

The dissertation is written in clear scientific English. Terminology is appropriate and consistent. While minor grammatical and stylistic corrections are recommended, the overall academic standard is satisfactory. Some impropriate terms should be revised

- References

The reference list consists of 79 research articles which is sufficient and highly relevant to the research topic.

- Scientific quality:

The present work demonstrated high scientific quality through 7 publications

Comments: Table 3.1. Quantitative levels of TPC, TFC, TSC, TAC. The candidate has quantified bioactive compounds in leaves and fruits of *P. tectorius* and *P. amaryllifolius*. However, the method, regarding sampling is confusing. TPC and TFC were measured by taking dried sample powders. The TAC was measured based on the extract (no information about the dried or wet extract). TSC was measured by 50 microliter extract. An explanation of the units for each measurement is necessary.

Table 4.7. The values of DPPH, hydroxyl, and alpha amylase assays were different from those in table 3.1. However, the method is same. You should make it consistently.

The optimization design in Table 5.1, regarding temperature at 80°C is not reasonable since ethanol is evaporated at 78°C

Some references format of author names are wrong and not consistent; check the hard copy of the manuscript

Discussion on extraction and biological activities in the manuscript is quite limited.

Questions:

1. Why did you try to approach saponin in these plants since the literature review did not mention saponin as a common compound of these species.

2. What would be the future formulation of health products that you suggest from these herbs?

Comment on the candidate ability (e.g. general scientific background, understanding on the research field and research topic, presentation skill, English level, etc)

The candidate demonstrates wide scientific background on chemical identification and biological activity investigation with strong experimental capacity with analytical techniques. English for presentation and writing is sufficient and good ability for scientific reasoning and explanation.

Conclusions (indicates whether the manuscript is accepted in the current form or accepted after minor/ major revisions; and whether the candidate deserves the USTH PhD degree)

The thesis satisfies the scientific and academic requirements for the award of the Doctor of Philosophy degree with minor revision as mentioned above

☐ **Accept the manuscript in the current form.**

☑ **Accept the manuscript with minor/ major revisions.**

☐ **The manuscript is not qualified to for the PhD degree.**

Hanoi 21th April, 2026

Jury Member's signature

Nguyen Huu Nghi

UNIVERSITY OF SCIENCE & TECHNOLOGY OF HANOI
UNIVERSITE DES SCIENCES ET DES TECHNOLOGIES DE HANOI
TRƯỜNG ĐẠI HỌC KHOA HỌC & CÔNG NGHỆ HÀ NỘI

USTH
VIETNAM FRANCE UNIVERSITY

PhD Thesis Examination Jury
Final Assessment

Time : April 24, 2026
Location : Meeting Room 402, USTH Building

I. PHD STUDENT:

Full name	**Do Hoang Giang**
Student ID	D22.PMAB.004
Program	Pharmacological, Medical and Agronomical Biotechnology
Thesis title	Phytochemical constituents and bioactivities of Pandanus tectorius and Pandanus amaryllifolius/ *Nghiên cứu thành phần hóa học và hoạt tính sinh học của loài dứa dại (Pandanus tectorius) và loài dứa thơm (Pandanus amaryllifolius)*
Supervisor	Assoc. Prof. Nguyen Tien Dat, Center for Research and Technology Transfer, Vietnam Academy of Science and Technology
Co-supervisor	Assoc. Prof. Nguyen Hai Dang, USTH

II. COMMENTS *(if any)*:

III. FINAL ASSESSMENT:

☐ Agree to award the PhD diploma to the candidate.

☒ Agree to award the PhD diploma to the candidate after revision.

☐ The thesis is not qualified for the PhD diploma. A second jury could be considered.

Jury member
(Signature & full name)

UNIVERSITY OF SCIENCE & TECHNOLOGY OF HANOI
UNIVERSITE DES SCIENCES ET DES TECHNOLOGIES DE HANOI
TRƯỜNG ĐẠI HỌC KHOA HỌC & CÔNG NGHỆ HÀ NỘI

USTH
VIETNAM FRANCE UNIVERSITY

PhD Thesis Examination Jury
Final Assessment

Time : April 24, 2026
Location : Meeting Room 402, USTH Building

I. PHD STUDENT:

Full name	**Do Hoang Giang**
Student ID	D22.PMAB.004
Program	Pharmacological, Medical and Agronomical Biotechnology
Thesis title	Phytochemical constituents and bioactivities of Pandanus tectorius and Pandanus amaryllifolius/ *Nghiên cứu thành phần hóa học và hoạt tính sinh học của loài dứa dại (Pandanus tectorius) và loài dứa thơm (Pandanus amaryllifolius)*
Supervisor	Assoc. Prof. Nguyen Tien Dat, Center for Research and Technology Transfer, Vietnam Academy of Science and Technology
Co-supervisor	Assoc. Prof. Nguyen Hai Dang, USTH

II. COMMENTS *(if any)*:

III. FINAL ASSESSMENT:

☐ Agree to award the PhD diploma to the candidate.

☑ Agree to award the PhD diploma to the candidate after revision.

☐ The thesis is not qualified for the PhD diploma. A second jury could be considered.

Jury member
(Signature & full name)

Nguyễn Hữu Nghị

UNIVERSITY OF SCIENCE & TECHNOLOGY OF HANOI
UNIVERSITE DES SCIENCES ET DES TECHNOLOGIES DE HANOI
TRƯỜNG ĐẠI HỌC KHOA HỌC & CÔNG NGHỆ HÀ NỘI

USTH
VIETNAM FRANCE UNIVERSITY

PhD Thesis Examination Jury
Final Assessment

Time : April 24, 2026
Location : Meeting Room 402, USTH Building

I. PHD STUDENT:

Full name	**Do Hoang Giang**
Student ID	D22.PMAB.004
Program	Pharmacological, Medical and Agronomical Biotechnology
Thesis title	Phytochemical constituents and bioactivities of Pandanus tectorius and Pandanus amaryllifolius/ *Nghiên cứu thành phần hóa học và hoạt tính sinh học của loài dứa dại (Pandanus tectorius) và loài dứa thơm (Pandanus amaryllifolius)*
Supervisor	Assoc. Prof. Nguyen Tien Dat, Center for Research and Technology Transfer, Vietnam Academy of Science and Technology
Co-supervisor	Assoc. Prof. Nguyen Hai Dang, USTH

II. COMMENTS *(if any)*:

- I accept the defence of the PhD Candidate, and his presentation today.
- The thesis should be revised according to the Jury member comments & suggestions

III. FINAL ASSESSMENT:

☐ Agree to award the PhD diploma to the candidate.

☑ Agree to award the PhD diploma to the candidate after revision.

☐ The thesis is not qualified for the PhD diploma. A second jury could be considered.

Jury member
(Signature & full name)

Nguyễn Phi Hùng

UNIVERSITY OF SCIENCE & TECHNOLOGY OF HANOI
UNIVERSITE DES SCIENCES ET DES TECHNOLOGIES DE HANOI
TRƯỜNG ĐẠI HỌC KHOA HỌC & CÔNG NGHỆ HÀ NỘI

USTH
VIETNAM FRANCE UNIVERSITY

PhD Thesis Examination Jury
Final Assessment

Time : April 24, 2026
Location : Meeting Room 402, USTH Building

I. PHD STUDENT:

Full name	**Do Hoang Giang**
Student ID	D22.PMAB.004
Program	Pharmacological, Medical and Agronomical Biotechnology
Thesis title	Phytochemical constituents and bioactivities of Pandanus tectorius and Pandanus amaryllifolius/ *Nghiên cứu thành phần hóa học và hoạt tính sinh học của loài dứa dại (Pandanus tectorius) và loài dứa thơm (Pandanus amaryllifolius)*
Supervisor	Assoc. Prof. Nguyen Tien Dat, Center for Research and Technology Transfer, Vietnam Academy of Science and Technology
Co-supervisor	Assoc. Prof. Nguyen Hai Dang, USTH

II. COMMENTS *(if any)*:

The PhD candidate have well presented the thesis, and satisfactorily responded to the Jury members questions. Very good presentation in general!

III. FINAL ASSESSMENT:

☐ Agree to award the PhD diploma to the candidate.
☑ Agree to award the PhD diploma to the candidate after revision.
☐ The thesis is not qualified for the PhD diploma. A second jury could be considered.

Jury member
(Signature & full name)

Pham Hoang Nam

UNIVERSITY OF SCIENCE & TECHNOLOGY OF HANOI
UNIVERSITE DES SCIENCES ET DES TECHNOLOGIES DE HANOI
TRƯỜNG ĐẠI HỌC KHOA HỌC & CÔNG NGHỆ HÀ NỘI

PhD Thesis Examination Jury
Final Assessment

Time : March 26, 2026
Location : Meeting Room 118, USTH Building

I. PHD STUDENT:

Full name	**Do Hoang Giang**
Student ID	D22.PMAB.004
Program	Pharmacological, Medical and Agronomical Biotechnology
Thesis title	Phytochemical constituents and bioactivities of Pandanus tectorius and Pandanus amaryllifolius/ *Nghiên cứu thành phần hóa học và hoạt tính sinh học của loài dứa dại (Pandanus tectorius) và loài dứa thơm (Pandanus amaryllifolius)*
Supervisor	Assoc. Prof. Nguyen Tien Dat, Center for Research and Technology Transfer, Vietnam Academy of Science and Technology
Co-supervisor	Assoc. Prof. Nguyen Hai Dang, USTH

II. COMMENTS *(if any)*:

- *regarding the structure*
- *regarding the content*
- *conclusions*
- *the reference list*

Questions and Discussions:

1. Why did the author not investigate all plant parts (leaves, fruits, roots, aerial parts) as described in the introduction for other species in the genus?
2. How do the absolute configurations of Pandanusfurans A/B influence their selective cytotoxicity against A549 cells? Were computational docking studies considered?
3. In the fruit optimization study, why were seven conditions presented instead of a single multi-objective optimum, and how do these conditions perform in scaled-up extractions?

For the proposed synergism in P. amaryllifolius, what specific phenolic-alkaloid interactions were hypothesized, and why was no further fractionation performed to confirm this?

III. FINAL ASSESSMENT:

☐ Agree to award the PhD diploma to the candidate.

☑ Agree to award the PhD diploma to the candidate after revision.

☐ The thesis is not qualified for the PhD diploma. A second jury could be considered.

Jury member
(Signature & full name)

Vu Duc Loi

UNIVERSITY OF SCIENCE & TECHNOLOGY OF HANOI
UNIVERSITE DES SCIENCES ET DES TECHNOLOGIES DE HANOI
TRƯỜNG ĐẠI HỌC KHOA HỌC & CÔNG NGHỆ HÀ NỘI

USTH
VIETNAM FRANCE UNIVERSITY

PhD Thesis Examination Jury
Final Assessment

Time : March 26, 2026
Location : Meeting Room 118, USTH Building

I. PHD STUDENT:

Full name	**Do Hoang Giang**
Student ID	D22.PMAB.004
Program	Pharmacological, Medical and Agronomical Biotechnology
Thesis title	Phytochemical constituents and bioactivities of Pandanus tectorius and Pandanus amaryllifolius/ *Nghiên cứu thành phần hóa học và hoạt tính sinh học của loài dứa dại (Pandanus tectorius) và loài dứa thơm (Pandanus amaryllifolius)*
Supervisor	Assoc. Prof. Nguyen Tien Dat, Center for Research and Technology Transfer, Vietnam Academy of Science and Technology
Co-supervisor	Assoc. Prof. Nguyen Hai Dang, USTH

II. COMMENTS *(if any)*:

As a reviewer for thes thesis, I am fully satisfied about the answers to the questions and the discussions about the coming steps of this work.

III. FINAL ASSESSMENT:

■ Agree to award the PhD diploma to the candidate.

☐ Agree to award the PhD diploma to the candidate after revision.

☐ The thesis is not qualified for the PhD diploma. A second jury could be considered.

Jury member
(Signature & full name)

UNIVERSITY OF SCIENCE & TECHNOLOGY OF HANOI
UNIVERSITE DES SCIENCES ET DES TECHNOLOGIES DE HANOI
TRƯỜNG ĐẠI HỌC KHOA HỌC & CÔNG NGHỆ HÀ NỘI

PhD Thesis Examination Jury
Final Assessment

Time : March 26, 2026
Location : Meeting Room 118, USTH Building

I. PHD STUDENT:

Full name	**Do Hoang Giang**
Student ID	D22.PMAB.004
Program	Pharmacological, Medical and Agronomical Biotechnology
Thesis title	Phytochemical constituents and bioactivities of Pandanus tectorius and Pandanus amaryllifolius/ *Nghiên cứu thành phần hóa học và hoạt tính sinh học của loài dứa dại (Pandanus tectorius) và loài dứa thơm (Pandanus amaryllifolius)*
Supervisor	Assoc. Prof. Nguyen Tien Dat, Center for Research and Technology Transfer, Vietnam Academy of Science and Technology
Co-supervisor	Assoc. Prof. Nguyen Hai Dang, USTH

II. COMMENTS *(if any)*:

III. FINAL ASSESSMENT:

☐ Agree to award the PhD diploma to the candidate.

☒ Agree to award the PhD diploma to the candidate after revision.

☐ The thesis is not qualified for the PhD diploma. A second jury could be considered.

Jury member
(Signature & full name)

Lê Nguyễn Thanh

VIETNAM ACADEMY
OF SCIENCE AND TECHNOLOGY
UNIVERSITY OF SCIENCE AND TECHNOLOGY OF HANOI
*

COMMUNIST PARTY OF VIETNAM

Hanoi, April 24, 2026

RESOLUTION OF THE UNIVERSITY'S DOCTORAL THESIS EXAMINATION JURY
(The 1st meeting)

Thesis title: Phytochemical constituents and bioactivities of Pandanus tectorius and Pandanus amaryllifolius/ *Nghiên cứu thành phần hóa học và hoạt tính sinh học của loài dứa dại (Pandanus tectorius) và loài dứa thơm (Pandanus amaryllifolius).*

PhD student's full name: Do Hoang Giang **Student ID:** D22.PMAB.004

Specialty: Pharmacological, Medical and Agronomical Biotechnology, Code: 9420201

Today, April 24, 2026., at USTH, after listening to the thesis presentation by PhD student Do Hoang Giang, the comments from 3 reviewers, the comments of the Jury's members and other participants, the Thesis Examination Jury reached the following conclusions:

1. The title of the thesis is appropriate for the program of Pharmacological, Medical and Agronomical Biotechnology, Code: 9420201.
2. The thesis does not overlap with any previously published works, theses, or thesis.
3. Main scientific conclusions, new points, new contributions of the thesis:

   - From *P. tectorius* leaves, two new benzofuran epimers (Pandanusfurans A and B) and four lignans were elucidated. The lignans contributed to antioxidant capacity, whereas the benzofurans, showed weaker antioxidant activity but exhibited α-amylase inhibition and showed selective cytotoxicity toward A549.
   - This study successfully optimized the extraction process of phenolic- and saponin enriched fractions from *Pandanus tectorius* fruit using the Box–Behnken Design. Phenolic-rich extracts obtained under high ethanol concentration and temperature conditions exhibited strong antioxidant activity.
   - Saponin-rich extracts obtained under lower ethanol concentration and longer extraction times, showed good nitric oxide inhibitory effects, albeit with potential cytotoxicity at higher doses
   - The phytochemical investigation of the phenolic enrichment from *P. amaryllifolius* leaves led to the isolation of 16 compounds, including 3 lignans and 9 benzoate derivatives, together with 3 shikimates and 1 glycoside. Except for 4-hydroxybenzoic acid, the other compounds were identified for the first time from the plant.
   - The optimized phenolic enrichment from *Pandanus amaryllifolius* leaves demonstrated substantial antioxidant and NO inhibition activities, surpassing the efficacy of its individual non-alkaloid and alkaloid fractions.
   - Contribution on Chemistry : expanding the phytochemical knowledge of the genus.

- Chemotaxonomic insights: The clear differentiation between species based on metabolite profiles (phenolics/saponins in *P. tectorius* vs. alkaloids in *P. amaryllifolius*) provides valuable chemotaxonomic markers.

After discussion, the committee unanimously voted to approve the Decision with the results of 7./7 votes in favor (accounting for 100%).

The Chairman of the Committee declared the end of the Thesis Examination Jury at USTH on the same day.

Chairman

Prof.Dr. Nguyen Van Hung

Secretary

Dr. Nguyen Huu Nghi

Director of Department of Academic Affairs

Assoc.Prof. Nguyen Hong Nam